

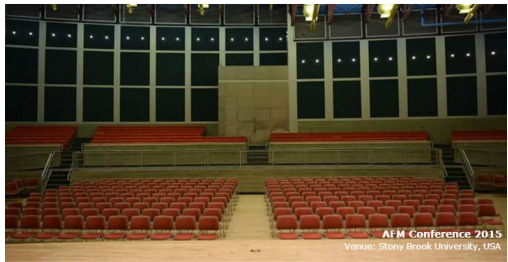
# Abstract Book

Advances  
in Functional *M*aterials



June 29 to July 3, 2015

**Stony Brook University**  
Stony Brook, New York, USA



## Overview

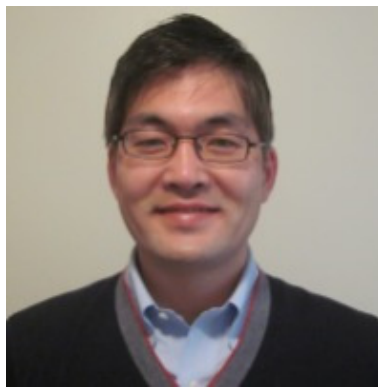
1<sup>st</sup> International Conference on Advances in Functional Materials (AFM 2015) was held on June 29<sup>th</sup> - 03<sup>rd</sup> July 2015, at Stony Brook University, Long Island USA. The objective of this international event was to present and share up to date researches and findings in the field of functional materials science. The conference provided a platform for the researchers to find global partners for future collaboration. More than 1000 abstracts were received from all over the world. A large number of participants including scientists, engineers, educators and students from all over the world attended this event.

The proceedings of the conference will be published in Elsevier journal Materials Today: Proceedings.

## 2015 CONFERENCE CO-CHAIRS



.....  
**PROF. DAE JOON KANG**  
Sungkyunkwan University, Korea

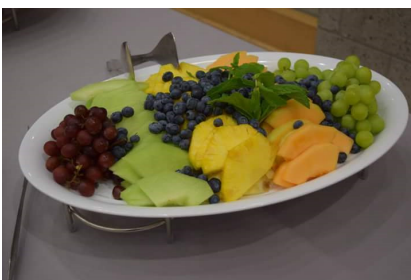


.....  
**PROF. TAE JIN KIM**  
Stony Brook University, USA



.....  
**PROF. IMRAN SHAKIR**  
King Saud University, Saudi Arabia

# PICTURE GALLERY



## ADVISORY COMMITTEE

Following well-known names in the field of Functional Materials and are part of our organizing committee:

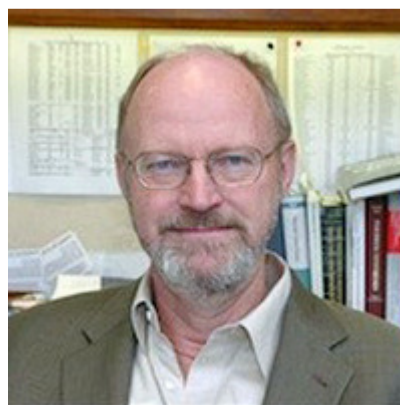
1. [Dr. Zhong Lin Wang](#) (Georgia Tech, USA)
2. [Prof. Hui-Ming Cheng](#) (Chinese Academy of Sciences, China)
3. [Prof. Kwanghee Lee](#) (Gwangju Institute of Science & Technology (GIST), Korea)
4. [Prof. In Sik Nam](#) (Pohang University of Science and Technology, Korea)
5. [Dr. Kazuhiro Takanabe](#) (King Abdullah University of Science and Technology (KAUST))
6. [Prof. Vivek Polshettiwar](#) (Tata Institute of Fundamental Research (TIFR), India)
7. [Prof. Arindam Ghosh](#) (Indian Institute of Science, India)
8. [Prof. Li Zhang](#) (The Chinese University of Hong Kong)
9. [Prof. Rizwan Raza](#) (COMSATS, Pakistan)
10. [Prof. Jason Jieshan Qiu](#) (Dalian University of Technology, China)
11. [Dr. Abbas Amini](#) (University of Western Sydney, Australia)
12. [Dr. Jose Rodriguez](#) (Brookhaven National Laboratory Upton, NY, USA)
13. [Dr. Rajeev S. Assary](#) (Argonne National Laboratory, Lemont IL, USA)
14. [Prof. Hyeon Suk Shin](#) (Ulsan National Institute of Science and Technology , Korea)
15. [Prof. Bin Zhu](#) (KTH, Stockholm, Sweden)
16. [Prof. N. Ali](#) (Chairman CNC Coatings, UK)
17. [Prof. Mohamed Bououdina](#) (University of Bahrain)
18. [Prof. Jean-Marie Basset](#) (Director, KAUST Catalysis Research Center)
19. [Prof. Fuat Celik](#) (Rutgers University, New Jersey, USA)
20. [Prof. Chang-Yong Nam](#) (Brookhaven National Lab, BNL)

## PLENARY SPEAKERS



**ALAN J. HEEGER**

*Recipient of the 2000 Nobel Prize in Chemistry "For the discovery and development of conductive polymers"*



**ROBERT HOWARD GRUBBS**

*Recipient of the 2005 Nobel Prize in Chemistry "For his work in the field of olefin metathesis"*

## KEYNOTE SPEAKERS



**ZHONG LIN (ZL) WANG**

*Director, Center for nanostructure Characterization (CNC), Georgia Tech, USA*



**DR. MIRIAM RAFAILOVICH**

*Director, Garcia materials research science and engineering center, Stony Brook University, USA*



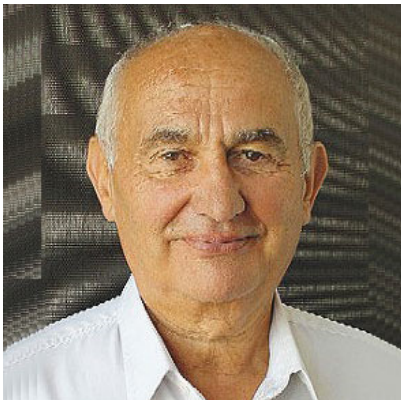
**PROF. ISRAEL E WACHS**

*Director, Operando Molecular Spectroscopy & Catalysis Research LAB, Lehigh University, USA*



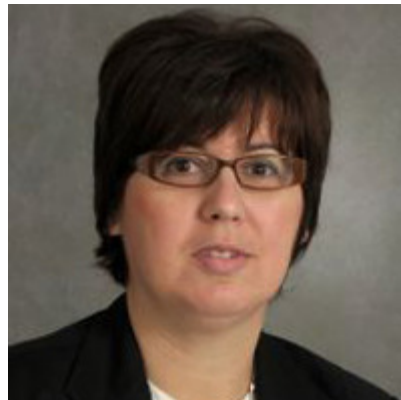
**PROF. STANISLAUS S. WONG**

*Professor of Chemistry, Stony Brook University, USA*



**PROF. JEAN MARIE BASSET**

*Director, KAUST Catalysis research center,  
KAUST, SA*



**PROF. PERENA GOUMA**

*Director of the Center for nanomaterials and sensor development,  
Stony Brook University, USA*



**PROF. LEE CRONIN**

*Regius Chair of Chemistry Laboratory,  
University of Glasgow, UK*



**MIGUEL A. BANARES**

*Deputy Vice President,  
Institute of Catalysis and Petrochemistry, Madrid, Spain*



**PROF. ESTHER TAKEUCHI**

*Professor of Stony Brook University,  
Stony Brook University, USA*



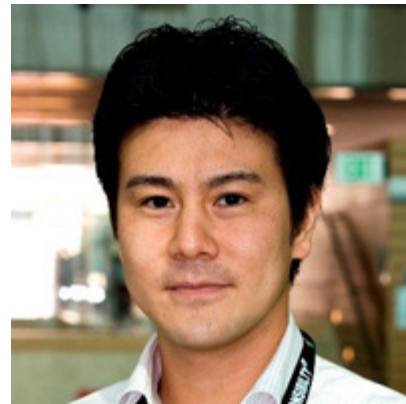
**PROF. HYEON SUK SHIN**

*Associate Professor,  
Ulsan National Institute of Science and Tech. (UNIST), South Korea*



**PROF. KWANGHEE LEE**

*Gwangju Institute of Science & Technology (GIST), Korea*



**PROF. KAZUHIRO TAKANABE**

*Assistant Professor of Chemical Sciences,  
King Abdullah University of Science & Technology (KAUST), KSA*



**JOSE RODRIGUEZ**

*Senior Chemist, Chemistry Dept.  
Brookhaven National Laboratory,  
UPTON, USA*



**DR. RAJEEV S. ASSARY**

*Assistant Scientist,  
Argonne National Laboratory, IL, USA*

## SESSION CHAIRS

### SYMPOSIUM S1

---

1. Dr. Abbas Amini, (University Of Western Sydney, Australia)
2. Dr. Amitesh Paul, (Tu Munich, Germany)
3. Dr. Haixue Yan, (Queen Mary University Of London, UK)
4. Dr. Imran Shakir, (King Saud University, KSA)
5. Dr. Jacques Noudem, (University Of Caen, France)
6. Dr. Mine Yurtsever, (Itu, Turkey)
7. Dr. Satnam Singh, (Thapar University Patiala, India)
8. Prof. Anil Ramdas Bari, (Arts, Commerce & Science College, Bodwad, India)
9. Prof. Dae Joon Kang (Sungkyunkwan University, Korea)
10. Prof. Danmin Liu, (Beijing University Of Technology, China)
11. Prof. Deore, Madhavrao, (Keshavrao Arts, Science And Commerce College, India)
12. Prof. Dr. Wilfred Wunderlich, (Tokai University, Japan)
13. Prof. Imran Shakir, (King Saud University, KSA)
14. Prof. John W. Bridge (University Of Washington, USA)
15. Prof. M V N Ambika Prasad, (Gulbarga University, India)
16. Prof. Pawan Tyagi, (University Of The District Of Columbia, USA)
17. Prof. Rajeevan N.E. (University Of Calicut, India)
18. Prof. Rajshree B Jotania (Gujarat University, India)
19. Prof. Ramesh Harishchandra Bari, (K.R.N.Commerce & M.D.Science College, India)
20. Prof. Wael Mamdouh Ahmed, (The American University In Cairo, Egypt)

### SYMPOSIUM S2

---

1. Dr. Emmanuel Ollier, (Grenoble, France)
2. Dr. Xiang Zhou, (Sun Yat-Sun University, China)
3. Dr. Xinhui Lu, (The Chinese University Of Hong Kong, HK)
4. Mr. Sergei Ovchinnikov, (Kirensky Institute Of Physics, Russia)
5. Prof. Elisa Camilla Dell'Orto, (University Of Milano-Bicocca, Italy)
6. Prof. Gotan Hiralal Jain, (S.P.H.J. Science College, USA)
7. Prof. Jason Trelewicz, (Stony Brook, USA)
8. Prof. Nupur Bahadur, (Amity University Uttar Pradesh, India)

### SYMPOSIUM S3

---

1. Dr. Imran Shakir, (King Saud University, KSA)
2. Dr. Muhammad Khan, (Sultan Qaboos University, Oman)
3. Dr. Prasanna Chandrasekhar, (Ashwin-Ushas Corporation, USA)
4. Prof. Dilip Kumar Kakati, (Gauhati University, India)
5. Prof. Muhammad S. Khan (Sultan Qaboos University, Oman)
6. Prof. Tadanori Koga, (Stony Brook University, USA)
7. Prof. Ubagaram Johnson Alengaram, (University Of Malaya, Malaysia)

### SYMPOSIUM S4

---

1. Dr. Amrit Pal Toor, (Panjab University, Chandigarh, India)
2. Dr. Chang-Yong Nam, (Brookhaven National Lab, USA)
3. Dr. Olga A Baturina, (US Naval Research Center, USA)
4. Dr. Yang, Weiyi, (Institute Of Metal Research, Chinese Academy Of Sciences, China)
5. Dr. Ying Yang, (Tsinghua University, China)
6. Prof. Jianlei Niu, (Hong Kong Polytechnic University, HK)
7. Prof. Jingli Luo, (University Of Alberta, Canada)
8. Prof. Jose Marques-Hueso, (Heriot Watt University, Scotland)
9. Prof. Steven E. Bottle, (Qut, Australia)

### SYMPOSIUM S5

---

1. Dr. Alexandra Rollett (University Of Natural Resources And Life Sciences, Vienna)
2. Ms. Bee Min Goh, (Newcastle University, UK)
3. Ms. Mitali Kakran, (IMRE, Singapore)
4. Prof. Shiladitya Das Sarma, (University Of Maryland, Singapore)



#### SYMPOSIUM S6

---

1. Prof. Rina Tannenbaum, (Stony Brook University, USA)
2. Dr. Louise Duhamel, (Université Lille, UCCS CNRS, France)
3. Dr. Philippe Vernoux, (Université Lyon, France)
4. Prof. Vasundhara Singh (PEC University of Technology, India)

#### SYMPOSIUM S7

---

1. Dr. Abdel Hadi Kassiba, (Univeristy Of Maine, France)
2. Dr. Andre Pereira, (Porto University, Portugal)
3. Dr. Antoine Hervier, (Laboratoire De Réactivité De Surface, France)
4. Dr. Eileen Fong, (Nanyang Technological University, Singapore)
5. Dr. Maria-Thereza Perez, (Lund University, Sweden)
6. Dr. Yuanhui Zheng, (Unsw, Australia)
7. Prof. D S Joag, (Emeritus Scientist, India)
8. Prof. Pervaiz Ahmad, (University Of Malaya, Malaysia)
9. Prof. Uttam K Sarkar, (Malda College, India)

#### SYMPOSIUM SP1

---

1. Prof. Giorgio Sberveglieri, (University of Brescia, Italy)

# Symposia 1

## Advances in Multifunctional Composite materials

---

- Synthesis and characterization of Composite materials
- Dielectric, Ferroelectric and Piezoelectric materials
- Electrostrictive and Magnetostrictive Materials.
- Shape-memory alloy (SMA), (smart metal, memory metal, memory alloy, muscle wire, smart alloy)
- Theoretical/Modelling/Computer Simulations Of Functional Materials
- Nano and mesostructured materials
- Carbon and metal oxide based composite materials
- Superconducting and magnetic materials
- Others

# INDEX PAGE

1. Synthesis And Characterization Of The Quaternary Thioaluminogermanates A(AlS <sub>2</sub> )(GeS <sub>2</sub> ) (A = Na, K) <b>AUTHOR:</b> Mr. Mohammed Abloushi	1
2. Dextran functionalized surfaces for high resolution label-free biosensors <b>AUTHOR:</b> Mr. András Saftics	2
3. Ferroelectricity And Ferromagnetism Of M-Type Lead Hexaferrite <b>AUTHOR:</b> Prof. Guolong Tan	3
4. Structural and magneto-mechanical properties of FeNiGa alloys <b>AUTHOR:</b> Prof. S. U. Jen	4
5. Hybrid Catalytic Membranes: Tunable And Versatile Materials For Fine Chemistry Applications <b>AUTHOR:</b> Dr. Jean-Francois Lahitte	5
6. Nanoscale phase transformation initiation sites in indented bulk of shape memory alloys <b>AUTHOR:</b> Dr. Abbas Amini	7
7. Phase selective synthesis of cobalt disulfide on reduced graphene oxide for hydrogen evolution reaction <b>AUTHOR:</b> Prof. Seongjoon Ahn	8
8. Microstructures and Properties of Piezoelectric Nanoceramics <b>AUTHOR:</b> Dr. Xiaohui Wang	9
9. Synthesis and characterization of the quaternary thioaluminogermanates A(AlS <sub>2</sub> )(GeS <sub>2</sub> ) (A = Na, K) <b>AUTHOR:</b> Dr. Bambar Davaasurenons	10
10. Structural and magnetic properties of X-type Ba <sub>2</sub> Zn <sub>2</sub> Mg <sub>2-x</sub> Fe <sub>28</sub> O <sub>46</sub> hexaferrite powder using citrate gel auto combustion technique <b>AUTHOR:</b> Prof. Rajshree Jotania	11
11. POLYANILINE -NANO ZINC OXIDE COMPOSITE AS A PIGMENT FOR CORROSION PROTECTION OF LOW CARBON STEEL <b>AUTHOR:</b> Dr. Pravin Deshpande	12
12. Dielectric relaxation of Sr <sub>2</sub> AlTaO <sub>6</sub> : Frequency and time domain approach <b>AUTHOR:</b> Dr. Alo Dutta	15
13. Hydroxyapatite with Amorphous Phosphate Phase versus Nano-structured Hydroxyapatite: Solid-State NMR, FTIR and Raman Study of Static and Dynamic Structures <b>AUTHOR:</b> Prof. Vytautas Balevicius	16
14. Effect of Particle Size and Titanium Content on the Fracture Toughness of Particle-Ceramic Composites <b>AUTHOR:</b> Dr. Enrique Rocha-Rangel	17
15. Synthesis of ZnO nanorods by spray pyrolysis for gas sensing application <b>AUTHOR:</b> Mr. Ganesh Patil	18
16. Experimental Investigations of Al-SiC-Gr hybrid metal matrix composites <b>AUTHOR:</b> Dr. Krishnaswamy Marimuthu	19
17. Mechanically Interlocked Derivatives of Carbon Nanotubes <b>AUTHOR:</b> Dr. Emilio Perez	20
18. Development of Braille Block for Visually Handicapped Person using Unsaturated Polyester Resin <b>AUTHOR:</b> Prof. Gwang-Won Lee	21
19. TEM Studies On RMnO <sub>3</sub> Multiferroic Materials <b>AUTHOR:</b> Prof. Richeng Yu	23

20. The influence of electric field induced on the oriented crystallization of Bi <sub>4</sub> Ti <sub>3</sub> O <sub>12</sub> grains in sintering process <b>AUTHOR:</b> Prof. Wanmei Sui	24
21. An advance towards the synthesis of Ag nanorod arrays with controlled surface roughness for SERS substrates <b>AUTHOR:</b> Dr Maria Isabel Gomez	25
22. Structural Properties Of [N(CH <sub>3</sub> ) <sub>4</sub> ] <sub>2</sub> Zn <sub>1-x</sub> CoxCl <sub>4</sub> (X=0, 0.5, 0.7, 0.9, And 1) Mixed Crystals By Mas Nmr <b>AUTHOR:</b> Prof. Ae Ran Lim	28
23. Ceria Mixed Oxides Prepared Through A Microwave-Assisted Synthesis For Co <sub>2</sub> Sensing In Low Power Work Function Sensors. <b>AUTHOR:</b> Mr. Elmar Laubender	29
24. Binder-Free Si Nanoparticle Electrode With 3-D Porous Structure Prepared By Electrophoretic Deposition For Lithium-Ion Batteries <b>AUTHOR:</b> Prof. Yang Yang	30
25. Variation of Crystalline parameters with capping agents and Optical study of Cadmium Sulphide Nanoparticles doped with Erbium ions . <b>AUTHOR:</b> Prof. Usha Kottarathil Thomas	32
26. Analytical Methods to Determine Chemical Changes in High-Oil Paraffin Binders used in Granular Composites <b>AUTHOR:</b> Dr. John Bridge	33
27. ELECTRICAL AND SENSOR BEHAVIOR OF PANI/In <sub>2</sub> O <sub>3</sub> NANO COMPOSITES. <b>AUTHOR:</b> Prof. M V N Ambika Prasad	35
28. Texture Formation in AZ magnesium alloy during High-temperature compression deformation <b>AUTHOR:</b> Prof. Kwonhoo Kim	36
29. Ferroelectrics for SERS Applications <b>AUTHOR:</b> Prof. Xiaoyan Liu	37
30. Pocop Pincer Ligands, Palladium Nanoparticles Composites Or Formal Organometallic Compounds <b>AUTHOR:</b> Prof. Rocio Redon	39
31. Study Of Electrical, Structural And Gas Sensing Properties Of Al <sub>2</sub> O <sub>3</sub> -Doped ZnO Composite Materials Thick Films. <b>AUTHOR:</b> Dr. Madhavrao Deore	40
32. Metal-Salen Polymers for Energy Storage and Conversion <b>AUTHOR:</b> Dr. Semyon Kogan	41
33. Characterization And Optical Study On Zinc Sulphide Nanostructures Doped With Gadolinium <b>AUTHOR:</b> Dr. George Varughese	42
34. Characterization Of Magnetorheological Elastomer (Mre) Engine Mounts. <b>AUTHOR:</b> Mr. Fadly Jashi Darsivan	43
35. Synthesis, Characterization of ZnO nanorods and its interaction with Albumin Protein. <b>AUTHOR:</b> Dr. Satyajit Saha	45
36. Synthesis of silver nanopaticles in thermoplastics <b>AUTHOR:</b> Dr. Jose Marques-Hueso	46
37. Polymeric vesicles for biomedical applications: View on pH- and size-controlled diffusion processes <b>AUTHOR:</b> Dr. Dietmar Appelhans	47
38. Coexistence of ferromagnetism and d-wave superconductivity in YBa <sub>2</sub> Cu <sub>3</sub> O <sub>7-x</sub> /La <sub>0.7</sub> Ca <sub>0.3</sub> MnO <sub>3</sub> bilayer. <b>AUTHOR:</b> Prof. Jiunn-Yuan Lin	48
39. Synthesis of Novel Keggin-type Tungstocobaltate-Functionalized Mesoporous Hybrid Materials and Their Catalytic Performance <b>AUTHOR:</b> Prof. Chun Yang	50

40. Synthesis of graphene/polymer composites by in situ intercalation polymerization and their functional behaviors . <b>AUTHOR:</b> Prof. Zuowan Zhou	51
41. Impact of Anisotropic Biaxial Compressive and Tensile Strain on the Properties of Epitaxial Ferroelectric Films <b>AUTHOR:</b> Prof. Roger Woerdenweber	52
42. Synthesis Of Zno Nanorods And Tripods By Hydrothermal Route For Gas Sensor <b>AUTHOR:</b> Dr. Sarika Shinde	53
43. Charge Relaxation in Titanium-Dioxide Filled High-Impact Polystyrene Films <b>AUTHOR:</b> Dr. Anna Guliakova	55
44. Removal and inactivation of virus and toxin using electrochemical multi-walled carbon nanotube yarns <b>AUTHOR:</b> Dr. Seung Hoon Nahm	56
45. Structure Of Interface Between Matrix Alloy And Reinforcement Particles In Al/Sicp + Cgp Hybrid Composites. <b>AUTHOR:</b> Dr. Anna Janina Dolata	57
46. Comparison of wear study of Al - Si (6% - 18%) - SiCp composites under continuous and reciprocating conditions <b>AUTHOR:</b> Dr. Rajeev Vamadevan	59
47. Hybrid double network Hydrogel for cartilage tissue engineering	61
48. X-ray and neutron scattering on disordered nanosize clusters: computational modelling of lead-zirconate-titanate solid solutions <b>AUTHOR:</b> Dr. Johannes Frantti	62
49. Parameters for Improving Titandioxid TiO2 as Photo catalysis material. <b>AUTHOR:</b> Prof. Wilfried Wunderlich	63
50. POSS-based fluoracrylate diblock copolymer for self-assembled film <b>AUTHOR:</b> Prof. Ling He	64
51. Graphite NanoPlatelets in poly(trimethylene terephthalate) (PTT) based nanocomposites: effect of flake size on electrical conductivity and barrier properties of thin polymer films. <b>AUTHOR:</b> Dr. Sandra Paszkiewicz	66
52. Relationship between damping capacity and texture in magnesium alloy <b>AUTHOR:</b> Prof. Sangpil Kim	68
53. Chemical Vapor Infiltration Of Stacked, Dry-Spun Carbon Nanotube Ribbons For Fabrication Of Multifunctional, Anisotropic Foams With Tunable Properties <b>AUTHOR:</b> Prof. Shaghayegh Faraji	69
54. Directed Metal Assembly using thio-G-Modified DNA for Nanoelectronic Materials <b>AUTHOR:</b> Ms. Samantha Lunn	71
55. Optimal Design of Functionally Graded Structures considering Dynamical Analysis <b>AUTHOR:</b> Prof. Wilfredo Montealegre-Rubio	72
56. EFFECT OF QUARTERNARY ELEMENT ON THE MICROSTRUCTURES AND SHAPE MEMORY PROPERTIES OF Cu-Al-Ni SHAPE MEMORY ALLOYS <b>AUTHOR:</b> Prof. Esah Hamzah	73
57. The use of MgO-paste as a biodegradable bone cement <b>AUTHOR:</b> Prof. Håkan Nygren	74
58. Singular thermal stress analysis of inhomogenous materials with irregular-shaped inclusions <b>AUTHOR:</b> Prof. Meng-Cheng Chen	75
59. Interaction Between Superconductor And Ferromagnetic Layers In Ybco-Lcmo Superlattices - Magnetic And Electrical Measurements. <b>AUTHOR:</b> Prof. Dayse Dos Santos	77
60. Selective uranium extraction from acidic solution using functionalized mesoporous silicas. <b>AUTHOR:</b> Mr. Alexandre Charlot	79

61. A Chiral Copper(Ii) Complex: Synthesis, Crystal Structure, Ferroelectric And Magnetic Properties <b>AUTHOR:</b> Prof. Guang-Xiang Liu	81
62. New Chiral Metal-Mesogenic Nanosystems <b>AUTHOR:</b> Prof. Tatiana Shabatina	83
63. Gold nanoparticles as drug delivery vehicle for Chondroitin sulphate (CS) to treat osteoarthritis. <b>AUTHOR:</b> Mr. Priyanka Dwivedi	84
64. Correction of Characteristics Obtained by Approximate Methods for Mechanical and Mechatronic Systems as Necessary Condition of their Synthesis <b>AUTHOR:</b> Prof. Andrzej Buchacz	86
65. SnO <sub>2</sub> @Graphene Nanocomposite As An Advanced Anode Materials For Lithium-Ion Batteries. <b>AUTHOR:</b> Prof. Haijiao Zhang	87
66. Characterization, Thermal Effects on Optical band gap energy and Photoluminescence in wurtzite Erbium doped Zinc Oxide Nanocrystallites <b>AUTHOR:</b> Mr. Anitha Thomas	89
67. Ether Based Electrolyte Improves The Performance Of CuFeS <sub>2</sub> Spike-Like Nanorod As A Novel Anode For Lithium Storage . <b>AUTHOR:</b> Prof. Jinbao Zhao	90
68. Optical silicones with quantum dots for sustainable lighting <b>AUTHOR:</b> Mr. Huanhuan Feng	91
69. Adsorption Of Bisphenol A From Aqueous Solution Onto Cationic Modified Zeolite <b>AUTHOR:</b> Prof. Jia-Qian Jiang	92
70. A model for high cycle fatigue damage based on a condensed approach for tetragonal ferroelectrics. <b>AUTHOR:</b> Mr. Stephan Lange	96
71. Carbon Nanomaterials via Ionothermal Hot-injection Synthesis <b>AUTHOR:</b> Dr. Yuanqin Chang	98
72. A pathway to optimize the properties of magnetocaloric Mn <sub>x</sub> Fe <sub>2-x</sub> (P <sub>1-y</sub> G <sub>y</sub> ) for magnetic refrigeration <b>AUTHOR:</b> Prof. Danmin Liu	100
73. Poly(trimethylene terephthalate-block-tetramethylene oxide) copolymer nanocomposites reinforced with carbon nanostructures <b>AUTHOR:</b> Dr. Anna Szymczyk	101
74. Superconducting properties of bulk MgB <sub>2</sub> cryo-magnet shaping by Spark Plasma Sintering <b>AUTHOR:</b> Prof. Jacques Noudem	102
75. Effect of TSI-POSS on thermal property of PU hybrid composites from molecular simulation combined with experimental results <b>AUTHOR:</b> Dr. Rui Pan	103
76. The computer analysis and experimental studies of layered composite structural elements in the repair process of railway wagons <b>AUTHOR:</b> Mr. Michał Majzner	104
77. Micromechanical Modeling of Piezoelectric-Piezomagnetic Composites using Computational Piezo-Grains (CPGs) <b>AUTHOR:</b> Dr. Peter Bishay	105
78. Electrical Properties Of Barium Titanate Dispersed Silver Sulphate <b>AUTHOR:</b> Dr. Shyamkant Anwane	106
79. Substitution of formaldehyde in phenolic resins with innovative and bio-based vanillin derived compounds <b>AUTHOR:</b> Mr. Gabriel Foyer	107
80. Microwave-Assisted Synthesis of Sr Al <sub>2</sub> O <sub>4</sub> :Eu <sup>2+</sup> , Dy <sup>3+</sup> Phosphor Powder by Citrate-gel Processing Route. <b>AUTHOR:</b> Dr. Masoud Rajabi	108

81. A Study For Eliminating The Pest Oxidation Of Mosi <sub>2</sub> In Severe Environments <b>AUTHOR:</b> Dr. Yagiz Uzunonat	109
82. Magnesium Silicide Based Materials For Energy Generation And Storage <b>AUTHOR:</b> Prof. Elzbieta Godlewska	110
83. Chemical and imaging surface analysis to improve biomolecule immobilization repeatability for on-chip Mach-Zehnder immunosensors. <b>AUTHOR:</b> Dr. Kamil Awsiuk	111
84. Hybrid Metal-Carbon Nanostructures for Spintronic Applications <b>AUTHOR:</b> Dr. Maria Del Carmen Gimenez Lopez	113
85. Micromechanical Analysis Of Novel Fuzzy Fiber-Reinforced Advanced And Smart Composites <b>AUTHOR:</b> Prof. Manas Ray	114
86. Functional Properties Of Aisi 316L Stainless Steel Processed By Spark Plasma Sintering <b>AUTHOR:</b> Mr. Kostiantyn Tabalaiev	116
87. Tailoring Optical and Rheological Properties of Host-Guest Systems based on an Epoxy Acrylate <b>AUTHOR:</b> Mr. Uwe Gleißner	117
88. Synthesis Mesoporous Silica Hollow Sphere for Transparency-Tunable Devices <b>AUTHOR:</b> Prof. Hong-Ping Lin	120
89. Dielectric behaviour of polyimide films containing TiO <sub>2</sub> nanotubes <b>AUTHOR:</b> Dr. Marius Andrei Olariu	122
90. Anisotropic Ordering in Polymeric Scaffolds via Magnetically Responsive Graphene Oxide/Iron Oxide Hybrid Nanomaterial <b>AUTHOR:</b> Mr. Louis Cheung	123
91. Self-assembling of non-ionic surfactants within the internal structure of layered materials. <b>AUTHOR:</b> Dr. Régis Guégan	125
92. Enzymatic Polyester Functionalization <b>AUTHOR:</b> Dr. Enrique Herrero Acero	126
93. Thin Oriented Polymer Carbon Nanotube Composite Films For Microwave Absorption. <b>AUTHOR:</b> Mr. Henok Mesfin	128
94. Synthesis, characterization and gas sensing properties of Ni <sub>1-x</sub> Zn <sub>x</sub> O nanoparticles and Ni <sub>1-x</sub> Zn <sub>x</sub> /ZnO nanocomposites <b>AUTHOR:</b> Mr. Roussin Lontio Fomekong	130
95. Baw Resonator As Tool Of Characterization Elastic Properties Of Wo <sub>3</sub> Thin Films <b>AUTHOR:</b> Dr. Madjid Arab	131
96. Rare Earth Nanoparticle Generation Via Laser Ablation And Investigation Of Its Stoichiometry Change <b>AUTHOR:</b> Dr. Kyung-Tae Kang	132
97. Studies on LPG Sensing Property of Polyaniline / BaZrO <sub>3</sub> Composites <b>AUTHOR:</b> Prof. Sasikala Mungamuri	133
98. Intermediate annealing of warm-rolled sheets and its influence on the texture evolution in the rolled columnar-grained Fe-Ga alloys <b>AUTHOR:</b> Dr. Chao Yuan	134
99. BULK NODAL-GAP IN OVERDOPED Y <sub>1-x</sub> Ca <sub>x</sub> BCO THIN FILMS <b>AUTHOR:</b> Dr. Eli Farber	135
100. Developing Nanocomposites Membranes, Targeted Drug Delivery Systems, and Novel Nanoscaffolds for Antibacterial and Tissue Regeneration Applications <b>AUTHOR:</b> Prof. Wael Ahmed	136
101. Dimensional Stability Of Alci/Sic+Cg Composites Under Heat Loading <b>AUTHOR:</b> Dr. Maciej Dyzia	137
102. Location of aromatic residue alters the structural and material characteristic of amyloid fibrils. <b>AUTHOR:</b> Prof. Myeongsang Lee	139

103.	Gold nanoparticles as drug delivery vehicle for Chondroitin sulphate (CS) to treat osteoarthritis <b>AUTHOR:</b> Dr. Vijayashree Nayak	140
104.	Encapsulation of Platinum Complex of Indole-7-Carbaldehyde Thiosemicarbazone into Nanolipid Carrier for Sustain Released Anti-Cancer Treatment <b>AUTHOR:</b> Ms. Hapipah Mohd Ali	141
105.	Bio-inspired design of the structure and mechanics of interfacial materials <b>AUTHOR:</b> Dr. Zhao Qin	142
106.	Neutron Diffraction Study on Magnetic Ordering in Bi doped Co <sub>2</sub> MnO <sub>4</sub> <b>AUTHOR:</b> Dr. Rajeevan N.E.	143
107.	On Spray Drying of Uniform Mesoporous Silica Microparticles <b>AUTHOR:</b> Dr. Cordelia Selomulya	145
108.	Electric field-induced transitions in lead-free Bi <sub>0.5</sub> Na <sub>0.5</sub> TiO <sub>3</sub> -based ceramics for energy storage. <b>AUTHOR:</b> Dr. Haixue Yan	147
109.	Microspinners: Controlling Rotational Frequency in Self-Phoretic Janus Devices <b>AUTHOR:</b> Mr. Richard Archer	148
110.	Surface-energy induced formation of bismuth nanowires at room temperature. <b>AUTHOR:</b> Dr. Mingzhao Liu	151
111.	Atomic-Scale Study of Precipitate in Photorefractive KTaO <sub>3</sub> <b>AUTHOR:</b> Mr. Yaobin Xu	152
112.	Supercritical hydrothermal synthesis and electrochemical performance analysis of Li <sub>Mx</sub> Mn <sub>2-x</sub> O <sub>4</sub> <b>AUTHOR:</b> Dr. Xuewu Liu	154
113.	Isotropy Verification of the C/PPS Samples Manufactured from Pellets by Image Processing Methods and Experiment. <b>AUTHOR:</b> Mr. Radek Sedlacek	155
114.	Functional polymer surfaces on performance materials <b>AUTHOR:</b> Dr. Nadia Grossiord	156
115.	Feasibility study on production of fibre cement board using waste Kraft pulp in corporation with Polypropylene and acrylic fibres. <b>AUTHOR:</b> Dr. Morteza Khorami	157
116.	Functionalization of 1D and 2D carbon materials with mixed-valence complexes. <b>AUTHOR:</b> Dr. Hiroaki Ozawa	158
117.	FE simulation of the electromagnetic poling process in multiferroic composites applying physically and phenomenologically motivated constitutive models <b>AUTHOR:</b> Mr. Artjom Avakian	159
118.	The water splitting efficiency of InVO <sub>4</sub> powders synthesized by the hydrothermal process with various InV molar ratio <b>AUTHOR:</b> Prof .Yu-Sheng Lai	160
119.	Synthetic Chemistry With Mesoporous Boron Nitride At High Pressure <b>AUTHOR:</b> Dr. Manik Mandal	161
120.	Molecular Dynamics Simulations on Synthesis of Zinc Oxide in Supercritical Water <b>AUTHOR:</b> Mr. Xiaojuan Wang	162
121.	Quasiparticle band structure and optical dielectric function of perovskite oxides. <b>AUTHOR:</b> Prof. Tripurari Prasad Sinha	163
122.	Non-collinear Spin Polarized Calculations for Multiferroic Bi <sub>2</sub> FeCrO <sub>6</sub> . <b>AUTHOR:</b> Prof. Liliana Braescu	164
123.	Damage and constitutive modelling of ferroelectrics including electrocaloric and thermomechanical effects <b>AUTHOR:</b> Mr. Marius Wingen	166



124.	Protective effects of green tea polyphenols nanoparticles on radiation induced cellular damage: A possible link of NF $\kappa$ B in radioprotection. <b>AUTHOR:</b> Dr. Ramovatar Meena	167
125.	A label-free and sensitive miRNA biosensor based on the electrocatalysis amplification on a Nanotip gold electrode <b>AUTHOR:</b> Dr. Gang Liu	168
126.	A Monte Carlo Study of Magnetic Tunnel Junction Based Molecular Spintronics Devices <b>AUTHOR:</b> Prof. Pawan Tyagi	170
127.	Template synthesis of p-n composite nanotubes for augmented properties. <b>AUTHOR:</b> Dr. Azzuliani Supangat	171
128.	Domain walls effective potential model and interaction with defects <b>AUTHOR:</b> Dr. Rolando Placeres Jimenez	172
129.	In-Situ Synthesis And Characterization Of Pani/Fe <sub>3</sub> O <sub>4</sub> Nanocomposites For Chromium Removal From Ground Water <b>AUTHOR:</b> Dr. Sujin Jose	173
130.	Homogeneous Dispersion Of Au Nanoparticles Into Mesoporous Sba-15 Exhibiting Improved Catalytic Activity For Nitroaromatic Reduction. <b>AUTHOR:</b> Dr. Satnam Singh	175
131.	Structural and electromagnetic interference (EMI) shielding properties of flexible polymer nanocomposite films including novel type functional nano fillers <b>AUTHOR:</b> Dr. Zehra Durmu	176
132.	Investigation Of Intermolecular Interactions Between Fluorene-Based Conjugated Polymers Using The Dispersion-Corrected Dft. <b>AUTHOR:</b> Prof. Jolanta Lagowski	177
133.	Multifunctional materials based on continuous macroscopic fibres of carbon nanotubes combined with polymers and inorganics <b>AUTHOR:</b> Dr. Juan José Vilatela	178
134.	Size control and photoluminescence enhancement of Mn <sup>2+</sup> -doped ZnS nanoparticles synthesized by AOT- reverse micelle modified by compressed CO <sub>2</sub> <b>AUTHOR:</b> Dr. Masturah Markom	179
135.	Tuning the nanostructure of highly functionalized silica using amphiphilic organosilane <b>AUTHOR:</b> Mr. Romain Besnard	180
136.	Photophysic Simulations of THz Wave Generator Originating From Infrared NLO Material SnGa <sub>4</sub> Se <sub>7</sub> . <b>AUTHOR:</b>	182
137.	Lead-Free Relaxor Ferroelectrics For Electrocaloric Cooling <b>AUTHOR:</b> Dr. Gunnar Suchanek	183
138.	Dielectric Relaxation Study of Diethanolamine with Triethanolamine at Melting Points Using Time Domain Reflectometry <b>AUTHOR:</b> Dr. Wei-Qi Huang	184
139.	A model for high cycle fatigue damage based on a condensed approach for tetragonal ferroelectrics <b>AUTHOR:</b> Mr. Andreas Ricoeur	
140.	A label-free and sensitive miRNA biosensor based on the electrocatalysis amplification on a Nanotip gold electrode. <b>AUTHOR:</b> Dr. Zhentao Wang	
141.	Exchange-bias-like coupling in a nondiluted and Cu-diluted-Fe/Tb multilayers <b>AUTHOR:</b> Dr. Amitesh Paul	
142.	Microspinners: Controlling Rotational Frequency in Self-Phoretic Janus Devices . <b>AUTHOR:</b> Mr. David Binns	
143.	Simulations of E-O Effect for Noncentrosymmetry Infrared Materials of SnGa <sub>4</sub> Q <sub>7</sub> (Q = S, Se) <b>AUTHOR:</b> Prof. Wen-Dan Cheng	

144. 146. Location of aromatic residue alters the structural and material characteristic of amyloid fibrils  
**AUTHOR:** Prof. Sungsoo Na
- 
145. An advance towards the synthesis of Ag nanorod arrays with controlled surface roughness for SERS substrates.  
**AUTHOR:** Dr. Daniel Hill
- 
146. Characterization, Thermal Effects on Optical band gap energy and Photoluminescence in wurtzite Erbium doped Zinc Oxide Nanocrystallites .  
**AUTHOR:** Mr. Anitha Thomas
- 
147. Characterization of perlite-epoxy foam cores for sandwich panels  
**AUTHOR:** Mr. Haleh Allameh Haery
- 
148. Ether Based Electrolyte Improves The Performance Of Cufes<sub>2</sub> Spike-Like Nanorod As A Novel Anode For Lithium Storage  
**AUTHOR:** Prof. Yunhui Wang
-

## Synthesis and characterization of the quaternary thioaluminogermanates $A(\text{AlS}_2)(\text{GeS}_2)$ ( $A = \text{Na}, \text{K}$ )

**Mohammed Al-Bloushi**

**Keywords:** Thioaluminogermanate; Semiconductor; Mixed position; Anionic Chain;

### Abstract

Novel quaternary thioaluminogermanates  $\text{Na}(\text{AlS}_2)(\text{GeS}_2)$  (**1**) and  $\text{K}(\text{AlS}_2)(\text{GeS}_2)$  (**2**) were synthesized by solid state reaction of starting materials at 850 °C. They crystallize in tetragonal space group  $I4/mcm$  (no. 140) with unit cell parameters,  $a = 7.4329(2)$  Å,  $c = 5.8352(4)$  Å for  $\text{Na}(\text{AlS}_2)(\text{GeS}_2)$  and  $a = 7.8826(2)$  Å,  $c = 5.8642(4)$  Å for  $\text{K}(\text{AlS}_2)(\text{GeS}_2)$ . The crystal structure comprises of one-dimensional  $[(\text{AlS}_2)(\text{GeS}_2)]^-$  anionic chains and alkali metal cations filling the square antiprismatic voids formed by sulfur atoms. The Raman spectra show characteristic  $\text{GeS}_4$  modes, whereas solid state  $^{27}\text{Al}$  NMR results clearly indicate the tetrahedral coordination of the aluminum. Both **1** and **2** are semiconductors with bandgap of 3.7 eV and 3.6 eV, respectively. They decompose above 680 °C under inert atmosphere, sensitive to air and hydrolyze in water.

## Dextran functionalized surfaces for high resolution label-free biosensors

A. Saftics<sup>1,2</sup>, S. Kurunczi<sup>1</sup>, K. Kamarás<sup>3</sup>, Zs. Szekrényes<sup>3</sup>, N. Q. Khanh<sup>1</sup>, A. Sulyok<sup>1</sup>, M. Fried<sup>1</sup>,  
P. Petrik<sup>1</sup>, R. Horváth<sup>1</sup>

<sup>1</sup>MTA TTK Institute for Technical Physics and Materials Science, Konkoly Thege M. út 29-33,  
H-1121 Budapest, HUNGARY

<sup>2</sup>BME, Faculty of Chemical Technology and Biotechnology, Műegyetem rkp. 3., H-1111  
Budapest, HUNGARY

<sup>3</sup>MTA Wigner Research Centre of Physics, Konkoly Thege M. út 29-33, H-1121 Budapest,  
HUNGARY

*Email of the presenting and corresponding author: saftics@mfa.kfki.hu*

Mode of presentation: poster. Topic: Advances in Biosensors and Biomaterials/Others.

OWLS (Optical Waveguide Lightmode Spectroscopy) sensor chips coated by dextran layer are proposed for various applications (label-free protein detection, cell adhesion studies). The purpose of this work is to investigate dextran layers prepared from 100 and 500 kDa molecular weight carboxymethyl dextran (CMD) on SiO<sub>2</sub>-TiO<sub>2</sub> based OWLS sensor chip surfaces and Si wafer model surfaces, and to demonstrate the stable grafting and wet conformation of the CMD. Several deposition methods of the CMD were applied on 3-aminopropyltriethoxysilane (APTES) and 3-glycidoxypropyltriethoxysilane (GOPS) surfaces. The efficiency of the surface functionalization was evaluated and the layers were characterized by *in situ* OWLS, AFM, ATR-IR, XPS, as well as QCM-D measurements. To extend the study towards biosensor applications, protein-repellent ability of the grafted CMD layers was also probed and the corresponding layer performance and its structure were revealed with unprecedented details.

**Keywords:** biosensor, carboxymethyl dextran, OWLS, grafting

## Ferroelectricity and Ferromagnetism of M-Type Lead Hexaferrite

Guo-Long Tan<sup>\*</sup>, Wei Li

*State Key Laboratory of Advanced Technology for Materials Synthesis and Processing,*

*Wuhan University of Technology, Wuhan 430070, China*

### Abstract

Polarization and related properties in M-type lead hexaferrites ( $\text{PbFe}_{12}\text{O}_{19}$ ) is reported for the first time. The remnant polarization of the  $\text{PbFe}_{12}\text{O}_{19}$  ceramic reaches as high as  $104\mu\text{C}/\text{cm}^2$ , exhibiting large spontaneous polarization at room temperature. Subsequent annealing of the  $\text{PbFe}_{12}\text{O}_{19}$  ceramics in oxygen atmosphere plays a key role on the saturation of its polarization hysteresis loop due to the great enhancement of its electric resistance. Two current peaks in I-V curve reveal the switching of polarization, which provides an effective evidence for the ferroelectricity of the  $\text{PbFe}_{12}\text{O}_{19}$  ceramics. Its temperature dependent dielectric constant demonstrates a colossal change near the vicinity of the transition temperature ( $518^\circ\text{C}$ ) of ferro- to para- phase, which follows modified Curie Weiss law, verifying its relaxor ferroelectric characterization. The ceramics also exhibit strong ferromagnetic characterization. These combined functional responses in  $\text{PbFe}_{12}\text{O}_{19}$  ceramics present an opportunity to create electric devices that actively couple the magnetic and ferroelectric orders.

---

<sup>\*</sup> Corresponding author; Tel: +86-27-87870271; fax: +86-27-87879468. Email address: gltan@whut.edu.cn

## Structural and magneto-mechanical properties of FeNiGa alloys

S. U. Jen<sup>1</sup>, F. L. Chiang<sup>1,2</sup>, W. C. Cheng<sup>2</sup>, L. Y. Yang<sup>1,2</sup> and P. L. Pai<sup>1,2</sup>

1. Institute of Physics, Academia Sinica, Taipei, Taiwan 11529, ROC
2. Dept. of Mechanical Engineering, NTUST, Taipei, Taiwan 106, ROC

$\text{Fe}_{81-x}\text{Ni}_x\text{Ga}_{19}$  alloys, with  $x = 0, 4, 11, 17, 22,$  and  $26$  at.%Ni, were made from an induction furnace, and then cooled slowly to room temperature. The structural property of each alloy was analyzed x-ray and selected area diffraction (SAD) within a plane-view transmission electron microscope (P-TEM) image. For the  $\text{Fe}_{81}\text{Ni}_{19}$  alloy, it contains the disordered A2 (matrix) and ordered  $\text{DO}_3$  phases, while after replacing Fe by Ni, e.g., the  $\text{Fe}_{64}\text{Ni}_{17}\text{Ga}_{19}$  alloy, it contains the disordered A2 (matrix), ordered B2, and ordered  $\text{DO}_3$  phases. All the FeNiGa alloys are highly (110) textured. The magneto-mechanical properties, such as the Young's modulus (E) and the shear modulus (G), were measured as a function of a magnetic field (H), respectively, by the impulse excitation technique. The  $\Delta E$  or  $\Delta G$  effect is defined as  $\Delta E/E \equiv [E_S - E_o]/E_S$ , or  $\Delta G/G \equiv [G_S - G_o]/G_S$ , where subscript "S" means the saturation state @H = 3.0 KOe, and the subscript "o" means the zero-field state. Moreover, the flexural magneto-mechanical coupling coefficient ( $K_E$ ) and the torsional magneto-mechanical coupling coefficient ( $K_G$ ) can be calculated from the following definitions:  $[1 - (K_E)^2]/(K_E)^2 \equiv \Delta E/E_S$  and  $[1 - (K_G)^2]/(K_G)^2 \equiv \Delta G/G_S$ . From the  $K_E$  vs.  $x$  and the  $K_G$  vs.  $x$  plots, we found that  $K_E$  reaches the maximum peak, about 17.9%, and  $K_G = 8.8\%$ , when  $x = 11$  at.%Ni. We also test the hardness ( $H_V$ ) of each alloy. The mechanical yield strength (Y) is defined as  $Y = (1/3)H_V$ . The Y vs.  $x$  plot shows that Y reaches the maximum peak, about 1.73 GPa, when  $x = 17$  at.%Ni, and  $Y = 1.42$  GPa, when  $x = 11$  at.%Ni. Thus, from this study, it is concluded that the  $\text{Fe}_{70}\text{Ni}_{11}\text{Ga}_{19}$  alloy should be a good functional material for the energy harvesting applications.

## Hybrid catalytic membranes: tunable and versatile materials for fine chemistry applications

Yingying Gu<sup>1</sup>, Clélia Emin<sup>1</sup>, Jean-Christophe Remigy<sup>1</sup>, Isabelle Favier<sup>2</sup>, Montserrat Gómez<sup>2</sup>, Richard D. Noble<sup>3</sup>, Jorge Macanás<sup>4</sup>, Berta Domènech<sup>5</sup>, Jean-François Lahitte<sup>1</sup>

<sup>1</sup>Université de Toulouse, INPT, UPS, CNRS, Laboratoire de Génie Chimique, France

<sup>2</sup>Laboratoire Hétérochimie Fondamentale et Appliquée, UMR CNRS 5069, Université de Toulouse, France

<sup>3</sup>Department of Chemical & Biological Engineering, University of Colorado, Boulder, United States

<sup>4</sup>Department of Chemical Engineering, Universitat Politècnica de Catalunya, UPC, Spain

<sup>5</sup>Chemistry Department, Universitat Autònoma de Barcelona, Spain

*E Mail/ Contact Détails : Jean-François LAHITTE, Université de Toulouse, France*

[lahitte@chimie.ups-tlse.fr](mailto:lahitte@chimie.ups-tlse.fr)

The aim of this collaborative international work is the synthesis of polymer-stabilized metallic nanoparticles (MNP, Au or Pd for instance) inside the functionalized polymeric porous membrane in order to develop hybrid catalytic membrane reactors and to test them in model metal-catalyzed organic reactions.

For this issue, a polymeric membrane support (Polyethersulfone on flat sheet or hollow fiber form) was functionalized with an ionogenic polymer capable to retain MNP or MNP precursors (i.e. poly(acrylic acid), poly(diallyldimethylammonium chloride) or poly(ionic liquid)) using an UV photo-grafting method. MNP were then generated inside the polymeric matrix by chemical reduction of salts (in situ synthesis) or captured by the polymeric matrix after a synthesis in solution (ex situ synthesis)[1-2].

For the in situ synthesis, small PdNP (mean diameter 3-4 nm) were found to be homogeneously dispersed in the polymeric grafted layer. For the ex situ synthesis, AuNP were also well dispersed (figure1). No leaching of MNP was detected during filtration processes. We observed that the amount of MNP included in the materials and the catalytic activity were influenced by the properties of the grafted network, from branched to gel-like structure.

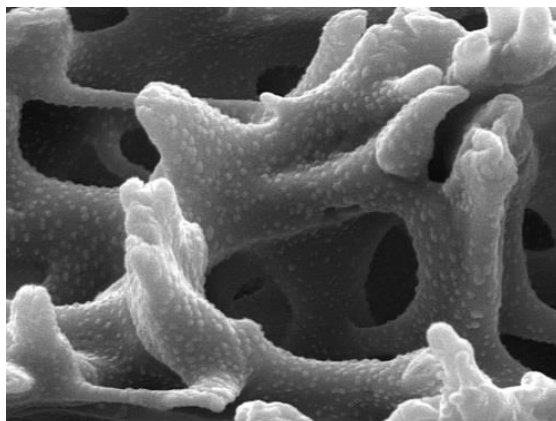


Fig. 1. SEM image of poly(diallyldimethylammonium chloride) grafted polyethersulfone membrane loaded with citrate-stabilized AuNP.

The catalytic performance of the PdNP catalytic membranes was evaluated using various reactions such as chemical reduction of nitrophenol, hydrogenation of (E)-4-phenylbut-3-en-2-one and Suzuki–Miyaura cross-coupling between 4-nitroiodobenzene and phenylboronic acid. The reactions were carried out by filtering solutions containing the reactants leading to full conversions within seconds compared to hours in batch reactors. The as-prepared catalytic membranes were much more efficient than batch reactors or colloidal nanoparticle systems, in terms of reaction time and selectivity. They were reusable more than 10 times without significant loss of their catalytic behaviour giving metal-free organic products.

**Keywords:** *Membrane, nanoparticle, catalysis, functionalisation, photografting*

[1] EMIN, C., REMIGY, J-C., LAHITTE, J-F., 2014. Influence of UV grafting conditions and gel formation on the loading and stabilization of palladium nanoparticles in photografted polyethersulfone membrane for catalytic reactions *C, J. Membrane Sci.*, 455, 55-63

[2] RUIZ, P., MUNOZ M., MACANAS J., TURTA C., PROIUS D., MURAVIEV D.N., 2010. Intermatrix synthesis of polymer stabilized inorganic nanocatalyst with maximum accessibility for reactants, *Dalton Trans.* 39, 1751-1757



## Nanoscale phase transformation initiation sites

### in indented bulk of shape memory alloys

Abbas Amini<sup>\*1</sup>, Chunhui Yang<sup>1,2</sup>, Yang Xiang<sup>1</sup>

<sup>1</sup>School of Computing, Engineering and Mathematics, University of Western Sydney,  
Locked Bag 1797, Penrith, NSW 2751, Australia

<sup>2</sup>Institute for Infrastructure Engineering, University of Western Sydney, Locked Bag  
1797, Penrith, NSW 2751, Australia

*E-mail : a.amini@uws.edu.au, Tel : +61 2 4736 0703*

A hypothesis is proposed for the solid-state phase transformation initiation and propagation in nanoscale bulk under small scale compressive loading during the cyclic spherical nanoindentation on NiTi shape memory alloy. At a low loading rate (isothermal) setup there is only one interface to propagate, however at a high loading rate setup, a jagged depth-load indentation curve concluded in numerous phase transition sites in the stressed bulk. The different responses of two setups are explained by the reorientation, thermal activation volume, as well as different propagation velocity of interface and latent heat exchange rates for two setups.

***Keywords: Shape memory alloy, cyclic loading, phase transition initiation, nanoscale heat transfer, nanoindentation***

## Phase selective synthesis of cobalt disulfide on reduced graphene oxide for hydrogen evolution reaction

Seongjoon Ahn<sup>1,2</sup>, Jieun Yang<sup>1,2</sup> and Hyeon Suk Shin<sup>1,2,3,4</sup>

<sup>1</sup>Department of Energy Engineering, <sup>2</sup>Low Dimensional Carbon Materials Center, <sup>3</sup>Department of Chemistry, <sup>4</sup>Center for Multidimensional Carbon Materials, Institute of Basic Science, Ulsan National Institute of Science and Technology (UNIST), UNIST-gil 50, Ulsan 689-798, Republic of Korea.

*E Mail/ Contact Détails ( sjahn@unist.ac.kr / shin@unist.ac.kr )*

Hybrid materials of transition metal dichalcogenides (TMDs) and reduced graphene oxide (rGO) have recently received considerable attention as good electrocatalytic materials. Among them, CoS<sub>2</sub>/rGO hybrid material has been expected to have higher catalytic ability due to metallic property of CoS<sub>2</sub>. Nevertheless, the selective synthesis of a single phase of CoS<sub>2</sub> has been difficult because the other phase of cobalt sulfides such as CoS, Co<sub>9</sub>S<sub>8</sub>, Co<sub>3</sub>S<sub>4</sub> and CoS<sub>1-x</sub> are co-synthesized with CoS<sub>2</sub>. Here, we present a facile synthetic method of single phase CoS<sub>2</sub>/rGO hybrid material by hydrothermal method using GO as the template with cobalt acetate and thioacetamide as precursors. We revealed that the other phase of cobalt sulfides including Co<sub>3</sub>S<sub>4</sub> and CoS was co-synthesized without GO, because divalent cations (Co<sup>2+</sup>) and dimer sulfur anion (S<sub>2</sub><sup>2-</sup>) are stabilized on the GO surface.<sup>1-2</sup> Furthermore, we measured the hydrogen evolution reaction (HER) performance which shows that CoS<sub>2</sub>/rGO hybrid exhibits a higher electrocatalytic activity compare to the multi-phase products synthesized without GO.

**Keywords:** *electrocatalysis, hybrid materials, hydrogen evolution reaction, cobalt disulfide, reduced graphene oxide*

[1] JIANG, X., MA, Y., LI, J., FAN, Q. & HUANG, W. 2010. Self-Assembly of Reduced Graphene Oxide into Three-Dimensional Architecture by Divalent Ion Linkage. *J. Phys. Chem. C.*, 114, 22462-22465.

[2] ROUT, C., KIM, B. H., XU, X., YANG, J., JEONG, H. Y., ODKHUU, D., PARK, N., CHO, J. & SHIN, H. S. 2013. Synthesis and Characterization of Patronite Form of Vanadium Sulfide on Graphitic Layer. *J. Am. Chem. Soc.*, 135, 8720-8725.

## Microstructures and Properties of Piezoelectric Nanoceramics

Xiao-Hui WANG

State Key Laboratory of New Ceramics and Fine Processing, School of Materials  
Science and Engineering, Tsinghua University, 100084 Beijing, China

### Abstract

There has been great progress in the last decade in the synthesis of nanopowders with highly controlled size and size distribution. Meanwhile, the development of an unconventional pressureless two-step sintering strategy enabling densification without grain growth provides a novel technology suitable for commercial production of nanograin ceramics. Combining the best powder synthesis and optimized two-step sintering, high-density  $(1-x)\text{BiScO}_3-x\text{PbTiO}_3$  (BSPT) solid-solutions with an average grain size down to 10 nm were prepared. Here we report the fabrication methods of high-density BSPT nanoceramics and the major findings of the size effect on their microstructure, phase transition and piezoelectric properties. High-resolution transmission electron microscopy revealed that the samples had dense and thin grain boundaries. Experimental evidence demonstrated that the polarisations of the BSPT nanoceramics were switchable and strong local piezoelectricity is present in 10 nm BSPT nanoceramics by APM. However, the local piezoelectric response showed a large fluctuation over different regions. Moreover, a significant difference between local and macro piezoelectric coefficients was observed. The properties of the grain boundary regions are the key factor to understanding the ferroelectric behaviours of BSPT nanoceramics.

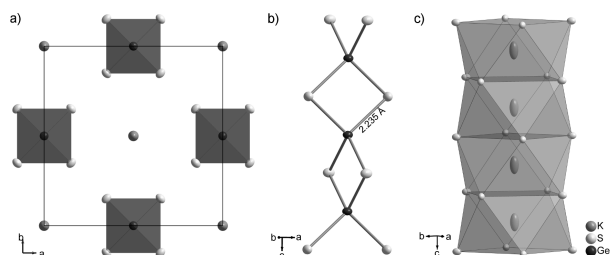
# Synthesis and characterization of the quaternary thioaluminogermanates $A(\text{AlS}_2)(\text{GeS}_2)$ ( $A = \text{Na}, \text{K}$ )

Mohammed Al-Bloushi,<sup>[a]</sup> Bambar Davaasuren,<sup>[a]</sup> Alexander Rothenberger\*<sup>[a]</sup>  
King Abdullah University of Science and Technology  
Thuwal-Jeddah Kingdom of Saudi Arabia

**Abstract:** Novel quaternary thioaluminogermanates  $\text{Na}(\text{AlS}_2)(\text{GeS}_2)$  (**1**) and  $\text{K}(\text{AlS}_2)(\text{GeS}_2)$  (**2**) were synthesized by solid state reaction of starting materials at 850 °C. They crystallize in tetragonal space group  $I4/mcm$  (no. 140) with unit cell parameters,  $a = 7.4329(2)$  Å,  $c = 5.8352(4)$  Å for  $\text{Na}(\text{AlS}_2)(\text{GeS}_2)$  and  $a = 7.8826(2)$  Å,  $c = 5.8642(4)$  Å for  $\text{K}(\text{AlS}_2)(\text{GeS}_2)$ . The crystal structure comprises of one-dimensional  $[(\text{AlS}_2)(\text{GeS}_2)]^-$  anionic chains and alkali metal cations filling the square antiprismatic voids formed by sulfur atoms. The Raman spectra show characteristic  $\text{GeS}_4$  modes, whereas solid state  $^{27}\text{Al}$  NMR results clearly indicate the tetrahedral coordination of the aluminum. Both **1** and **2** are semiconductors with bandgap of 3.7 eV and 3.6 eV, respectively. They decompose above 680 °C under inert atmosphere, sensitive to air and hydrolyze in water.

**Keywords:** Thioaluminogermanate; Semiconductor; Mixed position; Anionic Chain;

Figure 1: The thermal ellipsoid model of  $\text{K}(\text{AlS}_2)(\text{GeS}_2)$  showing the a) unit cell projection along [001], b) one-dimensional anionic partial structure and c) square-antiprismatic voids accommodating potassium cations.



## References:

- [1] a) B. Krebs, *Angew. Chem. Int. Ed.* **1983**, *22*, 113-134; b) W. S. Sheldrick, M. Wachhold, *Angew. Chem. Int. Ed.* **1997**, *36*, 206-224; c) W. S. Sheldrick, U. W. Michael, *Coord. Chem. Rev.* **1998**, *176*, 112; d) W. S. Sheldrick, M. Wachhold, *Coord. Chem. Rev.* **1998**, *176*, 211-322.
- [2] G. S. Armatas, M. G. Kanatzidis, *Nat Mater* **2009**, *8*, 217-222.
- [3] J. H. Liao, G. M. Marking, K. F. Hsu, Y. Matsushita, M. D. Ewbank, R. Borwick, P. Cunningham, M. J. Rosker, M. G. Kanatzidis, *J. Am. Chem. Soc.* **2003**, *125*, 9484-9493.
- [4] M. Tampier, D. Johrendt, *Z. Anorg. Allg. Chem.* **2001**, *627*, 312-320.
- [5] a) M. A. McGuire, T. K. Reynolds, F. J. DiSalvo, *Chem. Mater.* **2005**, *17*, 2875-2884; b) M. A. McGuire, T. J. Scheidemann, J. V. Badding, F. J. DiSalvo, *Chem. Mater.* **2005**, *17*, 6186-6191.
- [6] Y. Kim, I.-s. Seo, S. W. Martin, J. Baek, P. Shiv Halasyamani, N. Arumugam, H. Steinfink, *Chem. Mater.* **2008**, *20*, 6048-6052.
- [7] P. Wu, Y.-J. Lu, J. A. Ibers, *J. Solid State Chem.* **1992**, *97*, 383-390.
- [8] A. Rothenberger, M. Shafaei-Fallah, M. G. Kanatzidis, *Inorg. Chem.* **2010**, *49*, 9749-9751.
- [9] R. D. Shannon, *Acta Crystallogr. Sect. A: Found. Crystallogr.* **1976**, *32*, 751-767.
- [10] R. D. Shannon, *Acta Crystallogr. Sect. A: Found. Crystallogr.* **1976**, *32*, 751.
- [11] B. Eisenmann, A. Hofmann, *Z. Kristallogr.* **1991**, *197*, 161-162.
- [12] a) Y. Wu, C. Nather, W. Bensch, *Acta Crystallogr. Sect. E: Struct. Rep. Online* **2003**, *59*, i137-i138; b) K. O. Klepp, M. Zeitlinger, *Z. Kristallogr. - New Cryst. Struct.* **2000**, *215*, 7; c) K. O. Klepp, F. Fabian, *Z. Naturforsch., B: Chem. Sci.* **1999**, *54*, 1499-1504.
- [13] H. P. Preishuber, K. O. Klepp, *Z. Kristallogr. - New Cryst. Struct.* **2003**, 218-387.
- [14] J. F. Olivier, E. Philippot, M. Ribes, M. Maurin, *Rev. Chim. Miner.* **1972**, *9*, 757-770.
- [15] M. Melullis, S. Dehnen, *Z. Anorg. Allg. Chem.* **2007**, *633*, 2159-2167.
- [16] a) C. R. Nelson, S. A. Poling, S. W. Martin, *J. Non-Cryst. Solids* **2004**, *337*, 78-85; b) K. K. Rangan, M. G. Kanatzidis, *Inorg. Chim. Acta* **2004**, *357*, 4036-4044; c) X. Han, G. Sun, Y. Liu, H. Yang, Y. Liu, *Chalcogenide Letters* **2012**, *9*, 465-474.

**Structural and magnetic properties of X-type  $\text{Ba}_2\text{Zn}_2\text{Mg}_{2-x}\text{Fe}_{28}\text{O}_{46}$  hexaferrite powder using citrate gel auto combustion technique**

**R. B. Jotania and Amrin Kagdi**

**Department of Physics, University school of sciences, Gujarat University,  
Ahmedabad 380 009, India**

Magnesium doped barium zinc hexaferrite with composition  $\text{Ba}_2\text{Zn}_2\text{Mg}_{2-x}\text{Fe}_{28}\text{O}_{46}$  ( $x = 0.0, 0.4, 0.8, 1.2, 1.6$  and  $2.0$ ) have been prepared using citrate gel auto combustion technique. The prepared precursors samples sintered at various temperatures ( $950$  to  $1200$  °C) in order to get pure crystalline phase. Structural and Magnetic properties of Mg doped barium zinc hexaferrites were investigated using various experimental techniques. FTIR spectra of the samples (Calcined at  $1150$  °C) was recorded at room temperature in mid IR range show stretching of M-O band. XRD is used to check phase purity of prepared samples. SEM and VSM measurements used in order to investigate micro structural and magnetic properties.

Keywords: X-type hexaferrite, Citric acid sol-gel method, FTIR, XRD

## POLYANILINE -NANO ZINC OXIDE COMPOSITE AS A PIGMENT FOR CORROSION PROTECTION OF LOW CARBON STEEL

P. P. Deshpande  
Department of Metallurgy and Materials Science  
College of Engineering  
Shivajinagar, Pune- 411005 (M.S.) India  
\*E mail- [pravinpd@hotmail.com](mailto:pravinpd@hotmail.com)

### ABSTRACT

Conducting polyaniline -2 wt% nano zinc oxide based composite was synthesized by chemical oxidation technique in ortho phosphoric acid and the composite was used a pigment for making epoxy based paint coating. The composite was characterized by Fourier transform infrared spectroscopy and UV-VIS absorption spectroscopy which revealed the formation of conducting phase of polyaniline. The morphology of the pigment was studied using transmission electron microscopy.

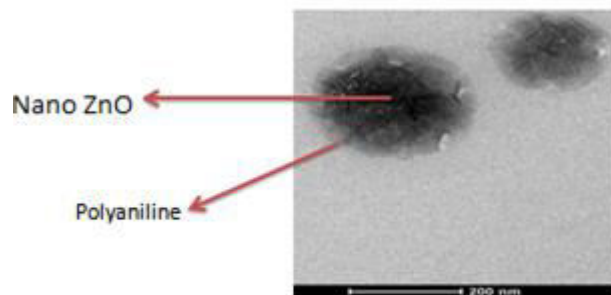


Figure 1: TEM Image of PANI- Nano Zn O composite

TEM investigations revealed in situ polymerization of conducting polyaniline around nano zinc oxide particles as shown in the figure 1. The conductivity of pigment was measured by four probe method and Hall effect measurements were conducted for calculating charge carrier concentration and to determine the semiconducting nature of the pigment. Hall effect measurements confirmed the formation of semiconducting junction. The corrosion protection aspects of the paint coating on low carbon steel were investigated in aqueous 3.5% NaCl solution by potentiodynamic polarization studies, open circuit potential measurements, electrochemical impedance spectroscopy, cyclic corrosion testing, salt spray testing and zero

resistance ammetry. Corrosion rate of conducting polyaniline - 2 wt% nano zinc oxide based paint coating in 3.5 % NaCl was found to be 1.7 mpy which is about 6.3 times lower than that of unpainted low carbon steel in same medium by potentiodynamic polarization studies.

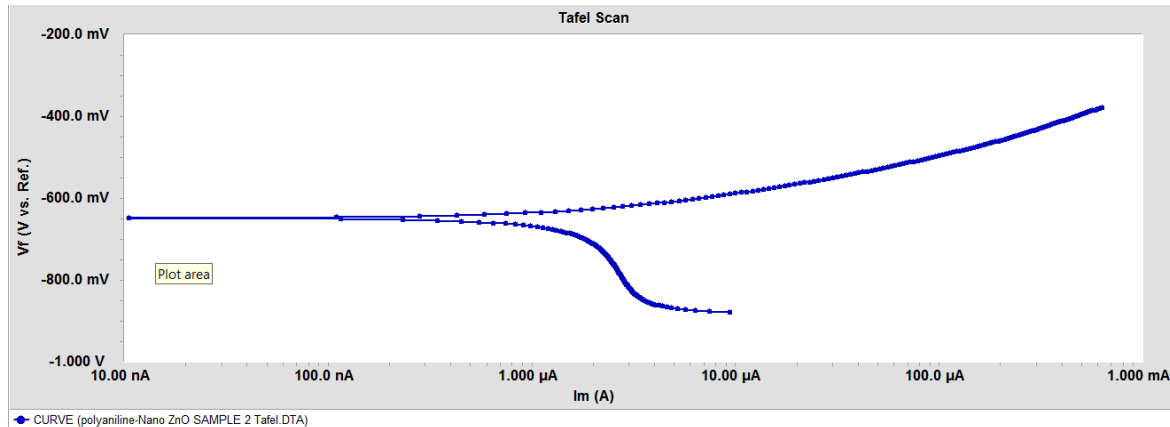


Figure 2 : Tafel plot - Conducting polyaniline - 2 wt% nano zinc oxide based paint coating in 3.5 % NaCl

Open circuit potential measurements, electrochemical impedance spectroscopy, cyclic corrosion testing, salt spray testing supported potentiodynamic polarization results.

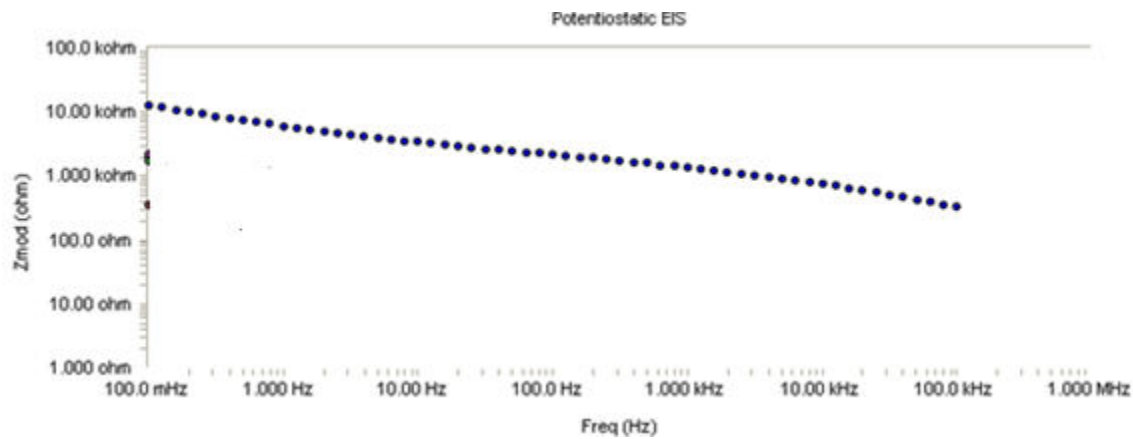


Figure 3 : Bode plot - Conducting polyaniline - 2 wt% nano zinc oxide based paint coating in 3.5 % NaCl

Zero resistance ammetry confirmed that the paint coating exhibited significant resistance to galvanic corrosion in 3.5 % NaCl. Enhanced corrosion protection can be attributed to the combined protection effect due to the redox activity of conducting polyaniline, increased surface area of conducting polyaniline based pigment for release of dopant and the P-N junction between conducting polyaniline and nano zinc oxide particle acting as a barrier for charge transport.



## Dielectric relaxation of $\text{Sr}_2\text{AlTaO}_6$ : Frequency and time domain approach

Alo Dutta\*, P. K. Mukhopadhyay and T. P. Sinha<sup>§</sup>

S. N. Bose National Centre for Basic Sciences  
Block-JD, Sector-III, Salt Lake, Kolkata-700098, India

<sup>§</sup>Department of Physics, Bose Institute, 93/1, A. P. C. Road, Kolkata-700009, India

\*Email: alo\_dutta@yahoo.com

The conduction mechanism in dielectric perovskites has been widely investigated by the various relaxation processes. Two formalisms are usually employed for relaxation: (i) the dipolar (or conductivity) formalism in the frequency domain originating from the motion of permanent dipoles, which can be described as a direct relationship between the dielectric constant and the admittance. The Cole–Cole or Davidson–Cole or Havriliak–Negami model is used to study the dipolar relaxation mechanism in the materials [1-3]. (ii) The electric modulus formalism, which uses electric modulus data to obtain a decay function  $\phi(t)$  in the time domain. The experimental data are converted from frequency domain into the time domain by using Fourier transform method [4, 5]. The relaxation function  $\phi(t)$  obtained by time domain method is usually found to be a stretched exponential decay function of Kohlrausch-Williams-Watts (KWW) type.

We present the effect of correlated hopping motion of charge carriers on the electrical conductivity relaxation of the complex perovskite oxide  $\text{Sr}_2\text{AlTaO}_6$  (SAT). The Rietveld refinement of the X-ray diffraction data at room temperature of SAT synthesized by solid-state reaction technique reveals the cubic  $\text{Fm}\bar{3}\text{m}$  phase. The conductance, capacitance, impedance and phase are measured in a temperature range from 303 to 503 K and in a frequency range from 50 Hz to 1 MHz. We have analyzed the conduction mechanism in SAT under frequency and time domains. In time domain, the time decay function  $\phi(t)$  is obtained from the imaginary part of electric modulus by using the Cole-Cole distribution function. The KWW function is used to analyse the time dependent behaviour of  $\phi(t)$ . The decreasing trend of  $\phi(t)$  with increasing temperature indicates the strong correlation between the hopping ion and their neighbouring ions. The frequency dependent conductivity spectra follow the power law. The power law regime is a description of the slowing down of the relaxation process as a result of cooperative effects, much in the same way as the KWW function does in the time domain.

[1] Alo Dutta, T. P. Sinha, S. Shannigrahi, *Phys. Rev. B* **76**, 155113 (2007).

[2] Alo Dutta, T. P. Sinha, B. Pahari, R. Sarkar, K. Ghoshray, S. Shannigrahi, *J. Phys.: Condens. Matter* **20**, 445206 (2008).

[3] P. Kumari, Alo Dutta, S. Shannigrahi, S. Prasad, T. P. Sinha, *J. Alloy. Compd.* **593**, 275 (2014).

[4] Alo Dutta, T. P. Sinha, *Physica B* **405**, 1475 (2010).

[5] C. Bharti, Alo Dutta, T. P. Sinha, *Solid State Sci.* **14**, 920 (2012).

## Hydroxyapatite with Amorphous Phosphate Phase *versus* Nano-structured Hydroxyapatite: Solid-State NMR, FTIR and Raman Study of Static and Dynamic Structures

Vytautas Klimavicius<sup>1</sup>, Laurynas Dagys<sup>1</sup>, Jonas Kausteklis<sup>1</sup>, Aleksandra Prichodko<sup>2</sup>, Aivaras Kareiva<sup>2</sup>, Valdemaras Aleksa<sup>1</sup>, Vytautas Balevicius<sup>1</sup>

<sup>1</sup>*Department of General Physics and Spectroscopy, Vilnius University, Sauletekio 9-3, LT-10222 Vilnius, Lithuania*

<sup>2</sup>*Department of Inorganic Chemistry, Vilnius University, Naugarduko 24, LT-03225 Vilnius, Lithuania*

Two calcium hydroxyapatites (containing amorphous phosphate phase (ACP-CaHA) and nano-structured (nCaHA)) have been prepared by sol-gel synthesis routes. Their structural organization respect to hydroxyl groups has been determined by means of solid-state NMR, FTIR and Raman spectroscopy. All these spectroscopic techniques confirm that the amount of structural –OH groups in nCaHA is significantly higher than that from adsorbed water and vice-verse in ACP-CaHA. A precise <sup>1</sup>H and <sup>31</sup>P NMR signal shape analysis has been carried out for both studied samples using a huge experimental dataset (> 4000 points per contour). The <sup>1</sup>H spin-lattice and spin-spin relaxation time measurements revealed the fast spin motion takes place in ACP-CaHA. The effect of MAS rate on the <sup>31</sup>P signal width confirms that the correlation time of this motion gets into the time scale of microseconds or even nanoseconds. Such fast dynamics can be attributed to the rotational diffusion of adsorbed water molecules. The magnitude of the inhomogeneous anisotropic broadening of  $1220 \pm 20$  Hz determined for nano-structured sample is very close to 1185 Hz that corresponds to the maximum of Gauss distribution of dipolar <sup>1</sup>H–<sup>31</sup>P coupling obtained using <sup>31</sup>P–<sup>1</sup>H CP MAS kinetics [1]. The dynamics of this interactions runs in the time scale of microseconds and it is much slower than in ACP-CaHA.

We acknowledge funding from the European Community's social foundation under Grant Agreement No. VP1-3.1-ŠMM-08-K-01-004/KS-120000-1756 and the financial support to A.P. from the Research Council of Lithuania under project "Postdoctoral Fellowship Implementation in Lithuania" (No. 004/102).

[1]. V. Klimavicius, A. Kareiva, V. Balevicius, *J. Phys. Chem. C*, 2014 (submitted).

## Effect of Particle Size and Titanium Content on the Fracture Toughness of Particle-Ceramic Composites

Rocha-Rangel Enrique<sup>1</sup>, Cruz-Sánchez Brianda<sup>1</sup>, Esparza-Vázquez Sergio<sup>1</sup>,  
Estrada-Guel Ivanovich<sup>2</sup> and Martínez-Sánchez Roberto<sup>2</sup>

<sup>1</sup>Polytechnic University of Victoria, Av. Nuevas Tecnología 5902, Parque Científico y Tecnológico de Tamulipas, Cd. Victoria, Tamaulipas 87138, México.

<sup>2</sup>CIMAV, Miguel de Cervantes 120, Complejo Industrial Chihuahua, Chihuahua, Chi. 31109, México.

*E Mail: erochar@upv.edu.mx*

Through the combination of an intense powder mixing in a planetary mill and pressureless sintering process they were manufactured Al<sub>2</sub>O<sub>3</sub>-ceramic composites strengthened with different amounts of Ti nano-particles (0.0, 0.5, 1.0, 2.0 and 3.0 wt. %). They were used three different times (1, 3 and 6 h) for mixing the materials. After milling, powders observations in a scanning electron microscopy show good dispersion of titanium in the mixture for the three milling times. From these observations it was estimated that the size of titanium particles is around 100nm, whereas, Al<sub>2</sub>O<sub>3</sub> presents sizes of 1-2µm. With these powders they were fabricated cylindrical samples by uniaxial pressing using 350MPa. Then samples were sintered at 1500°C during 2h. Resulting microstructures observed by optical and scanning electron microscopy, show dense composites formed by a fine Al<sub>2</sub>O<sub>3</sub>-ceramic matrix with homogeneous immerse distribution of titanium nano-particles. The behavior of fracture toughness of the composites is directly dependent with the titanium content in the ceramic-matrix. In this way as the titanium contents increased, the composites exhibited high values of fracture toughness.

***Keywords: Al<sub>2</sub>O<sub>3</sub>; Particle size; Ti nanoparticles; Fracture toughness.***

## Synthesis of ZnO nanorods by spray pyrolysis for gas sensing application

G. E. Patil and G. H. Jain

Department of Physics, SNJB's KKHA Arts, SMGL Commerce & SPHJ Science College, Chandwad District- Nashik MH INDIA

E-mail: ganeshpatil\_phy@rediffmail.com

### Abstract

Hexagonal pillar shaped ZnO nanorods with different sizes have been successfully synthesized by spray pyrolysis technique (SPT). The equal amount of methanol and water is used as a solvent to dissolve the AR grade Zinc acetate for precursor solution. This solution is sprayed on to the glass substrate heated at 350 °C. The films were characterized by ultra-violet spectroscopy (UV), X-ray diffraction (XRD), field emission scanning electron microscopy (FESEM) and transmission electron microscopy (TEM). The deposition of thin films results in a layer comprising well-shaped hexagonal ZnO nanorods with diameter of 90–120 nm and length of up to 200 nm. The gas sensing properties of these films have been investigated for various interfering gases such as CO<sub>2</sub>, CO, ethanol, NH<sub>3</sub> and H<sub>2</sub>S, etc. at operating temperature from 30° (room temperature) to 450 °C. The results indicate that the ZnO nanorods thin films showed much better response and stability than the conventional materials to H<sub>2</sub>S gas (100 ppm) at 50 °C.

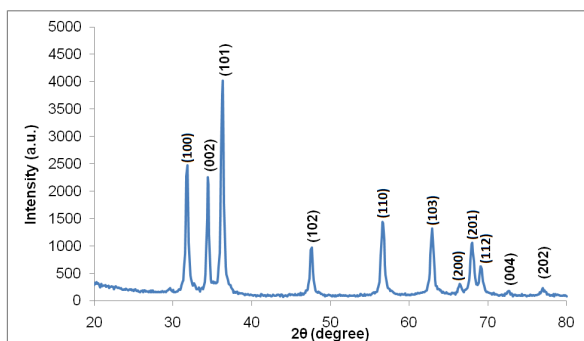


Figure 1: XRD pattern of ZnO thin film

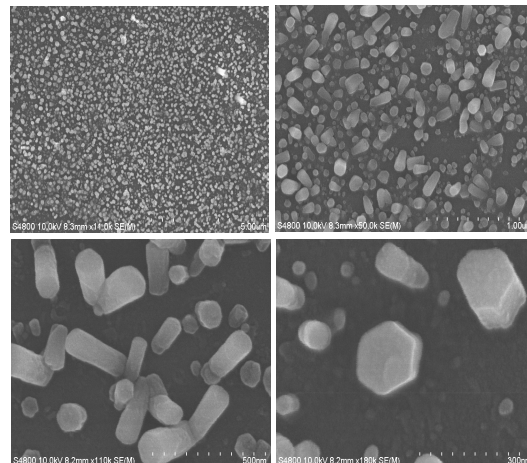


Figure 2: FESEM images of ZnO nanorods thin film

Nowadays due to increased threat of international terrorism and their use of toxic chemical attack, societies need to pay more attention on protecting their citizens from attack of toxic chemicals, either by accident or terrorist act. Therefore fast detection and identification of toxic chemicals is crucial for efficient protection of citizens. Therefore, these nanostructured thin films can be used to test the chemical warfare agents (CWA).

## Experimental Investigations of Al–SiC–Gr hybrid metal matrix composites

K. MARIMUTHU<sub>1</sub> P. SURESH<sub>2</sub>

1. Coimbatore Institute of Technology, Coimbatore 641014, Tamilnadu, India;

2. School of Mechanical Engineering, Galgotias University, Greater Noida 201306, Uttar Pradesh, India;

### **Abstract:**

Metal matrix composites reinforced with graphite particles provide better machinability and tribological properties. The present study attempts to find the optimal level of machining parameters for multi-performance characteristics in turning of Al–SiC–Gr hybrid composites using grey-fuzzy algorithm. The hybrid composites with 5%, 7.5% and 10% combined equal mass fraction of SiC–Gr particles were used for the study and their corresponding tensile strength values are 170, 210, 204 MPa respectively. Al–10%(SiC–Gr) hybrid composite provides better machinability when compared with composites with 5% and 7.5% of SiC–Gr. Grey-fuzzy logic approach offers improved grey-fuzzy reasoning grade and has less uncertainties in the output when compared with grey relational technique. The confirmatory test reveals an increase in grey-fuzzy reasoning grade from 0.619 to 0.891, which substantiates the improvement in multi-performance characteristics at the optimal level of process parameters setting.

**Key words:** hybrid mmc; machining; optimization; grey-fuzzy algorithm

## Mechanically Interlocked Derivatives of Carbon Nanotubes

A. de Juan, A. López-Moreno, S. Leret, M. Bernal, L. de Juan, E. M. Pérez

IMDEA Nanociencia, C/Faraday 9, Ciudad Universitaria de Cantoblanco, 28049 Madrid,  
SPAIN.

*emilio.perez@imdea.org*

Extensive research has been devoted to the chemical manipulation of carbon nanotubes. The attachment of molecular fragments through covalent-bond formation produces kinetically stable products, but implies the saturation of some of the C-C double bonds of the nanotubes.[1] Supramolecular modification maintains the structure of the SWNTs but yields labile species.[2] Here, we present a strategy for the synthesis of mechanically interlocked derivatives of SWNTs (MINTs).[3] In the key rotaxane-forming step, we employed macrocycle precursors equipped with two recognition units and terminated with bisalkenes that were closed around the nanotubes through ring-closing metathesis (RCM). The mechanically interlocked nature of the derivatives is probed by analytical, spectroscopic, and microscopic techniques, as well as by appropriate control experiments. Individual macrocycles were observed to circumscribe the nanotubes through HR-TEM.

**Keywords:** *Carbon nanotubes, mechanically interlocked molecules, rotaxanes, supramolecular chemistry, molecular machinery*

[1] SINGH, P., CAMPIDELLI, S., GIORDANI, S., BONIFAZI, D., BIANCO, A. & PRATO, M. 2009. Organic functionalization and characterization of single-walled carbon nanotubes. *Chem. Soc. Rev.*, 38, 2214-2230.

[2] ZHAO, Y.-L. & STODDART, J. F. 2009. Noncovalent Functionalization of Single-Walled Carbon Nanotubes. *Acc. Chem. Res.*, 42, 1161-1171.

[3] a) DE JUAN, A., POUILLON, Y., RUIZ-GONZALEZ, L., TORRES-PARDO, A., CASADO, S., MARTIN, N., RUBIO, A. & PEREZ, E. M. 2014. Mechanically Interlocked Single-Wall Carbon Nanotubes. *Angew. Chem., Int. Ed.*, 53, 5394-5400. b) LÓPEZ-MORENO & PÉREZ, E. M. 2014, Pyrene-based Mechanically Interlocked SWNTs. *Chem. Commun.* submitted by invitation to the 2015 Emerging Investigators Issue.

## Development of Braille Block for Visually Handicapped Person using Unsaturated Polyester Resin

Gwang-Won Lee<sup>1</sup>, Jun-Ho Choi<sup>1</sup>, Kwon-Hoo Kim<sup>1</sup>, Cheol-Jae Yoon<sup>2</sup>, Seong-Hwan Yoon<sup>3</sup>

<sup>1</sup>Pukyong National University, 45 Yongso-ro, Nam-gu, Busan 608-737, Korea

<sup>2</sup>Kyungpook National University, 80 Daehak-ro, Buk-gu, Daegu 702-701, Korea

<sup>3</sup>Pusan National University, 2 Busandaehak-ro, Geumjeong-gu, Busan 609-735, Korea

*E Mail/ Contact Détails (Corresponding Author: [jchoi@pknu.ac.kr](mailto:jchoi@pknu.ac.kr) (J. H. Choi))*

In this study, a braille block was developed from unsaturated polyester resin to overcome the disadvantages of cement-type braille blocks for visually handicapped persons. The two braille blocks were compared experimentally. The blocks were fabricated by mixing sand, crushed sand, blast furnace slag, unsaturated polyester resin, pigment, hardener, hardening accelerator, antifoaming agent, and polycarboxylic-type high-performance water-reducing agent. Unsaturated polyester resin hardens considerably slower than cement, and this produces many unaesthetic micropores on the exterior. These disadvantages were overcome by using the hardener, blast furnace slag, and antifoaming agent. In compression tests, the current cement-type braille block showed a strength of 6 MPa. It had a strength of 10 MPa when silica fume and high-performance water-reducing agent were added. The low compression strength was because the water/cement ratio was 12%, which means that the amount of water was inadequate. In contrast, the braille block with unsaturated polyester resin showed compression strengths of 91 and 51.7 MPa for the upper and lower parts, respectively. The large difference of 40 MPa was apparently caused by the difference in porosity. In an adsorption test, the braille block made from unsaturated polyester resin showed an adsorption of 0.95%, which is excellent compared to the 11% of the cement-type braille block. After the unsaturated polyester resin braille block was hardened at room temperature, it was alternately exposed to room temperature and sub-zero temperatures 1 day at a time for 1 week. The strength was then measured and found to be an average of 46.3 MPa. In brief, a braille block made from unsaturated polyester resin and a cement-type braille block were compared, and the former showed excellent results in terms of its compression strength, adsorption rate, and freeze/thaw resistance.

***Keywords: Unsaturated polyester resin, braille blocks, visually handicapped person***

[1] PARK, H. S., HWANG, K. R. & SOH, Y. S. 1995. Effect of filler on Strength Properties of Unsaturated Polyester Resin Mortar. Journal of Architectural Institute of Korea, v.11, n.1, 161-165. (Written in Korean Language)

[2] VALORE, R. C. & NAUS, D. J. 1976. Resin bound Aggregate Material System, Polymer in Concrete, Proceedings of the First International Congress on Polymer Concrete, The Construction Press, Lancaster, 216-222

[3] REBEIZ, K. S., FOWLER, D. W., & PAUL, D. R. 1994. Mechanical Properties of Polymer Concrete Systems Made with Recycled Plastic, ACI Materials Journal, v.91, n.1, 40-45



## TEM studies on $\text{RMnO}_3$ multiferroic materials

Q. H. Zhang<sup>1</sup>, G. T. Tan<sup>2</sup>, L. J. Wang<sup>1</sup>, L. Gu<sup>1</sup>, A. Hirata<sup>3</sup>, M. W. Chen<sup>3</sup>, C. Q. Jin<sup>1</sup>, Y. Yao<sup>1</sup>, Y. G. Wang<sup>1</sup>, X. F. Duan<sup>1</sup>, R. C. Yu<sup>1,\*</sup>

1. Beijing National Laboratory for Condensed Matter Physics, Institute of Physics, Chinese Academy of Sciences, Beijing 10090, China
2. Department of Physics, Beijing Normal University, Beijing 100875, China
3. WPI Advanced Institute for Materials Research, Tohoku University, Sendai, 980-8577, Japan

Multiferroic materials, displaying simultaneously ferromagnetism and ferroelectricity, have recently attracted growing interest due to their intriguing physical properties and potential applications.<sup>1,2</sup> In this presentation, we show our transmission electron microscopy results of  $\text{RMnO}_3$  multiferroic materials. Using state-of-the-art aberration-corrected annular-bright-field and high-angle annular-dark-field scanning transmission electron microscopy, we investigated the structure of multiferroic vortex domains in  $\text{YMnO}_3$  at atomic scale. Two types of displacements were identified among six domain walls; six translation-ferroelectric domains denoted by  $\alpha^+$ ,  $\gamma^-$ ,  $\beta^+$ ,  $\alpha^-$ ,  $\gamma^+$  and  $\beta^-$ , respectively, were recognized, demonstrating the interlocking nature of the anti-vortex domain. We found that the anti-vortex core is about four unit cells wide. We reconstructed the vortex model with three swirling pairs of domain walls along the [001] direction. Two types of 180 degree domain walls, i.e., the transverse and the longitudinal domain walls are identified, which is in consistency with the interlock between ferroelectric and structural translation domain wall predicted previously.<sup>3</sup> These wall structures are different from the polarization inversion in conventional ferroelectrics. These results<sup>4-6</sup> are very critical for the understanding of topological behaviors and unusual properties of the multiferroic vortex. In addition, we found a new ferroelectric phase induced by oxygen vacancy ordering. We proposed a proper structure model and examined its correctness.

### Rererences

- <sup>1</sup> A. J. Freedman and H. Schmid, *Magnetolectric Interaction Phenomena in Crystals*, Gordon and Breach: London (1975).
- <sup>2</sup> G. Srinivasan, E. T. Rasmussen, B. J. Levin, and R. Hayes, *Phys. Rev. B*, 65 (2002) 134402.
- <sup>3</sup> T. Choi, Y. Horibe, H. T. Yi, Y. J. Choi, W. D. Wu, and S. W. Cheong, *Nat. Mater.* 9 (2010) 253.
- <sup>4</sup> Q. H. Zhang, L. J. Wang, X. K. Wei, R. C. Yu, L. Gu, A. Hirata, M. W. Chen, C. Q. Jin, Y. Yao, Y. G. Wang, X. F. Duan, *Phys. Rev. B (R)*, 85 (2012) 020102.
- <sup>5</sup> Qinghua Zhang, Guotai Tan, Lin Gu, Yuan Yao, Changqing Jin, Yanguo Wang, Xiaofeng Duan, Richeng Yu, *Scientific Reports*, 3 (2013) 2471.
- <sup>6</sup> Qinghua Zhang, Sandong Guo, Binghui Ge, Peng Chen, Yuan Yao, Lijuan Wang, Lin Gu, Yanguo Wang, Xiaofeng Duan, Changqing Jin, Banggui Liu, and Richeng Yu, *J. Am. Ceram. Soc.*, 97(2014) 1264.

### Acknowledgements

This work was supported by 973 (2012CB932302) and NNSF of China (11174336). The sample was from Pengcheng Dai's group at UT/Rice supported by the US DOE, BES (DE-FG02-05ER46202).

## The influence of electric field induced on the oriented crystallization of $\text{Bi}_4\text{Ti}_3\text{O}_{12}$ grains in sintering process

Wanmei Sui<sup>1</sup>, Zhiwei Niu, Ranran Song, Hao Zhang

College of Physics Science, Qingdao University, 308 Ningxia Rd. Qingdao, 266071, China.

<sup>1</sup>E-mail: wlxswm@qdu.edu.cn

The piezoelectric and ferroelectric properties of functional ceramics can be strongly influenced by the orientation growth of grains because the spontaneous polarization and poling efficiency are better aligned than in a randomly orientation of grains. The preparation of textured ceramics are mainly including template grain growth, hot forging and tape casting methods and so on. These methods would result in a big size of oriented grains up to several ten centimeters. This ultra large grain would damage the electrical and mechanical properties of the ceramics.

To examine the effect of electric field on the texture evolution of functional ceramics in sintering process,  $\text{Bi}_4\text{Ti}_3\text{O}_{12}$  powder was synthesized by solid phase reaction route and then their compact were sintered and an electric field (dc) was or not was applied to these compacts in the sintering period. The measurement result shows that the density of the samples sintered with electric field was obviously lower than that of the sample with normal sintering. SEM investigation illustrate that the sample sintered at 1030°C for 1.5 hr and with the aid of 1.5kv/cm electric field (dc) present stronger oriented crystallization of grains in the direction of parallel with the direction of electric field applied. XRD analysis also shows that the intensity of the diffraction peak in the direction of parallel with the direction of electric field applied was largely stronger than that of the sample in the perpendicular direction for the same lattice face index. This experiment has shown that the increase of leakage electric current of the sample at high sintering temperature limits the intensity of electric field applied which leads to lower induce effect of electric field.

This study illustrate that an extra electric field applied in the sintering process is helpful for the oriented crystallization of  $\text{Bi}_4\text{Ti}_3\text{O}_{12}$  ceramics. Especially this technical route would be more effective for the preparation of textured ceramics with fine oriented grains when the starting powder is prepared by chemical methods and the powder size is in nano-scale.

**Keywords:** textured Ceramics, Electric Field, Grain Growth, Sintering.

## **An advance towards the synthesis of Ag nanorod arrays with controlled surface roughness for SERS substrates**

M. Gómez-Gómez<sup>1</sup>, J. Calderón<sup>2</sup>, R. Abargues<sup>2</sup>, P. J. Rodríguez-Canto<sup>1</sup>, I. Suarez<sup>1</sup>, J. P. Martínez Pastor<sup>1</sup>, D. Hill<sup>1</sup>

<sup>1</sup>Instituto de Ciencias de los Materiales, Universidad de Valencia, PO Box 22085, 46071 Valencia, Spain

<sup>2</sup>Intenanomat S. L., Catedrático José Beltrán 2, 46980 Paterna, Spain

*maria.i.gomez@uv.es*

The fabrication of metallic nanostructures on transparent substrates with high enhancement factors for SERS remains the focus of much research due to their potential integration into Lab on Chip devices, on their own, or as part of multiparameter sensing [1, 2]. The enhancement of the electric field for SERS is directly related to the morphology of a metallic surface with greater enhancement occurring in surface areas with high aspect ratios, or roughness [3]. Here we report a synthesis method to obtain on transparent substrates Ag nanorods (NRs) with controllable surface roughness and other characteristic morphological parameters (width, length, horizontal and vertical separation) in an array format. Three arrays of Ag NRs with different characteristic parameters were fabricated from a metal-polymer nanocomposite resist by a three step procedure: (i) fabrication of nanostructures (nanorods) by electron beam lithography followed by a wet-etch (ii) an in-situ synthesis of metal NPs during a post-bake step (iii) non electrochemical metallization of the nanocomposite nanorods [4, 5]. As a means to optimize the first step, and thereby control the characteristic parameters of the resulting nano-patterns, twelve different electron doses were used, one for each array, as shown in Figure 1 (a). Similarly for the third step it was repeated in several iterations with the effect of the metallization studied between each by scanning electron microscopy (SEM) and optical transmittance measurements. As expected, after each iteration the constituting Ag nanoparticles had increased in size, and subsequently surface roughness, demonstrating high reproducibility even for the smallest structures. Figures 1a and 1b

show the surface morphologies following the 4<sup>th</sup> and 5<sup>th</sup> iterations, respectively, whilst the optical transmittance measurements show that after the fourth round the plasmonic effects for the array with the smallest nanorod features are dominated by the particles on the surface of the NRs. From this thorough study, characterization results have been able to be successfully characterized with the parameters of the synthesis process. Finally, following on through previous LSPR modelling of other metallic nanostructures [6, 7] through Finite Element Method (FEM) simulations, the electric field enhancement factors arising in such nanostructures for different roughness (NPs size) have been compared to those for smooth Ag NRs with the same morphological characteristic parameters in order to see determine the granularity dependence of the SERS signal so as to compare with experimental data.

This method used to fabricate plasmonic nanostructures is a promising technique not only to overcome the usual fabrication limits of submicron features by lift-off but also to control the roughness of the nanostructures, thereby fine tuning the plasmon energy and linewidth and therefore the SERS enhancement.

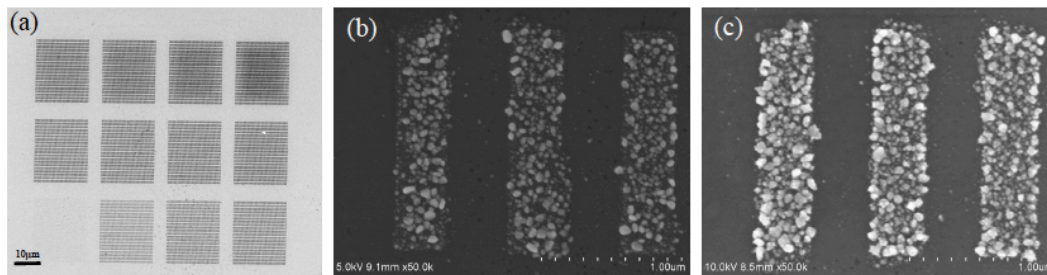


Figure 1 (a) SEM picture from 12 arrays of NRs with same characteristic parameters but different electron doses, after the (i) and (ii) steps of the process. (b) Representative results after 4<sup>th</sup> and 5<sup>th</sup> metallization rounds (b) and (c), respectively.

**Keywords:** *Functional, materials, plasmon, nanoparticle, SERS.*

[1] HSIEN WANG, H., YOU CHENG, T., SHARMA, T., FANG-YI, CH., YU CHIU, S. W., KAI WANG, J. & LIN WANG, Y. 2011 Transparent Raman-enhancing substrates for microbiological monitoring and in situ pollutant detection. *Nanotechnology* 38, 38570

[2] RODRÍGUEZ-LORENZO, L., FABRIS, L. & ÁLVAREZ-PUEBLA R. A. 2012. Multiplex optical sensing with surface-enhanced Raman scattering: A critical review, *Nanotechnology* 23, 10-23.

[3] MURRAY, W. A. & BARNES, W. L. 2007. Plasmonic Materials, *Advanced Materials*, 19, 3771-3782.

[4] ABARGUES, R., MARQUÉS-HUESO, J., CANET-FERRER J., PEDRUEZA, E., VALDÉS, J. L., JIMÉNEZ, E. & MARTÍNEZ-PASTOR, J. P. 2008. High-resolution electron-beam patternable nanocomposite containing metal nanoparticles for plasmonics. *Nanotechnology*, 19, 355308.

[5] ABARGUES, R., MARTÍNEZ-MARCO, M. L., ROGRÍGUEZ-CANTO, P. J., MARQUÉS-HUESO, J. & MARTÍNEZ-PASTOR, J. P. 2013. Metal-polymer nanocomposite resist: a step towards in-situ nanopatterns metallization. *Proc. SPIE*, 8682.

[6] CALDERÓN, J., ÁLVAREZ, MARTÍNEZ-PASTOR, J. P. & HILL, D. 2014. Modelling of polarimetric LSPR sensing with bowtie nanoantennas arrays. *Europtrode XII*.

[7] CALDERÓN, J., ÁLVAREZ, J., MARTÍNEZ-PASTOR, J. P. & HILL, D. 2014. Bowtie plasmonic nanoantenna arrays for polarimetric optical biosensing. *Frontiers in Biological Detection: From Nanosensor to Systema VI*, 893301.

## Structural properties of $[\text{N}(\text{CH}_3)_4]_2\text{Zn}_{1-x}\text{Co}_x\text{Cl}_4$ ( $x=0, 0.5, 0.7, 0.9,$ and $1$ ) mixed crystals by MAS NMR

Nam Hee Kim<sup>2</sup>, Ae Ran Lim<sup>1,2,\*</sup>

<sup>1</sup>Department of Science Education, Jeonju University, Jeonju 560-759, Korea

<sup>2</sup>Department of Carbon Fusion Engineering, Jeonju University, Jeonju 560-759, Korea

Temperature dependences of the chemical shift and spin-lattice relaxation time in the rotating frame  $T_{1\rho}$  were measured for  $^1\text{H}$  and  $^{13}\text{C}$  nuclei in mixed crystals of the form  $[\text{N}(\text{CH}_3)_4]_2\text{Zn}_{1-x}\text{Co}_x\text{Cl}_4$  ( $x=0, 0.5, 0.7, 0.9,$  and  $1$ ). The mixed crystals varied in color according to the amount of  $\text{Co}^{2+}$  ions, whereas the phase transition temperatures remained nearly unchanged.  $[\text{N}(\text{CH}_3)_4]_2\text{ZnCl}_4$  and  $[\text{N}(\text{CH}_3)_4]_2\text{CoCl}_4$  crystals contain two nonequivalent types of a- $\text{N}(\text{CH}_3)_4$  and b- $\text{N}(\text{CH}_3)_4$ . The two crystallographically different ions a- $\text{N}(\text{CH}_3)_4$  and b- $\text{N}(\text{CH}_3)_4$  were distinguished using  $^{13}\text{C}$  CP/MAS NMR spectroscopy. The existence of ferroelastic properties at low temperatures was also discussed. The NMR spectrum and  $T_{1\rho}$  for  $x=0.5$  and  $x=0.7$  were similar to those for  $[\text{N}(\text{CH}_3)_4]_2\text{ZnCl}_4$ , whereas those for  $x=0.9$  were absolutely different. Additionally,  $[\text{N}(\text{CH}_3)_4]_2\text{Zn}_{0.1}\text{Co}_{0.9}\text{Cl}_4$  exhibited the structural properties of both  $[\text{N}(\text{CH}_3)_4]_2\text{ZnCl}_4$  and  $[\text{N}(\text{CH}_3)_4]_2\text{CoCl}_4$ .

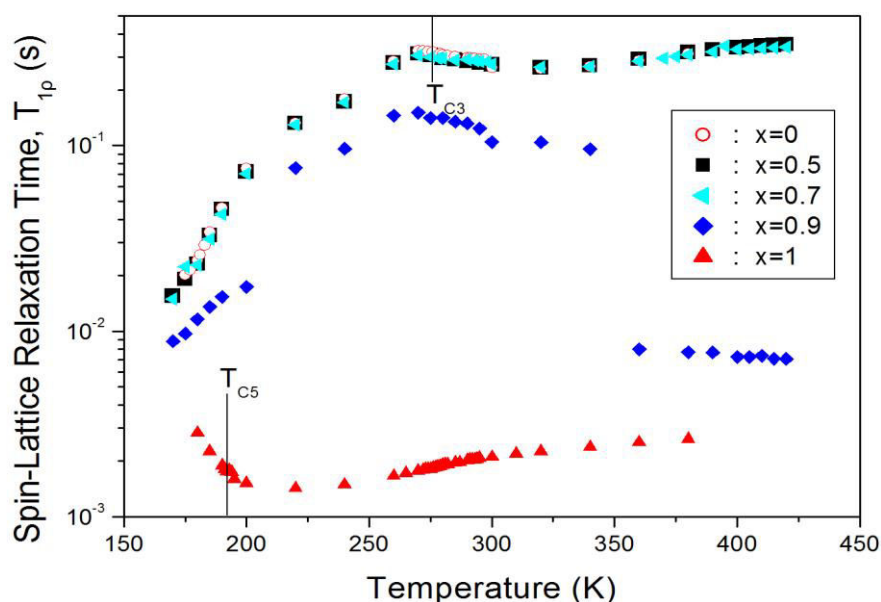


Figure. Temperature dependences of the  $^1\text{H}$  spin-lattice relaxation time in the rotating frame,  $T_{1\rho}$ , in  $[\text{N}(\text{CH}_3)_4]_2\text{Zn}_{1-x}\text{Co}_x\text{Cl}_4$  ( $x=0, 0.5, 0.7, 0.9,$  and  $1$ ).

## Ceria Mixed Oxides Prepared through a Microwave-Assisted Synthesis for CO<sub>2</sub> Sensing in Low Power Work Function Sensors

E. Laubender<sup>1</sup>, N.B. Tanvir<sup>1</sup>, G. Urban<sup>1</sup>, O. Yurchenko<sup>1</sup>

<sup>1</sup>Freiburg Materials Research Center, University of Freiburg, 79104 Freiburg, Germany.

*elmar.laubender@mf.uni-freiburg.de/ FMF, Stefan-Meierstr. 21, D-79104 Freiburg*

Cost-effective and fast CO<sub>2</sub> detection is currently in high demand. Solid state sensors can meet these requirements with suitable transducing materials. Presently, it is still a challenge to develop CO<sub>2</sub> sensors based on metal-oxide semiconductors (MOS) for the required concentration range. Ceria (CeO<sub>2</sub>) is most commonly used for the detection of CO and O<sub>2</sub> and at relatively high operating temperatures [1]. Here, in contrast, we present a nanocrystalline ceria-zirconia mixed oxide for CO<sub>2</sub> sensing at room temperature. Controlled nanoparticle size seems to be necessary to tune the sensitivity towards CO<sub>2</sub>.

A microwave assisted synthesis procedure under relatively mild conditions was chosen. Compared to precipitation and solid-state methods it is fast and has well-controllable synthesis parameters. This is crucial to obtain well-defined nanocrystalline material.

Capacitive based kelvin probe measurement was used to test the applicability in low power consumption field effect transistors (FET). The work function difference vs. a vibrating gold reference was monitored with an in-house developed setup using a lock-in Besocke kelvin probe at varying concentrations of CO<sub>2</sub> (between 400 and 4000 ppm) and different relative humidity. The synthesized CeO<sub>2</sub> nanoparticles showed a significantly higher response than commercial ceria. Furthermore, response time, signal size and stability was improved considerably by using a ceria-zirconia mixed oxide.

Possible reversible adsorption/desorption mechanisms will be discussed based on FTIR.

**Keywords:** *ceria nanoparticles, microwave synthesis, CO<sub>2</sub> detection, kelvin probe*

[1] FINE, G. F., CAVANAGH, L. M., AFONJA, A., AND BINIONS, R. 2010. Metal Oxide Semi-Conductor Gas Sensors in Environmental Monitoring. *Sensors* 10, 6, 5469–5502.

### Binder-free Si nanoparticle electrode with 3-D porous structure prepared by electrophoretic deposition for lithium-ion batteries

Yang Yang, Dingqiong Chen, Bo Liu, Jinbao Zhao\*

(State Key Lab of Physical Chemistry of Solid Surfaces, Department of Chemistry, Collaborative Innovation Center of Chemistry for Energy Materials, College of Chemistry and Chemical Engineering, Xiamen University, Xiamen, 361005, China, Email:jbzhao@xmu.edu.cn)

A binder-free Silicon (Si) based electrode for lithium ion battery was fabricated in an organic solvent through one-step electrophoretic deposition (EPD). The nano-sized Si and Acetylene black (AB) particles were bonded tightly together to form a homogeneous co-deposited film with 3-D porous structure through the EPD process. The 3-D porous structure provides buffer spaces to alleviate the mechanical stress due to silicon volume change during the cycling, and improves lithium ion conductivity by shortening ion diffusion length and better ion conducting pathway. Our results demonstrate that the Si nanoparticle electrode prepared through EPD exhibits smaller cycling capacity decay rate, and better rate capability than the electrode prepared by the conventional method (slurry coating method).

As shown in Fig. 1, The nano-sized Si and AB particles were bonded tightly together to form Interconnected macro/micropores which constructed a 3-D porous structure. Compared with EPD electrode, the conventional method electrode is much denser; the voids between the particles are much smaller. The EDX mapping of the EPD co-deposited film for the elements Si, C, Cu (substrate) is shown in Fig. 2. From these images, it is clear that both nano-Si and AB particles are uniformly deposited on the Cu foil to form a homogenous co-deposited film.

To evaluate the cycle ability of the electrode fabricated by EPD method and the conventional method, a charging and discharging current density of 0.1 C was used. As shown in Fig. 3(a), EPD electrode exhibits an initial charge/discharge capacity of 2520/3150 mAh g<sup>-1</sup>, respectively, and a much improved 1st Columbic efficiency of 80% as compared with 64% for the conventional method electrode. After 100 cycles, EPD electrode exhibits a discharge capacity of 1913 mAh g<sup>-1</sup> with a discharge capacity retention of 73%. On the other hand, the conventional method electrode only showed a discharge capacity of 1121 mAh g<sup>-1</sup> with a discharge capacity retention of 49%.

The cycle life of both EPD and conventional electrodes at high current densities were shown in Fig. 3(b). These cells were first cycled at 0.1 C for the initial 5 cycles, then the current density was increased to 1 C and 2 C for 200 cycles, respectively. EPD electrode exhibited a discharge capacity of 1516 mAh g<sup>-1</sup> at 1 C and 1231 mAh g<sup>-1</sup> at 2 C after 200 cycles, respectively, while the conventional electrode only showed much lower capacities of 204 and 14 mAh g<sup>-1</sup> after 200 cycles. Thus the EPD electrodes are much superior to conventional electrode. This superiority is attributed to the 3-D porous structure of electrode fabricated by EPD method: one is that the electrode has a higher specific surface area, resulting in the shorter diffusion path for lithium ions and improvement of transport between electrode and electrolyte of lithium-ions for better rate capability; two is that the higher porosity of

the electrode, the more void space to accommodate volume change of the electrode during cycling, thus more mechanically stable of the electrode to enable a longer cycle life.

We demonstrated here that a binder-free Si nanoparticle electrode for LIB can be successfully fabricated by simpler yet versatile one-step EPD process. Surface modified nano-sized Si and AB particles are bonded tightly together to form a 3-D porous structured thin film electrode on copper substrate through the EPD process. Our results demonstrate that with careful control of the co-deposition parameter, we can produce EPD electrode with much improved electrochemical performance, such as higher capacity, longer cycle life and better rate capability. These improvements stem from the 3-D porous structure of the electrode. The 3-D porous structure of the electrode is beneficial to alleviate volume expansion of silicon during the charge and discharge processes and facilitate faster transport kinetics of lithium-ions, which leads to better cycling and rate performances.

**Acknowledgment:** The National High Technology Research and Development Program of China (2012AA110204), National Natural Science Foundation of China (21321062) and Key Project of Science and Technology of Xiamen (2013H6022).

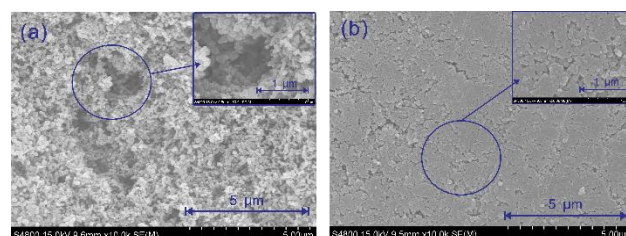


Fig. 1. SEM images of surface of (a) the electrode fabricated by EPD method. (b) the electrode fabricated by the conventional method.

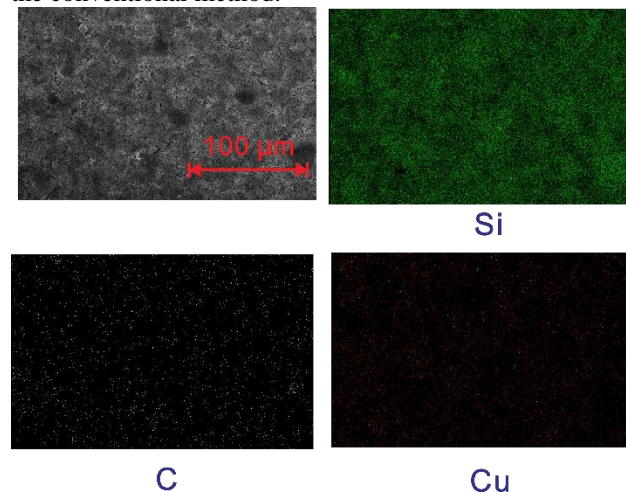


Fig. 2. EDX images of the electrode fabricated by EPD method.

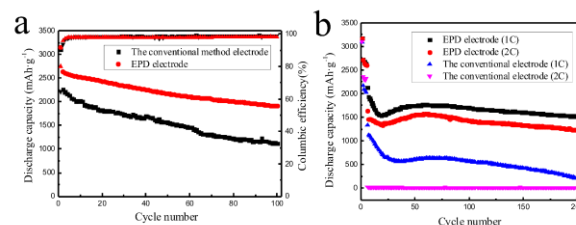


Fig. 3. (a) Discharge capacity versus cycle number plots for EPD and the conventional electrode. (b) Long-term rate performance of EPD and the conventional method



electrode at high current densities.

## Variation of Crystalline parameters with capping agents and Optical study of Cadmium Sulphide Nanoparticles doped with Erbium ions

<sup>1</sup>Usha, <sup>2\*</sup> Varughese, <sup>2</sup>Praveen, <sup>2</sup>Suraj, <sup>2</sup>Jithin

<sup>1</sup>Department of Chemistry, St. Cyrils College, Adoor, Kerala.

<sup>2</sup>Department of Physics, Catholicate College, Pathanamthitta, Kerala, India-689645

\*E-mail of corresponding author: [gvushakoppara@yahoo.co.in](mailto:gvushakoppara@yahoo.co.in)

Email of presenting author: [gvushakoppara@gmail.com](mailto:gvushakoppara@gmail.com)

**Abstract:** CdS is an important II-VI semiconductor with much optoelectronic application including solar cell, Photodiode, LED, Non linear optics heterogeneous photo catalysis. The prepared Erbium doped Cadmium Sulphide nanoparticle samples were characterized by XRD, FTIR, EDS and SEM. Optical properties are carried out using UV and PL studies. The size of the particles increased as the annealing temperature was increased. The crystallite size varied from 13.4 nm to 16.7nm as the calcination temperature increased. Band gap of Er doped CdS increases to 5.27 eV and remains constant at higher temperatures, due to the Burstein-Moss effect caused by the quantum confinement. While that of undoped CdS nanoparticle is 4.17eV. The UV-Vis Absorption spectra show a shift towards 505 nm which is considerably blue shifted relative to the absorption of bulk CdS indicating quantum size effect. The Er doped CdS is highly effective and can significantly enhance the photo catalytic degradation.

**Key words:** A: Semiconductor, Nanomaterial, Doping, Optical properties,

**PACS:** 81.05 Dz; 61.46+w; 61.72.Vv; 43.35.Bf

## Analytical Methods to Determine Chemical Changes in High-Oil Paraffin Binders used in Granular Composites

Bridge<sup>1,2,4</sup>, Fisher<sup>2</sup>, Weisshaupt<sup>2</sup>, Peterson<sup>3,4</sup>

<sup>1</sup>School of Science, Technology, Engineering & Mathematics, University of Washington, Bothell, WA 98011 USA

<sup>2</sup>Lab/Cor Materials LLC, 810 NW 45<sup>th</sup> Street, Seattle, WA 98107 USA

<sup>3</sup>Department of Mechanical Engineering, University of Maine, Orono, ME 04469 USA

<sup>4</sup>Racing Surfaces Testing Laboratory, 2 Summer Street, Orono, ME 04473 USA

*John W. Bridge, Ph.D., P.E.  
Associate Professor of Mechanical Engineering  
University of Washington, Bothell  
Phone: 425-352-5132  
E-mail: [jwbridge@uw.edu](mailto:jwbridge@uw.edu)*

The objective of this work is to assess the effectiveness and practicality of eight analytical tests used to observe chemical changes over time of a high-oil, paraffin wax binder used in synthetic sports surfaces. These surfaces are composed of granular composites used in many North American Thoroughbred horse racetracks. The mechanical properties of these surfaces do change over time which have safety implications for the horses and jockeys. The binder is a key component in equine contact interactions with the surface. One particular racetrack surface was studied over a six-year period. This surface did not have anything added to it over this time period and samples were taken from the same track location each year. The binder was removed from representative samples via solvent extraction and differences in chemical composition was determined through oil extraction, differential scanning calorimetry (DSC), gas chromatography (GCMS), Fourier transform infrared spectroscopy (FTIR), optical refraction, X-ray fluorescence and gel permeation chromatography (GPS). Previous work has focused on the temperature-

dependency of the binder and resulting changes in mechanical properties. Current work, for which this study is a part of, is material chemical degradation over time for these materials.

***Keywords: granular composites, synthetic horse racetracks, paraffin wax, degradation***

Preferred Mode of Presentation: Oral

Topic Area:

Composite Materials-Synthesis and Characterization

or

Advances in Thin Films

## ELECTRICAL AND SENSOR BEHAVIOR OF PANI/In<sub>2</sub>O<sub>3</sub> NANO COMPOSITES

Chakradhar Sridhar B<sup>1</sup>, Sasikala M<sup>2</sup>, Jakeer Husain<sup>3</sup> and M.V.N. Ambika Prasad<sup>3\*</sup>

<sup>1</sup>Department of Physics, Gulbarga University, Gulbarga-585 106, Karnataka, India

<sup>2</sup>Department of Electrical and Electronics Engineering, Godutai College of Engineering for Women, Gulbarga-585 103, Karnataka, India

<sup>3\*</sup>Department of Materials Science, Gulbarga University, Gulbarga-585 106, Karnataka, India

[chakradhar.rcr@gmail.com](mailto:chakradhar.rcr@gmail.com), [sasi\\_mun@rediffmail.com](mailto:sasi_mun@rediffmail.com), [Jakeerhusain21@gmail.com](mailto:Jakeerhusain21@gmail.com),  
[prasad1\\_amb@rediffmail.com](mailto:prasad1_amb@rediffmail.com)

### ABSTRACT

Indium oxide (In<sub>2</sub>O<sub>3</sub>) nanoparticles were successfully prepared by sol-gel method. Nanocomposites of polyaniline (PANI) and Indium oxide (In<sub>2</sub>O<sub>3</sub>) have been synthesized using in situ polymerization method for different concentrations of nano In<sub>2</sub>O<sub>3</sub> powder. The formation of polymer nanocomposite and changes in its structural and micro structural properties of the materials were investigated by X-ray diffractometry (XRD) and Fourier infrared spectroscopy (FTIR) techniques. The surface morphology of PANI–In<sub>2</sub>O<sub>3</sub> nanocomposite was elucidated using Scanning Electron Microscopy (SEM). DC conductivity studies of PANI-In<sub>2</sub>O<sub>3</sub> composites for different weight percentage (wt %) show thermally activated behaviour. The conductivity was found to increase with the increase in temperature indicating the semiconducting behaviour of all the compositions. Maximum conductivity was observed in 30 wt% of In<sub>2</sub>O<sub>3</sub> in polyaniline. A.C. conductivity studies reveal increase in conductivity of all the composites with increase in frequency. On exposure of the composites to liquefied petroleum gas (LPG), increase in resistance was observed with the increase in gas concentration. Maximum sensitivity for gas sensing was observed in the composite of 50 wt% In<sub>2</sub>O<sub>3</sub> in polyaniline.

**Keywords:** Polyaniline, Indium oxide, nano-crystalline, Conductivity, LPG sensing.

Author of correspondence: M.V.N.Ambika Prasad

Email id: [prasad1\\_amb@rediffmail.com](mailto:prasad1_amb@rediffmail.com), Phone: +919448405817

## Texture Formation in AZ magnesium alloy during High-temperature compression deformation

M. Park<sup>1,a</sup>, K. Okayasu<sup>2</sup>, H. Fukutomi<sup>2</sup>, K. Kim<sup>1,b</sup>

<sup>1</sup>Dep. of Metallurgical Engineering, Pukyong National University, 365 Sinseon-ro, Nam-gu, Busan 608-739, Korea

<sup>2</sup>Faculty of Engineering, Yokohama National University, 79-5 Tokiwadai, Hodogaya-ku, Yokohama 240-8501, Japan

E Mail/ [lklllklk@naver.com](mailto:lklllklk@naver.com)<sup>a</sup>, [mrppeng@pknu.ac.kr](mailto:mrppeng@pknu.ac.kr)<sup>b</sup>

Magnesium alloys have been paid attention as lightweight materials in various industrial fields. However, their use is limited by poor formability at room temperature which was caused by the limited number of slip systems. The texture control plays an important role in plastic workability of magnesium. Many studies have been conducted in order to understand the texture evolution in magnesium alloys [1]. Two authors reports the characteristics of texture formation deformation became clear with an increase of solute content during high-temperature deformation in Al-Mg alloys [2]. Therefore it is expected that the similar characteristic appear in AZ magnesium alloys with the solute and solvent element replacement relationship at high temperature deformation. In this study, three kinds of the AZ magnesium alloy with different solute aluminum concentration were experimentally investigated by uniaxial compression under various deformation conditions. Three kinds of specimens are AZ31, AZ61 and AZ91 magnesium alloys. Uniaxial compression is conducted at 673K and 723K with a strain rates ranging from  $5.0 \times 10^{-4} \text{ s}^{-1}$  to  $5.0 \times 10^{-2} \text{ s}^{-1}$ . In all the deformation conditions, working softening is observed for three types of AZ magnesium alloys. The results of the texture measurement reveal the main component of texture and the sharpness of texture varies depending on the deformation conditions. It is found that texture in AZ91 magnesium alloy is sharper than those in AZ31 and AZ61 as in the case of Al-Mg alloys.

**Keywords:** *High-temperature deformation, magnesium, compression, texture*

[1] Kaneko, J. and Sugamata, M., 2004. J. JILM, 54, 484-492.

[2] Okayasu, K., Takekoshi, H., Sakakibara, M. and Fukutomi, H., 2009. J. Japan Inst. Metals, 73, 58-63.

## Ferroelectrics for SERS Applications

X. Liu<sup>1</sup>, O. Minoru<sup>2</sup>, K. Kitamura<sup>2</sup>

<sup>1</sup>Chongqing University of Science & Technology, Chongqing, 401331, China; <sup>2</sup>National Institute for Materials Science, Tsukuba, 3050047, Japan  
E-mail: xliu7617@gmail.com

Surface-enhanced Raman spectroscopy (SERS) is a highly sensitive vibrational spectroscopy that allows for the detection of analytes at extremely low concentrations.<sup>1</sup> In SERS, the Raman signal of the probe molecule is amplified through excitation of localized surface plasmon resonances (LSPR) of the substrate, usually in the form of metal particles or a roughened metal film. Consequently, the magnitude of SERS enhancement is crucially dependent upon the SERS substrate. Many years of research have been devoted to creating and optimizing SERS substrates in order to provide the largest enhancement possible.<sup>2</sup> The fundamental metric for SERS activity is the enhancement factor (*EF*), which quantifies the increase in signal intensity per molecule. Applicable SERS substrates require both high *EF* and excellent spatial reproducibility. However, although high *EF* up to  $10^8$  can be achieved and several SERS substrates with signal relatively standard deviation (RSD) less than 7% were reported,<sup>3</sup> commonly used substrates based on metals, either prepared by corrosion or sol-gel methods, show very poor reproducibility with fluctuant *EF*s that may vary across several orders of magnitudes, which severely hinders the applications of SERS. A number of efforts have been made to improve the reproducibility of metallic substrates, but the most used techniques, such as electron beam lithography, nanosphere lithography, focused ion beam patterning, vacuum evaporation and soft-lithography, are limited by the high costs, the enormous difficulties to extend to large scales or complicated preparation steps.<sup>4</sup> Preparation of SERS substrates with both high sensitivity and high reproducibility still remains difficult and costly for routine SERS detection.

Here, we introduce a simple method based on ferroelectric lithography (top-down and bottom-up) assisted assembly of Ag/Au nanoparticle (NP) arrays to fabricate SERS substrates with excellent Raman enhancement and reproducibility. Ferroelectric materials have reversible spontaneous polarization. Polarization inversion results in domain patterns with polar surfaces that exhibit surface-bound charges. The different domains have surfaces with different electronic properties including electron affinity<sup>5</sup> and surface potential.<sup>6,7</sup> LiNbO<sub>3</sub> single crystal is favorable for fabrication of well-organized metal NP arrays due to its large polarization existing only along the crystallographic Z-axis. Figure 1(left) shows an example of AuNP arrays with the average particle diameter of 30 nm. High reproducible Raman signals of H2TMPyP, 5,10,15,20-tetrakis (1-methyl-4-pyridyl) porphyrin attaching onto the ferroelectric-based SERS substrate can be achieved up to  $10^8$  at the excitation wavelength of 568 nm as shown in figure 1(right).

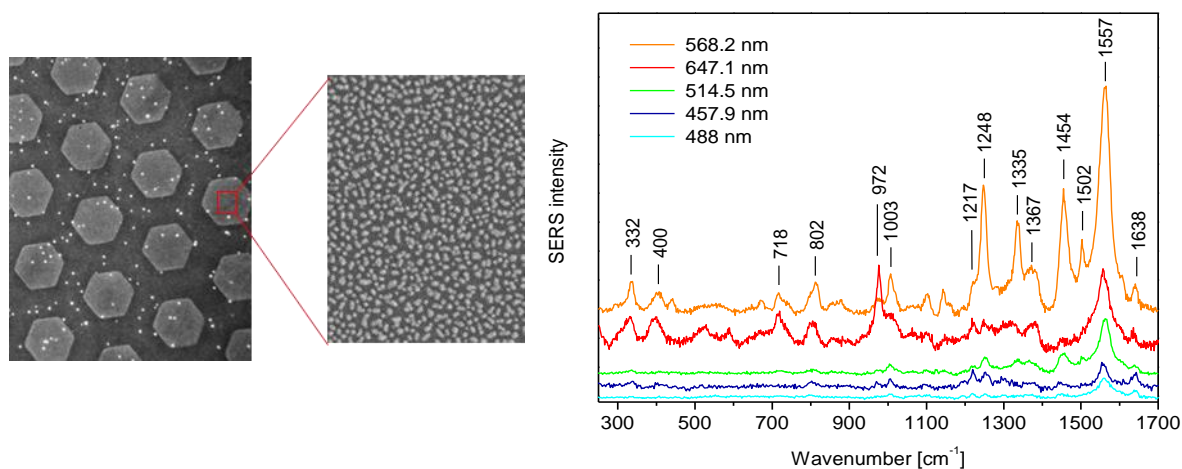


Fig.1(left) AuNP dot arrays on LiNbO<sub>3</sub> single crystal fabricated via ferroelectric lithography technique. Raman signals of H2TMPyP, 5,10,15,20-tetrakis (1-methyl-4-pyridyl) porphyrin attaching onto the substrate (left) obtained at different excitation wavelengths (right).

**References**

1. B. Sharma , R.R. Frontiera , A.-I. Henry , E. Ringe , R.P. Van Duyne , *Mater. Today* **15**, 16 ( 2012 ).
2. S.L. Kleinman , R.R. Frontiera , A.I. Henry , J.A. Dieringer , R.P. Van Duyne , *Phys. Chem. Chem. Phys.* **15**, 21 ( 2013 ).
3. U.S. Dinish, F.C. Yaw, A. Agarwal, M. Olivo, *Biosens. Bioelectron.* **26**, 1987–1992 (2011).
4. R.H. Que et al., *Adv. Funct. Mater.* **21**, 3337–3343 (2011).
5. Yang W C, Rodriguez B J, Gruverman A and Nemanich R J, *Appl. Phys. Lett.* **85** 2316 (2004).
6. Kalinin S V and Bonnell D A, *Phys. Rev. B* **63** 125411(2001).
7. Liu X Y, Kitamura K and Terabe K, *Appl. Phys. Lett.* **89** 132905 (2006).



## **POCOP Pincer ligands, palladium nanoparticles composites or formal organometallic compounds**

Rocío Redón<sup>1</sup>, Bernardo Mendoza-Pérez<sup>1</sup>

<sup>1</sup>Centro de Ciencias Aplicadas y Desarrollo Tecnológico, Universidad Nacional Autónoma de México, Cd. Universitaria A.P. 70-186, C.P. 04510, Coyoacán, México D. F., México.

*rredon@unam.mx (Rocío Redón), alexthedoors.quim@gmail.com (Bernardo Mendoza-Pérez)*

POCOP pincers have been used as ligands to obtain robust coordination/organometallic compounds, unfortunately the synthesis of this ligands is not the easiest thus researchers use similar but easier ligands to work with. In this paper, we present the synthesis and obtaining of composites and organometallic POCOP- Pd(0)/Pd(0) nanoparticles and the comparison on their catalytic behavior. The organometallic POCOP-Pd(II) compounds were better catalysts, than the composites Pd(0) nanoparticles-POCOP pincers with 80% yield compared with a 20% on the better yield of the composites. This might be because the nanoparticles does not have good protection from oxidation, before the catalyst reaction. Another good result on this materials is that depending on the catalyst employed, two different catalytic mechanisms can be applied depending on the material used, form the mechanism that uses Pd(II)/Pd(IV) with, organometallic Pd(II)-POCOP compounds and composites with Pd(II) nanoparticles with sodium citrate used as reductor, as catalysts and, the Pd(0)/Pd(II) mechanism with Pd(0) nanoparticles obtained with sodium borohydride as reductor, as catalyst.

***Keywords: POCOP, palladium composites, Susuki catalytic behavior, palladium-POCOP organometallic compounds, palladium nanoparticles***

## Study of Electrical, Structural and Gas Sensing properties of Al<sub>2</sub>O<sub>3</sub>-doped ZnO Composite Materials Thick Films

M. K. Deore

Department of Physics,  
Arts, Science and Commerce Collège, Ozar(Mig), India-422 206

*E Mail : deoremadhav@rediffmail.com, deoremadhav63@rediffmail.com*

*Contact Détails : +91 9860523315*

The thick films of undoped ZnO and Al<sub>2</sub>O<sub>3</sub> - doped ZnO were prepared by screen printing technique. AR grade (99.9% pure) Zinc Oxide powder was mixed mechanochemically with various weight percentages of Aluminium Chloride (AlCl<sub>3</sub>) powder ( 0.5, 1, 3 and 5 wt.% ) in acetone medium to obtain Al<sub>2</sub>O<sub>3</sub> - ZnO composite material. The prepared materials were sintered at 1000°C for 12h in air ambience and ball milled to ensure sufficiently fine particle size. The films were characterized by different techniques with respect to their crystal structure, surface morphology and compositional property by means of X-ray diffraction, Scanning Electron Microscope (SEM), Energy Dispersive Spectroscopy (EDAX). The X-ray diffraction analysis of pure and Al<sub>2</sub>O<sub>3</sub> - doped ZnO powders shows the polycrystalline nature. The surface morphology of the films was studied by SEM. The final composition of each film was determined by EDAX analysis. The gas response of undoped and Al<sub>2</sub>O<sub>3</sub>. doped ZnO films were studied for different gases such as CO, NH<sub>3</sub>, H<sub>2</sub>S, H<sub>2</sub> and Ethanol at operating temperature ranging from 50°C to 450°C. The pure film shows the response to H<sub>2</sub>S gas (500ppm) at 300°C while the film doped with 3 wt. % Al<sub>2</sub>O<sub>3</sub> gives the good response to H<sub>2</sub>S gas at ppb level at 350°C. The selectivity, response and recovery time of the sensor were measured and presented.

**Keywords:** *Thick films, ZnO, Al<sub>2</sub>O<sub>3</sub>, H<sub>2</sub>S gas, Sensitivity,*

## Metal-Salen Polymers for Energy Storage and Conversion

M. Karushev, I. Chepurnaya, A. Timonov, S. Kogan

Powermers Inc., 470 Olde Worthington Rd, Suite 200, Westerville, OH 43082, USA

*mkarushev@powermers.com / Phone: +1-614-4106769*

Electrodeposition of conducting polymer films at different substrates is widely acknowledged to be a powerful tool for surface functionalization, which affords development of novel composite materials for energy applications. In this work we describe the preparation of Metal-Salen type polymer films – 3D self-structured materials whose morphology and properties can be effectively controlled by the composition of Metal-Salen monomers and polymerization conditions – and polymer-based composites. Synthesized materials are investigated by means of cyclic voltammetry, dc charge-discharge cycling, scanning electron microscopy, and quartz crystal microbalance technique. We demonstrate that electrodeposition of Nickel-Salen type polymers into the pores of carbon-based materials results in the formation of composites that have up to 100% higher volumetric capacity than the original carbon materials. For the first time, we report that thin (~100 nm) Cobalt-Salen type polymer films show catalytic activity towards oxygen reduction reaction (ORR) in non-aqueous electrolytes by shifting the onset potential for the ORR up to as high as +0.4 V (vs. Ag/AgCl aqueous reference electrode) – the highest ORR potential reported to date – and confirm that the process is partially reversible. Finally, we demonstrate that the potential of the Nickel-Salen polymer-modified glassy carbon electrode immersed in the inert electrolyte solution is shifted by as high as 0.5 V when the electrode is exposed to sunlight. Discovered multiple functionalities of Metal-Salen type polymers, including but not limited to fast and reversible charge storage, catalytic activity towards ORR, and photoactivity afford a number of interesting possibilities in creating new designs for next generation energy storage and conversion systems, such as supercapacitors and Li-ion capacitors, Li-air batteries, photovoltaic (Gratzel type) and photogalvanic cells, respectively.

**Keywords:** *Conducting, polymers, energy storage, conversion*

## Characterization and Optical study on Zinc Sulphide nanostructures doped with Gadolinium

\*<sup>1</sup> George Varughese, <sup>1</sup>Jithin <sup>1</sup>Christy, <sup>2</sup>Usha,

<sup>1</sup>Crystalline Material Division, Department of Physics, Catholicate College,  
Pathanamthitta, Kerala-689 645, India

<sup>2</sup>Department of Chemistry, St. Cyril's College, Adoor, Kerala-691529, India

Corresponding author: \*E-mail: [gvushakoppara@yahoo.co.in](mailto:gvushakoppara@yahoo.co.in)

---

### ABSTRACT

Zinc Sulphide doped with Gadolinium (ZnS:Gd) quantum dots have various scientific and engineering applications in electronics, nonlinear optical devices for communication, and optical computers. It is effectively used for detecting cancer cells in human body. The material is an excellent light transmission material with high refractive index 2.27 also makes ZnS useful in photonic crystal devices that operate in the region from visible to near infrared. ZnS:Gd nano materials with an average particle size of 11-50 nm are synthesized by the reaction of zinc acetate and hydrogen sulphide by chemical route technique. XRD, SEM, FTIR and EDS characterize the samples. The percentage of doping material in the crystal is confirmed from the EDS spectra. The average crystal size of the prepared ZnS nanopowder is determined by XRD. Ultrasonic velocity through doped and undoped sample is measured and compressibility is computed. The compressibility is found to be increased. Also variation of compressibility of Zn S:Gd nanofluid with various grain size have been carried out and found that compressibility increases with decrease of particle size.

**Key words:** A: *Semiconductor, Nanomaterial, Doping, Optical properties*

**PACS:** 81.05 Dz; 61.46+w; 61.72.Vv; 43.35.Bf

## Characterization of Magnetorheological Elastomer (MRE) Engine Mounts

I.L Iadipo<sup>1</sup>, Fadly J.D<sup>2</sup> and Waleed Faris<sup>3</sup>

<sup>1,2,3</sup>College of Engineering, Department of Mechanical Engineering,

International Islamic University Malaysia

<sup>\*</sup>iadipo.ismail@live.iium.edu.my, fadlyjd@iium.edu.my, waleedfaris@iium.edu.my

**Abstract.** Modern cars have evolved with new requirements, designs and materials applications on every components of the automobile. These requirements have led to various further developments that can give better options and performance in new cars. The engine mounts is one of the most important components which has been continuously improved on to meet these new challenges. The use of smart materials is a new field and its applications in solving engineering issues especially in automobiles is also carefully been researched into. This study aims to apply the behavioral characteristics of Magnetorheological Elastomers (MRE)-a class of smart materials in solving engine mounts vibration. An adopted 4-Parameter model of the MRE is used in modelling the behavior of the automobiles engine characteristics and the significant improvement it provides when compared to traditional passive mounts is presented. The developed equations are compared using well known performance criteria of the engine mounts. The performance criteria at low and high frequencies shows 50% reduction or isolation of vibration at resonance frequencies of the low frequency region and an instantaneous frequency (which is selected) within the high frequency range. The improvements noted in these research is an apparent indication that the full adaptive nature of the MRE in the area of application such as an engine mounts system can be further studied.

**Keywords:** Engine Mounts, Magnetorheological Elastomers (MRE) Models, Vibration Isolation

### References

- [1] AZADI, M., BEHZADIPOUR, S. & FAULKNER, G. 2009. Antagonistic variable stiffness elements. *Mechanism and Machine Theory*, 44, 1746-1758.

- [2] CHANDRA, P. M. V., KUMAR SINGH., ABHISHEK, P., SINGH., R., RAJIT RAM, S. & KAPIL, J. 2005. A comparative study of engine mounting system for nvh improvement – Part-1.
- [3] CHOI, S., SONG, H., LEE, H., LIM, S., KIM, J. & CHOI, H. 2003. Vibration control of a passenger vehicle featuring magnetorheological engine mounts. *International Journal of Vehicle Design*, 33, 2-16.
- [4] CHOI, W. J. 2009. *Dynamic analysis of magnetorheological elastomer configured sandwich structures*. University of Southampton.
- [5] COLLETTE, C., KROLL, G., SAIVE, G., GUILLEMIER, V., AVRAAM, M. & PREUMONT, A. 2009. Isolation and damping properties of magnetorheologic elastomers. *Journal of Physics: Conference Series*, 149, 012091.
- [6] DARSIVAN, F. J., FARIS, W. F. & MARTONO, W. 2008. Active engine mounting controller using extended minimal resource allocating networks. *International Journal of Vehicle Noise and Vibration*, 4, 150-168.
- [7] DAVIS, L. C. 1999. Model of magnetorheological elastomers. *Journal of Applied Physics*, 85, 3348-3351.
- [8] GINDER, J. M., NICHOLS, M. E., ELIE, L. D. & TARDIFF, J. L. 1999. Magnetorheological elastomers: properties and applications. 131-138.
- [9] KIENCKE, U. & NIELSEN, L. 2005. *VEHICLE MODELLING*, SPRINGER.
- RIVIN, E. I. 1985. Passive Engine Mounts, Some Directions for Further Development.
- [10] SNOWDON, J. C. 1965. Rubberlike materials, their internal damping and role in vibration isolation. *Journal of Sound and vibration*, 2, 175-193.
- [11] SUCIU, C. V., TOBIISHI, T. & MOURI, R., 2011, P2P, Parallel, Grid, Cloud and Internet Computing (3PGCIC), Modeling and simulation of a vehicle suspension with variable damping and elastic properties versus the excitation frequency, International Conference on, 2011. IEEE, 402-407.
- [12] YU, Y., NAGANATHAN, N. G. & DUKKIPATI, R. V. 2001. A literature review of automotive vehicle engine mounting systems. *Mechanism and Machine Theory*, 36, 123-142.

## Synthesis, Characterization of ZnO nanorods and its interaction with Albumin Protein

A.K. Bhunia,<sup>1</sup> T. Kamilya<sup>2</sup> and S.Saha<sup>1</sup>

<sup>1</sup> Department of Physics & Technophysics, Vidyasagar University, Paschim Medinipur 721102, India.

<sup>2</sup> Department of Physics, Narajole Raj College, Paschim Medinipur 721211, India

*E Mail: [sahaphys.vu@gmail.com](mailto:sahaphys.vu@gmail.com)*

A simple wet chemical method has been successfully used to grow zinc oxide nanorods (ZnO NRs). The structural characteristics were investigated through TEM and XRD. The crystal unit cell of the nanorods is found to be hexagonal and the size of the ZnO NR  $\approx 27$  nm. UV- VIS spectrum was used to calculate the band gap of the ZnO NRs. The value of the band gap also suggests the confinement effect. The photoluminescence spectrum shows shallow deep level visible emission due to various defect states. The interaction as well as the formation of bioconjugate of Bovine Serum Albumin (BSA) and Zinc Oxide nanorods is investigated using optical spectroscopy. The zeta potential of ZnO NRs and ZnO-BSA bioconjugate were characterized. UV-VIS and fluorescence spectra show that a spontaneous binding process occurred between BSA and Zinc Oxide nanorod. A small red shift ( $\approx 4$  nm) of the absorption peak of BSA is observed due to binding of BSA with ZnO NRs<sup>1</sup>. Zinc Oxide nanorods quench the fluorescence emission of tryptophan residues in the structure of BSA. The Stern-Volmer quenching constant, the binding constant and the number of binding sites were also calculated.

**Keywords:** ZnO nanorod, protein, photoluminescence spectra, absorption spectra, high resolution transmission electron microscopy.

### Reference

1. Bhunia, A., Samanta, P. K., Saha, S., and Kamilya, T. 2013. ZnO nanoparticle-protein interaction: Corona formation with associated unfolding. Applied Physics Letters, 103, 43701(1-4).

## Synthesis of silver nanoparticles in thermoplastics

Jose Marques-Hueso, Marc P.Y. Desmulliez

Heriot-Watt University, School of Engineering & Physical Sciences (EPS), Institute of Signals, Sensors and Systems,  
Microsystems Engineering Centre (MISEC), Edinburgh, EH14 4AS, Scotland, UK

[J.Marques@hw.ac.uk](mailto:J.Marques@hw.ac.uk)

This work reports the synthesis and analysis of silver nanoparticles in some of the most common thermoplastics currently used by the industry. Silver nanoparticles have many different applications due to their particular properties. Their localised surface plasmon resonance confers them a strong interaction with visible light, which can be exploited for optical components such as light absorbers [1], filters, or colorimetric sensors [2], among others. The enhanced reactivity of the nanoparticles can also be used for other applications, such as catalysis or anti-bacteriological action [3]. On the other hand, thermoplastics constitute one of the most common materials in modern society, with ever-increasing new applications.

In this work, the synthesis of silver nanoparticles has been produced in some of the most commonly used thermoplastics, such as Acrylonitrile Butadiene Styrene (ABS), High Impact Polystyrene (HIPS) and Polyetherimide (PEI). The synthesis of the polymer/nanoparticle nanocomposites involves different stages. Firstly, the metallic ions of an ionic salt have been dispersed in a suspension of the polymer in an organic solvent. Next, different deposition techniques have been used to deposit the blend, such as spin-coating or drop-casting. Finally, the reduction of the metallic ions and the consequent in-situ synthesis of the nanoparticles have been induced by heating the samples on a hot plate at typically 150-240°C. Optical properties and nanoparticle morphology have been measured and correlated.

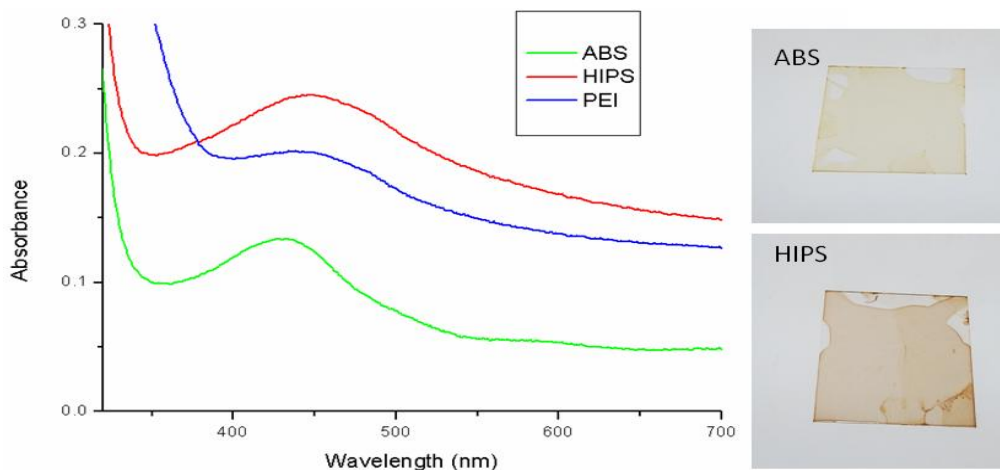


Fig.1. a) Absorbance of thin films of composite revealing the plasmon absorption peak of the silver nanoparticles, as well as a different absorbance baseline for each material, b) ABS-Ag NPs composite thin film on glass, c) HIPS-Ag NPs composite.

**Acknowledgement:** This work is part of the project “Photobioform” (EP/L022192/1) supported under the aegis of the Engineering and Physical Science Research Council (EPSRC) through the Programme “Manufacturing with Light”.

### References:

- [1] Wu, B., X. Wu, et al. *Nat Commun* **4**,. 2004 (2013)
- [2] J. Marques-Hueso, R. Abargues, et al., *Journal of Materials Chemistry*, **20**, 7436-7443 (2010)
- [3] S. Prabhu and E.K. Poulouse, *International Nano Letters*, **2**, 32 (2012)



## Polymeric vesicles for biomedical applications: View on pH- and size-controlled diffusion processes

D. Appelhans,<sup>a</sup> M. Yassin,<sup>a,b</sup> B. Iyisani,<sup>a,b</sup> D. Gräfe,<sup>a,b</sup> J. Kluge,<sup>a,b</sup> J. Gaitzsch,<sup>c</sup> B. Voit<sup>a,b</sup>

<sup>a</sup>Leibniz-Institut für Polymerforschung Dresden e.V., Hohe Str. 6, D-01069 Dresden, Germany

<sup>b</sup>Organische Chemie der Polymere, Technische Universität Dresden, D-01069 Dresden, Germany

<sup>c</sup>Department of Chemistry, University College London, 20 Gordon Street, London WC1H 0AJ, United Kingdom

Email of corresponding author: [applhans@ipfdd.de](mailto:applhans@ipfdd.de)

Over the last years, huge efforts have been undertaken to develop feasible polymer-based systems for biomedical applications and synthetic biology [1]. Polymeric capsules and polymersomes among other have been proven to be promising candidates for such purposes. Compared to their biological counterpart, the liposomes, the membrane from polymersomes is considerably thicker and shows increased mechanical and chemical strength [2]. In this context, our efforts were directed to establish pH-stable polymersomes over a broad pH range by the incorporation of two different photo-crosslinkable moieties in the membrane. This allows us for undergoing reversible switching of polymersome's membrane to trigger the uptake and release of small molecules under various pH values and to squeeze out dendritic glycopolymers under shear forces [3-4].

For developing even more complex polymeric vesicles usable in biomedical applications and synthetic biology, where post-non-covalent conjugation steps and/or de-conjugation/displacement steps are required, we will report further progress on pH- and size-controlled diffusion processes. Results are presented and discussed in respect to pH-dependent (multi-)enzymatic conversion steps [3,5,6] as well as enhanced folic acid-tailored uptake of doxorubicin-enclosed polymersomes by folic acid-sensitive cells [7]. Furthermore, examples are presented, where non-conjugation steps by using adamantane- $\beta$ -cyclodextrin inclusion complexes were established, to perform simultaneously and sequentially pH-controllable modification of the outer shell of polymersomes and polymersome's lumen. Such post-loading events also enabled us to carry out pH-dependent displacement steps where surface-tunable and versatile polymersomes can be used in future synthetic biology, cell engineering processes or lab-on-chip devices.

[1]J. C. M. van Hest et al., *Polym. Chem.* **2011**, 2, 1449.

[2]C. LoPresti et al., *J. Mater. Chem.* **2009**, 19, 3576.

[3]J. Gaitzsch et al., *Angew. Chem., Int. Ed.* **2012**, 51, 4448.

[4]M. A. Yassin et al., *Chem. Eur. J.* **2012**, 18, 12227.

[5]X. Huang et al., *ACS Nano* **2012**, 6, 9718.

[6]D. Gräfe et al., *Nanoscale* **2014**, 6, 10752.

[7]M. Yassin et al., *Small* **2014**, DOI: 10.1002/sml.201402581

## Coexistence of ferromagnetism and *d*-wave superconductivity in YBa<sub>2</sub>Cu<sub>3</sub>O<sub>7-x</sub>/La<sub>0.7</sub>Ca<sub>0.3</sub>MnO<sub>3</sub> bilayer

J.-Y. Lin<sup>1,2</sup>, Shih-Wen Huang<sup>2,3</sup>, L. Andrew Wray<sup>1</sup>, Horng-Tay Jeng<sup>4,5</sup>, V. T. Tra<sup>1</sup>, J. M. Lee<sup>6</sup>, M. C. Langner<sup>3</sup>, J. M. Chen<sup>6</sup>, S. Roy<sup>2</sup>, Y. H. Chu<sup>5,7</sup>, R. W. Schoenlein<sup>3</sup>, and Yi-De Chuang<sup>2</sup>

<sup>1</sup>*Institute of Physics, National Chiao Tung University, Hsinchu 30010, Taiwan*

<sup>2</sup>*Advanced Light Source, Lawrence Berkeley National Laboratory, Berkeley, CA 94720, USA*

<sup>3</sup>*Materials Sciences Division, Lawrence Berkeley National Laboratory, Berkeley, CA 94720, USA*

<sup>4</sup>*Department of Physics, National Tsing Hua University, Hsinchu 30013, Taiwan*

<sup>5</sup>*Institute of Physics, Academia Sinica, Taipei 11529, Taiwan*

<sup>6</sup>*National Synchrotron Radiation Research Center, Hsinchu 30076, Taiwan*

<sup>7</sup>*Department of Materials Science and Engineering, National Chiao Tung University, Hsinchu 30010, Taiwan*

Ferromagnetism and *d*-wave superconductivity are often regarded as incompatible to each other. With no crystalline materials showing the coexistence of these two orders, studying their mutual interactions remains restrictive to date. However, such studies can be performed on cuprate/manganite heterostructures where these two orders are brought into proximity. Here we show the coexistence of ferromagnetism and *d*-wave superconductivity in bulk superconducting YBa<sub>2</sub>Cu<sub>3</sub>O<sub>7-x</sub> (YBCO) grown on top of ferromagnetic La<sub>0.7</sub>Ca<sub>0.3</sub>MnO<sub>3</sub> (LCMO). The coexistence is present with MnO<sub>2</sub> interfacial termination, but absent with La<sub>0.7</sub>Ca<sub>0.3</sub>O interfacial termination. The difference originates from distinct energetics of CuO chain and CuO<sub>2</sub> plane next to LCMO layer at these two interfaces such that the spin-polarized electrons transferred from manganites to cuprates are influenced differently. As such, the ferromagnetic coupling inside YBCO layer can be sustained by the enhanced double-exchange interaction. Our findings demonstrate the far-reaching impacts of interfacial interactions to bulk physical properties, and open up a new paradigm of

using nanoscale heterogeneity to study the competing quantum orders in correlated electron systems.

## Synthesis of Novel Keggin-type Tungstocobaltate-Functionalized Mesoporous Hybrid Materials and Their Catalytic Performance

Jianping Zhang, Chun Yang

College of Chemistry and Material Science, Nanjing Normal University, Nanjing, 210097, P. R. China.

*E Mail: yangchun@njnu.edu.cn*

Keggin-type silanol substituted tungstocobaltate  $[\text{Co}^{\text{III}}\text{W}_{11}\text{O}_{40}(\text{SiOH})_2]^{5-}$ , a new polyoxometalate as shown in Fig.1, was synthesized by using  $\text{Co}^{\text{III}}\text{W}_{11}$  and TEOS as start materials. Then, it was grafted onto SBA-15 by surface condensation reaction between SiOH groups as illustrated in Fig.2 to obtain a novel tungstocobaltate-functionalized mesoporous hybrid material. The as-prepared hybrid materials were characterized by IR, UV-Vis/DRS, XRD,  $\text{N}_2$  adsorption-desorption and elemental analysis techniques. It is shown that  $[\text{Co}^{\text{III}}\text{W}_{11}\text{O}_{40}(\text{SiOH})_2]^{5-}$  had been linked on the surface of SBA-15, and Keggin unit and the order mesostructure remained intact.

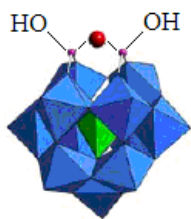


Fig.1

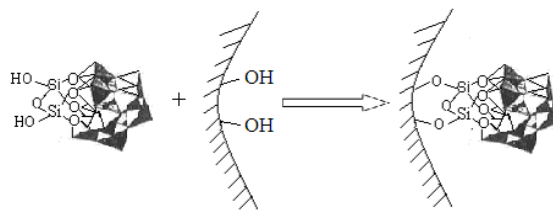


Fig.2

Furthermore, the catalytic performance of the mesoporous hybrid materials were investigated by acetalization of benzaldehyde and 1,2-propylene glycol. It was observed that the hybrid samples possessed obviously higher acetal yield (83.0%) than the corresponding pure  $[\text{Co}^{\text{III}}\text{W}_{11}\text{O}_{40}(\text{SiOH})_2]^{5-}$  compound (59.7%), and can be recycled 8 times without any apparent loss in catalytic activity and selectivity.

**Keywords:** tungstocobaltates, mesoporous hybrid materials, synthesis, catalysis.

# Synthesis of graphene/polymer composites by *in situ* intercalation polymerization and their functional behaviors

**Zuowan Zhou**<sup>\*</sup>, Xiangnan Chen, Liming Shan, Jingjing Chen, Xiaoling Xu, Man Jiang

Key Laboratory of Advanced Technologies of Materials (Ministry of Education), School of Materials Science and Engineering, Southwest Jiaotong University, Chengdu 610031, China

## ABSTRACT

It is of great importance to develop environmentally-friendly method for the preparation of graphene and graphene-contained composites for new functional applications. In this presentatin, a one-step method was realized for the preparation of graphene/polymer composites using intercalation polymerization of the monomeric molecules in-site the graphite layers. The structural and morphological characterizations were performed by X-ray diffraction analysis, transmission electron microscopy and field emission scanning electron microscopy. Firstly, the monomeric cations formed by monomer and  $H^+$  tends to be drawn towards the electron-enriched zone and to intercalate into the interlayer of graphite. Subsequently, *in situ* polymerizations lead to the graphite's separating into graphene as a result of the exothermic effect and more vigorous movements of the long chain molecules of the polymer. The interactions between polymer and graphene were confirmed by Fourier transformed infrared spectroscopy as well as Raman spectra.

As functionanl applications, this report will present the graphene composites hybridized by two kinds of conductive polymers, polyaniline and polypyrrole, and a thermal-conductive polymer, polyamide-6. The as-prepared conductive polymer composites showed an even lower conductivity compared to that of the hydrochloric acid doped polymer or the graphite, futher demonstrating that there were special interactions between polymer and graphene molecules. This can be reckoned that the hybridizing structures may be a good way towards new functional design with broad adjustable parameters of graphene and its composites. Besides, the graphene/polymer composites exhibited a breakthrough in improvement of microwave absorption and/or thermal conductivity.

---

<sup>\*</sup> Corresponding and attending author. E-mail: zwzhou@swjtu.edu.cn (Z. Zhou). Fax, Tel: +86 028-87600454.

## Impact of Anisotropic Biaxial Compressive and Tensile Strain on the Properties of Epitaxial Ferroelectric Films

R. Wördenweber<sup>1</sup>, J. Schwarzkopf<sup>2</sup>, B. Cai<sup>1</sup>, Y. Dai<sup>1</sup>, D. Braun<sup>2</sup>, J. Schubert<sup>1</sup>, E. Hollmann<sup>1</sup>

<sup>1</sup>Peter Grünberg Institute (PGI), Forschungszentrum Jülich, D-52425 Jülich, Germany

<sup>2</sup>Leibniz-Institute for Crystal Growth, Max-Born-Str. 2, D-12489 Berlin, Germany

Contact : [r.woerdenweber@fz-juelich.de](mailto:r.woerdenweber@fz-juelich.de)

The impact of anisotropic biaxial strain on the ferroelectric properties of thin oxide films (20-100nm) are examined using the example of epitaxial NaNbO<sub>3</sub> and SrTiO<sub>3</sub> films that are grown on single-crystalline oxide substrates with different lattice mismatch, leading to compressive and tensile in-plane strain, respectively. Generally, tensile in-plane strain leads to an increase of the ferroelectric in-plane transition temperature whereas compressive strain tends to decrease the transition temperature. Shifts of the transition temperature by several 100K can easily be obtained via this method leading to room-temperature permittivity of several 1000. Our investigations have shown that the phase transition itself and the ferroelectric states of the anisotropically strained films turn out to be highly complex. First, the transition temperature depends on the direction of the applied electric field which contradicts the concept of a uniform phase transition for a given system. Second, all systems, that we examined, showed relaxor properties which are usually expected for systems consisting of a mixture of phases. Third, most ferroelectric properties strongly depend on the applied electric field. This can partially be explained by Rayleigh law, however especially for the tensile strained SrTiO<sub>3</sub> terms of higher order in the field dependence of the permittivity indicate the strong impact of pinning of domain walls and polar regions (e.g. polar nano regions). Finally at elevated temperature an anisotropic conductivity is observed. The latter might attributed to domain wall conductance. The different observations are discussed in terms of existing models, potential application of the different properties will be sketched.

**Keywords:** *anisotropic strain, thin films, ferroelectrics, high-k material*

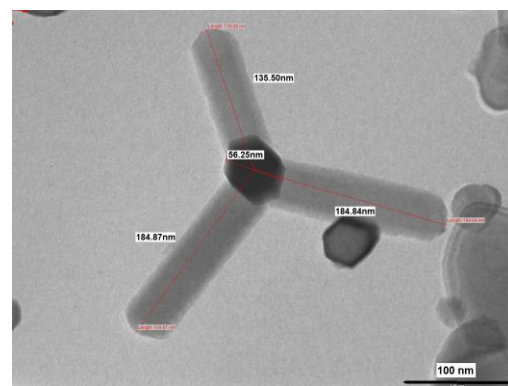
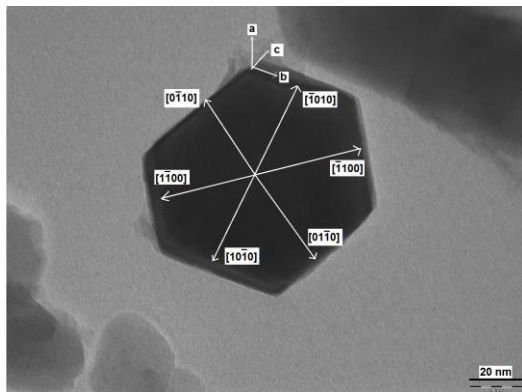
## Synthesis of ZnO nanorods and tripods by hydrothermal route for gas sensor

Ssarik D. Shinde

KKHA Arts, SMGL Commerce and SPHJ Science College, Chandwad 423101 India

Email: sarikagotan@rediffmail.com

**Abstract**— ZnO nanostructures with different sizes and shapes (Nanorods and tripods) have been successfully synthesized via a simple hydrothermal route, using zinc acetate and Cetyltrimmonium bromide (CTAB) as the reactants. The thick films of as prepared ZnO were prepared by screen-printing technique in desired pattern. The films are characterized by X-ray diffraction (XRD), scanning electron microscopy (SEM) and transmission electron microscopy (TEM). The gas sensing properties of the materials have been investigated for various interfering gases such as CO<sub>2</sub>, CO, Ethanol, NH<sub>3</sub> and H<sub>2</sub>S etc at operating temperature from 30° (room temperature) to 300°C. The results indicate that the ZnO nanorod and tripod thick films showed much better sensitivity and stability than the conventional materials to ethanol and LPG. The ZnO nanostructures can improve the sensitivity and selectivity of the sensors.



TEM images of ZnO rod tripod.

**Keywords:** Hydrothermal, ZnO nanorods, Tripods, H<sub>2</sub>S gas sensor.

## Abstract

Sandwich panels are a class of composite material fabricated by attaching two thin but stiff skins to a thick but lightweight core. They are widely used in structural applications where low density, high strength, and high damage tolerance are required. Several of their properties such as low density and high damage tolerance are attributable to the core material. The present study focuses on the development of an economical lightweight foam employed as the core material for sandwich composite panels. Foams are made of perlite particles (expanded siliceous volcanic glass) in a matrix of epoxy for a density range of 0.15 to 0.45 g/cm<sup>3</sup>. Compressive tests were conducted on the samples and the effect of density variation on compressive strength and modulus investigated. Results show that the compressive strength of the newly developed core is comparable to that of Polyurethane and Polypropylene closed cell foams but the new material has higher stiffness. Using macroscopic observations taken during the test, failure mechanisms of perlite foams under compression were studied and the presence of two failure modes was determined for the whole density range.



## Charge Relaxation in Titanium-Dioxide Filled High-Impact Polystyrene Films

Anna A. Guliakova<sup>1</sup>, Peter Frübing<sup>2</sup>, and Yuri A. Gorokhovatskiy<sup>1</sup>

<sup>1</sup> Department of General and Experimental Physics, Herzen State Pedagogical University, Moika River Embankment 48, 191186 St. Petersburg, Russia

<sup>2</sup> Applied Condensed-Matter Physics, Institute of Physics and Astronomy, University of Potsdam, Karl-Liebknecht-Strasse 24-25, 14476 Potsdam, Germany

*Anne\_Rut@mail.ru*

Relaxation processes and their influence on the electret-state stability in titanium-dioxide (TiO<sub>2</sub>, rutile modification) filled high-impact polystyrene (HIPS) films were investigated by means of dielectric relaxation spectroscopy (DRS), thermally stimulated depolarization current (TSDC), thermally stimulated surface-potential decay (TSSPD) as well as dynamic mechanical analysis (DMA) and differential scanning calorimetry (DSC). Three relaxation processes were observed. The first process corresponds to the glass-rubber transition, it is present in all samples and has no influence on the electret-state stability, no correlation with filler content was found. The second process can be related to trap-limited charge-carrier transport that determines the dc conductivity. The activation energy of conductivity is calculated by different methods which concordantly yield a value of about 1.1 eV. The improvement of charge-storage properties of HIPS by adding TiO<sub>2</sub> particles is supposed to be caused by formation of deep traps at the polymer-filler interfaces. The third process could represent the build-up of quasi-dipolar structures in the samples, caused by charge displacement between grain boundaries of the filler particles.

**Keywords:** *high-impact polystyrene, titanium-dioxide filler, dielectric relaxation*

## Removal and inactivation of virus and toxin using electrochemical multi-walled carbon nanotube yarns

Hoon-Sik (Jang)<sup>1</sup>, Sang Koo (Jeon)<sup>2</sup>, Nam Hee (Lee)<sup>2</sup>, Seung Hoon (Nahm)<sup>2\*</sup>

<sup>1</sup>DADA KOREA Co. Ltd., Daegu, Rep. of Korea.

<sup>2</sup>Center for Energy Materials Metrology, Korea Research Institute of Standards and Science, Daejeon, Rep. of Korea.

[physdrjhs@gmail.com](mailto:physdrjhs@gmail.com) (presenting author's),

\* [shnahms@kriss.re.kr](mailto:shnahms@kriss.re.kr) (corresponding author's)

Multi-walled carbon nanotube (MWCNT) may have the potential to provide solutions to critical problems in the biochemical field. Here, MWCNT yarns were produced by continuously pulling on well-aligned MWCNTs on a substrate, and then MWCNT sheet filter was prepared from MWCNT yarns. The efficacy of and anodic MWCNT sheet filter was developed to remove and inactivated the vaccinia virus and the botulinum toxin. MWCNT sheet filter was applied by the direct current(DC) power, during the removal and inactivation of virus and toxin. The MWCNT sheet filter were heated up to 100 °C by applying DC power of 10 V. We confirmed that the vaccine viruses and the botulinum toxin was removed and inactivated over 99 %. Virus and toxin could be effectively removed and inactivated by MWCNT sheet filter produced from yarns, as compared with other microfilters.

**Keywords:** Carbon nanotube yarn, Microfilter, electrochemical, Virus, Toxin.

[1] VECITIS, C. A., SCHNOOR, M. H., RAHAMAN, M. S., SCHIFFMAN, J. D., & ELIMELECH, M. 2011. Electrochemical multiwalled carbon nanotube filter for viral and bacterial removal and inactivation. Environ. Sci. Technol., 45, 3672-3679.

## Structure of interface between matrix alloy and reinforcement particles in Al/SiC<sub>p</sub> + Cg<sub>p</sub> hybrid composites

Anna J. Dolata<sup>1</sup>, Maciej Dyzia<sup>1</sup>, Sonia Boczek<sup>2</sup>

<sup>1</sup>Silesian University of Technology, Faculty of Materials Engineering and Metallurgy,  
ul. Krasińskiego 8, 40-019 Katowice, Poland

<sup>2</sup>Institute of Non-Ferrous Metals, Light Metals Division, ul. Piłsudskiego 19, 32-050  
Skawina, Poland

*anna.dolata@polsl.pl*

Presently, the most a new research are focus on the formation of structure and properties of functional hybrid aluminium matrix composites. Such composites (e.g: Al/SiC<sub>p</sub>+Cg<sub>p</sub> or Al/SiC<sub>p</sub>+GR<sub>p</sub>) have a better physical, mechanical, and tribological properties in comparison with composite materials reinforced by only one type of reinforcements [1-4]. Due to their beneficial ratio of strength to density and better wear resistance it can be used as parts in some vehicles (e.g.: pistons, sleeves, bearings), [5]. The fabrication process by the use of mechanical stirring of composite suspension is the one of the most economical method for manufacturing of such composite materials and has been used in the industrial practice [6].

Poor wetting and the interaction between liquid Al alloy and ceramic particles are main problems during the production of composite suspensions [7,8]. Because properties of composite materials depend on the interface microstructure therefore among other things: the proper selection of components - particularly the chemical composition of the Al alloy matrix and the kind of reinforcement particles - are necessary for to obtaining a high-quality composite castings.

The structure and properties of the interface between the components are the primary factor in determining the properties of composite materials, in addition to the properties of the matrix and reinforcing phase. The influence of aluminium matrix chemical composition and its modification on the interface microstructure in AlSi/SiC<sub>p</sub>+Cg<sub>p</sub> hybrid composite were presented. High-resolution scanning electron microscope (HR SEM) with

an attachment for the chemical analysis EDS in microregions were used for the microstructure characterization.

Scientific work financed from funds allocated for The National Centre for Research and Development as project no. PBS1/B6/13/2012

**Keywords:** *hybrid composites, stir casting, microstructure, interface*

- [1] DOLATA ANNA J. 2014. Hybrid Composites Shaped by Casting Methods. Light Metal and their Alloys III, Solid State Phenomena Vol. 211, 47-52, doi:10.4028/www.scientific.net/SSP.211.47.
- [2] DOLATA A.J., DYZIA M. 2012. Aspects of fabrication aluminium matrix heterophase composites by suspension method. IOP Conf. Series: Materials Science and Engineering 35 (2012) 012020 doi:10.1088/1757-899X/35/1/012020.
- [3] SURESHA S., SRIDHARA B.K. 2012. Friction characteristics of aluminium silicon carbide graphite hybrid composites, Materials & Design 34, 576-583.
- [4] YALCIN Y., AKBULUT H. 2006. Dry wear properties of A356-SiC particle reinforced MMCs produced by two melting routes. Materials and Design 27, 872-881.
- [5] DYZIA M. 2011. AlSi7Mg/SiC and Heterophase SiCp+Cg Composite for Use in Cylinder-Piston System of Air Compressor, Solid State Phenomena. 176, 49-54.
- [6] PRASADA S.V., ASTHANA R. 2004. Aluminum metal–matrix composites for automotive applications: tribological considerations. Tribology Letters, 17 (3), 445-453.
- [7] A. DOLATA-GROSZ 2011. Interaction of Al-Si alloys with SiC/C ceramic particles and their influence on microstructure of composites, Solid State Phenomena 176, 55-62.
- [8] LANDRY K., KALOGEROPOULOU S., EUSTATHOPOULOS N. 1998. Wettability of carbon by aluminum and aluminum alloys, Materials Science and Engineering A 254, 99-111.

## **Comparison of wear study of Al - Si (6% - 18%) - SiC<sub>p</sub> composites under continuous and reciprocating conditions**

G.L.Aswinikumar, V.R.Rajeev\*, K.Jayaraj, A.Farook

Mechanical Engineering Department, College of Engineering Trivandrum, Trivandrum,  
Kerala, India -695016  
\*rajeevcet@gmail.com

### **Abstract**

In the present study continuous and reciprocating sliding wear test were performed on Al-Si(6%-18%)-15%SiC<sub>p</sub> composites under similar conditions of load, speed and nominal area of contact in order to compare the wear rate for the two sliding modes under dry condition. Cumulative wear have been plotted against sliding distance for the three developed A319-15%SiC<sub>p</sub>, A336-15%SiC<sub>p</sub> and A390-15%SiC<sub>p</sub> composites. It was observed that the pattern of wear is similar for continuous and reciprocating sliding but a higher wear is noticed in the reciprocating process compared to continuous wear for all the three composites investigated. This is due to the enhanced chances of entrapment of wear particles in the case of reciprocating process compared to the continuous process which in turn cause differing amounts of three body abrasion in the two processes by the loose wear debris. Thus higher wear under reciprocating condition may be attributed to 3 body abrasive effects. Moreover during continuous sliding wear tests using pin-on-disc machine, some of the wear debris may flung from the rotating disc by the centrifugal force which during reciprocating sliding may entrapped between the sliding surfaces for longer times. Hence, higher wear in the case of reciprocating process compared to

continuous wear can be attributed to the greater amount of abrasion by the entrapped loose wear debris in the reciprocating process.

**Keywords:** Composite, Continuous wear, Reciprocating wear, Comparison, Three body abrasion.

## Hybrid double network Hydrogel for cartilage tissue engineering

RETHORE G.<sup>1</sup>, BOYER C.<sup>1</sup>, XIE F.<sup>1,2</sup>, GUICHEUX J.<sup>1</sup>, TASSIN J-F.<sup>2</sup>, WEISS P.<sup>1</sup>

<sup>1</sup> INSERM, U791, Université de Nantes, 1 Place Alexis Ricordeau, 44042 Nantes, France

<sup>2</sup> UMR CNRS 6120, Université du Maine, Avenue Olivier Messiaen, 72085 Le Mans, France.

*Pierre.weiss@univ-nantes.fr*

The good swelling property of Hydrogel gives it wide applications such as biosensors, drug delivery and tissue engineering. Weiss et al. developed an injectable scaffold by grafting silane on HPMC (Hydroxypropylmethylcellulose) leading to a self-cross-linkable hydrogel (Si-HPMC) without using any toxic chemical catalysts. The hydrogel (Si-HPMC) has excellent biocompatibility that makes it a good material for tissue engineering but with a low stiffness. Laponites are silicate particles in the form of disc-shaped crystals of about 25 X 1 nm. In this study, Si-HPMC/Laponite composite hydrogel was developed to propose a higher stiffness hydrogel scaffold for tissue engineering. The concentration of Si-HPMC was fixed at 2 wt% and the laponites content ranged from 0.5 to 5 wt%. The gelation processes and the viscoelastic properties of composite hydrogels with different laponites contents were studied by rheological methods. Biological investigations have been done with human adipose-derived stem cells (hASC) by determining the cell viability in 2D and in 3D. Confocal Laser Microscopy allowed us to observe the dispersion of Laponite particles in the composite hydrogels, showing there were two continuous parts: red light area and dark area. Adsorption experiments suggested that the red light area was the aggregation of Laponites caused by HPMC instead of high ionic strength. All the reinforcements that we used in this study showed no toxicity *in vitro*, both in 2D and 3D. After 6 weeks, of implantation of the composite hydrogels with human nasal chondrocytes (hNC), histological and immunohistological analysis showed the formation of cells nodules positively stained by Alcian blue and Masson's trichrome, suggesting the production of an extracellular matrix containing GAG and collagen respectively.

**Keywords:** *biomaterials, hydrogel, tissue engineering, nano reinforcement.*

## **X-ray and neutron scattering on disordered nanosize clusters: computational modelling of lead-zirconate-titanate solid solutions**

Johannes Frantti and Yukari Fujioka

Finnish Research and Engineering, Helsinki, Finland

*E Mail : johannes.frantti@fre.fi*

Defects and frequently used defect models of solids are summarized and signatures for identifying the disorder from x-ray and neutron scattering data are given. To give illustrative examples how technologically important defects contribute to x-ray and neutron scattering numerical method able to treat non-periodical solids possessing several simultaneous defect types is given for simulating scattering in nanosize disordered clusters. The approach takes particle size, shape, and defects into account and isolates element specific signals. As a case study a statistical approximation model for lead-zirconate titanate [ $\text{Pb}(\text{Zr}_x\text{Ti}_{1-x})\text{O}_3$ , PZT] is introduced. PZT is a material possessing several defect types, including substitutional, displacement and surface defects. Spatial composition variation is taken into account by introducing a model in which the edge lengths of each cell depend on the distribution of Zr and Ti ions in the cluster. The model is applied for computing the scattering from ellipsoid shaped PZT clusters and for simulating the structural changes as a function of composition. Two-phase co-existence, the so called morphotropic phase boundary (MPB), range is given correctly. The composition at which the rhombohedral and tetragonal cells are equally abundant was  $x \approx 0.51$ . Selected Bragg reflection intensities and line shapes were simulated. Examples of the effect of size and shape of the scattering clusters on diffraction patterns are given and the particle dimensions, computed through Scherrer equation, are compared with the exact cluster dimensions. Scattering from two types of  $180^\circ$  domains in spherical particles, one type assigned to Ti-rich PZT and the second to the MPB and Zr-rich PZT, is computed. We show how the method can be used for modeling polarization reversal.

**Keywords:** *Disorder, neutron scattering, x-ray scattering, ferroelectric, nanocluster*



## Parameters for Improving Titandioxid $\text{TiO}_2$ as Photo catalysis material

Wilfried Wunderlich 1),

1) Tokai University, Fac. Eng., Material Science Department, Kitakaname 4-1-1, 259-1292 Hiratsuka, Japan

Keywords: Photocatalyst, bandgap engineering, thin film, drug delivery

Titania, especially the rutile-phase, is a very widely used material in Photovoltaic DSSC-cells, as photo-catalyst and as transparent conductor. This overview paper summarizes solid-state physics principles which are necessary for improving the performance in applications such as water purification devices, self-cleaning surfaces, solar cell, and for photochemical water splitting etc. In this overview we describe 1) Band-gap engineering, 2) Searching for a suitable substrate 3) Doping with metal ions as three mechanism to improve the properties, see also the general overview on metal-ceramic interfaces [1]. All three enhances the photocatalytic efficiency

The mechanism for both, photovoltaic and photo-catalysts applications, can be divided into light absorption, excitation of carriers, carrier mobility, a proper p-n-junction and finally providing the carriers to the place where needed. Photo-catalysis is used for degradation of organic molecules like dust, or bacteria and water splitting. The main principle is that the reaction barrier in the excited state is smaller than in the ground state. Engineering can lower the band-gap (fig. 1) by applying strain provided by a substrate during thin-film growth [2,3]. Further change of the band-gap occurs when nano-particles are used. We examined the minimal achievable particle size as 2nm, see fig. 2. Depending on the surface curvature [4,5], in fact in most of such cases an increase in band gap occurs, nevertheless the improvement is achieved by increasing the interface area and the possibility of drug delivery directly into the bacteria [6,7]. Searching for suitable substrates can also increase the carrier concentration.

The largest effect can, however, be achieved by doping with electron donating atoms, mainly rare-earth ions and there have been published many papers on this issue: Si-, Al- [8] Nd- [9], Gd- [10], Ta-[11] doping. We summarize the findings by new outlines for this important research

[1] W. Wunderlich, Metal-ceramic-interfaces, *Metals* 2014, 4, 410-427; doi:10.3390/met4030410

[2] S.Tanemura, W.Wunderlich, et al. doi:10.1016/j.stam.2004.06.002

[3] W.Wunderlich, et al. *J.Cer. Proc.Res.* 5 [4] 343 (2004) NCF8

[4] W.Wunderlich, N. Hue, S. Tanemura (2004), doi: 10.2240/azojomo0208

[5] S. Winardi, W.Wunderlich, *Langmuir* (2009) DOI: 10.1021/la904619x

[6] T. Bak, et al., doi 10.1021/jp2027862,

[7] K. Sunada 10.1016/S1010-6030(02)00434-3

[8] K.V., Baiju et al., doi:10.1016/j.matlet.2006.07.124

[9] S.A.Moore, et al. doi: 10.1007/s10971-007-1590-2

[10] K.V. Baiju, et al., doi:10.1016/j.jallcom.2010.06.028

[11] K.V. Baiju et al. doi:10.1016/j.molcata.2007.06.017

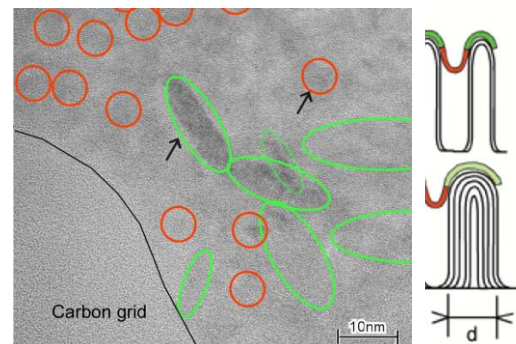
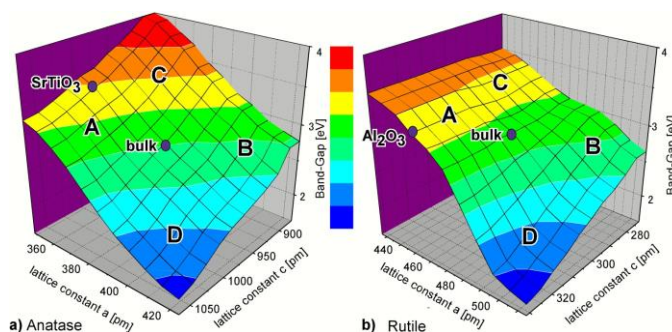


Fig. 1) Band gap as a function of the lattice constants [2] Fig. 2) Increase of amount of nano-sized Anatase

## POSS-based fluoracrylate diblock copolymer for self-assembled film

Ling He<sup>\*</sup>, Aizhao Pan, Shao Yang

Department of Chemistry, School of Science, Xi'an Jiaotong University, Xi'an, China

Corresponding Author, Ling He

Tel: +86-29-82668554, Fax: +86-29-82668559, E-mail: [helings@mail.xjtu.edu.cn](mailto:helings@mail.xjtu.edu.cn)

### ABSTRACT

In order to obtain self-assembled films in tailoring surface properties by migrating fluorinated block copolymer onto the surface of film and to improve the mechanical and thermal properties of film, 16-arm and single-arm POSS-based diblock fluoracrylate copolymers are synthesized by octakis(dibromoethyl) polyhedral oligomeric silsesquioxane (POSS-(Br)<sub>16</sub>) and aminopropylisobutyl POSS (ap-POSS) initiating atom transfer radical polymerization (ATRP) of methylmethacrylate (MMA) and dodecafluoroheptylmethacrylate (DFHM). The obtained POSS-(PMMA-b-PDFHM)<sub>16</sub> and ap-POSS-PMMA-b-PDFHM are proved with narrow distribution of molecular weight (PDI= 1.310 and 1.148) and high thermal stability (410-420°C). In THF solution, POSS-(PMMA-b-PDFHM)<sub>16</sub> and ap-POSS-PMMA-b-PDFHM could self-assemble into 200-250 nm micelles as POSS/PDFHM core and 70-80 nm PMMA shell. During these core/shell micelles self-assembling into films, PDFHM segments and POSS cages are surely competitive migrating onto the surface of film in the manner that PDFHM segments are much easy than POSS cages, so as both POSS-(PMMA-b-PDFHM)<sub>16</sub> and ap-POSS-PMMA-b-PDFHM to produce the typical films as fluorine-rich top layer/POSS enriched upper layer/PMMA bottom layer. Comparatively, ap-POSS-PMMA-b-PDFHM film is much more rough, fluorine-rich and oleophobicity than POSS-(PMMA-b-PDFHM)<sub>16</sub> film due to strong migrating of PDFHM segments onto the film surface in ap-POSS-PMMA-b-PDFHM. But POSS-(PMMA-b-PDFHM)<sub>16</sub> film shows obvious higher hydrophobicity. Therefore, ap-POSS-PMMA-b-PDFHM film gains higher water absorption and viscoelasticity than POSS-(PMMA-b-PDFHM)<sub>16</sub> film.

**KEYWORDS:** 16-arm and single-arm; POSS-based fluoracrylate diblock copolymers; Core/shell micelles; Self-assembled film; Surface wettability and viscoelasticity.

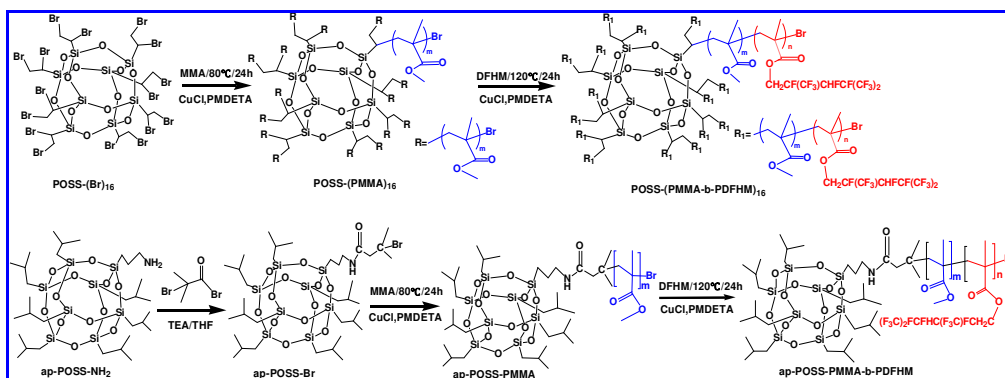


**Fig.1** Synthesis of POSS-(PMMA-b-PDFHM)<sub>16</sub> and ap-POSS-PMMA-b-PDFHM

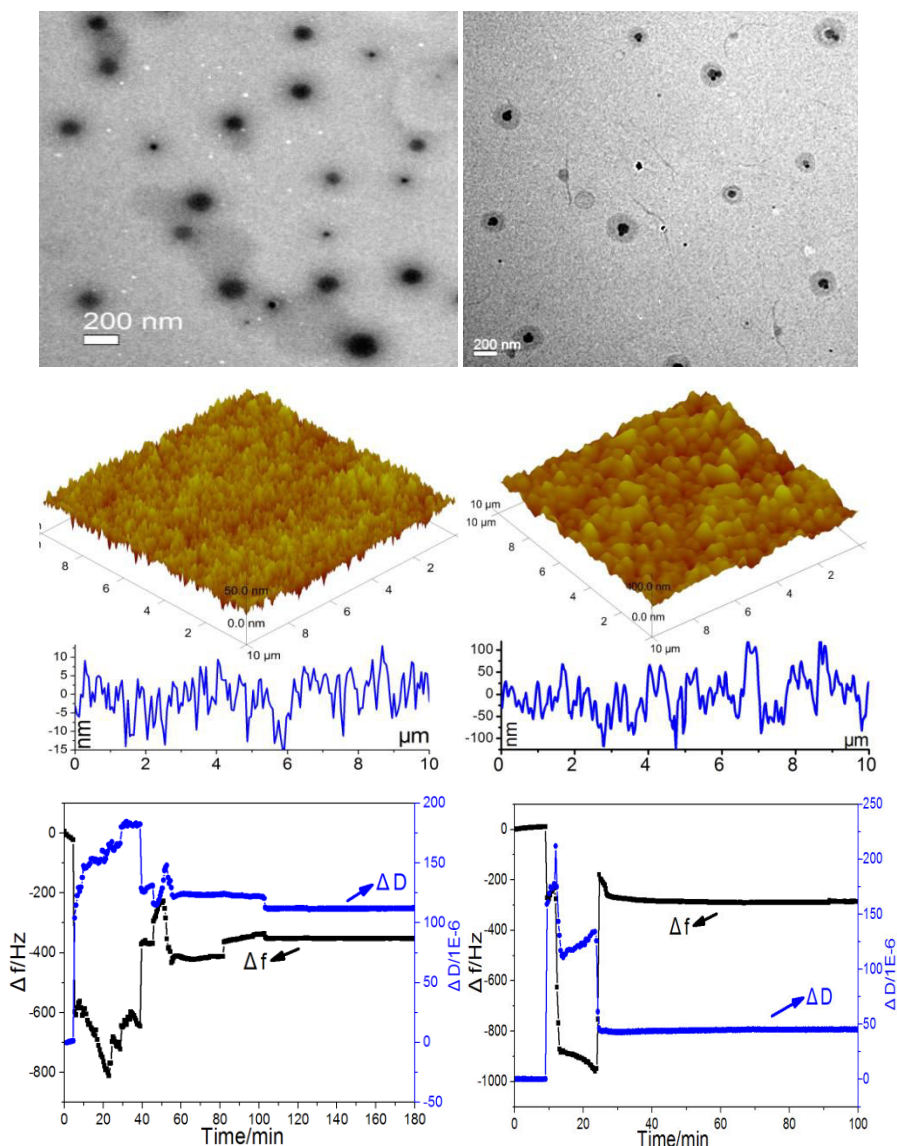


**Fig.2** The self-assembled micelles, the film surface, the Surface wettability and viscoelasticity of the self-assembled films by POSS-(PMMA-b-PDFHM)<sub>16</sub> (left) and ap-POSS-PMMA-b-PDFHM (right)

## Graphite NanoPlatelets in poly(trimethylene terephthalate) (PTT) based nanocomposites: effect of flake size on electrical conductivity and barrier properties of thin polymer films

Sandra Paszkiewicz<sup>a\*</sup>, Anna Szymczyk<sup>b</sup>, Zdenko Špitalský<sup>c</sup>, Jaroslav Mosnáček<sup>d</sup>, Tiberio A. Ezquerro<sup>e</sup>, Zbigniew Roslaniec<sup>a</sup>

<sup>a</sup>West Pomeranian University of Technology, Institute of Material Science and Engineering, Piastow Av. 19, PL-70310 Szczecin, Poland, <sup>b</sup>West Pomeranian University of Technology, Institute of Physics, Piastow Av. 19, PL-70310 Szczecin, Poland, <sup>c</sup>Polymer Institute, Slovak Academy of Sciences, Dúbravská cesta 9, 845 41 Bratislava 45, Slovakia, <sup>d</sup>Polymer Institute, Centre of Excellence FUN-MAT, Slovak Academy of Sciences, Dúbravská cesta 9, 845 41 Bratislava 45, Slovakia, <sup>e</sup>Instituto de Estructura de la Materia-Consejo Superior de Investigaciones Científicas, IEM-CSIC, Serrano 119-121, 28006 Madrid, Spain

\*Corresponding author. Tel.: +48 91 449 45 89; E-mail address: [spaszkwicz@zut.edu.pl](mailto:spaszkwicz@zut.edu.pl)

### Abstract

This work presents the preparation process of two batches of poly(trimethylene terephthalate) nanocomposites. Both synthesized by means of *in situ* polymerization with an addition of graphene nanoplatelets. The nanoplatelets used were 50 $\mu\text{m}$  (EG50) and 500 $\mu\text{m}$  (EG500) and a comparison of the influence of their size on processing, physicochemical properties, morphology and, most importantly, electrical conductivity and barrier properties of thin polymer films has been performed. It has been also confirmed that polymer films were amorphous, since crystallinity affects both barrier and electrical properties (Fig.1).

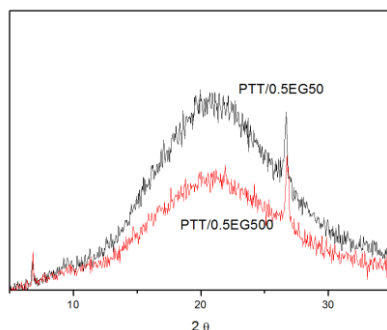


**Fig. 1** Wide angle X-ray scattering patterns of PTT based nanocomposites with the same concentration of nanofillers (0.5 wt %) submitted to both EG50 and EG500.

It was clearly found that smaller platelets i.e. EG50 enabled to obtain conductive thin polymer films with a nanoplatelet content of 0.3-0.5% wt. However, PTT/0.5EG500 nanocomposite proved to be non-conductive (Fig.2).

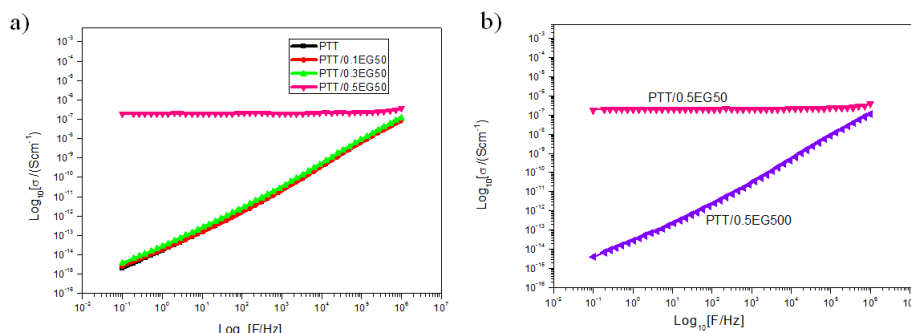


**Fig. 1** Broad band electrical conductivity,  $\sigma$  (F) as a function of frequency, F, for nanocomposites prepared by in situ polymerization with different fillers: (A) PTT/EG 50, (B) PTT with the same concentration (0.5wt.%) of EG50 and EG500.

At the same time smaller graphene platelets demonstrated a more uniform distribution in the PTT matrix, which was confirmed by means of Scanning Electron Microscopy (SEM) and Transmission Electron Microscopy (TEM), thus giving the samples in question barrier properties in respect to CO<sub>2</sub> and O<sub>2</sub>. Moreover, it has been shown that both EG50 as well as EG500 did not have a significant influence on the phase transition temperatures ( $T_g$ ,  $T_c$ ,  $T_m$ ) and on the long period (L). They caused however a slight decrease of crystallinity which is an evidence of an anti-nucleating character of those nanoparticles in the PTT matrix.

#### Acknowledgments

The studies were financed by the National Science Centre within project PRELUDE no 2013/11/N/ST8/00404. The experiments performed at A2 in Hasylab (DESY) were done using the beamline of the proposal II-20080143EC.

#### References

1. Kim H., Abdala A.A., Macosko C.W. *Macromolecules*, 2010, 43, 6515-6530.
2. Paszkiewicz S., Szymczyk A., Spitalsky Z., Soccio M., Mosnacek J., Ezquerro T.A., Roslaniec Z. *J Polym Sci Polym Phys*, 2012, 50, 1645-1652.
23. Zhang H-B. Zheng W-G., Yan Q., Yang Y., Wang J-W., Lu Z-H., Ji G-Y., Yu Z-Z. *Polymer*, 2010, 51(5), 1191-1196.
25. Paszkiewicz S. Roslaniec Z., Szymczyk A., Spitalsky Z., Mosnacek J. *Chemik*, 2012, 66(1), 26-30.
27. Paszkiewicz S., Szymczyk A., Špitalský Z., Mosnáček J., Janus E., Roslaniec Z. *Polimery/Polymers* 2013, 58(11-12), 893-899.

## Relationship between damping capacity and texture in magnesium alloy

S. Kim<sup>1,a</sup>, K. Okayasu<sup>2</sup>, H. Fukutomi<sup>2</sup>, H. Kwon<sup>3</sup>, C. kang<sup>4</sup>, K. Kim<sup>1,4,b</sup>

<sup>1</sup>Marine Design Co-Work, Pukyong National University, 45 Yongso-ro, Nam-gu, Basan 608-737, Korea.

<sup>2</sup>Faculty of Engineering, Yokohama National University, 79-5 Tokiwadai, Hodogaya-ku, Yokohama 240-8501, Japan

<sup>3</sup>Dep. of Materials System Engineering, Pukyong National University, 365 Sinseon-ro, Nam-gu, Busan 608-739, Korea.

<sup>4</sup>Dep. of Metallurgical Engineering, Pukyong National University, 365 Sinseon-ro, Nam-gu, Busan 608-739, Korea.

*E Mail/ ksp8909@nate.com<sup>a</sup>, mrppeng@pknu.ac.kr<sup>b</sup>*

Magnesium has excellent properties, such as low density, high specific strength, and good damping capacity. Because of these properties, magnesium has been attracted a lot of interest in various industrial parts. It was well-known that magnesium alloys have a good damping capacity compared to the other alloys [1]. Also, the damping properties of metals are generally recognized to be dependent on microstructural factors such as grain size and texture. However, there are very few studies on the relationship between the damping ability and texture of Mg alloys. Therefore, in this study, the AZ31 magnesium alloy which was carried out by heat treatment was experimentally investigated about the relationship between the texture and damping capacity. For damping test and texture measurement, specimens was machined out from commercial AZ31 magnesium alloy and hot-rolling and heat treatment was carried out. The damping capacity test was measured with a flexural internal friction measurement machine at room temperature. Texture measurement was carried out on the compression planes by the Schulz reflection method and EBSD measurement. It was found that the accumulation of pole density at center decreases with an increase of heat treatment temperature and time. Also, damping capacity increases.

**Keywords:** *Magnesium, damping capacity, texture, high-temperature deformation*

[1] Sugimoto, K., Matsui, K., Okamoto, T. and Kishitake, K., 1975. JIM, 16, 647-655.

## Chemical Vapor Infiltration of Stacked, Dry-Spun Carbon Nanotube Ribbons for Fabrication of Multifunctional, Anisotropic Foams with Tunable Properties

Faraji<sup>1</sup>, Yildiz<sup>1</sup>, Stano<sup>1</sup>, Li<sup>1</sup>, Zhu<sup>2</sup> and Bradford<sup>\*1</sup>

<sup>1</sup> Department of Textile Engineering, Chemistry and Science, North Carolina State University, Campus Box 8301, Raleigh, NC 27695, USA

<sup>2</sup> Department of Materials Science and Engineering, North Carolina State University, Campus Box 7907, Raleigh, NC 27695, USA

E-mail: [philip\\_bradford@ncsu.edu](mailto:philip_bradford@ncsu.edu)\*, [sfaraji@ncsu.edu](mailto:sfaraji@ncsu.edu)

Fabrication of macroscopic assemblies of carbon nanotubes (CNTs) is critical to realizing these materials in new practical applications. Among CNT assemblies, nanotube foams and aerogels have gained increased attention in recent years due to their applications in energy absorption materials, filtration and separation, sensors, supercapacitors and batteries. Despite this increased interest in porous, low-density CNT structures, there are only a few fabrication routes proposed for these materials. In this work we introduce a new approach for fabrication of CNT foams by stacking aligned sheets of CNTs, continuously drawn from spinnable nanotube arrays, and further infiltration of the stacked ribbon assembly with pyrolytic carbon (PyC). Although the idea of dry, continuous drawing of CNTs for production of yarns, fibers and aligned sheets has been studied before, no study has ever reported synthesis of CNT foam structures by dry spinning of nanotubes.

Microscopy characterizations showed that PyC deposition coated the junctions between nanotubes, while increasing surface roughness of CNTs. These morphological changes helped to explain the transition from non-elastic behavior to foam-like recovery. Complete shape and structural recovery of the foams was observed after 100 cycles of compression testing at 90% strain. Dynamic Mechanical Analysis showed no degradation in compressive mechanical properties over the large temperature range of -100 to 300 °C.

Alignment of the nanotubes resulted in anisotropic mechanical and thermal behavior of the foams. The properties of these anisotropic carbon nanotube/carbon (ACNT/C) foams could be tuned for specific applications through altering the PyC coating duration. Samples with longer PyC coating duration exhibited much greater compressive strength and energy absorption while

having lower thermal diffusivity. Furthermore, the dependence of electrical resistance of the foams to applied pressure was investigated in situ for compressive strains up to ~ 90%. Results showed that electrical resistance of ACNT/C foams has stable, linear dependency to applied compressive strain, making these foams acceptable for use as pressure sensors.

***Keywords: Carbon nanotube, foam, anisotropic, tunable, multi-functional***



## Directed Metal Assembly using thio-G-Modified DNA for Nanoelectronic Materials

Andrew Pike<sup>1</sup>, [Samantha Lunn](mailto:s.m.l.lunn@newcastle.ac.uk)<sup>1</sup>

<sup>1</sup>Newcastle University, Newcastle upon Tyne, Tyne and Wear, NE1 7RU

[s.m.l.lunn@newcastle.ac.uk](mailto:s.m.l.lunn@newcastle.ac.uk), [andrew.pike@newcastle.ac.uk](mailto:andrew.pike@newcastle.ac.uk)

The functionalization of DNA with modified bases that interact with metal ions has potential applications in nanoelectronics and molecular materials.<sup>[1]</sup> This poster describes the site specific incorporation of 2-deoxy-6-thioguanosine (tG) bases into a self-complementary oligonucleotide sequence, d(T<sub>6</sub>tG<sub>4</sub>A<sub>6</sub>), via solid phase DNA synthesis. Modifications to DNA are routinely achieved by the use of commercially available modified-phosphoramidites,<sup>[2]</sup> or via an additional step after oligonucleotide synthesis.<sup>[3]</sup> We describe here, a method allowing the conversion of guanine (G) to thio-guanine (tG), during mid-synthesis of the oligonucleotide. The tG bases are able to act as multiple metal binding sites, through the N(7) and S(6) positions, and specifically coordinate to Cd<sup>2+</sup> forming interstrand S-Cd-N bridges between adjacent nucleobases. The binding of Cd<sup>2+</sup> ions was investigated to assess the ability of the DNA to assemble 1D nanomaterials and the resulting effects on the structure of the double helix.

**Keywords:** *modified nucleobases, nanoelectronic materials, metal-mediated base pairing*

[1] TANAKA, K., TENEGHIA, A., KATO, T., TOYAMA, N., SHIONOYA, M. (2003). A Discrete Self-Assembled Metal Array in Artificial DNA. *Science*, 299, 1212-1213.

[2] GOODCHILD, J. (1990). Conjugates of oligonucleotides and modified oligonucleotides: A review of their synthesis and properties. *Bioconjugate Chem.*, 1, 165-187.

[3] BEILSTEIN, E. A., GRINSTAFF, W. M. (2001). Synthesis and characterization of ferrocene-labeled oligodeoxynucleotides. *J. Organomet. Chem.*, 637-639, 509-510.

## Optimal Design of Functionally Graded Structures considering Dynamical Analysis

Wilfredo Montealegre Rubio<sup>1</sup>

<sup>1</sup> Department of Mechanical Engineering, Faculty of Mines, Universidad Nacional de Colombia, Núcleo el Río, Carrera 64 No. 63 – 120, bloque 04, oficina 219, Medellín, Antioquia, Colombia, wmontealegrer@unal.edu.co

**Presenting and corresponding author: Wilfredo Montealegre Rubio, Department of Mechanical Engineering, Universidad Nacional de Colombia, Car. 80 No. 65-223, M8, oficina 211, Medellín, Colombia**

Functionally Graded Materials (FGM) are advanced materials, whose properties change continuously in a specified direction. These materials combine desirable features of their constituent phases; for instance, high temperature resistance typical of ceramics with mechanical strength of metals. Usually, graded structures (based on FGM concept) are designed considering trial and error techniques or their topologies are optimized by using a-priori gradation functions. However, the performance of these structures change according to gradation function considered. Accordingly, it is a very important issue to find the optimal gradation law for achieving specific performances. This work is focused on finding the optimal gradation function of mechanical structures by using the topology optimization method (TOM). The TOM combines optimization algorithms with the Finite Element Method (FEM) in order to maximize a user-defined objective function. For exemplifying the proposed methodology, the optimal gradation function of a structure is found, which maximizes their resonance frequency while the properties are graded from Cooper to Nickel. Several relevant aspects are treated for achieving goals, which includes: (i) the Graded Finite Element Concept; (ii) the Continuous Approximation of Material Distribution (CAMD); (iii) the Material Projection technique; and (iv) the Modal Assurance Criterion. An example is presented to illustrate the method.

**Keywords:** *Functionally Graded Materials, Topology Optimization Method, Material Gradation Function, Cu-Ni.*

## EFFECT OF QUARternary ELEMENT ON THE MICROSTRUCTURES AND SHAPE MEMORY PROPERTIES OF Cu-Al-Ni SHAPE MEMORY ALLOYS

E.Hamzah<sup>\*</sup>, Safaa.N.Saud, T. Abu Bakar

*Faculty of Mechanical Engineering, Universiti Teknologi Malaysia,*

*81310 UTM Johor Bahru, Johor, MALAYSIA*

### ABSTRACT

The microstructures and mechanical properties of the Cu-Al-Ni shape memory alloys (SMA) with addition of different quaternary element, namely, Fe, Mn, Ti, and Co were studied. The microstructure variations were characterized and analyzed by means of optical microscopy, field emission electron microscopy, and x-ray diffraction. It was found that the morphology of Cu-Al-Ni SMA changes in terms of martensite phase shape, volume fraction, and distribution associated with the existence of different types of precipitates formed with the addition of the fourth element. Meanwhile, the mechanical properties were investigated using Vickers hardness and shape memory effect test. A large hysteresis and shape recovery were obtained with the addition of the fourth element, especially with cobalt, which has recovered 100 % of the original shape after heating at 300°C which was mainly attributed to the presence of high volume fraction of  $\gamma_2$  phase. An increase in fracture strain and ductility were obtained with the Fe addition, which was attributed to presence of  $\alpha$  martensite. The evolution of the transformation temperatures of the alloys was studied by differential scanning calorimetry. It was found that the transformation temperatures and the thermodynamic parameters were slightly varied due to the addition of the alloying element. These changes were mainly linked to the variations of the structure, morphology, and existence of the precipitates that were generated after the addition of the fourth alloying elements. The main advantage of this work is to enhance the properties of Cu-based SMAs and thus reduce its limitation for engineering applications.

---

\*  
*Corresponding author: Tel No: 607-5554855; Fax No: 607-5566159*

*E-mail address: [esah@fkm.utm.my](mailto:esah@fkm.utm.my)*

## The use of MgO-paste as a biodegradable bone cement

Biel<sup>1</sup> A., Chaudhry<sup>2</sup> M., Gustafsson<sup>3</sup>, S., Johansson<sup>4</sup>, K-E., Nygren<sup>2</sup> H.

<sup>1</sup>Department of Engineering Sciences, University of Skövde, 541 28 Skövde, Sweden.

<sup>2</sup>Department of Cell Biology and Medical Chemistry, Institute of Biomedicine, University of Gothenburg, Gothenburg P.O.Box 420, 405 30 Göteborg, Sweden.

<sup>3</sup>Department of Applied Physics, Chalmers University of Technology, 412 96 Göteborg, Sweden.

<sup>4</sup>Elos Medtech Inc, 540 16 Timmersdala, Sweden.

*Contact: Professor Håkan Nygren, Institute of Biomedicine, University of Gothenburg, Sweden. E-mail: hakan.nygren@gu.se*

The low bone mass and altered bone microarchitecture of osteoporotic fracture patients gives a high risk of delayed fracture healing and bone non-union. In the aging population of the western world of today, this is an increasing problem now and in the future, and a motivation to intense research in the field of regulation of bone mass.

Magnesium and its alloys have been proposed as a novel class of highly bone-active and biodegradable materials. That is, these materials are supposed to temporarily aid the healing process of a diseased tissue and then progressively disappear after a certain time of function.

The use of MgO-paste as bone cement was tested on titanium cylinders implanted into rat tibia. The primary evaluation of the effect was made with the retention force (pull-out) test. Preimplantation of the MgO-paste into drill perforations of rat tibia increased the retention of the titanium implant 6-fold. The force was normalized to the bone-covered area of the cylinder (N/mm<sup>2</sup>). The error was expressed as the 95% confidence interval of means (n=10 bones in each group). The observed difference between 3.46±0.71 N/mm<sup>2</sup> for Ti-cylinders implanted with MgO-paste and 0.56±0.26 N/mm<sup>2</sup> for Ti-cylinders implanted directly into the bone, is statistically significant (p<0.01).

The effect of implanted MgO on bone healing was analysed by SEM/EDX and light microscopy. The results suggest that the increase of retention force, caused by MgO is due to an increased thickness of the compact cortical bone and compact bone surrounding the implant, due to anabolic formation of compact bone in the advanced phases of bone remodeling. The EDX analysis indicates that the Mg is resorbed from the bone marrow cavity within 2 weeks of healing and taken up into the bone mineral phase.

The advancement of MgO compared to previous materials used as bone cements is the rapid adsorption from the bone marrow cavity into bone mineral and its anabolic effect on bone tissue resulting in higher bone mass of compact bone.

**Keywords:** *Bone formation, bone cement, Magnesium, bone healing, osteoporosis*

## Singular thermal stress analysis of heterogeneous medium with irregular-shaped inclusions

Mengcheng Chen<sup>1</sup>, Xuecheng Ping<sup>2</sup>, Weixing Wu<sup>1</sup>

<sup>1</sup> School of Civil Engineering, East China Jiaotong University, Nanchang 330013, China

<sup>2</sup> School of Mechanical and Electronical Engineering, East China Jiaotong University,  
Nanchang 330013, China

919367042@qq.com / Prof. Mengcheng Chen

When composite structures subjected to thermo-mechanical loads undergo large localized deformations, reinforcements can adversely affect their failure properties, e.g., durability and fracture toughness. Cracks may nucleate at or near the particle-matrix interface. Such detrimental behavior has spurred critical examination of the mechanical properties and deformation characteristic of inclusions, resulting in a number of models emphasizing failure mechanisms. Until now, we have not been aware of any reports on numerical results of multi-polygonal inclusions for thermo-mechanical loads in the literatures. In this paper, a new *ad hoc* finite element method based on the numerical eigenanalysis technique is developed to investigate stress intensity factors around the inclusion corners of double periodic rectangular inclusions in 0-3 and 1-3 composites. The effects of inclusion spacings, material mismatches, temperature changes and thermal expansion mismatches on the field intensity factors are discussed in detail. The research results will be useful for the life prediction of 0-3 and 1-3 composites subjected to thermo-mechanical loads and the design of composite materials.

**Keywords:** *Sharp inclusion, thermo-mechanical stress, corner apex element, unit cell*

[1] CHEN, M.C., PING, X.C. 2009. Analysis of the interaction within a rectangular array of rectangular inclusions using a new hybrid finite element method, Eng. Fract. Mech. 76, 580-593.

*Topic considered : Advances in Multifunctional Composite materials*

## Interaction between superconductor and ferromagnetic layers in YBCO-LCMO superlattices - magnetic and electrical measurements

Yonamine, A. H.<sup>1</sup>, Fedoseev, S. A.<sup>2</sup>, Dos Santos, D. I.<sup>3</sup>, Pan, A. V.<sup>2</sup>

<sup>1</sup> POSMAT Programa de Pós Graduação em Ciência e Tecnologia de Materiais,  
São Paulo State University UNESP, Brazil.

<sup>2</sup> Institute for Superconducting and Electronic Materials - University of Wollongong,  
Australia.

<sup>3</sup> Department of Physics - São Paulo State University UNESP, Bauru, SP, Brazil.

*dayse@fc.unesp.br*

The interaction between superconductor and ferromagnetic ultrathin layers prepared by pulsed laser deposition on LaAlO<sub>3</sub> substrate was studied in YBa<sub>2</sub>Cu<sub>3</sub>O<sub>6+d</sub>/La<sub>2/3</sub>Ca<sub>1/3</sub>MnO<sub>3</sub> superlattices. The superconductor and ferromagnetic layers have (YBCO-20nm/LCMO-20nm)<sub>x20</sub> architecture and were separated by a layer of insulator having a variety of thicknesses. A few insulators (SrTiO<sub>3</sub>, CeO<sub>2</sub> and others) were tested in order to investigate the tuning of the overall superlattice property. The coexistence of both ferromagnetism and superconductivity was observed for most of the samples using zero field and field cooling measurements. The critical and Curie temperatures showed to be dependent of the insulator thickness, but in different ways for each type of insulator. Surface and cross section micrographs showed distinct interfaces and in a few cases evidenced lattice mismatch, which may be responsible for unexpected phenomena observed in magnetic and electrical measurements. MPMS equipment was used to obtain curves of resistance as a function of temperature with applied and no applied magnetic field and for different insulating layers and for a much defined thickness colossal magnetoresistance was observed. No specific tendency was observed for growing insulators thicknesses until 16 nm thick. The critical temperatures as well as the magneto phenomena were observed for the resistivity, below critical temperature, depending on the chosen lattice architectures.

**Keywords:** *High temperature Superconductor; YBCO-LCMO Superlattice; YBCO-LCMO interaction; Superconductor-Ferromagnetic proximity.*





## Selective uranium extraction from acidic solution using functionalized mesoporous silicas

A. Charlot<sup>1</sup>, F. Cuer<sup>1</sup>, A. Grandjean<sup>1</sup>

<sup>1</sup>French Alternative Energies and Atomic Energy Commission, DEN, Marcoule, F30207  
Bagnols-sur-Cèze, France.

*E mail:* [alexandre.charlot@cea.fr](mailto:alexandre.charlot@cea.fr) / *Phone:* +33 466 397 679

Mesoporous structured organo-silica materials are known for their adsorption capacities since the 90's. Indeed, researches are continuously evolving on novel adsorbents with a perfect selectivity, a fast uptake process, and a high chemical resistance to a targeted compound such as heavy metals or organic pollutants[1]. Then, in a context of an important growth of energetic demand in the next decades, recent works have shown that silica hybrid material could be attractive for the recovery of uranium from acidic solutions[2] to be used as nuclear fuel. Hybrid materials couple inorganic and organic properties with a very large specific surface areas, tuneable pore sizes and specific reactivity.

Tailoring of silica mesoporous materials is based on a soft way: hydrolyse and condensation of an inorganic precursor occurs around surfactant that acts as a structuration template. Then calcination leads to a silica mesoporous material with a narrow pore size distribution. By post-grafting method, the surface could be functionalized by complexing compounds leading to precise applications[3].

In our case, we design hybrid materials to extract selectively uranium from acidic solution. In order to achieve this goal, it is necessary to choose organic ligands showing a higher affinity to uranyl ions than counterions (phosphate, sulphate). The combinations of amido and phosphonate groups are well known for their affinity with actinides. We adapt this result to design a tridentate ligand. Materials are characterized by CP-MAS NMR (<sup>29</sup>Si, <sup>13</sup>C, <sup>31</sup>P), small-angle X-ray scattering (SAXS), adsorption of nitrogen (BET, BJH methods), TGA and elementary analyses.

Synthetic effluents have been treated in order to demonstrate the selective extraction of uranium with these hybrid materials. Results show clearly an efficient extraction capacity, and it has been proved that iron in solution does not affect uranium extraction. Also, uranium stripping was broached by sulphuric acid solution (3M). Results show a recovery up to 90% of

the uranium previously uptakes. Finally, these hybrid materials could be attractive in a near future for this application.

**Keywords:** *Hybrid mesoporous silica, Uranium, Extraction, acid solutions.*

[1] A. Walcarius et al, *Mesoporous organosilica adsorbents: nanoengineered materials for removal of organic and inorganic pollutants*. Journal of Materials Chemistry, 2010. **20**(22): p. 4478.

[2] A. Charlot et al., *From phosphate rocks to uranium raw materials: hybrid materials designed for selective separation of uranium from phosphoric acid*. RSC Advances, accepted, 2014.

[3] F. Hoffmann et al., *Silica-based mesoporous organic-inorganic hybrid materials*. Angew Chem Int Ed Engl, 2006. **45**(20): p. 3216-51.

## A chiral copper(II) complex: Synthesis, crystal structure, ferroelectric and magnetic properties

Guang-Xiang Liu<sup>1,2</sup>, Xiao-Feng Wang<sup>1</sup>, Hong Zhou<sup>1</sup>

<sup>1</sup> School of Chemistry and Environmental Engineering, Nanjing Xiaozhuang University, Nanjing 211171, P. R. China

<sup>2</sup> State Key Laboratory of Coordination Chemistry, School of Chemistry and Chemical Engineering, Nanjing University, Nanjing 210093, P. R. China

E Mail: [njuliugx@126.com](mailto:njuliugx@126.com); [zhouhong@njxzc.edu.cn](mailto:zhouhong@njxzc.edu.cn)

The reaction of phenyl 2-pyridyl ketoxime (PhPyCNOH) with  $\text{Cu}(\text{NO}_3)_2 \cdot 3\text{H}_2\text{O}$  in methanol results in the chiral trinuclear complex  $[\text{Cu}_3(\text{OH})(\text{PhPyCNO})_3(\text{NO}_3)(\text{CH}_3\text{OH})] \cdot (\text{NO}_3)$  (**1**), which has been characterized by elemental analysis, IR spectra and single-crystal X-ray diffraction. The structure of **1** exhibits a triangle of Cu(II) ions, centered by a triply bridging hydroxo ligand and with three edge-bridging oximate groups from the three PhPyCNO<sup>-</sup> ions. Preliminary variable-temperature magnetic susceptibility studies reveal an antiferromagnetically-coupled system showing antisymmetric exchange. Complex **1** crystallizes in an acentric space group ( $P2_1$ ) which belongs to a polar point group, which displays second harmonic generation response and ferroelectric behavior. Moreover, complex **1** exhibits interesting magnetic features and the antisymmetric exchange interaction has to be taken into account to describe the magnetic behavior of the cluster properly. A full magnetic analysis of **1** is in progress.

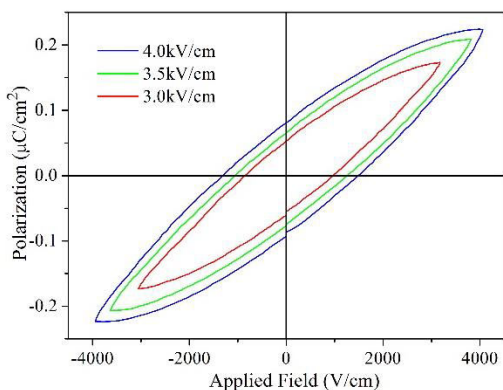


Figure 1. Electric hysteresis loops for a

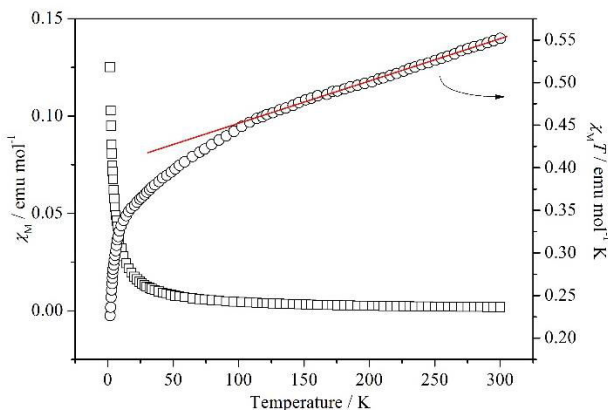


Figure 2. Plots of  $\chi_M T$  and  $\chi_M$  as a function of  $T$  of

pellet obtained from a powdered sample of complex **1**. Solid line above the experimental data is the theoretical curve derived from the Hamiltonian.

**Keywords:** *Oxime complex, crystal structure, ferroelectric properties, magnetic properties*

- [1] ZHAO, H. X., ZHUANG, G. L., WU, S. T., LONG, L. S., GUO, H. Y., YE, Z. G., HUANG, R. B., ZHENG, L. S. 2009. Experimental and theoretical demonstration of ferroelectric anisotropy in a one-dimensional copper(II)-based coordination polymer. *Chem. Commun.*, 1644-1646.
- [2] OHKOSHI, S., TOKORO, H., MATSUDA, T., TAKAHASHI, H., IRIE, H., HASHIMOTO, K. 2007. Coexistence of ferroelectricity and ferromagnetism in a rubidium manganese hexacyanoferrate. *Angew. Chem., Int. Ed.*, 46, 3238-3241.
- [3] MILIOS, C. J., PILIGKOS, S., BELL, A. R., LAYE, R. H., TEAT, S. J., VICENTE, R., MCINNES, E., ESCUER, A., PERLEPES, S. P., WINPENNY, R. E. P. 2006. A rare mixed-valence state manganese(II/IV) tetranuclear cage formed using phenyl 2-pyridyl ketone oxime and azide as ligands. *Inorg. Chem. Commun.*, 9, 638-641.
- [4] STAMATATOS, T. C., FOGUET-ALBIOL, D., STOUMPOS, C. C., RAPTOPOULOU, C. P., TERZIS, A., WERNSDORFER, W., PERLEPES, S. P., CHRISTOU, G. 2007. New Mn<sub>3</sub> structural motifs in manganese single-molecule magnetism from the use of 2-pyridyloximate ligands. *Polyhedron*, 26, 2165-2168.

## New Chiral Metal-Mesogenic Nanosystems

T.I.Shabatina, A.A.Belyaev, E.S.Anistratova, Ya.A.Gromova

*Department of Chemistry, M. V. Lomonosov Moscow State University,*

*119991 Moscow, Russian Federation*

*E Mail: tatyana-shabatina@yandex.ru*

New metal-mesogenic nanosystems based on mesogenic derivatives of cholesterol and its heteroatomic analog thiocholesterol including nanosized silver particles of  $d=5,0\pm 0,5$  nm and  $d=2,5\pm 0,5$  nm, correspondingly, have been obtained by two-phase chemical synthesis. Ordered 1D-, 2D- and 3D-structures including silver nanoparticles were formed on different support surfaces by removing of inert solvent from triple metal/ligand/solvent system and by cooling of binary metal/ligand system from isotropic state to liquid crystalline mesophase [1]. The microstructure and composition of the hybrid nanosystems were characterized by FTIR, UV-Vis spectroscopy and transmission electron microscopy (TEM). Supramolecular organization of the ligand molecules allows us to use the obtained nanoparticles for self-assembling in binary superlattices and for the formation of ordered 1D-, 2D-, and 3D nanostructures. The optical properties of nanosystems obtained belong to the plasmon absorption of individual silver nanoparticles and possess modified plasmonic bands of hybrid nanostructures of nanoparticle superlattices. Integrating of silver nanoparticles of exact size and shape and of their aggregates of definite morphology with biological molecules and blocks opens new perspectives for obtaining of new biocompatible instruments for imaging and sensing of biological objects in living organisms and targeted medical therapy.. The work is financially supported by RFBR grant 2013-03-00792 a/

***Keywords: Metal-mesogenic nanosystems, metal nanoparticles, hybrid nanomaterials, optical properties***

[1] SHABATINA, T.I., BELYAEV, A.A., SERGEEV, G.B. 2013. Self-assembled nanostructures in silver/cholesterol and silver/thiocholesterol systems. *BioNanoScience*, **3**, N3, pp/289-294.

## **Gold nanoparticles as drug delivery vehicle for Chondroitin sulphate (CS) to treat osteoarthritis.**

**Authors : Priyanka Dwivedi <sup>a</sup>, Meenal kowshik<sup>a</sup>, Ashok kumar <sup>b</sup>, Vijayashree Nayak <sup>a</sup>**

**<sup>a</sup>Department of Biological Sciences, Birla Institute of Technology and Science-Pilani, K. K. Birla Goa Campus, Zuarinagar Goa 403726, India.**

**<sup>b</sup>Department of Biological Sciences and Bioengineering, Indian Institute of Technology Kanpur, 208016-Kanpur, India**

### **Abstract**

Osteoarthritis (OA) is a disease which is characterized by joint pain, swelling and stiffness due to wear and tear of articular cartilage and has limited self repair capacity due to its avascular and aneural nature. Nanotherapeutics use nanomaterials for various biomedical applications such as drug delivery, diagnostics and biosensors. This work focuses on the use of gold nanoparticles for enhancing the delivery of chondroitin sulphate (CS)-a drug used in the treatment of Osteoarthritis (OA). CS has already shown many benefits in treating osteoarthritis. Gold nanoparticles were synthesized and combined with CS. Gold nanoparticles were characterized by Transmission electron microscopy (TEM), XRD analysis. Further *invitro* analyses of this combination of Gold nanoparticles with CS (AuNp-CS) on primary goat chondrocytes were done by various assays like MTT, Hoescht staining, Glycosaminoglycan and collagen studies. Cell viability studies by MTT revealed that Gold nanoparticles –CS (AuNp-CS) stimulated cell proliferation. There was increase in cell viability observed by Gold nanoparticles-CS than Native CS at same concentration. Similar Results were also observed with GAG and Collagen assay. There was 2.18 and 2.05 fold increase observed in GAG and collagen production when gold nanoparticles–CS (AuNp-CS) was added in combination than native CS. So this study shows that this combination of gold nanoparticles-CS stimulates chondrocyte proliferation and enhances Extracellular matrix production (ECM). Thus giving us the insight for the applicability of gold nanoparticles as a carrier for osteoarthritic drug CS which can hold potential for treatment of disease.

Presenting author

Priyanka Dwivedi

Ph.D Scholar ,BITS PILANI K.K. BIRLA GOA(INDIA)

Priya.dwivedi15@gmail.com



## Correction of Characteristics Obtained by Approximate Methods for Mechanical and Mechatronic Systems as Necessary Condition of their Synthesis

Andrzej Buchacz<sup>1</sup>

<sup>1</sup>Silesian University of Technology, Faculty of Mechanical Engineering, Institute of Engineering Processes Automation and Integrated Manufacturing Systems  
44-101 Gliwice, Konarskiego 18A, Poland

andrzej.buchacz@polsl.pl

The main aim of this paper is to compare the transients of characteristics - of the mechatronic system - obtained by exact and approximate methods. At first the torsionally or longitudinally vibrating mechanical subsystems are considered. The mechatronic system composed from many continuous mechanical and discrete-continuous mechatronic subsystems having the same length and variable cross section, loaded by the focused moment was analysed. The main subject of deliberation was to determine the flexibility of the mechanical system with constant cross section using the exact and approximate methods. Next the comparison method and the correction of approximate method were made. Analysing the diagrams of characteristics of confirmed system it has been determined that in case of approximate method the resonance frequencies cover with those which have been determined with exact method. However the values of the characteristic in other areas are different. Therefore there is the mistake of approximate method, which in case of studying the single system does not have any influence because in resonance areas the characteristic values of the system approach to the infinity. However the difference between values of flexibility within two methods has the great influence on the result of complex systems. The characteristic of the elementary subsystems using the exact and approximate methods has been determined according to accepted frequencies and the correction coefficient. The frequencies were chosen from the spectrum in which the synthesis of complex systems will be conducted. It was very important that the difference of flexibility values in the spectrum was minimal. The coefficient of the correction has been determined according to the flexibility values of chosen points and it is equal to quotient of flexibility calculated using the exact method across the flexibility delivered by using the approximate method. After determination the correction coefficient the medium value has been calculated which has been afterwards considered in dynamic characteristics correlation. The problems presented in this paper is the introduction to the synthesis of torsionally or longitudinally vibrating mechatronic systems with assume frequency spectrum.

**Keywords:** *Analysis, Modeling, Approximate and exact methods, Vibrating shafts, Piezoelectric*



## **SnO<sub>2</sub>@graphene nanocomposite as an advanced anode materials for Lithium-ion batteries**

Renmei Gao, Zheng Jiao, Haijiao Zhang

*Institute of Nanochemistry and Nanobiology, School of Environmental and Chemical  
Engineering, Shanghai University, Shanghai 200444, P. R. China*

*E-mail: hjzhang128@shu.edu.cn*

In recent years, lithium-ion batteries (LIBs) have been extensively applied as an important energy-storage device because of their well-known advantages. Very recently, many metal oxides have widely investigated as the high-capacity anode material for LIBs, such as Co<sub>3</sub>O<sub>4</sub>, TiO<sub>2</sub>, and SnO<sub>2</sub>, etc. Among these materials, SnO<sub>2</sub> is considered as one of the most promising candidate due to its abundance, safe lithiation potential and high theoretical capacity (780 mAhg<sup>-1</sup>). However, its practical application is still hindered by fast capacity fading and poor rate capability owing to the low conductivity and large volume change in the lithiation-delithiation process. To solve the problem, one effective way is the construction of the SnO<sub>2</sub>@carbon nanocomposites, for example, graphene with the large surface area, excellent charge carrier and good mechanical properties is a very attractive carbon nanomaterial. Herein, we demonstrate a one-step and in-situ chemical route for synthesis of SnO<sub>2</sub>@graphene nanocomposite starting from SnCl<sub>2</sub>•2H<sub>2</sub>O and graphene as the raw materials with the assistance of cetyltrimethylammoniumbromide (CTAB). The products were characterized by SEM, TEM, XRD, and BET techniques. The resulting SnO<sub>2</sub>@graphene showed uniform morphology and high surface area. Moreover, the SnO<sub>2</sub> nanoparticles were homogeneously anchored onto the surface of graphene nanosheets. Additionally, the particle sizes of SnO<sub>2</sub> nanoparticles were readily adjusted by varying the reaction temperature. More importantly, the nanocomposite exhibited an extremely high storage capability and a good retention capacity. After 20th cycle, the discharge capacities are still kept as high as 1176 mAhg<sup>-1</sup>. The excellent electrochemical performance was mainly attributed to the

conducting, buffering and protective effects of graphene nanosheets on the SnO<sub>2</sub> nanoparticles, as well as the uniform morphology and high specific surface area. We believe that the materials prepared will have more potential applications in various fields, including the dye-sensitized solar cell, sensor, and optical devices.

**Keywords:** *SnO<sub>2</sub>@graphene, nanocomposite, In-situ hydrothermal synthesis, Lithium-ion batteries*

[1] ZHANG, H., XU, P., DU, G., CHEN, Z., OH, K., PAN, D. & JIAO, Z. 2011. A facile one-step synthesis of TiO<sub>2</sub>/graphene composites for photodegradation of methyl orange. *Nano Research*, 4, 274-283.

[2] ZHANG, H., XU, P., NI, Y., GENG, H., ZHENG, G., DONG, B. & JIAO, Z. 2014. In situ chemical synthesis of SnO<sub>2</sub>/reduced graphene oxide nanocomposites as anode materials for lithium-ion batteries. *Journal of Materials Research*, 29, 617-624.

## Characterization, Thermal effect on Optical band gap energy and Photoluminescence in wurtzite Erbium doped Zinc Oxide Nanocrystallites

<sup>1</sup>Anitha <sup>1</sup>Usha <sup>2\*</sup>Varughese, <sup>2</sup>Jithin <sup>2</sup>Christy,

<sup>1</sup>Department of Chemistry, St.Cyrils College Adoor, Kerala- 691 529, India

<sup>2</sup>Department of Physics, Catholicate College, Pathanamthitta, Kerala-689 645, India.

\*Email-Corresponding author: gvushakoppara@yahoo.co.in

Email-Presenting author: anithajose65@gmail.com

---

### ABSTRACT

Zinc Oxide is an extensively studied group II-VI Semiconductor with optical properties that permits stable emission at room temperature having immense application in sensors, field emission and photonic devices. It exhibits a wide variety of morphologies in the nano regime. XRD, FTIR, EDAX and TEM spectra have been used for characterizing the rare earth element Erbium doped Zinc oxide nanomaterial. The percentage of doping material is confirmed from the EDAX spectrum. The XRD results indicated that the particle size of nano ZnO: Er is much small as compared to that of pure ZnO and decreases with the Erbium loading. XRD has shown that as temperature increases, particle size also increases. The UV Absorption spectra showed blue shift towards 208 nm due to doping with Er. The peak position of the absorption spectra is shifted towards the lower wavelength side or blue-shifted relative to undoped ZnO. The band gap energy of Er-doped ZnO nanoparticles at 120 and 200°C are determined using Tauc plot and found to be in the range 3.321 eV. It was found that energy band gap  $E_g$  increases with doping of Er. As temperature increases the band gap energy decreases. Doping of Er changed the free carrier concentration in the ZnO nanoparticles. The Photo-Luminescence study was carried out on this material and observed longer wavelength shift for emission peaks on calcination. The analysis of optical properties shows that ZnO: Er is a promising material and has potential application in optoelectronic devices.

**Key words:** A: Semiconductor, Nanomaterial, Doping, Optical properties,

**PACS:** 81.05 Dz; 61.46+w; 61.72.Vv; 43.35.Bf

## Ether based electrolyte improves the performance of CuFeS<sub>2</sub> spike-like nanorod as a novel anode for lithium storage

Yunhui Wang, Xue Li, Jinbao Zhao\*

State Key Laboratory of Physical Chemistry of Solid Surfaces, Collaborative Innovation Center of Chemistry for Energy Materials, College of Chemistry and Chemical Engineering, Xiamen University, Xiamen, 361005, China  
\*Corresponding author: Tel: +86 5922186935; fax: +86 5922186935. Email: [jbzhao@xmu.edu.cn](mailto:jbzhao@xmu.edu.cn)

Nowadays, the metal sulfides are attractive electrode materials for lithium-ion battery because of their high capacity and energy density. However, to the best of our knowledge, there are no reports about the electrochemical study of CuFeS<sub>2</sub> as anode material in Li ion battery fields.<sup>[1]</sup> As a new class of electrode material, CuFeS<sub>2</sub> has a high theoretical capacity (the specific capacity is 587 mAh/g and the specific energy is 881 Wh/kg) and a good electrical conductivity (10<sup>3</sup> S/cm at 100 K)<sup>[1]</sup>.

This paper firstly reports the study of CuFeS<sub>2</sub> spike-like nanorods as a promising anode material for lithium ion batteries. When being evaluated as an anode material in traditional carbonate-based (EC/ DEC/ DMC) and ether-based (DOL/ DME) electrolytes, we find that the type of the electrolytes is the key factor contributes to the electrochemical performance. It shows the electrochemical reversibility is much better in ether-based electrolyte and an outstanding rate capability can be obtained at a high rate of 10 C.

SEM structural study of the prepared CuFeS<sub>2</sub> is shown in Fig. 1. From the figure, we can see all the CuFeS<sub>2</sub> nanorods are spike-like and are composed of micron-size secondary particles stacked with nanometer-size primary particles, which is optimal for practical usage as electrode materials. From Fig. 1c-d, it could be observed that the Cu, Fe and S elements are uniformly distributed.

The XRD patterns of the CuFeS<sub>2</sub> powders are shown in Fig. 1g with good crystallization. All diffraction peaks in the synthetic sample can be indexed to the CuFeS<sub>2</sub> standard card (PDF card No.065-1573) except the two little peaks (31.9°, 33.1°) which are ascribed to CuS (PDF card No.065-3931).

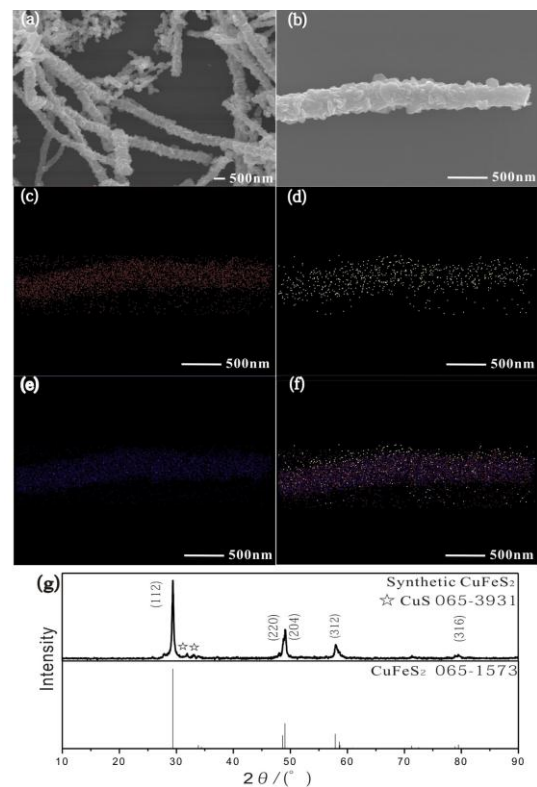
Fig. 2a-2b shows the cycling performance of the Li/CuFeS<sub>2</sub> cells at the current rate of 0.2 C. In Fig. 3a, the dramatic capacity decay is observed and the capacity retention is 10.1% after 50 cycles (as shown in Table S2). However, although a slight decay in capacity occurs upon the cells cycling in the DOL/DME electrolyte, no sign of severe capacity failure is found. The capacity retention is 63.0% after 50 cycles.

Fig. 2c-2d shows the cycling stability and corresponding charge-discharge curves of the Li/CuFeS<sub>2</sub> cell from 0.2 C to 10 C rate (1C = 587mA/g). As seen, the discharge capacity of the first cycle at 0.2 C is 585.3 mAh/g. With cycling, the discharge capacities at the current rates of 0.5 C, 1C, 2C, 5C and 10 C are about 415, 380, 320, 260 and 190 mAh/g, respectively, suggesting the rate performance is good.

In summary, the CuFeS<sub>2</sub> spike-like nanorods were successfully prepared by a simple hydrothermal method and were firstly used as an anode material in LIBs. In traditional carbonate electrolytes (EC/DEC/DMC), the capacity of the spike-like nanorod CuFeS<sub>2</sub> electrode fades quickly, but shows a much better electrochemical

performance in the ether-based electrolytes (DOL/DME). The capacity retention cycling in EC/DEC/DMC at 0.2 C is 10.1% after 50 cycles, while the other is 63.0% at the same condition. And the discharge specific capacity still remains about 190 mAh/g at 10 C. Thus, we believe that such a facile hydrothermal method could be applied in a wide range of fields and the binary metal sulfide CuFeS<sub>2</sub> could be promising anode materials for high-rate lithium batteries.

**Acknowledgment:** We gratefully acknowledge the financial support of National Natural Science Foundation of China (Grant Nos. 21273185 and 21321062).



**Fig. 1** SEM images of the synthetic CuFeS<sub>2</sub> (a, b) and elemental mapping of Cu(c), Fe(d), S(e) & superposed one (f), (g) XRD pattern of synthetic CuFeS<sub>2</sub> compared with the corresponding standard material card.

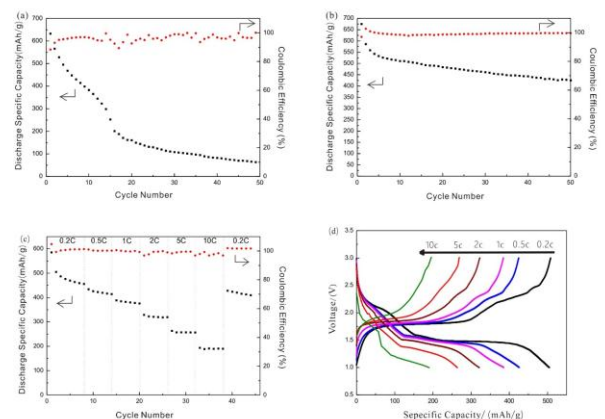


**Fig. 2** The cycling performance of Li/CuFeS<sub>2</sub> cells performed in: a) EC/DEC/DMC. b) DOL/DME current rate of 0.2 C in the voltage range of 1-3 V and (c) rate capabilities and (d) voltage profiles of CuFeS<sub>2</sub> at various current rates from 0.2 C to 10 C.

## References

- [1] T. Teranishi, K. Sato, K.i. Kondo, Optical Properties of a Magnetic Semiconductor: Chalcopyrite CuFeS<sub>2</sub>: I. Absorption Spectra of CuFeS<sub>2</sub> and Fe-Doped CuAlS<sub>2</sub> and CuGaS<sub>2</sub>, Journal of the Physical Society of Japan, 36 (1974) 1618-1624.

## Optical silicones with quantum dots for sustainable lighting

Huanhuan Feng & Joris Sprakel

Responsive Colloidal Systems Group, Laboratory of Physical Chemistry and Colloid Science, Wageningen University

New LED lighting solutions require integration of optical elements for spectral conversion, light diffusion and focussing. Under the harsh conditions to which these elements are exposed in close proximity to the LED module, most polymer materials exhibit rapid degradation, mechanical failure and discoloration; thereby limiting the life time of the LED-based lighting product. Silicones prove to be promising candidates being able to withstand the high light fluxes and temperature for hundreds of thousands of hours.

Their efficient application as optical elements requires incorporation of light emitting elements, for spectral conversion, and of high refractive index particles for refractive index tuning. In both cases however, particles, up to large volume fractions, need to be homogeneously dispersed throughout the silicone matrix, to maintain optical transparency.

In this presentation we highlight our recent work in exploring new pathways to create these optical silicones, using a combination of theoretical calculations and experiments. We theoretically predict the stability and instability of surface functionalised nanoparticles, using self-consistent field theory, to establish design rules for creating homogeneous composites of quantum dots and silicones. We then use these design rules to synthesize, coat and surface functionalise quantum dots using simple, yet effective, novel methods and show how this can be effectively used to achieve the desired materials.



Figure1. The QDs dispersed in silicone with different polymer chain length

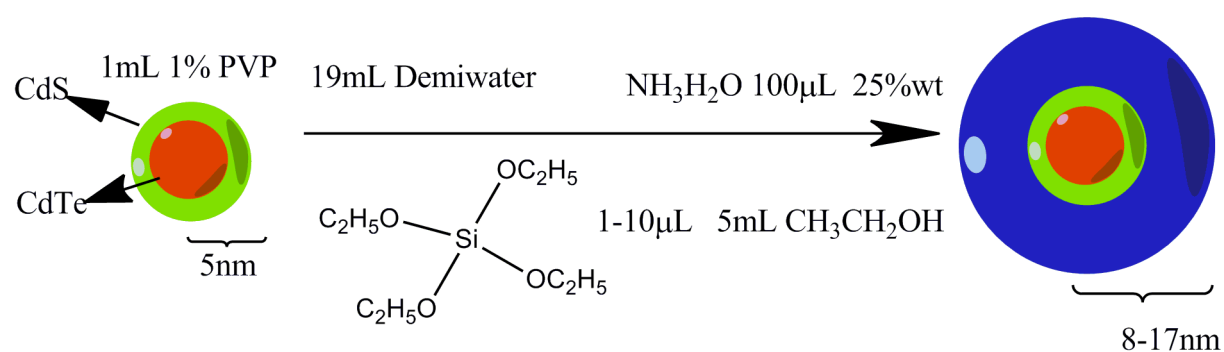


Figure2. The protocol of aqueous QDs' silica coating

## Adsorption of Bisphenol A from Aqueous Solution onto Cationic Modified Zeolite

Hongyu Wang,<sup>1</sup> Hangli Zhang,<sup>1</sup> Jia-Qian Jiang<sup>2,†</sup>, Xiaoyan Ma<sup>1</sup>

<sup>1</sup>School of Civil Engineering and Architecture, Zhejiang University of Technology, Hangzhou, 310014, China

<sup>2</sup>School of Engineering and Built Environment, Glasgow Caledonian University, Glasgow, Scotland

†Corresponding authors Email: [jiaqian.jiang@gcu.ac.uk](mailto:jiaqian.jiang@gcu.ac.uk)

This paper concerns with the adsorption of bisphenol-A (BPA) by modified zeolites which were prepared using an orthogonal experimental design. The preparation process was optimized by the defined conditions, i.e., that 10% of cetyltrimethyl ammonium bromide was used as the optimal modifier and processing time and temperature were 36 h and 25<sup>o</sup>C, respectively. The adsorption equilibrium of BPA onto the modified zeolite fits the Freundlich isotherm with a high correlation coefficient 0.996 and was defined by a second-order rate constant ( $K_v$ ) of 1.07 g/mg h. Furthermore, the effects of solution chemical properties on the adsorption of BPA by modified zeolites were examined. The result reveals that the best adsorption temperature was 25<sup>o</sup>C, and the optimal pH ranged from 5.0 to 10.0. In addition, the adsorption capacity of BPA increased with concentrations of HCO<sub>3</sub><sup>-</sup> and decreased with increasing in concentrations of NO<sub>3</sub><sup>-</sup>, OH<sup>-</sup>, and Al<sup>3+</sup> in the test solution.

**Characterization of zeolite.** Chemical compositions and BET surface areas of natural zeolite (PZ) and CTAB modified zeolite (CTABZ) are summarized in Table 1. The inorganic elemental composition of PZ and CTABZ are listed in Table 2. The content of carbon and nitrogen containing groups on the surfaces of CTABZ was higher than that of PZ, reflecting that the modifier, CTAB, which consists of C, H, N and Br, was attached onto the surface of zeolite. Therefore, after modifying, the content of Br element was increase from 0 to 0.94 % (Table 2), and the surface area was reduced from 16.39 to 9.78 m<sup>2</sup> g<sup>-1</sup> as shown in Table 1, since CTAB occupies a part of zeolite's surface

**Table 1.** Surface organic elemental composition and surface areas of PZ and CTABZ

Adsorbents	Surface elemental composition			Surface area (m <sup>2</sup> g <sup>-1</sup> )
	C (%)	O (%)	N (%)	
PZ	10.49	89.51	0.00	16.39
CTABZ	46.06	51.67	2.27	9.78

**Table 2.** Inorganic elemental composition of PZ and CTABZ

Adsorbents	Elemental composition (%)							
	Si	Al	Na	Ca	K	Br	Fe	Mg
PZ	35.54	7.58	2.46	1.77	1.61	0	0.58	0.41
CTABZ	35.23	7.75	2.00	1.72	1.58	0.94	0.58	0.49

**Adsorption kinetics and isotherms.** The process of adsorption of BPA onto CTABZ could be divided into three stages. As shown in Figure 1, the first stage was identified by a fast intake of BPA in the initial 30 minutes of the reaction (Table 3), which was followed by a second stage of a sluggish approach to equilibrium lasting approximately 210 min, and a final stage characterized by a slight inversion approximately after 240 minutes of contact. Sorption data were fitted well to the pseudo second-order kinetic model described. A suitable fitness between calculated and experimental data indicated that the sorption of BPA by CTABZ follows the pseudo-second-order reaction kinetics ( $R^2 = 0.996$ ) with a rate constant of ( $K_v$ ) of  $1.07 \text{ g mg}^{-1} \text{ h}^{-1}$  (Table 4). The pseudo second-order kinetic model can thus be described by Equation 3, where  $q_t$  is the amount adsorbed at given time,

$$dq_t = 1.07(22.46 - q_t)^2 \quad [3]$$

Equilibrium adsorptions of BPA by CTABZ were analyzed by the Langmuir and Freundlich models (Table 4). The Langmuir isotherm showed a deviation from linearity ( $R^2 = 0.9626$ ). The Freundlich isotherm gave a good fit ( $R^2 = 0.9956$ ). The Freundlich isotherm can thus be described by Equation 4 where  $C_{eq}$  is the concentration of adsorbate at equilibrium in the liquid phase,  $Q_m$  is the corresponding amount of adsorbate in the solid phase, and two coefficients,  $K_f$  and  $n$ , have been established.

$$Q_m = 16.47C_{eq}^{0.19} \quad [4]$$

**Table 3.** Kinetics of adsorption between 0-30 minutes

t(min)	1.00	3.00	5.00	10.00	20.00	30.00
q(mg g <sup>-1</sup> )	17.81	19.13	19.62	19.88	20.73	21.01

**Table 4.** Adsorption models parameters of BPA by CTABZ

Pseudo-Second-order kinetic			Langmuir isotherm			Freundlich isotherm		
$K_v$ (g mg <sup>-1</sup> h <sup>-1</sup> )	$q_e$	$R^2$	$Q_m$ (mg g <sup>-1</sup> )	$b$ (L g <sup>-1</sup> )	$R^2$	$K_f$	$1/n$	$R^2$
1.07	22.46	0.999	37.85	0.65	0.963	16.47	0.19	0.996

**The effect of solution chemical properties on BPA adsorption by modified zeolite.** The effects of solution chemical properties on the adsorption of BPA onto CTABZ were examined and discussed below. Batch adsorption experiments were carried 4h at 150 rpm and given temperatures (e.g., 25 °C).

**Initial BPA concentration.** The sorption of BPA onto CTABZ was investigated for the initial concentrations from 50 to 200 mg L<sup>-1</sup> at various temperatures as shown in Figure 2. The adsorption capacity of BPA increased from 4.88 to 40.72 mg L<sup>-1</sup> with increasing the initial concentration from 50 to 200 mg L<sup>-1</sup>. Higher BPA initial concentration provided the power to overcome the resistance to mass transfer from water phase to solid surface, and also had effects on the efficiency and ability of sorption. Generally, increase in the initial concentrations would elevate the adsorption capacity until a critical initial concentration reaches when adsorbate is quickly saturated in the surface and inter layer of the zeolite.

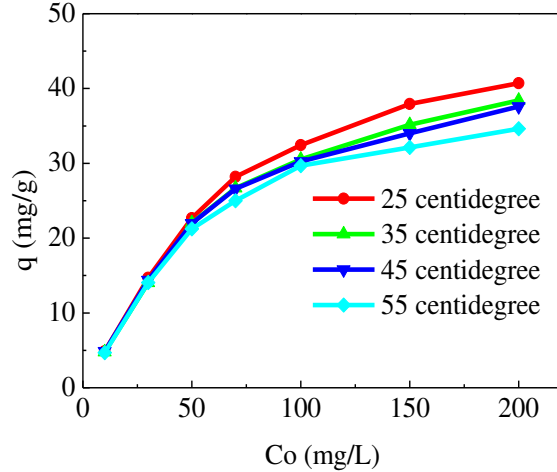
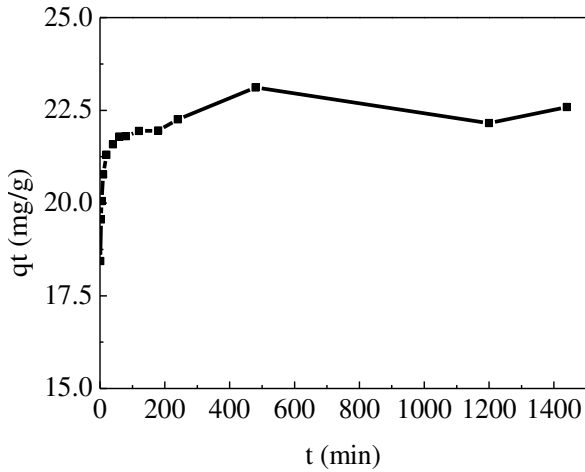
**Temperature.** The adsorption of BPA onto CTABZ was investigated at temperature of 25, 35, 45 and 55 °C. The results of sorption isotherms were illustrated in Figure 2. The results showed that adsorption capacity of BPA at 25 °C was the largest, and increasing in temperature slightly decreased the adsorption capacity. This can be attributed to the exothermic sorption mechanism; that the adsorption capacity of BPA by surfactant-modified zeolite and activated carbon was diminished with increasing in solution temperatures. Thus, further studies were conducted at temperature of 25 °C.

**Solution pH.** The effect of solution pH on the adsorption of BPA onto CTABZ was investigated at the pH range from 2.0 to 11.0. Results shown in Figure 3 indicated that adsorption efficiency of BPA onto the CTABZ was good, and the adsorption capacity increased with increasing in solution pH ranging from 3-10. However, when solution pH was greater than 10.0, the adsorption capacity decreased. The phenomena can be interpreted based on the concept of first and second deprotonation equilibriums of BPA, which were occurred at pH 9.6 and pH 11.3, respectively. When solution pH was less than 10, the BPA was dissociated to form H<sup>+</sup> and BPA anions which will be easily bonded by the cationic modified CTABZ via the charge neutralisation and thus the adsorption efficiency of BPA on CTABZ increased in raising solution pH. While pH was greater than 10, major compound of BPA was to be anions and this increased the solubility of BPA and thus leading to the decrease in adsorption efficiency of BPA by CTABZ. It is observed that the relative low adsorption capacity of BPA was observed when solution pH was less than 5 (Figure 3). Lower pH solutions (higher H<sup>+</sup> concentration) intend to exchange cationic ions of the modifiers combined with CTABZ and this changes CTABZ to be less hydrophobic on its surface and leads to the decrease in the reactions between BPA and CTABZ and thus adsorption efficiency. pH 10 was determined to be the optimal pH to adsorb BPA by the CTABZ.

**The presence of anions in the test solution.** The influence of representative inorganic anions on the BPA sorption by CTABZ was investigated and the results are shown in Figure 4. It can be seen that the adsorption capacity did not change in the presence of CO<sub>3</sub><sup>2-</sup>, SO<sub>4</sub><sup>2-</sup>, Cl<sup>-</sup>. However, it increased from 21.95 to 23.72 mg L<sup>-1</sup> with the presence of HCO<sub>3</sub><sup>-</sup>, and decreased from 21.95 to 17.78 mg L<sup>-1</sup> and 21.95 to 11.07 mg L<sup>-1</sup> respectively, in the presence of NO<sub>3</sub><sup>-</sup> and OH<sup>-</sup> with their concentrations up to 500 mg L<sup>-1</sup>.

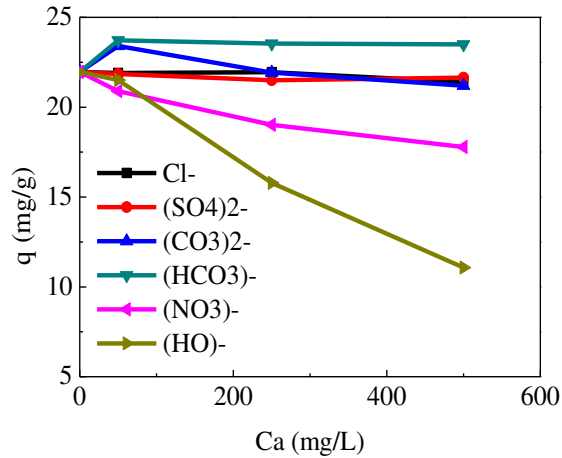
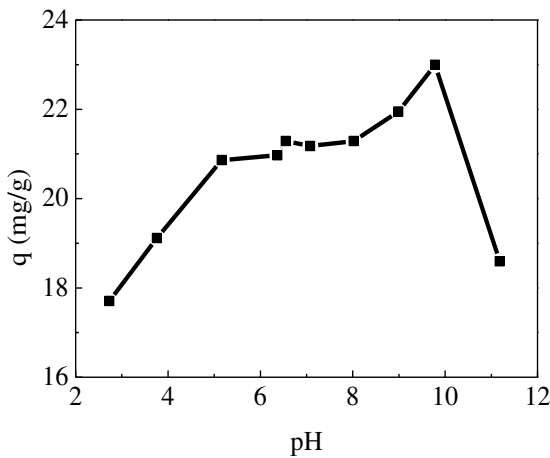
**The presence of cation in solution.** The influence of several inorganic cations in solution on BPA sorption by CTABZ was studied and the result is shown in Figure 5. Obviously, the presence of the monovalent (K<sup>+</sup>, Na<sup>+</sup>) and bivalent cations (Ca<sup>2+</sup>, Mg<sup>2+</sup>) made no difference to the adsorption capacity. However, it decreased from 21.95 to 17.72 mg L<sup>-1</sup> with increasing in the concentration of Al<sup>3+</sup> up to 500 mg L<sup>-1</sup>. Possible reasons of this would be that solution pH decreased to below 10 resulting from hydrolyzing reactions of Al<sup>3+</sup> in aqueous solutions and then adsorption capacity decreases as demonstrated in Figure 3.





Left: FIG. 1. Kinetics of adsorption. 50 mL of 50 mg L<sup>-1</sup> BPA solution, 100 mg CTABZ, T=25 °C, 150 rpm. q<sub>t</sub>, adsorption capacity, t, adsorption equilibrium time (min).

Right: FIG. 2. The effect of BPA initial concentration and temperature on the adsorption capacity. 50 mL of 50 mg L<sup>-1</sup> BPA solution, 100 mg CTABZ, 150 rpm. q, adsorption capacity, C<sub>0</sub>: initial concentration.



Left: FIG. 3. The effect of pH on the adsorption capacity. 50 mL of 50 mg L<sup>-1</sup> BPA solution, 100 mg CTABZ, T=25 °C, 150 rpm. q<sub>t</sub>, adsorption capacity.

Right: FIG. 4. The effect of anions on the adsorption capacity. 50 mL of 50 mg L<sup>-1</sup> BPA solution, 100 mg CTABZ, T=25 °C, 150 rpm. q<sub>t</sub>, adsorption capacity, C<sub>a</sub>, the concentration of anions.

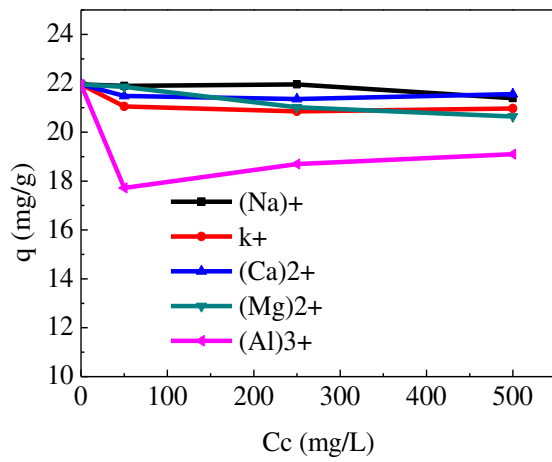


**FIG. 5.** The effect of cations on the adsorption capacity. 50 mL of 50 mg L<sup>-1</sup> BPA solution, 100 mg CTABZ, T=25 °C, 150 rpm.  $q_t$ , adsorption capacity,  $C_c$ , the concentration of cations.

## A model for high cycle fatigue damage based on a condensed approach for tetragonal ferroelectrics

S. Lange<sup>1</sup>, A. Ricoeur<sup>1</sup>

<sup>1</sup>Institute of Mechanics, Chair of Engineering Mechanics / Continuum Mechanics,  
University of Kassel, Moenchebergstr. 7, 34109 Kassel, Germany

[stephan.lange@uni-kassel.de](mailto:stephan.lange@uni-kassel.de)

Ferroelectric materials such as barium titanate are widely used in smart structures and devices as actuators, sensors, etc. To investigate the material behavior, a condensed model for ferroelectric solids with tetragonal unit cells is presented. The approach is microelectromechanically and physically motivated, considering discrete switching processes on the level of unit cells and quasi-continuous evolution of inelastic fields on the domain wall level. To calculate multiple grain interactions, an averaging technique is applied [1,2]. Hysteresis loops are simulated for a pure electric and an electromechanical loading to demonstrate the influence of a compression preload on the poling and stress-strain behavior. Further, residual stresses are calculated as a result of switching processes and interactions between crystallites. To study the high cycle fatigue damage and to predict life time of ferroelectric devices, an accumulation model is proposed based on the growth of microcracks [2].

**Keywords:** *High cycle fatigue damage, life time prediction, grain interaction, residual stress*

[1] LANGE, S. & RICOEUR, A. 2014. A condensed microelectromechanical approach for modeling tetragonal ferroelectrics. International Journal of Solids and Structures, accepted for publication

[2] LANGE, S. & RICOEUR, A. 2014. A condensed microelectromechanical constitutive and damage model for tetragonal ferroelectrics. Proceedings in Applied Mathematics and Mechanics, in press.

## Carbon Nanomaterials via Ionothermal Hot-injection Synthesis

Yuanqin Chang, Tim-Patrick Fellingner, Markus Antonietti

Max-Planck-Institut für Kolloid- und Grenzflächenforschung

Am Mühlenberg 1, 14476 Potsdam, Deutschland

E-Mail: [Yuanqin.Chang@mpikg.mpg.de](mailto:Yuanqin.Chang@mpikg.mpg.de)

Carbon nanomaterials, due to their unique properties, are one of the most important materials in applications including adsorption, separation, energy conversion and storage. Typically carbon nanomaterials are synthesized in bulk processes using precursors with low volatility. Bulk processes and solid state transformations however always have the disadvantages of restricted mass transport and missing reorganizational dynamics so that mainly disordered but also heterogeneous products are obtained. A liquid solution route for carbon materials would indeed solve many of the above mentioned problems, and nanomaterials other than carbons, such as metal nanoparticles, can be synthesized using nucleation and growth mechanisms. However, the key-drawback of solution route is that the final carbon structures undergo significant shrinkage due to the mass loss and high surface energy.

Recently we reported on a novel “wet-chemical” synthesis route using inorganic salt melts as solvents for the ionothermal synthesis of high surface area and aerogel-like nanocarbons, showing superior electrocatalytic activity. The inorganic salt melts act as solvents and porogens, where the carbonaceous material mechanically stabilizes against shrinkage. The precursors need to be thermally stable, miscible with the salt melt and carbonizable. So far this could only be realized using task-specific ionic liquids or acrodam.

In order to synthesize carbon nanomaterials even more economically and efficiently, we introduce herein a salt melt-based carbonization via a combination of hot injection technique with ionothermal chemistry, which dramatically expands the number of possible carbon precursors down to most simple organic solvents. 10 organic solvents were successfully converted into carbonaceous nanomaterials in sometimes surprisingly high yields. Heteroatom containing solvents lead to respectively doped carbons with doping level of up to 14 wt.% N and 13 wt.% S. Surface areas and pore volumes of solvent carbons are as high as  $1666 \text{ m}^2 \text{ g}^{-1}$  and  $2.80 \text{ cm}^3 \text{ g}^{-1}$ .

More importantly, the solvent nanocarbons are obtained in three different interesting morphologies including aerogels, hyper-branches and nanosheets. (Figure 1)

Converting commonly used organic solvents into carbons directly, this approach opens a new synthetic pathway of advanced functional carbon materials with unique nanoscopic morphologies, suggesting great importance in the field of nanomaterial synthesis and potential applications for energy conversion and storage. A comparison of different carbon precursors will be presented and the role of chemical properties in defining the final carbon morphology will be discussed. Some preliminary results in electrochemical testing will be presented as well.

**Keywords:** *ionothermal, hot-injection, carbon nanomaterials, morphology control*

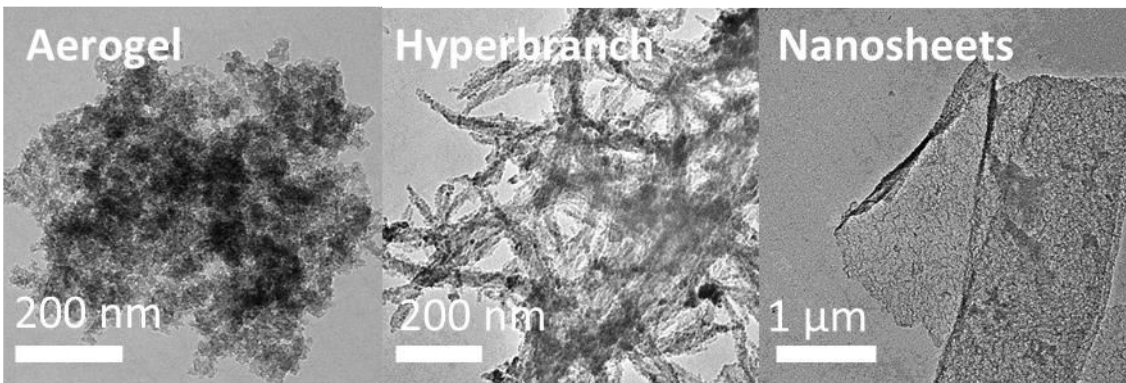


**Figure 1.** TEM images of carbons with three different morphologies.

[1] DAI, L., CHANG, D. W., BAEK, J.-B. & LU, W. 2012. Carbon Nanomaterials for Advanced Energy Conversion and Storage. *Small*, 8, 1130-1166.

[2] ELUMEEVA, K., FECHLER, N., FELLINGER, T. & ANTONIETTI, M. 2014. Metal-free ionic liquid-derived electrocatalyst for high-performance oxygen reduction in acidic and alkaline electrolytes. *Materials Horizons*, 1, 588-594.

[3] FECHLER, N., FELLINGER, T. P. & ANTONIETTI, M. 2013. "Salt Templating": A Simple and Sustainable Pathway toward Highly Porous Functional Carbons from Ionic Liquids. *Advanced Materials*, 25, 75-79.

## A pathway to optimize the properties of magnetocaloric

### $\text{Mn}_x\text{Fe}_{2-x}(\text{P}_{1-y}\text{Ge}_y)$ for magnetic refrigeration

D. M. Liu<sup>a</sup>, Z.L.Zhang<sup>a</sup>, Q. Z. Huang<sup>c</sup>, M. Yue<sup>b</sup>, J. X. Zhang<sup>b</sup>, and J. W. Lynn<sup>c</sup>

<sup>a</sup> Institute of Microstructure and Property of Advanced Materials, Beijing University of Technology, 100 Pingleyuan, Chaoyang District, Beijing 100124, China

<sup>b</sup> College of Materials Science and Engineering, Beijing University of Technology, 100 Pingleyuan, Chaoyang District, Beijing 100124, China

<sup>c</sup> NIST Center for Neutron Research, National Institute of Standards and Technology, Gaithersburg, Maryland 20899 (USA)

Magnetocaloric materials can be useful in magnetic refrigeration applications, but to be practical the magneto-refrigerant needs to have a very large magnetocaloric effect (MCE) near room temperature for modest applied fields (<2 Tesla) with small hysteresis and magnetostriction, and should have a complete magnetic transition, be inexpensive, and environmentally friendly. One system that may fulfill these requirements is  $\text{Mn}_x\text{Fe}_{2-x}(\text{P}_{1-y}\text{Ge}_y)$ , where a combined first-order structural and magnetic transition occurs between the high temperature paramagnetic and low temperature ferromagnetic phase. We have used neutron diffraction, differential scanning calorimetry, and magnetization measurements to study the effects of Mn and Ge location in the structure on the ordered magnetic moment, magnetocaloric effect, and hysteresis for a series of compositions of the system near optimal doping. The diffraction results indicate that the Mn ions located on the 3f site enhance the desirable properties, while those located on the 3g sites are detrimental. The phase fraction that transforms, hysteresis of the transition, and entropy change can be controlled by both the compositional homogeneity and the particle size, and an annealing procedure has been developed that substantially improves the performance of all three properties of the material. On the basis of these results we have identified a pathway to optimize the MCE properties of this system for magnetic refrigeration applications.

**Poly(trimethylene terephthalate-*block*-tetramethylene oxide) copolymer nanocomposites reinforced with carbon nanostructures**

Anna M. Szymczyk<sup>1</sup>, Sandra Paszkiewicz<sup>2</sup>, Zbigniew Roslaniec<sup>2</sup>

<sup>1</sup>Institute of Physics, <sup>2</sup>Institute of Material Science and Engineering, West Pomeranian University of Technology, Piastow Av. 19, PL-70310 Szczecin, Poland

The influence of the addition of single walled-carbon nanotubes (SWCNT), graphene nanosheets (GNS), and mixtures of both, on the mechanical, thermal and electrical properties of poly(trimethylene terephthalate-*block*-tetramethylene oxide) (PTT-*block*-PTMO) copolymer nanocomposites was studied. The obtained polymer nanocomposites with mentioned carbon nanostructures were prepared by *in situ* polymerization method. It was established that the addition of single-wall carbon nanotubes and graphene nanosheets with a concentration of not higher than 0.6 wt % to the polyester thermoplastic elastomer (PTT-*block*-PTMO) allows obtaining lightweight, electrically conductive composite materials with improved thermal stability and improved mechanical properties. The positive hybrid (SWCNT+GNS) effect has been observed, for both, improvement in mechanical properties and electrical conductivity.

## Superconducting properties of bulk MgB<sub>2</sub> cryo-magnet shaping by Spark Plasma Sintering

J. G. Noudem<sup>1,2\*</sup>, L. Dupont<sup>1</sup>, M. Aburas<sup>1</sup>, L. Gozzelino<sup>3</sup>, and P. Bernstein<sup>1</sup>

<sup>1</sup>CRISMAT-ENSICAEN (CNRS-UMR6508) and Université de Caen, Caen, France

<sup>2</sup>LUSAC, Université de Caen, Caen, France

<sup>3</sup>Department of Applied Science and Technology, Politecnico di Torino, 10129, Torino, Italy

\*Email : [Jacques.noudem@ensicaen.fr](mailto:Jacques.noudem@ensicaen.fr) ; fax : +33 231 451 366

### Abstract:

The MgB<sub>2</sub> bulk superconductors were shaped by non-conventional “Spark Plasma Sintering-SPS” process. The obtained material is denser (98 % relative density of the theoretical value) than the samples obtained by Hot-Pressing (HP) and/or Conventional Sintering-CS. Superconducting properties were measured and the influence of the processing conditions on the properties was evidenced. SPS favours shorter elaboration times and produces samples with superconducting characteristics enhanced due to better grains connection and densification of the bulk material.

Trapped field higher than 1.4 T has been measured at 20 K for a single disc of bulk MgB<sub>2</sub> with 20 mm diameter and 10 mm thick at a distance of 1.5 mm above the disk surface. On the other hand, the feasibility to use the MgB<sub>2</sub> in Maglev vehicle has been investigated. Here we present preliminary results that show that it presents interesting characteristics. The samples were located in a cryostat and cooled down below T<sub>c</sub> at 30 mm from a 45 mm NdFeB magnet. Their levitation force was investigated between 17 to 35 K. While the magnetic field was equal to 0.22T at the minimum magnet-superconductor separation of 13mm, the levitation force was in the range of 13 N between 17 K and 32 K at this distance that corresponds to a magnetic pressure near 20000 Pa. The results show that, the bulk MgB<sub>2</sub> superconductors could be a viable variant for magnetic levitation applications and/or as cryo-magnets.



## Effect of TSI-POSS on thermal property of PU hybrid composites from molecular simulation combined with experimental results

Rui Pan<sup>1</sup>, Yong Liu<sup>2</sup>, Lingling Wang<sup>1</sup>

<sup>1</sup>Chemistry and Material Science College, Sichuan Normal University, Chengdu City, PRC, 610041.

<sup>2</sup>Key Laboratory of Special Waste Water Treatment, Sichuan Province Higher Education System, Chengdu City, PRC, 610041.

[panrui546@gmail.com](mailto:panrui546@gmail.com)

Combined with experimental results, molecular simulation approach was applied in elucidating the structure-thermal property relationship of PU hybrid composites with various concentration of trisilanolisobutyl polyhedral oligomeric silsesquioxane (TSI-POSS) at molecular level. These hybrid composites models were characterized by mean square displacement, radial distribution function and volume-temperature behavior analysis. According to the experimental and simulation data, the stiff open cage of TSI-POSS linked to the polymer backbones acts as a rigid node with less mobility and leads to the steric hindrance of polymer chain apparently. Furthermore, as TSI-POSS concentration increasing, the distance of neighboring chains is shortened due to the humping cage self-interaction in TSI-POSS fractures and thus, the motion of the whole chain is retarded, which leads to the T<sub>g</sub> increasing and broadens the glass transition region of hybrid composites.

**Keywords:** *Molecular mechanics, molecular dynamics, POSS, polyurethane,*

[1] Rui Pan, Robert Shanks et al. 2014. Trisilanolisobutyl POSS/Polyurethane Hybrid Composites: Preparation, WAXS and Thermal Properties. *Polymer Bulletin*, 71, 2453-2464.

[2] Xueyu Song, Yi Sun et al. 2011. Molecular dynamics simulation of a novel kind of polymer composite incorporated with polyhedral oligomeric silsesquioxane (POSS). *Comput. Mater. Sci.* 50, 3282-3289.

## **The computer analysis and experimental studies of layered composite structural elements in the repair process of railway wagons**

Andrzej Buchacz<sup>1</sup>, Andrzej Baier<sup>1</sup>, Michał Majzner<sup>1</sup>

<sup>1</sup>Silesian University of Technology, Faculty of Mechanical Engineering, Institute of Engineering Processes Automation and Integrated Manufacturing Systems, Konarskiego 18A, 44-100 Gliwice, Poland

*E Mail/ Contact Détails [michal.majzner@polsl.pl](mailto:michal.majzner@polsl.pl)*

The paper presents a methodology for the selection of composite components, in the design of the structure of composite panels. Composite panels are used to repair and modify the internal space of the loading of freight wagons. In order to identify the strength parameters of composite panels, was conducted a series of studies, which were divided into the following steps:

- identification of the forces acting on the sheathing of a freight wagon during normal operation. The simulation of driving the wagon on trackway, include the different loads from the load and changing the parameters of the movement - the maximum speed and the profile of the track.
- simulation and experimental studies, which performed the analysis and synthesis of layered composites structures. For the synthesis modeling method has been applied a methodology of using elementary objects (called Feature or ontologies) For this purpose has been developed a method, which is called (Feature Based Modeling Composite).
- simulation and experimental studies of the methods of connecting the composite panels to existing construction of the load space , which is made from steel, in repaired wagon in most cases corroded. Was conducted research on the, methods of joining composite panels including the tabs, assembled and mounted to the structural elements with use of bonding and screwing.

***Keywords: Composite Panels, Feature based methods, Railway wagons, Laminates, FEM***

Acknowledgements The work was carried out under the project number PBS2/A6/17/2013 realized as a part of the Applied Research Program, funded by the National Research and Development Centre

## Micromechanical Modeling of Piezoelectric-Piezomagnetic Composites using Computational Piezo-Grains (CPGs)

Peter L. Bishay<sup>a,\*</sup> and Satya N. Atluri<sup>b</sup>

<sup>a</sup> The Hal and Inge Marcus School of Engineering, Saint Martin's University, Lacey, WA, USA.

<sup>b</sup> Center for Aerospace Research and Education (CARE), University of California, Irvine, CA, USA.

---

### Abstract:

Accurate micromechanical modeling of particle and fibrous composite samples with large number of defects (inclusions, voids, cracks, etc.) using the regular finite elements is very expensive because of the mesh-refinement used around each defect. In this work we develop new type of finite elements that has two important features: (1) each element can have an arbitrarily polygonal shape to mimic the shape of grains in the microscale, (2) each element may contain a defect (void or inclusion) embedded in its domain. These new elements are named "Computational Piezo-Grains" (CPGs). CPGs can accurately capture the fields around each defect without mesh refinement, since each defect is already embedded in a single element (or grain), thus saving a lot of computational time especially when the number of defects is very large. In this work, the materials of the matrix and inclusions in the composite could be elastic, piezoelectric, or piezomagnetic, thus allowing for variety of composite types and configurations to be modelled. Mathematically, the fields in the matrix and inclusion in each grain are expressed based on Lekhnitskii formulation.

**Keywords:** Finite elements; inclusion; composite; piezoelectric; piezomagnetic; Lekhnitskii; Trefftz; multiferroic;

---

\* Corresponding author. Tel.: +1 (360) 688-2741; fax: +1 (360) 438-4548.

E-mail address: PBishay@stmartin.edu (P. Bishay).

## Electrical Properties of Barium Titanate dispersed Silver Sulphate

S W Anwane

*Department of Physics, Shri Shivaji Science College, Congress Nagar, Nagpur, India 440 012*

### ABSTRACT

Composite materials obtained by dispersing insulating phase in host silver sulphate offer value added properties over the basic material. Silver sulphate, possessing moderate silver ion conducting features, when dispersed with barium titanate insulating particles, the electrical conductivity is found to increase thereby decreasing activation enthalpy of ion migration. In the present work,  $(100-x) \text{Ag}_2\text{SO}_4:(x) \text{BaTiO}_3$  for  $x=0, 10, 20, 30, 40\text{wt}\%$  have been synthesized and characterized using complex impedance spectroscopy followed by Arrhenius Plot. We found that the conductivity has been increased however the ionic transference number remains unchanged. The optimum composition, 30 Wt%  $\text{BaTiO}_3$  dispersed in  $\text{Ag}_2\text{SO}_4$  is the most promising material found out of present study that may be further considered for device applications.

**Keywords:** dispersion, silver sulphate, complex impedance spectroscopy, electrical properties

## Substitution of formaldehyde in phenolic resins with innovative and bio-based vanillin derived compounds

Gabriel FOYER<sup>1</sup>, Ghislain DAVID<sup>1</sup>, Sylvain CAILLOL<sup>1</sup>.

<sup>1</sup>*Institut Charles Gerhardt Montpellier - Equipe Ingénierie et Architectures  
Macromoléculaires, 8 rue de l'Ecole Normale, 34296 Montpellier Cedex 5, FRANCE.*

Gabriel FOYER, [gabriel.foyer@enscm.fr](mailto:gabriel.foyer@enscm.fr), +33(0)467144320.

Phenolic resins are industrially used in a wide range of applications from commodity and construction materials to high-technology aerospace industry. They are mainly produced from the reaction between phenolic compounds and formaldehyde. Nevertheless, formaldehyde is a highly volatile and hazardous compound, classified as a Carcinogenic, Mutagenic and Reprotoxic chemical (CMR). Vanillin is a bio-based and non-toxic aromatic aldehyde compound obtained from the abundant lignin resources. Also, its aromaticity is very interesting for the synthesis of phenolic resins with high thermal stability. However, because of the relatively low reactivity of its aldehyde function toward phenolic compounds, it has never been used to synthesize phenolic resins.

We developed innovative functionalization reactions[1] and designed new bio-based aromatic aldehyde compounds from vanillin. Those innovative compounds present improved reactivity toward phenolic compounds compared to vanillin. Moreover, they have target structures to synthesize highly cross-linked phenolic resins with high aromatic densities. We have obtained phenolic resins from substituted vanillin, thus without the use of any aldehyde compound classified as CMR. The analytical tests of the cured resins confirmed that those bio-based resins exhibit high levels of performance with high thermal stability and high rigidity properties.

**Keywords:** *Phenolic resins, formaldehyde-free, vanillin, bio-based, non-toxic.*

[1] FOYER, G., DAVID, G., CAILLOL, S., patent pending.

## Microwave-Assisted Synthesis of Sr Al<sub>2</sub> O<sub>4</sub>:Eu<sup>2+</sup>, Dy<sup>3+</sup> Phosphor Powder by Citrate-gel Processing Route

M.R. Johary<sup>1</sup>, and M.Rajabi<sup>1\*</sup>

1-Materials & Metallurgy Engineering Department, Engineering and Technology Faculty, Imam Khomeini International University (IKIU), Qazvin, Iran

P.O.Box:288

\*corresponding Author: m.rajabi@eng.ikiu.ac.ir

### Abstract

Citrate -gel processing of SrAl<sub>2</sub>O<sub>4</sub>:Eu<sup>2+</sup>, Dy<sup>3+</sup> has been carried out by varying the pH and the fuel ratio (the molar ratio of H<sub>3</sub>Cit/Al<sup>3+</sup>+Sr<sup>+4</sup>). The best conditions for pure monoclinic SrAl<sub>2</sub>O<sub>4</sub> phase formation are achieved at pH of the precursors solution equal to 7 and the fuel ratio (at 900C<sup>o</sup> for 2h in the furnace ) equal to 3. In addition, calcinations at higher temperatures (T > 900 C<sup>o</sup>) showed that temperature and pH play an important role in formation of pure monoclinic SrAl<sub>2</sub>O<sub>4</sub> phase as the optimum conditions is achieved at pH 7 and by calcinations at 1250 C<sup>o</sup>. Photoluminescence properties such as emission, excitation, decay time were examined. The optimum synthesis time has been determined, as samples synthesized by microwave at shorter time in comparison with conventional processing route.

## **A Study for Eliminating the Pest Oxidation of MoSi<sub>2</sub> in Severe Environments**

Uzunonat, Y.<sup>1</sup>

<sup>1</sup>Anadolu University, Transportation Vocational School, Basin Sehitleri Caddesi No:152  
Eskisehir/Turkey

*yuzunonat@anadolu.edu.tr/ Phone : +90 222 224 13 91*

Pest oxidation phenomena is the major drawback of MoSi<sub>2</sub> for the applications of this material over gas turbine elements. Therefore, addition of Si<sub>3</sub>N<sub>4</sub> does not only eliminate the structural disintegration behavior which can only be observed between relatively low temperatures (673-873K) but also improves the fracture toughness at elevated temperatures. In this study, after giving some significant properties of MoSi<sub>2</sub>, effect of processing conditions to microstructural morphology and oxidation characteristics at gas turbine operating temperatures will be discussed within a composite approach.

***Keywords: Molybdenum Disilicide, Pest Oxidation, Controlled Consolidation Process***

## Magnesium silicide based materials for energy generation and storage

Godlewska, Mars, Pichor, Mitoraj, Zych

AGH University of Science and Technology, Faculty of Materials Science and Ceramics, Al. A.

Mickiewicza 30, 30-059 Krakow, Poland.

*e-mail address:* [godlewsk@agh.edu.pl](mailto:godlewsk@agh.edu.pl), *contact phone:* +48 126172536

Magnesium silicide is continually under investigation as a component of materials for thermoelectric generators, cathode material for Li-ion batteries and component of lightweight composites. In this paper we present an attractive technological route leading to a nanostructured product, which can be further processed to receive porous sinters, dense bodies or lightweight composites. The starting materials in all mentioned technologies are elemental powders, possibly with fine particle sizes. The proposed self-propagating synthesis bears features of combustion. It is completed in a short time and proceeds without melting of the components. Several examples are given to demonstrate flexibility of the proposed approach: manufacturing of doped Mg<sub>2</sub>Si dense bodies from pure commercial silicon and recycled Si/SiC powders, in-situ composites based on aluminosilicate cenospheres (by-product of coal combustion) and doped Mg<sub>2</sub>Si, nanostructured powder of Mg<sub>2</sub>Si suitable for battery applications or spraying. Final products are characterized in terms of phase composition and structure (XRD, SEM/TEM, EDS), selected physical and mechanical properties (density, thermal/electrical conductivity, Seebeck coefficient, hardness). It is indicated that the procedure can be further modified to obtain more complex (*multi*)functional materials.

**Keywords:** *Magnesium silicide, synthesis, processing, thermoelectrics, composites*

The authors acknowledge financial support from the National Science Center in Poland, grant **N N507 406039**, **N N507 609938** and ThermoMag Project co-funded by the European Commission in the 7th Framework Programme (contract NMP4-SL-2011-263207), by the European Space Agency and individual partner organizations.



## Chemical and imaging surface analysis to improve biomolecule immobilization repeatability for on-chip Mach-Zehnder immunosensors

K. Gajos<sup>1</sup>, M. Angelopoulou<sup>2</sup>, P. Petrou<sup>2</sup>, K. Awsiuk<sup>1</sup>, S. Kakabakos<sup>2</sup>, W. Haasnoot<sup>3</sup>, A. Bernasik<sup>4</sup>, J. Rysz<sup>1</sup>, K. Misiakos<sup>5</sup>, I. Raptis<sup>5</sup>, A. Budkowski<sup>1</sup>

<sup>1</sup>M. Smoluchowski Institute of Physics, Jagiellonian University, Łojasiewicza 11, 30-348 Kraków, Poland

<sup>2</sup>Institute of Nuclear & Radiological Sciences & Technology, Energy & Safety NCSR Demokritos, P. Grigoriou & Neapoleos St, Aghia Paraksevi 15310, Athens, Greece

<sup>3</sup>RIKILT Wageningen UR, Akkermaalsbos 2, 6708 WB Wageningen, Netherlands

<sup>4</sup>Academic Centre for Materials and Nanotechnology, AGH University of Science and Technology, Mickiewicza 30, 30-059 Kraków, Poland

<sup>5</sup>Department of Microelectronics, Institute of Nanoscience and Nanotechnology, NCSR Demokritos, P. Grigoriou & Neapoleos St, Aghia Paraksevi 15310, Athens, Greece

*kamil.awsiuk@uj.edu.pl*

Label-free detection of analytes using optical devices based on miniaturized planar waveguides functionalized with biomolecules has increased demands for homogeneous biomolecule immobilization. In this work, time-of-flight secondary ion mass spectrometry (imaging, micro-analysis), X-ray photoelectron spectroscopy (angle-resolved, normal mode) and atomic force microscopy were employed to evaluate effective and homogeneous biofunctionalization of the sensing arm areas of Mach-Zehnder interferometers [1] and correspondent planar Si<sub>3</sub>N<sub>4</sub> surfaces for the detection of bovine κ-casein in goat milk. Surfaces were examined after the sequential steps: modification with (3-aminopropyl)triethoxysilane, spotting of κ-casein solutions, blocking with 1/100 diluted goat milk, and reaction with monoclonal anti-casein antibodies in 1/100 diluted goat milk. Protein distribution after spotting of κ-casein solutions of different concentrations was examined and the concentration provided

homogeneous sensing arm coverage was determined. Multi-molecular coverage of biosensor surfaces was evaluated. Thicker layer, abundant in glycerides, was observed when the  $\kappa$ -casein spotted surfaces were blocked with diluted goat milk, whereas a thinner film, rich in amino acids, was found after the reaction with Mabs solution. Uniformly immobilized  $\kappa$ -casein and specifically bonded Mabs were confirmed on the sensing arms. A multivariate Principal Component Analysis of ToF-SIMS data resolved protein amino acids from milk glycerides, and amino acids characteristic for Mabs from those specific for  $\kappa$ -casein. ToF-SIMS results for spotted planar surfaces formed 3 groups that spanned PCA score plot, with well separated data referring to sensing arms after spotting, blocking and immuno-reaction.

**Keywords:** *biosensor,  $\kappa$ -casein, PCA*

[1] MISIAKOS, K., RAPTIS, I., SALAPATAS, A., MAKARONA, E., BOTSIALAS, A., HOEKMAN, M., STOFFER, R. & JOBST, G. 2014. Broad-band Mach-Zehnder interferometers as high performance refractive index sensors: Theory and monolithic implementation, *Opt. Express*, 22, 8856–8870

## Hybrid Metal-Carbon Nanostructures for Spintronic Applications

Dr. Maria Gimenez Lopez

Royal Society Dorothy Hodgkin Research Fellow, School of Chemistry, University of Nottingham, NG72RD, UK

*Maria.Gimenez-Lopez@nottingham.ac.uk*

Spintronics is an emerging field of electronics aiming at exploiting the property of the spin of the electron in addition to its charge. Information is stored as one of two possible orientations (up and down). In principle, manipulating spin is faster and requires far less energy than pushing charges around and it can take place at smaller scales. Spintronics also offers the possibility to create computer memories that can retain the stored information even when not powered. However, fundamental understanding of the control, manipulation and detection of the spin of the electron appears to be extremely challenging, as scientist from different disciplines have been tackling these problems for several years. Moreover, many practical aspects in this area are hindered because of the lack of suitable materials. The external decoration of carbon nanotubes with magnetic nanocomponents has been proposed for the development of nanoscale spintronic applications. In my talk I will present examples of the encapsulation of magnetic nanoparticles<sup>1</sup> and molecule magnets<sup>2</sup> within the internal cavities of hollow 1D tubular carbon nanostructures such as carbon nanotubes and carbon nanofibers.

**Keywords:** *Carbon nanotubes, magnetic nanoparticles, single-molecule magnets, self-assembly.*

[1] GIMENEZ-LOPEZ, M., LA TORRE, A., FAY, M.W., BROWN, P.D. & KHLOBYSTOV, A.N. 2013. Assembly and Magnetic Bistability of Mn<sub>3</sub>O<sub>4</sub> Nanoparticles Encapsulated in Hollow Carbon Nanofibers, *Angew. Chem. Int. Ed.*, 52, 2051 –2054.

[2] GIMENEZ-LOPEZ, M., MORO, F., LA TORRE, A., GOMEZ-GARCIA, C.J., BROWN, P.D., VAN SLAGEREN, J. & KHLOBYSTOV, A.N. 2011. Encapsulation of single-molecule magnets in carbon nanotubes, *Nature Communications*. 2:407 doi: 10.1038/ncomms1415

# Micromechanical Analysis of Novel Fuzzy Fiber-Reinforced Advanced and Smart Composites

M. C. Ray

*Mechanical Engineering Department, Indian Institute of Technology, Kharagpur-721302, India*

A novel unidirectional continuous fuzzy fiber reinforced composite (**FFRC**) and a novel short fuzzy fiber reinforced composite (**SFFRC**) have been proposed and analyzed. The distinct constructional feature of these composites is that the uniformly spaced straight or sinusoidally wavy carbon nanotubes (**CNTs**) are radially grown on the circumferential surfaces of the carbon fiber reinforcements. Such an advanced fiber augmented with radially grown **CNTs** is called a fuzzy fiber. Micromechanical models have been developed to predict the effective elastic properties of these novel **FFRC** and **SFFRC** with and without the consideration of an interphase between a **CNT** and the polymer matrix. Such an interphase is the continuum representation of the non bonded van der Waals interaction between a **CNT** and the polymer matrix. The micromechanical analyses reveal that the values of the transverse effective elastic constants of the **FFRC** and the **SFFRC** are significantly improved over their values without **CNTs**. Such enhancement is attributed to the transverse stiffening of the polymer matrix surrounding the carbon fiber by the radially grown **CNTs**. The non-bonded van der Waals interaction between a **CNT** and the polymer matrix does not affect the in-plane effective elastic coefficients of the **FFRC** and the **SFFRC** and its effects on the other effective elastic coefficients of the **FFRC** and the **SFFRC** are also not pronounced. Pronounced effects of the waviness of the radially grown **CNTs** on the values of the effective elastic properties of the **FFRC** are observed. If the plane of the radially grown wavy **CNTs** is coplanar with the plane of the carbon fiber such that amplitudes of the **CNTs** are parallel to the length of the carbon fiber then the axial effective elastic properties of the **FFRC** are significantly improved while the transverse effective elastic properties of the **FFRC** are decreased as compared to those with straight **CNTs**. Analytical micromechanics models have also been developed to estimate the effective thermoelastic properties of the continuous **FFRC** containing straight **CNTs**. It is found that the transverse effective thermal expansion coefficients of the **FFRC** are significantly decreased due to the radially grown **CNTs** on the surface of the carbon fiber over their values without **CNTs**. Effect of temperature deviation on the effective thermal expansion coefficients of the **FFRC** is found to be negligible.

Finally, concept of a novel continuous unidirectional piezoelectric fuzzy fiber reinforced composite (**PFFRC**) comprised of single-walled **CNTs** and piezoelectric fibers as reinforcements embedded in a conventional polymer matrix will be presented. Micromechanical analysis has been carried out to estimate the effective piezoelectric and elastic properties of this novel smart composite have been estimated. It is found that the effective in-plane piezoelectric coefficient and elastic coefficients of the **PFFRC** are significantly improved over those of the

existing 1-3 piezoelectric composite without reinforced with carbon nanotubes. The micromechanical analyses reveal that the excellent properties of CNTs can be exploited to develop advanced and smart composites for structural applications and high performance smart structures, respectively.

## Functional properties of AISI 316L stainless steel processed by spark plasma sintering

Kostiantyn Tabalaiev<sup>1\*</sup>, G. Marnier<sup>1</sup>, C. Keller<sup>1</sup>, E. Hug<sup>2</sup>, J. G. Noudem<sup>2</sup>

<sup>1</sup>GPM-ERMECA, INSA Rouen, Avenue de l'Université 76800 Saint-Etienne du Rouvray

<sup>2</sup>CRISMAT-UMR 6508 CNRS, ENSICAEN-UCBN, 6 bd M<sup>al</sup> Juin 14050 Caen Cedex 04

\* [kostiantyn.tabalaiev@insa-rouen.fr](mailto:kostiantyn.tabalaiev@insa-rouen.fr)

**Abstract:** The unconventional Spark Plasma Sintering (SPS) was used to consolidate micrometric and submicrometric austenitic stainless steel 316L powders. Samples of various shapes (figure below) were in-situ produced in order to perform the mechanical properties without additional sample shaping. Process parameters (time, temperature and pressure) were varied over wide ranges and the impact of such variations on processed materials was studied through the investigation of their microstructures, densities, hardness, and corrosion resistance. The results show that, the SPS allows: (i) to control the grain growth and (ii) to obtain the high dense samples. The mechanical characterization shows also the enhancement of hardness (annealed  $145 \pm 4$  HV; micrometric  $209 \pm 3$  HV [1]; submicrometric  $390 \pm 5$  HV) with respect to the conventional of the sintered samples. The correlation between processing conditions, microstructures generated and mechanical strength behavior using Hall-Petch law of the stainless steel are discussed. The corrosion experiments performed in acid medium show the similar behavior than annealed or sintered 316L stainless steel.



**Figure:** Complex shape samples consolidated by Spark Plasma Sintering.

[1] Marnier G., Keller C., Noudem J., Hug E. "Functional properties of a spark plasma sintered ultrafine-grained 316L steel". *Materials and Design* 2014 ; 63 : 633-640

## **TAILORING OPTICAL AND RHEOLOGICAL PROPERTIES OF HOST-GUEST SYSTEMS BASED ON AN EPOXY ACRYLATE**

U. Gleißner<sup>1</sup>, T. Hanemann<sup>1,2</sup>

<sup>1</sup> Laboratory for Materials Processing, IMTEK, University of Freiburg,  
Georges-Köhler-Allee 102, 79110 Freiburg, Germany,

<sup>2</sup> Material and Process Development, Institute for Applied Materials, Karlsruhe Institute  
of Technology, Hermann-von-Helmholtz-Platz 1, 76344 Eggenstein-Leopoldshafen,  
Germany.

*E-Mail: uwe.gleissner@imtek.uni-freiburg.de*

In this paper, we report on an easy and precise method to tune refractive index and viscosity of an epoxy acrylate based host-guest system. Refractive index tuning plays an important role in waveguide development, whereas viscosity adjustment is a critical parameter in replication methods such as hot embossing and inkjet printing. In combination with previous results presented at the Photonics Europe Conference 2014 [1] our latest research established high achievable refractive index differences while retaining the specific viscosity needed for replication. Characterization of the expanded system with respect to viscosity, refractive index, Abbe number, glass transition temperature and optical damping was performed.

In literature, several different approaches have been shown for tuning the refractive index. Carlos et al. reviewed several different inorganic-organic multi-component hybrid materials for optical applications which are partly very complex [2]. Plasma-polymerization of co-polymers is another method which was used to realize thin, scratch-resistant layers with modified refractive indices [3]. These methods result in high costs

for layer thicknesses of more than 1  $\mu\text{m}$  and their thermoset properties which prevent further shaping.

In our research we investigated Syntholux, which was used as matrix polymer and which is a commercially available UV-curable epoxy acrylate. Refractive index and viscosity tuning was achieved using benzyl methacrylate (BMA). Additionally, phenanthrene was used as dopant for further increase of refractive index and as UV-sensitive initiator Diphenyl(2,4,6-trimethylbenzoyl)phosphine oxide was used.

Experimental results showed a direct relation between refractive index and comonomer content. Starting at  $n = 1.55$  for pure Syntholux refractive increased to almost 1.57 for pure BMA (each measured at 589 nm and 20 °C). Further increase of refractive index of approx. 0.01 was achieved due to the addition of phenanthrene. As refractive indices were measured at different wavelengths the respective Abbe numbers for the different compositions were calculated to a corresponding mean of around 37. In contrast, viscosity was seen to sharply decrease with increasing BMA content. At 20 °C the viscosity decreased from 46 Pa·s for pure Syntholux down to 4 mPa·s for pure BMA. Viscosity measurements were taken in a temperature range of 20 to 80 °C.

By combining our experimental inferences with previously established results, it is now possible to tune the refractive index over  $\Delta n = 0.06$  while maintaining viscosity. This is of great importance and has potential applications in several types of replication methods.

**Keywords:** *refractive index, epoxy acrylate, Abbe number, viscosity, waveguide*



- [1] Uwe Gleissner and Thomas Hanemann. "Tailoring the optical and rheological properties of an epoxy acrylate based host-guest system". *Proc. SPIE*, 9130:913016–913016–8, 2014.
- [2] R.A.S. Ferreira, P.S. Andre, and L.D. Carlos. "Organic-inorganic hybrid materials towards passive and active architectures for the next generation of optical networks". *Optical Materials*, 32(11):1397 – 1409, 2010.
- [3] H. Jiang, W. E. Johnson, J. T. Grant, K. Eyink, E. M. Johnson, D. W. Tomlin, and T. J. Bunning. "Plasma polymerized multi-layered photonic films". *Chemistry of Materials*, 15(1):340–347, 2003.

## Synthesis Mesoporous Silica Hollow Sphere for Transparency-Tunable Devices

Hong-Ping Lin<sup>1\*</sup>, Duo-Wen Chen<sup>1</sup>, Jia-Sheng Chang<sup>1</sup>, Shao-Nai Lin<sup>1</sup>, and Kuang-Yao Lo<sup>2,3</sup>

1. Department of Chemistry, National Cheng Kung University, Tainan, Taiwan 701
2. Department of Physics, National Cheng Kung University, Tainan, Taiwan 701
3. Advanced Optoelectronic Technology Center, National Cheng Kung University, Tainan, Taiwan 701

### Abstract:

Complex materials are usually produced by mixing together different distinct components, the interactions between which can give rise to unusual optical and physical properties of the whole system. Dispersion of particles in anisotropic fluids, such as liquid crystals (LC), is an important state of matter, and the behaviors of such materials have attracted much research interest in recent decades.

To synthesize the mesoporous silica hollow spheres, 30.0 g of 0.5 wt.% gelatin aqueous solution was added to 50.0 g of 1.0 wt.% PMMA beads (diameter = 100–500 nm) solution to form a stable colloid solution. After stirring for about 30 min at 40°C, the PMMA-gelatin colloid solution was poured into an acidified silicate solution at pH  $\approx$  4.0. The acidified silicate solution was obtained from simply mixing a sodium silicate solution (0.60 g sodium silicate form Aldrich and 30.0 g water) and a diluted sulfuric acid solution (0.3 g of 6.0 M H<sub>2</sub>SO<sub>4</sub> and 30.0 g water), followed by pH tuning to 4.0 and aging for 4 min. After further stirring for 6 h, the gel solution was transferred to a polypropylene bottle and hydrothermally treated at 100°C for 1-2 d. Filtration, drying and calcination at 500°C produced the mesoporous silica hollow spheres (denoted as MSPHS). The high-resolution TEM images show wormhole-like nanopores distributed on the shell of the MPSHS. The thickness of the shell is about 15~20 nm. Obviously, the wormhole-like nanopores exist among the interconnected silica particulates.

A novel configuration of MSPHS which will isotropize LCs with random fields created by the disordered nanopores in the shell of MPSHS to generate a novel MPSHS-LC phase. Based on an analysis of the differential scanning calorimetry (DSC) results, the MPSHS-LC phase should have multi-domains due to the isotropized LCs around MSPHS. In practice, we used the homogeneous and stable MPSHS-LC phase to assemble a transparency-tunable smart window, without using any of the critical production conditions for polymer matrix formation in PDLC devices.

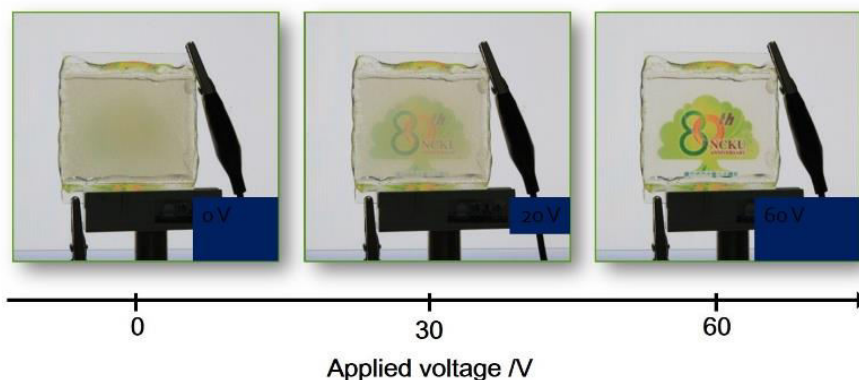


**Fig. 1** Photographs of the HSMSs-LC display with an HSMS/LC weight ratio of 4.5 wt.% at different applied voltages.

## Dielectric behaviour of polyimide films containing TiO<sub>2</sub> nanotubes

Corneliu Hamciuc<sup>1</sup>, Elena Hamciuc<sup>1</sup>, Iuliana Stoica<sup>1</sup>, Marius Olariu<sup>2,\*</sup>, Lidia Okrasa<sup>3</sup>,  
Lubomir Dimitrov<sup>4</sup>, Yuri Kalvachev<sup>4</sup>

<sup>1</sup>”Petru Poni” Institute of Macromolecular Chemistry, 41A Ghica Voda, 700487 Iasi, RO

<sup>2</sup>Technical University of Iasi, 67 D. Mangeron, 700050, Iasi, RO

<sup>3</sup>Lodz University of Technology, Zeromskiego 116, 90-924 Lodz, PL

<sup>4</sup>Institute of Mineralogy and Crystallography, Acad. G. Bonchev 107, 1113 Sofia, BG

\**molariu@tuiasi.ro, Technical University of Iasi, 67 D. Mangeron 67, 700050, Iasi, RO*

To date, TiO<sub>2</sub> nanotubes (TNTs) have not been extensively studied in spite of their good chemical, physical and electrical properties. Within the herein study polyimide composite dielectrics containing TNTs of 10-12nm diameter and several hundreds of nanometers in length were prepared and characterized. TNTs content influence upon composite's properties was investigated. The good compatibility between the filler and the polyimide matrix is demonstrated via AFM and SEM. Moreover, the composite films exhibited flexibility, toughness as well as high thermal stability. The dielectric properties, dielectric constant,  $\epsilon$ , and dissipation/loss factor,  $\tan \delta$ , were investigated via broadband dielectric spectroscopy. Dielectric behavior was studied while varying frequency between 10<sup>-2</sup>Hz and 10<sup>7</sup>Hz and temperature from -100°C up to 300°C. At moderate temperatures a secondary relaxation  $\beta$  was observed while introduction of TNTs decreased the activation energy and facilitated the appearance of an additional  $\beta_1$  process. At higher temperature an  $\alpha$  relaxation was visible. The increase of TNTs content raised the values of dielectric constant and dissipation factor while the maximum of  $\sigma$  relaxation peak shifted to higher temperatures.

**Keywords:** *TiO<sub>2</sub>, TNTs based composites, dielectric behavior*

**Acknowledgement:** The herein study was realized within Partnership in S&T priority domains, financially supported by MEN-UEFISCDI through contract no. 43/2014.

## Anisotropic Ordering in Polymeric Scaffolds *via* Magnetically Responsive Graphene Oxide/Iron Oxide Hybrid Nanomaterial

Louis Cheung<sup>1</sup>, Xiaowu (Shirley) Tang<sup>1</sup>

<sup>1</sup>Department of Chemistry & Waterloo Institute for Nanotechnology, University of Waterloo,  
200 University Avenue West, Waterloo, Ontario N2L 3G1, Canada.

*Email (presenting author): l6cheung@uwaterloo.ca*

*Email (corresponding author): tangxw@uwaterloo.ca*

Tissue engineering involves the rational design of artificial substitutes for damaged tissues and organs. The ultimate goal is to reproduce the 3D anisotropic and hierarchical structures of native tissues, such as cardiac muscle and bone, in artificial constructs, which remains tantalizingly out of reach. One promising strategy is to create cell-laden hierarchical scaffolds, with cells encapsulated inside natural and synthetic polymer matrices with ordered microstructures, to template/guide anisotropic cell growth and organization. Introducing “order” to otherwise homogeneous scaffolds has become a new focus of tissue engineering. Herein, we present an approach to incorporate magnetically responsive nanoparticles into hydrogels and introduce anisotropic ordering in the hydrogel scaffolds via magnetic fields.

A hybrid nanocomposite material consisting of graphene oxide decorated with iron oxide nanoparticles (GO-Fe<sub>3</sub>O<sub>4</sub>) has been synthesized through a high-temperature reduction method. Subsequent characterization revealed graphene oxide (GO) flakes with highly loaded, homogeneously dispersed, uniformly sized magnetite nanoparticles owing to the innately high surface area and density of hydrophilic functional groups of GO. In addition, the material was shown to be superparamagnetic at room temperature with an appreciable saturation magnetization. This nanocomposite can be readily dispersed into aqueous polymer precursor solutions, allowing for anisotropic orientation of the GO-Fe<sub>3</sub>O<sub>4</sub> as directed by magnetic field-induced ordering followed by the *in situ* crosslinking of polymer chains into a hydrogel network. The alignment of the GO-Fe<sub>3</sub>O<sub>4</sub> was retained upon removal of the magnetic field. It is anticipated that this novel hybrid nanomaterial will be a biocompatible tissue scaffold suitable for the encapsulation of cells and their improved organization in a 3D environment. Also, by virtue of the presence of the highly ordered microstructures within the polymeric matrix, it is expected that the material will exhibit anisotropic mechanical reinforcement, in contrast with

past work demonstrating enhanced isotropic mechanical properties as a result of the homogeneous distribution of nanoparticles.

The present work shows the versatility and feasibility of utilizing relatively low magnetic fields to control the microstructure of hydrogel matrices to more accurately emulate the physiological environment. The concepts elucidated in this work show promise in the field of tissue engineering for the creation of complex 3D tissue constructs.

***Keywords: Graphene oxide, magnetic nanoparticles, anisotropic ordering, hybrid nanocomposites, tissue constructs***

## Self-assembling of non-ionic surfactants within the internal structure of layered materials

Régis Guégan<sup>1</sup>, Sylvian Cadars<sup>2</sup>, Makoto Ogawa<sup>3</sup>

<sup>1</sup>ISTO, 1A Rue de la Férellerie, 45071 Orléans cedex 2, France

<sup>2</sup>CEMHTI, 1D Avenue de la Recherche Scientifique, 45071 Orléans cedex 2, France

<sup>3</sup>The University of Waseda, Nishiwaseda 1, Tokyo 169-8050, Japan

*regis.guegan@univ-orleans.fr*

Nonionic surfactants tend to form aggregates on interfaces, which determine various applications in the area of detergency, ore flotation, oil recovery agents, or composite materials. Aggregation mechanisms on solid surfaces differs from bulk solution by involving additional forces with the surface. Among non-ionic surfactants, amphiphilic molecules containing  $n\text{-C}_n\text{H}_{2n+1}(\text{OCH}_2\text{CH}_2)_m\text{OH}$  (abbreviated as  $\text{C}_n\text{E}_m$ ) surfactant have received particular attention due to their ability to self-assemble in various liquid crystalline phases above the critical micelle concentration. The recent intercalation of a  $\text{C}_{10}\text{E}_3$  bilayer in a clay mineral resulting to the condensation of a bulk lamellar phase points out the link between the packing of the surfactant and its bulk phase state [1, 2]. The aim of this work is to study the role of the surfactant state in bulk solution for the adsorption onto layered materials, by focusing on the structure and the dynamics of aggregates made by several  $\text{C}_n\text{E}_m$  surfactants. The results obtained with different complementary techniques highlight the importance of the bulk phase state for the adsorption and the structure of the confined aggregates within the interlayer space of the host layered materials.

**Keywords:** *layered materials, nonionic surfactants, adsorption, aggregation*

[1] GUEGAN, R. 2010. Intercalation of Nonionic Surfactant ( $\text{C}_{10}\text{E}_3$ ) bilayer into a Na-Montmorillonite Clay. *Langmuir*, 26, 19175-19180.

[2] GUEGAN, R. 2013. Self-assembly of a non-ionic surfactant onto a clay mineral for the preparation of hybrid layered materials. *Soft Matter*, 9 10913-10920.

## Enzymatic polyester functionalization

Enrique (Herrero Acero)<sup>1</sup>, Alessandro (Pellis)<sup>1,2</sup>, Sara (Vecchiato)<sup>1</sup>, Andreas (Ortner)<sup>1,2</sup>,  
Caroline (Gamerith)<sup>1</sup>, Georg M. (Guebitz)<sup>1,2</sup>

<sup>1</sup>ACIB GmbH, Konrad-Lorenz Strasse 20, 3430, Tulln (Austria)

<sup>2</sup>Institute for Environmental Biotechnology, University of Natural Resources and Life Sciences, Vienna, Konrad-Lorenz Strasse 20, 3430, Tulln (Austria)

*enrique.herreroacero@acib.at*

Polymers are essential materials in a wide range of applications in modern life due to their excellent properties. Regardless what polymer type, natural or synthetic origin, often the material shows excellent bulk properties, like mechanical or chemical resistance; whereas the surface properties are not optimal for the final application or challenge the material processing. Typical methods used to adjust the surface properties of a certain material involve the use of chemical methods or plasma approaches. For some materials like polyesters the use of harsh chemicals, like concentrated NaOH, leads to material loss which dramatically decreases the mechanical properties and generates irregular surfaces [1]. Enzymatic partial hydrolysis of PLLA membranes followed by chemical grafting of human serum albumin (HSA) lead to a higher polymer biocompatibility [2]. Recently we have developed a new approach to directly enzymatically graft functional molecules to PLA films in a single step, which in addition of shorten the reaction steps reduces the use of aggressive and/or toxic chemicals. The development of new enzyme variants with improved sorption properties [3,4] and consequently higher activity towards the polymers of interest allows extrapolation of these approaches to even more challenging polyesters like polyethylene terephthalate (PET). In this presentation the latest achievements and industrial applications of enzymatically functionalized technical PET materials will be presented

**Keywords:** *Enzymes, polymer functionalization*



- [1] PELLIS, A., HERRERO ACERO, E.; WEBER, H. J.; OBERSRIEBNIG, M.; BREINBAUER, R.; SREBOTNIK, E.; GUEBITZ, G. M. 2014. Enzymatic functionalization of poly(L-lactic acid) films. under review.
- [2] NYANHONGO, G. S., RODRÍGUEZ, R. D., PRASETYO, E. N., CAPARRÓS, C., RIBEIRO, C., SENCADAS, V., LANCEROS-MENDEZ, S., HERRERO ACERO, E. & GUEBITZ, G. M. 2013. Bioactive albumin functionalized polylactic acid membranes for improved biocompatibility. *Reactive and Functional Polymers*, 73, 1399-1404.
- [3] HERRERO ACERO, E., RIBITSCH, D., DELLACHER, A., ZITZENBACHER, S., MAROLD, A., STEINKELLNER, G., GRUBER, K., SCHWAB, H. & GUEBITZ, G. M. 2013. Surface engineering of a cutinase from *Thermobifida cellulosilytica* for improved polyester hydrolysis. *Biotechnology and Bioengineering*, 110, 2581-2590.
- [4] RIBITSCH, D., ORCAL YEBRA, A., ZITZENBACHER, S., WU, J., NOWITSCH, S., STEINKELLNER, G., GREIMEL, K., DOLISKA, A., OBERDORFER, G., GRUBER, C. C., GRUBER, K., SCHWAB, H., STANA-KLEINSCHEK, K., HERRERO ACERO, E. & GUEBITZ, G. M. 2013. Fusion of Binding Domains to *Thermobifida cellulosilytica* Cutinase to Tune Sorption Characteristics and Enhancing PET Hydrolysis. *Biomacromolecules*, 14, 1769-1776.

## **Thin oriented polymer carbon nanotube composite films for microwave absorption.**

Henok M (Mesfin)<sup>1</sup>, Sophie (Herman)<sup>2</sup>, Isabelle (Huynen)<sup>3</sup>, Arnaud (Delcorte)<sup>1</sup>,  
Christian Bailly<sup>1</sup>

<sup>1</sup> Institute of Condensed Matter and Nanosciences (IMCN), Division of Bio and Soft Matter (BSMA), Croix du Sud 1, Université catholique de Louvain, B-1348 Louvain-la-Neuve, Belgium.

<sup>2</sup> Institute of Condensed Matter and Nanosciences (IMCN), Division of Molecules, Solids and Reactivity (MOST), Place Louis Pasteur 1, Université catholique de Louvain, B-1348 Louvain-la-Neuve, Belgium.

<sup>3</sup> Institute of Information and Communication Technologies, Electronics and Applied Mathematics (ICTEAM), Place du Levant 3, Université catholique de Louvain, B-1348 Louvain-la-Neuve, Belgium

*E Mail/ henok.mesfin@uclouvain.be*

Wireless microwave electronic devices are widespread and exacerbate the issue of electromagnetic interference (EMI). As classical EMI shielding by reflection becomes problematic for compact electronic systems, the alternative of shielding by absorption is receiving increased attention. This paper presents an approach for shielding by absorption based on thin polycarbonate films containing in plane oriented carbon nanotubes (CNT). The films were obtained by squeezing the corresponding randomly distributed nanocomposites, with concentrations ranging from 0.5 to 5 wt%, in the melt to form 170  $\mu\text{m}$  thick films with planar CNT orientation due to biaxial flow. For comparison, reference 400  $\mu\text{m}$  thick samples without orientation were also prepared. The electromagnetic absorption index was calculated based on measured scattering parameters. The results reveal that the random nanocomposites have highest average absorption in the vicinity of 1wt%. For planar oriented samples the maximum average absorption is achieved around 3wt%. Essentially the same level of absorption is achieved for an oriented 3wt% composite as a random 1wt% sample and despite its much lower thickness (170  $\mu\text{m}$  vs. 400  $\mu\text{m}$ ). Moreover, thanks to the reduced thickness for the same EM absorption per unit area, the oriented composite contains a comparable weight of CNT per unit area (1.28 times the amount in the random composite) despite the three

times higher volumetric concentration. In addition to that above 2.5wt% planar oriented sample have higher absorption as compared to their corresponding weight percentage random composites. Hence, the planar oriented films are much thinner, lighter, and more flexible at the same absorption efficiency. In all cases higher CNT concentration leads to less the absorption since reflection is increased due to higher conductivity. The out of plane conductivity of the planar oriented samples is lower than for the randomly dispersed samples, indicating the expected planar arrangement is indeed achieved.

***Keywords: EM Absorption, EMI shielding, Carbon nanotubes, Nanocomposites***

## Synthesis, characterization and gas sensing properties of Ni<sub>1-x</sub>Zn<sub>x</sub>O nanoparticles and Ni<sub>1-x</sub>Zn<sub>x</sub>O/ZnO nanocomposites

LONTIO F.R.<sup>1,2</sup>, NGOLUI J.L.<sup>1</sup>, DELCORTE A.<sup>2</sup>, DEBLIQUY M.<sup>3</sup>, LAHEM D.<sup>4</sup>, DUPONT V.<sup>5</sup>

- 1) Laboratoire de Physico-chimie des Matériaux, département de Chimie Inorganique, Université de Yaoundé I, P.O BOX 812, Yaounde, Cameroon
- 2) Pole Bio & Soft Mater, Institut de la Matière Condensée et des Nanosciences, Université Catholique de Louvain, Croix du Sud 1, 1348, Louvain-La-Neuve, Belgium
- 3) Service de Science des Matériaux, UMONS, 20, Place du Parc, 7000-Mons, Belgium
- 4) Materia Nova ASBL, Rue de l'Épargne 56, B-7000 Mons, Belgium
- 5) Belgian Ceramic Research Centre, 4, Avenue du Gouverneur Cornez 7000 Mons, Belgium  
roussin.lontio@uclouvain.be

The selectivity of oxide based resistive gas sensors remains a challenging issue as they suffer from low selectivity. Researchers have suggested various ways to overcome this problem of cross-sensitivity. Thus it was established that a significant improvement can be reached by using mixed metal oxide system [1], by microstructural modification and by the use of dopants and catalysts [2] or by controlling the size and the shape of the oxide grains. Among mixed metal oxides, the nanocomposite materials and the doped materials are very promising for gas sensor applications. Indeed, various authors have reported sensitive and selective gas sensing characteristics of composite oxide materials made by different methods [3]. According to our knowledge, reports on the NiO-ZnO systems are limited [4] and the literature on Zn doped NiO used as gas sensor is very scarce.

In this work we report for the first time, the synthesis of Ni<sub>1-x</sub>Zn<sub>x</sub>O nanoparticles and Ni<sub>1-x</sub>Zn<sub>x</sub>O/ZnO nanocomposites at relatively low temperature using corresponding metal malonate as single batch precursors. These materials were obtained by thermal decomposition (~ 360°C) of the corresponding metal malonate presynthesized by coprecipitation in aqueous solution. All the precursors were characterized by ICP-AES, FTIR, and TGA and these analyses confirm the structure of the precursors as Ni<sub>1-x</sub>Zn<sub>x</sub>(OOCCH<sub>2</sub>COO).2H<sub>2</sub>O. The presence of mixed phase nanoparticles after thermal decomposition of the precursor was confirmed by a combination of characterization techniques (SEM, XRD, XPS and ToF-SIMS). The gas sensing properties of the synthesized materials were examined using some reducing and oxidant gases showing significant changes in behavior in function of the doping.

**Keyword:** *Nanocomposite, mixed metal oxide, coprecipitation, gas sensor.*

[1] L. I. TRAKHTENBERG, G. N. GERASIMOV, V. F. GROMOV, T. V. BELYSHEVA and O. J. ILEGBUSI, "Gas Semiconducting Sensors Based on Metal Oxide Nanocomposites", J. Mater. Sci. Res., **1** (2012) 56-68.

[2] HAENG J. Y., GYEONG M. C. "Selective CO gas detection of CuO- and ZnO-doped SnO<sub>2</sub> gas Sensor", Sensors and Actuators B, **75** (2001) 56-61.

[3] H. WOO, C. W. NA, I. D. KIM, J. LEE, "Highly sensitive and selective trimethylamine sensor using one-dimensional ZnO-Cr<sub>2</sub>O<sub>3</sub> hetero-nanostructures", Nanotechnology, **23** (2012) 245501.

[4] L. YANLI, L. GUIZHI, M. RIDING, D. CONGKUN, G. PENGZHAO, "An environment-benign method for the synthesis of p-NiO/n-ZnO heterostructure with excellent performance for gas sensing and photocatalysis", Sensors and Actuator B, **191** (2014) 537-544.

## **BAW resonator as tool of characterization elastic properties of WO<sub>3</sub> thin films**

Madjid Arab

Université de Toulon, IM2NP, UMR CNRS 7334, BP 20132, 83957, La Garde, France

Corresponding author: [madjid.arab@univ-tln.fr](mailto:madjid.arab@univ-tln.fr)

Bulk acoustic wave (BAW) gas sensors generally require the use of a reactive layer for molecule adsorption. Tungsten trioxide WO<sub>3</sub> has been identified for a long time as a high potential sensitive layer particularly for NH<sub>3</sub>, NO<sub>x</sub>, CO, etc. The exploited principle consists in the change of dielectric properties of the film when adsorbing specific molecules. The design of such sensors requires the knowledge of the actual properties of the detection film as it is directly deposited atop the resonator electrodes, yielding modal dispersion which must be accounted for to guaranty the device operation according given requirements.

In this work, we report the characterization of elastic properties of such material using the dispersion behavior of BAW propagating under gratings passivated with WO<sub>3</sub> films of various thicknesses. Quartz Cristal Microbalance QCM as well as BAW devices are used in that purpose, allowing for the derivation of a reliable data set. WO<sub>3</sub> thin films were characterized using X-ray diffraction/Rietveld refinement and the samples morphology were analyzed by atomic force and electron microscopy. The diffract pattern showed the monophasic layers with the same crystallinity and they reveal a pseudo cubic phase (isotropic behaviour). We then have measured the piezoelectric coefficient of the resonators allowing for fitting the coating elastic properties by model updating. This fit has been first achieved using quartz resonators and we have obtained the fitted coefficients (apparent elastic constants C<sub>11</sub>, C<sub>12</sub>, C<sub>44</sub> and mass density).

## Rare Earth Nanoparticle Generation via Laser Ablation and Investigation of its Stoichiometry Change.

Yoonsoo Rho<sup>1,a</sup>, David J. Hwang<sup>2</sup>, Kyung-Tae Kang<sup>1,b\*</sup>

<sup>1</sup>Korea Institute of Industrial Technology, KITECH

<sup>2</sup>Department of Mechanical Engineering, State University of New York at Stony Brook

<sup>a</sup>[hirho@kitech.re.kr](mailto:hirho@kitech.re.kr), Tel : +82-31-8040-6427, Fax : +82-31-8040-6430

<sup>b</sup>[ktkang@kitech.re.kr](mailto:ktkang@kitech.re.kr), Tel : +82-31-8040-6435, Fax : +82-31-8040-6430

Rare earth materials are essential to realize many significant industrial applications. However, the separation based on chemical solution bring problems such as environmental pollution, time consuming process and high prices. In this study, we utilized laser as a promising tool for alternative route to effective separating of rare earth materials from erbium contained glasses. The ultraviolet nanosecond laser can ablate the glasses and generate nanoparticles. The morphological, optical, stoichiometric and spectroscopic changes of the nanoparticles were investigated with different laser focal point and power intensity. The results show discrepancy of latent heat of elements may cause non-stoichiometric change with lower laser fluence while the composition was almost maintained with high laser fluence. The experimental studies show the stoichiometry was also affected by laser-plasma interactions.

**Keywords:** *Rare Earth Materials, Laser Ablation, Nanoparticles, Stoichiometry*

[1] K. Hiromatsu, D.J. Hwang & C.P. Grigoropoulos. Active glass nanoparticles by ultrafast laser pulses. *Micro & Nano Letters*, 2008, Vol3, No.4, pp.121-124.

[2] J. Koch,\* A. von Bohlen, R. Hergenroder and K. Niemax Particle size distributions and compositions of aerosols produced by near-IR femto- and nanosecond laser ablation of brass. *J. Anal. At. Spectrom.*, 2004, 19, 267-272.

## Studies on LPG Sensing Property of Polyaniline / BaZrO<sub>3</sub> Composites

Khened B.S<sup>1</sup>, Machappa.T<sup>2</sup>, M.V.N.Pradeep<sup>3</sup>, M.V.N. Ambika Prasad<sup>4</sup>, Sasikala. M.<sup>5</sup>

<sup>1</sup>Department of Electrical and Electronics Engineering, Ballari Institute of Technology & Management, Bellary-583 104, Karnataka, India

<sup>2</sup>Department of Physics, Ballari Institute of Technology & Management Bellary-583 104, Karnataka, India.

<sup>3</sup>Department of Instrumentation and Control, Manipal Institute of Technology, Manipal- 576104, Karnataka, India.

<sup>4</sup>Department of Materials Science, Gulbarga University, Gulbarga-585 106, Karnataka, India

<sup>5</sup>Department of Electrical and Electronics Engineering, Godutai Engineering College for Women, Gulbarga-585103, Karnataka, India

[bskhened@yahoo.co.in](mailto:bskhened@yahoo.co.in),

[machappat@rediffmail.com](mailto:machappat@rediffmail.com), [pradeep.mungamuri@gmail.com](mailto:pradeep.mungamuri@gmail.com), [prasad1\\_amb@rediffmail.com](mailto:prasad1_amb@rediffmail.com),

[sasi\\_mun@rediffmail.com](mailto:sasi_mun@rediffmail.com)

### Abstract

Polyaniline (PANi) / Barium zirconate (BaZrO<sub>3</sub>) composites were prepared by insitu polymerization with 10, 20, 30, 40 and 50 weight percentage (wt%) of BaZrO<sub>3</sub> in polyaniline and characterized by FTIR spectra, X-ray diffraction and scanning electron microscopy. Thermally activated behavior was seen in DC conductivity measurements, where increase in conductivity with increase in temperature was observed. Maximum conductivity was seen in 40 wt% of BaZrO<sub>3</sub> in polyaniline. AC conductivity studies reveal increase in conductivity of all the composites with increase in frequency. On exposure to LPG gas, variation in resistance of the composites was observed. The change in resistance was found to be maximum in 40 wt% and 50 wt% of BaZrO<sub>3</sub> in polyaniline compared to other composites.

**Key words:** Polyaniline, Barium zirconate, composites, LPG sensing.

Intermediate annealing of warm-rolled sheets and its influence on the texture evolution in the rolled columnar-grained Fe-Ga alloys

Chao Yuan, Xuexu Gao \* , Jiheng Li, Wenlan Zhang, Xiaoqian Bao, Yanli Sui

*State Key Laboratory of Advanced Metals and Materials, University of Science and Technology*

*Beijing 100083, China*

Abstract:

The magnetostrictive Fe-Ga sheets were prepared by rolling processes on the <001> oriented columnar-grained alloys along the rolling direction, and the texture evolution was investigated. During the rolling processes without intermediate annealing processes, the  $\eta$ -fiber texture can be inherited from the original <001> orientation of the columnar grains in the hot-rolled slabs. However, the  $\eta$ -fiber texture has a strong tendency to cluster in the primary annealed sheets, and a strong {001}<130> texture was developed after final annealing processes. Intermediate annealing processes, 850 °C for 5 min, on the warm-rolled sheets during rolling processes can affect the evolution of recrystallization textures. Strong  $\gamma$ -fiber, {111}<110> and {111}<112>, was obtained in the primary annealed sheets with intermediate annealing processes, and sharp Goss orientation with magnetostriction above 200 ppm was achieved in the sheets after the final annealing processes.

Key words: Fe-Ga alloys; Magnetostriction; Intermediate annealing; Rolling; Texture evolution

---

\* corresponding author. Tel.:+86 10 62334343; fax: +86 10 62334327; e-mail: gaox@skl.ustb.edu.cn



BULK NODAL-GAP IN OVERDOPED  $Y_{0.9}Ca_{0.1}Ba_2Cu_3O_{7-\delta}$  THIN FILMSN. Bachar<sup>1</sup> and E. Farber<sup>1</sup><sup>1</sup>. Laboratory for Superconductivity and Optical Spectroscopy, Ariel University , Ariel, 40700, Israel.

The complex conductivity of overdoped  $Y_{0.9}Ca_{0.1}Ba_2Cu_3O_{7-\delta}$  thin films was measured in the Terahertz frequency range using frequency and time domain methods. The films were measured in the frequency range of 3 to 100  $cm^{-1}$  and in temperature range of 20 to 300 K. Results show a possible deviation from a pure  $d_{x^2-y^2}$ -wave superconductor, indicated by the existence of an energy sub-gap in overdoped  $Y_{0.9}Ca_{0.1}Ba_2Cu_3O_{7-\delta}$  films. Evidence for this sub-gap appears as non-monotonic behavior of  $\sigma_1(\omega, T)$  as a function of frequency followed by a sharp decrease at low frequencies, and a dip in the imaginary part of the optical conductivity multiplied by frequency,  $\omega\sigma_2(\omega, T)$ . The mentioned features were observed at energy of about 1.2 meV in 10% Ca doped YBCO thin films. Our complex conductivity spectra are in agreement with the theoretical prediction obtained by using a mixed symmetry order parameter within the Born limit, shown by Schürer et al. We suggest that these observations are direct evidence for a nodal gap obtained in a  $d_{x^2-y^2}$ -wave superconductor and can be theoretically clarified by adding an imaginary component as  $is$  or  $id_{xy}$  to the main  $d_{x^2-y^2}$ -wave order parameter.

## Developing Nanocomposites Membranes, Targeted Drug Delivery Systems, and Novel Nanoscaffolds for Antibacterial and Tissue Regeneration Applications

**Wael Mamdouh\***<sup>1,3</sup>, Irene Fahim,<sup>1,2</sup> Hanadi Salem,<sup>1,2</sup> Nancy El-Baz,<sup>1</sup> Laila Zeiko,<sup>1,4</sup> Rania Siam,<sup>1,4</sup> Isra Ali,<sup>1</sup> Marwa Moro,<sup>1</sup> Walaah Wahbi,<sup>1,3</sup>

<sup>1</sup>*Yousef Jameel Science and Technology Research center (YJSTRC), School of Sciences and Engineering (SSE), The American University in Cairo (AUC), AUC Avenue, P.O. Box 74, New Cairo 11835, Egypt*

<sup>2</sup>*Department of Mechanical Engineering, School of Sciences and Engineering (SSE), The American University in Cairo (AUC), AUC Avenue, P.O. Box 74, New Cairo 11835, Egypt.*

<sup>3</sup>*Department of Chemistry, School of Sciences and Engineering (SSE), The American University in Cairo (AUC), AUC Avenue, P.O. Box 74, New Cairo 11835, Egypt*

<sup>4</sup>*Department of Biology, School of Sciences and Engineering (SSE), The American University in Cairo (AUC), AUC Avenue, P.O. Box 74, New Cairo 11835, Egypt*

Polymer nanocomposites (PNCs) are polymers reinforced with nanofiller materials which can be organic, inorganic compounds or metals. These PNCs exhibit unique properties that are completely different from the analogue composites with larger particles such as stiffness, toughness, heat distortion, temperature and mold shrinkage and show a significant enhancement in thermal, electrical, mechanical, physical, optical, flammability and gas-barrier properties according to their applications [1-3].

Polymer nanocomposites (PNC) membranes are the future for the global packaging industry. This is due to the presence of nanoparticles in the polymer matrix which improve the packaging properties of the PNC membranes such as: flexibility, gas barrier, temperature/moisture stability, mechanical stress, chemical stability, recyclability, dimensional stability, heat resistance, and optical clarity. [4-5]

In this talk, the work which has been conducted by the Biomedical Polymer Nanocomposites, Hydrogels and tissue Engineering research group at the American University in Cairo (AUC) on PNCs will be presented. A special focus on designing novel membranes with controlled porosity and permeability will be discussed. In addition, the effect of nanofiller material and weight percentage on the PNC membrane's properties (e.g. mechanical, chemical, physical, and electrical) will be highlighted.

Moreover, the latest results on preparing different silver nanoparticles-based combinatorial therapies and evaluating their cytotoxicity on MCF-7 breast cancer cells will be presented. These results highlight that combining DOX and Ag/polymeric nanocarriers (NCs) at very low doses probably induced a synergic anticancer effect on MCF-7 cells. To the best of the authors' knowledge, this is the first time to report on these significantly higher cytotoxic effects of lower doses of DOX on MCF-7 cells. [6]

More recent results on Electrospun nanofibers and nanocomposites as Nanoscaffolds for wound dressings and antibacterial applications as well as tissue regeneration will also be presented.

### References

- [1] Polymeric Nanocomposites: Theory and Practice. S. N. Bhattacharya, R. K. Gupta, M. R. Kamal, ©Carl Hanser Verlag, Munich **2008**
- [2] Recent developments in bio-nanocomposites for biomedical applications. Tiwari A. New York: Nova Science Publishers, Inc.; **2011**.
- [3] Okada K, Usuki A. *Macromol. Mater. Eng.* **2006**, 291, 1449–76.
- [4] Irene S. Fahim, Wael Mamdouh\*, Hanadi Salem. *American Journal of Nanoscience and Nanotechnology*, **2013**, 1, 31-40
- [5] Tarek M. Madkour, Fatma M. Hagag, Wael Mamdouh, Rasha A. Azzam. *Polymer* **2012**, 53, 5788-5797
- [6] Nancy Mohamed ElBaz, Wael Mamdouh, Laila Zeiko, Rania Siam, a Provisional U.S. patent filled on September 19, 2014, Application No. 62/052841 (Nanoparticle-based Combinatorial Therapy)

## Dimensional stability of Al<sub>2</sub>O<sub>3</sub>/SiC+Cg composites under heat loading

Maciej Dyzia<sup>1</sup>, Anna Dolata<sup>1</sup>, Jan Szymuszal<sup>1</sup>

<sup>1</sup>Silesian University of Technology, Faculty of Materials Engineering and Metallurgy,  
ul. Krasińskiego 8, 40-019 Katowice, Poland  
*maciej.dyzia@polsl.pl*

Proper selection of reinforcing components allows to designed material properties of composite materials. In the case of the materials for application in tribosystem, not only the friction coefficient and degree of the wear of friction partners, but is also important dimensional stability at elevated temperatures. The thermal dimensional stability of the composite material is very often referred to as one of the advantages of these materials compared to the unreinforced matrix material [1-5].

An example of operation at elevated temperature may be a connection piston and the cylinder sleeve in the air compressors. In the cycle sized test measurement system is charged for 1 hour at 300 ° C

The main objective of the research carried out was to evaluate the behavior of the cast composite material under a temperature change in the heating and cooling cycles similar to the operating conditions. The test specimens were in the form of rings cuted from the sleeve casted into a mold of 80 mm diameter. The skin layer of cast has been removed by turning. To the surface of the samples were welded K-type thermocouple (insulated wire 2 x 0.50mm 740 type GH, ABB). Before the cycle thermal loads were measured diameter of the samples - five measurements with an accuracy of 5 µm for each point. The test cycle consisted of heating the sample to 250 ° C, annealing them at this temperature for one hour and cooling in a stream of flowing air 230 m<sup>3</sup>/h. After completion of the test samples was again measured diameters in designated areas. As the dimensional stability criterion adopted changes to the dimensions of the rings before and after four cycles of thermal loads. The data obtained allowed to estimate the basic characteristics of descriptive statistics composite castings diameter change after four cycles of temperature changes. Analyzing the changes in the diameters of samples

measured at 20 ° C after four cycles of temperature changes in the range of 20-250 °C can be concluded that the test composite materials have greater dimensional stability compared to the unreinforced matrix material:

Scientific work financed from funds allocated for The National Centre for Research and Development as project no. PBS1/B6/13/2012

**Keywords:** *hybrid composites, thermal cycles, dimensional stability*

[1] UJU W. A., OGUOCHA I. N. A, Thermal cycling behaviour of stir cast Al–Mg alloy reinforced with fly ash, *Materials Science and Engineering A* 526 (2009) 100–105.

[2] REN S., HE X., QU X., HUMAIL I., S., LI Y., Effect of Mg and Si in the aluminum on the thermo-mechanical properties of pressureless infiltrated SiCp/Al composites, *Composites Science and Technology* 67 (2007) 2103–2113.

[3] HUANG Y.D., HORT N., KAINER K.U., Thermal behavior of short fiber reinforced AlSi12CuMgNi piston alloys, *Composites: Part A* 35 (2004) 249–263.

[4] PONIEWIERSKI Z., RYLSKI A., Dimensional changes in AlSi alloys under thermal processes, *Solidification of Metals and Alloys*, No.28. 1996, 174-179 (in Polish)

[5] BALCH D.K., FITZGERALD T.J., MICHAUD V.J., MORTENSEN A., SHEN Y.-L., SURESH S., Thermal expansion of metals reinforced with ceramic, *Particles and microcellular foams Metallurgical And Materials Transactions A*, vol 27A, (1996) 3700-3717

## Location of aromatic residue alters the structural and material characteristic of amyloid fibrils

Myeongsang Lee<sup>1</sup>, Hyun Joon Chang<sup>1</sup>, Inchul Baek<sup>1</sup> and Sungsoo Na<sup>1,\*</sup>

<sup>1</sup>Division of mechanical engineering, Korea University, Seoul, Korea, 136-713

\*Corresponding author : nass@korea.ac.kr

Amyloidosis is the hallmark symptoms of neuro-degenerative and degenerative diseases which are known as Alzheimer's disease, Parkinson's disease, type II diabetes and cardiovascular diseases<sup>1,2</sup>. The source of amyloidosis is amyloid proteins, which existed from 1D structures to 3D structures under physiological conditions. These amyloid proteins have insoluble characteristic which proteins are not easily degraded in spite of external environment conditions. Using this insoluble characteristic, amyloid proteins have been developed as the functional materials with biocompatibility such as conductive nanowires and drug delivery components.

For the usage of the functional materials, structural stability of amyloid proteins is important. Typically, hydrogen bonds have been recognized as a crucial agent for amyloid protein stability through several computational and experimental studies. However, role of the aromatic characteristic such as phenylalanine residue has also been recognized as the main source of amyloid fibrils. For example, experiment study of A $\beta$  amyloid fibrils with aromatic residue mutation study was conducted to reveal the aggregation and formation tendencies. Furthermore, location of amyloid proteins, which is known as the polymorphic characteristic, varies the structural morphologies and their characteristic.

Here, we found the function of aromatic residue location on the A $\beta$  and hIAPP fibrils through the material properties using molecular dynamics simulations (MD). Through the MD simulation and analysis, not only the increased material characteristic of amyloid proteins affected by aromatic residue can be revealed, but the different material behavior also can be observed. Our study provides the importance of aromatic residue on amyloid fibrils for the utilization of functional materials.

### Acknowledgement

S.N. gratefully acknowledges the Basic Science Research Program, through the National Research Foundation of Korea (NRF) and funded by the Ministry of Science, ICT & Future Planning (MSIP) (No. 2007-0056094) and (No. 2014R1A2A11052389).

### Reference

1. C. Soto, *Nat Rev Neurosci* **4** (1), 49-60 (2003).
2. M. B. Pepys, *Annual Review of Medicine* **57** (1), 223-241 (2006).

## **Gold nanoparticles as drug delivery vehicle for Chondroitin sulphate (CS) to treat osteoarthritis.**

**Authors : Priyanka Dwivedi <sup>a</sup>, Meenal kowshik<sup>a</sup>, Ashok kumar <sup>b</sup>, Vijayashree Nayak <sup>a</sup>**

**<sup>a</sup>Department of Biological Sciences, Birla Institute of Technology and Science-Pilani, K. K. Birla Goa Campus, Zuarinagar Goa 403726, India.**

**<sup>b</sup>Department of Biological Sciences and Bioengineering, Indian Institute of Technology Kanpur, 208016-Kanpur, India**

### **Abstract**

Osteoarthritis (OA) is a disease which is characterized by joint pain, swelling and stiffness due to wear and tear of articular cartilage and has limited self repair capacity due to its avascular and aneural nature. Nanotherapeutics use nanomaterials for various biomedical applications such as drug delivery, diagnostics and biosensors. This work focuses on the use of gold nanoparticles for enhancing the delivery of chondroitin sulphate (CS)-a drug used in the treatment of Osteoarthritis (OA). CS has already shown many benefits in treating osteoarthritis. Gold nanoparticles were synthesized and combined with CS. Gold nanoparticles were characterized by Transmission electron microscopy (TEM), XRD analysis. Further *invitro* analyses of this combination of Gold nanoparticles with CS (AuNp-CS) on primary goat chondrocytes were done by various assays like MTT, Hoescht staining, Glycosaminoglycan and collagen studies. Cell viability studies by MTT revealed that Gold nanoparticles –CS (AuNp-CS) stimulated cell proliferation. There was increase in cell viability observed by Gold nanoparticles-CS than Native CS at same concentration. Similar Results were also observed with GAG and Collagen assay. There was 2.18 and 2.05 fold increase observed in GAG and collagen production when gold nanoparticles–CS (AuNp-CS) was added in combination than native CS. So this study shows that this combination of gold nanoparticles-CS stimulates chondrocyte proliferation and enhances Extracellular matrix production (ECM). Thus giving us the insight for the applicability of gold nanoparticles as a carrier for osteoarthritic drug CS which can hold potential for treatment of disease.

## Encapsulation of Platinum Complex of Indole-7-Carbaldehyde Thiosemicarbazone into Nanolipid Carrier for Sustain Released Anti-Cancer Treatment

Tiew Shu Xian, Woo Juin Onn, Misni Misran, Hapipah Mohd Ali

*CENAR, Department of Chemistry, Faculty of Science, University of Malaya,  
50603 Kuala Lumpur, Malaysia.  
Email: [misni@um.edu.my](mailto:misni@um.edu.my)*

Platinum complex of indole-7-carbaldehyde thiosemicarbazone Pt(L)(PPh<sub>3</sub>) which possess significant cytotoxicity towards cancer cell lines was encapsulated in nanolipid carrier (NLC) prepared by melt-emulsification technique. Larger particles size and increasing loading efficiency were obtained when the drug amount in formulation was increased. Larger particle size of higher amount of Pt(L)(PPh<sub>3</sub>) revealed that direct participation of platinum complex in the formation of NLC, as in agreement with the result of loading efficiency. The zeta potential of the Pt(L)(PPh<sub>3</sub>) loaded nanolipid is lower than the unloaded nanolipid, could be attributed by neutralization effect from the complex and increase with the increasing amount of Pt(L)(PPh<sub>3</sub>). From MTT assay evaluation, Pt(L)(PPh<sub>3</sub>) loaded nanolipid exhibited lower toxicity rather than free drug for 24, 48 and 72 hours of treatment, showing slower release of Pt(L)(PPh<sub>3</sub>) from the lipid matrix. The study suggested that the nanolipid could be a promising carrier for Pt(L)(PPh<sub>3</sub>) to lower its toxicity and enhancement of the therapeutic efficacy in the anti-cancer treatment.

**Keywords:** Platinum Complex, nanolipid carrier, encapsulation, slow release, anti-cancer

**Bio-inspired design of the structure and mechanics of interfacial materials**Zhao Qin<sup>1</sup>

<sup>1</sup> Department of Civil and Environmental Engineering, Massachusetts Institute of Technology, 77 Massachusetts Ave., Rm 1-239, Cambridge, MA 02139

Biomaterial covers a range of materials that are expressed by genetic information and play functional roles for the biological system such as DNA origami, cytoskeleton network, bone, silk and wood. These materials have fascinating mechanical and biological functions built up from simple basic material building blocks. Such ability to synergistically integrate multiple advantages in materials goes far beyond our current understanding of using synthesizing engineered materials. While it is known that the specific structure of an interface plays an important role in defining its mechanical properties, less clear is whether or not there exist universal scaling laws that govern the structural evolution of a very broad range of natural interfaces that lead to its biological functions. Here we show that cooperativity of interacting elements, causing great strength with synergistic material use, is a key concept that leads to the exceptional mechanical property of many natural materials. By translating this insight gained from the study of natural materials such as spider web, cocoon, mussel thread or cytoskeleton network to engineered materials such as composites composed of graphene and other polymers, we demonstrate an engineering paradigm that facilitates the design of multifunctional materials starting from the molecular level. To generalize our findings, by utilizing the integrated combination of experimental characterization, mathematical modeling, massive computational calculation and advanced additive manufacturing, we illustrate the concept to realize materials of functions by design.



## Neutron Diffraction Study on Magnetic Ordering in Bi doped $\text{Co}_2\text{MnO}_4$

N. E. Rajeevan<sup>1</sup>, S. D. Kaushik<sup>2</sup>, Ravi Kumar<sup>3</sup>

<sup>1</sup>Department of Physics, Z. G. College, University of Calicut, Kerala-673014, India.

<sup>2</sup>UGC-DAE CSR Mumbai Centre, R-5 Shed, BARC, Mumbai-400085, India.

<sup>3</sup>BCET, Gurdaspur Punjab 143521, India.

*E-mail: rajeevneclt@gmail.com*

The materials possessing the simultaneous existence of more than one ferroic order (termed as 'multiferroics') are of specific interest due to the possible technological applications in transducers, magnetic field sensors, and multiple state memories etc. [1]. Doping of  $\text{Bi}^{3+}$  nonmagnetic ion at Co site in  $\text{Co}_2\text{MnO}_4$  series of  $\text{AB}_2\text{O}_4$  spinel family of compounds where structurally A and B occupies the tetrahedral and octahedral positions respectively, have shown the promising feature of multiferroicity [2,3]. Crystal structure and magnetic structure of  $\text{Co}_2\text{MnO}_4$  is scarcely studied by employing neutron diffraction (ND) technique. In this work, the results on the ND studies of  $\text{Bi}_x\text{Co}_{2-x}\text{MnO}_4$  ( $x = 0, 0.05, 0.10, 0.15$ ) are presented, which clearly signifies the phase purity of the samples and low temperature ND study of the compounds show onset of ferrimagnetic ordering. ND study was carried out on powder samples at the National Facility for Neutron Beam Research (NFNBR), Dhruva Reactor, Mumbai (India). ND patterns were recorded at room temperature (300K) and at 2.9K. The Reitveld Refined room temperature ND pattern of polycrystalline samples of  $\text{Bi}_x\text{Co}_{2-x}\text{MnO}_4$  showed that the samples are phase pure and exhibit cubic crystal structure (space group 'Fd-3m'). The low temperature (at 2.9 K) ND pattern of the  $\text{Bi}_x\text{Co}_{2-x}\text{MnO}_4$  series clearly indicated the emergence of new superstructure peak and enhancement in the structural Bragg peak, depicting the ferrimagnetic ordering in the series. These additional peaks have been refined for magnetic structure. This analysis will further augment in understanding the multiferroic behavior in the Bi doped  $\text{Co}_2\text{MnO}_4$  compound.

**Keywords:** *Multiferroics, Neutron diffraction, Magnetization*

[1] ERENSTIEN, W., MATHUR, N. D., & SCOTT, J. F. 2006. Multiferroic and magnetoelectric materials. *Nature*, 442, 759-765.

[2] RAJEEVAN, N. E., RAVI KUMAR., SHUKLA, D. K., THAKUR, P., BROOKES, N. B., CHAE, K. H., CHOI, W. K., GAUTAM,S., ARORA, S. K., SHVETS, I. V., & PRADYUMNAN, P. P. 2009. Bi-substitution induced magnetic moment distribution in spinel  $\text{Bi}_x\text{Co}_{2-x}\text{MnO}_4$  multiferroic. *J Phys Condens. Matter* 21, 406006 (6pp).

[3] RAJEEVAN, N. E., RAVI KUMAR., SHUKLA, D. K. 2012. Combining Magnetism and Ferroelectricity towards Multiferroicity. *Solid State Phenomena* 189, 15-40.

## On Spray Drying of Uniform Mesoporous Silica Microparticles

Waldron, K.<sup>1</sup>, Wu, Z.<sup>1,2</sup>, Wu, D. W.<sup>2</sup>, Liu, W.<sup>1</sup>, Zhao, D.<sup>1,3</sup>, Chen, X. D.<sup>2</sup>, and Selomulya, C.<sup>1\*</sup>

<sup>1</sup> Department of Chemical Engineering, Monash University, Clayton Campus, Victoria 3800, Australia.

<sup>2</sup> College of Chemistry, Chemical Engineering and Material Science, Soochow University, Jiangsu 215123, China

<sup>3</sup> Department of Chemistry and Laboratory of Advanced Materials, Fudan University, Shanghai, 200433, China

\* Email: [cordelia.selomulya@monash.edu](mailto:cordelia.selomulya@monash.edu)

### Abstract

A protocol to synthesise monodisperse mesoporous silica microparticles via a microfluidic jet spray-drying route is reported. The first example used CTAB as the templating agent, with microparticles demonstrating highly ordered hexagonal mesostructures of surface areas from ~ 900 up to 1500 m<sup>2</sup>/g and pore volumes from ~ 0.6 to 0.8 cm<sup>3</sup>/g. Highly ordered mesoporous silica microparticles were produced even at a relatively low drying temperature of 92 °C. The uniform particle size could be varied from ~ 60 to 100 μm by changing the initial solute content, or changing the drying temperature. The ratio of the surfactant (CTAB) and silica (TEOS), and the amount of water in the precursor affected the degree of ordering of mesopores by promoting either the self-assembly of surfactant-silica micelles or silica condensation in the evaporation-induced self-assembly. The spray-dried microparticles showed a comparable controlled release performance with that of MCM-41 particles (Waldron et al., 2014). In the second example, large (~ 50 μm) and uniform SBA-15 microspheres were produced using amphiphilic Pluronic block co-polymer F127 as the surfactant. The size, morphology, and mesostructure of particles can be controlled from inlet drying temperature, initial solute content, hydrolysis time of the precursor, and the choice of solvent. The particles produced at 160 °C exhibited long-range ordering and were ~ 50 % larger than those generated at 120 °C due to a faster evaporation rate. Increasing hydrolysis time of the precursor solution allowed more cross-linking of silica, resulting in hollow, “bowl-like” particles. The use of water instead of ethanol as a solvent resulted in disordered “worm-like” mesostructure due to the slower evaporation rate. Analyses via SAXS and TEM indicated that the mesostructures were still mobile immediately after spray drying,

confirming the so-called “wet-pocket” phenomenon that determined the final mesostructures (Waldron et al., *accepted*).

**Keywords:** *spray drying; silica microparticles; mesoporous; uniform size*

**References:**

- WALDRON, K., WU, W. D., WU, Z., LIU, W., SELOMULYA, C., ZHAO, D. & CHEN, X. D. 2014. Formation of monodisperse mesoporous silica microparticles via spray-drying. *Journal of Colloid and Interface Science*, 418, 225-233.
- WALDRON, K., WU, W. D., WU, Z., LIU, W., SELOMULYA, C., ZHAO, D. & CHEN, X. D. Formation of Uniform Large SBA-15 Microspheres via Spray Drying. *Journal of Materials Chemistry A*, *accepted*.

## Electric field-induced transitions in lead-free $\text{Bi}_{0.5}\text{Na}_{0.5}\text{TiO}_3$ -based ceramics for energy storage

Giuseppe Viola<sup>1</sup>, Ruth McKinnon<sup>1</sup>, Vladimir Koval<sup>2</sup>, Arturas Adomkevicius<sup>1</sup>, Steve Dunn<sup>1</sup> and Haixue Yan\*<sup>1</sup>

<sup>1</sup> School of Engineering and Materials Science, Queen Mary University of London, 380 Mile End Road, London E1 4NS, UK

<sup>2</sup> Institute of Materials Research, Slovak Academy of Sciences, Watsonova 47043 53 Kosice, Slovak Republic

**ABSTRACT:** Lithium substituted  $0.95[0.94(\text{Bi}_{0.5}\text{Na}_{(0.5-x)}\text{Li}_x)\text{TiO}_3-0.06\text{BaTiO}_3]-0.05\text{CaTiO}_3$  materials include the polar rhombohedral  $R3c$  and weakly polar tetragonal  $P4bm$  phases. On increasing lithium content, the ( $R3c/P4bm$ ) phase ratio decreased, while the rhombohedral and tetragonal lattice distortions remained the same. The temperature corresponding to the shoulder in the dielectric permittivity shows no clear shift with respect to lithium substitution, due to the rhombohedral distortion remaining constant. Electrical poling produced an increase of the rhombohedral phase fraction, together with a rise of the rhombohedral and tetragonal distortion. This confirmed the occurrence of a phase transition from the weakly polar to the polar phase during electrical poling. Four peaks found in the current-electric field ( $I$ - $E$ ) loops are related to reversible electric field-induced transitions. As a consequence of a reversible transition induced by an alternating electric field, competitive energy densities with those of lead-based and lead-free bulk ceramics recently developed was obtained, indicating bismuth-based perovskites as potential lead-free systems for energy storage applications.

**KEYWORDS:** ferroelectrics, polarization, dielectrics, energy storage.

## Microspinners: Controlling Rotational Frequency in Self-Phoretic Janus Devices

Richard Archer<sup>1</sup>, Stephen Ebbens<sup>1</sup>

<sup>1</sup>The University of Sheffield

[rjarcher1@sheffield.ac.uk](mailto:rjarcher1@sheffield.ac.uk)

[s.ebbens@sheffield.ac.uk](mailto:s.ebbens@sheffield.ac.uk)

Autonomous micron scale swimming devices are a class of active materials which show directed propulsion at low Reynolds numbers, giving translational displacements far exceeding that of Brownian motion without the need for external actuation. Such devices use catalytic decomposition of dissolved fuels by spatially separated inert and active sections to generate motion by phoretic or bubble release phenomena.

Here we consider spherical Janus particles with one hemisphere coated in Platinum which produce motion by decomposing hydrogen peroxide. In usual conditions these devices have been shown to produce a thrust vector orientated away from their active cap. However a small increase in rotational diffusion rate as fuel concentration increases above that expected for pure Brownian diffusion has also been reported, thought to be caused by physical imperfections in the hemispherical cap generating angular velocity (Howse et al. 2007). Extending this idea, here we control the active cap shape using a glancing angle metal deposition method described by Pawar et al (Pawar & Kretzschmar 2008). Specifically we look at the effect of breaking the active hemisphere symmetry to unbalance the propulsive force and generate an angular velocity. Recently, rapidly

spinning particles have been shown in a range of applications such as causing cell apoptosis (Domenech et al. 2013) and directing nerve growth through generation of sheer forcers in the microfluidic environment (Wu et al. 2011), however, deploying these phenomena is currently limited by a reliance on external fields to generate well controlled spin, motivating this study to develop an autonomous alternative.

Our results demonstrate that tilting colloidal crystals on a planar surface between 0 and 80°, with respect to the directional platinum vapor results in propulsive Janus particles with average rotational frequencies tunable from 0.25 up to 2.62 Hz. Simple geometrical analysis shows that the cap symmetry is broken due to shadowing effects of neighboring particles in the crystal lattice. This is confirmed by repeating the experiment at sparse colloidal coverage, where particles show low angular velocity at all tilt angles.

While autonomous micron scale spinning devices have been previously reported by random self-assembly of two or more Janus particles, the resulting angular velocity was not well controlled (Ebbens et al. 2010) Consequently this work extends the potential to investigate and deploy many interesting driven rotational phenomena.

***Keywords: Active matter, nanotechnology, colloids, Janus.***

Domenech, M. et al., 2013. Lysosomal membrane permeabilization by targeted magnetic nanoparticles in alternating magnetic fields. *ACS nano*, 7(6), pp.5091–101.

Ebbens, S. et al., 2010. Self-assembled autonomous runners and tumblers. *Physical Review E*, 82(1), p.015304.

Howse, J. et al., 2007. Self-Motile Colloidal Particles: From Directed Propulsion to Random Walk. *Physical Review Letters*, 99(4), p.048102.

Pawar, A.B. & Kretzschmar, I., 2008. Patchy particles by glancing angle deposition. *Langmuir : the ACS journal of surfaces and colloids*, 24(2), pp.355–8.

Wu, T. et al., 2011. A photon-driven micromotor can direct nerve fibre growth. *Nature Photonics*, 6(1), pp.62–67.



**Surface-energy induced formation of bismuth nanowires at room temperature***Mingzhao Liu*

Center for Functional Nanomaterials, Brookhaven National Laboratory, Upton, NY 11973

Bismuth nanowire is a material of many intriguing electronic properties but remains a challenge for scalable and high quality fabrication. In this talk I will present a novel catalyst-free and template-free technique to grow single crystalline bismuth nanowires in high yield, through spontaneous release of surface energy by embedded nanometer-sized bismuth domains. The discovery starts from the unexpected formation of vertical bismuth nanowires array over a continuous vanadium film held at room temperature, during thermal evaporation of bismuth in vacuum, a technique conventionally reserved for thin film fabrication. Responsible for this novel technique is a previously unknown nanowire growth mechanism that roots in the mild porosity of the vanadium thin film. Infiltrated into the pores, bismuth forms nanometer-sized domains, which carry excessive surface energy that continuously expels them out of the vanadium matrix to form nanowires. The simplicity of the technique and the universality of the mechanism open a new avenue for the growth of nanowire arrays of a variety of materials, which I will discuss in the later part of this talk.

## Atomic-Scale Study of Precipitate in Photorefractive $\text{KTaO}_3$

Y.B. Xu<sup>\*</sup>, Y.L. Tang, Y.L. Zhu and X.L. Ma

Shenyang National Laboratory for Materials Science, Institute of Metal Research,  
Chinese Academy of Sciences, 110016 Shenyang, China

\*Corresponding. Tel.: +86 24 23971850. E-mail: [xuyb10s@imr.ac.cn](mailto:xuyb10s@imr.ac.cn) (Y.B. Xu).

Perovskite  $\text{KTaO}_3$  oxide is a prototype photorefractive crystal widely used in doping of photorefractive crystals. In addition, recent studies have revealed novel intriguing prosperities in  $\text{KTaO}_3$  as incipient ferroelectricity and superconductivity [1]. Particularly, the performance of  $\text{KTaO}_3$  and related crystals are dramatically affected by corresponding defects and purity of  $\text{KTaO}_3$ , which is still an obstacle for optimizing photorefractive property of  $\text{KTaO}_3$  related materials, since the volatile potassium tend to loss and thus impure precipitates forms. For example, the general formed tantalum-rich  $\text{K}_6\text{Ta}_{10.8}\text{O}_{30}$  secondary phase with tetragonal tungsten bronze structure greatly blocks the promising applications of  $\text{KTaO}_3$  crystal [2]. However, the precipitate configurations and corresponding interface structures of the  $\text{K}_6\text{Ta}_{10.8}\text{O}_{30}$  secondary phase are still elusive, which impact the preparations of low defect density crystals. In this work,  $\text{K}_6\text{Ta}_{10.8}\text{O}_{30}$  precipitates in  $\text{KTaO}_3$  crystal was systematically investigated by aberration-corrected scanning transmission electron microscopy (STEM). Orientation relationships between  $\text{K}_6\text{Ta}_{10.8}\text{O}_{30}$  and  $\text{KTaO}_3$  and atomistic structures of  $\text{K}_6\text{Ta}_{10.8}\text{O}_{30}$  and corresponding interface structures were determined at the atomic level.

Figure 1(a) is a bright-field image of  $\text{KTaO}_3$  crystal with  $\text{K}_6\text{Ta}_{10.8}\text{O}_{30}$  precipitates exhibiting different configurations featured with stark square and lamellar appearances, as marked with two arrows.

Figure 1(b) and Figure 1(c) are HAADF-STEM images of the fine interface structures. The interface between a square precipitate (yellow arrow in Figure 1(a)) and  $\text{KTaO}_3$  was characterized with atomic scale facets probably along high index planes. Corresponding orientation relationship is:  $\text{K}_6\text{Ta}_{10.8}\text{O}_{30}$  [001] //  $\text{KTaO}_3$  [001] and  $\text{K}_6\text{Ta}_{10.8}\text{O}_{30}$  (310) //  $\text{KTaO}_3$  (100). Figure 1(c) is the magnified HAADF-STEM image of

precipitate with lamellar shape marked with green arrow in Figure 1(a). The interface between this precipitate and  $\text{KTaO}_3$  is completely straight with well defined crystallographic planes, yet another specific orientation relationship was identified:  $\text{K}_6\text{Ta}_{10.8}\text{O}_{30}$   $[310] \parallel \text{KTaO}_3$   $[001]$  and  $\text{K}_6\text{Ta}_{10.8}\text{O}_{30}$   $(001) \parallel \text{KTaO}_3$   $(100)$ . This interface is terminated by  $\text{TaO}_2$  plane of  $\text{KTaO}_3$  crystal. This structure information will be useful for growing perfect  $\text{KTaO}_3$  and related crystals and help to understand the impurity induced performance depression.

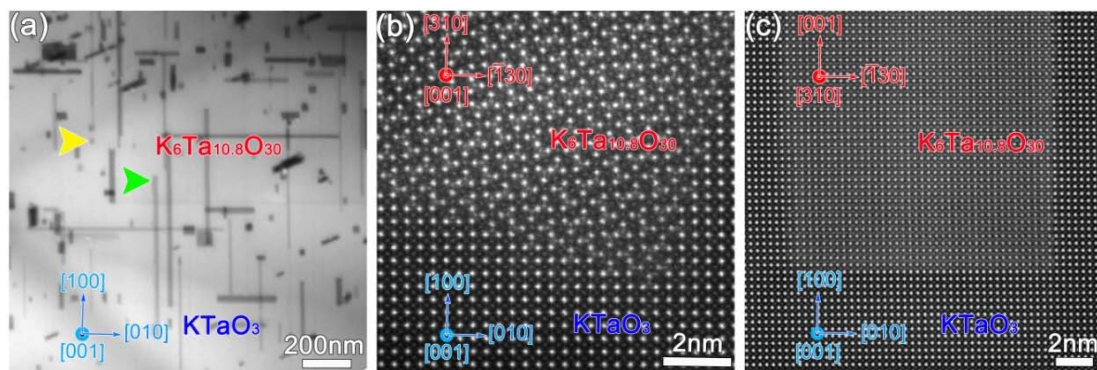


Figure 1. (a) Low-magnification of bright-field TEM image taken along the  $[001]$  direction of  $\text{KTaO}_3$  crystal. (b) High resolution of HAADF-STEM image of  $\text{KTaO}_3$  crystal and  $\text{K}_6\text{Ta}_{10.8}\text{O}_{30}$  precipitate taken along  $[001]$  direction of  $\text{K}_6\text{Ta}_{10.8}\text{O}_{30}$ . (c) High resolution of HAADF-STEM image of  $\text{KTaO}_3$  crystal and  $\text{K}_6\text{Ta}_{10.8}\text{O}_{30}$  precipitate taken along  $[310]$  direction of  $\text{K}_6\text{Ta}_{10.8}\text{O}_{30}$ .

## References

- [1] Ueno K, Nakamura S, Shimotani H, Yuan HT, Kimura N, Nojima T, Aoki H, Iwasa Y, Kawasaki M. *Nat. Nanotechnol.* 2011;6:408.
- [2] Axelsson AK, Pan YY, Valant M, Alfordz N. *J. Am. Ceram. Soc* 2009;92:1773.

**Preferred contribution: Oral**

## Supercritical hydrothermal synthesis and electrochemical performance analysis of $\text{LiM}_x\text{Mn}_{2-x}\text{O}_4$

Xuewu Liu (Liu)<sup>1,3</sup>, Xiaojuan Wang (Wang)<sup>1</sup>, Shuhua Chen (Chen)<sup>2</sup>, Xusong Qin (Qin)<sup>3</sup>

<sup>1</sup>School of chemical machinery, Dalian University of Technology, Dalian 116024, China.

<sup>2</sup>College of Environmental and Chemical Engineering, Dalian University, Dalian 116622, China.

<sup>3</sup>Guangzhou HKUST Fok Ying Tung Research Institute, Guangzhou 511458, China.

*Presenting and corresponding author: liuxuewu@dlut.edu.cn*

$\text{LiM}_x\text{Mn}_{2-x}\text{O}_4$  with different doping cations was prepared via a batch hydrothermal synthesis process at supercritical water conditions. The structure, morphology and electrochemical performance of  $\text{LiM}_x\text{Mn}_{2-x}\text{O}_4$  were characterized by X-ray diffraction, scanning electron microscope and charge and discharge test, respectively. The effects of doping ions and doping rate on the structure, morphology and electrochemical performance of the material were investigated. The results showed that: the cyclic performance of doping material improved in different degrees. Compared with material doping with Al and Fe, the material doping with Co has better performance: it has uniform particle size, good dispersity and stable electrochemical performance. The material doping with Co has initial discharge capacity of 111.7mAh/g at 1C discharge rate, capacity retention rates is 87.2% after 200 cycling. With the increasing of doping amounts, the stability of the material increased and cycle performance improved, but the capacity decreased as the active material  $\text{Mn}^{3+}$  is replaced by  $\text{Co}^{3+}$ , and the dispersity get worse as particle size reduced, overmuch doping may lead to other secondary phase generate. So the amount doping of 5% is optimal value.

**Keywords:** *supercritical hydrothermal; doping;  $\text{LiM}_x\text{Mn}_{2-x}\text{O}_4$ ; cyclic performance*

## Isotropy Verification of the C/PPS Samples Manufactured from Pellets by Image Processing Methods and Experiment

Padovec, Z.<sup>1</sup>; Chlup, H.<sup>1</sup>; Sedláček, R.<sup>1</sup>; Král, M.<sup>1</sup>; Růžička, M.<sup>1</sup>; Růžička, P.<sup>1</sup>

<sup>1</sup>Department of Mechanics, Biomechanics and Mechatronics, Faculty of Mechanical Engineering, Czech Technical University in Prague, Technická 4, Praha 6, 166 07, Czech Republic.

*Zdenek.Padovec@fs.cvut.cz/+420 224 352 519*

The main goal of this work is to determine isotropy (anisotropy) of the samples which were manufactured from C/PPS pellets with random orientation. Image processing analysis of the samples was done to detect the orientation of the pellets on the surface area. Image was transformed into binary map which was discretized on facets with rotating abscissa with length of  $N$  pixels. The evaluation of the frequency of detected peaks depending on the angle of the abscissa was done and isotropy of the material was confirmed. Then mechanical characteristics of the samples were analytically calculated with the modification of classic lamination theory for randomly reinforced composites according to [1]. FE simulation of the tensile test was done in software ABAQUS with material characteristics obtained by the analytical calculation. Verifying tensile tests based on ASTM D3039 were done on specimens cut from flat plates in both longitudinal and transversal direction [2]. Tests were done on TIRA 2300 universal test machine with clamped jaws and evaluated. Isotropy which was confirmed from image processing analysis has not been fully confirmed from the verifying tensile tests due to great dispersion in measured values. Future work will focus on the tests with bigger group of specimens and measuring  $G$  modulus using ultrasound methods.

**Keywords:** *image processing, FEM, experiment, random orientation, thermoplastic composite*

[1] BARBERO, E., J. 2011. Introduction to Composite Materials Design Second Edition. CRC Press. Boca Raton, 978-1-4200-7915-9.

[2] PADOVEC, Z. *et al.* 2014. Stress and Strength Analysis of Flat Samples Manufactured from Pellets. Proceedings of 30<sup>th</sup> Conference Computational Mechanics.

## Functional polymer surfaces on performance materials

Nadia Grossiord<sup>1</sup>

<sup>1</sup> SABIC Innovative Plastics; Materials & Polymer Physics T&I; Plasticolaan 1; 4612 PX

Bergen op Zoom; the Netherlands

*nadia.grossiord@sabic-ip.com; tel: +31 (0)164 293441*

This abstract is preferably meant for an oral presentation in Symposium 2 “Advances in Thin Films”.

Modifications aimed at adding (stimulus-triggered) functionality to surfaces have enabled many new applications such as self-cleaning, self-replenishing, self-healing, thermal regulation, energy scavenging and anti-(bio)fouling. Nature appears to be an inexhaustible source of inspiration as many biological species display remarkable surface structures and chemistry, enabling extraordinary properties. Some of the most famous examples of such surfaces are the super-hydrophobic lotus leaf and the water-repellent butterfly wing, the hydrodynamic drag-reducing shark skin as well as the super-adhesive gecko foot.

Surface functionality tuning is typically achieved by chemical functionalization/modification, by surface patterning/roughening or particle self-assembly, or by deposition of smart coatings. As a result, wettability, weldability, friction, conductivity, optical absorption, printability and adhesion, a.o., can be adjusted. Depending on the targeted utilization, modifications can be reversible or permanent.

Nowadays, the demand for surfaces with new functional properties is becoming more and more prominent in many industrial branches. This trend is expected to increase in the future. The most targeted functionalities are: (i) easy-to-clean, self-cleaning and anti-microbial material surfaces, (ii) self-healing surfaces (iii) environment-responsive sensors and actuators and (iv) surfaces exhibiting defined tribological and/or mechanical properties. Developments and competencies needed to realize the realization and production of these novel surfaces will be discussed, supported by relevant examples from academia and the performance polymer industry.

***Keywords: Self-cleaning, self-healing, sensor, tribology, performance polymer surfaces***

**Feasibility study on production of fibre cement board using waste Kraft pulp in corporation with Polypropylene and acrylic fibres**

**Dr. Morteza Khorami<sup>1</sup> , Dr.Eshmaeil Ganjian<sup>2</sup> , Dr. Anupam Srivastav<sup>1</sup>**

<sup>1</sup>: The middle east College, Muscat, Oman

<sup>2</sup>: Coventry University, Coventry, UK

**Keyword:**

**Cement composite, Waste Material, Natural fibres, Polymeric fibres, Cement board, nano silica.**

Fibre cement board is one of famous construction products that can be used as an internal/external wall as well as materials for roofing. However, over the past two decades, the use of asbestos fibres has been forbidden in the production of fibre cement board in many of developed country, those carcinogenic fibres are still used in many of developing countries. This research attempts to find the cheap and accessible materials and fibres as an asbestos replacement in the production of fibre cement board.

In this research, waste Kraft pulp and which gained from waste cardboard in corporation with two polymeric fibres; acrylic and polypropylene fibres which are normally used in fabric industry, were used as two different alternatives for asbestos fibres in the production of fibre cement board. In both groups, nano silica were used as additives.

Mechanical and physical characteristics of specimens were tested and analysed according to relevant standards.

The results showed that the specimens made out of waste cardboard and acrylic fibres could meet the standard's requirements and have adequate potential to be used as an alternative of asbestos.

## Functionalization of 1D and 2D carbon materials with mixed-valence complexes

Hiroaki Ozawa<sup>1</sup>, Norihiko Katori<sup>1</sup>, Masa-aki Haga<sup>1</sup>

<sup>1</sup> Department of Applied Chemistry, Chuo University, 1-13-27 Kasuga, Bunkyo-ku, Tokyo, 112-8551, Japan.

*E Mail/ mhaga@kc.chuo-u.ac.jp*

Mixed-valence complexes have attracted great interest because of the understanding of intramolecular electron transfer events and conductivity, and electric dipole moment of their solid state. These complexes have great potential for a functional unit in the field of molecular electronics. Recently, composites of functional metal complex and carbon materials such as SWNT and graphene have been studied for the application of electronics and sensor; however, there has been no report of composites consisting of mixed-valence complexes as building block. Thus, it is important to evaluate the mixed-valence states of the complexes on carbon materials surfaces. Here we report synthesis of dinuclear ruthenium complex containing two cyclometalated Ru bridge and pyrene anchors to a SWNT, HOPG, or graphene surface, and investigated the composite formation between carbon materials and the ruthenium complex through noncovalent  $\pi$ - $\pi$  interactions of pyrene anchors. The mixed-valence Ru complex was attached on these surfaces strong enough to measure the electrochemical measurements. After the SWNT composite formation, the composite was deposited on a Pt electrode by simple solvent evaporation. This complex/SWNT-modified showed two reversible oxidation waves at  $E_{\text{pox}} = -0.32$  and  $0.16$  V in  $\text{CH}_3\text{CN}$  (0.1 M TBAPF<sub>6</sub>), which can be assigned to the Ru(II/III) oxidation of the ruthenium complex attached on SWNTs. The oxidation potentials of the composites are consistent with those in solution, indicating conservation of the electrochemical properties of the binuclear Ru cores on carbon nanotube surface. Details of adsorption behaviors of complex to carbon materials surface and electronic properties of composites will be discussed at the meeting. **Keywords:** *Mixed-valence complex, single walled carbon nanotube, HOPG, graphene, composite.*



## **FE simulation of the electromagnetic poling process in multiferroic composites applying physically and phenomenologically motivated constitutive models**

Artjom Avakian<sup>1</sup> and Andreas Ricoeur<sup>2</sup>

<sup>1,2</sup> Institute of Mechanics, University of Kassel, Moenchenbergstr. 7, Kassel 34125, Germany.

<sup>1</sup> [artjom.avakian@uni-kassel.de](mailto:artjom.avakian@uni-kassel.de)

The coupling of magnetic and electric fields due to the constitutive behavior of a material is commonly denoted as magnetoelectric (ME) effect. The latter is only observed in a few crystal classes exhibiting a very weak coupling, mostly at low temperatures, which can hardly be exploited for technical applications. Much larger coupling coefficients are obtained at room temperature in composite materials with ferroelectric and ferromagnetic constituents. The ME-effect is then induced by the strain of matrix and inclusions converting electrical and magnetic energies based on the piezoelectric and magnetostrictive effects.

In this paper, the theoretical background of nonlinear constitutive multifield behavior as well as the Finite Element (FE) implementation are presented. Nonlinear material models describing the magneto-ferroelectric or electro-ferromagnetic behaviors are presented. Both physically and phenomenologically motivated constitutive models have been developed for the numerical calculation of the nonlinear magnetostrictive and ferroelectric behaviors. On this basis, the polarization in the ferroelectric and magnetization in the ferromagnetic respectively magnetostrictive phases are simulated and the resulting effects analyzed. Numerical simulations focus on the prediction of local domain orientations and residual stress going along with the poling process, thus supplying information on favorable electric-magnetic loading sequences. Goals are to improve the efficiency of ME coupling and to reduce damage associated with the poling process. Further, the developed tools enable the prediction of the electromagnetomechanical properties of smart multiferroic composites and supply useful means for their optimization. The resulting final state of a poling simulation can be implemented as a starting condition for approximate linear simulations and multifield homogenization procedures.

**Keywords:** *Multiferroics, magnetoelectric effect, ferromagnetics, ferroelectrics, homogenization.*

## The water splitting efficiency of InVO<sub>4</sub> powders synthesized by the hydrothermal process with various In/V molar ratio

Yu-Sheng Lai, Chih-Hsiang Yang, Jih-Mirn Jehng\*

<sup>1</sup> *Department of Chemical Engineering, National Chung Hsing University, 250 Kuo Kuang Rd., Taichung 402, Taiwan R.O.C.*

*\*e-mail address of corresponding author: [jmjehng@dragon.nchu.edu.tw](mailto:jmjehng@dragon.nchu.edu.tw)*

Hydrogen is an important green energy. It is clean and contains high energy (285.8 J/mol). The production of hydrogen with photocatalysis is a potential technology. In this study, InVO<sub>4</sub> has been chosen as a photocatalyst to split the water into hydrogen. By controlling the synthesis conditions such as the compositions, the ammonia contains, synthesized time, pH and temperature to study the formation of the surface features and crystalline phase and the efficiency for the water splitting.

Hydrothermal method has been used to prepare InVO<sub>4</sub> catalysts. The control parameters of hydrothermal method include the composition ratio of In/V to 1:1; the ammonia contains of 0.5g and 1g; hydrothermal time 1hr、2hr、4hr、8hr; pH value 5, and hydrothermal temperature 160°C、180°C、200°C、220°C. The catalysts were characterized by FE-SEM and XRD to determine the structure of the catalysts, and GC for analyzing the water splitting efficiency. When the addition amount of urea is 0.5g and hydrothermal process is 4hr, there is a maximum concentration of hydrogen 113.9 μmole/g·cat in water splitting; while increasing the amount of urea addition to 1g, the catalysts forms byproducts (NH<sub>4</sub>)<sub>2</sub>V<sub>6</sub>O<sub>16</sub> and the reactivity decreases than that of the 0.5g ammonia addition, but this crystal form can also be used as catalysts for the production of hydrogen. Due to the literature search, this results haven't been reported before. This new crystal catalyst can maintain the hydrogen concentration of 94.7 μmole/g·cat in the water splitting reaction. This study concludes that the best preparation conditions for the pH5 hydrothermal temperature 200°C, while its 4hr hydrogen concentration 113.9 μmole / g·cat. In addition, the byproducts (NH<sub>4</sub>)<sub>2</sub>V<sub>6</sub>O<sub>16</sub> could also possess the efficiency of hydrogen production in this reaction.

Keywords : Hydrothermal synthesis, Photolysis, Hydrogen production, urea, InVO<sub>4</sub>, (NH<sub>4</sub>)<sub>2</sub>V<sub>6</sub>O<sub>16</sub>

## Synthetic Chemistry with Mesoporous Boron Nitride at High Pressure

**Manik Mandal**,<sup>1</sup> **Cong Liu**<sup>1</sup>, **Yingwei Fei**,<sup>2</sup> **Kai Landskron**<sup>1,\*</sup>

<sup>1</sup> *Department of Chemistry, Lehigh University, 6 E Packer Ave, Bethlehem, PA 18015, USA*

<sup>2</sup> *Geophysical Laboratory, Carnegie Institution of Washington, Washington, DC 20015, USA*

We report on synthetic chemistry using mesoporous boron nitride material under high-pressure and high-temperature (HPHT). Mesoporous boron nitride was synthesized using mesoporous carbon as hard template. The synthesized mesoporous BN material has BET surface area of  $\sim 600 \text{ m}^2/\text{g}$ , pore volume of  $0.66 \text{ cm}^3/\text{g}$  and pore size of  $\sim 5.2 \text{ nm}$ . It was observed that upon HPHT treatment, the amorphous boron nitride was transformed completely into cubic boron nitride (cBN) nanocrystals at a pressure of 14 GPa and temperature of  $1300 \text{ }^\circ\text{C}$  for 3 h. The synthesized cBN nanocrystals have average size of  $\sim 50 \text{ nm}$  as confirmed by TEM and SEM. Further optimization of synthesis conditions, it was observed that cBN could be synthesized even at lower pressure of 10 GPa and temperature of  $1000 \text{ }^\circ\text{C}$  for 30 min. Further, lowering pressure and temperature, however, hexagonal BN was synthesized. All the materials were characterized by X-ray diffraction, Raman, TEM, and SEM.

## Molecular Dynamics Simulations on Synthesis of Zinc Oxide in Supercritical Water

Xiaojuan Wang (Wang), Xiaofei Xu(Xu), Zhu A-lei(Zhu), Zhiyi Li (Li), Zhijun Liu\* (Liu)

R&D Institute of Fluid and Powder Engineering, School of Chemical Machinery,

Dalian University of Technology, Dalian 116023, P. R. China

Presenting author: Xiaojuan Wang, [xjwang@dlut.edu.cn](mailto:xjwang@dlut.edu.cn).

Corresponding author: Zhijun Liu, [liuzj@dlut.edu.cn](mailto:liuzj@dlut.edu.cn)

Hydrothermal synthesis of ZnO under supercritical conditions from zinc-containing solution (or solution directly) is an environmentally safe process. Two reaction steps are involved, zinc hydroxide sol formation and dehydration from the sol. However, little is known about the underlying mechanism. In this study, experiments were conducted to investigate the effects of process parameters on particle size, and the molecular dynamics simulations were performed to investigate the structural and thermodynamic changes for the hydrolysis process of zinc acetate, i.e.,  $\text{Zn}(\text{CH}_3\text{COO})_2$ , in supercritical water (SCW). ZnO particles with an average size of 10 nm can be produced, and the products are characterized with XRD, FE-SEM, TEM and FT-IR. Our simulation results show that  $\text{Zn}(\text{CH}_3\text{COO})_2$  is prone to aggregate in SCW. On average, one  $\text{Zn}^{2+}$  ion is coordinated with five  $\text{CH}_3\text{COO}^-$  species and one  $\text{H}_2\text{O}$  molecule, forming an octahedral configuration. Whereas more water molecules were found to be able to bind  $\text{Zn}^{2+}$  in the interface of SCW and the  $\text{Zn}(\text{CH}_3\text{COO})_2$  clusters. The total potential energy of each system decreases after the hydrolysis of  $\text{Zn}(\text{CH}_3\text{COO})_2$ , suggesting it is a thermally favorable process in SCW. The reaction product of  $\text{OH}^-$  is observed to incorporate into the amorphous  $\text{Zn}(\text{CH}_3\text{COO})_2$  cluster and  $\text{CH}_3\text{COOH}$  is found to be in the SCW phase. Our results provide a general theoretical framework to the hydrothermal synthesis in SCW.

**Keywords:** *Zinc oxide, Supercritical water, Hydrothermal synthesis, Molecular dynamics simulation*

## Quasiparticle band structure and optical dielectric function of perovskite oxides

T. P. Sinha

Department of Physics, Bose Institute, 93/1 A. P. C. Road, Kolkata –700009, India.  
Email: sinha\_tp@yahoo.com

Perovskite oxides of general formula  $ABO_3$  have been the subject of extensive investigation in recent years. Its ideal structure is cubic, where O ions lie on the face centres and the B cation lies at the centre of O octahedra. When the octahedrally coordinated B-cation is occupied by two kinds of B' and B'' cations, it forms double perovskite oxides of general formula  $A_2B'B''O_6$ . These perovskite oxides possess very high values of dielectric constant and are widely used in memory devices based on capacitive components. The physics underlying the observed dielectric effect in these materials can be extracted by its optical conductivity analyses.

It is well known that the linear response of any perovskite oxide to an external electromagnetic field with a small wave vector is measured through the complex dielectric function  $\epsilon(\omega)$ . The optical dielectric functions of the perovskite oxides are calculated by density functional theory (DFT) in its generalized gradient approximation. The calculated results have been compared with the observed experimental data [1-4]. The DFT band gaps are found to be 1.63 eV and 1.71 eV for cubic and tetragonal phases of  $BaTiO_3$  (BT) respectively. While the dispersion of the bands is in reasonable agreement with photoemission measurements, the calculated band gap is well below the measured optical band gap of 3.3 eV (cubic BT). In order to address these discrepancies, we have calculated the electronic and optical properties of BT accounting for quasiparticle effects within the GW approach, and for electron-hole attraction by solving the Bethe-Salpeter equation [3]. Quasiparticle effects open the BT band gap significantly. The experimental optical spectra are compared with the theoretical results obtained from electronic energy band calculation and the density of states of the systems. The role of electronic band structure to understand the optical properties of double perovskite oxides [5-7] will also be presented.

- [1] S. Saha, T. P. Sinha and A. Mookerjee, *Phys. Rev. B*, 62 (2000) 8828.
- [2] K. K. Saha, T. Saha-Dasgupta, A. Mookerjee, S. Saha and T. P. Sinha, *J. Phys.: Condens. Matter*, 14 (2002) 3849.
- [3] S. Sanna, C. Thierfelder, S. Wippermann, T. P. Sinha and W. G. Schmidt, *Phys. Rev. B*, 83 (2011) 054112-1.
- [4] T. P. Sinha, A. Dutta, S. Saha, K. Tarafder, B. Sanyal, O. Eriksson and A. Mookerjee, *Physica B*, 407 (2012) 4615.
- [5] Alo Dutta and T. P. Sinha, *Solid State Commun.*, 150 (2010) 1173.
- [6] Alo Dutta, T. P. Sinha and S. Shannigrahi, *Phys. Rev. B*, 88 (2013) 075129-1.
- [7] Alo Dutta and T.P.Sinha, *Compt. Mat. Sci.*, 83 (2014) 303.

## Non-collinear Spin Polarized Calculations for Multiferroic $\text{Bi}_2\text{FeCrO}_6$

Braescu<sup>1,2,3</sup>, Vidal<sup>2</sup>, Pignolet<sup>2</sup>

<sup>1</sup>Dept. of Mathematics & Computer Science, Alfaisal University, Riyadh 11533, KSA

<sup>2</sup>Institut National de la Recherche Scientifique – Centre Énergie, Matériaux et Télécommunications, 1650 Boulevard Lionel-Boulet, Varennes, J3X 1S2, QC, Canada

<sup>3</sup>Radiological Technologies University-VT, 100 Wayne St., South Bend, IN 46601, USA

*E Mail: [lbraescu@alfaisal.edu](mailto:lbraescu@alfaisal.edu) / Contact details: Department of Mathematics & Computer Science, Alfaisal University, P. O. Box 50927, Riyadh 11533, Takhassusi Road, KSA, Phone: +966-11-215-7978*

For application in integrated sensors or devices, functional materials are used in the form of thin films. Ferroelectricity and many other properties of multiferroic materials, such as the magnetocrystalline anisotropy, are strongly related to the material crystal structure. Because fundamental physics of multiferroic materials is rich, theoretical studies are of great importance, since it is extremely difficult to understand the intrinsic material properties using only experimental data. An example of multiferroic material having the potential to revolutionize electronic industry is the rhombohedral double-perovskite  $\text{Bi}_2\text{FeCrO}_6$  (BFCO) owing to its good ferroelectric and magnetic properties at room temperature that were both theoretically predicted by ab-initio calculations [1] and experimentally demonstrated on epitaxial thin films [2]. To complement these studies, theoretical investigations have been performed in order to analyze the spin-orbit coupling (SOC) effects on the magnetic and ferroelectric properties of BFCO. Using first-principles density functional theory (DFT) calculations within the VASP package, investigations were performed for both collinear and non-collinear spin structures of BFCO, respectively. Exchange and correlation effects were treated using the local density approximation plus Hubbard potential, on the different possible high spin (HS) and low spin (LS) states of the ferromagnetic (FM) and ferrimagnetic (FiM) spin arrangements.

In the case of collinear spin calculations without SOC, the existence of four competing phases (FMHS, FMLS, FiMHS and FiMLS) with distinct electronic and magnetic

properties was found, in agreement with recent published theoretical results [3]. The FiMHS state was found to be the most stable, with a total magnetic moment  $|M_{\text{BFCO}}| \sim 2\mu_{\text{B}}/\text{cell}$ , and a computed spontaneous polarization of  $P_s = 79.1 \text{ } [\mu\text{C}/\text{cm}^2]$  in agreement with reported data [1]. When SOC was considered, the calculations also showed the existence of the above four stable states, FiMHS remaining the most stable state. It was found that magnetization is somewhat higher, namely  $|M_{\text{BFCO}}| = 2.005 \mu_{\text{B}}/\text{cell}$ , when the total magnetization vector is parallel to the direction (1 1 -2). It was also shown that, the obtained magnetizations does not have a preferred direction in the HS states, but show deviation from the direction (1 1 1) in the LS states, due to structural distortions, with energy minimized in the direction  $\sim(2 \ 1 \ 1)$ . Spontaneous polarizations computed for optimized structures using the Berry-phase method, were found to be slightly higher when SOC is considered, namely  $P_s \sim 81.5 \text{ } [\mu\text{C}/\text{cm}^2]$  for FiMHS.

Additionally, comparing the Fe-O and Cr-O bond lengths in the  $\text{FeO}_6$  and  $\text{CrO}_6$  octahedra, it was found that the Cr-O bonds and  $\text{Cr}^{3+}$  magnetic moments have non-significant changes (smaller than 0.7% of the bond length) when SOC is considered, while Fe-O bonds and  $\text{Fe}^{3+}$  magnetic moments exhibit substantial changes (up to 6.9% of the bond length).

**Keywords:** *multiferroic, DFT, spin-orbit coupling, distortions*

[1] BAETTIG, P., EDERER, C. & SPALDIN, N. A. 2005. First principles study of the multiferroics  $\text{BiFeO}_3$ ,  $\text{Bi}_2\text{FeCrO}_6$ , and  $\text{BiCrO}_3$ : Structure, polarization, and magnetic ordering temperature. *Phys Rev B*, 72, 214105-1-8.

[2] NECHACHE, C., HARNAGEA, C. & PIGNOLET, A. 2012. Multiferroic properties - structure relationships in epitaxial  $\text{Bi}_2\text{FeCrO}_6$  thin films: recent developments. *J. Phys.: Condensed Matter*, 24, 096001-1-13.

[3] GOFFINET, M., INIGUEZ, J. & GHOSEZ, P. 2012. First-principles study of a pressure-induced spin transition in multiferroic  $\text{Bi}_2\text{FeCrO}_6$ . *Phys Rev B*, 86, 024415-1-6.

## Damage and constitutive modelling of ferroelectrics including electrocaloric and thermomechanical effects

M. Wingen<sup>1</sup>, R. Gellmann<sup>2</sup>, A. Ricoeur<sup>2</sup>

<sup>1,2</sup> Institute of Mechanics, Chair of Engineering Mechanics / Continuum Mechanics,  
University of Kassel, Moenchebergstr. 7, Kassel 34109, Germany

<sup>1</sup> *maris.wingen@uni-kassel.de*

Due to their special electromechanical properties, nowadays ferroelectric materials are widely used in many technical applications, mostly as actuators or sensors. Advantages compared to other smart devices are the extremely fast reaction times in a range of  $\mu\text{s}$  – ms and large actuation forces. Influences of temperature and heat flux due to electrocaloric and thermomechanical effects are mostly neglected in models, although they may have a non-negligible impact on issues like phase transitions, domain wall motion or reliability and lifetime.

In this paper, the theoretical background and the Finite Element (FE) implementation of a micromechanically and physically based constitutive model are presented. In addition to the nonlinear ferroelectric behavior and the evolution of damage in terms of microcrack growth, the model considers the mutual nonlinear coupling of thermal and electromechanical fields. The numerical calculations reveal switching processes in ferroelectric and associated heating or cooling, enable the prediction of crack initiation e.g. at electrode tips in stack actuators and demonstrate the hysteresis characteristics of mechanical, electrical and thermal fields.

**Keywords:** *ferroelectrics, electrocaloric effects, domain switching, damage, crack growth*



## Protective effects of green tea polyphenols nanoparticles on radiation induced cellular damage: A possible link of NF kB in radioprotection

Ramovatar Meena<sup>1</sup>, Sumit Kumar<sup>2</sup>, Paulraj R<sup>1\*</sup>

<sup>1</sup> School of Environmental Sciences, Jawaharlal Nehru University, New Delhi 110067

<sup>2</sup> School of Life Science, Jawaharlal Nehru University, New Delhi 110067

The effectiveness of cancer treatment by radiation along with chemotherapeutic drugs is frequently limited due to its toxicity to the normal tissue. Identification of the possible chemosensitizer that could lead to the protecting normal tissue along with sensitizing the cancerous tissue. Green tea polyphenols, the second largest beverage has strong anticancer and antitumor potential. Present study aimed to evaluate the radio-modulatory potential of green tea polyphenols nanoparticles in murine splenocytes and wistar rat. In-vitro studies were done using primary rat splenocytes culture and effect of radiation on ROS, DNA damage, protein expression and apoptosis were studied. For In-vivo studies rats were pretreated with green tea polyphenols nanoparticles for 15 days followed by irradiation (5Gy). Micronuclei formation, hematopoietic stem cells survival, level of antioxidant enzyme and protein expression was studied during the post-irradiation period. Green tea polyphenols NPs significantly decreased the radiation induced ROS, DNA damage and apoptosis in murine splenocytes. Meanwhile in *in-vivo* results it reduces the radiation induced micronuclei formation, apoptosis besides modulating the level of antioxidant enzymes. The radio-protective nature of green tea polyphenols nanoparticles at molecular level was found to be due to decreased expression of NF-kB and its downstream genes p53, p21 and Bax, cytochrome-c, iNOS by scavenging free radicals in in-vitro studies. However in case of in-vivo system the reduction in the radiation induced apoptosis was found to be due to its interference in the expression of NF-kB. The interference in the radiation induced NF kB was found to be protective in nature as lower the levels of the p53, p21 and Bax, cytochrome-c, iNOS. These protective effects of green tea polyphenols NPs on radiation induced damage can be ascribed to the modulation of NF-kB induced gene expression. In conclusion, green tea polyphenols NPs are promising to be used as radio-mitigators or radioprotectors in clinical settings.

## A label-free and sensitive miRNA biosensor based on the electrocatalysis amplification on a Nanotip gold electrode

Lele Wang<sup>a,b</sup>, Yanli Wen<sup>a</sup>, Li Xu<sup>a</sup>, Qin Xu<sup>a</sup>, Gang Liu<sup>\*a</sup>, Nengqin Jia<sup>b</sup>

<sup>1</sup> Shanghai Institute of Measurement and Testing Technolog, 1500 Zhangheng Road, Shanghai, 201203, P.R.China

<sup>2</sup> Shanghai Normal University, 100 Guilin Road, Shanghai,200234, P.R.China

MicroRNAs (miRNAs) are key regulators of a wide range of cellular processes, and identified as promising cancer biomarkers. However, for the diagnostic application of miRNAs, there is still urgent need for the research of sensitive and specific miRNA assays especially in real samples, which still remain a challenge due to the low abundance and short length of miRNAs. Electrochemical biosensors have attracted tremendous research interest for their advantages of high sensitivity, low economy/time cost and portability. Whereas, the signal/noise ratio of miRNA electrochemical biosensors is often limited by mass transport and the surface crowding effect at the water-electrode interface. Recently, our study showed that the subuliform surface of nanotip electrodes at about 100 nm dimension could help to regulate the oligonucleotide self-assembling and improve the recognition [1].

In this work, we applied the gold nanotip electrode for highly sensitive miRNA detection based on the electrocatalytic reaction between  $\text{Ru}(\text{NH}_3)_6^{3+}$  absorption and  $\text{Fe}(\text{CN})_6^{3-}$  amplification. Figure 1 showed the principle of the electrocatalytic miRNA detection based on a gold nanotip electrode. Firstly,  $\text{Ru}(\text{NH}_3)_6^{3+}$  stoichiometrically bound to the phosphate backbone of single DNA probes through electrostatic interaction, and thus generate a redox current signal, which would be then increased when miRNA hybridized to the probes and adsorbed more  $\text{Ru}(\text{NH}_3)_6^{3+}$ .  $\text{Fe}(\text{CN})_6^{3-}$  will dramatically amplify the electrochemical signal by regenerating reduced  $\text{Ru}(\text{NH}_3)_6^{3+}$ .

After the single strand capture probe was immobilized onto the nanotip electrodes, cyclic voltammetry was exploited to characterize the electrocatalytic effect

in the  $10 \mu\text{M Ru}(\text{NH}_3)_6^{3+}$  solution, and an obvious electrocatalytic reductive current was observed in the presence of the  $4 \text{ mM Fe}(\text{CN})_6^{3-}$ . Results showed that the unique surface morphology and dimension of the nanotip electrode obviously improved the catalysis by facilitating the Ru-Fe reaction and decreasing the background signal. Scanning electron microscopy (SEM) was used to characterize these electrodes with a tip end in the nanometer scale ( $< 100 \text{ nm}$ ). (Fig 2A)

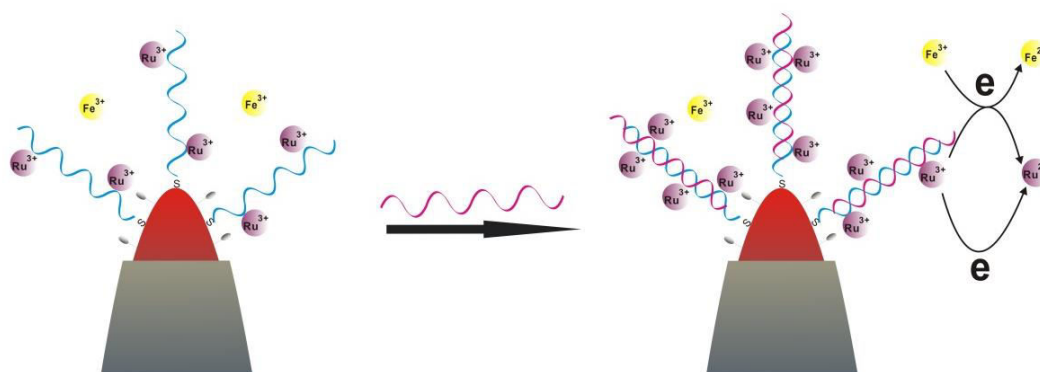


Figure 1. schematic illustration of electrocatalytic detection of miRNA based on a gold nanotip electrode.

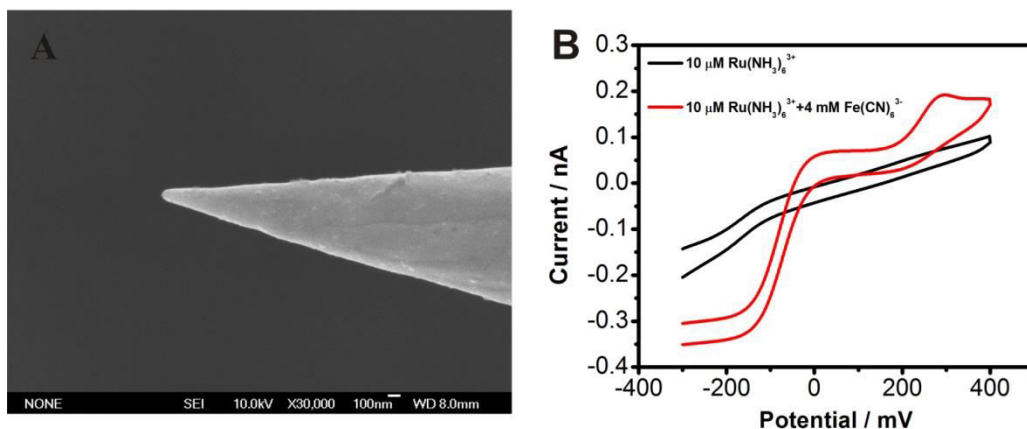


Figure 2. (A) SEM image for bare gold nanotip electrode. (B) Cyclic voltammogram of single strand DNA modified nanotip electrode in RuHex /  $\text{K}_3\text{Fe}(\text{CN})_6$  system.

**Keywords:** *microRNA, nanotip electrode, electrocatalysis*

[1] Gang Liu, Chunfeng Sun, Di Li, Shiping Song, Bingwei Mao, Chunhai Fan, and Zhongqun Tian, "Gating of Redox Currents at Gold Nanoelectrodes via DNA Hybridization", *Adv. Mater.* 2010, 22, 2148–2150

## **A Monte Carlo Study of Magnetic Tunnel Junction Based Molecular Spintronics Devices**

<sup>1</sup>Pawan Tyagi\*, <sup>2</sup>Christopher D'Angelo and <sup>1</sup>Collin Baker

<sup>1</sup>*Department of Mechanical Engineering, University of the District of Columbia, Washington DC-20008*

<sup>2</sup>*Department of Mathematics, University of the District of Columbia, Washington DC-20008*

**Molecule spintronics devices (MSDs) are expected to be capable of harnessing the controllable transport and magnetic properties of molecular device elements and can revolutionize computer logic and memory. A MSD is realized by placing magnetic molecule(s) between the two ferromagnetic electrodes. Recent experimental studies exhibited that some magnetic molecules yielded unparalleled strong exchange couplings between the two ferromagnets, leading to interesting magnetic and transport properties in a MSD. Further growth of MSDs will be governed by gaining an in-depth understanding of the molecule induced exchange coupling, and its impact on MSD's switchability, functional temperature range, stability etc. However, the large size of MSD systems and unsuitable device designs are the two biggest hurdles in theoretical and experimental studies of magnetic attributes produced by molecules in a MSD. This paper theoretically studies the MSD systems by performing Monte Carlo simulations (MCS). The effect of magnetic molecule induced exchange coupling was studied at different temperature using continuous MCS. For these studies MSDs were represented by a 3D Ising model. Our MCS shows that thermal energy strongly influenced the molecular coupling effect in a MSD. We studied the effect of a wide range of molecule-metal electrode couplings on the fundamental properties of MSDs.**

## Template synthesis of p-n composite nanotubes for augmented properties

Azzuliani (Supangat)<sup>1</sup>, Abdullah Haaziq (Ahmad Makinudin)<sup>1</sup>

<sup>1</sup>Low Dimensional Materials Research Centre, Faculty of Science, University of Malaya,  
50603 Kuala Lumpur, MALAYSIA

*azzuliani@um.edu.my* (**Azzuliani Supangat**)

In this study, the template synthesis of metal phthalocyanine:fullerene composite nanotubes is realized and compared with its bulk heterojunction counterpart. Metal phthalocyanine:fullerene composite nanotubes have been synthesized from the solution concentration of 5 mg/ml via the template-assisted method of immersion and spin coating. HRTEM images show that metal phthalocyanine (p-type) nanotubes synthesized by immersion technique were first produced which led to the infiltration of fullerene (n-type) of spin-coated. If compared to the metal phthalocyanine:fullerene bulk heterojunction, metal phthalocyanine:fullerene composite nanotubes show a wider band absorption and the peak absorption was shifted to the longer wavelength. This could be due to the improved interaction between small molecules and fullerene at their interfaces. The enhanced absorption that portrayed by composite nanotubes was supported by the quenching of intense peak in photoluminescence spectrum. Owing to the quenching, the photo-induced charge transfer and charge carrier dissociation in the composite nanotubes is better than in the bulk heterojunction.

***Keywords: template, metal phthalocyanine, fullerene, composite nanotubes***

**Domain walls effective potential model and interaction with defects**Rolando Placeres Jiménez<sup>1</sup>, José Pedro Rino<sup>1</sup>, André Marino Gonçalves<sup>2</sup>, JoséAntonio Eiras<sup>2</sup>

<sup>1</sup>Grupo de Simulação Computacional. Departamento de Física. Universidade Federal de São Carlos, São Carlos-SP, Brazil.

<sup>2</sup>Grupo de Materiais Ferroelétricas. Departamento de Física. Universidade Federal de São Carlos, São Carlos-SP, Brazil.

Domain wall motion can be modelled as a rigid body moving in dissipative medium under the action of the effective potential  $W(l)$ . From this model it is possible to derive the dispersion relationships. An analytical expression for the effective potential is found assuming that the dielectric permittivity depends on the electric field strength as  $\epsilon \propto 1/(\alpha + \beta E^2)$ . Multidomain configuration and polarization hysteresis can be taking account through the effective field approximation  $E_{\text{eff}} \equiv E + \kappa P(E)$ . An analytic expression is found for the dependence of permittivity on the electric field strength that reproduces its hysteretic behaviour. Minor loop under subswitching alternating electric field are simulated and they are compared with experimental data obtained from PZT thin films. Losses due to point defect are simulated considering defects as perturbation of the effective potential.

## **In-situ synthesis and characterization of PANI/Fe<sub>3</sub>O<sub>4</sub> nanocomposites for Chromium removal from ground water**

### **Abstract**

Aruna Ramachandran<sup>1</sup>, S.Sivaprakash<sup>1</sup>, T. Prasan Kumar, R.Ilangovan<sup>2</sup> and Sujin P. Jose<sup>1,3\*</sup>

<sup>1</sup> School of Physics, Madurai Kamaraj University, Madurai - 625021, Tamil Nadu, India.

<sup>2</sup>Department of Nano science and Nanotechnology, Alagappa University, Karaikudi, India

<sup>3</sup>Department of Materials Science and Nanoengineering, Rice University, Texas, USA.

*\*sujamystica@yahoo.com*

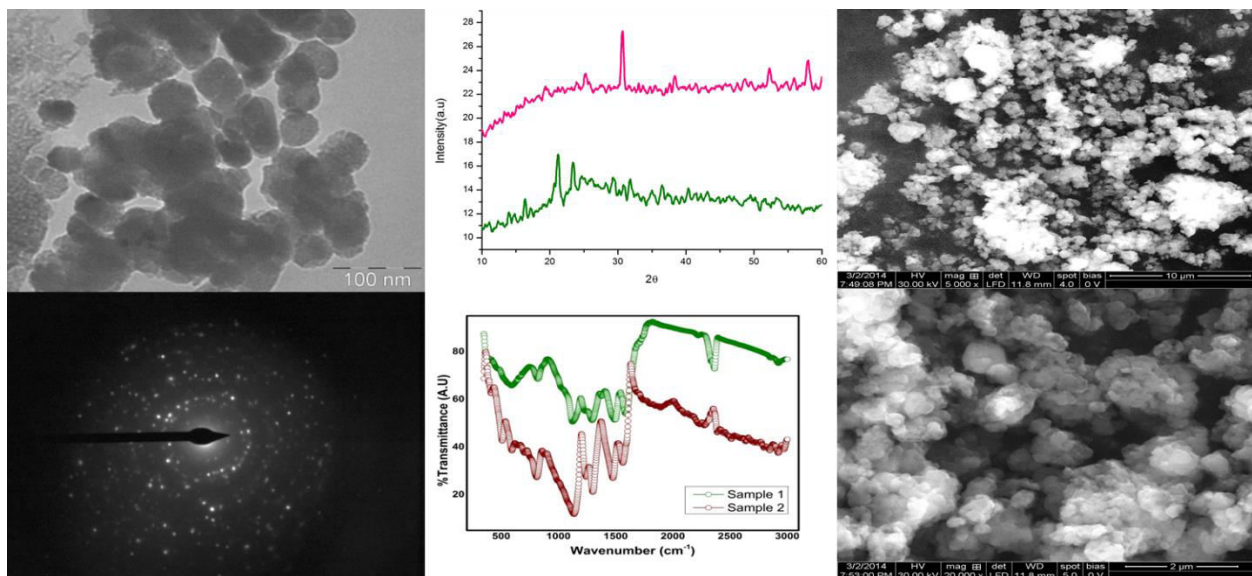
Potable ground water is an important environmental issue faced by our planet now-a-days. Chromium, one of the heavy metals, is generated from a wide range of anthropogenic sources in effluent streams. A variety of methods and materials have been developed for environmental remediation of chromium from wastewater. The present study is focused to assess the chromium level in groundwater of Madurai Kamaraj University area, which is mainly used for drinking purpose and also demonstrates the feasibility of Cr removal in these ground water samples by the synthesized PANI/Fe<sub>3</sub>O<sub>4</sub> nanocomposites. The US Environmental Protection Agency (EPA) has recommended a maximum limit of 0.1 mg L<sup>-1</sup> for total chromium in drinking water to reduce human exposure to toxic chromium.

The Fe<sub>3</sub>O<sub>4</sub> nanoparticles were prepared by microwave irradiation technique, followed by the synthesis of PANI/Fe<sub>3</sub>O<sub>4</sub> nanocomposites by in-situ polymerization. The prepared samples were analyzed using XRD, FTIR, SEM, TEM and TGA for their structural, morphological and topological studies. The XRD revealed a decrease in intensity of the composite compared to bare magnetite due to the amorphous coating of aniline polymer. But the crystal phase of magnetite core is well maintained even after polymerization. The broad peaks around 20-30° are ascribed to the polymer chain of PANI. The combination of magnetite with polymer is also verified with FTIR. The characteristic bands of Fe-O vibrations are assigned to 574-580 cm<sup>-1</sup> for the bare and treated samples. The nanocomposites exhibit C=N, C-N and C-H stretching vibration modes.

The SEM analysis showcases the formation of aggregated nanospheres overlapped with each other. TEM image shows coarse surface indicating the magnetite core and shell structure of PANI. The thermal stability of the composite was further investigated by thermo-gravimetric analysis(TGA).

The next phase of the work reports the use of Fe<sub>3</sub>O<sub>4</sub>/PANI nanocomposite in treating the ground water samples. The untreated and treated groundwater samples were further analysed by atomic absorption spectroscopy(AAS) to measure the Cr content. The Cr content is found to be decreased dramatically after the treatment with Fe<sub>3</sub>O<sub>4</sub>/PANI from 0.295 mg L<sup>-1</sup> to 0.190 mg L<sup>-1</sup> and 0.144 mg L<sup>-1</sup> respectively. This aforementioned analysis confirms the removal of chromium successfully from the ground water samples and will open up new avenues in the preparation of hybrid nanocomposites for environmental remediation.

**Keywords:** Magnetite, in-situ polymerization, polyaniline nanocomposites, ground water, Cr removal.





## Homogeneous dispersion of Au nanoparticles into mesoporous SBA-15 exhibiting improved catalytic activity for nitroaromatic reduction

Satnam Singh<sup>a</sup>, Bonamali Pal<sup>a</sup>, Shweta Sareen<sup>a</sup> and Vishal Mutreja<sup>b</sup>

<sup>a</sup>School of Chemistry & Biochemistry, Thapar University, Patiala – 147 004, Punjab, India

<sup>b</sup>Chemistry Department, MM University, Mullana – 133 207, Haryana, India

### Abstract:

Mesoporous silica SBA-15 having pore size (~8 nm) was prepared using Pluronic P123 triblock copolymer followed by its surface modification with 2 wt.% of 3-aminopropyltriethoxysilane (APTES). The Au (1-10 wt.%) impregnation led to the formation of homogeneously dispersed Au nanospheres of size 5-6 nm, and nanorods of length 90-180 nm (and width 6-9 nm) throughout the APTES-modified SBA-15 without any distortion in the long range ordering of mesochannels. It was found that increasing amount (1-10 wt.%) of Au loading followed by calcination at 350 °C resulted in change of spherical morphology to rod like Au nanostructures beyond 5 wt.% loading. The surface area (664 m<sup>2</sup>/g) and pore volume (1.33 cm<sup>3</sup>/g) of bare SBA-15 were significantly reduced to 292 m<sup>2</sup>/g and 0.6031 cm<sup>3</sup>/g for Au nanosphere, and 457 m<sup>2</sup>/g and 0.7677 cm<sup>3</sup>/g for Au nanorod dispersed SBA-15, respectively, due to partial filling of mesopores. The catalytic activity of APTES-modified SBA-15 for the reduction of m- and p-dinitrobenzene is abruptly enhanced, after optimum amount (4-10 wt.%) of Au dispersion following a pseudo first order kinetic law that exhibited the best yield and 89 % selectivity for m-phenylenediamine and 81% for p-nitroaniline formation, respectively.

## Structural and electromagnetic interference (EMI) shielding properties of flexible polymer nanocomposite films including novel type functional nano fillers

**Zehra Durmus<sup>1</sup>, Muhammed Yunus Bektay<sup>1</sup>, Alper Kasgoz<sup>2</sup>, Ali Durmus<sup>2</sup>, Huseyin Kavas<sup>3</sup>, Bekir Aktas<sup>4</sup>**

<sup>1</sup>Faculty of Pharmacy, Bezmialem Vakıf University, Fatih, 34093 Istanbul, Turkey.

<sup>2</sup>Department of Chemical Engineering, Faculty of Engineering, Istanbul University, Avcılar, 34160 Istanbul, Turkey.

<sup>3</sup>Department of Engineering Physics, Istanbul Medeniyet University, Kadıköy-Istanbul, Turkey.

<sup>4</sup>Department of Physics, Gebze Technical University, 41400, Gebze, Kocaeli, TURKEY

[zdurmus@bezmialem.edu.tr](mailto:zdurmus@bezmialem.edu.tr)

### Abstract

It is a simple fact that all electrical and electronic devices emit electromagnetic (EM) signals. These devices and communication instruments are more widely used in the modern society. Nowadays, it has been remarked that the electromagnetic pollution originated from the electromagnetic waves spreading out from the electronic devices which are become daily-life necessity in modern era brings many damaging effects on the human health, communication and environment. Research studies related to the developing of electromagnetic interference (EMI) shielding materials have been increased considerably for minimizing such damaging effects of EM waves and providing data security in the communication industry and the confidential issues in the military applications. Light weight EMI shielding materials are needed to protect the workspace and environment from radiation coming from computers and telecommunication equipment as well as for protection for sensitive circuits. An effective shielding could be conventionally achieved by metals, or metal-based materials. Polymer composites have recently attracted much interest because of their light weight, resistance to corrosion, flexibility and processing advantages.

In this study, structural and physical properties of flexible polymer nanocomposite films including novel type magnetic nanoparticles were investigated in detail. Thermoplastic polyurethane (TPU) and “carbon-magnetic nanoparticles” were used as matrix material and functional nano filler in the nanocomposite film structure, respectively. The new type functional fillers were formed via the decoration of magnetic nanoparticles ( $\text{Fe}_3\text{O}_4$ ), synthesized by the reflux method, onto a carbon template, carbon nano fiber (CNF). Flexible films consisting of various amounts of nano filler were prepared via solution casting method. Micro-structural features, physical properties and EMI shielding effectiveness of the nanocomposite films were characterized by the scanning electron microscopy (SEM), X-Ray diffraction (XRD), dynamic mechanical analysis (DMA) and vibrating sample magnetometer (VSM) methods. Microwave absorption performances of the films will also be concluded depending on the compositional parameters and the structural properties of the samples.

**Keywords:** *EMI shielding; polymer film; nanocomposite; carbon related materials*

## Investigation of intermolecular interactions between fluorene-based conjugated polymers using the dispersion-corrected DFT

Sarah Ayoub<sup>1</sup> and Jolanta B. Lagowski<sup>1</sup>

<sup>1</sup>Department of Physics and Physical Oceanography, Memorial University of Newfoundland, St. John's, NL, A1B 3X7, Canada.

[saa038@mun.ca](mailto:saa038@mun.ca)/[jolantal@mun.ca](mailto:jolantal@mun.ca)

Alternating triphenylamine-fluorene, TPAFn (n=1-3), and fluorene-oxadiazole OxFn (n=1-3) conjugated copolymers are important components of novel high-efficiency multi-layer organic light-emitting diodes (OLEDs).[1,2] In this work, we investigate the intermolecular interactions between the various combinations of monomers of OxFn-TPAFn (n=1-3) copolymers using the dispersion-corrected density functional theory (B97D) method. The monomer combinations are taken with and without the presence of long alkyl chains in order to study the effect of side-chains on the polymer backbone intermolecular interactions. The dispersion effect is determined by comparing the structures of the interacting monomers with those in vacuum. In addition, we calculate intermolecular distances, energy gaps and binding energies of monomer dimers corresponding to different pairings of OxFn-TPAFn (n=1-3) monomers. Our results show that the combination of OxF3-TPAF2 monomers exhibits the highest binding energy, closest intermolecular distance, and the best matching in chain length among the all the combinations of OxFn-TPAFn (n=1-3) monomers. Experiments have shown that OxF3-TPAF2 combination gives the best performance for OLEDs made of OxF-TPAF polymer layers.

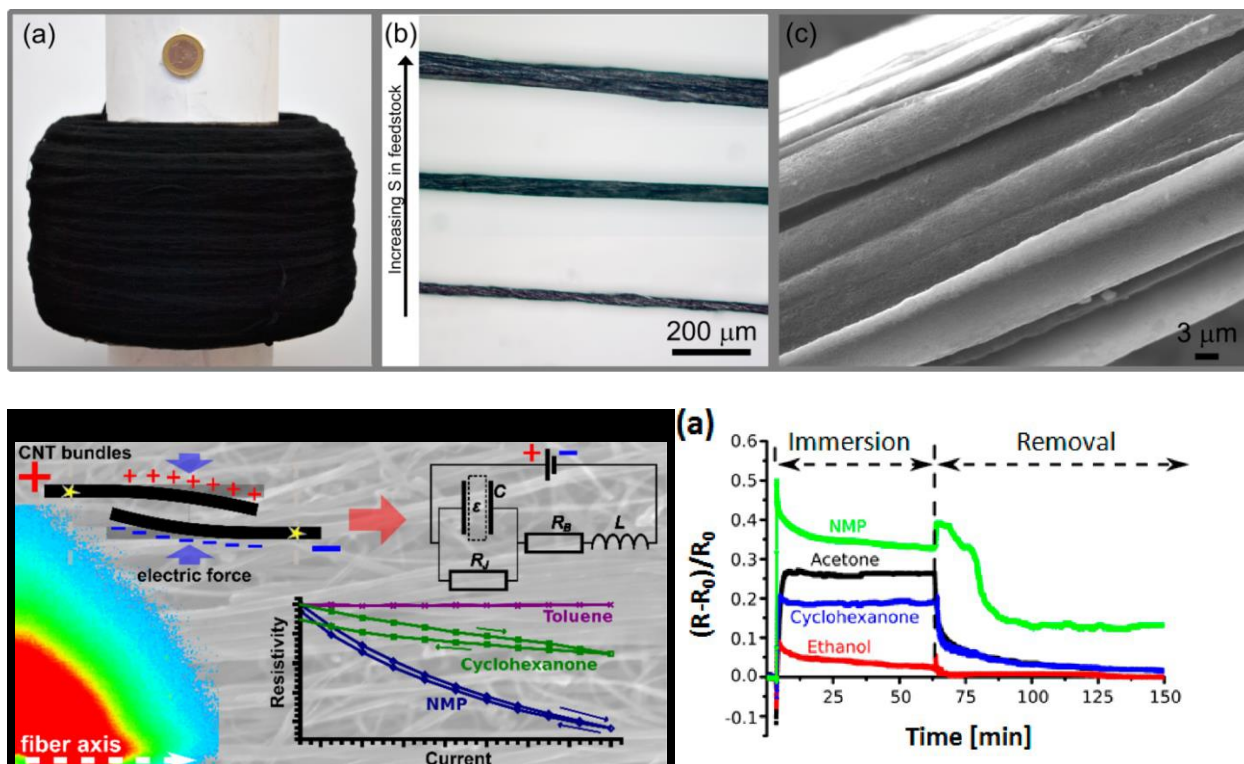
**Keywords:** *Conjugated Polymers, Interfacial Interactions, Dispersion Corrected DFT*

[1] Lin Ling and Jolanta B. Lagowski, 2013, "DFT Study of Electronic Band Structure of Alternating Triphenylamine-fluorene copolymers," *Polymer*, 54, 2535-2543.

[2] Lin Ling and Jolanta B. Lagowski, 2010, "Electronic Band Structure of Alternating Fluorene-Oxadiazole Conjugated Copolymer – A 1D Solid-State DFT Study," *J. Mol. Struct. (Theochem)*, 944, 146-155.

Multifunctional materials based on continuous macroscopic fibres of carbon nanotubes combined with polymers and inorganics.

Juan J. Vilatela, IMDEA Materials Institute, Madrid, Spain 28906



We report on the synthesis of kilometers of continuous macroscopic fibers made up of carbon nanotubes (CNT) of controlled number of layers, ranging from singlewalled to multiwalled, tailored by the addition of sulfur as a catalyst promoter during chemical vapor deposition in the direct fiber spinning process. The progressive transition from single-walled through collapsed double-walled to multiwalled is clearly seen by an upshift in the 2D ( $G'$ ) band and by other Raman spectra features<sup>1</sup>. Through control of CNT structure and orientation in the fibre we obtain fibre strengths  $> 1\text{GPa/SG}$  and modulus  $> 60\text{GPa/SG}$  and composite reinforcement levels beyond the rule of mixtures.

These fibres are good electrical conductors, chemically resistant and have a specific surface area in excess of  $100\text{m}^2/\text{g}$ . They are thus ideal to host large amounts of additional phases within the fibre itself, such as liquids, polymers and inorganics. The ingress of foreign liquids produces reversible changes in electrical resistance due to modest fibre swelling<sup>2</sup> and to the effect of the medium on the probability of electron tunnelling between adjacent CNTs, setting the basis to use this materials as a liquid sensor<sup>3</sup>.

We then show examples of hybrids materials where the fibres are combined with either polymers or inorganics. In the case of polymer matrices, we show how the large fibre surface induces fast nucleation of crystalline lamella and the formation of a transcrystalline layer. The CNT fibre/inorganic materials is characterised in terms of interfacial charge transfer processes. A few examples of application of these materials in energy management are presented.

- (1) Reguero, V.; Alemán, B.; Mas, B.; Vilatela, J. J. *Chem. Mater.* **2014**, *26*, 3550–3557.
- (2) Qiu, J.; Terrones, J.; Vilatela, J. J.; Vickers, M. E.; Elliott, J. A.; Windle, A. H. *ACS Nano* **2013**, *7*, 8412–8422.
- (3) Terrones, J.; Elliott, J. A.; Vilatela, J. J.; Windle, A. H. *ACS Nano* **2014**, *8*, 8497–8504.

## Size control and photoluminescence enhancement of Mn<sup>2+</sup>-doped ZnS nanoparticles synthesized by AOT- reverse micelle modified by compressed CO<sub>2</sub>

Rahizana Ibrahim<sup>a</sup>, Masturah Markom<sup>a,\*</sup> and Huda Abdullah<sup>b</sup>

<sup>a</sup>*Department of Chemical and Process Engineering, Faculty of Engineering and Built Environment, Universiti Kebangsaan Malaysia, 43600 Bangi, Selangor Malaysia*

<sup>b</sup>*Department of Electrical, Electronic and System Engineering, Faculty of Engineering and Built Environment, Universiti Kebangsaan Malaysia, 43600 Bangi, Selangor Malaysia*

### Abstract

Uniform Mn<sup>2+</sup>-doped ZnS nanoparticles with reduced surface defects and improved optical properties have been synthesized in a system of AOT-reverse micelle modified by compressed CO<sub>2</sub>. This process utilized sub-critical CO<sub>2</sub> at relatively low pressure of 20-60 bars at constant temperature of 40<sup>0</sup>C and adjustment of dopant ratio value (*W*). Physical characterization was carried out using UV-vis, XRD and TEM. Compared with the conventionally prepared Mn<sup>2+</sup>-doped ZnS, the particles synthesized by the modified reverse micelle method produced particles with mean particle diameter of 2 - 3 nm and significant enhancement of optical properties at 600 nm wavelength. The ZnS:Mn<sup>2+</sup> particles also exhibited a narrow band size dependent excitation emission, indicating dissolution of CO<sub>2</sub> into the micelle solution and effective surface modification, thus producing high photoluminescence (PL) efficiency of 41% .

**Keywords:** Mn<sup>2+</sup>-doped ZnS, reverse micelle, sub-critical CO<sub>2</sub>, photoluminescence

## Tuning the nanostructure of highly functionalized silica using amphiphilic organosilane

R. Besnard, J. Cambedouzou, G. Arrachart, and S. Pellet-Rostaing

Institut de Chimie Séparative de Marcoule, UMR 5257 CEA/CNRS/UM2/ENSCM,  
BP17171, F-30207 Bagnols-sur-Cèze, France.

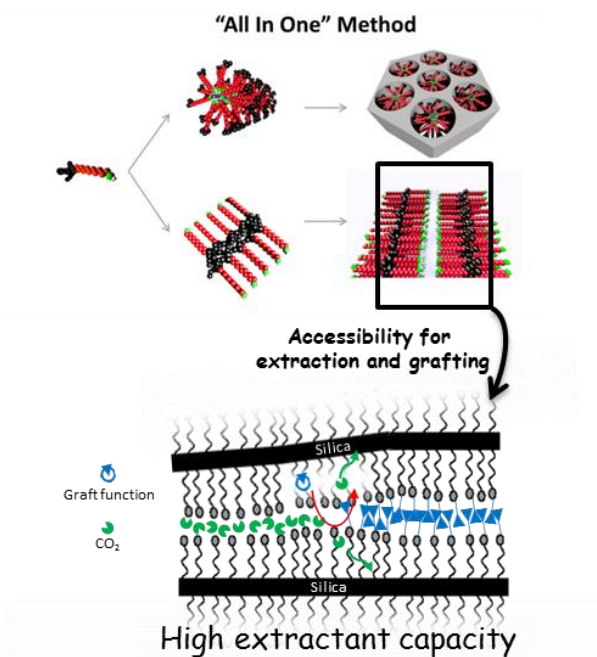
romain.besnard@cea.fr

In the context of solid-phase extractants, the organically functionalized silica should have a high density of functional groups with a satisfying homogeneity and accessibility. These requirements are usually difficult to obtain with conventional approaches.

Nanoporous silica-based materials with a densely functionalized surface have recently been prepared from organosilane amphiphile molecules.[1] Based on their amphiphilic properties, such organosilica precursors could be hydrolyzed to spontaneously give structured materials without requiring further addition of external surfactant.

The aim of our study was to develop suitable “all-in-one” approach using condensable surfactant precursors either for preparation of hybrid materials. Recently, we described the self-assembly of a simple amine (amino-undecyl-triethoxysilane) as a model, leading to hybrid organic-inorganic materials of hexagonal and lamellar structure.[2]

The mechanism of organization will be described as function of catalyst involved in sol-gel process, silica precursor (TEOS) adding and aging temperature. The study shows that the structure of such amino@silica material is enhanced by the presence



of cohesion agent like carbon dioxide for instance which can be released to unzip bilayers for the grafting of functional group and extraction of ions.

The method was extended on similar amphiphilic precursors with different functional groups which modify the amphiphilic behavior and the final structure.

Extraction tests on such materials exhibit a very high extractant capacity and without any degradation of the structure. This study presents a very promising result for hybrids materials used for solid-liquid extraction.

***Keywords: hybrid materials, highly functionalized silica, bilayers, mesostructured materials, SAXS experiment.***

[1] ZHANG, Q., ARIGA, K., OKABE, A., AIDA, T. 2004. J. Am. Chem. Soc., 126, 988–989.

[2] BESNARD, R., CAMBEDOUZOU, J., ARRACHART, G., DIAT, O., and PELLET-ROSTAING, S. 2013. Langmuir, 29, 10368-10375.

## Photophysics Simulations of THz Wave Generator Originating From Infrared NLO Material SnGa<sub>4</sub>Se<sub>7</sub>

Wen-Dan Cheng<sup>\*a</sup>, Chen-Sheng Lin<sup>b</sup>, Hao Zhang<sup>c</sup>

State Key Laboratory of Structural Chemistry, Fujian Institute of Research on the Structure of Matter, Chinese Academy of Sciences, Fuzhou 350002, P. R. China.

**a** [cwd@fjirsm.ac.cn](mailto:cwd@fjirsm.ac.cn), **b** [cslin@fjirsm.ac.cn](mailto:cslin@fjirsm.ac.cn), **c** [hzh@fjirsm.ac.cn](mailto:hzh@fjirsm.ac.cn) ([cwd@fjirsm.ac.cn](mailto:cwd@fjirsm.ac.cn))

Mid/far infrared nonlinear optical crystal can be used to produce a source of terahertz (THz) radiation by different frequency generation. For the generation of THz radiation based on the photonic way, it is strongly dependent on the optimal nonlinear optical (NLO) crystal with wide infrared wavelength converge. Photophysical properties of a new infrared NLO crystal SnGa<sub>4</sub>Se<sub>7</sub> obtained by our group [1] are investigated in order to consider it as a generation of THz radiation source. The measured and calculated infrared spectra show the wide transparent regions in the mid-infrared (MIR) zone up to 25 μm and 33 μm for SnGa<sub>4</sub>Se<sub>7</sub> powder and single crystal, respectively. The second harmonic generation (SHG) conversion efficiencies and the laser-induced damage thresholds (LIDTs) are about 3.8 times and 4.6 times of that of AgGaS<sub>2</sub> at the same particle size, respectively. The measurements of the SHG intensities depending on particle size of SnGa<sub>4</sub>Se<sub>7</sub> show that it is a phase matching material. The calculated energy band structure and density of states show that the compound is an indirect bandgap material with the gap of 2.588 eV. The micro-mechanism studies indicate that the NLO response mainly originates from the charge transfer of Se<sup>2-</sup> to Ga<sup>3+</sup> ions, and mixed with some amount of charge transfers from Se<sup>2-</sup> to Sn<sup>2+</sup> for this material. The SnGa<sub>4</sub>Se<sub>7</sub> material appearing these characteristics will be fit for the NLO crystal producing THz radiation source.

**Keywords:** THz generator, metal chalcogenides, DFT calculations

[1] LUO, Z.-Z., LIN, C.-S., CUI, H.-H., ZHANG, W.-L., ZHANG, H., HE, Z.-Z., CHENG, W.-D. 2014. SHG Materials SnGa<sub>4</sub>Q<sub>7</sub> (Q = S, Se) Appearing with large conversion efficiencies, high damage thresholds, and wide Transparencies in the mid-infrared region, *Chem. Mater.* **26**, 2743–2749.



## Lead-free Relaxor Ferroelectrics for Electrocaloric Cooling

Gunnar Suchaneck, Gerald Gerlach

TU Dresden, Solid State Electronics Lab, 01062 Dresden, Germany.

*E Mail/ Contact Details* (**Gunnar.Suchaneck@tu-dresden.de**)

Since the electrocaloric (EC) effect possesses a maximum near the ferroelectric-paraelectric phase transition, EC research is mainly focused on materials with a first-order phase transition. However, polar-domain related and dielectric losses make the temperature change of adiabatic heating larger than that of adiabatic cooling. This is not suitable for devices subjected to repeated thermodynamic cycles.

In this work, we consider an alternative approach: EC device operation at high electric fields  $E$  above the temperature  $T_m$  of the maximum dielectric permittivity. Here, the EC response is determined by the steepness of the electric compliance,  $d\epsilon/dT$ , with  $\epsilon$  as the dielectric permittivity, while dielectric losses are comparably low. Above  $T_m$ , relaxor ferroelectrics exhibit a much larger  $d\epsilon/dT$  than classical ferroelectrics. This is attributed to polar nanoregions not present in the ordinary paraelectric phase. At large fields ( $E > 5$  MV/m), the Devonshire equation of electric state in relaxors yields a much steeper  $E$ -field dependence of the EC effect,  $\Delta T_{EC} \sim E^{4/3}$ , than in ferroelectrics,  $\Delta T_{EC} \sim E^{2/3}$ . For example, at 25 MV/m, a ca. 50% higher  $\Delta T_{EC}$  of  $(\text{Ba}_{0.6}\text{Sr}_{0.3}\text{Ca}_{0.1})\text{TiO}_3$  occurs compared to ordered  $\text{Pb}(\text{Sc}_{0.5}\text{Ta}_{0.5})\text{O}_3$ . The latter was already used in an EC demonstrator device.

We discuss materials design strategies for lead-free relaxor EC materials based on stability and distortion of crystal structures with respect to a maximum of  $d\epsilon/dT$ .

Different thermodynamic cycles (Carnot, Brayton, Ericsson, Stirling and Olsen) will be analyzed for EC device application. Thin film EC devices show the most promising properties when operated with higher cycle frequency employing lower thin film thermal relaxation times.

**Keywords:** *Electrocaloric cooling, relaxor ferroelectrics, materials design*

## Dielectric Relaxation Study of Diethanolamine with Triethanolamine at Melting Points Using Time Domain Reflectometry

Pawar V. P.<sup>1</sup>, Patil A. V.<sup>2</sup>

<sup>1</sup>Department of Physics and Electronics, Maharashtra Udayagiri Mahavidyalaya, Udgir-413 517, India

<sup>2</sup>Department of Physics, I.C.S. College of Arts, Commerce and Science, Khed-415 709, India.

*Pawar\_vyankat@yahoo.com*

The dielectric relaxation study of diethanolamine with triethanolamine binary mixture have been determined over the frequency range of 10 MHz to 20 GHz, at 15, 20, 25, 28, and 30°C using time domain reflectometry (TDR) method for 11 concentrations of the system. The present work reveals molecular interaction between same multi-functional groups [–OH and –NH<sub>2</sub>] of the alkanolamines (diethanolamine and triethanolamine) using different models (Such as Debye model, Excess model, Kirkwood model and Bruggeman model). The dielectric parameters viz. static dielectric constant ( $\epsilon_0$ ), dielectric constant at high frequency ( $\epsilon_\infty$ ) and relaxation time ( $\tau$ ) have been obtained with Debye equation characterized by a single relaxation time without relaxation time distribution by the least squares fit method. The values of static dielectric constant increases up to their melting points and then it decreases with increasing temperatures. This behavior of the static dielectric constant indicates the change of phase from semi-solid to liquid state of the system. At the melting points, the values of relaxation time suddenly drop down.

**Keywords:** *Dielectric properties, Excess properties, Kirkwood properties, TDR*

# Symposia 2

## Advances in Thin Films

---

- Organic Thin Films
- Superconducting Thin Films
- Metal oxide, carbon, nitrides etc based thin Films
- Innovative Methods for the Structural Characterization of Thin films
- Theory of Structure, Surface and Interface of thin films
- Devices for acoustic wave modulation, sensing and actuating
- Plasma-Surface Interactions for Thin Film Engineering
- Advances in Deposition Techniques for thin films
- Structure Formation in Multi-Component thin films
- Optical, electrical and magnetic properties of thin films
- Synthesis, Characterization and modeling of the atomic processes of bulk and thin-film oxide film formation
- Nanostructured and Architecturally Designed Coatings, Smart Surfaces
- Protective Coatings in Severe Environments
- Thin films for optoelectronics, nanoelectronics and spintronics
- Thin films in Energy Harvesting and Storage
- Thin Films in Biological and environmental Applications
- Applications of Electrochemical and Electroless Depositions
- Advances in Deposition Techniques
- Others

# INDEX PAGE

1. Microstructure and mechanical properties of Ti6Al4V coatings deposited using high-pressure cold spraying process <b>AUTHOR:</b> Dr. Erjia Liu	1
2. Electrochemically etched porous Silicon Carbide for micro device applications <b>AUTHOR:</b> Prof. Gaël Gautier	3
3. Microstructure and mechanical properties of Ti6Al4V coatings deposited using high-pressure cold spraying process <b>AUTHOR:</b> Dr. Nicholas Weeks	4
4. Gold Wire-networks : Particle Array Guided Evaporation Lithography <b>AUTHOR:</b> Dr. Saifullah Lone	6
5. Fatigue Crack Arrest via Electrochemical Crack Infiltration <b>AUTHOR:</b> Dr. Henry Cardenas	7
6. Removal Of Zn <sup>+2</sup> From Aqueous Solutions Onto Polypyrrole Modified Reticulated Vitreous Carbon Electrodes <b>AUTHOR:</b> Dr. Clarisse Piatnicki	8
7. Novel reflection-type optical fiber methane sensor based on a no-core fiber structure <b>AUTHOR:</b> Ms. Shanya Li	9
8. Preparation of nanostructured NiO by hydrothermal for H <sub>2</sub> S gas sensor <b>AUTHOR:</b> Dr. Gotan Hiralal Jain	10
9. Doped MWCNTs thin films as electrode materials <b>AUTHOR:</b> Prof. Uwe Ritter	11
10. Effects of Oxynitridation Temperatures on the Physical and Electrical Properties of Sputtered Zr on Si Substrate <b>AUTHOR:</b> Dr. Yew Hoong Wong	12
11. Functional films of granular metal-carbon for sensing applications <b>AUTHOR:</b> Prof. Guenter Schultes	13
12. Metal oxide semiconductors thin films deposition by Supersonic Plasma Jet Source for energetic applications <b>AUTHOR:</b> Dr. Elisa Camilla Dell'Orto	15
13. Metal oxide semiconductors thin films deposition by Supersonic Plasma Jet Source for energetic applications <b>AUTHOR:</b> Dr. Claudia Riccardi	18
14. Surface modification by a graded carbon thin film for better tribological and anti-oxidation properties <b>AUTHOR:</b> Dr. Abdul Samad Mohammed	21
15. Ferroelectric and structural properties of lanthanides-doped tetragonal tungsten bronze Ba <sub>2</sub> LnFeNb <sub>4</sub> O <sub>15</sub> thin films prepared by pulsed laser ablation <b>AUTHOR:</b> Mr. Thameur Hajlaoui	22
16. Mixed Matrix Membranes Incorporated With Zif-12 For Improved Polymeric Gas Separation Membranes: Synthesis And Characterization <b>AUTHOR:</b> Dr. Mehtap Safak Boroglu	24
17. Physical Properties Of Chemically Sprayed ZnO Films <b>AUTHOR:</b> Dr. Maria De La Luz Olvera Amador	26
18. A novel method of producing field-assisted wide bandgap transparent conductive electrodes, and its application to GaN-based lateral-type light-emitting diodes <b>AUTHOR:</b> Prof. Taeho Lee	27
19. Hierarchical Cassie states on superhydrophobic micropillar arrays <b>AUTHOR:</b> Dr. Noemí Encinas García	29

20. Quorum quenching and matrix degrading enzymes in multilayer coatings prevent bacterial biofilm formation on urinary catheters <b>AUTHOR:</b> Prof. Kristina Ivanova	30
21. Relationships between structure and electrical sensitivity of breathable membranes <b>AUTHOR:</b> Dr. Annarosa Gugliuzza	32
22. Nanostructured thin films for solar selective absorbers and infrared selective emitters <b>AUTHOR:</b> Dr. Dmitry Grigoriev	34
23. Effect of Layering on pH-Triggered Swelling of Nanothin Hydrogels <b>AUTHOR:</b> Dr. John Ankner	38
24. Novel strategies for the prevention of Pseudomonas aeruginosa biofilms on urinary catheters <b>AUTHOR:</b> Dr. Tzanko Tzanov	40
25. Unprecedented tuning of the in-plane easy axis in (100) magnetite films grown by IR-PLD <b>AUTHOR:</b> Dr. Alberto Bollero	41
26. Pulsed laser deposition and characterization of Epitaxial Thin Films of $\hat{\mu}$ -Fe <sub>2</sub> O <sub>3</sub> and $\hat{\mu}$ -Al <sub>x</sub> Fe <sub>2-x</sub> O <sub>3</sub> <b>AUTHOR:</b> Mr. Luca Corbellini	43
27. The Structural And Magnetic Characterization Of Nio/Co <sub>90</sub> Fe <sub>10</sub> Bilayers. <b>AUTHOR:</b> Prof. Yu-Chi Chang	45
28. Anisotropic Chiral Colloidal Lithography <b>AUTHOR:</b> Dr. Sabine Portal	47
29. Structural and Magnetic Study of Mn-doped CeO <sub>2</sub> Diluted Magnetic Semiconductor Prepared by Sol-gel Method <b>AUTHOR:</b> Prof. Yang Shenghong	49
30. Synthesis And Magnetic Properties Of Co Thin Films. <b>AUTHOR:</b> Prof. Ahmed Kharmouche	50
31. Structure, optical, and magneto-optical properties of magnetic silicide Fe <sub>3</sub> Si and Fe <sub>5</sub> Si <sub>3</sub> <b>AUTHOR:</b> Prof. Sergei Ovchinnikov	52
32. Unprecedented tuning of the in-plane easy axis in (100) magnetite films grown by IR-PLD <b>AUTHOR:</b> Dr. Federico J. Mompean	53
33. Effect of Changed Structure as well as Composition on the Behaviour of Sn(Se,Te) Compound Semiconductor Thin Films and Schottky Diodes for Solar Cell Applications <b>AUTHOR:</b> Prof. Naresh Padha	55
34. Deposition-controlled enhancement of green emission of hydrogen annealed ZnO thin films <b>AUTHOR:</b> Miss Olga Chichvarina	56
35. Effect of Porosity on resistivity of Silver Nanoparticle Ink during Laser Sintering <b>AUTHOR:</b> Dr. Jun Y Hwang	58
36. Improving Performance of Organic Light-emitting Diodes by Combing Both MoO <sub>3</sub> Hole Injection Layer and MoO <sub>3</sub> Doped Hole Transport layer <b>AUTHOR:</b> Prof. Xiang Zhou	59
37. Synchrotron X-Ray Studies On The Morphology Of Ternary Organic Polymer Solar Cells <b>AUTHOR:</b> Dr. Xinhui Lu	60
38. Optical and Electrical Characterizations of Silicon Phthalocyanine dichloride thin films <b>AUTHOR:</b> Dr. Regimol Joseph	61
39. Fabrication Of A Coupled Silicon-Gold Plasmonic Structure Using Remote Plasma Enhanced Chemical Vapor Deposition And Sputtering <b>AUTHOR:</b> Dr. Arturo Rodriguez Gomez	62
40. Silicon Containing Layer On Ti-46Al-8Ta Alloy For Hot Corrosion Protection. Kinetic Studies Of Layer Deposition <b>AUTHOR:</b> Ms. Katarzyna Rubacha	65
41. Overview Of Superhydrophilic, Photocatalytic And Anti-Corrosive Properties Of TiO <sub>2</sub> Thin Films Doped With Multiwall Carbon Nanotubes And Deposited On 316L Stainless Steel	66

<b>AUTHOR:</b> Ms. Géraldine Léonard	
42. Rapid Prototyped Biomimetic Antifouling Surfaces for Marine Applications	
<b>AUTHOR:</b> Mr. Paul O'Neill	67
43. Investigation on Correlation between Adhesion and Electrochemical Impedance Spectroscopy for Acrylate-Epoxy Paint System...	
<b>AUTHOR:</b> Dr.Vengadaesvaran Balakrishnan	68
44. Development and characterization of hydrophobic anticorrosive acrylic - silicone/SiO <sub>2</sub> nanoparticles hybrid nanocomposite coatings	
<b>AUTHOR:</b> Dr. Ramesh Kasi	69
45. Diffusion and Diffusion-Controlled Transformations in Intermetallic Nanolayers: Atomistic Modelling	
<b>AUTHOR:</b> Prof. Piotr Sowa	70
46. First order phase transition in epitaxial Ni-Mn-Ga-Co films on ferroelectric substrates	
<b>AUTHOR:</b> Mr. Benjamin Schleicher	71
47. Effect Of Annealing To Oxidation State Of Sr <sub>2</sub> Femoo <sub>6</sub> Double Perovskite Film	
<b>AUTHOR:</b> Prof. Dong-Hyun Kim	72
48. Josephson generation of coherent THz stimulated emission on Planar Superconducting Multilayer Films (PSMF)	
<b>AUTHOR:</b> Dr. Leonid Muravey	73
49. Effects Of Hydrothermal Ageing On Structure And Adhesion Properties Of Tio <sub>2</sub> -Nanotubes	
<b>AUTHOR:</b> Dr. Tobias Mertens	74
50. Structural and magnetic properties of single graphene film with magnetic Co deposition	
<b>AUTHOR:</b> Prof. Min Zhai	75
51. Improvement in Structural and Optical Properties of InGaN/GaN LEDs Using Grid Patterns Realized by Laser Treatments	
<b>AUTHOR:</b> Mr. Kwanjae Lee	76
52. Properties Of Zns:Cu Thin Films Grown By Chemical Bath Deposition	
<b>AUTHOR:</b> Dr. Amanda Carrillo	77
53. Carbon nanotubes modified with gold nanoparticles in biosensing	
<b>AUTHOR:</b> Dr. Nikos Tsierkezos	78
54. Zeolite Impregnated Polysulfone Membrane For The Removal Of Metals In Wastewater	
<b>AUTHOR:</b> Dr. Yilmaz Yurekli	79
55. Piezoelectric Thin Film Layer Integrated Microdiaphragm For The Dynamic Sensing Viscosity And Density Of Liquid For Bio Applications	
<b>AUTHOR:</b> Dr. Kyo Seon Hwang	81

## Microstructure and mechanical properties of Ti<sub>6</sub>Al<sub>4</sub>V coatings deposited using high-pressure cold spraying process

Adrian Wei-Yee Tan<sup>1,2</sup>, Nay Win Khun<sup>1,2</sup>, Rupert Adams<sup>1,3</sup>, Nicholas Weeks<sup>1,3</sup>,  
Erjia Liu<sup>1,2,\*</sup>

<sup>1</sup>Rolls-Royce@NTU Corporate Lab, Nanyang Technological University, 50 Nanyang Avenue, Singapore 639798, Singapore

<sup>2</sup>School of Mechanical & Aerospace Engineering, Nanyang Technological University, 50 Nanyang Avenue, Singapore 639798, Singapore

<sup>3</sup>Advanced Technology Centre, Rolls-Royce Singapore Pte Ltd, 1 Seletar Aerospace Crescent, Singapore 797575, Singapore

*Email: mejliu@ntu.edu.sg, Tel: +65-67905504*

**Abstract:** Cold spray is an additive technology that is capable of dense coating for surface repair or protection in the aerospace industry. It uses a high pressure (40 to 50 bar) preheated (to 1000°C) gas stream (nitrogen or helium) to accelerate the microparticles (40 to 60 μm) via a converging-diverging nozzle to supersonic speeds (600 to 800 m/s) and impact the particles onto the substrate. The micro-particles will then plastically deform and bond with the substrate. Although preheat temperatures as high as 1000°C are used, the gas rapidly cools as it expands in the diverging section of the nozzle. Hence, the dwell time of the particles in contact with hot gas is brief, and the temperatures of the solid micro-particles at impact remain substantially below the initial gas preheat temperature. Therefore, unlike current thermal-based method such as welding and plasma spray, cold spray minimises the residual thermal stresses and surface oxidation of the coatings.

Ti<sub>6</sub>Al<sub>4</sub>V is a commonly used aerospace metal alloys due to its high specific strength, high toughness, high thermal stability, and high corrosion resistance along with other excellent properties. However, deposition of good quality Ti<sub>6</sub>Al<sub>4</sub>V coatings on aerospace alloys via cold spray is a challenge because of the high hardness of Ti<sub>6</sub>Al<sub>4</sub>V particles (350 HV). The window of deposition for particles depends on the critical particle velocity, which is highly influenced by the particle hardness. It is difficult to plastically deform micro-particles with high hardness like Ti<sub>6</sub>Al<sub>4</sub>V and bond them to the substrate surface with a high adhesive strength. Part of hard particles might also rebound away.

This work investigates the cold sprayed Ti6Al4V coatings on Ti6Al4V substrates. The effect of cold spraying on the microstructure and mechanical properties of the Ti6Al4V coatings is systematically investigated. The coating thickness and surface roughness are measured using surface profilometry. The microstructural characteristics of the coatings are analyzed using optical microscopy, scanning electron microscopy and X-ray diffraction. The hardness and modulus of elasticity of the coatings are measured using micro- and nano-indentation.

***Keywords: High-pressure cold spray, Ti<sub>6</sub>Al<sub>4</sub>V coating, Ti<sub>6</sub>Al<sub>4</sub>V substrate, Microstructure, Mechanical properties***



## **Electrochemically etched porous Silicon Carbide for micro device applications**

G. Gautier<sup>1</sup>, T. Defforge<sup>1</sup>, J. Biscarrat<sup>1</sup>, D. Valente<sup>1</sup>, F. Cayrel<sup>1</sup>, S. Menard<sup>2</sup>, A. Gary<sup>1</sup>, A. Fèvre<sup>1,2</sup>, K. Venga<sup>1</sup>, J.F. Michaud<sup>2</sup>, D. Alquier<sup>2</sup>.

<sup>1</sup> Université François Rabelais de Tours, CNRS, CEA, INSA CVL, GREMAN UMR  
7347, 16 rue P. et M. Curie, 37071 Tours.

<sup>2</sup>STMMicroelectronics, 16 rue P. et M. Curie, 37071 Tours.

*gael.gautier@univ-tours.fr*

For decades, silicon carbide (SiC) has been studied knowing that this material has high electron velocity, high critical electric field and high thermal conductivity. As a consequence, SiC, especially 4H-SiC polytype, is a very attractive material for power applications. Moreover, SiC is very stable in many chemical etching solutions even at high temperatures and hence, is highly promising for harsh environment sensors or devices. Electrochemical etching is known to be an efficient technique to form porous regions in SiC substrates [1]. This material shows remarkable and very specific properties. It can be used as active material for ultraviolet light emitting diodes and chemical or physical sensors. In addition, porous semi-conductors exhibit low electrical conductivity compared with the bulk, even for low porosities. As a consequence, porous SiC layer is an interesting alternative as passivation in high-power SiC devices or as an isolating substrate under RF devices. In this communication, we present an overview of our work in the field of SiC electrochemical etching (experimental setup description, influence of anodization parameters such as current density, electrolyte composition, or UV lighting, on porous SiC morphology). In addition, we emphasize on the electrical performances of such material in DC or RF.

***Keywords: Porous SiC, electrochemical etching, electrical characteristics***

[1] SHOR, J.S., GRIMBERG, I., WEISS, B.-Z. & KURTZ, A.D. 1993. Appl. Phys. Lett., 62, 2836- 2838.

## Microstructure and mechanical properties of Ti<sub>6</sub>Al<sub>4</sub>V coatings deposited using high-pressure cold spraying process

Adrian Wei-Yee Tan<sup>1,2</sup>, Nay Win Khun<sup>1,2</sup>, Rupert Adams<sup>1,3</sup>, Nicholas Weeks<sup>1,3</sup>,  
Erjia Liu<sup>1,2,\*</sup>

<sup>1</sup>Rolls-Royce@NTU Corporate Lab, Nanyang Technological University, 50 Nanyang Avenue, Singapore 639798, Singapore

<sup>2</sup>School of Mechanical & Aerospace Engineering, Nanyang Technological University, 50 Nanyang Avenue, Singapore 639798, Singapore

<sup>3</sup>Advanced Technology Centre, Rolls-Royce Singapore Pte Ltd, 1 Seletar Aerospace Crescent, Singapore 797575, Singapore

*Email: mejliu@ntu.edu.sg, Tel: +65-67905504*

**Abstract:** Cold spray is an additive technology that is capable of dense coating for surface repair or protection in the aerospace industry. It uses a high pressure (40 to 50 bar) preheated (to 1000°C) gas stream (nitrogen or helium) to accelerate the microparticles (40 to 60 μm) via a converging-diverging nozzle to supersonic speeds (600 to 800 m/s) and impact the particles onto the substrate. The micro-particles will then plastically deform and bond with the substrate. Although preheat temperatures as high as 1000°C are used, the gas rapidly cools as it expands in the diverging section of the nozzle. Hence, the dwell time of the particles in contact with hot gas is brief, and the temperatures of the solid micro-particles at impact remain substantially below the initial gas preheat temperature. Therefore, unlike current thermal-based method such as welding and plasma spray, cold spray minimises the residual thermal stresses and surface oxidation of the coatings.

Ti<sub>6</sub>Al<sub>4</sub>V is a commonly used aerospace metal alloys due to its high specific strength, high toughness, high thermal stability, and high corrosion resistance along with other excellent properties. However, deposition of good quality Ti<sub>6</sub>Al<sub>4</sub>V coatings on aerospace alloys via cold spray is a challenge because of the high hardness of Ti<sub>6</sub>Al<sub>4</sub>V particles (350 HV). The window of deposition for particles depends on the critical particle velocity, which is highly influenced by the particle hardness. It is difficult to plastically deform micro-particles with high hardness like Ti<sub>6</sub>Al<sub>4</sub>V and bond them to the substrate surface with a high adhesive strength. Part of hard particles might also rebound away.

This work investigates the cold sprayed Ti6Al4V coatings on Ti6Al4V substrates. The effect of cold spraying on the microstructure and mechanical properties of the Ti6Al4V coatings is systematically investigated. The coating thickness and surface roughness are measured using surface profilometry. The microstructural characteristics of the coatings are analyzed using optical microscopy, scanning electron microscopy and X-ray diffraction. The hardness and modulus of elasticity of the coatings are measured using micro- and nano-indentation.

***Keywords: High-pressure cold spray, Ti<sub>6</sub>Al<sub>4</sub>V coating, Ti<sub>6</sub>Al<sub>4</sub>V substrate, Microstructure, Mechanical properties***

## Gold Wire-networks : Particle Array Guided Evaporation Lithography

Saifullah Lone, Jiaming Zhang, Ivan U. Vakarelski, & Sigurdur T. Thoroddsen

**High-Speed Fluids Imaging Laboratory, Division of Physical Sciences and Engineering, King Abdullah University of Science & Technology (KAUST), Thuwal 23955-6900, Saudi Arabia. [Email Saifullah.lone@kaust.edu.sa](mailto:Saifullah.lone@kaust.edu.sa).**

We exploited the combination of dry deposition of monolayer of 2D (two dimensional) templates, lift-up transfer of 2D template onto flat surfaces and evaporation lithography [1] to fabricate gold micro- and submicron size wire networks. The approach relies upon the defect free dry deposition of 2D monolayer of latex particles [2] on patterned silicon template and flat PDMS-substrate to create square centered and honey-comb wire networks respectively. The process is followed by lift-up transfer of 2D latex crystal on glass substrate. Subsequently, a small amount of AuNP-suspension is doped on top of the transferred crystal; the suspension is allowed to spread instantaneously and dried at low temperature. The liquid evaporates uniformly to the direction perpendicular to glass substrate. During evaporation, AuNPs are de-wetted along with the movement of liquid to self-assemble in-between the inter-particle spaces and therefore, giving rise to liquid-bridge networks which upon delayed evaporation, transforms into wire networks. The approach is used to fabricate both micro- and submicron wire-networks by simply changing the template dimensions. One of the prime motives behind this study is to down-scale the existing particle array template-based evaporation lithography process to fabricate connected gold wire networks at both micro- and submicron scale. Secondly, the idea of combining the patterned silicon wafer with lifted latex particle template creates an opportunity to clean and re-use the patterned wafer more often and thereby, saving fabrication time and resources. Finally, we illustrated the validity of this approach by creating an easy and high-speed approach to develop gold wire networks on a flexible substrate with a thin deposited adhesive. These advances will not only serve as a platform to scale up the production, but also demonstrated that the fabrication method can produce metallic wire networks of different scale and onto a variety of substrates.

**Keywords:** *Dry Deposition, Lift-up, Doping, Evaporation, Self-Assembly, Wires*

[1] VAKARELSKI, I. U., CHAN, D.Y. C., NONOGUCHI, T., SHINTO, H., & HIGASHITANI, K. 2009. Assembly of Gold Nanoparticles into Microwire Networks Induced by Drying Liquid Bridges. PRL, 102, 2009, 058303- 058303-4

[2] KHANH N. N., & YOON J. K. B. 2009. Facile Organization of Colloidal Particles into Large, Perfect One & Two-Dimensional Arrays by Dry Manual Assembly on Patterned. J. AM. CHEM. SOC., 131, 14228–14230.

## Fatigue Crack Arrest via Electrochemical Crack Infiltration

Konstantin Dolgan, David E. Hall, Henry E. Cardenas

The aim of this work was to alter the structure of a fatigue crack so as to slow or arrest crack growth. Nickel was electroplated onto the crack surfaces of ASTM A36 steel that had been machined into ASTM E399 Compact tension specimens. Prior to treatment, fatigue cracks were developed using an R ratio of zero. During the plating operation the cracks were held open at 95% of the load utilized during fatigue cycling. A Watt's plating bath was utilized for a 1-hour electrodeposition period. Upon returning the specimens to cyclic loading the arrest of fatigue cracks was observed. The arrest state was maintained for several tens of thousands of cycles. It was also found that reapplication of the treatment was repeatedly effective at re-inducing crack arrest. In many cases the specimens behaved as if the crack was removed and only the chevron notch of the specimen remained. This called into question whether the crack re-initiation life was dominated by the treated crack or by the notch from which the original crack had initiated. The prediction of crack re-initiation is a key question that was explored. This answer is vital for determining how frequently a treatment needs to be repeated in order to maintain cracks in an arrested state. Subsequent analysis revealed that a power law relationship existed between the number of cycles required to re-initiate a crack and a modified version of the stress intensity factor. This new factor was altered to reflect the intended electroplating dosage. Future work will build on the success of these findings by examining electrodeposition candidates that will provide enhanced corrosion resistance coupled with effective crack arrest properties.

### Removal of Zn<sup>2+</sup> from aqueous solutions onto polypyrrole modified reticulated vitreous carbon electrodes

Vanessa Villela, Jucelânia Tramontina, Denise S. Azambuja, \*Clarisse M. S. Piatnicki  
 Instituto de Química, Universidade Federal do Rio Grande do Sul, Av. Bento Gonçalves, 9500,  
 CP 15003, 91501-970, Porto Alegre-RS, Brazil. \*e-mail: clarisse@iq.ufrgs.br

Industrial activities are the most important sources of environmental contamination by heavy metals, the removal of which from dilute aqueous effluents is a relevant concern. Materials such as reticulated vitreous carbon (RVC) have been employed as porous electrodes obtaining high conversion rates.<sup>1,2</sup> On the other hand, during the last decade, there has been widespread interest in conducting polymers such as polypyrrole, both for academic purposes and for potential applications.<sup>3</sup> The aim of this work is to investigate removal of Zn<sup>2+</sup> from aerated sulfuric-sulfate synthetic solutions through electrochemical reduction at polypyrrole coated RVC electrodes. It must be emphasized that 16 mg L<sup>-1</sup> is the lowest initial concentration of Zn<sup>2+</sup> reported in the literature<sup>4</sup> while in the present study it is 10 mg L<sup>-1</sup>. The electrochemical cell was a conventional three-electrode assembly, the working electrodes being either 60 or 100 ppi RVC prisms of approximately 1.0 cm x 1.0 cm x 1.5 cm, either bare or polypyrrole modified, fixed to a graphite rod using a conducting graphite paint. The PPy films were electrodeposited on the RVC surface and electroreduced to PPy<sup>0</sup> before use. Samples containing 10 mg L<sup>-1</sup> in K<sub>2</sub>SO<sub>4</sub> 0.1 mol L<sup>-1</sup> were prepared from a 1000 mg L<sup>-1</sup> ZnSO<sub>4</sub> stock solution in sulfuric medium. Reduction of Zn<sup>2+</sup> was then carried out at -1.10, -1.40 and -1.50 V vs. SCE, under stirring, between 60 to 90 minutes, in aerated solution, at several pH values. Monitoring of Zn<sup>2+</sup> decay was carried out by anodic stripping voltammetry using a model 303A polarograph from EGG. An aliquot of the sample was electrolyzed at a hanging mercury drop electrode, the anodic stripping peak current being used to determinate the Zn<sup>2+</sup> ion concentration.

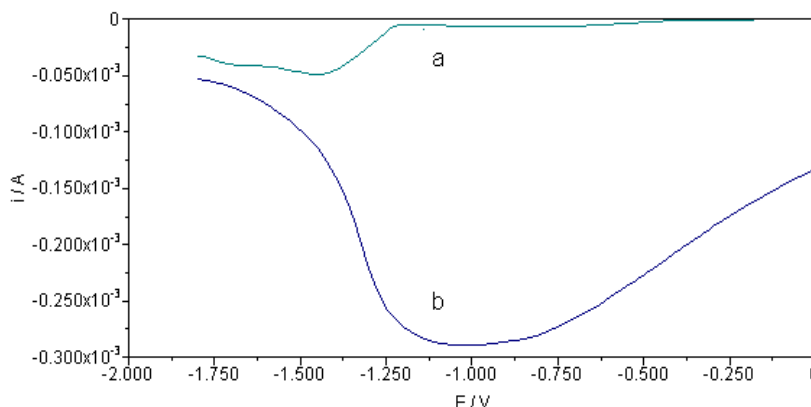


Figure 1. Linear voltammetry in sulfuric-sulfate solution at pH 4.8 containing Zn<sup>2+</sup> 10 mg L<sup>-1</sup>. a) RVC electrode and b) RVC/PPy<sup>0</sup> modified electrode scanned between 0.000 and -1.750 V vs. SCE, under stirring. Scan rate 0.020 V s<sup>-1</sup>.

The highest Zn<sup>2+</sup> removal value found is 79.6 % at 100 ppi RVC/PPy<sup>0</sup> electrolyzed for 90 minutes at -1.1 V and pH 6.5. The removal efficiency depends on the electrodeposition potential and the RVC porosity, the reduction reaction being a mixed mass transport-kinetic controlled one. The higher overpotential needed for the H<sub>2</sub> evolution reaction to occur in the experimental condition favors zinc deposition even at low pH values. The proposed procedure presents practical interest in the development of flow systems for removal of low heavy metals concentration from effluents.

#### References

1. Lanza, M.R.V., Bertazzoli, R., J. Appl. Electrochem., 2000, **30**,61-70.
2. Ruotolo, L. A. M., Gubulin, J. C., Chemical Engineering Journal, 2011, **171**, 1170-1177.
3. Mohsen G., Hossein E., Synthetic Metals, 2012, **162**,1429–1433.
4. Mohsen G., Hossein E., J. Vinyl & Additive Technology, 2013,**19**, 213-218.

## Novel reflection-type optical fiber methane sensor based on a no-core fiber structure

Li Shanya<sup>1</sup>, Li Xueming<sup>1\*</sup>, Zhou Lang<sup>2</sup>, Yang Jianchun<sup>2</sup>, Luo Binbin<sup>1</sup>

<sup>1</sup>College of Chemistry and Chemical Engineering, <sup>2</sup>College of Optoelectronic Engineering, Chongqing University, Chongqing, 400044

*E-mail: Lishanyacqu@163.com; xuemingli@cqu.edu.cn.*

Early detection of methane concentration in coal mine is particularly important. A novel and simple reflection-type optical fiber methane sensor based on a no-core fiber structure is reported. Cryptophanes A/polysiloxane is used to form methane-sensitive film on the surface of no-core fiber by automatically dip-coating technique. The dip-coating solution was composed by 600  $\mu\text{mol}$  cryptophane A, 1 g siloprene K1000, 0.2 g siloprene cross-linking agent K11 and 15 mL dichloromethane. The nickel reflecting layer was plated on the end of no-core fiber by electroless deposition method, the other end of no-core fiber was spliced with SMF-28 optical fiber. Both thickness and refractive index of the sensitive film were measured by using F20-UVX thickness meter. The result showed that the film thickness was about 300 nm and the refractive index reduces 0.01 with increasing 1% methane concentration. The sensing experiments indicated that the peak wavelength of reflection interference spectra showed a significant blue-shift linearly with the increase in the methane concentration from 0 to 3.5%(v/v), and the sensitivity was about 1.5 nm/% CH<sub>4</sub> and the minimal detection limit for methane gas was confirmed as approximately 0.2 % for 5 cm sensing region, which agreed well with that of numerical simulate by OptiFDTD software. Compared with the other optical fiber methane sensors, this fiber sensor has simple structure, lower cost, better sensitivity and selectivity.

**Keywords:** methane sensor, supra-molecular, cryptophanes A, thin film, refractive index

[1] AMIR, H. K., PAUL, C. H. L., NABLY, M., BEHRAAD, B. 2012. Highly Sensitive Supra-molecular Thin Films for Gravimetric Detection of Methane. Sensors and Actuator B-Chemical, 161, 954-960.

The work was supported by the National Natural Science Foundation of China (61271059)

## Preparation of nanostructured NiO by hydrothermal for H<sub>2</sub>S gas sensor

**Gotan H. Jain**

KKHA Arts, SMGL Commerce and SPHJ Science College,

Chandwad- 423101, India

*ail : gotanjain@rediffmail.com, Contact Détails : +919423474476*

A hydrothermal process was used for the synthesis of nanostructured NiO with and without capping reagent (surfactant). All reagents were purchased from Sigma-Aldrich and used as received. First, 0.1 M of the Nickel Chloride (NiCl<sub>2</sub>) a precursor of Nickel was dissolved in 20 mL of deionised water-ethanol (1:1 volume ratio), a 5 M NaOH solution was prepared in deionised water for maintaining pH of the reaction, a 0.2 M Thioglycerol, a capping reagent, solution was prepared in isopropyl alcohol with constant stirring to make clear solution. Then these prepared homogeneous solutions (25 ml each with surfactant and without surfactant) were transferred in 50 ml capacity autoclaves with Teflon liner by uniform heating at 200 °C for 15 h. These reaction mixtures were heated at a rate of 5 °C min<sup>-1</sup>. After completion of the reaction, it was cooled to room-temperature and powdered samples were collected by centrifugation. Powdered sample was thoroughly washed with deionised water and ethanol. Samples were dried at 80 °C for 12 h. The materials were characterized by XRD, UV, SEM and TEM techniques. The thick films of these materials were prepared by screen printing and proposed for gas sensor applications. The gas sensing performance of NiO thick films (with and without surfactant) was tested to H<sub>2</sub>S, LPG, H<sub>2</sub>, NH<sub>3</sub>, Ethanol, CO, CO<sub>2</sub>, and O<sub>2</sub>, at the operating temperature ranging from 100 °C to 450 °C, they showed maximum response to H<sub>2</sub>S for 10 ppm gas concentration.

**Keywords:** *Hhydrothermal, Nano NiO, Thick film, H<sub>2</sub>S.*



# Surface modification by a graded carbon thin film for better tribological and anti-oxidation properties

M Abdul Samad<sup>1</sup>

<sup>1</sup>) Department of Mechanical Engineering, King Fahd University of Petroleum and Minerals, Dhahran - 31261, KSA

## Abstract

An ultra-thin film of carbon using filtered cathodic vacuum arc technique with a graded structure in the top layer ( $\leq 1.5$  nm) of a cobalt surface is evaluated for its tribological and anti-oxidation properties. A unique approach of embedding carbon in the top layer of a cobalt surface with a ion energy of 90 eV using filtered cathodic vacuum arc technique (FCVA) was established in our previous studies [1,2]. Even though the embedded layer was less than 1 nm, it exhibited excellent tribological and antioxidation properties. Hence, looking at the potential of the above developed method and the scope of further improvement, the present study is undertaken whereby the main objective is to embed carbon into the cobalt surface using different ion energies.

Two different ion energies of 60 eV and 90 eV respectively are used in succession to achieve carbon embedding in the top layer of the cobalt surface. The developed technique showed promising results in terms of tribology and anti-oxidation, demonstrating its potential to be used in the surface modification of different surfaces such as the magnetic media for higher areal densities.

Auger electron spectroscopy (AES) and transmission electron microscopy are used to characterize the graded layer in terms of its thickness and chemical composition. Ball-on-disk wear tests are conducted on the bare cobalt and modified cobalt surface to characterize the wear resistance. The modified cobalt surface with the graded structure showed a low coefficient of friction of  $\sim 0.2$  when compared to the bare cobalt surface ( $\sim 0.7$ ). AES analysis on the modified surface showed a significant improvement in the oxidation resistance of the surface when compared to the bare cobalt surface.

**Key words:** Nanotribology, surface modification, cobalt, anti-oxidation, carbon

- [1]. ABDUL SAMAD, M., RISMANI, E., YANG, H., SINHA, S. K., & BHATIA, C. S. 2011. Overcoat free surface modification for lower magnetic spacing and improved tribological properties for higher areal densities, *Tribology Letters*, 43(3) p.247-256
- [2]. ABDUL SAMAD, M., YANG, H., SINHA, S. K., & BHATIA, C. S. 2011. Effect of carbon embedding on the tribological properties of magnetic media surface with and without a perfluoropolyether (PFPE) layer, *Journal of Physics D: Applied Physics*, 44

## Effects of Oxynitridation Temperatures on the Physical and Electrical Properties of Sputtered Zr on Si Substrate

Yew Hoong Wong<sup>1,a</sup> and Kuan Yew Cheong<sup>2</sup>

<sup>1</sup> Department of Mechanical Engineering, Faculty of Engineering, University of Malaya, 50603 Kuala Lumpur, Malaysia.

<sup>2</sup> Electronic Materials Research Group, School of Materials and Mineral Resources Engineering, Engineering Campus, Universiti Sains Malaysia, 14300 Nibong Tebal, Seberang Perai Selatan, Penang, Malaysia.

<sup>a</sup> E-mail: [yhwong@um.edu.my](mailto:yhwong@um.edu.my) / Tel.: +603-7967-7022 ext 2654 / Fax: +603-7967-5317

### Abstract

In this work, thermally oxynitrided Zr thin films on Si have been produced. The thickness of the produced films was approximately 12 nm. This nanometre-scaled film was applied as gate dielectric in metal-oxide-semiconductor-based devices. Physical and electrical properties of the films on Si have been systematically investigated. Simultaneous oxidation and nitridation of sputtered Zr thin films on Si was performed in N<sub>2</sub>O environment for 5 min at 500–1100°C in order to optimize the oxynitride properties. The atomic microscopy force results indicated that the surface root-mean-square roughness of the sample increased with the increasing oxidation and nitridation temperature. Positive effective oxide charges were revealed in all investigated oxides. The electrical results showed that the sample oxidized and nitrided at 700°C had the highest breakdown field, owing to its lowest positive effective oxide charge, interface-trap density, and total interface-trap density.

**Keywords:** *Nanometre film; high- $\kappa$  gate dielectric; metal-oxide-semiconductor*

## Functional films of granular metal-carbon for sensing applications

Guenter Schultes<sup>1,2</sup>

<sup>1</sup> University of Applied Sciences, Goebenstrasse 40, 66117 Saarbruecken, Germany

<sup>2</sup> ZeMA gGmbH, Eschberger Weg, 66121 Saarbruecken, Germany

*guenter.schultes@htwsaar.de*

This contribution demonstrates the benefits of thin granular metal-carbon systems as strain sensing thin films. These materials consist of metal clusters of nanometer scale embedded in a matrix of carbon. The clusters are electrically insulated from each other, i.e. the conduction is hindered by barriers and may be influenced strongly by applying strain. We are able to demonstrate gauge factors of 20 to 30 in some metal-carbon systems [1], that is a tenfold sensitivity compared to common strain gauge materials. In addition, the temperature coefficient of resistivity (TCR) is small and adjustable, if Ni as a metal is used. Thin films of this composition are deposited by means of sputtering technology onto several substrates as steel, polymers, ceramics and glass, allowing the construction of different sensors. Fig. 1a gives an impression of the films microstructure. Some atomic layers of graphite like carbon surround nickel clusters, which are insulated from each other. Pattern definition is the next step to design a grid of adequate resistance with small tolerances, length and overall dimensions. Laser ablation by means of an ultrafast-pulsed ( $< 10$  ps) laser beam with a wavelength of 355 nm is an appropriate method. The process can be adjusted to remove just the thin film from the polyimide as shown in Fig. 1b or from some other substrate materials.

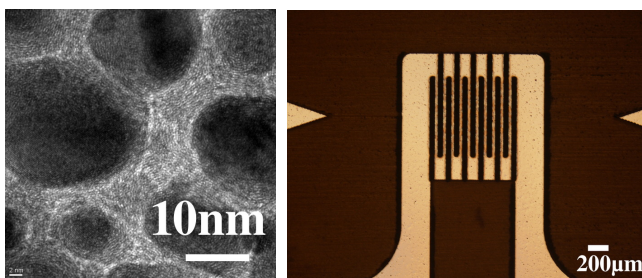


Fig. 1: (a) Transmission electron micrograph of a nickel-carbon composite. (b) The pattern definition is performed with an ultrafast-pulsed laser system. The photograph shows an example of a grid on polyimide.

The results of prototypes with these foil strain gauges on force transducers and load cells in a Wheatstone bridge circuit are discussed.

An innovative technological approach for pressure sensors is presented as well. Membrane and sensor body are based on the ceramic material  $ZrO_2$  stabilized with  $Y_2O_3$  yielding very good mechanical properties. Due to the ceramics inherent electrical insulation and the use of granular metal-carbon thin films a simplified set-up is feasible. The membrane carries a highly sensitive layer that is structured to a Wheatstone bridge just by some laser cuts. Electrical contacts are securely bonded directly on the sensor layer without the need for contact layers. We further demonstrate a construction and assembling technique of the complete pressure sensor including threat and housing. Raw results and signals processed by means of an embedded electronic are discussed.

***Keywords: metal carbon thin film, pressure sensor, force sensor,***

***LASER structuring, strain gauges***

[1] R. KOPPERT, H. SCHMID-ENGEL, ST. UHLIG, A.-C. PROBST, D. GOETTEL, G. SCHULTES, U. WERNER, Structural and physical properties of highly piezoresistive nickel containing hydrogenated carbon thin films, *Diamond & Related Materials*, 25 (2012) 50-58, <http://dx.doi.org/10.1016/j.diamond.2012.01.03>

**Topic: Symposium 2: *Advances in Thin Films,*  
Metal oxide, carbon, nitrides etc based thins Films**

**Preferred mode of presentation: oral**

## **Metal oxide semiconductors thin films deposition by Supersonic Plasma Jet Source for energetic applications**

Dell'Orto<sup>1</sup>, Caldirola<sup>1</sup>, Roman, Riccardi<sup>1</sup>

<sup>1</sup>University of Milano-Bicocca, Physics Department, Piazza della Scienza 3, Milano-Italy

*elisa.dellorto@unimib.it* (Dell'Orto Elisa)

In the last years nanotechnologies have proved to be extremely promising for the development of new functional materials for technological applications of great importance, such as in the energetical, biological and environmental sections [1]–[4]. Metal oxides are widely used for environmental and energy applications, including self-cleaning surfaces, sensors, generation of hydrogen through the photo-electrolysis of water, lithium batteries and the third generation photovoltaics (e.g. Dye Sensitized Solar Cell (DSSC) and solid state solar cells). It has been shown that the properties of these materials are strongly dependent on the size of the clusters and their nanometric morphology. TiO<sub>2</sub> and ZnO are two of the mainly studied oxides, due to their low cost, versatility, availability, low toxicity and chemical stability [5]–[7]. Thin films are produced mainly by sol-gel methods and different types of Chemical Vapor Deposition (CVD) and Physical Vapor Deposition (PVD) [8]–[11]. Despite the developments made in this field, it is difficult to find a deposition method that allows making films with precise control of the morphology, the chemical structure and the porosity. Another open challenge is to point out a process that is easily reproducible on a large scale, allowing a production at industrial level and cost containment.

We propose an innovative deposition process (Supersonic Plasma Jet Deposition), that allows to realize thin films with a hierarchically structured morphology and a controlled chemistry. The innovative idea is to separate the process of synthesis of the material in the gas phase, starting from a precursor that interacts with a cold plasma, and the process of growth of the film, that will happen in a supersonic jet. In this way the control of the stoichiometry and the control of the morphology are decoupled, and they could be optimized independently. In this communication we present the deposition technique and

the characterization of chemical, morphological and electric properties of ZnO, TiO<sub>2</sub> and Zn/TiO<sub>2</sub> thin films realized. The peculiar properties of these films make them suitable for applications in solid state solar cell devices and lithium batteries.

**Keywords:** *Functional, template, materials, edition, solar cell (Maximum Five)*

[1] E. COMINI, "Metal oxide nano-crystals for gas sensing." *Anal. Chim. Acta*, vol. 568, no. 1–2, pp. 28–40, May 2006.

[2] M. SUZUKI, T. ITO, AND Y. TAGA, "Photocatalysis of sculptured thin films of TiO<sub>2</sub>," *Appl. Phys. Lett.*, vol. 78, no. 25, p. 3968, 2001.

[3] T. MIYAGI, M. KAMEI, T. MITSUHASHI, T. ISHIGAKI, AND A. YAMAZAKI, "Charge separation at the rutile/anatase interface: a dominant factor of photocatalytic activity," *Chem. Phys. Lett.*, vol. 390, no. 4–6, pp. 399–402, Jun. 2004.

[4] O. BRIAN AND M. GRATZEL, "A low-cost, high-efficiency solar cell based on dye-sensitized colloidal TiO<sub>2</sub> film," *Nature*, vol. 353, p. 737, 1991.

[5] J. XU, Z. CHEN, J. A. ZAPIEN, C.-S. LEE, AND W. ZHANG, "Surface Engineering of ZnO Nanostructures for Semiconductor-Sensitized Solar Cells." *Adv. Mater.*, vol. 26, no. 31, pp. 5337–67, Aug. 2014.

[6] Z. L. WANG, "Zinc oxide nanostructures: growth, properties and applications," *J. Phys. Condens. Matter*, vol. 16, no. 25, pp. R829–R858, Jun. 2004.

[7] J.-H. YUM, P. CHEN, M. GRÄTZEL, AND M. K. NAZEERUDDIN, "Recent developments in solid-state dye-sensitized solar cells." *ChemSusChem*, vol. 1, no. 8–9, pp. 699–707, Jan. 2008.

[8] M. PAZOKI, N. TAGHAVINIA, Y. ABDI, F. TAJABADI, G. BOSCHLOO, AND A. HAGFELDT, "CVD-grown TiO<sub>2</sub> particles as light scattering structures in dye-sensitized solar cells," *RSC Adv.*, vol. 2, no. 32, p. 12278, 2012.

[9] J. ALTMAYER, S. BARTH, AND S. MATHUR, "Influence of precursor chemistry on CVD grown TiO<sub>2</sub> coatings: differential cell growth and biocompatibility," RSC Adv., vol. 3, no. 28, p. 11234, 2013.

[10] R. SCOTTI, L. CONZATTI, M. D'ARIENZO, B. DI CREDICO, L. GIANNINI, T. HANEL, P. STAGNARO, A. SUSANNA, L. TADIELLO, AND F. MORAZZONI, "Shape controlled spherical (0D) and rod-like (1D) silica nanoparticles in silica/styrene butadiene rubber nanocomposites: Role of the particle morphology on the filler reinforcing effect," Polymer (Guildf.), vol. 55, no. 6, pp. 1497–1506, Mar. 2014.

[11] S. MANN, S. L. BURKETT, S. A. DAVIS, C. E. FOWLER, N. H. MENDELSON, S. D. SIMS, D. WALSH, AND N. T. WHILTON, "Sol - Gel Synthesis of Organized Matter," Chem. Mater., vol. 4756, no. 97, pp. 2300–2310, 1997.

## **Metal oxide semiconductors thin films deposition by Supersonic Plasma Jet Source for energetic applications**

Dell'Orto<sup>1</sup>, Caldirola<sup>1</sup>, Riccardi<sup>1</sup>

<sup>1</sup>University of Milano-Bicocca, Physics Department, Piazza della Scienza 3, Milano-Italy

*elisa.dellorto@unimib.it (Dell'Orto Elisa)*

In the last years nanotechnologies have proved to be extremely promising for the development of new functional materials for technological applications of great importance, such as in the energetical, biological and environmental sections [1]–[4]. Metal oxides are widely used for environmental and energy applications, including self-cleaning surfaces, sensors, generation of hydrogen through the photo-electrolysis of water, lithium batteries and the third generation photovoltaics (e.g. Dye Sensitized Solar Cell (DSSC) and solid state solar cells). It has been shown that the properties of these materials are strongly dependent on the size of the clusters and their nanometric morphology. TiO<sub>2</sub> and ZnO are two of the mainly studied oxides, due to their low cost, versatility, availability, low toxicity and chemical stability [5]–[7]. Thin films are produced mainly by sol-gel methods and different types of Chemical Vapor Deposition (CVD) and Physical Vapor Deposition (PVD) [8]–[11]. Despite the developments made in this field, it is difficult to find a deposition method that allows making films with precise control of the morphology, the chemical structure and the porosity. Another open challenge is to point out a process that is easily reproducible on a large scale, allowing a production at industrial level and cost containment.

We propose an innovative deposition process (Supersonic Plasma Jet Deposition), that allows to realize thin films with a hierarchically structured morphology and a controlled chemistry. The innovative idea is to separate the process of synthesis of the material in the gas phase, starting from a precursor that interacts with a cold plasma, and the process of growth of the film, that will happen in a supersonic jet. In this way the control of the stoichiometry and the control of the morphology are decoupled, and they could be optimized independently. In this communication we present the deposition technique and



the characterization of chemical, morphological and electric properties of ZnO, TiO<sub>2</sub> and Zn/TiO<sub>2</sub> thin films realized. The peculiar properties of these films make them suitable for applications in solid state solar cell devices and lithium batteries.

**Keywords:** *Functional, template, materials, edition, solar cell (Maximum Five)*

[1] E. COMINI, "Metal oxide nano-crystals for gas sensing." *Anal. Chim. Acta*, vol. 568, no. 1–2, pp. 28–40, May 2006.

[2] M. SUZUKI, T. ITO, AND Y. TAGA, "Photocatalysis of sculptured thin films of TiO<sub>2</sub>," *Appl. Phys. Lett.*, vol. 78, no. 25, p. 3968, 2001.

[3] T. MIYAGI, M. KAMEI, T. MITSUHASHI, T. ISHIGAKI, AND A. YAMAZAKI, "Charge separation at the rutile/anatase interface: a dominant factor of photocatalytic activity," *Chem. Phys. Lett.*, vol. 390, no. 4–6, pp. 399–402, Jun. 2004.

[4] O. BRIAN AND M. GRATZEL, "A low-cost, high-efficiency solar cell based on dye-sensitized colloidal TiO<sub>2</sub> film," *Nature*, vol. 353, p. 737, 1991.

[5] J. XU, Z. CHEN, J. A. ZAPIEN, C.-S. LEE, AND W. ZHANG, "Surface Engineering of ZnO Nanostructures for Semiconductor-Sensitized Solar Cells." *Adv. Mater.*, vol. 26, no. 31, pp. 5337–67, Aug. 2014.

[6] Z. L. WANG, "Zinc oxide nanostructures: growth, properties and applications," *J. Phys. Condens. Matter*, vol. 16, no. 25, pp. R829–R858, Jun. 2004.

[7] J.-H. YUM, P. CHEN, M. GRÄTZEL, AND M. K. NAZEERUDDIN, "Recent developments in solid-state dye-sensitized solar cells." *ChemSusChem*, vol. 1, no. 8–9, pp. 699–707, Jan. 2008.

[8] M. PAZOKI, N. TAGHAVINIA, Y. ABDI, F. TAJABADI, G. BOSCHLOO, AND A. HAGFELDT, "CVD-grown TiO<sub>2</sub> particles as light scattering structures in dye-sensitized solar cells," *RSC Adv.*, vol. 2, no. 32, p. 12278, 2012.

[9] J. ALTMAYER, S. BARTH, AND S. MATHUR, “Influence of precursor chemistry on CVD grown TiO<sub>2</sub> coatings: differential cell growth and biocompatibility,” *RSC Adv.*, vol. 3, no. 28, p. 11234, 2013.

[10] R. SCOTTI, L. CONZATTI, M. D’ARIENZO, B. DI CREDICO, L. GIANNINI, T. HANEL, P. STAGNARO, A. SUSANNA, L. TADIELLO, AND F. MORAZZONI, “Shape controlled spherical (0D) and rod-like (1D) silica nanoparticles in silica/styrene butadiene rubber nanocomposites: Role of the particle morphology on the filler reinforcing effect,” *Polymer (Guildf.)*, vol. 55, no. 6, pp. 1497–1506, Mar. 2014.

[11] S. MANN, S. L. BURKETT, S. A. DAVIS, C. E. FOWLER, N. H. MENDELSON, S. D. SIMS, D. WALSH, AND N. T. WHILTON, “Sol - Gel Synthesis of Organized Matter,” *Chem. Mater.*, vol. 4756, no. 97, pp. 2300–2310, 1997.

# Surface modification by a graded carbon thin film for better tribological and anti-oxidation properties

M Abdul Samad<sup>1</sup>

<sup>1</sup>) Department of Mechanical Engineering, King Fahd University of Petroleum and Minerals, Dhahran - 31261, KSA

## Abstract

An ultra-thin film of carbon using filtered cathodic vacuum arc technique with a graded structure in the top layer ( $\leq 1.5$  nm) of a cobalt surface is evaluated for its tribological and anti-oxidation properties. A unique approach of embedding carbon in the top layer of a cobalt surface with a ion energy of 90 eV using filtered cathodic vacuum arc technique (FCVA) was established in our previous studies [1,2]. Even though the embedded layer was less than 1 nm, it exhibited excellent tribological and antioxidation properties. Hence, looking at the potential of the above developed method and the scope of further improvement, the present study is undertaken whereby the main objective is to embed carbon into the cobalt surface using different ion energies.

Two different ion energies of 60 eV and 90 eV respectively are used in succession to achieve carbon embedding in the top layer of the cobalt surface. The developed technique showed promising results in terms of tribology and anti-oxidation, demonstrating its potential to be used in the surface modification of different surfaces such as the magnetic media for higher areal densities.

Auger electron spectroscopy (AES) and transmission electron microscopy are used to characterize the graded layer in terms of its thickness and chemical composition. Ball-on-disk wear tests are conducted on the bare cobalt and modified cobalt surface to characterize the wear resistance. The modified cobalt surface with the graded structure showed a low coefficient of friction of  $\sim 0.2$  when compared to the bare cobalt surface ( $\sim 0.7$ ). AES analysis on the modified surface showed a significant improvement in the oxidation resistance of the surface when compared to the bare cobalt surface.

**Key words:** Nanotribology, surface modification, cobalt, anti-oxidation, carbon

- [1]. ABDUL SAMAD, M., RISMANI, E., YANG, H., SINHA, S. K., & BHATIA, C. S. 2011. Overcoat free surface modification for lower magnetic spacing and improved tribological properties for higher areal densities, *Tribology Letters*, 43(3) p.247-256
- [2]. ABDUL SAMAD, M., YANG, H., SINHA, S. K., & BHATIA, C. S. 2011. Effect of carbon embedding on the tribological properties of magnetic media surface with and without a perfluoropolyether (PFPE) layer, *Journal of Physics D: Applied Physics*, 44

## Ferroelectric and structural properties of lanthanides-doped tetragonal tungsten bronze $\text{Ba}_2\text{LnFeNb}_4\text{O}_{15}$ thin films prepared by pulsed laser ablation

T. Hajlaoui<sup>1</sup>, C. Harnagea<sup>1</sup>, and A. Pignolet<sup>1</sup>

<sup>1</sup>Institut National de la Recherche Scientifique – Centre Énergie, Matériaux,  
Télécommunications,  
1650 Boulevard Lionel-Boulet, Varennes, Québec, J3X 1S2, Canada

Contact author: [thameur.hajlaoui@emt.inrs.ca](mailto:thameur.hajlaoui@emt.inrs.ca) (Thameur Hajlaoui)

### Abstract:

Tetragonal tungsten bronze ferroelectrics are currently studied for the elaboration of new multifunctional materials. Recent studies on  $\text{Ba}_2\text{LnFeNb}_4\text{O}_{15}$  (TTB-Ln) bulk ceramics demonstrate that these materials display the spontaneous formation of a magnetic phase of Barium hexaferrite within the TTB phase during the ceramic processing, producing a novel multiferroic composite at room temperature [1]. Using bulk ceramic as targets, TTB-Ln thin films have been obtained by radiofrequency magnetron sputtering and they displayed dielectric permittivities comparable to bulk ceramics [2]. The main objective of our study is to investigate the physical properties of thin films of TTB-Ln grown by pulsed laser deposition (PLD) in order to optimize their multiferroic properties.

Epitaxial thin films of  $\text{Ba}_2\text{LnFeNb}_4\text{O}_{15}$  (Ln = Eu, Sm, and Nd) have been successfully obtained using many substrates by PLD. Among of those substrates we have used  $\text{SrTiO}_3\text{:Nb}$  STO:Nb (100), MgO (100) and  $\text{Gd}_3\text{Ga}_5\text{O}_{12}$  GGG (100) in order to study the effect of the substrate on the structural and functional properties. The optimum conditions of deposition have been established, which are  $T_s \approx 750^\circ\text{C}$  and  $\text{PO}_2 \approx 7.5$  mTorr. The surface morphology and structural properties were investigated. The thickness of all thin films was estimated to be about 380 nm. A structure of grains having diameters of 100 nm was observed. The lattice parameters have been estimated to be around  $a \approx 12.422$  Å and  $c \approx 3.921$  Å which are slightly smaller than those observed in the bulk [1], indicative of a compressive stress buildup in the films during the deposition. Ferroelectric macroscopic P-E hysteresis loops have demonstrated the existence of a spontaneous polarization at room temperature in TTB-Ln thin films. The measured remnant

polarization in the  $\text{Ba}_2\text{EuFeNb}_4\text{O}_{15}$  thin films deposited on STO:Nb (100) is  $0.46 \mu\text{C}/\text{cm}^2$ , only slightly smaller than the remnant polarization in the bulk reported to be  $0.6 \mu\text{C}/\text{cm}^2$  [1]. An investigation of the microscopic electromechanical properties of the studied thin films showed the existence of a piezoelectric signal and of piezoelectric hysteresis loops, which confirm the ferroelectric behavior of the prepared thin films.

**Keywords:** *thin film, pulsed laser deposition, multiferroic*

[1] M. Josse, O. Bidault, F. Roulland, E. Castel, A. Simon, D. Michau, R. Von der Muhll, O. Nguyen, M. Maglione, *Solid State Sciences* 11 (2009) 1118–1123.

[2] R. Bodeux, D. Michau, M. Josse, M. Maglione, accepted in *Solid State Sciences*

## **Mixed matrix membranes incorporated with ZIF-12 for improved polymeric gas separation membranes: Synthesis and characterization**

Safak Boroglu M., Ugur M., Boz I.

Istanbul University, Faculty of Engineering, Chemical Engineering Department, Avcilar, 34320, Istanbul, Turkey.

[mehtap@istanbul.edu.tr](mailto:mehtap@istanbul.edu.tr)

Gas separation using membranes has been extensively studied because it is considered to be one of the most energy-efficient separation processes. Among candidate materials for membrane fabrication, polymers remain the most practical and economical choice. The demand for the development of new polymeric materials for gas storage and gas separations has been rapidly increasing. Metal organic frameworks (MOFs) have recently gained considerable attention as promising nanoporous materials for gas storage and gas separation applications due to their exceptional physical and chemical properties such as high porosity, large surface area, a wide range of pore sizes, high gas uptake capacities, and good chemical and mechanical stability. As a subfamily of MOFs zeolitic imidazolate frameworks (ZIFs) not only exhibit the advantages of MOFs but also have exceptional high thermal and chemical stability. Studies on ZIF membranes with supports have shown promising gas separation properties for various gas pairs. ZIFs are built by connecting metal clusters (mainly Zn or Co) through functionalized imidazole linkers. Because of the organic linkers presented in ZIF structure, it is believed that ZIFs can achieve better affinity and interaction with polymeric materials [1]. Polyetherimide (PEI) is a promising polymeric membrane material because of its outstanding physical, thermal, and chemical stability. In addition, PEI membrane could be easily fabricated because it is soluble in solvents such as N-methyl-2-pyrrolidone (NMP) and N,N-dimethylacetamide (DMAc).

In this study, the preparation of polyetherimide (PEI)/ZIF-12 nanocomposite membranes were studied in different nanoparticles compositions (0-5-10-15-30 wt. %). The membrane morphologies were observed by the scanning electron microscopy (SEM).

Thermal properties of membranes were determined by thermogravimetric analyses (TGA). The gas permeabilities of PEI/ ZIF-12 nanocomposite membranes were measured for H<sub>2</sub>, CH<sub>4</sub> and CO<sub>2</sub> pure gases at 35°C and the selectivities of all membranes were calculated.

ZIF-12 nanoparticles were prepared by a modified recipe reported by Wang et al. [2]. The phase structure of the ZIF-12 sample was confirmed by the powder X-ray diffraction patterns. The characteristic peaks of the as-prepared ZIF-12 particles are in good agreement with good crystallinity in the literature [2-3]. The newly synthesized ZIF-12 nano-particles with a particle size of ~200 nm were compatibly incorporated in PEI membranes as novel mixed matrix membranes (MMMs).

**Keywords:** *Metal–organic frameworks, polymer membranes, ZIF-12, gas separation.*

[1] HUANG, X.-C., ZHANG, J.-P., CHEN, X.-M. 2003. [Zn(bim)<sub>2</sub>](H<sub>2</sub>O)<sub>1.67</sub>: a metalorganic open-framework with sodalite topology. Chinese Science Bulletin, 48, 1531–1534.

[2] HE, M., YAO, J., LIU, Q., ZHONG, Z., WANG, H. 2013. Toluene-assisted synthesis of RHO-type zeolitic imidazolate frameworks: synthesis and formation mechanism of ZIF-11 and ZIF-12. Dalton Transactions, 42, 16608-16613.

[3] PARK, K.S., NI, Z., COTE, A.P., CHOI, J.Y., HUANG, R., URIBE-ROMO, F.J., CHAE, H.K., O'KEEFE, M., YAGHI, O.M. 2006. Exceptional chemical and thermal stability of zeolitic imidazolate frameworks. Proceedings of the National Academy of Science, 103, 10186-10191.

## Physical Properties of Chemically Sprayed ZnO Films

Olvera M. de la L., Maldonado Arturo

Departamento de Ingeniería Eléctrica-SEES, Centro de Investigación y de Estudios Avanzados del Instituto Politécnico Nacional, CINVESTAV-IPN, D. F., MEXICO.

Email: molvera@cinvestav.mx (Olvera M. de la L)

Undoped ZnO thin films were deposited on sodocalcic glass substrates by the spray pyrolysis technique. Atomization of the starting solution was carried out by ultrasonic excitation. The effect of the water content in the starting solution on the structural, optical, and morphological properties of the films was studied. All films showed mirror-like finish with good adherence on the substrate. A preferential (002) growth was observed in the films, although the increase in the water content leads to a slight increase in the (101) peak intensity. From photoluminescence measurements at room temperature it was found that, as the water content in the starting solution increases, both the UV and the green emission increase at a constant substrate temperature; at high substrate temperature increases, the green PL peak intensity shows an increase, reaching a maximum at 425 °C. Surface morphology changes slightly with water content variation in the starting solution, since films deposited with low water content show hexagonal shaped grains with round edges and a wide distribution in the average size; whereas well defined rod-shaped grains are present in films manufactured from a starting solution with high water content.

**Keywords:** *Thin Solid Films, Zinc Oxide, Spray Pyrolysis, Semiconductor Oxide.*



## **A novel method of producing field-assisted wide bandgap transparent conductive electrodes, and its application to GaN-based lateral-type light-emitting diodes**

TaeHo Lee<sup>1</sup>, Ju Hyun Park<sup>1</sup>, Kyoung Heon Kim<sup>1</sup>, Byeong Ryong Lee<sup>1</sup>, MinJu Kim<sup>1</sup>, Hee Woong Shin<sup>1</sup>, Tae Geun Kim<sup>1</sup>

<sup>1</sup>School of Electrical Engineering, Korea University, Anam-dong 5-ga, Sungbuk-gu, Seoul 136-701, Republic of Korea

[jp6018@korea.ac.kr](mailto:jp6018@korea.ac.kr) and [tgkim1@korea.ac.kr](mailto:tgkim1@korea.ac.kr)

Gallium nitride (GaN) based light-emitting diodes (LEDs) have gained much attention, especially for solid state lightings. There are many applications including automotive headlights, various types of displays, and indoor/outdoor lightings [1]. In spite of various applications, further enhancement regarding the efficiency and power of LED is required to replace conventional lighting systems. This can be achieved by improving the performance of transparent conductive electrodes (TCEs) in the way of increasing the current injection and current spreading while maintaining high optical transparency. Significant efforts have been made to overcome this challenge for many years. A materialistic approach for solving the problem has led to the development of various TCEs. Indium-doped tin oxide (ITO), in particular, has been widely used as TCEs for GaN based LEDs [2]. But the indium is a rare earth and light absorption material which lowers the light extraction efficiency. Therefore, a novel TCE with both high optical transparency and low contact resistivity is highly demanded as a breakthrough for high performance LEDs.

Accordingly, our group has developed the novel field assisted method of producing a wide bandgap TCE having both high optical transparency and low contact resistivity [3-4]. Field assisted electrical breakdown process (EBD) was used for wide bandgap materials such as silicon oxide. After EBD process, a conductive filament is formed in the TCE layer which improves the current injection while maintaining the optical

transmittance. Consequently, we applied this novel method to GaN based lateral-type LEDs, and their electrical and optical characteristics will be presented at the conference.

**Keywords:** *Gallium nitride (GaN), light-emitting diode (LED), transparent conductive electrodes (TCE), electrical breakdown process (EBD)*

[1] TAN, S. T., SUN, X. W., DEMIR, H. V. & DENBAARS, S. P. 2012. Advances in the LED materials and architectures for energy-saving solid-state lighting toward “lighting revolution”. IEEE Photonics Journal, 4, 613-619.

[2] YANG, Y., HUANG, Q., METZ, A. W., NI, J., JIN, S., MARKS, T. J., MADSEN, M. E., DIVENERE, A. & HO, S. T. 2004. High-Performance Organic Light-Emitting Diodes Using ITO Anodes Grown on Plastic by Room- Temperature Ion-Assisted Deposition. Advanced Materials, 16, 321-324.

[3] KIM, H. D., AN, H. M., KIM, K. H., KIM, S. J., KIM, C. S., CHO, J. H., SCHUBERT, E. F. & KIM, T. G. 2013. A Universal Method of Producing Transparent Electrodes Using Wide-Bandgap Materials. Advanced Functional Materials, 24, 1575-1581.

[4] KIM, S. J., KIM, H. D., KIM, K. H., Shin, H. W., HAN, I. K. & KIM, T. G. 2014. Fabrication of wide-bandgap transparent electrodes by using conductive filaments: performance breakthrough in vertical-type GaN LED. Scientific Reports, 4, 5827.

## **Hierarchical Cassie states on superhydrophobic micropillar arrays**

N. Encinas<sup>1</sup>, L. Mammen<sup>1</sup>, F. Schellenberger<sup>1</sup>, C. K. Weiss<sup>1</sup>, D. Vollmer<sup>1</sup>, H.-J. Butt<sup>1</sup>

<sup>1</sup>Max Planck Institute for Polymer Research, Ackermannweg 10, D-55128, Mainz,  
Germany

*encinas@mpip-mainz.mpg.de*

Control over the wettability properties of a surface is a matter of high importance in microfluidics, fog harvesting, self-cleaning materials or anti-biofouling coatings. In the present work we follow a strategy to modify wetting behavior of patterned surfaces by decorating with colloids. Flat-top SU-8 photoresist micropillars with different diameters and surface fractions were prepared by means of photolithography. After silica coating following the Stöber reaction the arrays were decorated in a Langmuir trough with monolayers of hexagonally arranged polystyrene particles. The final step was the hydrophobization of the surfaces under chemical vapor deposition of a fluorosilane. Mono- and multilayers of particles were prepared in order to reduce the roll-off angle and the contact angle hysteresis on the micropillars. This effect is attributed to the overhangs in which air pockets are entrapped between micropillars and the interstitials of the particles. The stabilization of the Cassie state by a particle layer is also evaluated by reducing the size, thus contact of particles in an oxygen plasma chamber. The Cassie states, the pinning of droplets and the transition to the Wenzel state were imaged by laser scanning confocal microscopy. A hierarchy of Cassie states was observed.

***Keywords: Superhydrophobicity, Patterned surfaces, Colloids, Confocal microscopy***

[1] MAMMEN, L., BLEY, K., PAPADOPOULOS, P., SCHELLENBERGER, F., ENCINAS, N., BUTT, H.-J., WEISS, C. & VOLLMER, D. 2014.. Functional superhydrophobic surfaces made of Janus micropillars. *Soft Matter*, DOI: 10.1039/c4sm02216e.

## **Quorum quenching and matrix degrading enzymes in multilayer coatings prevent bacterial biofilm formation on urinary catheters**

*Kristina Ivanova<sup>‡</sup>, Margarida M. Fernandes<sup>‡</sup>, Antonio Francesko<sup>‡</sup>, Tzanko Tzanov<sup>\*‡</sup>*

<sup>‡</sup> Group of Molecular and Industrial Biotechnology, Department of Chemical Engineering, Universitat Politècnica de Catalunya, Rambla Sant Nebridi 22, 08222, Terrassa, Spain

Bacteria that grow in complex biofilm communities embedded in a self-produced extracellular polymeric matrix are a global health concern. When these microorganisms colonize indwelling medical devices they cooperate through a quorum sensing mechanism and form well-established biofilms that resist antibiotic treatments and cause difficult to treat infections. Despite the recent advances in antimicrobial research, efficient antibiofilm strategies for control of bacteria adhesion and proliferation on the surfaces of medical devices are still needed. In this study, quorum quenching acylase and exopolysaccharide-degrading  $\alpha$ -amylase enzymes were deposited on silicone urinary catheters in a layer-by-layer fashion in order to investigate their potential to prevent bacterial biofilm formation. The assembling of the hybrid multilayer coatings on the catheter surface was achieved by alternate deposition of negatively charged enzymes and positively charged polyethylenimine. The hybrid coatings simultaneously interfered with the bacterial quorum sensing and degraded the biofilm polysaccharide matrix, enhancing up to 30 % the inhibition of *Pseudomonas aeruginosa* biofilm formation when compared to the enzymes applied individually on the silicone material. Furthermore, the dual-species biofilm occurrence (*Pseudomonas aeruginosa* and

*Escherichia coli*) on silicone urinary catheters was significantly reduced under dynamic conditions in an *in vitro* catheterized bladder model. The developed antibiofilm coatings did not cause toxicity on the human fibroblasts cell line (BJ-5ta) over seven days and thus constitute a viable alternative to control bacterial biofilms on urinary catheters.

## Relationships between structure and electrical sensitivity of breathable membranes

Annarosa Gugliuzza<sup>1</sup>, Valentino Pingitore<sup>2</sup>, Enrico Drioli<sup>1,3,4</sup>

<sup>1</sup> Research Institute on Membrane Technology-National Research Council (ITM-CNR),  
Via Pietro Bucci 17C, Rende (CS), 87036, Italy

<sup>2</sup>Department of Physics, University of Calabria, Via Pietro Bucci, 33C, Rende (CS),  
87036, Italy

<sup>3</sup>Department of Chemical Engineering and Materials, University of Calabria, Via Pietro  
Bucci, 33C, Rende (CS), 87036, Italy

<sup>4</sup>WCU Energy Engineering Department, College of Engineering, Hanyang University,  
Korea

*a.gugliuzza@itm.cnr.it / Ph +39 0984 492026 (presenting and crossponding author's)*

Membranes are ideal microarrays where different and complementary functions can be accommodated, taking the privilege to combine surface and bulk transport in a unique layer. Here, the fabrication of outstanding electrically responsive membranes is discussed together with their ability to work as humidity sensors and microclimate regulators. Designated nano-assembly approaches have generated highly ordered microporous membranes, which support electrical charge pathways. A pH-assisted build up has deposited functional carbon nanotubes in hybrid networks, while pendant chemical moieties have directed nanotubes stratification and aggregation, resulting in a different number of interconnections and quality-electrical charge pathways. An electrical current passage of the order of mA is measured at very low voltages through better-quality nanotubes networks, while a variation of the electrical resistance up to 28% can be detected as a response to severe changes in the surrounding environment. Assisted proton diffusion with resulting doping effect by water is envisioned as a potential mechanism for the responsive behavior. Also, the nanotubes moieties are identified as transport regulators due to their different ability to interact with water molecules through

donor/acceptor interactions, thus yielding modular moisture exchange. These membranes are candidate to provide attractive solutions to the construction of ultra-smart devices.

**Keywords:** *Smart membranes, sensors, carbon nanotubes, layer-by-layer, electrical conduction*

[1] GUGLIUZZA, A. 2014. Smart Membranes and Sensors, Wiley-Scrivener Publishing, Salem, Massachusetts, USA.

[2] PINGITORE, V., GUGLIUZZA, A. 2013. Fabrication of Porous Semiconductor Interfaces by pH-Driven Assembly of Carbon Nanotubes on Honeycomb Structured Membranes. J. Phys. Chem. C. 117, 26562.

[3] PINGITORE, V., DRIOLI, E., GUGLIUZZA, A. 2014. Electro-responsive membranes for humidity comfort sensors. Submitted

[4] GUGLIUZZA A., DRIOLI, E. 2013. A review on membranes engineering for innovation in wearable fabrics and protective textiles. J. Membr. Sci., 446, 350.

## **Nanostructured thin films for solar selective absorbers and infrared selective emitters.**

E. Ollier<sup>1</sup>, N. Dunoyer<sup>1</sup>, H. Szambolics<sup>1</sup>, G. Lorin<sup>1</sup>

<sup>1</sup>Institute of New Energy Technologies and Nanomaterials LITEN - French Alternative Energies and Atomic Energy Commission CEA, 17 rue des martyrs, 38054 Grenoble Cedex 9, France.

[Emmanuel.ollier@cea.fr](mailto:Emmanuel.ollier@cea.fr) / Phone: +33 7 87 04 65 61

Engineering of the optical functions of surfaces and thin films is becoming critical for many applications, especially for renewable energy technologies. Selective solar absorbers are key elements of all existing solar thermal systems. Solar thermal panels and Concentrated Solar Power (CSP) systems aim at producing heat and electricity. In both technologies, a surface receives the solar radiation and the material is designed to have the highest optical absorptivity of the solar radiation in the visible wavelength range where the solar intensity is the highest. It also has a low emissivity in the infrared range in order to avoid radiative losses. Infrared emitter materials are used in the domain of thermophotovoltaics (TPV) and more recently for solar thermophotovoltaics. In both cases, an accurate control of the optical function of the infrared emitter material is mandatory for TPV conversion efficiency. Current material solutions usually consist in depositing interferential thin films or cermet materials for solar absorbers [1] [2] and in materials patterned with expensive microtechnology techniques for TPV [3]. Structured surfaces consisting in 2D photonic crystals have been proposed [4] because they present interesting properties compared to interferential solutions as high acceptance angle for absorption and directionality for infrared emission. Even if processes for low cost production are being investigated [5], most realizations still use expensive lithography paths needed for structuring materials at nanoscale.

This work presents a low cost pathway to realize 2D nanophotonic crystals with tunable cut-off wavelength. They are realized with refractory materials able to sustain high temperatures like molybdenum. Fabrication process mechanisms are detailed. These nanostructured materials have a dual function as selective solar absorber and/or selective



infrared emitters. Optical properties are investigated by spectrophotometry in the visible and infrared ranges at room temperature. Very high absorptivity is obtained with more than 95% absorption in the visible range. The cut-off wavelength can be tuned in the 1 to 2 micron wavelength range. In addition, infrared emissivity is investigated at high temperatures. This novel pathway for producing low cost nanostructured tunable selective absorbers and emitters provides new opportunities for solar absorption in Concentrated Solar Power, Solar Thermophotovoltaics, Solar Thermo-Electrical Generators and for infrared emission control in thermophotovoltaic technologies.

**Presenting author:** [Emmanuel.oilier@cea.fr](mailto:Emmanuel.oilier@cea.fr); CEA-LITEN; France

**Preferred Mode of presentation:** Oral

**Topic:** Symposia 2: Advances in Thin Films (Nanostructured and Architecturally Designed Coatings, Smart Surfaces)

**Keywords:** *thin films, nanostructuration, photonic crystals, optical absorbers, infrared emitters.*

[1] KENNEDY, C.E. 2002. Review of Mid- to High-Temperature Solar Selective Absorber Materials. NREL/TP-520-31267.

[2] SELVAKUMAR, N., BARSHILIA, H.C. 2012. Review of physical vapor deposited (PVD) spectrally selective coatings for mid- to high-temperature solar thermal applications. Sol. Energy Mater. Sol. Cells, 98, p. 1.

[3] FLEMING, J. G., LIN, S. Y., EL-KADY, I., BISWAS, R., HO K.M. 2002. All-metallic three-dimensional photonic crystals with a large infrared bandgap. Nature 417(6884), 52–55.

[4] WANG, J., CHEN, Z., LI, D. 2010. Simulation of two-dimensional Mo photonic crystal surface for high-temperature solar-selective absorber. Phys. Status Solidi A 207, No. 8, 1988–1992 / DOI 10.1002/pssa.200925573.

- [5] OLLIER, E., DUNOYER, N., DELLEA, O., SZAMBOLICS, H. 2014. Nanostructured refractory thin films for solar applications. SPIE Optics + Photonics symposium 17 - 21 August 2014, San Diego.

## **Self-lubricating organic coatings via embedded submicrocontainers: preparation and functionalities**

*D. Grigoriev<sup>1</sup>, M. Schenderlein<sup>1</sup>, S. Aidarova<sup>2</sup>, A. Tleuova<sup>2</sup> and H. Möhwald<sup>1</sup>*

*<sup>1</sup>Max-Planck Institute of Colloids and Interfaces, Am Muehlenberg 1, 14476 Potsdam-Golm, Germany*

*<sup>2</sup>Kazakh National Technical University, Satpaev Street 22a, 050013, Almaty, Republic of Kazakhstan*

Development of materials having an ability to restore their function in response to destructive impacts is nowadays one of most rapidly growing fields in the modern material engineering. Polymeric materials and coatings with the features to heal their integrity or to recover their protective function autonomously are of great interest in counteracting and combating diverse deterioration processes like fatigue, corrosion, wear etc.

Embedding of micro-, submicro- or even and nanocontainers in the coating matrix is today most frequently used approach to impart to this coating one or several specific feedback active features. Depending on the type of the active ingredient loaded in containers, on their size and morphology, coatings with the properties aimed at various kinds of self-recovering may be prepared.

In this contribution, we present the preparation of organic coatings with self-lubricating function. A key element of these is the lubricant filled organic/inorganic submicrocontainers prepared via emulsion route on the basis of oil-in-water Pickering emulsions.

Morphology, size and surface charge of containers filled with several lubricants as well as the efficiency of their enclosure were investigated using modern experimental methods such as dynamic light scattering (DLS), Zeta-potential measurements, scanning electron microscopy (SEM), transmission electron microscopy (TEM), thermogravimetric analysis (TGA) etc.

The benefits of new containers based self-lubricating coatings in comparison with common ones were shown by means of tribological measurements revealing at least 20% reduce of friction coefficient for the former.

## Effect of Layering on pH-Triggered Swelling of Nanothin Hydrogels

V. Kozlovskaya<sup>1</sup>, E. Kharlampieva<sup>1</sup>, and J.F. Ankner<sup>2</sup>

<sup>1</sup>Dept. of Chemistry, U. of Alabama at Birmingham, Birmingham, AL 35294

<sup>2</sup>Spallation Neutron Source, Oak Ridge National Lab, Oak Ridge, TN, 37831

*E-mail: anknerjf@ornl.gov*

Stimuli-responsive hydrogels have numerous applications in drug delivery, tissue engineering, and sensing [1]. Layer-by-Layer (LbL) assembly performed via alternating adsorption of polymers at surfaces enables fabrication of films on almost any substrate, with nano-scale control over film composition, structure, and properties [2]. The stimuli-triggered behaviors of these systems are provided by functional groups not involved in covalent binding [3-5]. Ultrathin multilayer-derived hydrogels have been investigated for responsiveness by varying chemical composition, assembly routes, and charge balance, rather than internal organization. The absence of studies on hydrogel architecture is due at least partly to the difficulty of controlling the structural organization of randomly chemically linked networks. Another challenge is the inability of conventional probes to resolve internal structure at the nanoscale. This lack of knowledge prevents rational design of surface nanogels. In the present study, we demonstrate tunable swelling of ultrathin hydrogels via controlled internal structure. The hydrogel films are composed of pH-sensitive poly(methacrylic acid) (PMAA) networks produced by chemical cross-linking of PMAA layers within hydrogen-bonded LbL templates [6]. We have produced highly swollen hydrogels, swelling to almost twenty times the original dry thickness at pH=7.5, from well-stratified ‘spin-assisted’ templates. Analogous films created by conventional LbL ‘dipping’ exhibited a three-fold smaller swelling. Neutron reflectivity measurements of these films as-grown, after cross-linking, and in contact with pH-controlled buffer solutions have provided the crucial structural information needed to comprehend how their swelling behavior relates to layer quality and interdiffusion.

**Keywords:** *hydrogel, layer-by-layer growth, neutron reflectometry, stimulus responsive*

[1] TOKAREV, I. and MINKO, S. 2009. *Adv. Mater.*, 21, 241-47.

[2] *Multilayer Thin Films: Sequential Assembly of Nanocomposite Materials* (Eds. DECHER, G. and SCHLENOFF, J.), Wiley & Sons, 2012.

[3] KOZLOVSKAYA, V., HIGGINS, W., CHEN, J., and KHARLAMPIEVA, E. 2011. *Chem. Commun.*, 47, 8352-54.

[4] KOZLOVSKAYA, V., WANG, Y., HIGGINS, W., CHEN, J., CHEN, Y., and KHARLAMPIEVA, E. 2012. *Soft Matter*, 8, 9828-39.

[5] WANG, Y., KOZLOVSKAYA, V., ARCIBAL, I., CROPEK, D., and KHARLAMPIEVA, E. 2013. *Soft Matter*, 9, 9420-29.

[6] KOZLOVSKAYA, V., ZAVGORODNYA, O., WANG, Y., ANKNER, J.F., and KHARLAMPIEVA, E. 2013. *ACS Macro Lett.*, 2, 226-29.

## **Novel strategies for the prevention of *Pseudomonas aeruginosa* biofilms on urinary catheters**

Margarida M. Fernandes, Kristina Ivanova, Antonio Francesko, Tzanko Tzanov

Group of Molecular and Industrial Biotechnology, Department of Chemical Engineering, Universitat Politecnica de Catalunya, Rambla Sant Nebridi 22, 08222, Terrassa, Spain

Biofilms are bacterial communities embedded in a self-produced polymeric matrix that commonly grow on urinary catheters. This mode of growing is regulated by a quorum-sensing (QS) system, a unique mechanism of communication that bacterial cells use through the secretion and uptake of small hormone-like molecules, called autoinducers. Due to their innate resistance to the immune system and low susceptibility to antibiotics, the microbial biofilms are difficult to treat and are a major factor in the morbidity and mortality of most infectious diseases. Methods by which the initial stages of bacterial attachment and biofilm formation can be restricted or prevented are therefore needed. This work is about the creation of alternative strategies to coat silicone urinary catheters and thus control *P. aeruginosa* biofilm formation. The developed integrated technological platform is comprised of: i) a quorum quenching enzyme, previously shown to be able to degrade and thus scramble the *P. aeruginosa* signals and delay the process of biofilm formation, and ii) nanoantibiotics, commonly used antibiotics to which bacteria has developed resistance that once transformed into nanospheres regained their ability to kill and eradicate *P. aeruginosa* biofilms. The functionalization of the urinary catheters was achieved with a layer-by-layer technique by alternate deposition of the enzymes and nanoantibiotics. The coating prevented the biofilm formation on the catheters, measured both under static and dynamic conditions in an *in vitro* catheterized bladder model. Moreover, by measuring the minimum biofilm eradication concentration, the quorum-quenching enzyme was found to increase the susceptibility of *P. aeruginosa* biofilm to the nanoantibiotics. This work underscores the potential of such combined treatment/coatings in preventing and eradicating biofilms at the same time avoiding the development of resistance mechanisms.

## Unprecedented tuning of the in-plane easy axis in (100) magnetite films grown by IR-PLD

A. Bollero<sup>1</sup>, F.J. Pedrosa<sup>1</sup>, J.L.F. Cuñado<sup>1</sup>, J. Rial<sup>1</sup>, M. Sanz<sup>2</sup>, M. Oujja<sup>2</sup>, E. Rebollar<sup>2</sup>, J.F. Marco<sup>2</sup>, J. de la Figuera<sup>2</sup>, M. Monti<sup>2</sup>, M. Castillejo<sup>2</sup>, M. Garcia-Hernandez<sup>3</sup>, F. Mompean<sup>3</sup>, N.M. Nemes<sup>4</sup>, T. Feher<sup>5</sup>, B. Nafradi<sup>6</sup>, L. Forro<sup>6</sup>, J. Camarero<sup>1</sup>

<sup>1</sup> IMDEA Nanoscience, Madrid, Spain.

<sup>2</sup> Instituto Química Física Rocasolano, CSIC, Madrid, Spain.

<sup>3</sup> Instituto Ciencias de Materiales de Madrid, CSIC, Madrid, Spain.

<sup>4</sup> Dep. Física Aplicada III, UCM, Madrid, Spain.

<sup>5</sup> Dep. Theoretical Physics, BUTE, Budapest, Hungary.

<sup>6</sup> Institute of Condensed Matter Physics, EPFL-SB-ICMP-LPMC, Lausanne, Switzerland.

*E-Mail: alberto.bollero@imdea.org*

Thin films can be considered as ideal cases for the design of improved bulk magnets [1]. Magnetite ( $\text{Fe}_3\text{O}_4$ ) is attracting much interest in the last years due to its robust ferrimagnetism down to nanometer thickness, good electrical conductivity and presumed half-metal character. In particular,  $\text{Fe}_3\text{O}_4$  films have been tentatively used in spin-valves and spin-LEDs.  $\text{Fe}_3\text{O}_4$  presents a low-temperature metal-insulator transition, the Verwey transition ( $T_V$ ) which has also been proposed for spintronic applications. An open question is to what extent the preparation of  $\text{Fe}_3\text{O}_4$  films can affect their detailed magnetic properties, such as the magnetic anisotropy axis. This information is required to efficiently apply  $\text{Fe}_3\text{O}_4$  films in spintronic applications.

Most of studies dealing with bulk and  $\text{Fe}_3\text{O}_4$  thin film systems show room temperature (RT) in-plane  $\langle 110 \rangle$  magnetic easy axis. By contrast, we show in this work the preparation of pure stoichiometric  $\text{Fe}_3\text{O}_4$  thin films with RT easy axes along the in-plane  $\langle 100 \rangle$  directions [2], i.e. rotated by  $45^\circ$  respect to previous studies.

$\text{Fe}_3\text{O}_4$  films have been grown by ablation from a sintered hematite target using a nanosecond infrared (IR) laser at 1064 nm and a substrate temperature of 750 K [3]. Single crystal substrates of  $\text{SrTiO}_3$ ,  $\text{MgAl}_2\text{O}_4$  and  $\text{MgO}$  have been used. All films consisted of stoichiometric  $\text{Fe}_3\text{O}_4$  and presented a Verwey transition at  $T_V=115-118$  K.

RT in-plane hysteresis loops were measured by vectorial-MOKE as a function of the direction of the applied magnetic field in the 0-360° range with an angular step of 5°. For all epitaxial films under study, the highest coercivity and remanence are found at 0, 90, 180 and 270°, thus orthogonal to each other, while the lowest coercivity values are found between them. This results in a well-defined four-fold symmetry indicative of biaxial magnetic anisotropy [2]. In order to verify this result, ferromagnetic resonance (FMR) experiments have been carried out at 9.4 GHz frequency. The angular dependence of the in-plane resonance field at RT for the Fe<sub>3</sub>O<sub>4</sub> layers proves that the easy axes are indeed the in-plane <100> directions.

All angular studies here shown in addition to spin-polarized low-energy electron microscopy experiments demonstrate easy-axis orientation along in-plane <100> directions, i.e., differing from that of bulk magnetite or films prepared by other techniques, and thus demonstrating the possibility of tuning the easy axis orientation.

**Keywords:** *Thin films, magnetite, spintronics, magnetic properties*

[1] *NANOPYME*: [www.nanopyme-project.eu](http://www.nanopyme-project.eu)

[2] MONTI, M., SANZ, M., OUJJA, M., REBOLLAR, E., CASTILLEJO, M., PEDROSA, F.J., BOLLERO, A., CAMARERO, J., CUÑADO, J.L.F., NEMES, N. M., MOMPEAN, F.J., GARCIA-HERNANDEZ, M., NIE, S., MCCARTY, K.F., N'DIAYE, A.T., CHEN, G., SCHMID, A.K, MARCO J.F. & DE LA FIGUERA J. 2013. Room temperature in-plane 100 magnetic easy axis for Fe<sub>3</sub>O<sub>4</sub>/SrTiO<sub>3</sub>(001):Nb grown by infrared pulsed laser deposition. *J. Appl. Phys.* 114, 223902.

[3] SANZ, M., OUJJA, M., REBOLLAR, E., MARCO, J.F., DE LA FIGUERA, J., MONTI, M., BOLLERO, A., CAMARERO, J., PEDROSA, F.J., GARCIA-HERNANDEZ, M. & CASTILLEJO, M. 2013. Stoichiometric magnetite grown by infrared nanosecond pulsed laser deposition. *Applied Surface Science* 282, 642.



## Pulsed laser deposition and characterization of Epitaxial Thin Films of $\epsilon$ -Fe<sub>2</sub>O<sub>3</sub> and $\epsilon$ -Al<sub>x</sub>Fe<sub>2-x</sub>O<sub>3</sub>.

**L. Corbellini<sup>1</sup>, C. Harnage<sup>1</sup>, C. Lacroix<sup>2</sup>, A. Morin<sup>3</sup>, X. Ropagnol<sup>1</sup>, T. Ozaki<sup>1</sup>, D. Menard<sup>3</sup> and A. Pignolet<sup>1</sup>**

<sup>1</sup>*Institut National de la Recherche Scientifique, Université du Québec  
Varenes, Québec, Canada J3X 1S2*

<sup>2</sup>*Department of Electrical Engineering, Polytechnique Montréal,  
Montréal, Québec, Canada H3C 3A7*

<sup>3</sup>*Department of Engineering Physics, Polytechnique Montréal,  
Montréal, Québec, Canada H3C 3A7*

$\epsilon$ -Fe<sub>2</sub>O<sub>3</sub> is a metastable intermediate phase of iron (III) oxide, between maghemite ( $\gamma$ -Fe<sub>2</sub>O<sub>3</sub>) and hematite ( $\alpha$ -Fe<sub>2</sub>O<sub>3</sub>). Epsilon ferrite has been investigated essentially because of its ferrimagnetic ordering with a Curie temperature of circa 500 K<sup>[1]</sup>. However, given its orthorhombic crystal structure that belongs to the non centrosymmetric space group *Pna2<sub>1</sub>*, it should exhibit ferroelectric behavior along with magnetoelectric coupling of the two orders (potentially making it one of the few room temperature multiferroic materials)<sup>[2,3]</sup>. Moreover, the material is characterized by strong magnetic anisotropy, resulting in a ferromagnetic resonance (FMR) frequency in the THz range in the absence of magnetic field and at room temperature. This is of particular interest given its potential use in short-range wireless communications (e.g. 60GHz WiFi) and ultrafast computer non-volatile memories<sup>[4-6]</sup>.

Due to its metastable nature,  $\epsilon$ -Fe<sub>2</sub>O<sub>3</sub> needs to undergo size confinement in order to be stabilized: that is the reason why it has been mainly synthesized by sol-gel as nanoparticles embedded inside a SiO<sub>2</sub> matrix. Recently however, deposition of epitaxial thin films of  $\epsilon$ -Fe<sub>2</sub>O<sub>3</sub> on SrTiO<sub>3</sub> (111) was demonstrated<sup>[7]</sup>; in this case the stabilization is thought to be due to both epitaxial strain and interface interaction between the substrate and the film.

We report the growth by Pulsed Laser Deposition of epitaxial thin films of  $\epsilon$ -Fe<sub>2</sub>O<sub>3</sub> and  $\epsilon$ -Al<sub>x</sub>Fe<sub>2-x</sub>O<sub>3</sub> on different single crystal substrates, and the study of the influence of aluminum doping on the structural, magnetic and dielectric properties. In particular, we focused our attention on the effect of Al inclusion inside the  $\epsilon$ -Fe<sub>2</sub>O<sub>3</sub> lattice, which should result in the improvement of the electric properties, given the ferroelectric nature of the isostructural AlFeO<sub>3</sub>, and lowering of the FMR frequency due to non-magnetic nature of Al. Electric and magnetic properties were probed both macroscopically and locally through ferroelectric measurements/vibrating sample magnetometer and piezoelectric/magnetic force microscopy (PFM – MFM), while measurements of the ferromagnetic resonance were conducted by direct FMR probing and through THz light absorption.

[1] S. Ohkoshi *et al.*, *Angew. Chem. Int. Ed.* **46**, 8392 (2007);

[2] E. Tronc *et al.*, *J. Solid State Chem.* **139**, 93 (1998);

[3] M. Gich *et al.*, *Nanotechnology* **17**, 687 (2007);

[4] M. Nakajima, A. Namai, S. Ohkoshi, T. Suemoto, *Optics Express* **18**, 18260 (2010);

- [5] H.C. Siegmann *et al.*, J. Magn. Magn. Mater. **151**, L8 (1995);
- [6] C.H. Back *et al.*, Science **285**, 864 (1999);
- [7] M. Gich *et al.*, Appl. Phys. Lett. **96**, 112508 (2012).

## The structural and magnetic characterization of NiO/Co<sub>90</sub>Fe<sub>10</sub> bilayers

Yu-Chi Chang<sup>1</sup>, Ko-Wei Lin<sup>1,\*</sup>, Johan van Lierop<sup>2,\*</sup>

<sup>1</sup> Department of Materials Science and Engineering, National Chung Hsing University,  
Taichung 402, Taiwan

<sup>2</sup> Department of Physics and Astronomy, University of Manitoba, Winnipeg, R3T 2N2,  
Canada

*kwlin@dragon.nchu.edu.tw/ johan@physics.umanitoba.ca*

The exchange bias effect [1] usually refers to the exchange coupling between a ferromagnetic (FM) material and an antiferromagnetic (AF) or ferrimagnetic material. In this work, we investigate the effects of post deposition magnetic field annealing on modifying the magnetic properties of NiO (~ 30 nm)/Co<sub>90</sub>Fe<sub>10</sub> (~ 20 nm) bilayers prepared by using a dual-ion beam sputtering deposition technique [2]. The top NiO layer consisted of fcc structure while the bottom Co<sub>90</sub>Fe<sub>10</sub> (at%) layer consisted of hcp structure, as characterized by XRD and TEM. The NiO/Co<sub>90</sub>Fe<sub>10</sub> bilayer exhibited soft magnetic property with a coercivity,  $H_c \sim 10$  Oe, as characterized by VSM. The post deposition magnetic field annealing processes (at different applied field (1-3 kG) and temperatures (up to 400 °C) under vacuum) were carried out in order to set the exchange bias coupling between AF NiO and FM CoFe. Results have shown that the NiO/Co<sub>90</sub>Fe<sub>10</sub> bilayer exhibited similar soft magnetic properties under  $H_{app.} = 3$  kG at 300 °C for 1 hour. However, with further increasing the annealing temperature to 400 °C, an enhanced  $H_c$  (~ 550 Oe) with no observed loop shift was measured for an annealed NiO/Co<sub>90</sub>Fe<sub>10</sub> bilayer. Our results indicate that the magnetization reversal mechanism was affected strongly by exchange coupling between the Co<sub>90</sub>Fe<sub>10</sub> and NiO layers and by modified spin structures as they are aligned during the field annealing processes.

Research was supported by Ministry of Science and Technology (MOST) of Taiwan and NSERC of Canada.

***Keywords: exchange bias, ion-beam sputtering deposition technique, magnetic thin films***

[1] NOGUES, J. et al., 2005, Phys. Rep. 422, 65.

[2] LIN, K.-W. et al., 2012, Appl. Phys. Lett. 100, 122409.

## **Anisotropic Chiral Colloidal Lithography**

Sabine Portal<sup>1</sup>, Carles Corbella<sup>2</sup>, Oriol Arteaga<sup>3</sup>, Bart Kahr<sup>4</sup>

<sup>1</sup>Dep. Photonics and Terahertztechnology, Ruhr-University Bochum, Universitystr. 150,  
44780 Bochum, Germany.

<sup>2</sup>Research Group Reactive Plasmas, Ruhr-University Bochum, Universitystr. 150, 44780  
Bochum, Germany.

<sup>3</sup>Dep. Applied Physics and Optics, Barcelona University, 647 Diagonal Av., 08028  
Barcelona, Spain.

<sup>4</sup>Kahr Research Group, NYU Department of Chemistry, Brown 656, Molecular Design  
Institute, New York, NY 10003-6688

*E Mail/ Contact Details (sabineportal@hotmail.com)*

Preferred mode of presentation: Oral

**Symposia 2:** *Advances in Thin Films*

Abstract

Surfaces with optical activity were produced in large area by combining bottom-up and top-down material synthesis.

In a previous work, surface nanopatterning was realized by colloidal lithography which consists in a dry-etching process with argon ions using colloidal crystals as sacrificial templates, the incidence angle was varied and the azimuthal angle remained constant [1]. Silica sub-micron particles produced by sol-gel synthesis were assembled in triangular arrays by Langmuir-Blodgett technique to produce the colloidal template [2]. Then, the template pattern was transferred onto the underlying substrate by dry-etching.

The novelty of this work is the fabrication of optically active surfaces by production of chiral patterns. Chiral anisotropy was introduced in the material during the etching process by using oblique incidence and changing the azimuthal angle. The etched material presented screw-shaped pillars and it showed circular dichroism and circular birefringence in the visible range and near infrared. The anisotropic active materials were characterized by scanning electron microscopy (SEM), confocal microscopy, polarimetry and Fourier transform infrared spectroscopy (FTIR). Finally, thin films of gold of 10 to 30 nm were deposited on top of the pillars in order to enhance the optical activity by plasmon resonance: circular dichroism and circular birefringence present both an amplitude enhancement and a red shift after deposition of the gold layer. These trends are amplified at oblique polarimetric measurement.

**Keywords:** *Colloidal lithography, anisotropy, chirality, polarimetry, plasmon resonance*

[1] PORTAL, S., RUBIO-ROY, M., CORBELLA, C., VALLVE, M.A., IGNES-MULLOL, J., BERTRAN, E. 2009. Influence of incident ion beam angle on dry etching of silica sub-micron particles deposited on Si substrates. *Thin Solid Films*, 518 (5),1543-1548.

[2] PORTAL-MARCO, S., VALLVE, M.A., ARTEAGA, O., IGNES-MULLOL, J., CORBELLA, C., BERTRAN, E. 2012. Structure and physical properties of colloidal crystals made of silica particles. *Colloids and Surfaces A: Physicochem. Eng. Aspects* 401, 38–47.

## Structural and Magnetic Study of Mn-doped CeO<sub>2</sub> Diluted Magnetic Semiconductor Prepared by Sol-gel Method

Yang Sheng-hong<sup>a</sup>, Zhang Yue-li

State Key Laboratory of Optoelectronic Materials and Technologies // School of Physics & Engineering, Sun Yat-sen University, Guangzhou 510275, P.R. China

<sup>a</sup>E-mail: [stsyshh@mail.sysu.edu.cn](mailto:stsyshh@mail.sysu.edu.cn) (Yang SH)

In this paper, Mn-doped CeO<sub>2</sub> diluted magnetic semiconductor were prepared by the sol-gel method. The magnetic and structural properties were studied. The magnetic measurements of Mn-doped CeO<sub>2</sub> clearly indicate the ferromagnetic behavior, and the Curie temperature of the samples is above room temperature. The magnetization saturations were 0.11  $\mu_B$ /Mn, 0.53  $\mu_B$ /Mn and 0.56  $\mu_B$ /Mn for samples with 1%, 3% and 5% of Mn, respectively. We attribute this ferromagnetic state to the presence of dilute localized magnetic moments inside the semiconductor matrix. In fact, within the accuracy of our measurements, X-ray diffraction data reveal the formation of single-phase structurally isomorphous CeO<sub>2</sub>, indicating there are not any secondary phases of Mn substituted for Ce in CeO<sub>2</sub> host. Furthermore, our analysis on the optical absorbance measurements and Raman scattering shows a change in the band gap and an increase in the oxygen vacancies. As the content of Mn increases, the crystallite size and the optical band gap decrease, but the ferromagnetic behavior increase.

**Keywords:** *Mn-doped CeO<sub>2</sub>, Diluted magnetic semiconductor, Sol-gel method, Room temperature ferromagnetism*

[1] SINGHAL R. K., KUMARI P., KUMAR SUDHISH, DOLIA1 S. N., XING Y. T., ALZAMORA M., DESHPANDE U. P., SHRIPATHI T. & SAITOVITCH ELISA 2011. Room Temperature Ferromagnetism in Pure and Co- and Fe-doped CeO<sub>2</sub> Dilute Magnetic Oxide: Effect of Oxygen Vacancies and Cation Valence. J. Phys. D: Appl. Phys., 44, 165002.

# Synthesis and magnetic properties of Co thin films

A. Kharmouche

Laboratory of Surfaces and Interfaces Studies of Solid Materials (LESIMS),  
Department of Physics, Faculty of Technology, Ferhat Abbas University Sétif1, 19000, Sétif, Algeria

[kharmouche\\_ahmed@yahoo.fr](mailto:kharmouche_ahmed@yahoo.fr) & [kharmouche\\_ahmed@univ-setif.dz](mailto:kharmouche_ahmed@univ-setif.dz)

## Abstract.

We synthesized series of thin layers of cobalt on semiconductor, conductor and insulator substrates, using thermal heating process, under a pressure of  $10^{-7}$  mbar. The incident beam strikes the substrates under normal and oblique incidences within a home-made design. The thickness ranges from 18 to 400 nm. To investigate the static magnetic properties, the hysteresis loops are performed by means of Physical Property Measurement System (PPMS) with Quantum Design Instrument and Alternating Gradient Field Magnetometer (AGFM). The zero-field magnetic structure has been investigated by Magnetic Force Microscopy (MFM), using a Veeco 3100 apparatus. To investigate the dynamic magnetic properties, and particularly the magnetic anisotropy in Co/Si films, we used Brillouin Light Scattering (BLS) experiments, using a (2x3)-pass tandem Fabry-Perot interferometer, and Ferromagnetic Resonance (FMR) technique. All the films are polycrystalline and exhibit a hexagonal close packed (hcp) structure, with the  $\langle 0001 \rangle$  texture. Many films are under stress. The easy magnetization axis lies in the plane of the film whatsoever is the substrate nature. Coercivity is very sensitive to surface roughness, stress and crystallite size. In Co evaporated on glass, coercivity evolution versus thickness follows a  $t^{-n}$  Néel law, symptomatic of Bloch domain motion. MFM images reveal well-defined stripe patterns, mainly for the thickest films. Good agreement is found between the experimental and the calculated spectra in the BLS measurements (fig.1). This satisfactory accord was obtained by fitting the magneto-crystalline anisotropy field  $H_a$ , assumed to be uniaxial ( $H_a = 2K_u/M_s$  with  $K_u$  the uniaxial anisotropy constant). From FMR spectra (derivative of the absorption power vs. applied magnetic field  $H$ ) for the perpendicular configuration, and specifically from the position of the peak (corresponding to the resonant field value) we computed the uniaxial magnetocrystalline anisotropy constant  $K_u$  (fig.2). Values of  $K_u$  greater than  $7 \times 10^6$  erg.cm $^{-3}$  were found for the Co/Si thin films, evaporated under normal incidence. In the obliquely evaporated Co thin films, anisotropy field  $H_a$  (and magnetic anisotropy constant  $K_u$ ) has been improved comparative to Co thin films evaporated at a normal incidence.  $K_u$  value as high as  $13 \times 10^6$  erg/cm $^3$  has been measured. All these results and others will be presented and discussed.

**Keywords:** Thermal evaporation; Co thin films; magnetization; anisotropy factors;

## References

- [1] A. Kharmouche, *J. Magn. Magn. Mater.* **327**(2013) 91.
- [2] A. Kharmouche, S.-M. Chérif, Y. Roussigné, G. Schmerber, *Appl. Surf. Sci.* **255** (2009) 6173–6178.
- [3] A. Kharmouche, S.-M. Chérif, G. Schmerber, and A. Bourzami, *J. Magn. Magn. Mater.* **310**(2007) 152.
- [4] R. D. Fisher, V. S. Au-Yeung, and B. B. Sabo, *IEEE Trans. Magn.* **MAG-20**, 806 (1984).
- [5] Y. Endo, O. Kitakami, S. Okamoto, and Y. Shimada, *Appl. Phys. Lett.* **77**, 1689 (2000).



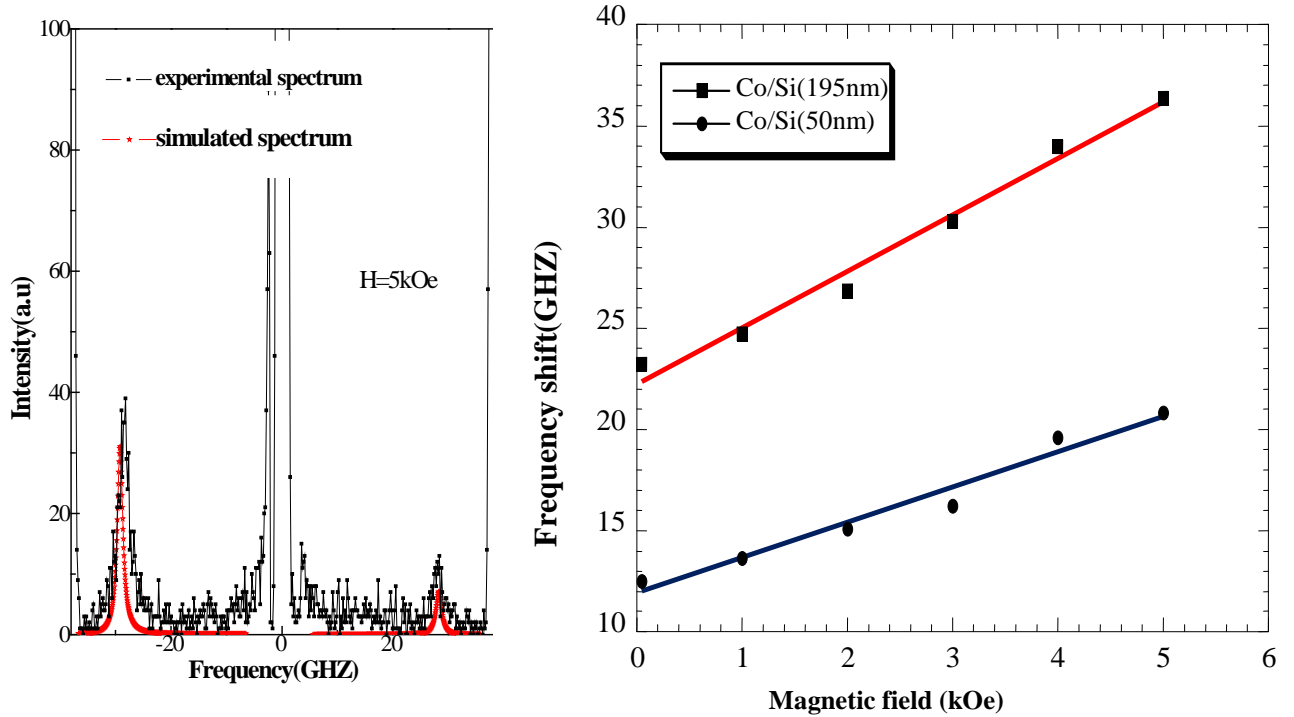


Fig.1. Examples of BLS spectrum for applied magnetic field  $H = 5 \text{ kOe}$ , and Damon-Eschbach mode frequency versus applied magnetic intensity field.

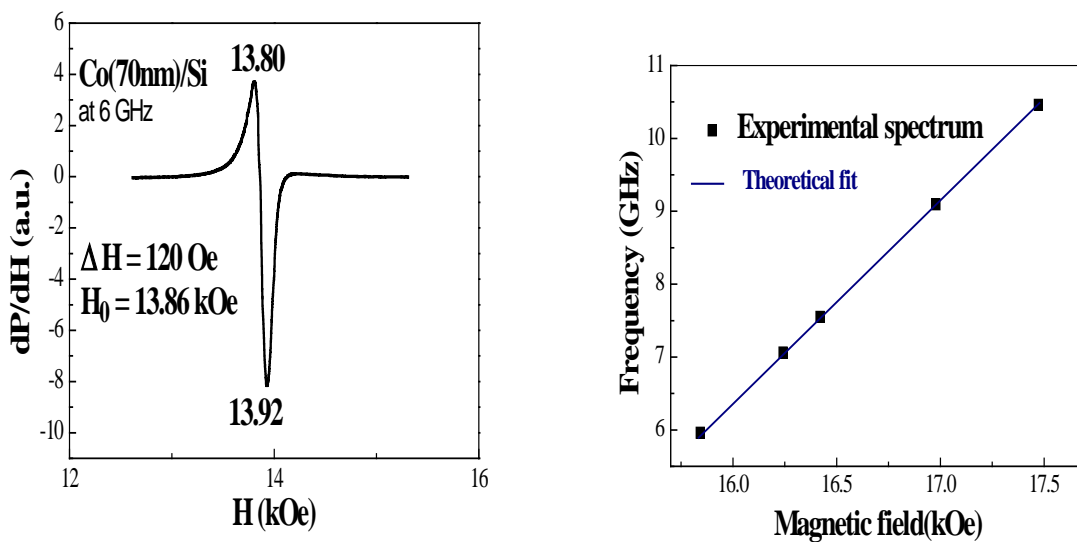


Fig.2 Example of experimental FMR spectrum, recorded at a frequency of 6 GHz, and Frequency evolution versus magnetic field.

**Structure, optical, and magneto-optical properties of magnetic silicide Fe<sub>3</sub>Si and Fe<sub>5</sub>Si<sub>3</sub>**

Varnakov S.N., Yakovlev I.A., Tarasov I.A., Popov Z.I., Molokeyev M.S., Zharkov S.M., Ovchinnikov S.G.

Kirensky Institute of Physics, Siberian Branch, Russian Academy of Science, Krasnoyarsk, 660036, Russia

[sgo@iph.krasn.ru](mailto:sgo@iph.krasn.ru)

Fe/Si nanostructures are attractive materials for spintronics due to combination the magnetic and semiconductor properties. The formation of Fe silicides in the interface may decrease the required characteristics of the material. Here we report the results of the in situ optical and magneto-optical properties for the MBE grown single crystalline Fe<sub>3</sub>Si and polycrystalline Fe<sub>5</sub>Si<sub>3</sub> films on Si(111) substrate. The high resolution TEM and XRD of Fe<sub>3</sub>Si( 27nm)/Si(111)7x7 have shown the epitaxial film. The Fe<sub>3</sub>Si film has saturation magnetization 875 Gauss and single axis anisotropy Ha=26 Oe. The Fe<sub>5</sub>Si<sub>3</sub> is unstable in the bulk and has been obtained by thermal evaporation of (Fe/Si)<sub>n</sub> multilayer film with subsequent heating at 700K, its crystal structure has been confirmed by the XRD spectra. For both films we have measured the spectral dependence of complex refractive index  $n+ik$  and the magneto-optical Fogy parameters by the home-made magnetoellipsometer in the photon energy 1.5-4.9 eV. For both silicides magneto-optical spectra contain several resonance peaks found by gaussian decomposition of the spectra. We have carried out *ab initio* band structure calculation for both silicides. The spin-polarised density of states reveals several intraband excitation for the spin up and spin down bands. There is a qualitative agreement between calculated intraband excitation energies and gaussian peaks in the magneto-optical spectra.

**Keywords:** *Spintronics, magnetic multilayers, molecular beam epitaxy, magnetoellipsomet*

- [1] YAKOVLEV I.A., VARNAKOV S.N., BELYAEV B.A., ZHARKOV S.M., MOLOKEEV M.S., TARASOV I.A., OVCHINNIKOV S.G. 2014. Study of structural and magnetic properties of epitaxial Fe<sub>3</sub>Si/Si(111) films. JETP letters, 99, 527-531.
- [2] TARASOV I.A., POPOV Z.I., VARNAKOV S.N., MOLOKEEV M.S., FEDOROV A.S., YAKOVLEV I.A., FEDOROV D.A. and OVCHINNIKOV S.G. 2014. Optical characteristics of an epitaxial Fe<sub>3</sub>Si(111) iron silicide film. JETP Letters. 99. 565-569.

## Unprecedented tuning of the in-plane easy axis in (100) magnetite films grown by IR-PLD

A. Bollero<sup>1</sup>, F.J. Pedrosa<sup>1</sup>, J.L.F. Cuñado<sup>1</sup>, J. Rial<sup>1</sup>, M. Sanz<sup>2</sup>, M. Oujja<sup>2</sup>, E. Rebollar<sup>2</sup>, J.F. Marco<sup>2</sup>, J. de la Figuera<sup>2</sup>, M. Monti<sup>2</sup>, M. Castillejo<sup>2</sup>, M. Garcia-Hernandez<sup>3</sup>, F. Mompean<sup>3</sup>, N.M. Nemes<sup>4</sup>, T. Feher<sup>5</sup>, B. Nafradi<sup>6</sup>, L. Forro<sup>6</sup>, J. Camarero<sup>1</sup>

<sup>1</sup> IMDEA Nanoscience, Madrid, Spain.

<sup>2</sup> Instituto Química Física Rocasolano, CSIC, Madrid, Spain.

<sup>3</sup> Instituto Ciencias de Materiales de Madrid, CSIC, Madrid, Spain.

<sup>4</sup> Dep. Física Aplicada III, UCM, Madrid, Spain.

<sup>5</sup> Dep. Theoretical Physics, BUTE, Budapest, Hungary.

<sup>6</sup> Institute of Condensed Matter Physics, EPFL-SB-ICMP-LPMC, Lausanne, Switzerland.

*E-Mail: alberto.bollero@imdea.org*

Thin films can be considered as ideal cases for the design of improved bulk magnets [1]. Magnetite ( $\text{Fe}_3\text{O}_4$ ) is attracting much interest in the last years due to its robust ferrimagnetism down to nanometer thickness, good electrical conductivity and presumed half-metal character. In particular,  $\text{Fe}_3\text{O}_4$  films have been tentatively used in spin-valves and spin-LEDs.  $\text{Fe}_3\text{O}_4$  presents a low-temperature metal-insulator transition, the Verwey transition ( $T_V$ ) which has also been proposed for spintronic applications. An open question is to what extent the preparation of  $\text{Fe}_3\text{O}_4$  films can affect their detailed magnetic properties, such as the magnetic anisotropy axis. This information is required to efficiently apply  $\text{Fe}_3\text{O}_4$  films in spintronic applications.

Most of studies dealing with bulk and  $\text{Fe}_3\text{O}_4$  thin film systems show room temperature (RT) in-plane  $\langle 110 \rangle$  magnetic easy axis. By contrast, we show in this work the preparation of pure stoichiometric  $\text{Fe}_3\text{O}_4$  thin films with RT easy axes along the in-plane  $\langle 100 \rangle$  directions [2], i.e. rotated by  $45^\circ$  respect to previous studies.

$\text{Fe}_3\text{O}_4$  films have been grown by ablation from a sintered hematite target using a nanosecond infrared (IR) laser at 1064 nm and a substrate temperature of 750 K [3]. Single crystal substrates of  $\text{SrTiO}_3$ ,  $\text{MgAl}_2\text{O}_4$  and  $\text{MgO}$  have been used. All films consisted of stoichiometric  $\text{Fe}_3\text{O}_4$  and presented a Verwey transition at  $T_V=115-118$  K.

RT in-plane hysteresis loops were measured by vectorial-MOKE as a function of the direction of the applied magnetic field in the 0-360° range with an angular step of 5°. For all epitaxial films under study, the highest coercivity and remanence are found at 0, 90, 180 and 270°, thus orthogonal to each other, while the lowest coercivity values are found between them. This results in a well-defined four-fold symmetry indicative of biaxial magnetic anisotropy [2]. In order to verify this result, ferromagnetic resonance (FMR) experiments have been carried out at 9.4 GHz frequency. The angular dependence of the in-plane resonance field at RT for the Fe<sub>3</sub>O<sub>4</sub> layers proves that the easy axes are indeed the in-plane <100> directions.

All angular studies here shown in addition to spin-polarized low-energy electron microscopy experiments demonstrate easy-axis orientation along in-plane <100> directions, i.e., differing from that of bulk magnetite or films prepared by other techniques, and thus demonstrating the possibility of tuning the easy axis orientation.

**Keywords:** *Thin films, magnetite, spintronics, magnetic properties*

[1] *NANOPYME*: [www.nanopyme-project.eu](http://www.nanopyme-project.eu)

[2] MONTI, M., SANZ, M., OUJJA, M., REBOLLAR, E., CASTILLEJO, M., PEDROSA, F.J., BOLLERO, A., CAMARERO, J., CUÑADO, J.L.F., NEMES, N. M., MOMPEAN, F.J., GARCIA-HERNANDEZ, M., NIE, S., MCCARTY, K.F., N'DIAYE, A.T., CHEN, G., SCHMID, A.K, MARCO J.F. & DE LA FIGUERA J. 2013. Room temperature in-plane 100 magnetic easy axis for Fe<sub>3</sub>O<sub>4</sub>/SrTiO<sub>3</sub>(001):Nb grown by infrared pulsed laser deposition. *J. Appl. Phys.* 114, 223902.

[3] SANZ, M., OUJJA, M., REBOLLAR, E., MARCO, J.F., DE LA FIGUERA, J., MONTI, M., BOLLERO, A., CAMARERO, J., PEDROSA, F.J., GARCIA-HERNANDEZ, M. & CASTILLEJO, M. 2013. Stoichiometric magnetite grown by infrared nanosecond pulsed laser deposition. *Applied Surface Science* 282, 642.

## **Effect of Changed Structure as well as Composition on the Behaviour of Sn(Se,Te) Compound Semiconductor Thin Films and Schottky Diodes for Solar Cell Applications**

Naresh Padha\*, Narinder Kumar\*, Anjali Devi\*, Ramesh Sachdeva\* and Chetal J Panchal\*\*

\*Department of Physics & Electronics, University of Jammu, Jammu-180006, J&K, INDIA.

\*\*Department of Applied Physics, M.S. University of Baroda, Vadodara, Gujarat, INDIA.

### **ABSTRACT**

There has been a great motivation to achieve new material types and fabricate electronic devices which show unusual properties in the field of energy generation and transformation. The recent investigations in this area are directed towards the development of cost-effective, non-toxic and abundant materials, the chalcogenide materials have emerged as a convenient choice in the regard. IV-VI chalcogenide semiconductors have exhibited flexibility to possess varied bandgap energies (bandgap tailoring) which allowed the materials to tap different regions of the solar spectrum. These Devices have achieved highest energy conversion efficiencies among the thin film technologies (above 20%). Further, Sn(S,Se,Te) chalcogenide thin films have been reported to possess the optical and electrical properties suitable for applications for solar harvesting. These have also been reported to be used in infrared LEDs/Detectors, fast switches and optoelectronic Devices.

Comparative analysis of some Sn(Se, Te) compound semiconductor thin films and schottky diodes have been made. SnSe used as primary material has transformed to SnSe<sub>2</sub> on changing its structure from orthorhombic to hexagonal. It, however, attained SnTeSe (Orthorhombic) composition on replacement of some of the Se atoms with Te. Films of all the three types of materials have been deposited at different substrate temperatures and changed thickness. These were then characterized on the basis of their structural, morphological, electrical and optical properties. The grain size of SnSe films increased on its transformation to SnTeSe as well as SnSe<sub>2</sub>. The electrical as well as optical analysis of the films showed that the bandgap and resistivity decrease for SnSeTe, the same however increase for SnSe<sub>2</sub>. Further, the conductivity type remained p-type for SnSeTe but changed to n-type for SnSe<sub>2</sub> films. The Schottky Barrier Diodes of the deposited films were formed and their characteristics studied for the temperature dependent current-voltage (I-V) and capacitance-voltage(C-V) behaviour. The current voltage characteristics of Al/n-SnSe<sub>2</sub> Schottky diodes demonstrated better diode parameters (ideality factors, barrier heights and breakdown voltage) in comparison Ag/p-SnSe and Ag/p-SnSeTe Schottky Diodes. Further, the ideality factors decreased and barrier heights increased with increase in temperature in all types. The temperature dependence of the barrier heights and ideality factors has been explained on the basis of "barrier inhomogenities" existing over the metal-semiconductor interface. Further, there have been variations between the theoretically generated data (on the basis Gaussian Distribution Function) to that from the experimental results which indicated the possibility of the existence of tunneling current component existing in the current transport of the Schottky Diodes. The breakdown voltages of all the three types of undertaken diodes were increased with decrease in temperature and provided negative temperature coefficient and depicted soft breakdown due to 'Defect Assisted Tunneling' phenomenon existing over the Schottky interface.

## **Deposition-controlled enhancement of green emission of hydrogen annealed ZnO thin films.**

Chichvarina O., Heng T.S., Ding J.\*

Department of Materials Science and Engineering, National University of Singapore,  
7 Engineering Drive 1, Singapore 117574, Singapore.

\* *Corresponding author, email: [msedingj@nus.edu.sg](mailto:msedingj@nus.edu.sg)*

*Presenting author, email: [a0092791@nus.edu.sg](mailto:a0092791@nus.edu.sg)*

Hydrogen treatment has been reported to enhance green emission in ZnO thin films [1]. Due to high diffusivity at elevated temperatures hydrogen is claimed to form interstitial and substitutional defects in ZnO which tend to act as shallow donors [2], leading to an increase in the localization of excitons. However, the effect of the preliminary ZnO thin film growth conditions on the emission efficiency is not well understood. Here, we report the results of our systematic study on optical properties of ZnO thin films grown on quartz substrates via pulsed laser deposition in different conditions and subsequently annealed in H<sub>2</sub> atmosphere. One series of ZnO/quartz films was deposited at 600°C at oxygen partial pressure  $2 \times 10^{-4}$  mbar while another series was grown at room temperature in very high vacuum ( $\sim 10^{-7}$  mbar) without oxygen supply. As the deposition conditions vary the films exhibit different structural and optical properties after hydrogen annealing. The PL measurements revealed red-shift and significant increase of the intensity for the samples prepared at room temperature without oxygen. The study shows that the deposition conditions play an important role in controlling green emission intensity of ZnO thin films.

**Keywords:** ZnO, green emission, hydrogen annealing.

[1] LI, T., HERNG, T. S., LIANG, H. K., BAO, N. N., CHEN, T. P., WONG, J. I., XUE, J. M. & DING, J. 2012. Strong green emission in ZnO films after H<sub>2</sub> surface treatment. *Journal of Physics D-Applied Physics*, 45.

[2] KOCH, S. G., LAVROV, E. V. & WEBER, J. 2014. Interplay between interstitial and substitutional hydrogen donors in ZnO. *Physical Review B*, 89.

## Effect of Porosity on resistivity of Silver Nanoparticle Ink during Laser Sintering

Yoon Jae Moon<sup>1,2</sup>, Kyung Tae Kang<sup>1</sup>, Heuseok Kang<sup>1</sup>, Jun Young Hwang<sup>1</sup>,  
and Seung Jae Moon<sup>2</sup>

<sup>1</sup>Korea Institute of Industrial Technology 143, Hanggaul-ro, Sangnok-gu, Ansan-si,  
Gyeonggi-do, 426-910, KOREA

<sup>2</sup>The school of Mechanical Engineering, Hanyang University, 222, Wangsimni-ro,  
Seongdong-gu, Seoul, 133-791, KOREA

*ktkang@kitech.re.kr/ Tel. +82-31-8040-6427, Fax. +82-31-8040-6430, jyhwang@kitech.re.kr/ Tel.  
+82-31-8040-6434, Fax. +82-31-8040-6430*

The printed metal nanoparticles should be sintered to have high electrical conductivity. The electrical conductivity of metal electrode is affected by grain size and porosity. The printed metal nanoparticles have the porosity inherently. The change of resistivity of laser-sintered silver nanoparticles with porosity was examined with various beam intensities. A 532-nm continuous wave laser was irradiated onto inkjet-printed silver lines on a glass substrate. As laser intensity increased, porosity and resistivity decreased. At very high laser intensity, porosity begins to increase and resistivity of silver nanoparticles did not decrease any more. When porosity effect was removed from the measured resistivity, the resistivity of silver is the same as that of bulk silver. Because of the porosity increase of printed metal nanoparticles at high laser intensity, the resistivity of printed metal nanoparticles cannot reach the specific resistance of bulk silver.

**Keywords:** *Silver nanoparticles, Inkjet printing, Laser sintering, Porosity, Resistivity*



## Improving Performance of Organic Light-emitting Diodes by Combing Both MoO<sub>3</sub> Hole Injection Layer and MoO<sub>3</sub> Doped Hole Transport layer

Wei Liu, Guohong Liu, Zhonggui Gao, Jianhua Liang, and Xiang Zhou\*

State Key Lab of Optoelectronic Materials and Technologies, School of Physics and Engineering, Sun Yat-Sen University, Guangzhou, 510275, P. R. China

\*E-Mail ( [stszx@mail.sysu.edu.cn](mailto:stszx@mail.sysu.edu.cn) )

We improved the performance of the organic light-emitting diodes (OLEDs) by combing both MoO<sub>3</sub> hole injection layer (HIL) and MoO<sub>3</sub> doped hole transport layer (HTL) to improve both the hole injection and transport efficiency. Comparing with the OLEDs with only MoO<sub>3</sub> HIL or MoO<sub>3</sub> doped HTL, the OLEDs with both MoO<sub>3</sub> HIL and MoO<sub>3</sub> doped HTL showed superior performance in driving voltage, power efficiency, and stability. Based on the typical NPB/Alq<sub>3</sub> heterojunction structure, the OLEDs with both MoO<sub>3</sub> HIL and MoO<sub>3</sub> doped HTL showed a driving voltage of 5.4 V and a power efficiency of 1.4 lm/W for 1000 cd/m<sup>2</sup>, and a lifetime of around 0.8 hour with an initial luminance of around 5000 cd/m<sup>2</sup> under room temperature in air without encapsulation. While the OLEDs with only MoO<sub>3</sub> HIL or MoO<sub>3</sub> doped HTL showed a little higher driving voltage of 6.4 V or 5.8 V and lower power efficiency of 1.2 lm/W or 1.3 lm/W for 1000 cd/m<sup>2</sup>, and shorter lifetime of around 0.3 hour or 0.5 hour with an initial luminance of around 5000 cd/m<sup>2</sup> under room temperature in air without encapsulation. Our results demonstrate clearly that combing both MoO<sub>3</sub> HIL and MoO<sub>3</sub> doped HTL is a simple and effective approach to simultaneously improve both the hole injection and transport efficiency in the OLEDs, and thus results in further improvements in the driving voltage, power efficiency, and stability of the OLEDs.

**Keywords:** OLEDs, MoO<sub>3</sub>, hole injection, hole transport, doped,

## Synchrotron X-ray Studies on the Morphology of Ternary Organic Polymer Solar Cells

Jiangquan Mai<sup>1</sup>, Tsz Ki Lau<sup>1</sup>, Xinhui Lu<sup>1\*</sup>

<sup>1</sup>Department of Physics, The Chinese University of Hong Kong

*xhlu@phy.cuhk.edu.hk/+852-39436350*

Nowadays, solar industry becomes the fastest growing industry due to the rising demands to solve energy crisis and environmental problems. Organic photovoltaic (OPV) devices, as one of the most promising technologies offering low-cost, light weight and flexible solar cells, have attracted more and more attentions. One major limitation to OPV devices is the insufficient light absorption, which lies in two-folds: 1. the narrow absorption spectrum of organic semiconductors, which merely spans a few hundred nm, unable to fully cover the solar spectrum. 2. the limited optimal thickness of active layer (<110 nm), which is only capable to absorb less than 80% of incident photons with higher energy than the absorber's band gap. Here, we report our recent work on a ternary organic polymer system to address the aforementioned issues. High efficiency for thick-film devices has been realized by combining poly(3-hexylthiophene) (P3HT), which can maintain high charge carrier mobility with thick film and polythieno[3,4-b]-thiophene-co-benzodithiophene (PTB7) which has shown high PCE. Grazing incidence X-ray scattering techniques have been employed to investigate the ternary morphology: grazing incidence wide-angle X-ray scattering (GIWAXS) for molecular level ordering and grazing incidence small-angle X-ray scattering (GISAXS) for nano-scale ordering.

**Keywords:** *OPV, ternary, morphology, GIWAXS, GISAXS*

[1] MAI J., LAU TK., LU X.H., Ternary morphology facilitated thick-film organic solar cell, in preparation.

[2] LU X. H., HLAING H., GERMACK D., PEET J., JO W. H., ANDRIENKO D., KREMER K. AND OCKO B. M., Bilayer ordering in a polycarbazole conjugated polymer : a new structural motif, *Nature Communications*, 3, 795 (2012).

## Optical and Electrical Characterizations of Silicon Phthalocyanine dichloride thin films

Regimol (Joseph)<sup>1</sup>, Menon(C S)<sup>2</sup>

<sup>1</sup>Assumption College, Changanacherry P O, Kottayam, Kerala-686101, India

<sup>2</sup>School of Pure and Applied Physics, Mahatma Gandhi University, Priyadarshini Hills P. O, Kottayam, Kerala-686560, India

*E mail- regijose2004@yahoo.co.in*

The phthalocyanines [Pc] are a class of planar aromatic organic compounds that have hetero-aromatic  $\pi$  system and readily form complexes with many groups and transitions metals. The versatility, architectural flexibility, non-toxicity and ease of processing make them eligible for use in microelectronics and also in nano-technology.

The present paper discusses the optical and electrical characterizations of Silicon Phthalocyanine dichloride thin films. It is observed that the electrical and optical properties of phthalocyanines are critically dependent on film morphology, which in turn is determined by preparation parameters such as deposition rate, substrate temperature and post deposition annealing. The direct optical transition takes place in these films. The optical energy gap remains unaffected due to annealing both in air and vacuum. For longer wavelength greater than 800nm, the film becomes transparent. The film also shows anomalous dispersion.

The variation of thermal activation energy with thickness and annealing temperature is studied. An Arrhenius plot shows two linear regions. Activation energy decreases with increase of annealing temperature in vacuum. By optimizing the growth conditions, the applicability of this halogenated metal phthalocyanine as active layer in organic semiconductor thin film devices can be improved.

**Keywords:** *Phthalocyanines, optical properties, optical band gap, thermal activation energy*

## **Fabrication of a coupled silicon-gold plasmonic structure using Remote Plasma Enhanced Chemical Vapor Deposition and Sputtering**

Arturo Rodríguez-Gómez<sup>1\*</sup>, Jesús Ángel Arenas-Alatorre<sup>1</sup>, Juan Carlos Alonso-Huitrón<sup>2</sup>

<sup>1</sup>Instituto de Física, Universidad Nacional Autónoma de México, A.P.20-364,  
Coyoacán01000, México D. F., Mexico

<sup>2</sup>Instituto de Investigaciones en Materiales, Universidad Nacional Autónoma de México,  
A.P.70-360, Coyoacán04510, México D. F., Mexico

\*[arodriguez@fisica.unam.mx](mailto:arodriguez@fisica.unam.mx)

It has been observed a considerable improvement of the integrated emission intensity from silicon nanostructures which are coupled with a thin film of nanostructured noble metal particles (Biteen *et al.*, 2007; Walters *et al.*, 2010). This enhancement is due to the surface plasmon of the metal particles. The fabrication of coupled silicon-metal nanostructures could be a possible solution for the manufacture of multiple luminescent devices based silicon, because the enhancement provided by the noble metal particles makes the silicon efficient enough to be a suitable material to built a wide range of luminescent artifacts.

However, to get luminescence enhancement from the surface plasmon is not a simple task. To achieve the enhancement is necessary condition to set the plasmon into resonance. The resonance frequency of the system depends of multiple factors among which are: size and volume of the noble-metal nanoparticles, the dielectric constant of the medium and the distance between silicon nanoparticles and metal particles (Jain *et al.*, 2007).

For this conference, our work presents a controlled method for depositing a coupled silicon-gold structure (Si-Au structure). The Si-Au structure shows a PL Enhancement of 87% compared with the silicon nanoparticles without coupling. We use Remote Plasma Enhanced Chemical Vapor Deposition (RPECVD) for depositing the silicon quantum dots (SQDs) and the dielectric made of silicon nitride (NH<sub>3</sub>) used to separate gold

nanoparticles (AuNPs) from the SQDs. Meanwhile, the AuNPs were deposited by sputtering.

We carried out three major characterizations: A) Ultraviolet–visible spectroscopy, using a double beam PerkinElmer Lambda 35 spectrophotometer to find the plasmon location of the AuNPs. B) Excitation with a Kimmon He-Cd laser beam with a wavelength of 325nm and a power of 25 mW to obtain the PL curves from all deposited structures. And C) High-Resolution Transmission Electron Microscopy (HRTEM) using a JEOL JEM-2010F FasTEM microscope equipped with a GATAN digital micrograph system for image acquisition (version 3.7.0) to analyze the density and distribution of both silicon and gold nanoparticles.

There are some common methods for attaching a layer of AuNPs that use colloidal solutions as sources of gold (Wu *et al.*, 2011; Lim *et al.*, 2007). Unlike these methods, ours offers several advantages such as: a dry deposit that allows its adaptation to the techniques commonly used in the manufacture of microchips. Meanwhile, AuNPs density is uniform over the entire film, which allows a PL Enhancement all over the surface and not only in certain areas. Finally, the gold target used for Sputtering is solid and reusable, therefore, is a more economical source of gold than the gold salts required to formulate the colloidal solutions.

**Keywords:** *PL Enhancement, RPECVD, Plasmonic Structure, Silicon Quantum Dots.*

### **References:**

- Biteen, J.S., Sweatlock, L. a., Mertens, H., Lewis, N.S., Polman, a. & Atwater, H. a. (2007) Plasmon-Enhanced Photoluminescence of Silicon Quantum Dots: Simulation and Experiment [online]. *Journal of Physical Chemistry C*. 111 (36), pp. 13372–13377.
- Jain, P.K., Huang, X., El-Sayed, I.H. & El-Sayed, M. a. (2007) Review of Some Interesting Surface Plasmon Resonance-enhanced Properties of Noble Metal Nanoparticles and Their Applications to Biosystems [online]. *Plasmonics*. 2 (3), pp. 107–118. [Accessed 21 January 2014].

- Lim, S.H., Mar, W., Matheu, P., Derkacs, D. & Yu, E.T. (2007) Photocurrent spectroscopy of optical absorption enhancement in silicon photodiodes via scattering from surface plasmon polaritons in gold nanoparticles [online]. *Journal of Applied Physics*. 101 (10), pp. 104309. [Accessed 8 December 2014].
- Walters, R.J., van Loon, R.V. a, Brunets, I., Schmitz, J. & Polman, a (2010) A silicon-based electrical source of surface plasmon polaritons. [online]. *Nature materials*. 9 (1), pp. 21–25. [Accessed 11 December 2014].
- Wu, J., Lee, S., Reddy, V.R., Manasreh, M.O., Weaver, B.D., Yakes, M.K., Furrow, C.S., Kunets, V.P., Benamara, M. & Salamo, G.J. (2011) Photoluminescence plasmonic enhancement in InAs quantum dots coupled to gold nanoparticles [online]. *Materials Letters*. 65 (23-24), pp. 3605–3608. [Accessed 31 December 2013].

## **Silicon containing layer on Ti-46Al-8Ta alloy for hot corrosion protection. Kinetic studies of layer deposition.**

Rubacha<sup>1</sup>, Godlewska<sup>1</sup>, Mars<sup>1</sup>, Mitoraj<sup>1</sup>

<sup>1</sup> AGH University of Science and Technology, Faculty of Materials Science and Ceramics, Al. A. Mickiewicza 30, 30-059 Krakow, Poland

*e-mail address: rubacha@agh.edu.pl, contact phone: +48 126174787*

Titanium alloys have been extensively investigated for many years as potential lightweight structural materials. They are characterized by low density, high Young modulus and good resistance to oxidation at moderate temperatures. One of their important drawbacks is insufficient oxidation resistance at elevated temperatures (800-900°C), especially in contact with mineral deposits (hot corrosion). In spite of numerous coating systems investigated, the satisfactory protection against hot corrosion has not been attained. The objective of this work was to develop a novel technological route and assess the growth kinetics of a silicon-rich layer on the surface of a Ti-46Al-8Ta (at. %) alloy belonging to 4th generation of titanium alloys based on intermetallic phases. The silicon-containing coating was deposited on a Ti-46Al-8Ta (at%) alloy in a two-step process, comprising physical and chemical vapour deposition (magnetron sputtering and pack cementation, respectively). The kinetics was determined by coating thickness measurements as a function of deposition time. The good-quality coating was about 40 µm thick and consisted of silicide phases with different composition and stoichiometry. To evaluate the protective properties of the coating, the samples were contaminated with NaCl or Na<sub>2</sub>SO<sub>4</sub> and oxidized in thermal cycling conditions in air at 800°C. Reaction progress was followed by thermogravimetric measurements. Post-exposure examination included scanning electron microscopy (SEM) with energy dispersive X-ray analysis (EDS/EDAX) and X-ray diffraction (XRD). Significant improvement in hot corrosion resistance was noted for the coated samples compared with the uncoated reference.

**Keywords:** *hot corrosion, intermetallics, pack cementation*

The author gratefully acknowledges financial support from National Science Centre project number 2013/11/N/ST8/01345

## Overview of superhydrophilic, photocatalytic and anti-corrosive properties of TiO<sub>2</sub> thin films doped with multiwall carbon nanotubes and deposited on 316L stainless steel

Géraldine L.-M. Léonard<sup>a,\*</sup>, Simon Remy<sup>a</sup>, Benoît Heinrichs<sup>a</sup>

<sup>a</sup>Laboratoire de Génie Chimique, B6a, Université de Liège, B-4000 Liège, Belgium  
(\* e-mail : geraldine.leonard@ulg.ac.be).

In this work, a coating is developed to prevent the corrosion of stainless steel. The coating is based on TiO<sub>2</sub> material. The TiO<sub>2</sub> is known for its photocatalytic activity and superhydrophilicity. These two properties of TiO<sub>2</sub> provide the “easy-to-clean” property. Indeed, superhydrophilicity induces a very low contact angle between TiO<sub>2</sub> and water leading to the formation of a water film at the surface of the material. The photocatalytic activity, responsible for the pollutant decomposition, is explained by the excitation of the semiconductor under UV light leading to the formation of electron-hole pairs.

The combination of these three properties (anti-corrosive, photocatalytic and superhydrophilic) allows to develop a material with low fouling and with a reduced corrosion. The final material, that can be set in inaccessible places, has so a longer lifetime.

Multiwall carbon nanotubes (MWCNTs) are electrical conductors and their introduction in TiO<sub>2</sub> could increase the conductivity of photogenerated electrons. MWCNTs can prevent the corrosion by driving the electron, photogenerated by UV, from the TiO<sub>2</sub> to the stainless steel. These electron can so slow down the oxidation process by keeping a low potential. Moreover, the incorporation of MWCNTs can modify the superhydrophilicity of TiO<sub>2</sub>. Finally, the photoactivity can be improved by reducing the electron-hole recombination rate. MWCNTs play a role in electron transfer and allow to decrease the recombination of electron-hole pairs.

Two sol-gel syntheses were studied in alcohol and water respectively. In the alcoholic medium, monolayer films are obtained by dip-coating on stainless steel substrate. In some cases, those films are calcined at 400°C. The thermal treatment allows to crystallize TiO<sub>2</sub> in the anatase form but induces an oxidation of the stainless steel. In the aqueous synthesis, monolayer films are obtained by dip-coating stainless steel substrate too. The TiO<sub>2</sub> shows already the anatase structure at room temperature.

The characterizations of the samples have confirmed the presence of nanotube in the aqueous synthesis and in the alcoholic synthesis (calcined and no-calcined films).

TiO<sub>2</sub> alone induces a decrease of the corrosion due to its photogenerated electron and by simple barrier effect. Introduction of MWCNTs enhances the anti-corrosive property of TiO<sub>2</sub> by reducing the corrosion potential and corrosion current. The best samples are the aqueous samples.

For both synthesizes, the films without MWCNTs are superhydrophilic but the contact angle increases with the incorporation of MWCNTs. The superhydrophilicity is lost with MWCNTs introduction.

When MWCNTs are introduced, the improvement of photocatalytic activity is higher in the case of aqueous synthesis than in the case of alcoholic synthesis. The aqueous synthesis leads to more active photocatalysts than the alcoholic synthesis.



## Rapid Prototyped Biomimetic Antifouling Surfaces for Marine Applications

Paul (O'Neill)<sup>1,3</sup>, Tim (Sullivan)<sup>2</sup>, Ronan (McCann)<sup>1,3</sup>, Komal (Bagga)<sup>1,3</sup>, Mercedes (Vazquez)<sup>1,3</sup>, Fiona (Regan)<sup>1,2</sup>, Dermot (Diamond)<sup>4</sup>, Dermot (Brabazon)<sup>1,3</sup>

<sup>1</sup>Advanced Processing Technology Research Centre, School of Mech. & Manu. Eng.,

<sup>2</sup>Marine and Environmental Sensing Technology Hub, School of Chemical Sciences,

<sup>3</sup>Irish Separation Science Cluster, National Centre for Sensor Research

<sup>4</sup>Insight Centre for Data Analytics, National Centre for Sensor Research

Dublin City University, Glasnevin, Dublin 9, Ireland

E-mail: paul.oneill37@mail.dcu.ie Tel.: +353 (1) 700 7674

Prevention of biofouling can be achieved by applying antifouling coatings or technologies that are biocidal in nature or can deter settlement or adhesion of biofouling in some way. Polydimethylsiloxane (PDMS) has shown great potential as an antifouling material in marine applications. Antifouling capabilities can be improved by infusing the Polydimethylsiloxane (PDMS) with a lubricant, such as silicone oil, as demonstrated by Howell et al. [1]. However, over time the infused lubricant is lost due to environmental conditions and needs to be replenished. Here, we present a solution for the replenishment of the lubricating medium using a microfluidic network in PDMS. This dynamic microfluidic network containing fluid inlets was assessed on its ability to replenish lubricant under controlled lubrication loss rate conditions. In addition, the effects of potentially biocidal nanomaterial additives (silver, carbon, and titanium) to the silicon oil were investigated. Results demonstrate the enhanced antifouling capabilities of this novel combined approach over standard PDMS coatings.

**Keywords:** *Biofouling, biomimetic, rapid prototyped, marine, nanoparticle*

[1] C. HOWELL, T. L. VU, J. J. LIN, S. KOLLE, N. JUTHANI, E. WATSON, J. C. WEAVER, J. ALVARENGA, AND J. AIZENBERG, Aug 2014, Self-replenishing vascularized fouling-release surfaces., ACS Appl. Mater. Interfaces, vol. 6, no. 15, pp. 13299–307

## Investigation on Correlation between Adhesion and Electrochemical Impedance Spectroscopy for Acrylate-Epoxy Paint System

**B. Vengadaesvaran, S. Ramis Rau, K. Ramesh, S. Ramesh and A.K. Arof**

Centre For Ionics, Faculty of Science, Physics Department, University of Malaya, 50603 Kuala Lumpur, Malaysia

Corresponding Author\* : [venga@um.edu.my](mailto:venga@um.edu.my)

Strict environment regulations and human health protection have put considerable pressure on the paint industry to reconsider the current paint trends. Apart from that to maintain the adhesion of the paint to the metal substrate under environmental exposure is a key performance which can be used to evaluate the capability of the paint system. Interfacial chemical reaction involved in the establishment of paint adhesion, in the suppression of corrosion processes, and in the degradation and loss of paint adhesion have been extensively studied using modern surface analytical technique. In the current study, the best performing hybrid systems were prepared by blending an acrylic polyol resin (A) with an epoxy polyol resin (E) in ratio of 90 wt%:10 wt% respectively which was earlier published in the journal of adhesion [1]. In this hybrid system, TiO<sub>2</sub> pigment have been introduced using different Pigment Volume Concentration (PVC) to obtain a Critical Pigment Volume Concentration (CPVC) by performing corrosion resistance test and mechanical test. The dry film thickness of the paint was maintained within the range of 40 µm to 80 µm. The panels were allowed to cure under ambient air condition for one week prior to testing. The correlation between electrochemical impedance spectroscopy, acid resistance test and adhesive properties of the paint to the metal substrate has been studied and analyzed extensively until a clear correlation between adhesion and Electrochemical Impedance spectroscopy studies established for the above said paint systems. From the Electrochemical Impedance Spectroscopy, the paint system consist of 30% PVC has portrayed a high coating resistance and low coating capacitance. Apart from that this paint system also has shown a good acid resistance property up to 360 hours.

**Keywords:** *Hybrid coating; Paint adhesion; Corrosion protection; Adhesion; EIS; Mild steel panel*

### ACKNOWLEDGEMENT

The authors would like to thank the University Malaya Research Grant Scheme RG143-11AFR.

[1] **Development of Organic Resins Hybrid System Using Epoxy Polyol Resin for Mild Steel Protective Coating.** S. Ramis Rau, B. Vengadaesvaran, R. Puteh and A.K. Arof, *Journal of Adhesion*, Vol. 87, Issue 7-8, 2011, Pg:755-765

# Development and characterization of hydrophobic anticorrosive acrylic - silicone/SiO<sub>2</sub> nanoparticles hybrid nanocomposite coatings

Ammar Shafaamri, S.Ramesh, K. Ramesh\*

Centre for Ionics University of Malaya, Department of Physics, Faculty of Science, University of Malaya, Kuala Lumpur, 50603 Malaysia.

\* Corresponding author: rameshkasi@um.edu.my

## **Abstract**

In this study, acrylic-silicone (AS) coatings containing SiO<sub>2</sub> nanoparticles at various concentrations have been successfully prepared with the assistance of ultrasonication process. The surface morphology and the effect of the ultrasonication process in introducing the nano fillers into the acrylic-silicone matrix were evaluated by Field Emission Scanning Electron Microscopy (FESEM). The chemical structures of AS/ SiO<sub>2</sub> nanocomposite were examined via Fourier transform infrared (FT-IR) spectroscopy and the mechanical property of the blend has been carried out by using pull-off tester and adhesion tester (Cross Hatch- Cutter). The wettability of the surface was examined by measuring the water contact angle (CA). Electrochemical Impedance Spectroscopy (EIS) was used to investigate the anti-corrosion properties of the developed nanocomposite coatings on pre-treated cold rolled mild steel panel. The results indicated that the incorporation of SiO<sub>2</sub> nanoparticles in acrylic-silicone matrix improve the wetting properties and make the surface able to consider as hydrophobic with CA up to 97° when it exist at 1 wt.%. Also, the addition of SiO<sub>2</sub> nano fillers leads to superior anticorrosive performance when it present as 1, 3, 5 or 8 wt. %.

Keywords: coatings, corrosion, nanocomposite, hydrophobic coatings, silicone, acrylic.

## **Diffusion and Diffusion-Controlled Transformations in Intermetallic Nanolayers: Atomistic Modelling.**

A. Biborski<sup>1</sup>, M. Kozłowski<sup>2</sup>, P. Sowa<sup>2</sup>, S. Brodacka<sup>2</sup>, R. Kozubski<sup>2</sup>, Ch. Goyhenex<sup>3</sup>,  
V. Pierron-Bohnes<sup>3</sup>, J. Janczak-Rusch<sup>4</sup>, E.V. Levchenko<sup>5</sup>, A.V. Evteev<sup>5</sup>, I.V. Belova<sup>5</sup>,  
G.E. Murch<sup>5</sup>

<sup>1</sup>Academic Centre for Materials and Nanotechnology, AGH University of Science and Technology, Krakow, Poland

<sup>2</sup>M. Smoluchowski Institute of Physics, Jagiellonian University in Krakow, Poland

<sup>3</sup>Institut de Physique et Chimie des Materiaux de Strasbourg, UMR 7504, Strasbourg, France

<sup>4</sup>EMPA, Swiss Federal Laboratories for Materials Science and Technology, Dübendorf, Switzerland,

<sup>5</sup>University Centre for Mass and Thermal Transport in Engineering Materials, School of Engineering, The University of Newcastle Callaghan, Australia

*rafal.kozubski@uj.edu.pl*

Decomposition, precipitation, chemical ordering and surface segregation in nanolayered intermetallics have been modeled at the atomistic scale using hybrid Monte Carlo – Molecular Statics (MC/MS) algorithms. Three particular results are reported: (i) The discontinuous transformation from “in-plane” to “off-plane” L1<sub>0</sub> variant in [001]-oriented FePt nano-layers previously presumed by “rigid-lattice” Ising-model-based MC simulations and then observed experimentally now modelled with Analytic Bond-Order Potentials (ABOP) dedicated to FePt; (ii) The configuration of the eutectic mixture of Ag and Cu precipitates in nano-layered Ag-40at.%Cu modelled with many-body potential derived for Ag-Cu within the Second-Moment-Approximation; (iii) Kinetics of “order-order” and surface segregation processes modelled by means of Semigrand Canonical Monte Carlo (SGCMC) and Kinetic Monte Carlo (KMC) simulations in B2-ordering stoichiometric A-50at.%B thin films mimicking NiAl. The SGCMC simulations provided equilibrium vacancy concentration and atomic configuration in the films with B-atom termination of both free surfaces achieved at high temperatures by the generation of an antiphase boundary. KMC simulations implemented with the SGCMC-determined equilibrium vacancy concentration revealed very slow relaxation of the films towards equilibrium configuration.

**Keywords:** *intermetallics, nanolayers, atomistic modelling*

- [1] KOZŁOWSKI M., KOZUBSKI R., GOYHENEX C. 2013. Surface induced superstructure transformation in L1<sub>0</sub> FePt by Monte Carlo simulations implemented with Analytic Bond-Order Potentials. *Materials Letters*, 106, 273–276.
- [2] BRODACKA S., KOZŁOWSKI M., KOZUBSKI R., JANCZAK-RUSCH J. 2014. Atomistic simulation of the eutectic mixture in bulk and nano-layered Ag-40at.%Cu alloy. *Comput.Mater.Sci.*, 89, 30–35.
- [3] SOWA P., BIBORSKI A., KOZUBSKI R., LEVCHENKO E.V., EVTEEV A.V., BELOVA I.V., MURCH G.E. 2014. Semigrand Canonical and Kinetic Monte Carlo simulations of binary B2-ordered nano-films with triple defects. *Intermetallics*, 55, 40-48.

## First order phase transition in epitaxial Ni-Mn-Ga-Co films on ferroelectric substrates

B. Schleicher<sup>1,2</sup>, R. Niemann<sup>1,2</sup>, A. Diestel<sup>1</sup>, L. Schultz<sup>1,2</sup>, S. Fähler<sup>1,2</sup>

<sup>1</sup> IFW Dresden, Inst. for Metallic Mat., P.O. Box 270116, D-01171 Dresden, Germany.

<sup>2</sup> TU Dresden, Institute for Solid State Physics, D-01062 Dresden, Germany.

Contact: [b.schleicher@ifw-dresden.de](mailto:b.schleicher@ifw-dresden.de)

One of the challenges today is the constantly growing demand for energy. A significant amount is used for industrial and private cooling applications. Therefore new cooling devices with a higher efficiency are needed. Solid-state cooling cycles relying on magnetic field induced phase transitions have been proposed [1]. Promising materials are Heusler alloys such as Ni-Co-Mn-X (X=Ga, In, Sb, Sn) which show an inverse magnetocaloric effect with a structural and magnetic phase transition between a ferromagnetic austenite at high temperature and a weak magnetic martensite at low temperature. Additionally to high external magnetic fields, the transformation can also be induced by the application of mechanical stress. This can be achieved by the deposition of a magnetocaloric thin film on a ferroelectric substrate. Thin films are of particular interest since their high surface to volume ratio allows fast heat transfer and high cycling frequencies which leads to higher cooling power using less material.

We present first results on sputter deposited epitaxial Ni-Mn-Ga-Co thin films on ferroelectric  $\text{Pb}(\text{Mg}_{1/3}\text{Nb}_{2/3})_{0.72}\text{Ti}_{0.28}\text{O}_3$  (PMN-PT) substrates. Temperature dependent texture and magnetic measurements show the magnetic and structural phase transition in the material. By applying an electric field at the ferroelectric PMN-PT substrate we can induce the martensitic transformation in Ni-Mn-Ga-Co electrically which changes the magnetization significantly. This work is supported by DFG through SPP 1599 [www.FerroicCooling.de](http://www.FerroicCooling.de).

**Keywords:** magnetocaloric, thin film, Ni-Mn-Ga-Co, Heusler, PMN-PT

[1] FÄHLER, S., RÖSSLER, U. K., KASTNER, O., ECKERT, J., EGGELER, G., EMMERICH, H., ENTEL, P., MÜLLER, S., QUANDT, E., & ALBE, K. 2012. Caloric Effects in Ferroic Materials: New Concepts for Cooling. *Advanced Engineering Materials*, 14, 10-19.

## Effect of Annealing to Oxidation State of $\text{Sr}_2\text{FeMoO}_6$ Double Perovskite Film

D. Handoko<sup>1</sup>, S.-C. Yu<sup>1</sup>, S. K. Oh<sup>1</sup>, D.-H. Kim<sup>1</sup>, D. S. Yang<sup>2</sup>, S. E. Demyanov<sup>3</sup>,  
N. A. Kalanda<sup>3</sup>, A. Petrov<sup>3</sup>, M. V. Yarmolich<sup>3</sup> and L. V. Kovalev<sup>3</sup>

<sup>1</sup> Department of Physics Chungbuk National University, Cheongju 361-763, South Korea

<sup>2</sup> Department of Physics Education, Chungbuk National University, Cheongju 361-763, South Korea

<sup>3</sup> Scientific-Practical Research Centre of NAS of Belarus, BY-220072 Minsk, Belarus

*E-mail:* [donghyun@chungbuk.ac.kr](mailto:donghyun@chungbuk.ac.kr)

$\text{Sr}_2\text{FeMoO}_6$  double perovskite films have been investigated by means of extended X-ray fine structure (EXAFS) and X-ray absorption near-edge spectra (XANES). The films were deposited on a  $\text{SrTiO}_3$  substrate with different annealing temperatures. Fe K- and Mo K-edge XANES were measured to determine the oxidation state modification due to an annealing at 1173 K, compared to the case of annealing at 973 K, as shown in Fig. 1. It is observed that the oxidation state becomes more deficient for a lower annealing temperature, indicating less number of unoccupied Fe states with decreasing Mo coordination number. From the Fourier transform spectra, it has been found that the films also have intense binding of O to Fe than Mo. Ordering degree of Fe and Mo ions in  $\text{Sr}_2\text{FeMoO}_6$  films is found to strongly correlated to the oxidation state.

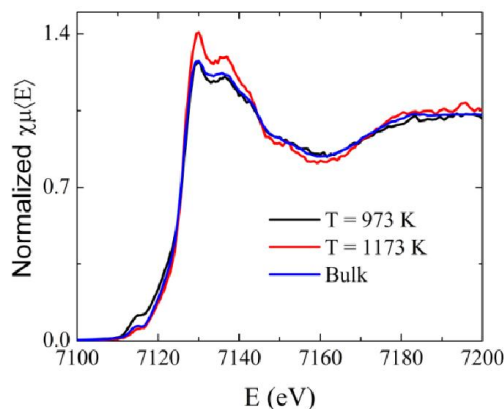


Figure 1. Fe K-edge absorption spectra measured for  $\text{Sr}_2\text{FeMoO}_6$  films at different annealing temperatures.

**Keywords:** double perovskite, oxidation state, EXAFS, XANES

## Josephson generation of coherent THz stimulated emission on Planar Superconducting Multilayer Films (PSMF)

V.E. Grishin<sup>1</sup>, L.A. Muravey<sup>2</sup>

<sup>1</sup>Australian National University ANU, Canberra, ACT-0200

<sup>2</sup>MATI- RSTU, Moscow, Russia

### Abstract

The transmission fluxon waves and plasmon waves are considered on Planar Superconducting Multilayer Films (PSMF). The Josephson array defectivity is considered with the frustration parameter. The number of states in these models shows a wide variety of critical behavior as a function of the frustration  $f$  ( $0 < f < 1$ ). In particular, the phenomenon of stimulation of superconductivity (growth of  $T_c(n)$ ) is expounded and specific dependence on the number of oxide evaporated layers and their thickness is obtained. In addition, the movement and vibrations of fluxons in Josephson junctions is accompanied by stimulated emission in the range up to 10 THz. Using RVB model, one can estimate the maximum values of the upper critical field  $H_{c2}$  and  $T_c(n)$  for the metal oxide ceramics  $Yb_{a_2}Cu_3O_{(7-d)}$ , (YBCO) thin films deposited on  $LaAlO_3$  substrates is observed. According to estimate of the superconducting loop for area  $S=100 \text{ mm}^2$ ,  $H_{c2}=0.1 \text{ Oe}$ . For a mean granule size of  $0.7 \cdot 10^{-6} \text{ m}$  in  $LaSrCuO$ ,  $H_{c1}=0.2 \text{ Oe}$ . From nonlinearity of magnetization low-temperature isotherms in weak fields, the magnetic field penetrates first into the intergranular space  $H_{c1} < 1 \text{ Oe}$ , then into the superconducting granules ( $H_{c1} > 100 \text{ Oe}$ )

## Effects of Hydrothermal Ageing on Structure and Adhesion Properties of TiO<sub>2</sub>-Nanotubes

**Tobias Mertens<sup>1</sup>, Beatriz Rico-Oller<sup>1</sup>, Max Kolb<sup>1</sup>, Jürgen Wehr<sup>1</sup>**

<sup>1</sup> Airbus Group, Airbus Group Innovations, Dept. Metallic Technologies & Surface Engineering, 81663 Munich/Germany, tel: +49 89 607 21440, email: tobias.mertens@airbus.com

In the aerospace industry new design concepts offering weight savings are high in demand. In the recent generation of aircrafts (e.g. Airbus 350 XWB, Boeing 787), composite materials have shown new perspectives in terms of structural efficiency and performance. Due to the increasing amount of composite materials used in the aircraft structure, new corrosion concepts have to be developed. Composite materials with carbon fibres can induce galvanic corrosion when attached to an aluminium structure. In order to avoid this kind of galvanic corrosion, titanium alloys have to be used in aerospace. However, it is well-known in aerospace industry that titanium materials exhibit critical issues in regard to long-term stable adhesion. Reflecting this, the surface treatment is the most important step to ensure durable joints.

Within this work, the anodisation of TiO<sub>2</sub>-nanotubes in a fluoride-containing electrolyte is used as a pre-treatment of the titanium alloy Ti6Al4V. Using this anodising process, the surface area could be enlarged, compared to the initial surface after the alkaline etching

As shown within this work, the TiO<sub>2</sub>-nanotube anodising leads to an oxide layer that features an amorphous structure. The exposure of the amorphous TiO<sub>2</sub>-nanotubes under hydrothermal conditions (40 °C and 100 % rh) revealed that the TiO<sub>2</sub>-nanotubes are instable. At these conditions, the TiO<sub>2</sub>-nanotubes crystallise to the TiO<sub>2</sub> modifications anatase and rutile. This process is initiated by the rearrangement of TiO<sub>6</sub> octahedrons, due to the interaction between the water molecules and the OH groups of the different TiO<sub>6</sub> octahedrons. Nevertheless, the resultant adhesion properties are not affected by the described instability of the nanotubes under hydrothermal conditions. Due to the reaction of the oxide OH groups with the organic molecules of the coating, the OH groups are not available for the interaction with the water molecules and hence, the rearrangement of TiO<sub>6</sub> octahedrons cannot be initiated.

The investigations show that in principle the TiO<sub>2</sub>-nanotubes can be used as pre-treatment of Ti6Al4V. However, if the Nanotubes are not covered by an organic coating, a crystallisation process takes place at hydrothermal conditions.



## Structural and magnetic properties of single graphene film with magnetic Co deposition

Min Zhai<sup>1</sup>, Shuangli Ye<sup>2,\*</sup>, Feng Liu<sup>2</sup>, Chang Qi<sup>2</sup>, Xinzhi Shi<sup>2</sup>, Gaofeng Wang<sup>2</sup>

<sup>1</sup>*School of Physics and Technology, Wuhan University, Wuhan 430072, P. R. China*

<sup>2</sup>*Institute of Microelectronics and Information Technology, Wuhan University, Wuhan 430072, P. R. China*

The magnetic Co deposited on the CVD-grown pristine p-type single graphene film/SiO<sub>2</sub> and on the CVD-grown Nitrogen-doped n-type graphene film/SiO<sub>2</sub> nanostructures have been fabricated, respectively. The composition, structure and magnetic properties of these nanostructures are investigated by the XRD, Raman, XPS and HRTEM and SQUID experiments. It can be found that the Co nanoparticles are formed on the surface of the single layer graphene, which is demonstrated by XRD and SEM measurements. On the other hand, the XPS result reveals the existence of bivalent Cobalt ions. The Raman spectroscopy shows the enhanced disorder effects and the large red shift of the 2D peak after the Co deposition process. These results confirm that the Co is embedded into the graphene film as well. With the temperature decreasing, the G peak is stiffened and sharpened for the pristine single graphene film. In contrast, hardly temperature dependence can be found for the G peak of the graphene film after Co deposition. This phenomenon indicates the inhomogeneous local disorder effect induced by the Co atoms embedded in the graphene film. Moreover, the larger disorder effect induced by the Co deposition can be found for the single graphene film with higher original vacancies, illustrating the possibility for the formation of the Co atom-vacancy complexes, which can contribute the local magnetic moment in graphene. On the other hand, with the carriers of the graphene film changed from p-type to n-type by Nitrogen doping, the interplay between the local magnetic moment and the itinerant  $\pi$  carriers in graphene film have been investigated by magneto-transport measurements. The formation of the magnetic Co nanoparticles and the magnetic Co atom-vacancy complexes in graphene offers a possibility for the graphene-based spintronic device application.

**Corresponding author:** Prof. Shuangli Ye, Institute of Microelectronics and Information Technology, Wuhan University, No.37, Luoyu Rd., Wuhan 430079, P. R. China. Phone: ++86-(0)27-68778588-804, fax: ++86-(0)27-68778588-807, email:slye@whu.edu.cn.

## Improvement in Structural and Optical Properties of InGaN/GaN LEDs Using Grid Patterns Realized by Laser Treatments

Kwanjae Lee<sup>1</sup>, Cheul-Ro Lee<sup>1</sup>, and Jin Soo Kim<sup>1,\*</sup>

<sup>1</sup>Division of Advanced Materials Engineering & Research Center of Advanced Materials Development, Chonbuk National University, Jeonju 561-756, Korea

*E-mails:* [dlrhksw01012@naver.com](mailto:dlrhksw01012@naver.com) and [kjinsoo@jbnu.ac.kr](mailto:kjinsoo@jbnu.ac.kr)

When growing GaN-based epitaxial layers on a sapphire substrate, there is inherently bowing largely due to difference in lattice constants and thermal expansion coefficients [1]. In the present work, we report the influences of grid-patterned sapphire substrate realized by laser treatment on the structural and optical properties including bowing characteristics of GaN-based epitaxial layers. The sizes and depths of grid patterns (GPs) fabricated on sapphire substrates were manipulated by changing laser power. The spacings between adjacent GPs were 1, 2, and 3 mm. After realizing the GPs on a substrate, the InGaN/GaN light-emitting diode (LED) structures were grown by Thomas-Swan vertical-metal-organic chemical-vapor deposition. A conventional InGaN/GaN LED (C-LED) without the GPs was prepared as a reference. The optical and electrical properties of the LED samples were evaluated by photoluminescence (PL) and electroluminescence (EL) mapping spectroscopies for the entire substrate. The amount of bowing for the LEDs with respect to the grid spacings (GSs) of 1 (GS1-LED), 2 (GS2-LED), and 3 mm (GS3-LED) were measured to be 100.05, 100.43, and 101.59  $\mu\text{m}$ , respectively, which were significantly improved compared to that of the C-LEDs (108.06  $\mu\text{m}$ ). From the PL mapping results, the standard deviations in wavelength with respect to the main peak for the GS1-LED, GS2-LED, and GS3-LED were evaluated to be 1.02, 1.38, and 1.06 nm, respectively. These deviations are relatively smaller than that of the C-LED sample (2.04 nm) indicating that the uniformity was effectively enhanced using the laser treatments. Also, the emission wavelength for all the GS-LEDs was blue-shifted compared to the C-LED (445 nm) at room temperature mainly due to the strain relaxation caused by the decrease in initial bowing.

**Keywords:** *Initial bowing, laser treatment, InGaN/GaN LEDs*

[1] OHNO, Y., KUZUHARA, M. 2001. Application of GaN-Based Heterojunction FETs for Advanced Wireless Communication, IEEE Transactions on Electron Devices, 48, 517–523.

## Properties of ZnS:Cu thin films grown by chemical bath deposition

C. Barraza Ramos<sup>1</sup>, K. Sáenz Gutiérrez<sup>1</sup>, F. S. Aguirre Tostado<sup>2</sup>, R. C. Ambrosio Lázaro<sup>1</sup>, M. de L. Mota González<sup>1</sup>, A. Carrillo Castillo<sup>1\*</sup>

<sup>1</sup>*Instituto de Ingeniería y Tecnología, Universidad Autónoma de Ciudad Juárez. Cd. Juárez Chih. CP 32310, México.*

<sup>2</sup>*Centro de Investigación en Materiales Avanzados, S. C., Unidad Monterrey, Alianza Norte 202, Parque de Investigación e Innovación Tecnológica, Apodaca, Nuevo León, C.P. 66628, México.*

*E Mail/ Contact Détails:* [amanda.carrillo@uacj.mx](mailto:amanda.carrillo@uacj.mx)

Zinc sulphide (ZnS) multilayer films were prepared by chemical bath at 80 °C on glass substrates. In order to grow ZnS multilayer films with different thickness, the films were deposited at different times and the chemical process was repeated two consecutive times with fresh solutions used for every deposition. After complete chemical bath deposition 10 nm of copper was deposited by sputter technique. The films were annealed for 20 min at 200 °C in air.

The films obtained were structural, optical and electrical characterized. Homogeneous ZnS thin films with amorphous structure were obtained, The optical band gap was determined by UV-Vis absorption around 3.6 eV for ZnS films and 3.1 eV for ZnS:Cu films. The electrical resistivity on the ZnS showed values greater than 100 MΩ, and for ZnS:Cu films the electrical resistivity varied in the range from 10 and 37 MΩ, it decreasing with the deposition time and number dip increase for ZnS films. These characteristics obtained in the amorphous ZnS:Cu thin films make them a suitable candidate for device and optoelectronic device applications that require low processing temperature.

***Keywords:* ZnS:Cu, thin films, chemical bath deposition, amorphous films**

## Carbon nanotubes modified with gold nanoparticles in biosensing

Nikos G. Tsierkezos, Uwe Ritter

Ilmenau University of Technology, Department of Chemistry, Ilmenau, Germany

E Mail: [nikos.tsierkezos@tu-ilmenau.de](mailto:nikos.tsierkezos@tu-ilmenau.de)

Pristine and nitrogen-doped multi-walled carbon nanotubes were fabricated and modified with gold nanoparticles possessing different diameters. The fabricated nanotubes, further denoted as MWCNTs/AuNPs and N-MWCNTs/AuNPs, were initially characterized using  $[\text{Fe}(\text{CN})_6]^{3-/4-}$ . Within the two different types of films probed, N-MWCNTs/AuNPs reveals improved response towards  $[\text{Fe}(\text{CN})_6]^{3-/4-}$  due to nitrogen that is incorporated into the structure of nanotubes and enhances their electro-catalytic activity. The findings exhibit that the electrochemical response of films enhance with their decoration with AuNPs. Thus, the response of MWCNTs/AuNPs and N-MWCNTs/AuNPs is improved for about ~40% and ~20%, respectively, upon modification. N-MWCNTs/AuNPs with AuNPs possessing various diameters (5, 14, and 35 nm) were applied for simultaneous analysis of ascorbic acid, uric acid, and dopamine. The findings reveal strong dependence of films' response on AuNPs diameter. It was recognized that onto N-MWCNTs/AuNPs (14 nm) greater separation between oxidation waves of biomolecules occurs permitting thus their simultaneous analysis in a single experiment [1].

**Keywords:** carbon nanotubes, gold nanoparticles, electrochemical biosensors

[1] TSIERKEZOS, N.G., SZROEDER, P., RITTER, U. 2014. Voltammetric study on pristine and nitrogen-doped multi-walled carbon nanotubes decorated with gold nanoparticles. *Microchim. Acta*, 181, 329-337.

## **Zeolite Impregnated Polysulfone Membrane for the Removal of Metals in Wastewater**

Yılmaz Yürekli

Celal Bayar University, Bioengineering Department, 45140, Manisa/ TURKEY

[yilmazyurekli@gmail.com](mailto:yilmazyurekli@gmail.com) / +90-2362012454

In this study, separation capabilities of zeolite nano-particles added polysulfone (PSf) membranes against metal ions ( $\text{Pb}^{2+}$  and  $\text{Ni}^{2+}$ ) were determined under dynamic conditions by using dead-end stirred cell. Zeolite nano-particles were synthesized using conventional hydrothermal method [1]. X-ray diffraction (XRD), scanning electron microscopy (SEM) and energy dispersive X-ray (EDX) analysis revealed that the synthesized nanoparticles are pure NaX zeolite with particle sizes around 200 nm and Si/Al ratio is 1.24. According to the results obtained from batch adsorption experiments at 25°C, the maximum adsorbed amount of lead and nickel ions were determined as 443 and 279 mg/g respectively. Water hydraulic permeability of the PSf membrane was increased from 23 to 45 L/m<sup>2</sup>.h.bar with the addition of NaX-nanoparticles indicates that hydrophilicity of the membrane was improved which was proved by FTIR-ATR and water contact angle measurements. Filtration results revealed that the increased amount of NaX-nanoparticles from 0 to 5 w% (PSf to PSf5) in the membrane increased the adsorbed amount of metal from 0.2 to 0.8 mg for the filtration of nickel in which the initial feed concentration was 500 mg/L and transmembrane pressure was constant at 1 bar. When the NaX content of the PSf membrane was increased to 10 w% (PSf10), the adsorbed amount of nickel was almost twice than it was achieved with PSf5 membrane. The maximum adsorbed amount of metals have been achieved as 56 and 110 mg/g for nickel and lead ions respectively at the end of 60 min filtration of 100 mg/L feed solutions at 1 bar. As a conclusion, with the addition of NaX-nanoparticles both hydraulic permeability and adsorption capacity of the PSf membrane was improved.

**Keywords:** *NaX-nanoparticles, membrane filtration, metal ions removal*

[1] ZHAN B.Z., WHITE M.A., LUMSDEN M., MUELLER-NEUHAUS J., ROBERTSON K.N., CAMERON T.S., GHARGHOURI M., 2002. Control of particle

size and surface properties of crystals of NaX zeolite, Chem. Mater. 14, 3636–3642.

## Piezoelectric thin film layer integrated microdiaphragm for the dynamic sensing viscosity and density of liquid for bio applications

Hye Jin Kim<sup>1,2</sup>, Jinsik Kim<sup>1</sup>, Myung-Sic Chae<sup>1,2</sup>, Yong Kyoung Yoo<sup>1,3</sup>, Gangeun Kim<sup>1,2</sup>, Dahye Jeong<sup>1</sup>, Jung Ho Park<sup>2</sup> and Kyo Seon Hwang<sup>1</sup>

<sup>1</sup>Center for BioMicrosystems, Korea Institute of Science and Technology, Seoul 136-791, Korea

<sup>2</sup>Department of Electrical Engineering, Korea University, Seoul 136-713, Korea

<sup>3</sup>Department of Electrical Engineering, Kwangwoon University, Seoul 139-701, Korea

*kshwang@kist.re.kr/ Kyo Seon Hwang*

A microdiaphragm sensor have been grown up as a promising sensor in bio applications [1]. A resonant frequency of microdiaphragm sensor would be changed by loaded materials such as biomolecules [2, 3]. And detecting the resonant frequency was the principle of detecting biomolecules with microdiaphragm. Many variables such as a spring constant, damping ratio, loaded mass, and a loading position of the mass can affect to the changes of resonant frequency. To detect the changes of resonant frequency with more efficiency, higher sensitivity and accuracy, the integrated dynamic actuating layer of microdiaphragm was needed [4].

Here, we introduced a piezoelectric layer of lead zirconate titanate (PZT;  $\text{Pb}(\text{Zr}_{0.52}\text{Ti}_{0.48})\text{O}_3$ ) embedded microdiaphragm resonating sensor for detecting viscosity and density of human blood. The effective mechanical factors are analyzed to change the resonant frequency of microdiaphragm. The acting of microdiaphragm with integrated PZT acting layer was also confirmed with the analysis. The microdiaphragm has uniform resonant frequency in (1,1) and (2,2) modes without any loading of biomolecules by PZT acting layer. The microdiaphragm with dynamic actuating layer has hundreds kHz range of resonant frequency with microdiaphragm which has dimension of  $500\mu\text{m}$  by  $500\mu\text{m}$ . Viscous solutions of mixture with glycerol and deionized water were prepared to verify the basic characteristics of microdiaphragm with a viscosity and density in the range from 1 to 1414 cP and 0.998 to  $1.263 \times 10^3 \text{ kg/m}^3$ , respectively. The solution was injected at

the bottom side of the microdiaphragm and the changes of resonant frequency was occurred by the loading of viscous solution. The resonant frequencies decreased according to the density and viscosity of liquid in the both (1,1) and (2,2) modes. The sensitivities of density (range:  $0.998 \sim 1.146 \times 10^3 \text{ kg/m}^3$ ) of microdiaphragm were respectively  $28.03 \text{ Hz/kg}\cdot\text{m}^{-3}$  and  $81.85 \text{ Hz/kg}\cdot\text{m}^{-3}$  in (1,1) and (2,2) modes. The full width of half maximum had been changed with the viscosity of liquid and the liquid has viscosity-range from 1 to 8.4 cP. The microdiaphragm with PZT actuating layer can measure the density and viscosity of a liquid within the ranges of density and viscosity of blood as generally known as  $1.060 \times 10^3 \text{ kg/m}^3$  and 3–4 cP. The microdiaphragm sensor were also demonstrated with a real human serum. The mixture of human serum and deionized water was also used to verify the suitability of measuring the viscosity and density of human blood. The sensitivity of viscosity and density were also similar with human blood serum as simulant viscous solutions.

Consequently, the PZT layer embedded microdiaphragm resonating sensor could be actuated and detected the liquid in various density and viscosity range and even the human blood serum. We hope that the microdiaphragm sensor could be used for early diagnosis of diseases associated with the physical properties of blood.

***Keywords: Piezoelectric layer, diaphragm sensor, viscosity and density of blood, resonance frequency***

[1] Ioana Voiculescu, Anis Nurashicin Nordin, 2012. Acoustic wave based MEMS devices for biosensing applications. *Biosensors and Bioelectronics*, 33, 1-9.

[2] Shaokang Li, Wei Ren, Xu Lu, Zhuo Xu, Zhongyang Cheng, Xiaofeng Chen, Peng Shi, Xiaoqing Wu and Xi Yao, 2011. Ferroelectric Thin Film Diaphragm Resonators for Bio-Detection. *Ferroelectrics*, 410, 145-151.



[3] Guo-Hua Feng, Zhi-Dian Lin, 2013. A droplet-based piezoelectric concave diaphragm biosensor with self-enhancing functionality for label-free detection of protein-ligand interactions. *Sensors and Actuators B : Chemical*, 182, 809-817.

[4] Yang Xin, Zhimin Li, LeVar Odum and Z. -Y. Cheng. 2006. Piezoelectric diaphragm as a high performance biosensor platform. *APL*, 89, 223508.

# Symposia 3

## Advances in Polymers and Ceramics

---

- Progress in the synthesis of polymers and ceramics
- Advances in the characterization techniques for polymer and ceramics
- Theoretical Studies and Modeling of polymer and ceramics
- Biomedical and Cosmetic Applications of polymers
- Optoelectronics, sensing, energy and electronic Applications of polymers
- Polymer materials from renewable resources
- Nanofabrication and Nanopatterning of polymers: Challenges and Innovation
- Porous Polymers and ceramics
- Electroactive polymers (ionic and electronic), shape memory polymers, and ionic gels
- Advanced Ceramic Materials and Processing for Photonics and Energy
- Next Generation Bioceramics and Biocomposites
- Modelling of processes and properties of polymers and ceramics
- Others

# INDEX PAGE

1. 2 mol% Mn-doped zinc phosphate used as irreversible thermal sensor <b>AUTHOR:</b> Dr. Salek Guillaume	1
2. Infrared microscopy: time-resolved chemical mapping in light-emitting electrochemical cells <b>AUTHOR:</b> Dr. Mohammadjavad Jafari	2
3. Synthesis Of Novel Chemosensors Based On Xanthene Molecules And Its Functionalized Platform <b>AUTHOR:</b> Prof. Young-A Son Son	3
4. 4.Ultra-Responsive Soft Matter From Strain-Stiffening Hydrogels <b>AUTHOR:</b> Dr. Paul Kouwer	4
5. Study on the CMC/PLA composite foam as wound packing materials <b>AUTHOR:</b> Dr. Song Jun Doh	5
6. Study on the CMC/PLA composite foam as wound packing materials <b>AUTHOR:</b> Dr. Yoon Jin Kim	6
7. Development of conducive polymer electrodes for biomedical applications <b>AUTHOR:</b> Dr. Ernesto Suaste	7
8. Engineering PEEK bioactivity: Effect of plasma and gold sputtered interface <b>AUTHOR:</b> Dr. Alena Reznickova	9
9. Pva/ Zno Nanoparticles Via Sol Gel Process For Biomedical Applications <b>AUTHOR:</b> Dr. Amanda Carrillo	11
10. Study on the CMC/PLA composite foam as wound packing materials <b>AUTHOR:</b> Dr. Jungyeon Kim	12
11. Study on the CMC/PLA composite foam as wound packing materials <b>AUTHOR:</b> Dr. Jung Nam Im	13
12. Architecture Design of Dynamic Networks with Shape-memory Effect <b>AUTHOR:</b> Prof. Ke-Ke Yang	14
13. Emittance Variation and IR Electrochromism in Skins Comprised of Unique Conducting Polymers, Ionic Liquid Electrolytes, Microporous Polymer Membranes and Semiconductor/Polymer Coatings, for Spacecraft Thermal Control <b>AUTHOR:</b> Dr. Prasanna Chandrasekhar	16
14. All organic modified relaxor ferroelectric terpolymers: Towards Low Electric Field Dielectric Actuators <b>AUTHOR:</b> Dr. Jean Fabien Capsal	17
15. Mediating gel formation from structurally controlled poly(ionic liquids): towards ionic gel electrolytes for energy storage <b>AUTHOR:</b> Dr. Hassan Srour	18
16. Conducting polymers as biomimetic reactive sensors of the working conditions: Evidence from Polyaniline <b>AUTHOR:</b> Dr. Yahya Ismail	19
17. All organic modified relaxor ferroelectric terpolymers: Towards Low Electric Field Dielectric Actuators <b>AUTHOR:</b> Dr. Florent Ganet	20
18. Epoxy-Based Shape Memory Composites Containing Carbon-Based Additives <b>AUTHOR:</b> Prof. Goknur Bayram	21
19. Active Water Vapor Transport across Functionalized Conducting Polymer Microporous Membranes at Very High Rates, Using the Electroosmotic Effect, with Simultaneous Chemical Warfare (CW) Agent Blocking, for Use in Soldier Uniforms <b>AUTHOR:</b> Mr. Brian Zay	23
20. Electrically triggered release of amoxicillin from polyacrylamide/polyaniline and	24

polyacrylamide/polypyrrole hydrogels <b>AUTHOR:</b> Dr. Teresa Del Castillo Castro	
21. Piezoresistive NBR-Polypyrrole composites prepared by swelling method <b>AUTHOR:</b> Dr. José Carmelo Encinas	25
22. Crystallization induced self-assembly of amphiphilic copolymer based on poly(p-dioxanone) controlled by solvent mixing and its application in electrospun nanofiber <b>AUTHOR:</b> Prof. Si Chong Chen	26
23. Novel Foam Structures for Personalized Bone Replacement Materials <b>AUTHOR:</b> Mr. Matthias Ahlhelm	29
24. Biomimetic synthesis of rosette-like calcite mesocrystals mediated by a marine-derived recombinant glycine-rich protein <b>AUTHOR:</b> Prof. Yoo Seong Choi	30
25. Optoelectronic Fast Response Properties Of Pq/Pmma Polymer <b>AUTHOR:</b> Prof. Xiudong Sun	31
26. Organometallics for Opto-electronic Device Applications <b>AUTHOR:</b> Prof. Muhammad Khan	32
27. Ultra-Fast Response Polyaniline Memristor By One Pot Synthesis Using FeCl <sub>3</sub> As Oxidant And Doping Agent <b>AUTHOR:</b> Dr. Sergio Bocchini	33
28. Covalent Superabsorbent Hydrogel Based On Alginate For Removal Of Dye From Environmental Samples <b>AUTHOR:</b> Prof. Adley Forti Rubira	35
29. SUSTAINABLE GEOPOLYMER MORTAR USING LOCAL INDUSTRIAL WASTE MATERIALS <b>AUTHOR:</b> Dr. Ubagaram Johnson Alengaram	37
30. High-Performance Polyimides Derived From Bio-Derived Eccentric Amino Acid <b>AUTHOR:</b> Prof. Tatsuo Kaneko	38
31. Cellulose nanocrystals and nanofibers for renewable active materials <b>AUTHOR:</b> Prof. Jaehwan Kim	39
32. Novel thermo-reversible polymers from furan-modified vegetable oils via Diels-Alder reactions <b>AUTHOR:</b> Dr. Talita Martins Lacerda	40
33. Isolation of Macromolecular Polymeric Ingredients from Waste Biomass Materials and their Characterization <b>AUTHOR:</b> Dr. Hanzade Acma	41
34. Synthesis of alkyd resins from ceiba pentandra L. (kapok) seed oil and an investigation on their biodegradation <b>AUTHOR:</b> Prof. Dilip Kumar Kakati	42
35. Biodegradable Plastic Compounded with Oil Palm Biomass to Produces Bioplastic Fertilizer (BpF) Composites <b>AUTHOR:</b> Mr. Harmaen Ahmad Saffian	44
36. Preparation Of Ultra-Anisotropic Hydrogels Of Cyanobacterial Polysaccharides, Sacran <b>AUTHOR:</b> Dr. Maiko Okajima	46
37. Tuning the degradation of PLA through the use of hybrid organic-inorganic coatings <b>AUTHOR:</b> Dr. Andrea Sacconi	47
38. Effect of the addition of chitosan on the physicochemical properties of extruded polypropylene films <b>AUTHOR:</b> Dr. Dora Evelia Rodríguez Félix	48
39. TiO <sub>x</sub> Magneli phases as anode material for the degradation of refractory pollutants <b>AUTHOR:</b> Dr. Bechelany Mikhael	49
40. TiO <sub>x</sub> Magneli phases as anode material for the degradation of refractory pollutants <b>AUTHOR:</b> Dr. Sophie Cerneaux	50
41. A Porous TiO <sub>2</sub> -Coated Silica Glass Tube And Its Application For Compact Air- And Water-Purification Units	51

<b>AUTHOR:</b> Dr. Tsuyoshi Ochiai	
42. Fabrication of Hierarchically Structured Porous Films of Metal Oxides and Carbonates through Coffee Ring Effect	53
<b>AUTHOR:</b> Prof. Sachin Khapli	
43. Nanofibers/ Microporous Kevlar® Films For Separator Technology	55
<b>AUTHOR:</b> Dr. Chi Ho Kwok	
44. A new synthesis scaffolds route with sol-gel bioactive glass and addition of porogen agents for bone tissue regeneration	56
<b>AUTHOR:</b> Ms.Fabiana Barbosa Amaral Pereira Guimarães	
45. Functionalized oligomers and block copolymers synthesis using Catalytic Chain Transfer Polymerization	58
<b>AUTHOR:</b> Prof. Andre Mortreux	
46. The Controlled/Living Radical Homopolymerization Of Multivinyl Monomers: Toward Single Chain Cyclized Polymers	59
<b>AUTHOR:</b> Mr. Yongsheng Gao	
47. High coercive CoFe <sub>2</sub> O <sub>4</sub> powders for technological permanent magnet applications	62
<b>AUTHOR:</b> Mr. José Luis F. Cuñado	
48. Fabrication And Characterization Of Superparamagnetic Maghemite/Pmma Nanofibrous Composite	64
<b>AUTHOR:</b> Dr. Bee Chin Ang	
49. Mechanical Properties of Non-cement Mortars fabricated under Supercritical Carbonation Conditions without Alkali Activators and Composed of Fly Ash and Fused Waste Slag	65
<b>AUTHOR:</b> Prof. Yootaek Kim	
50. Comparative study of Iron-catalyzed ATRP Systems Using Various Highly Active Bidentate P-N Ligands	66
<b>AUTHOR:</b> Dr. Mohd Yusuf Khan	
51. Computational Investigation Of Multi Phase Formation In Segmented Polyurethane Copolymers	68
<b>AUTHOR:</b> Prof. Mine Yurtsever	
52. Highly water soluble nanostructured Boron Nitride for anticancer drug delivery	69
<b>AUTHOR:</b>	
53. The Use Of Kenaf Fiber Reinforced Composite To Confine The Concrete Cylinder	70
<b>AUTHOR:</b> Dr. Reza Mahjoub	

## 2 mol% Mn-doped zinc phosphate used as irreversible thermal sensor

Salek G<sup>1</sup>, Gaudon M.<sup>1</sup>, Demourgues A.<sup>1</sup>, Garcia A<sup>1</sup>, Jubera, V<sup>1</sup>.

1 CNRS, Univ. Bordeaux, ICMCB, UPR9048, F-33600 Pessac, France

[salek@icmcb-cnrs.bordeaux.cnrs](mailto:salek@icmcb-cnrs.bordeaux.cnrs)/[gaudon@icmcb-cnrs.bordeaux.fr](mailto:gaudon@icmcb-cnrs.bordeaux.fr)/[demourg@icmcb-bordeaux.cnrs.fr](mailto:demourg@icmcb-bordeaux.cnrs.fr)

Over the past few decades, research on phosphors based thermometry systems are becoming increasingly important in different fields: engineering, nanosciences, etc.<sup>1</sup> The temperature dependence characteristics of the thermographic phosphors can be evaluated by a spectral and/or a temporal modification of the phosphorescence emission. Within the different thermometric phosphors,  $Zn_3(PO_4)_2$  doped by phosphor activator can be used as an irreversible thermographic sensor. Three allotropic monoclinic forms with notations:  $\alpha$ ,  $\beta$ ,  $\gamma$  exist for the anhydrous compound. For Mn-doped  $Zn_3(PO_4)_2$  compound, the phase transitions between these allotropic forms are associated with a change of the emission spectrum due to a modification of the  $Mn^{2+}$  ions coordination. Indeed, the main visible emission of this phosphor dopant corresponds to a  ${}^4T_1 \rightarrow {}^6A_1$  transition, which is strongly dependent on the ligand field and the coordination number. The relationship between the annealing temperature and the phosphorescence was established combining X-ray diffraction and luminescence spectroscopy. Thus, the evolution of the compound chromaticity versus thermal history was fully interpreted and then evaluated in regard of the potentiality of the this compound to be used as a thermographic phosphor.

**Keywords:** *Thermal sensors, Luminescence, Pigment, Orthophosphate*

[1] Aldén, M.; Omrane, A.; Richter, M.; Särner, G. *Prog. Energy Combust. Sci.* **2011**, *37*, 422–461.



## Synthesis of Novel Chemosensors based on Xanthene Molecules and its Functionalized Platform

Jongwoo Jeong<sup>1</sup>, Haksoo Kim<sup>1</sup>, Jiyong Hwang<sup>1</sup>, Chang-Soo Lee<sup>2</sup> and Young-A Son<sup>1,\*</sup>

<sup>1</sup>Department of Advanced Organic Materials Engineering, Chungnam National University, Daejeon 305-764, South Korea

<sup>2</sup>Department of Chemical Engineering, Chungnam National University, Daejeon 305-764, South Korea

*E Mail : yason@cnu.ac.kr*

We report the design and synthesis of a novel chemosensor rhodamine-based indicator for selective detection of hazardous cation. Sensing behavior toward various metal ions was investigated by UV-Vis and fluorescence spectroscopy. The indicator exhibited highly selective and sensitive colorimetric and “turn-on” fluorescent responses toward Al<sup>3+</sup> cations based on the ring-opening mechanism of the rhodamine spirolactam. The obvious change from colorless to pale pink upon the addition of Al<sup>3+</sup> could make it a suitable “naked eye” indicator for Al<sup>3+</sup>. More significantly, the sensor displayed a remarkable colorless to yellowish green fluorescence switch in the presence of Al<sup>3+</sup> cations. Finally, we proposed a reversible ring-opening mechanism (OFF–ON) of the rhodamine spirolactam induced by Al<sup>3+</sup> binding and forming a 1:1 stoichiometric complex of CS- Al<sup>3+</sup> which is supported by the material studio theory calculations.

**Keywords:** *rhodamine 6G, phenyl semicarbazide, Fluorescent Chemosensor, molecular modeling.*

[1] D.MAITY, D. KARTHIGEYAN, T.K.KUNDU, AND T.GOVINDARAJU. 2013. Sensors and Actuators, B 176, 831 (2013).



## Ultra-responsive soft matter from strain-stiffening hydrogels

Paul H. J. Kouwer

Radboud University, Institute for Molecules and Materials, Heyendaalseweg 135,  
6525 AJ Nijmegen, the Netherlands

*E Mail: p.kouwer@science.ru.nl*

The stiffness of hydrogels is crucial for their applications. Nature's hydrogels become stiffer as they are strained. This stiffness is not a constant but increases when the gel is strained. This stiffening is used, for instance, by cells that actively strain their environment to modulate their function. When optimised, such strain-stiffening materials become extremely sensitive and very responsive to stress. Strain-stiffening, however, is unexplored in synthetic gels since the structural design parameters are unknown. We uncover how readily tuneable parameters such as concentration, temperature and polymer length impact the stiffening behaviour. Our work also reveals the marginal point, a well-described, but never observed, critical point in the gelation process. Around this point, we observe a transition from a low-viscous liquid to an elastic gel upon applying minute stresses. Our experimental work in combination with network theory yields universal design principles for future strain-stiffening materials.

***Keywords: Responsive soft matter, hydrogels, mechanical properties, cytoskeleton & ECM***

- [1] JASPERS, M., DENNISON, M., MABESOONE, M. F. J., MACKINTOSH, F. C., ROWAN, A. E. & KOUWER, P. H. J. Ultra-responsive soft matter from strain-stiffening hydrogels, *Nat. Commun.* **2014**, doi: 10.1038/ncomm6808.
- [2] KOUWER, P. H. J., KOEPF, M. LE SAGE, V. A. A., JASPERS, M., VAN BUUL, A. M., EKSTEEN-AKEROYD, Z. H., WOLTINGE, T. SCHWARTZ, E., KITTO, H. J., HOOGENBOOM, R., PICKEN, S. J. NOLTE, R. J. M., MENDES, E. & ROWAN, A. E. Responsive biomimetic networks from polyisocyanopeptide hydrogels, *Nature* **2013**, 493, 651.
- [3] DENNISON, M., JASPERS, M., KOUWER, P. H. J., STORM, C., ROWAN, A. E. & MACKINTOSH, F. C. Critical behaviour in the elastic response of hydrogels, *arXiv*, **2014**, 1407.0543.

## Study on the CMC/PLA composite foam as wound packing materials

Yoon Jin (Kim)<sup>1</sup>, Jung Nam (Im)<sup>1</sup>, Tae Hee (Kim)<sup>1</sup>, Song Jun (Doh)<sup>1</sup>

<sup>1</sup>Korea Institute of Industrial Technology, 143 Hangeul-ro, Ansan, South Korea, 426-910

*wolfpack@kitech.re.kr*

Carboxymethyl cellulose(CMC)/poly(lactic acid)(PLA) composite foam was obtained by lyophilization of PLA-dispersed CMC solution and post-treatment. The aim of the study was to prepare CMC/PLA composite foams and to investigate the liquid handling properties and their applicability to wound packing materials. Structural analyses were performed through SEM, FT-IR, DSC and so on. The mechanical properties were analyzed by measuring compressional strength and compression recovery. The liquid handling properties were studied by liquid absorption measurement under a certain pressure condition. As the proportion of PLA increased, the compressional strength and recovery increased while the liquid absorption capacity decreased. Gamma ray radiation process was introduced after the foam manufacturing as means of controlling biodegradability and sterilization. The degradation period decreased with increasing amount of the radiation. However, the mechanical properties were not affected by the amount of the radiation significantly.

***Keywords:*** Carboxymethyl cellulose, Foam, Liquid handling properties, wound packing, acid treatment

## Study on the CMC/PLA composite foam as wound packing materials

Yoon Jin (Kim)<sup>1</sup>, Jung Nam (Im)<sup>1</sup>, Tae Hee (Kim)<sup>1</sup>, Song Jun (Doh)<sup>1</sup>

<sup>1</sup>Korea Institute of Industrial Technology, 143 Hangeul-ro, Ansan, South Korea, 426-910

*wolfpack@kitech.re.kr*

Carboxymethyl cellulose(CMC)/poly(lactic acid)(PLA) composite foam was obtained by lyophilization of PLA-dispersed CMC solution and post-treatment. The aim of the study was to prepare CMC/PLA composite foams and to investigate the liquid handling properties and their applicability to wound packing materials. Structural analyses were performed through SEM, FT-IR, DSC and so on. The mechanical properties were analyzed by measuring compressional strength and compression recovery. The liquid handling properties were studied by liquid absorption measurement under a certain pressure condition. As the proportion of PLA increased, the compressional strength and recovery increased while the liquid absorption capacity decreased. Gamma ray radiation process was introduced after the foam manufacturing as means of controlling biodegradability and sterilization. The degradation period decreased with increasing amount of the radiation. However, the mechanical properties were not affected by the amount of the radiation significantly.

***Keywords:*** Carboxymethyl cellulose, Foam, Liquid handling properties, wound packing, acid treatment

## **Development of conductive polymer electrodes for biomedical applications.**

E. Suaste-Gomez<sup>1</sup>, O. Teran-Jimenez<sup>1</sup>, D. Hernández-Rivera<sup>1</sup>, H. Reyes-Cruz, C. J.<sup>1</sup>  
Rodríguez-Montoya<sup>1</sup>

<sup>1</sup>A Center for Research and Advanced Studies of the National Polytechnic Institute. Av IPN, #. 2508, San Pedro Zacatenco, Del. Gustavo A. Madero, D.F. Mexico, C.P 07360<sup>1</sup>

*esuaste@cinvestav.mx* / presenting and corresponding author

*omartjnz@hotmail.com* / corresponding author

The use of electrodes in the process of register physiological signals is very important for medical and research areas. Actually exists a variety of electrodes according to the use or the requirements of the biosignal that need to be registered. However, many electrodes are still based on Ag/AgCl which is very problematic for registers where the patient require stay in movement or for long term monitoring due to the aging process.

With the discovering of conductive polymers, the possibilities of use have reached the development of monitoring electrodes which have growth in the last years. However, the fabrication process for many of them are still expensive in their production by the specialized equipment reducing the chances for massive production. In this wok have been proposed the fabrication of conductive polymer electrodes based on PPY with an effective and lowcost fabrication process which have been demonstrated excellent results in compare with a typical Ag/AgCl electrodes. The PPY electrodes fabricated were also used after months of its first use to probe their capability of be a reusable electrode. ECG and impedanciometry registers are reported.

The potential of uses can be expanded to EOG, EEG, TENs, or another medical purpose where an skin electrode are required without the limitation of shape and size cause the electrodes proposed can be designed to be rigid or flexible according to the application requirements.

**Keywords:** *Conductive polimer, electrodes, impedanciometry, ECG, pollypirrolePPY*

- [1] KANIUSAS, E. 2012. *Biomedical Signals and Sensors I: Linking Physiological Phenomena and Biosignals*, Springer.
- [2] BOR-SHYH, L., CHOU, W., HSING-YU, W., YAN-JUN, H. & JENG-SHYANG, P. 2013. Development of novel non-contact electrodes for mobile electrocardiogram monitoring system. *IEEE Journal of Translational Engineering in Health and Medicine*, 1, 2700108 (8 pp.)-2700108 (8 pp.).
- [3] CUNICO, F. J., MARQUEZ, J. C., HILKE, H., SKRIFVAR, M., SEOANE, F. & IOP 2013. Studying the Performance of Conductive Polymer Films as Textile Electrodes for Electrical Bioimpedance Measurements. *Xv International Conference on Electrical Bio-Impedance (Icebi) & Xiv Conference on Electrical Impedance Tomography (Eit)*, 434.
- [4] HONDA, W., ARIE, T., AKITA, S. & TAKEI, K. 2014. Printable and foldable electrodes based on a carbon nanotube-polymer composite. *Physica Status Solidi A - Applications and Materials Science*, 211, 2631-2634.
- [5] HONG-CHANG, T., JING-QUAN, L., DAI-XU, W., XIAO-YANG, K., CHUAN, Z., JING-CHENG, D., BIN, Y., XIANG, C., HONG-YING, Z., YAN-NA, N. & CHUN-SHENG, Y. 2014. Graphene oxide doped conducting polymer nanocomposite film for electrode-tissue interface. *Biomaterials*, 35, 2120-2129.

## Engineering PEEK bioactivity: Effect of plasma and gold sputtered interface

A. Reznickova<sup>1</sup>, Z. Novotna<sup>1</sup>, J. Siegel<sup>1</sup>, S. Rimpelova<sup>2</sup>, V. Svorcik<sup>1</sup>

<sup>1</sup>Department of Solid State Engineering, Institute of Chemical Technology, 166 28 Prague 6, Czech Republic

<sup>2</sup>Department of Biochemistry and Microbiology, Institute of Chemical Technology, 166 28 Prague 6, Czech Republic

Contact Details [reznicka@vscht.cz](mailto:reznicka@vscht.cz), tel. +420 220 445 159, fax: +420 220 444 330

Polyetheretherketone (PEEK) has been used as an alternative to metallic implants for orthopaedic and active medical implant applications, e.g. Eon spinal cord device. PEEK has shown neither cytotoxicity nor mutagenicity *in vitro*. Surface properties playing the most important role in cell adhesion are: surface hydrophilicity, morphology, roughness, energy, charge, and chemical composition. Plasma treatment has been previously used to modify polymer surface to improve its biocompatibility [1, 2].

In our recent work, we have investigated the use of Ar plasma etching to structure the PEEK surface in order to enhance adhesion of mouse fibroblast (L929) and human osteoblast (U-2 OS). We present a novel way of PEEK modification resulting in asymmetric samples with two different types of the surface plasma activated and gold sputtered. The objective of this study was to investigate the effect of the interface between plasma activated and gold coated PEEK on adhesion and spreading of cells. The surface properties of pristine PEEK and its modified counterparts were studied by different experimental techniques: XPS spectroscopy and goniometry which were used for characterization of surface chemical structure and polarity. Further, AFM microscopy was employed to study the surface morphology and roughness of the interface created on PEEK. The biological response of the two model cell lines seeded on untreated and plasma treated PEEK matrices was quantified in terms of the cell adhesion, density, and metabolic activity. Cell spreading and morphology were assessed by SEM microscope.

Plasma treatment leads to the ablation of the polymer surface layers. Despite of the fact that the plasma treatment proceeds in inert Ar plasma, the oxidized degradation products are created on the polymer surface which contribute to increased hydrophilicity of the plasma treated polymer. Cell adhesion measured on the interface between plasma activated and gold coated PEEK was the higher the gold layer on the sample was thicker.

**Keywords:** *PEEK, interface, plasma, sputtering, cell spreading*

*This work was supported by GACR 14-18149P.*

[1] REZNICKOVA, A., MAKAJOVA, Z., SLEPICKOVA KASALKOVA, N., KOLSKA, Z., SVORCIK, V. 2014. Growth of vascular smooth muscle cells on plasma treated and gold nanoparticles grafted polytetrafluorethylene. *Iran. Polym. J.*, 23, 227-236.

[2] AWAJA, F., BAX, D.V., ZHANG, S., JAMES, N., MCKENZIE, D. R. 2012. Cell Adhesion to PEEK Treated by Plasma Immersion Ion Implantation and Deposition for Active Medical Implants. *Plasma Process. Polym.*, 9, 355–362.

## **PVA/ ZnO nanoparticles via sol gel process for biomedical applications**

K. A de la Torre Sáenz<sup>1</sup>, J. M Guerrero Villalba<sup>1</sup>, C. López Díaz<sup>1</sup>, C. A. Rodríguez González<sup>1</sup>, R. C. Ambrosio Lázaro<sup>1</sup>, M. de L. Mota González<sup>1</sup>, A. Carrillo Castillo<sup>1\*</sup>

<sup>1</sup>*Instituto de Ingeniería y Tecnología, Universidad Autónoma de Ciudad Juárez. Cd. Juárez Chih. CP 32310, México.*

*E Mail/ Contact Details:* [amanda.carrillo@uacj.mx](mailto:amanda.carrillo@uacj.mx)

Polyvinyl alcohol (PVA) is a semicrystalline synthetic polymer, which is soluble in water and slightly soluble in ethanol. It is tasteless, odorless, has good mechanical properties, a high ability to form films and a good compatibility and biodegradability in human tissues and fluid. PVA is known as an aliphatic polymer with a carbon chain backbone with hydroxyl groups attached to methane carbons, where the hydroxyl group can interact with different types of ions, including other organic compounds and even metals, this expands the implementation are of PVA to biomedical and electrical engineering. In the same way zinc oxide nanoparticles are used in different applications due to their easy fabrication; environmentally friendly nature, and non-toxic synthesis route, ZnO nanoparticles can provide a better option for various biological applications. Recent studies about PVA, focus on the synthesis via sol gel route, this process is a method for producing solid materials from small molecules, and involves the conversion of monomers into a colloidal solution (sol) that act as the precursor for an integrated network (gel) of either discrete particles or network polymers. This method has improved the synthesis of hybrid materials based on PVA. Many of these hybrid materials focus on the synthesis and characterization of PVA with silica nanocomposites among others, using sol-gel technique.

Here we report the synthesis of a PVA hydrogel polymer with zinc oxide nanoparticles by the sol-gel method. The hydrogel was chemical, optical and thermal characterized in order to evaluate its potential applications in the biomedical area. We evaluated the PVA concentration with a constant TEOS: ethanol and ZnO nanoparticles concentrations. Compared with PVA, PVA-ZnO hydrogel composite exhibit remarkable improvement in the chemical and optical properties and thermal stability.

***Keywords:*** PVA, ZnO nanoparticles, sol gel process, hydrogel



## Study on the CMC/PLA composite foam as wound packing materials

Yoon Jin (Kim)<sup>1</sup>, Jung Nam (Im)<sup>1</sup>, Tae Hee (Kim)<sup>1</sup>, Song Jun (Doh)<sup>1</sup>

<sup>1</sup>Korea Institute of Industrial Technology, 143 Hanggaul-ro, Ansan, South Korea, 426-910

*wolfpack@kitech.re.kr*

Carboxymethyl cellulose(CMC)/poly(lactic acid)(PLA) composite foam was obtained by lyophilization of PLA-dispersed CMC solution and post-treatment. The aim of the study was to prepare CMC/PLA composite foams and to investigate the liquid handling properties and their applicability to wound packing materials. Structural analyses were performed through SEM, FT-IR, DSC and so on. The mechanical properties were analyzed by measuring compressional strength and compression recovery. The liquid handling properties were studied by liquid absorption measurement under a certain pressure condition. As the proportion of PLA increased, the compressional strength and recovery increased while the liquid absorption capacity decreased. Gamma ray radiation process was introduced after the foam manufacturing as means of controlling biodegradability and sterilization. The degradation period decreased with increasing amount of the radiation. However, the mechanical properties were not affected by the amount of the radiation significantly.

***Keywords: Carboxymethyl cellulose, Foam, Liquid handling properties, wound packing, acid treatment***

## Study on the CMC/PLA composite foam as wound packing materials

Yoon Jin (Kim)<sup>1</sup>, Jung Nam (Im)<sup>1</sup>, Tae Hee (Kim)<sup>1</sup>, Song Jun (Doh)<sup>1</sup>

<sup>1</sup>Korea Institute of Industrial Technology, 143 Hanggaul-ro, Ansan, South Korea, 426-910

*wolfpack@kitech.re.kr*

Carboxymethyl cellulose(CMC)/poly(lactic acid)(PLA) composite foam was obtained by lyophilization of PLA-dispersed CMC solution and post-treatment. The aim of the study was to prepare CMC/PLA composite foams and to investigate the liquid handling properties and their applicability to wound packing materials. Structural analyses were performed through SEM, FT-IR, DSC and so on. The mechanical properties were analyzed by measuring compressional strength and compression recovery. The liquid handling properties were studied by liquid absorption measurement under a certain pressure condition. As the proportion of PLA increased, the compressional strength and recovery increased while the liquid absorption capacity decreased. Gamma ray radiation process was introduced after the foam manufacturing as means of controlling biodegradability and sterilization. The degradation period decreased with increasing amount of the radiation. However, the mechanical properties were not affected by the amount of the radiation significantly.

***Keywords: Carboxymethyl cellulose, Foam, Liquid handling properties, wound packing, acid treatment***

## Architecture Design of Dynamic Networks with Shape-memory Effect

Ke-Ke Yang\*<sup>1</sup>, Min-Wei<sup>1</sup>, Tian-Hao Zhang<sup>1</sup>

<sup>1</sup> Center for Degradable and Flame-Retardant Polymeric Materials (ERCPM-MoE),  
College of Chemistry, Sichuan University, 29 Wangjiang Road, Chengdu 610064, China.

\*E-mail: kkyangscu@126.com/Phone: +86-28-85410755, Fax: +86-28-85410755

Shape memory polymers (SMPs) are a promising class of intelligent materials which can respond to appropriate external stimuli (such as pH, light, electricity, heat etc.) by changing from a temporary shape to a permanent shape. To achieve a SMP, more attention is focused on the design of the molecular switch, actually, the architecture of the network is also very important for the shape-memory effect. Recently, the dynamic networks draw tremendous attention of researchers for their triggerable and reversible nature. In present work, Diels-Alder reaction, hydrogen bonding and metal-ligand coordination have been chosen to construct dynamic networks, the crystallization behavior, dynamic thermal mechanical behaviors and shape-memory effects of dynamic networks have also been addressed<sup>[1,2]</sup>.

**Keywords:** *Dynamic network, shape-memory, hydrogen bonding, D-A reaction, metal-ligand coordination*

[1] XIAO, L.P., WEI, M., ZHAN, M.Q., ZHANG, J.J., XIE, H., DENG, X.Y., YANG, K.K., AND WANG, Y.Z. 2014. Novel triple-shape PCU/PPDO interpenetrating polymer networks constructed by selfcomplementary quadruple hydrogen bonding and covalent bonding, *Polymer Chemistry*, 5, 2231-2241

[2] ZHANG, J.J., Niu, y., HUANG, C.L., XIAO, L.P., CHEN, Z.T., YANG, K.K., AND WANG, Y.Z. 2012. Self-Healable and Recyclable Triple-Shape PPDO-PTMEG Co-network Constructed through Thermoreversible Diels-Alder Reaction, *Polymer Chemistry*, 3,1390-1393

# Emittance Variation and IR Electrochromism in Skins Comprised of Unique Conducting Polymers, Ionic Liquid Electrolytes, Microporous Polymer Membranes and Semiconductor/Polymer Coatings, for Spacecraft Thermal Control

Prasanna Chandrasekhar,<sup>1\*</sup> Brian J. Zay,<sup>1</sup> David Lawrence,<sup>1</sup> Edmonia Caldwell,<sup>2</sup> Rubik Sheth,<sup>3</sup> Ryan Stephan<sup>3</sup> and John Cornwell<sup>3</sup>

<sup>1</sup> Ashwin-Ushas Corporation, 2 Timber Lane, Unit 301, Marlboro, NJ 07746, USA

<sup>2</sup> National Aeronautics and Space Administration (NASA)- Goddard Space Flight Center (NASA-GSFC), Greenbelt Road, Greenbelt, MD 20771, USA

<sup>3</sup> NASA-Johnson Space Flight Center (NASA-JSFC), 2101 NASA Parkway, Houston, TX 77058, USA

The ability to vary emittance ( $\epsilon$ ) of spacecraft surfaces is a vital if uncelebrated requirement for spacecraft thermal control. Here, we describe fabrication and performance of thin-film, flexible, variable-  $\epsilon$  (V-E) IR-electrochromic skins having a conducting polymer/-Au/-microporous membrane (CP/Au/ $\mu$ P) base and unique ionic liquid electrolyte (IonEl). A unique, patented device design yields no barrier between the active, electrochromic CP surface and the external environment, except for a thin, IR-transparent semiconductor/polymer film that lowers solar absorptance ( $\alpha(s)$ ) and protects from atomic-O/far-UV. Use of the IonEl requires special methods to activate the skins. Typical performance includes tailorable  $\epsilon$  variations (0.19 to 0.90),  $\Delta\epsilon$  values of  $> 0.50$  (highest reported thus far for functional V-E materials, to our knowledge),  $\alpha(s) < 0.35$ , cyclability of  $>10,000$  cycles. Extended space durability testing and continuous light/dark cycling over  $> 7$  months under space conditions ( $< 10^{-5}$  Pa vacuum, far-UV) show excellent durability. Other data show resistance to solar wind, atomic-O, electrostatic discharge (ESD), micrometeoroids. These lightweight, inexpensive, advanced polymeric skins represent the only technology that can work with micro- ( $< 20$  kg) and nano- ( $< 2$  kg) spacecraft; this will eventually allow for much greater flexibility in their design, potentially “democratizing” the entire space industry.

## KEYWORDS

conducting polymer, applications, microporous, polymer membrane, spacecraft, thermal, control, variable, emittance

**All organic modified relaxor ferroelectric terpolymers:****Towards Low Electric Field Dielectric Actuators**

Jean-Fabien Capsal\*<sup>1</sup>, Pierre-Jean Cottinet<sup>1</sup>, Minh Quyen Le<sup>1</sup>, Mickaël Lallart<sup>1</sup>

<sup>1</sup> *Laboratoire de Génie Electrique et Ferroélectricité (LGEF), INSA Lyon, 69621  
Villeurbanne, France*

*jean-fabien.capsal@insa-lyon.fr* (**presenting and crossponding author's**)

Electroactive polymers (EAPs) have recently showed promising potential in various applications especially for electromechanical conversion such as low-frequency actuation, for instance micropumps or long stroke actuators. These polymers reach large strain response to an electric field, making them good candidates as low frequency active actuators. Fluorinated terpolymer P(VDF-TrFE-CFE/CTFE), which has been investigated in this study, is considered as a semi-crystalline polymer possessing the highest level of conversion from electrical to mechanical energy thanks to its excellent dielectric permittivity ( $\epsilon_r \sim 50$ ) and high mechanical modulus ( $\sim 200$  MPa). However, significant electrical field should be required ( $E > 100\text{V}/\mu\text{m}$ ) to obtain high strain level ( $> 2\%$ ). In this work, fluorinated terpolymer P (VDF-TrFE-CFE) was plasticized with (2-ethylhexyl) phtalate (DEHP). Such an organic modification of the terpolymer enables a 28 fold increase of the electrostrictive strain under low applied electric field as well as a 233 fold increase of the mechanical energy compared to the neat polymer [Sensors and Actuators A 207, 25– 31(2014), Patent application FR1353537, 04/18/2013]. Indeed, this simple chemical doping allows to benefit the exceptional properties of the terpolymer at an electric field of 5.5 times lower than the one of the pure terpolymer. In addition, the proposed modification has a reduced effect on the dielectric strength of the EAP with respect to conventional inorganic/organic composites. Furthermore, the process is relatively cheap, industrially used and could potentially break a technological lock as the performance recorded at low electric field are greater than any conventional electroactive polymer.

**Keywords:** *Electrostrictive polymer, soft actuators, materials, relaxor ferroelectric*

## Mediating gel formation from structurally controlled poly(ionic liquids): towards ionic gel electrolytes for energy storage

Hassan Srour,<sup>1</sup> Olivier Ratel,<sup>2</sup> Mathieu Leocmach,<sup>1</sup> Sandrine Denis-Quanquin,<sup>1</sup> Nicolas Taberlet,<sup>1</sup> Jean-Charles Majesté,<sup>2</sup> Christian Carrot,<sup>2</sup> and Cyrille Monnereau\*<sup>1</sup>

<sup>1</sup>Ecole Normale Supérieure de Lyon, 46 Allée d'Italie, 69007 Lyon, France.

<sup>2</sup>Ingénierie des Matériaux Polymères, 42023 Saint-Etienne, France.

[hassan.srou@ens-lyon.fr](mailto:hassan.srou@ens-lyon.fr) and [cyrille.monnerau@ens-lyon.fr](mailto:cyrille.monnerau@ens-lyon.fr)

Poly(ionic liquids) (PILs) and ionic gels made thereof constitute an increasingly sought-after category of materials, as they are expected to replace leakage-prone liquid electrolytes in future energy storage devices, and other electroactive materials.

In this communication, we will present a novel methodology, involving an initial Atom Transfer Radical Polymerization (ATRP) step, which provides an easy access to a broad range of PILs from a common monomeric precursor. We will show how the introduction of an anionic functional group on the ATRP initiator is enough to mediate gel formation at low concentrations in water through electrostatic interactions and demonstrate that the incorporation of additives along the polymer backbone helps optimizing ionogel properties in various solvents.<sup>[1]</sup> Finally, we will illustrate the potential of the ionogels as materials for energy storage devices through studying their rheological behaviour, electrochemical stability, diffusion and ionic conductivity.

**Keywords:** *Poly(electrolytes) • ionic gel • supramolecular interactions • rheology • electrochemistry*

[1] SROUR, H., RATEL, O., LEOCMACH, M., ADAMS, E.-A., DENIS-QUANQUIN, S., TABERLET, M., MAJESTÉ, J.-C., CARROT, C., ANDRAUD, C. & MONNEREAU, C. 2014. Mediating Gel Formation from Structurally Controlled Poly(Electrolytes) Through Multiple “Head-to-Body” Electrostatic Interactions, *Macromol. Rapid Commun*, DOI: 10.1002/marc.201400478.

## **Conducting polymers as biomimetic reactive sensors of the working conditions: Evidence from Polyaniline**

Yahya Ahmed Ismail<sup>1</sup>, Jose Gabriel Martinez<sup>2</sup>, Toribio Fernandez Otero<sup>2</sup>

(1) Division of Chemistry, Department of Basic Sciences, A'Sharqiyah University, Ibra, Oman.

(2) Centre for Electrochemistry and Intelligent Materials (CEMI), Universidad Politécnica de Cartagena, Cartagena, Murcia, Spain.

*E Mail : aiyahya@asu.edu.om*

Conducting polymers are reactive dense gels whose composition -reactive polymer chains, ions and water- mimic the intracellular matrix of biological cells. The gel reactions shift its composition and the related properties mimicking similar functions from biological organs. Devices driven by those reactions (artificial muscles, smart membranes, batteries or electro chromic windows etc.) can sense any physical or chemical variable acting on the chemical equilibrium or on the reaction rate. The sensing ability of conducting polymers arises from their reactive nature, through the unique electrochemical reaction. This work is a first time report on the reactive sensing ability of an electroactive polymer (polyaniline) other than polypyrrol. A polyaniline/silk hybrid microfibrinous mat was fabricated through electrospinning followed by in-situ chemical polymerization. The sensing characteristics were studied as a function of the working conditions: applied current, electrolyte concentration and temperature in aqueous acidic solution. The chronopotentiometric responses were studied by applying square electrical currents for a specified time. Inside the reversible range the chronopotentiometric responses change with (sense) the reaction variables: electrolyte concentration, pH, temperature and driving current. The potential of the materials, or the consumed electrical energy, for a constant reaction time follow the linear or semi logarithmic relationships with each of the experimental variables - electrolyte concentration, temperature or driving electrical current -predicted by the electrochemical kinetics. Thus, the conducting polymers are the sensors of the working conditions which is a general property. Since the input and output signals (current and potential) are simultaneously sent and received back through the same two connecting wires as natural muscles do, conducting polymers can mimic the permanent feedback communication between brain and biological muscles.



**All organic modified relaxor ferroelectric terpolymers:****Towards Low Electric Field Dielectric Actuators**

Jean-Fabien Capsal\*<sup>1</sup>, Pierre-Jean Cottinet<sup>1</sup>, Minh Quyen Le<sup>1</sup>, Mickaël Lallart<sup>1</sup>

<sup>1</sup> *Laboratoire de Génie Electrique et Ferroélectricité (LGEF), INSA Lyon, 69621  
Villeurbanne, France*

*jean-fabien.capsal@insa-lyon.fr* (**presenting and crossponding author's**)

Electroactive polymers (EAPs) have recently showed promising potential in various applications especially for electromechanical conversion such as low-frequency actuation, for instance micropumps or long stroke actuators. These polymers reach large strain response to an electric field, making them good candidates as low frequency active actuators. Fluorinated terpolymer P(VDF-TrFE-CFE/CTFE), which has been investigated in this study, is considered as a semi-crystalline polymer possessing the highest level of conversion from electrical to mechanical energy thanks to its excellent dielectric permittivity ( $\epsilon_r \sim 50$ ) and high mechanical modulus ( $\sim 200$  MPa). However, significant electrical field should be required ( $E > 100\text{V}/\mu\text{m}$ ) to obtain high strain level ( $> 2\%$ ). In this work, fluorinated terpolymer P (VDF-TrFE-CFE) was plasticized with (2-ethylhexyl) phtalate (DEHP). Such an organic modification of the terpolymer enables a 28 fold increase of the electrostrictive strain under low applied electric field as well as a 233 fold increase of the mechanical energy compared to the neat polymer [Sensors and Actuators A 207, 25– 31(2014), Patent application FR1353537, 04/18/2013]. Indeed, this simple chemical doping allows to benefit the exceptional properties of the terpolymer at an electric field of 5.5 times lower than the one of the pure terpolymer. In addition, the proposed modification has a reduced effect on the dielectric strength of the EAP with respect to conventional inorganic/organic composites. Furthermore, the process is relatively cheap, industrially used and could potentially break a technological lock as the performance recorded at low electric field are greater than any conventional electroactive polymer.

**Keywords:** *Electrostrictive polymer, soft actuators, materials, relaxor ferroelectric*

## Epoxy-based Shape Memory Composites Containing Carbon-based Additives

Irem Sengor<sup>1</sup>, Ozcan Koysuren<sup>2</sup>, Goknur Bayram<sup>1</sup>

<sup>1</sup>Department of Chemical Engineering, Middle East Technical University,  
Ankara 06800, Turkey

<sup>2</sup>Department of Chemical Engineering, Selcuk University, Konya 42031, Turkey

*E-Mail : gbayram@metu.edu.tr*

Shape memory polymers (SMP) have attracted a certain attention as smart materials. They have potential to store a deformed shape and recover their original shape by the application of an external stimulus such as heat, electricity, light, magnetic field, etc. The various advantages of SMPs, which are structural versatility, low manufacturing cost, easy processing and high elastic deformability above transition temperature, have caused a great interest among researchers.<sup>[1, 2]</sup> The versatility of SMPs led to their usage in different application areas such as; civil, electrical and aerospace engineering, automobile, textile and medical industries.

Among various types of polymers, epoxy shows shape memory capability in addition to its outstanding mechanical properties. When monomers and also carbon-based fillers are added to the neat epoxy, better shape memory properties of the composites may be obtained due to their effects in soft and hard segments of the composite. Monomer addition causes toughness and lower transition temperature since they act as soft segments in the composite structure. Carbon-based fillers such as carbon nanotubes (CNTs), carbon black (CB), carbon nanofibers, etc. should contribute to hard segments of the composite and actuate the shape memory behavior through the electrical triggering mechanism. In literature, the studies on the effect of both monomer and carbon filler together on the properties of epoxy-based systems are limited.<sup>[3]</sup>

The aim of this study is to prepare SMP composites using epoxy as the matrix material, low molecular weight additive (monomer) and separate/hybrid fillers of CB and CNTs. It is also aimed to characterize the composites and the neat material in terms of their shape memory (shape recovery and fixity), mechanical (tensile and impact), thermal properties and morphology.

Neat epoxy matrix and monomer added epoxy matrix were prepared as follows: epoxy and curing agent were degassed individually, mixed for 25 mins, the matrix was poured into molds and cured at room temperature for 1 hr, 90°C for 17 hrs and 130°C for 3 hrs. Monomer was added to epoxy resin prior to mixing. The composite specimens were prepared through solvent assisted sonication method. Carbon-based fillers were mixed with acetone and ultrasonicated, afterwards epoxy was added to the mixture and ultrasonication was continued. Acetone was removed by heating the mixture for 6 hrs in total at 60°C and 65°C. The mixture was vacuumed and mixed with the curing agent, then same steps was followed as in the matrix preparation.

Impact strength of the neat epoxy improved and glass transition temperature lowered with the addition of monomer. Shape recovery and shape fixity of the composites containing both monomer and the filler together or separately had the values in the range between 97-99 %. Lowest recovery time of 88s was obtained for the composite containing 15% monomer, 1% CB and 0.5% CNT together.

**Keywords:** *Shape memory polymer, composite, epoxy, carbon black, carbon nanotubes*

[1] LUO, X., MATHER, P.T. 2010. Conductive Shape Memory Nanocomposites for High Speed Electrical Actuation. *Soft Matter*, 6, 2146-2149.

[2] YU, K., ZHANG, Z., LIU, Y., LENG, J. 2011. Carbon Nanotube Chains in a Shape Memory Polymer/Carbon Black Composite: To Significantly Reduce the Electrical Resistivity. *Applied Physics Letters*, 98, 074102-1,3.

[3] SENGOR, I. 2013. Shape Memory Polymer Composites Containing Carbon-Based Fillers. M.Sc. Thesis, Middle East Technical University, Ankara, Turkey.

## Active Water Vapor Transport across Functionalized Conducting Polymer Microporous Membranes at Very High Rates, Using the Electroosmotic Effect, with Simultaneous Chemical Warfare (CW) Agent Blocking, for Use in Soldier Uniforms

Brian J. Zay<sup>1\*</sup>, Prasanna Chandrasekhar<sup>1</sup>, Petar Pirgov<sup>1</sup>, David Lawrence<sup>1</sup>, Sean Morefield<sup>2</sup>, Tilghman L. Rittenhouse<sup>3</sup>, Quoc Truong<sup>4</sup>, Salvatore G. Clementi<sup>3</sup>, Russell R. Greene<sup>5</sup>

<sup>1</sup>Ashwin-Ushas Corporation, Marlboro, USA

<sup>2</sup>US Army Engineer Research and Development Center, Construction Engineering Research Laboratory (ERDC-CERL), Champaign, USA

<sup>3</sup>Chemical and Biological Technologies Directorate, US Defense Threat Reduction Agency (DTRA), Fort Belvoir, USA

<sup>4</sup>Warrior Science, Technology, and Applied Research Directorate, US Army Natick Soldier Research, Development, and Engineering (RD&E) Center, Natick, USA

<sup>5</sup>Hazardous Materials Research Center (HMRC), Battelle Columbus Laboratories, Battelle Memorial Institute, Columbus, USA

Email: \*chandra.p2@ashwin-ushas.com

Electroosmosis, one of the four electrokinetic effects, describes the movement of a liquid or condensed vapor relative to a stationary charged surface (as in a capillary). Here, we report electroosmotic water vapor transport (WVT) across very thin, flexible, functionalized conducting polymer (CP) microporous ( $\mu\text{P}$ ) membranes at a very high rate. Both *passive* and *active* (6 VDC applied, power  $<1 \text{ W}\cdot\text{m}^{-2}$ ) WVT are reported, the latter for the first time. WVT occurs with simultaneous, effective blocking of chemical warfare (CW) agents. Initial active liquid||membrane||liquid interface studies demonstrated WVT rates of  $>1.7 \times 10^{-5} \text{ g}\cdot\text{mm}^{-2}\cdot\text{s}^{-1}$ , vs. the highest prior reported values of  $5 \times 10^{-6} \text{ g}\cdot\text{mm}^{-2}\cdot\text{s}^{-1}$ . Subsequent vapor||membrane||vapor interface studies using industry-standard methods, ASTM E96B Upright Cup (“WVT”), ASTM F2298 (“Dynamic Moisture Permeation Cell”), ASTM F1868 (“Sweating Guard Hotplate”), yielded WVT values of  $2564.4 \text{ g}\cdot\text{m}^2\cdot\text{d}^{-1}$  (passive) and  $3706.7 \text{ g}\cdot\text{m}^2\cdot\text{d}^{-1}$  (active), to be compared with the highest (passive) prior reported value,  $984.8 \text{ g}\cdot\text{m}^2\cdot\text{d}^{-1}$ . More than 20 different membrane configurations, porosities and types were studied, including membranes containing CP with impregnated enzymes. Efficient blocking of CW agents GB, HD, VX is also reported. Membranes also passed all industry-standard durability tests, e.g. ASTM D2261 (Tearing), ASTM D5034 (Breaking), ASTM D3886 (Abrasion), ASTM F392 (Gelbo Flex). Incorporation into “smart” soldiers’ garments was demonstrated. Proposed mechanisms of enhanced WVT and CW agent blocking in the membranes are presented.

**Keywords:** Electroosmotic; Transport; Smart; Microporous; Membrane; Conducting; Polymer; Functionalized

## **Electrically triggered release of amoxicillin from polyacrylamide/polyaniline and polyacrylamide/polypyrrole hydrogels**

Del Castillo Castro T.<sup>1,\*</sup>, Pérez Martínez C.J.<sup>2,3</sup>, Valencia Castro L.E.<sup>3</sup>, Castillo Ortega M.M.<sup>1</sup>,  
Rodríguez Félix D.E.<sup>1</sup>

<sup>1</sup>Departamento de Investigación en Polímeros y Materiales, Universidad de Sonora, C.P. 83000  
Hermosillo, Sonora, México.

<sup>2</sup>Centro de Investigación en Materiales Avanzados, S. C. Unidad Chihuahua, C.P. 31109  
Chihuahua, Chihuahua, México.

<sup>3</sup>Departamento de Ciencias Químico Biológicas, Universidad de Sonora, C.P. 83000 Hermosillo,  
Sonora, México.

\*e-mail: [terecat@polimeros.uson.mx](mailto:terecat@polimeros.uson.mx)

Drug delivery systems based on controlled release under an electrical stimulus offer the promise of new treatments for chronic diseases that require periodic and precise doses of medication. Electroactive materials obtained from the dispersion of an electroconductive polymer into a hydrogel matrix are suitable for drug delivery systems, particularly, in implantable and transdermal devices. In this work, composite hydrogels were prepared by the individually entrapment of amoxicillin-loaded polyaniline or amoxicillin-loaded polypyrrole into polyacrylamide networks. The drug release profile from composite hydrogels under electrical stimulation showed that the antibiotic molecules can be subsequently released (or sustained) in response to application (or removal) of the electrical stimulation. Drug delivery was associated to the electrochemical reduction of the electroconductive polymer, which causes changes in the charge density of the particles, with the concomitant volume contraction and synergistically release of noncovalently bonded amoxicillin molecules.

**Keywords:** *Electrically controlled drug release, electroactive polymer*

## Piezoresistive NBR-Polypyrrole composites prepared by swelling method

Encinas J.C.<sup>1</sup>, Urrea J.<sup>1</sup>, Huitrón J.A.<sup>1</sup>, Madera T.<sup>2</sup>

<sup>1</sup>Universidad de Sonora, Colonia Centro, 83000, Hermosillo, Sonora, México.

<sup>2</sup>Centro de Investigación en Alimentación y Desarrollo, A.C. Carr. a La Victoria, Km 0.6, 83304 Hermosillo, Sonora, México.

**carmelo@polimerosa.uson.mx**

Composite material of acrylonitrile butadiene rubber (NBR) and polypyrrole was prepared by in situ polymerization of pyrrole swollen in NBR film. The polymerization was carried out by immersing the swollen NBR films in a solution of copper(II) perchlorate hexahydrate. The material produced had strain at break similar to original NBR and has potential strain sensing application piezoresistive properties. Only small shifts in the onset temperature of the major exotherm are observed indicating that the miscibility is limited in this blend at room temperature however scanning electron microscope images fractured surface show no granular morphology. In order to know the piezoresistivity response films were subjected to cycling loading uniaxial tensile up to 22% strain. The composite responds with an increase in electrical resistance when stretching it at each cycle and then resiliently returns to resistance values close to the original value by removing the stretching effort. Recovery of electrical resistance quite close to the initial values for each cycle was achieved. This can be related to maintenance of the elastic properties without actually plastic behavior. A linear resistance change response was obtained by deforming up to 20% elongation and this linear piezoresistive effect is maintained over 100 cycles. Our group is currently studying optional material composites with piezoresistive properties [1].

**Keywords:** *piezoresistive material, polypyrrole, elastomer, swelling*

[1] DEL CASTILLO-CASTRO, T., CASTILLO-ORTEGA, M. M. ; ENCINAS, J. C., HERRERA FRANCO, P. J., CARRILLO-ESCALANTE, H. J. 2012. Piezo-resistance effect in composite based on cross-linked polydimethylsiloxane and polyaniline: potential pressure sensor application. *Journal of Materials Science*, 47, 1794-1802.

## **Crystallization induced self-assembly of amphiphilic copolymer based on poly(p-dioxanone) controlled by solvent mixing and its application in electrospun nanofiber**

Si-Chong Chen, Mei-Jia Wang, Hao Wang, and Ya Liu

National Engineering Laboratory of Eco-Friendly Polymeric Materials (Sichuan),  
College of Chemistry, State Key Laboratory of Polymer Materials Engineering, Sichuan  
University, Chengdu 610064, China.

*E Mail:* [chensichong@scu.edu.cn](mailto:chensichong@scu.edu.cn); *Tel/Fax:* +86-28-85410755

The crystallization of the core forming blocks of the crystalline-coil copolymer in selective solvent, which result in nanostructures with very unique anisotropic morphology, have attracted great attentions because their potential application in controlled delivery of pharmaceuticals and bottom-up design of hierarchical assemblies.

We have been particularly interested in the amphiphilic crystalline-coil copolymer using poly(p-dioxanone) (PPDO) as core forming crystalline block, which can form nano particles in aqueous medium with very special “star anise”-like morphology.[1-3] The temperature dependent phase transition and morphological evolution suggested that the formation mechanism of the “star anise”-like nano particles is a hierarchical assembly process from flake-like nano particles.[4,5] However, there is still requirement to deeply understand the kinetic process of nano particle formation in order to develop a simple solution protocol for preparing of nano particles with controlled morphology.

In this work, we developed a very facile strategy for nanofabrication of polymeric 1-D nanomaterial by controlling the nano particle morphology of PPDO containing block copolymer in mixed solvent depending on the sequence and rate of solvent mixing. DMF is a good solvent for both PPDO and PEG blocks, while water is a selective solvent for PEG block. Therefore, when adding water into the DMF solution of PPDO-b-PEG copolymer, the PPDO blocks of the copolymer may self-assemble and crystallize because of the change in solvent quality. We used two different ways to accomplish solvent mixing: quickly pouring or slowly dropping water into DMF solution of the copolymer

under stirring. The copolymer could form “star anise”-like, “chrysanthemum”-like and sphere-like nano particles at different solvent mixing conditions, which could be attributed to stepwise aggregation-crystallization mechanism and simultaneously aggregation-crystallization mechanism, respectively owing to the different rate of solvent mixing.

Nanofibers from poly(lactic acid) (PLA) homopolymer and PPDO-b-PEG copolymer with different phase separation morphologies depending on the crystallization induced self-assembly of PPDO-b-PEG were therefore prepared by single spinneret electrospinning. Mixing solvents with different composition were used for controlling the crystallization of PPDO block and therefore the phase separation in obtained nanofibers.

***Keywords: Crystallization induced self-assembly, nanofabrication, electrospun nanofiber, PPDO-b-PEG copolymer***

[1] CHEN, S. C., WU, G., SHI, J. & WANG, Y. Z.\* 2011. Novel “Star anise”-like Nano Aggregate Prepared by Self-assembling of Preformed Microcrystals from Branched Crystalline-coil Alternating Multi-block copolymer. *Chem. Comm.*, 47, 4198-4200.

[2] CHEN, S. C.\*, LI, L. L., WANG, H., WU, G. & WANG, Y. Z.\* 2012. Synthesis and micellization of amphiphilic multi-branched Poly(p-dioxanone)-block-poly (ethylene glycol). *Polym. Chem.*, 3, 1231-1238.

[3] ZHAI, F. Y., HUANG, W., WU, G., JING, X. K., WANG, M. J., CHEN, S. C.\*, WANG, Y. Z., CHIN, I. J. & LIU, Y.\* 2013. Nanofibers with Very Fine Core-Shell Morphology from Anisotropic Micelle of Amphiphilic Crystalline-Coil Block Copolymer. *ACS Nano*, 7, 4892-4901.

[4] WU, G.; CHEN, S. C.\*, WANG, X. L., YANG, K. K. & WANG, Y. Z.\* 2012. Dynamic Origin and Thermally Induced Evolution of New Self-Assembled Aggregates from an Amphiphilic Comb-Like Graft Copolymer: A Multiscale and Multimorphological Procedure. *Chem. Eur. J.*, 18, 12237-12241.



[5] WANG, H., LIU, C. L., WU, G., CHEN, S. C.\*, SONG, F. & WANG, Y. Z.\* 2013. Temperature Dependent Morphological Evolution and the Formation Mechanism of Anisotropic Nano-Aggregates from a Crystalline-Coil Block Copolymer of Poly(p-dioxanone) and Poly(ethylene glycol). *Soft Matter*, 9, 8712-8722.

## Novel Foam Structures for Personalized Bone Replacement Materials

Ahlhelm, M.<sup>1</sup>, Scheithauer, U., Gorjup, E.<sup>2</sup>, von Briesen, H.<sup>2</sup>, Moritz, T.<sup>1</sup>, Michaelis, A.<sup>1</sup>

<sup>1</sup>Fraunhofer IKTS, Winterbergstrasse 28, 01277 Dresden, Germany.

<sup>2</sup>Fraunhofer IBMT, Ensheimer Strasse 48, 66386 St. Ingbert, Germany.

*matthias.ahlhelm@ikts.fraunhofer.de/ Fraunhofer IKTS, Winterbergstrasse 28, 01277 Dresden, Germany, Tel. : +49351 2553 7572*

The objective of the presented work is to develop novel porous, near-net shaped foam structures for personalized bone replacement materials allowing the ingrowth and differentiation of human mesenchymal stem cells (hMSCs). The so-called freeze-foaming process offers the possibility to achieve mainly open porous and interconnected sponge-like structures without any CO<sub>2</sub>-producing pore formers or similar volatile whole PU-scaffolds. Furthermore, the near-net shaping feasibility of these Freeze Foams allows to foam for instance, the inner contours of additive manufactured (AM) ceramic scaffolds which are then combined in a co-sintering step to a single personalized, complex 3D-structure. As results, ceramic biomaterials, in this case hydroxyapatite (HAp) and/or zirconia (ZrO<sub>2</sub>), probably allow the osteogenic differentiation of hMSCs on the detection of alkaline phosphatase and collagene-1 on the one hand. Foamed as a hybrid mixture on the other hand, achieved ZrO<sub>2</sub>/HAp composites exhibit significantly increased compressive strength whilst biocompatibility is retained. Within an oral presentation the author wants to show the potential of this novel bone replacement structures as possible next generation bioceramics/-composites used as personalized implants which allow an adaption according to the needs of customers.

***Keywords: Freeze Foaming, Additive Manufacturing, Bioceramics, Bone Replacement Material, Personalization***

## **Biomimetic synthesis of rosette-like calcite mesocrystals mediated by a marine-derived recombinant glycine-rich protein**

**Wooho Song, Yoo Seong Choi\***

*Biomolecular Engineering Laboratory, Department of Chemical Engineering,  
Chungnam National University, Daejeon 305-764, South Korea*

[\\*biochoi@cnu.ac.kr](mailto:biochoi@cnu.ac.kr)

### **Abstract**

The layer of molluscan shells consists of structure of highly organized calcium carbonate crystals, which provides remarkable strength and toughness compared to pure mineral calcium carbonate. It has been known that the organized biomineral is controlled by 1~5% organic templates. Here, we successfully produced a recombinant acidic protein in *E coli*, which are expected to be involved in the control of calcium carbonate biomineralization. Calcium carbonate binding properties of the recombinant were investigated, and it was tried to regulate the morphology in calcium carbonate crystallization. As a result, rosette-like spherical calcite mesocrystals were uniformly obtained, and possible mechanism was suggested based on the evolution of the crystal morphology. From this study, we expect that the recombinant protein can regulate *in vitro* biomineralization for the production of calcium carbonate with superior mechanical properties. This study can give potential to understand biomineralization mechanism and to fabricate marine-inspired notable materials.

## Optoelectronic fast response properties of PQ/PMMA polymer

Sun<sup>1,2</sup>, Fu<sup>1,2</sup>, Pei<sup>1,2</sup>

<sup>1</sup>Department of Physics, Harbin Institute of Technology, Harbin 150001, China.

<sup>2</sup>Key Lab of Micro-Optics and Photonic Technology of Heilongjiang Province, Harbin 150001, China.

*xdsun@hit.edu.cn*

The organic photopolymer is ideal for volume holographic storage due to its high diffraction efficiency, not post-processing, simple preparation method and cheap cost et al. The phenanthrenequinone doped poly(methyl methacrylate) (PQ/PMMA) photopolymer is able to effectively inhibit the shrinkage by unique fabrication method, and attract more attentions among numerous polymers due to its high thicknesses with millimeter even centimeter magnitudes. In this paper, the PQ/PMMA polymer and doped ones are prepared. Its high optical response properties can obtained through dark enhancement process after recording. Furthermore, it is demonstrated that PQ/PMMA polymer can be used in fast recording using nanosecond pulse inputs with wavelength of 532nm.

***Keywords: photopolymer, holographic memory, dark enhancement effect, nanosecond pulse***

## Organometallics for Opto-electronic Device Applications

Muhammad S. (Khan)<sup>1</sup>, Rayya A. (Al-Balushi)<sup>1</sup>

<sup>1</sup>Department of Chemistry, College of Science, Sultan Qaboos University, Oman.

*E Mail: msk@squ.edu.om*

Conjugated organometallics have emerged as a new class of novel materials for opto-electronic (O-E) devices such as solar cells (SCs), light-emitting diodes (LEDs), and memory devices. In this context, Pt(II) poly-yne and bis(ferrocenylethynyl)s are widely investigated in our laboratory (**Chart 1**). Pt(II) poly-yne provide very efficient light emission from the triplet excited state. The long-lived triplets promote charge generation and enhance efficiency of the O-E devices. The redox-active ferrocene moiety facilitates long-range intra-molecular electronic communication in bis(ferrocenylethynyl)s. Inter-chain interactions, interaction parameters and structure/property relationships in Pt(II) poly-yne and bis(ferrocenylethynyl)s will be discussed.

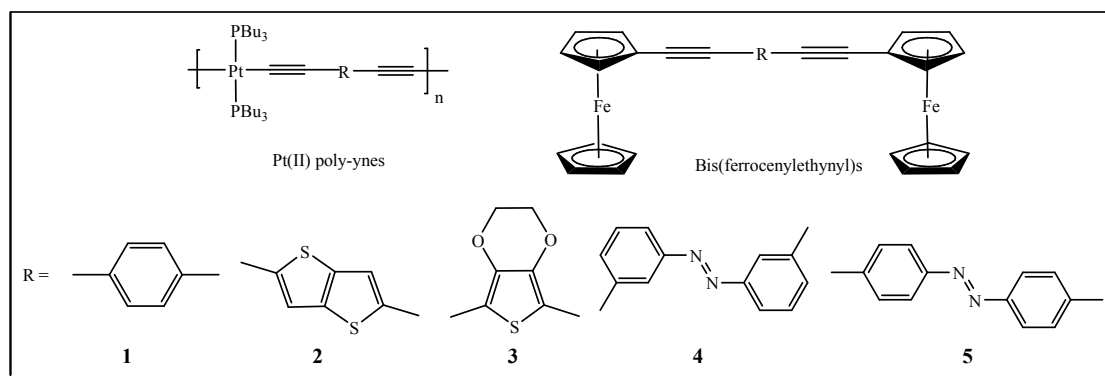


**Chart 1.** Pt(II) poly-yne and bis(ferrocenylethynyl)s

**Keywords:** Pt(II) poly-yne, bis(ferrocenylethynyl)s, opto-electronic, structure/property

[1] SHAH, H. H., AL-BALUSHI, R. A., AL-SUTI, M. K., KHAN, M. S., WOODALL, C. H., MOLLOY, K. C., RAITHBY, P. R., ROBINSON, T. P., DALE, S. E. & MARKEN, F. 2013. Long-Range Intramolecular Electronic Communication in Bis(ferrocenylethynyl) Complexes Incorporating Conjugated Heterocyclic Spacers: Synthesis, Crystallography and Electrochemistry. *Inorg. Chem.*, 52(9), 4898-4908.

## **Ultra-fast response polyaniline memristor by one pot synthesis using FeCl<sub>3</sub> as oxidant and doping agent**

Sergio Bocchini, Katarzyna Bejtka, Alessandro Chiolerio

Center for Space Human Robotics, Istituto Italiano di Tecnologia, Corso Trento 21,  
Torino 10129, Italy

*Sergio.bocchini@iit.it Tel: +39 011 0903433 Fax: +39 011 0903401 Center for Space  
Human Robotics, Istituto Italiano di Tecnologia, Corso Trento 21, Torino 10129, Italy*

Memristors represent the fourth type of two-terminal elemental components, completing the classical set of electronic passive elements, they are predicted to revolutionize in the near future the current approaches in computer electronics architecture, moreover they are indicated as the first brick to create neuromorphic devices and artificial intelligence. Polyaniline (PANI) was already used to produce organic memristive systems composed by conducting polymers realizing a solid electrolyte heterojunction and used for the realization of systems imitating synaptic learning. However in this case the memristive response being linked to ionic charge transfer through heterojunction results slow. Memristive properties based on local rearranging of charges in order to induce a faster switching between the high resistance state (HRS) and the low resistance state (LRS) will allow to spread their use without changing the peculiar properties of these organic memristors. For this purpose ferric chloride can be used as oxidizing agent and, at the same time as doping agent that allows a shift from HRS and LRS. The bi-stability in the electrical response, i.e. the ability to have two states with low/high conductivity (high/low resistivity) is due to the bi-stable oxidation state of the PANI and iron, it can be supposed that in the electric field the equilibrium between polyaniline in the emeraldine form and iron (III) is changed producing polyaniline in the pernigraniline form and iron (II) whose conductivity is strongly influenced. The huge on/off ratio that can exceed  $5 \cdot 10^5$ , makes practically feasible a soft memristive device based on this composition. Moreover multiple analyses on the system shows presence of both short term neuroplasticity (STP) and long term neuroplasticity (LTP) making the material able to “learn” by experiencing a feature typical of neuronal systems.

***Keywords: Polyaniline, Memristor, Neuroplasticity, Inkjet printings, Organic electronic***

## **Covalent superabsorbent hydrogel based on alginate for removal of dye from aqueous solutions**

Pablo G. Costa, Marcos R. Mauricio, Marcos R. Guilherme, Adley F. Rubira

Department of Chemistry, State University of Maringá, Av. Colombo, 5790, CEP 87020-900 Maringá, Paraná, Brazil

*Corresponding Author: afrubira@uem.br*

Superabsorbent hydrogels (SH), which is a class of hydrogel with high water absorption performance, can absorb and retain up to ca. 1,000 g of water per gram of dry sample. In recent years, SH incorporating polysaccharides has been widely studied, because it appears as a viable ecologically economically alternative.

Color removal from effluents polluted with dyes of textile industries has been considered a challenge due to the difficulty of treating such wastewaters by conventional methods. SH based on polysaccharides may be used as an ecological and economical alternative for removal of some aqueous solutes. As SH possesses ionic functional groups, it can absorb ionic dyes, such as methylene blue (MB), from wastewaters. In other words, in the same way that SH absorbs water, molecules of different sizes can be absorbed by and retained in its 3D structure.

Sodium alginate is a polysaccharide of relatively low cost. The sodium alginate is obtained from alginic acid. There are several possible arrangements of chains segments of alginic acid because it contains two different kinds of monomers having carboxylic groups. These segments are designated as L-mannuronic and L-guluronic acid. The carboxylic groups in alginate are expected to play an important role in the water absorption power of SH.

This work aimed at investigating an alternative method for removal of dyes from an aqueous environment using a reasonably priced and biodegradable SH based on sodium alginate and *N,N'*-dimethylacrylamide (DMAAm). In such a hydrogel, sodium alginate is the key constituent acting as a pillar for polymer network. DMAAm was used owing to its good gel-forming capacity. To prepare SH, sodium alginate was vinyl-modified for introduction of covalent cross-links and subsequently cross-linked/polymerized with DMAAm. Although sodium alginate shows a remarkable gelation in aqueous solution in



the presence of some divalent cations, we used a covalent approach to prepare SH, because the cross-links are stable with time, preserving the gel properties. The main idea was introduce alginate into SH as a key constituent, serving as a support on polymer network. In other words, if its chains break, the whole hydrogel unmake.

The potential applications of SH were demonstrated by determining their water transport profile and ability to remove color from aqueous solutions. Power law and Weibull equations, which are swelling-based models, were used for treating the experimental data. Alginate-based SH showed high efficiency of water absorption. For experiments of color removal, dry SH was immersed into the solutions of MB. In all cases, SH became blue while the solution became almost colorless. This phenomenon was accomplished by an increase in the volume of SH, indicating that the removal of dye is driven by swelling.

***Keywords: Alginate, Hydrogel, functionalization, wastewater, swelling.***

## SUSTAINABLE GEOPOLYMER MORTAR USING LOCAL INDUSTRIAL WASTE MATERIALS

Iftekhair Ibnul (Bashar)<sup>1</sup>, U. Johnson ([Alengaram](#))<sup>2</sup>, Mohd Zamin Jumaat<sup>3</sup> Azizul Islam<sup>4</sup>

<sup>1,2,3,4</sup>Department of Civil Engineering  
University of Malaya  
50603, Kuala Lumpur, Malaysia

*Email : [ujohnrose@yahoo.com](mailto:ujohnrose@yahoo.com)*

### Abstract

The use of alternative geopolymer binders from industrial waste products, namely palm oil fuel ash (POFA), fly ash (FA) and ground granulated blast furnace slag (GGBS) to wholly replace conventional ordinary portland cement and the effect on the use of processed quarry waste, alternatively known as manufactured sand (M-sand) as fine aggregate replacement in the development of compressive strength of POFA-FA-GGBS based geopolymer mortar was investigated. The variables investigated include the quantities of replacement levels of M-sand with normal sand and the different proportion of POFA, FA and GGBS. The alkaline solution, water, and curing condition remained constant. The results show that the silica rich POFA and FA increased the rate of strength development of the mortar and an average of 76% of the 28-day compressive strength was found at the age of 3-day. Based on the compressive strength, the use of 100% M-sand shows a comparable strength as that of mortar prepared with mixes of 100% normal sand. The particle size of fine aggregates play significant role in the strength development due to the filling and packing ability. The use of industrial waste materials such as POFA-FA-GGBS and M-sand as binders and fine aggregate respectively could be viable alternative to conventional concrete that could lead to sustainable geopolymer material.

***Keywords: Geopolymer binder, palm oil fuel ash, fly ash, ground granulated blast furnace slag, geopolymer mortar, manufactured sand***

[1] DAVIDOVITS J., 2011. Geopolymer chemistry and applications. 3 ed. France: Geopolymer Institute.

[2] LLOYD N, RANGAN V. Geopolymer Concrete-Sustainable Cementless Concrete. ACI Special Publication. 2009;261:33-54.

## High-performance polyimides derived from bio-derived eccentric amino acid

Tatsuo Kaneko<sup>1</sup>, Naoki Takaya<sup>2</sup>

<sup>1</sup>School of Materials Science, Japan Advanced Institute of Science and Technology (JAIST), Nomi, Ishikawa, 923-1292, Japan. E-mail: [kaneko@jaist.ac.jp](mailto:kaneko@jaist.ac.jp)

<sup>2</sup>School of Life and Environmental Science, College of Agro-Biological Resource Sciences, University of Tsukuba, Tsukuba, Ibaraki, 305-8577. Japan

Bio-based polymers obtained by a polymerization of biomolecules are indispensable for establishment of sustainable green society<sup>[1,2]</sup>. Conventional bio-based polymers such as poly(lactic acid)s have a worse hand comparing to commodity-type plastics in terms of the

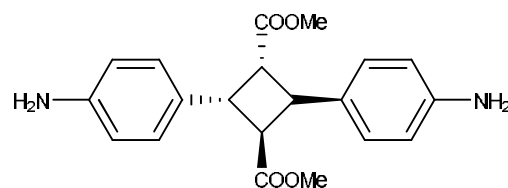


**Figure 1:** Photodimer of biomolecules usable as an aromatic diamine biomonomer for polyimides

balance of cost with performance in materialization. Development of high-performance biopolyimides should be effectual on overcoming this problem because higher performance plastics circulate in higher price than biological matters such as food additives.

Here we produce an aromatic monoamine 4-aminocinnamic acid from glucose by using metabolically engineered *E. coli*<sup>[3]</sup>. Quantitative photodimerization of 4-aminocinnamic acid generated diacid- and diamino biomonomers, both of which had functionalized a rigid  $\alpha$ -truxillate structure and then were used to synthesize series of aromatic polyamides (Figure 1). These aromatic polyamides and polyimides were processed into highly-transparent plastic films with thermal stability and mechanical performance as high as super engineering plastic films, in spite of amorphous structures. Combined photolysis and hydrolysis efficiently degraded them into the monomers, which we recover and re-polymerize into the polyamides/polyimides..

**Acknowledgement** The researches have been financially supported by ALCA (5100270) and CREST of JST and *Grant-in-Aid* for challenging *Exploratory Research*.

**References** [1] T. Kaneko, et al. *Nature Mater*, 5, 966 (2006). [2] M. Chauzar, T. Kaneko, et al. *Adv. Funct. Mater.* 22, 3438 (2012). [3] P. Suvannasara, T. Kaneko, et al. *Macromolecules*, 47, 1586 (2014).

# Cellulose nanocrystals and nanofibers for renewable active materials

Jaehwan Kim, Kishor Kumar Sadasivuni, Lindong Zhai, Seongcheol Mun, Hyun Chan Kim, Seung-Ki Min

Center for EAPap Actuator  
Inha University  
Incheon 402-751, Republic of Korea  
jaehwan@inha.ac.kr

Cellulose is one of abundant renewable biomaterials in the world. Over 100 billion tons of cellulose is produced per year in nature. In nature, cellulose is produced from plants by biosynthesis, forming microfibrils which in turn aggregate to form cellulose fibers. Using new effective methods these fibrils can be disintegrated from the fibers to nanosized materials, so called cellulose nanocrystal (CNC) and cellulose nanofiber (CNF), which can be a new building block of new materials. The CNC and CNF have extremely good strength properties, dimensional stability, thermal stability and good optical properties on top of their renewable behavior. The bio-based one dimensional CNCs and CNF are versatile materials since it can be applied in many different fields, for example, new lightweight composite materials to be used in transport, electronic applications but they can also be used in food, cosmetics, medicine, packaging and many other applications.

This presentation reports recent advancement of cellulose nanocrystals and cellulose nanofibers, followed by their possibilities as well as challenges for renewable active materials. Natural behaviors, extraction, modification of cellulose nanocrystals and fibers are explained and their synthesis with nanomaterials is introduced, which is necessary to meet the technological requirements for smart materials. Also, its possibilities and challenges for smart materials are addressed.

Keywords—Renewable material; cellulose; active materials; smart materials

## Novel thermo-reversible polymers from furan-modified vegetable oils via Diels-Alder reactions

Talita M. Lacerda<sup>1,2\*</sup>, Antonio J. F. Carvalho<sup>2</sup> and Alessandro Gandini<sup>1,2</sup>

<sup>1</sup>São Carlos Institute of Chemistry and <sup>2</sup>São Carlos School of Engineering, University of São Paulo – São Carlos, SP, Brazil.

*E-mail: talita@iqsc.usp.br*

The application of the thermo-reversible Diels-Alder (DA/rDA) reaction to the realm of furan polymers is of great potential for the preparation of a wide variety of novel mendable and recyclable macromolecular materials based on renewable resources [1]. Furthermore, the use of vegetable oils (VO) for the synthesis of monomers and polymers is the focus of many studies, and this interest lies on the carbon-carbon double bonds that are present in most of the fatty acid chains, notoriously known as active sites for chemical substitution and functionalization [2]. As part of an ongoing study that deals with the concurrent exploitation of furans and VO for the synthesis of macromonomers, to be further polymerized via DA reactions with bismaleimides, the use of epoxidized linseed oil and tung oil were previously reported [3]. Based on the same principles, we describe here the thiol-ene modification of castor oil (CO) and its aminolysis reaction for the insertion of furan moieties, aimed at the preparation of renewable macromonomers to be polymerized with bismaleimides in thermally reversible systems. FTIR analysis showed the successful insertion of furan moieties into CO, and its thermo-reversible polymerization with a commercial aromatic bismaleimide, as shown by the increase, followed by a drastic reduction, of the viscosity of the medium at 65 °C and 110 °C, respectively. This ongoing study represents a significant contribution to the preparation of polymers from renewable resources using the concepts of click-chemistry.

**Keywords:** *Furan, Vegetable oils, Click-chemistry, Diels-Alder polymerization.*

[1] GANDINI, A. 2013. *Progress in Polymer Science*, 38, 1-29.

[2] GANDINI, A., LACERDA, T.M. 2014. *Polymers from plant oils*. Shawbury: Smithers Rapra, in press.

[3] GANDINI, A., LACERDA, T.M., CARVALHO, A.J.F. 2013. A straightforward double coupling of furan moieties onto epoxidized triglycerides: synthesis of new monomers based on two renewable resources. *Green Chemistry*, 15, 1514-1519. LACERDA, T.M., CARVALHO, A.J.F., GANDINI, A. 2014. Two alternative approaches to the Diels-Alder polymerization of tung oil. *RSC Advances*, 4, 26829-26837.

## **Isolation of Macromolecular Polymeric Ingredients from Waste Biomass Materials and their Characterization**

**E.Bilgic, S.Yaman\*, H.Haykiri-Acma**

**Istanbul Technical University, Chemical and Metallurgical Engineering Faculty, Chemical Engineering Department, 34469, Maslak, Istanbul, Turkey**

**Phone: 90 212 2853351**

**Fax: 90 212 2852925**

**e-mail: yamans@itu.edu.tr**

### **ABSTRACT**

Waste biomass species such as woody remnants, agricultural leftovers, food processing wastes, and forestry by-products are comprised of the combinations of several polymeric constituents. That is, the macromolecular polymeric ingredients such as cellulose, hemicellulosics and lignin that are the most abundant natural polymers in the world are mixed in different ratios in waste biomass materials.

In this study, we tried to isolate the macromolecular polymeric ingredients from waste biomass species such as sunflower seed shell and hazelnut shell. For this purpose, biomass samples were treated in sequential extraction procedures using various chemical reagents, and the individual polymers were isolated.

The polymeric ingredients were then characterized considering the physical and chemical properties, and compared with the parent materials from which they were isolated. The results of proximate and ultimate analyses as well as SEM (Scanning Electron Microscopy) micrographs, FTIR (Fourier Transform Infrared Spectroscopy) spectra of the isolated ingredients were interpreted. In addition, thermal reactivities of the materials were also regarded applying DTA (Differential Thermal Analysis) and TGA (Thermogravimetric Analysis) techniques.

It was concluded that each of the isolated polymers has quite different characteristics. For instance, functional group distributions which play significant role on the surface characteristics differ considerably. Besides, SEM images revealed the difference in morphologies of the polymers that lignin has very amorphous but strong structure, while cellulosics have cylindrical and highly ordered texture. On the other hand, thermal analysis profiles showed that cellulosics are likely to become decomposed easily by thermal effects, while lignin resists against the thermal decomposition, and the thermal reactivity of each polymer takes part in the apparent characteristics of the parent material.

## Synthesis of alkyd resins from *ceiba pentandra* L. (kapok) seed oil and an investigation on their biodegradation

Montu Moni Bora, Dilip Kumar Kakati

Department of Chemistry, Gauhati University, Assam - 781014, India

Email: [dilip\\_kakati2003@yahoo.co.in](mailto:dilip_kakati2003@yahoo.co.in)

Vegetable oil based biodegradable polymers have drawn the attention of academia and industry in recent years because of their non-petroleum origin, renewability and eco-friendly nature. A good number of seed oils have been used in the synthesis of various polymeric resins like polyester, epoxy, polyurethane and polyester amide which are used in paint, coating, adhesives etc.<sup>[1,2,3]</sup> The use of non-edible oil as raw materials for polymer synthesis is considered more important as they do not put pressure on the food-chain.

*Ceiba pentandra* L. locally known as kekabu or kapok belongs to the Malvaceae family is a drought resistant tree cultivated in Southeast Asia, Malaysia, India and Sri Lanka. Kapok seed is found to contain 25% of oil. The present work describes the biodegradation studies of alkyd resin synthesized from kapok seed oil.

The oil from kapok seed is subjected to glycerolysis reaction by reacting with glycerol at 235<sup>0</sup> C ( $\pm$  5<sup>0</sup> C) in presence of PbO catalyst. The monoglyceride thus formed was reacted with phthalic anhydride to synthesize the alkyd resins.<sup>[4]</sup> The product was characterized by FTIR and <sup>1</sup>H NMR. The physico-chemical properties like acid value, iodine value, drying properties were evaluated. The resins have also been tested for thermal stability, chemical resistance and pencil hardness. Biodegradability of the synthesized alkyd resins is tested by broth culture technique using *Pseudomonas aeruginosa* and *Bacillus subtilis* strains.<sup>[5]</sup> The SEM images revealed biodegradation of the resin materials. The

results indicate the possibility of synthesis of biodegradable alkyd resins from a renewable natural resource, for use in surface coatings, paints etc.

*Keywords:* *Ceiba pentandra*, Biodegradability, Alcoholysis-polyesterification, Alkyd resin.

#### References:

1. N. Dutta, N. Karak, S.K. Dolui, *Prog. Org. Coat*, 49 (2004) 146–152.
2. M. M. Bora, P. Gogoi, D. C. Deka, D. K. Kakati, *Ind. Crops Prod.* 52 (2014) 721–728.
3. S. Ahmed, S.M. Ashraf, S. Yadav, A. Jamal, *J. Appl. Polym. Sci*, 82 (2001) 1855–1858.
4. M. M. Bora, R. Deka, N. Ahmed, D. K. Kakati, *Ind. Crops Prod.* 61 (2014) 106–114.
5. B. Das, U. Konwar, M. Mandal, N. Karak, *Ind. Crops Prod.* 44 (2013) 396– 404.



## **Biodegradable Plastic Compounded with Oil Palm Biomass to Produces Bioplastic Fertilizer (BpF) Composites**

A.S. Harmaen<sup>1</sup>, A. Khalina<sup>2</sup>, I. Azowa<sup>3</sup>, M.A. Hassan<sup>4</sup>, and M. Jawaid<sup>1</sup>

<sup>1</sup>Institute of Tropical Forestry and Forest Products (INTROP), Universiti Putra Malaysia, 43400 UPM, Serdang, Selangor. Malaysia.

<sup>2</sup>Faculty of Engineering, University Putra Malaysia, 43400 UPM, Serdang, Selangor. Malaysia.

<sup>3</sup>Faculty of Science, Universiti Putra Malaysia, 43400 UPM, Serdang, Selangor. Malaysia.

<sup>4</sup>Faculty of Biotechnology and Biomolecular Science, Universiti Putra Malaysia, 43400 UPM, Serdang, Selangor. Malaysia.

\*[harmaen@upm.edu.my](mailto:harmaen@upm.edu.my) (Harmaen Ahmad Saffian)

### **Abstract**

Bioplastic fertilizer (BpF) composites produced by processing Poly (hydroxybutyrate-co-valerate) (PHBv) using supercritical processed or extrusion and it can be processed controlled by formulation and temperature through extrusion method. The aim of this study, to produced Bioplastic fertilizer (BpF) composites for slow released fertilizer control by blending. NPK fertilizer blends with bioplastic composites and oil palm biomass to produced bioplastic fertilizer (BpF) composites at 150°C processing temperature for 3 to 5 min using twin screw extruder. Thermal and biodegradation study of BpF composites was investigated. Soil burial study of BpF composites were collected after 4 weeks and followed until 16 weeks and morphological properties of BpF were determined. Results obtained in this study showed thermal stability of the BpF composites shifted towards the lower temperature, which indicated that the presence of EFB fibre made PHBv little thermally unstable than neat PHBv. Biodegradation study showed that 98% weight loss after 16 weeks completed in soil. Scanning electron microscopy showed that compounding of PHBv between the EFB fibre and

NPK fertilizer evidence of poor bonding and weak interfacial adhesion at the interface. BpF composites product for slow release fertilizer expected to have wide potential applications in agriculture and horticulture activities.

**Keywords:** Biodegradable plastic; oil palm biomass; fertilizer; Bioplastic composites.

## Preparation of ultra-anisotropic hydrogels of cyanobacterial polysaccharides, sacran

Maiko K. Okajima, Ryosuke Mishima, Tatsuo Kaneko\*

*School of Materials Science, Japan Advanced Institute of Science and Technology (JAIST),  
Ishikawa 923-1292 Japan*

*Phone: +81-761-51-1633, Fax : +81-761-51-1635, \*E-mail: kaneko@jaist.ac.jp*

**Keywords:** Polysaccharide, Hydrogels, Anisotropy, In-situ gelation, Cyanobacteria

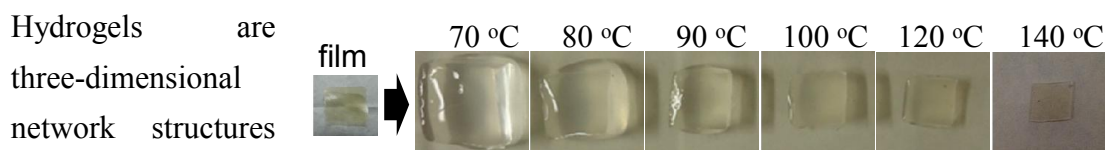


Fig. Digital images of gels prepared from in-situ gelation of films annealed at various temperatures

Hydrogels are three-dimensional network structures obtained from a class of synthetic and/or natural polymers which can absorb and retain significant amount of water. The hydrogels have been used extensively in various biomedical applications such as drug delivery, cell carriers and/or entrapment, wound management, and tissue engineering. Sacran is a cyanobacterial-polysaccharide extracted from *Aphanothece sacrum* and contains 11 % of sulfate group, 22 % of carboxyl group, and about 250 % of hydroxyl group to sugar residues [1]. Moreover sacran has a very high molecular weight of 29 Mg/mol and then a super-absorbent property to induce an anti-inflammatory activity [2]. We prepared the physical hydrogel made by following method; 1) 0.5 % sacran solution was dried at 60 °C for 12 h to create the thin film (about 50 μm). 2) The film was heated at 70, 80, 90, 100, 120, and 140 °C for 2 hours. 3) The film was then immersed into pure water to form anisotropic hydrogels (this phenomenon was specifically observed in sacran but not in other polysaccharides). The swollen degree of the gels to the dry weight was controlled from 20 to 800 times by the heating temperature of the film at 70-140 °C. The following properties of the hydrogels were evaluated: structural orientation, mechanical properties, swelling ratio, and anisotropy in pure water and other aqueous solution with various compositions.

### References

- [1] Okajima M.K., Ono M., Kabata K., Kaneko T. *Pure Appl Chem.* **2007**, *79*, 2039.
- [2] Ngatu N.R., Okajima M.K., et al. *Annals of Allergy, Asthma & Immunology.* **2012**, *108*, 117.

## **Tuning the degradation of PLA through the use of hybrid organic-inorganic coatings**

Maurizio (Toselli)<sup>1</sup>, Andrea (Saccani)<sup>1</sup>

<sup>1</sup> Dipartimento di Ingegneria Civile, Ambientale e dei Materiali

Viale Terracini 28, 40131, Bologna – ITALY

*E Mail/ Contact Détails (andrea.saccani@unibo.it)*

PLA is one of the polymers deriving from renewable sources that has been extensively investigated in the last years. Conceived to be used in the packaging industry, its durability is supposed to be rather limited. However, in view of the possible application in other industrial fields (houseware, mobile phones, automotive) the rate of degradation becomes an important issue. As an alternative to the bulk modification (conventional or nano additivation) we have investigated the possibility to protect the materials through the use of hybrid organic-inorganic coatings derived by sol-gel reactions. The composition of the coatings can be formulated against a specified environmental stress and allows some flexibility and the technology of deposition can be quite simple (spin or dip coating). In this work, we present data concerning the thermo-oxidative degradation of coated PLA samples and some preliminary results on photo-oxidative degradation.

***Keywords: Hybrid organic inorganic coatings, , degradation, PLA, durability, thermoplastics.***

[1] M. TOSELLI, A. SACCANI, F. PILATI “Thermo-oxidative resistance of crosslinked polyethylene coated by hybrid coatings containing graphene oxide” *in press* on Surface and Coating Technology.

[2] A. SACCANI, M. TOSELLI, F. PILATI. 2011. Improvement of the thermo-oxidative stability of LDPE films by organic-inorganic hybrid coatings. *Polymer Degradation Stability* 96, 212-219.

**Effect of the addition of chitosan on the physicochemical properties of extruded polypropylene films**

Rodríguez Félix D.E.<sup>1</sup>, Carrasco Guigón F.J.<sup>1</sup>, Castillo-Ortega M.M.<sup>1</sup>,  
Herrera Franco P.J.<sup>2</sup>

<sup>1</sup>Departamento de Investigación en Polímeros y Materiales, Universidad de Sonora, C.P.83 000, Hermosillo, Sonora, México.

<sup>2</sup>Unidad de Materiales, Centro de Investigación Científica de Yucatán, C.P. 97200 Mérida, Yucatán, México

[dora@polimeros.uson.mx](mailto:dora@polimeros.uson.mx)

The mixture of natural and synthetic polymers is a simple and practical way of producing new materials with useful properties. Films formed by blending two or more polymers usually have physicochemical properties different from those of the initial components. Furthermore, since the synthetic polymers are easily obtained and have low production costs, the mixture of natural and synthetic polymers may improve the cost-performance ratio of the resulting films.

In this work extruded films of polypropylene, one of the most widely used synthetic polymer and chitosan, a biodegradable polymer, were prepared. The effect of chitosan in the mixture was analyzed as a function of thermal, mechanical and morphological properties using Polypropylene-graft-maleic anhydride as a compatibilizer and glycerol as a plasticizer.

**Keywords:** *polypropylene, chitosan, polypropylene-graft-maleic anhydride, extrusion*

[1] QUIROZ-CASTILLO J.M., RODRIGUEZ-FELIX D.E., GRIJALVA-MONTEVERDE H., DEL CASTILLO-CASTRO T, PLASCENCIA JATOMEA M, RODRIGUEZ-FELIX F., HERRERA-FRANCO P.J. 2014. Preparation of extruded polyethylene/chitosan blends compatibilized with polyethylene-graft-maleic anhydride. Carb Polym, 101,1094-1100

[2] RODRIGUEZ-FELIX D.E., QUIROZ-CASTILLO J.M., GRIJALVA-MONTEVERDE H., DEL CASTILLO-CASTRO T., BURRUEL-IBARRA S.E., RODRIGUEZ-FELIX F., MADERA-SANTANA T., CABANILLAS R.E., HERRERA-FRANCO P. J., 2014. Degradability of Extruded Polyethylene/Chitosan Blends Compatibilized with Polyethylene-graft-Maleic Anhydride under Natural Weathering. J. Appl. Polym. Sci., 131/22

## TiOx Magneli phases as anode material for the degradation of refractory pollutants

Samuel Leleu<sup>1</sup>, Roseline Esmilaire<sup>1</sup>, Stéphane Raffy<sup>2</sup>, Marc Cretin<sup>1</sup>, Sophie Cerneaux<sup>1</sup>  
<sup>1</sup>IEM (Institut Européen des Membranes), UMR 5635 (CNRS-ENSCM-UM2),  
Université de Montpellier 2, Place E. Bataillon, F- 34095, Montpellier, France  
<sup>2</sup> Saint Gobain CREE, F-84000 Cavaillon, France

*E Mail/ Contact Details (sophie.cerneaux@univ-montp2.fr)*

Scarcity of pure water worldwide is dramatically affecting the economic development of Third Countries but also the industrial growth of others. Towards the water recycling and reuse, new technologies are to be developed, such as Advanced Oxidation Process (AOP). Indeed, electrochemical processes are of high interest since they are very efficient in the degradation of refractory pollutants that cannot be eliminated by conventional techniques. They allow the *in situ* generation of highly reactive and non-selective  $\cdot\text{OH}$  radicals through water oxidation that induce thus the total mineralization of pollutants.

Boron Doped Diamond (BDD) electrodes are currently used for this purpose. One of our objectives was to prepare electrodes at lower cost keeping the same efficiency towards the electrochemical degradation of pollutants. TiOx Magneli phases have shown their ability to play this role and are now developed in our team as porous electrode membrane material. Our aim would be to couple ultrafiltration (UF) and depollution of solutions to enhance system performance toward the degradation of persistent emerging pollutants like pharmaceutical residues.

Several strategies are thus being developed: (i) synthesis of TiOx powders of various compositions, (ii) preparation of pellets from these powders and (iii) elaboration of porous tubular membranes from the selected formulation. The challenge in this work is to find out the Magneli phase but also the required additives that will lead to the electrode material with the highest electronic conductivity, largest over potential window but still chemically and mechanically resistant to be designed as tubular porous membranes.

Textural, structural and electrochemical properties of the powders, pellets and tubular membranes were determined as a function of the formulation of the Magneli TiOx powders and the thermal treatment applied. TiOx membranes are characterized by an open porosity around 40 vol.% and a mean pore size diameter of 200 nm. As a preliminary study, pellets were examined in terms of electrochemical degradation of a model dye and behavior after many cycles of utilization. The next step will be the UF of polluted solutions under current with the optimized porous TiOx membrane and the characterization of recovered water.

**Keywords:** AOP, Magneli TiOx, Ultrafiltration, Electrochemistry

## TiOx Magneli phases as anode material for the degradation of refractory pollutants

Samuel Leleu<sup>1</sup>, Roseline Esmilaire<sup>1</sup>, Stéphane Raffy<sup>2</sup>, Marc Cretin<sup>1</sup>, Sophie Cerneaux<sup>1</sup>  
<sup>1</sup>IEM (Institut Européen des Membranes), UMR 5635 (CNRS-ENSCM-UM2),  
Université de Montpellier 2, Place E. Bataillon, F- 34095, Montpellier, France  
<sup>2</sup> Saint Gobain CREE, F-84000 Cavaillon, France

*E Mail/ Contact Details (sophie.cerneaux@univ-montp2.fr)*

Scarcity of pure water worldwide is dramatically affecting the economic development of Third Countries but also the industrial growth of others. Towards the water recycling and reuse, new technologies are to be developed, such as Advanced Oxidation Process (AOP). Indeed, electrochemical processes are of high interest since they are very efficient in the degradation of refractory pollutants that cannot be eliminated by conventional techniques. They allow the *in situ* generation of highly reactive and non-selective  $\cdot\text{OH}$  radicals through water oxidation that induce thus the total mineralization of pollutants.

Boron Doped Diamond (BDD) electrodes are currently used for this purpose. One of our objectives was to prepare electrodes at lower cost keeping the same efficiency towards the electrochemical degradation of pollutants. TiOx Magneli phases have shown their ability to play this role and are now developed in our team as porous electrode membrane material. Our aim would be to couple ultrafiltration (UF) and depollution of solutions to enhance system performance toward the degradation of persistent emerging pollutants like pharmaceutical residues.

Several strategies are thus being developed: (i) synthesis of TiOx powders of various compositions, (ii) preparation of pellets from these powders and (iii) elaboration of porous tubular membranes from the selected formulation. The challenge in this work is to find out the Magneli phase but also the required additives that will lead to the electrode material with the highest electronic conductivity, largest over potential window but still chemically and mechanically resistant to be designed as tubular porous membranes.

Textural, structural and electrochemical properties of the powders, pellets and tubular membranes were determined as a function of the formulation of the Magneli TiOx powders and the thermal treatment applied. TiOx membranes are characterized by an open porosity around 40 vol.% and a mean pore size diameter of 200 nm. As a preliminary study, pellets were examined in terms of electrochemical degradation of a model dye and behavior after many cycles of utilization. The next step will be the UF of polluted solutions under current with the optimized porous TiOx membrane and the characterization of recovered water.

**Keywords:** AOP, Magneli TiOx, Ultrafiltration, Electrochemistry

## **A porous TiO<sub>2</sub>-coated silica glass tube and its application for compact air- and water-purification units**

Tsuyoshi Ochiai<sup>1,2</sup>, Mio Hayashi<sup>1</sup>, Hiromasa Tawarayama<sup>3</sup>, Toshifumi Hosoya<sup>4</sup>, Akira Fujishima<sup>1,2</sup>

<sup>1</sup>Kanagawa Academy of Science and Technology, KSP building East 407, 3-2-1 Sakado, Takatsu-ku, Kawasaki, Kanagawa 213-0012, Japan

<sup>2</sup>Photocatalysis International Research Center, Tokyo University of Science, 2641 Yamazaki, Noda, Chiba 278-8510, Japan

<sup>3</sup>Optical Communications R&D Laboratories, Sumitomo Electric Industries, Ltd., 1 Taya-cho, Sakae-ku, Yokohama 244-8588, Japan

<sup>4</sup>Sumitomo Electric Industries, Ltd., 1-1-3, Shimaya, Konohana-ku, Osaka 554-0024, Japan

*E-mail:* [pg-ochiai@newkast.or.jp](mailto:pg-ochiai@newkast.or.jp); *Tel.:* +81-44-819-2040; *Fax:* +81-44-819-2070

A simple, handy, reusable and inexpensive air- and water-purification unit including a one-end sealed porous amorphous-silica (a-silica) tube coated with TiO<sub>2</sub> photocatalyst layers has been developed. The porous a-silica layers were formed through outside vapor deposition (OVD). TiO<sub>2</sub> photocatalyst layers were formed through OVD or vacuum impregnation onto a-silica layers surface (Figure 1)<sup>1</sup>. Developed porous TiO<sub>2</sub>-coated a-silica glass tubes have been evaluated for the air- and water-purification activity by using of acetaldehyde gas and methylene blue solution, respectively. The tubes also have been assayed for the tube filtering feature against *Escherichia coli* (*E. coli*) solution used as one of the typical bacteria size species or Q $\beta$  phage also used as typical virus size species and compared with the feature of porous a-silica tubes alone. The tubes removed *E. coli* completely from the aqueous suspension which contained 10<sup>6</sup> CFU/mL of *E. coli* without UV irradiation. The porous TiO<sub>2</sub>-coated a-silica glass tube with UV-C lamps reduced Q $\beta$  phage amount in the suspension successfully from 10<sup>9</sup> to 10<sup>3</sup> PFU/mL. Therefore, the tubes has great potential as compact air-purification, water-purification, and disinfection units.



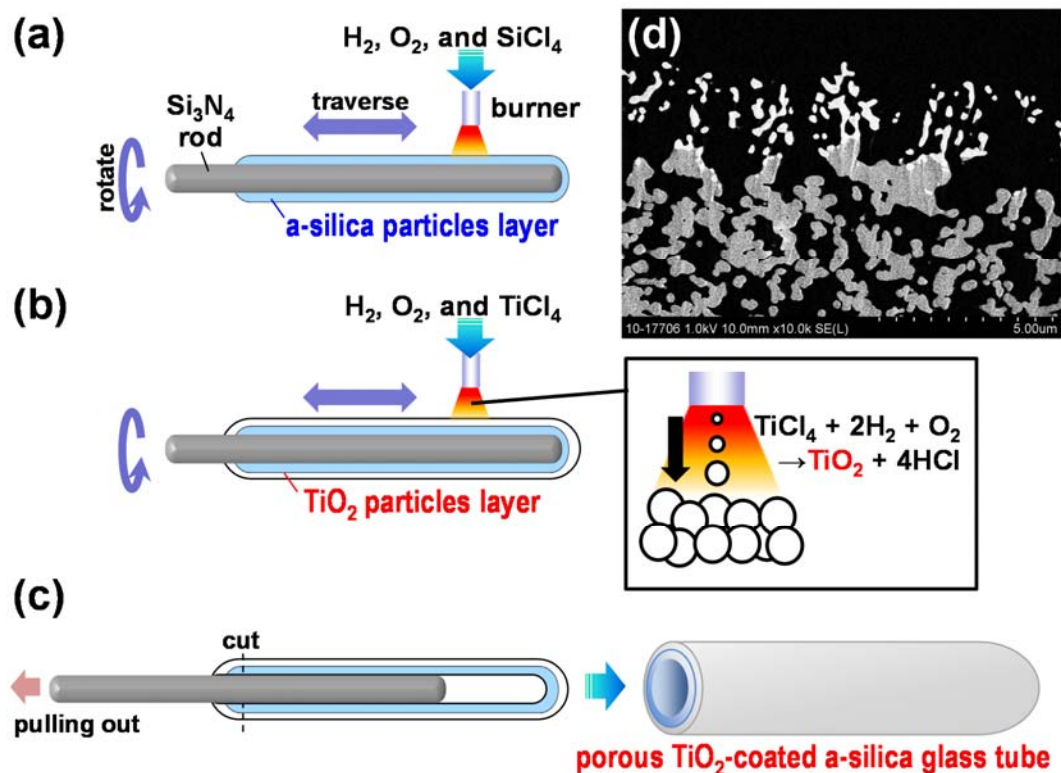


**Fig. 1.** The fabrication method for the porous  $\text{TiO}_2$ -coated a-silica glass tube by the OVD method and a SEM image of the tube. (a) Fine a-silica particles synthesized by hydrolysis of  $\text{SiCl}_4$  were deposited on a  $\text{Si}_3\text{N}_4$  rod target with a diameter of 6 mm. (b)  $\text{TiO}_2$  particles synthesized by hydrolysis of  $\text{TiCl}_4$  were deposited onto the porous a-silica glass layer. (c) A one-end sealed porous tube was obtained by pulling out the rod target from the soot body. (d) A high-magnification Secondary Election Image of cross-section of stacked  $\text{TiO}_2$  layers over a-silica layers.

**Keywords:** photocatalysis, porous amorphous-silica, air-purification, water-purification, disinfection

[1] OCHIAI, T., TAGO, S. TAWARAYAMA, H., HOSOYA, T., ISHIGURO, H. & FUJISHIMA, A. 2014. Fabrication of a Porous  $\text{TiO}_2$ -Coated Silica Glass Tube and Its Application for a Handy Water Purification Unit. International Journal of Photoenergy, 2014, Article ID 584921, 6 pages, doi:10.1155/2014/584921.

## **Fabrication of Hierarchically Structured Porous Films of Metal Oxides and Carbonates through Coffee Ring Effect**

Sachin Khapli<sup>1,\*</sup>, Ina Rianasari<sup>1</sup>, Sudhir Sharma<sup>1</sup>, Tom Blanton<sup>2</sup>, Ramesh Jagannathan<sup>1</sup>

<sup>1</sup>Engineering Division, New York University Abu Dhabi, Abu Dhabi, United Arab Emirates.

<sup>2</sup>International Centre for Diffraction Data, Newtown Square, Pennsylvania, United States.

\* Presenting and corresponding author

*Email : [sachin.khapli@nyu.edu](mailto:sachin.khapli@nyu.edu) / Phone : +971 56 749 1980*

We report a versatile method for the fabrication of hierarchically structured porous films from a wide variety of metal oxide, mixed metal oxide, and metal carbonates through a non-vacuum, spray-based deposition technique. Our method consists of evaporation of CO<sub>2</sub>-enriched water microdroplets (diameter ~ 3 μm) containing dissolved organic salts on superheated substrates (T = 120°C) at atmospheric pressure. A novel supercritical CO<sub>2</sub> (sc-CO<sub>2</sub>) based nebulization technique is used to generate microdroplets with control over droplet size and composition. A variety of porous scaffolds with 1-3 micron sized pores are generated because of the enhanced coffee ring effect during the evaporation of gas-enriched microdroplets. Subsequent sintering of the scaffolds is shown to generate nano-sized pores in the walls of the porous scaffold, creating a dual hierarchy of pore sizes (~50 nm & 1-3 μm). We demonstrate the fabrication of such hierarchically porous films for a wide variety of ceramic materials such as CaCO<sub>3</sub>, ZnO, CuO, Co<sub>3</sub>O<sub>4</sub>, Co-doped ZnO, and Ag<sub>2</sub>O. We also demonstrate the formation of thin films consisting of a network of nanowires from these materials by tuning the deposition conditions. Novel morphologies are also obtained through the application of Ostwald ripening process after deposition. For example, thin films consisting of a network 2-dimensional crystals of CaCO<sub>3</sub> that are one unit cell thick are obtained through this procedure. We report the influence of various process parameters on the morphology of films and provide a mechanism for their formation based on the results of extensive characterization using the techniques of scanning electron microscopy, optical and Raman microscopy, atomic force microscopy, photoluminescence measurements, and X-ray diffraction. Our process

utilizes sc-CO<sub>2</sub> and hence provides a sustainable, green process platform for processing a wide variety of ceramic materials. It is also advantageous for the fabrication of mixed-oxide and carbonate films since several pre-cursor materials could be co-dissolved and precipitated from a single source stream, thereby increasing the chemical uniformity in the final structures. Unlike the conventional, template based methods, our method is amenable to scale-up by assembling arrays of spray nozzle heads to coat on wide-format, roll-to-roll, moving surfaces. The resulting hierarchically structured films with interesting morphologies can lead to improved performance in applications that require high specific surface area, such as catalysis, sensors, solar cells, fuel cells, electrodes with improved properties, and biocompatible scaffolds for promoting cell adhesion. We demonstrate the utility of our technique through the application of CaCO<sub>3</sub> scaffolds in tissue engineering (Khapli et al., 2014) and the applications of ZnO films with strong near band edge (NBE) emission in optoelectronic devices.

**Keywords:** *Hierarchically porous materials, nanowires, two-dimensional crystals, calcium carbonate, zinc oxide*

[1] KHAPLI, S., RIANASARI, I., BLANTON, T., WESTON, J., GILARDETTI, R., NEIVA, R., TOVAR, N., COELHO, P., & JAGANNATHAN, R. 2014. Fabrication of Hierarchically Porous Materials and Nanowires through Coffee Ring Effect. ACS Applied Materials and Interfaces, Just Accepted Manuscript, DOI: 10.1021/am505318d, Publication Date (Web): November 7, 2014.

**Submission to Symposia 3:** Advances in Polymers and Ceramics

**Presentation Mode:** Oral / ~~Poster~~

**Topics Covered in Talk:** Porous Polymers and ceramics / Advanced Ceramic Materials and Processing for Photonics and Energy / Next Generation Bioceramics and Biocomposites

## Nanofibers/ Microporous KEVLAR<sup>®</sup> films for separator technology

Chi Ho (KWOK), Chenmin (LIU), Ning (TU)

Units 608-609, 6/F, Lakeside 2, No. 10 Science Park West Avenue,  
Hong Kong Science Park, Shatin, New Territories, Hong Kong

The Nano and Advanced Materials Institute Limited (NAMI), Hong Kong

[erickwok@nami.org.hk](mailto:erickwok@nami.org.hk); [chmlcm@nami.org.hk](mailto:chmlcm@nami.org.hk)

Separator for lithium-ion batteries, being a porous membrane sandwiched between electrodes of opposite polarity, which allow the Li<sup>+</sup> ions to flow but preventing the direct contact of electrodes. Today, a variety of polymers have been used. Materials such as polypropylene (PP) and polyethylene (PE) films are commonly used as microporous separators. More recently, some aromatic polyamides (i.e. polyparaphenylene terephthalamide) are being used to develop separators for battery purpose. Owing to their special structure-property relationship, these fibers provide an outstanding strength-to-weight property, which is suitable for battery application.

Electrospinning has been regarded as the most effective and versatile technology to develop nanofibers with controlled morphology and dimension from polymeric materials. In this study, we will make use of DuPont KEVLAR<sup>®</sup> to develop separators for lithium ion battery. The separator can be produced by 1) electrospinning to form fibrous film or 2) phase separation technique to develop polymeric film. By controlling the electrospinning parameters, such as solution concentration, flow rate, spinning distance and applied voltage, nano-scaled KEVLAR<sup>®</sup> fibrous films have been produced (Figure A). On the contrary, by controlling the concentration of the phase separation material, microporous KEVLAR<sup>®</sup> films have also been produced (Figure B). In addition, their batteries and the key performance parameters for both separators will be discussed.

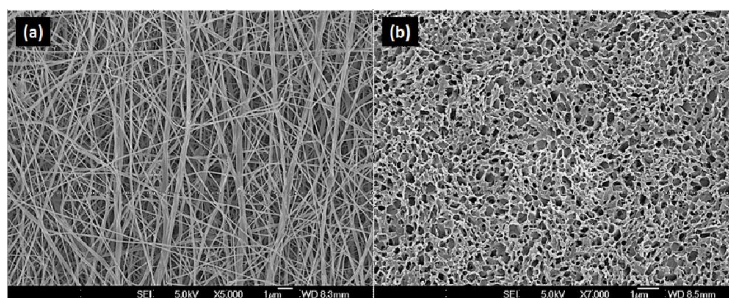


**Figure** Scanning electronic micrographs of KEVLAR<sup>®</sup> separator used in lithium ion batteries. Separator prepared by (a) electrospinning and (b) phase separation technique.

**Keywords:** Separator, electrospinning, phase-separation, lithium battery

## **A new synthesis scaffolds route with sol-gel bioactive glass and addition of porogen agents for bone tissue regeneration**

Guimarães, F. B. A. P.<sup>1</sup>, Oliveira, A. A. R.<sup>1</sup>, Pereira, M. M.<sup>1</sup>

<sup>1</sup> Dpto. Engenharia Metalúrgica e de Materiais, Escola de Engenharia, Universidade Federal de Minas Gerais, Belo Horizonte, BRAZIL.

*fabianabapg@gmail.com, agdalinero@gmail.com, mpereira@demet.ufmg.br*

The use of biomaterials capable of generating a biological response has been one of the biggest progresses in regenerative medicine, due to their ability to support growth stimulation and damaged tissue regeneration. In this context, ceramics – and particularly bioactive glass, were the subjects of multiple studies because of their known capacity to promote strong bonds between the tissues and the implant. Since the discovery of bioactive glass in the 1970s, various *in vitro* studies confirmed a high compatibility, osteoconductive and osteoinductive properties of this material.

The addition of porogen agent techniques for the synthesis of scaffolds is an interesting procedure because several types of porogen agents can be used.

The aim of this present work was to obtain scaffolds using four porogen agents: two types of paraffin, (I): paraffin 1 with average size 608,5  $\mu\text{m}$  until 993,3 $\mu\text{m}$ , (II): paraffin 2, with size 1,929mm until 2,307mm, (III): wax, with size 9,272 $\mu\text{m}$  until 204 $\mu\text{m}$  and (IV): CMC (carboxy methyl cellulose), with size 27,74 $\mu\text{m}$  until 382 $\mu\text{m}$ .

This study prepared and characterized scaffolds sol-gel bioactive glass 100S more porogen agents. Bioactive glass 100S (100%  $\text{SiO}_2$ ) was proposed in order to obtain only the porosity of the porogen agents. The calcium and phosphorus are silicate network modifiers and enhance material porosity. The scaffolds were submitted to different treatment temperatures: 700, 800 and 900°C to evaluate the effects that a change in treatment temperature can have on their crystallinity.

The porogen agents were characterized using scanning electron micrographs (SEM). The scaffolds were characterized using micro-computed tomography ( $\mu\text{CT}$ ), scanning electron micrographs (SEM), infrared spectroscopy (FTIR) and X-ray powder diffraction (XRD).

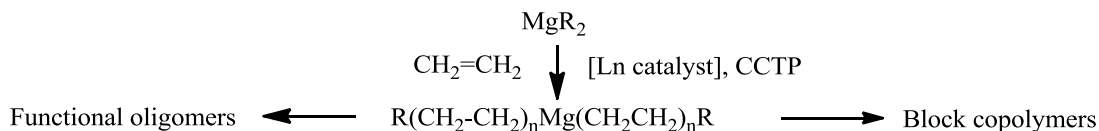
The results showed that the development of these scaffolds is possible and successful. Three-dimensional interconnected porous structures were obtained. These can be considered potential biomaterials for bone tissue regeneration.

***Keywords: Biomaterials, bioactive glass, porogen agents, sol-gel***

## Functionalized oligomers and block copolymers synthesis using Catalytic Chain Transfer Polymerization

André Mortreux, Thomas Chenal, Marc Visseaux,  
 UCCS, Unité de Catalyse et Chimie du Solide, UMRCNRS 8181, Université Lille1,  
 ENSCL, BP 90108 59652, Villeneuve d'Ascq Cedex France  
*andre.mortreux@ensc-lille.fr*

Since the seminal work on ethylene oligomerization and polymerization using magnesium dialkyls and lanthanidocene  $Cp^*_2LnCl_2Li(OEt_2)_2$  based catalysts [1], the use of CCTP as a tool for the synthesis of narrow distribution controlled synthesis of oligomers and polymers has attracted much attention in the last two decades [2]. Using dialkyl magnesium as starting main metal reagent, one of the major interests of this living transfer process using ethylene as the substrate is to provide higher molecular weight polyethylenyl  $Mg(PE)_2$  Grignard reagents of well controlled chain length leading by further functionalization to the synthesis of end-capped functionalized oligomers of narrow molecular weight distribution. The aim of this communication will be to present some of our results in this field, including a straightforward procedure for the catalyst synthesis, allowing a rapid screening of different cyclopentadienyl ligands on the lanthanide and their effect on the reactivity and selectivity in the ethylene polymerization and transfer reactions [3], as well as applications in the synthesis of block copolymers.



Special attention will be given to the synthesis of high molecular weight fatty alcohols which may compete with the ALFOL process, and allows to synthesize in high yield perfectly linear alcohols of the UNILIN<sup>®</sup> range, up to C50 with a polydispersity of 1.1.

**Keywords:** *ethylene, functionalization, chain transfer, catalysis, coordination*

[1] PELLETIER, J.F., MORTREUX, A., OLONDE, X., BUJADOUX, K. 1996. Synthesis of new dialkylmagnesium compounds by living transfer ethylene oligo- and polymerization with lanthanidocene catalysts, *Angew.Chem.*, 35, 1854-1856.

[2] VALENTE, A., MORTREUX, A., VISSEAU, M., ZINCK, P. 2013; *Chemical Reviews, Coordinative Chain Transfer Polymerization*, 113 (5), 3836-3887.

[3] CHENAL, T., MORTREUX, A., VISSEAU, M. 2013. Method for preparing dialkylmagnesium compounds and use thereof, *PCT Appl. WO2013/014383-A1*

## **The controlled/living radical homopolymerization of multivinyl monomers: toward single chain cyclized polymers**

Yongsheng Gao, Tianyu Zhao, Dezhong Zhou and Wenxin Wang\*

Charles Institute of Dermatology, School of Medicine and Medical Science, University College Dublin, Belfield, Dublin 4, Ireland.

*E Mail/ Contact Details :*

**Presenting author: [yongsheng.gao@ucdconnect.ie](mailto:yongsheng.gao@ucdconnect.ie)**

**Corresponding author: [wenxin.wang@ucd.ie](mailto:wenxin.wang@ucd.ie)**

The ability to control the homopolymerization of multivinyl monomers (MVMs) has always been a challenge. However, our initial studies has demonstrated a kinetically controlled strategy can be utilized to control both the gelling point and the macromolecular architecture in the homopolymerization of MVMs without the need for a diluted reaction condition<sup>1,2</sup>. Here, we present the homopolymerization of acrylate based MVMs can be kinetically controlled *via* Cu<sup>0</sup>-mediated controlled/living radical polymerization in the presence of additional Cu<sup>II</sup>, which enables the efficient regulation of chain propagation, intramolecular cyclization and intermolecular crosslinking. The gelation was effectively delayed over *ca.* 50% monomer conversion in the concentrated polymerization system ([M] = 40.9 wt %), which is far higher than the Flory–Stockmayer theory<sup>3</sup> predicted. Moreover, directed by this kinetically controlled strategy, novel single chain cyclized polymers were formed by this one-pot self-assembly reaction due to the promotion of intramolecular cyclization and the suppression of intermolecular crosslinking (Fig 1)<sup>4</sup>. This facile method opens a new avenue to the design and synthesis of a broad range of novel single chain cyclized polymeric materials.



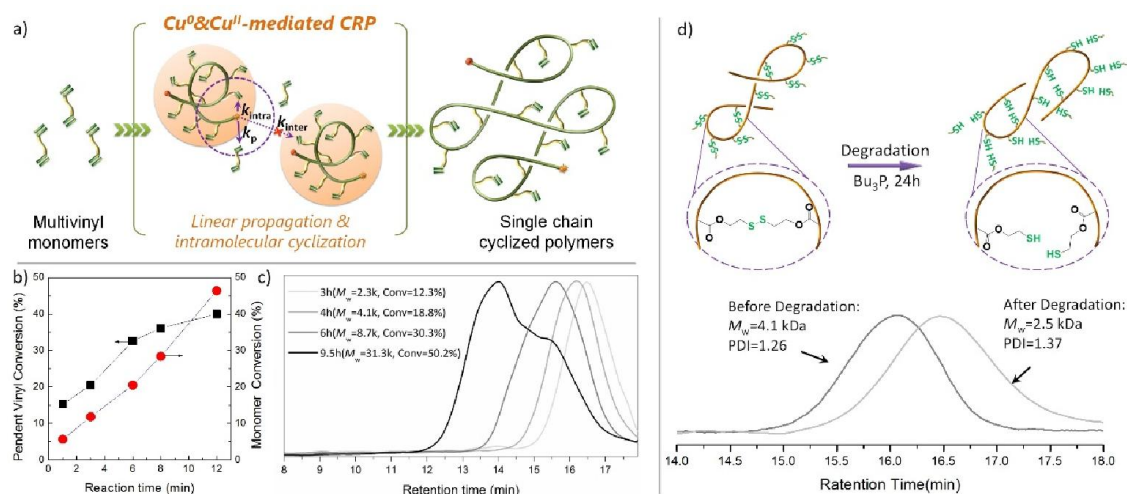


Figure 1 (a) Illustration of the formation of the single chain cyclized polymer structure. The intramolecular cyclization is promoted due to the small kinetic chain length and the high local vinyl concentration near the active centre. (b) Evolution of the monomer conversion and pendant vinyl conversion. *Ca.* 15-20% of pendant vinyl groups were reacted even at the onset of the reaction with a very low yield (< 5%). (c) GPC trace of the poly(bis(2-acryloyl)oxyethyl disulphide) showing the unimodal peaks typically at initial stages (<6 h) and multimodal peaks appearing later. (d) Schematic representation and degradation profiles of the poly(bis(2-acryloyl)oxyethyl disulphide) using reduction of tributylphosphine ( $\text{Bu}_3\text{P}$ ).

**Keywords:** *Controlled/living polymerization, multivinyl monomers, single chain polymers, cyclized polymers*

[1] ZHENG, Y., CAO, H., NEWLAND, B., DONG, Y., PANDIT, A., WANG, W., 2011. 3D single cyclized polymer chain structure from controlled polymerization of multi-vinyl monomers: beyond Flory-Stockmayer theory. *J. Am. Chem. Soc.* 133, 13130–13137.

[2] ZHAO, T., ZHENG, Y., POLY, J., WANG, W., 2013. Controlled multi-vinyl monomer homopolymerization through vinyl oligomer combination as a universal approach to hyperbranched architectures. *Nat. Commun.* 4, 1873.

[3] STOCKMAYER, W.H., 1944. Theory of Molecular Size Distribution and Gel Formation in Branched Polymers II. General Cross Linking. J. Chem. Phys. 12, 125.

[4] GAO, Y., ZHAO, T., ZHOU, D., MCMAHON, S., GREISER U., WANG, W. 2014. The homopolymerization of acrylate based multivinyl monomers *via* Cu<sup>0</sup>-mediated controlled/living radical polymerization: toward single chain cyclized polymers. *Submitted*

## High coercive $\text{CoFe}_2\text{O}_4$ powders for technological permanent magnet applications

K. Golasinski<sup>1</sup>, F.J. Pedrosa<sup>1</sup>, J. Rial<sup>1</sup>, A. Quesada<sup>2</sup>, F. Rubio-Marcos<sup>2</sup>, M.N. Guzik<sup>3</sup>, S. Deledda<sup>3</sup>, J.F. Fernández<sup>2</sup>, J. Camarero<sup>1</sup>, A. Bollero<sup>1</sup>

<sup>1</sup> IMDEA Nanoscience, Madrid, Spain.

<sup>2</sup> Electroceramic Department, Instituto de Cerámica y Vidrio, CSIC, Madrid, Spain.

<sup>3</sup> Institute for Energy Technology, 2027 Kjeller, Norway.

*E-Mail: karol.golasinski@imdea.org*

Rare earth-based permanent magnets (RE-PM) are used in a large number of nowadays technological applications. The rapidly increasing market of emerging technologies (wind turbines, electric vehicles...) demands increased amounts of this type of magnets [1,2]. This demand in combination with the strategically geographical distribution of RE (especially critical for heavy RE elements) make necessary the search of alternatives to these PMs in as many applications as possible.

*NANOPYME* (“*Nanocrystalline PMs based on Hybrid Metal-Ferrites*”) is a European project (with multidisciplinary participation of 11 institutions) that addresses the design and development of high quality PMs based on ferrites, with no REs content and with a larger energy product,  $(\text{BH})_{\text{max}}$ , compared to currently used ferrites [3]. Implementation of these new materials in the PM market will require low cost and efficient processing routes. High energy ball milling is a long tradition technique used in the synthesis and refinement of magnetic materials. One of its main disadvantages is the relatively long milling time (1h – tenths of hours) required to achieve adequate magnetic properties through an optimized microstructure.

In this work authors will show the possibility of obtaining a fourfold increase in coercivity for isotropic cobalt ferrite ( $\text{CoFe}_2\text{O}_4$ ) powders with a mean grain size of 10 nm by using milling times as short as 1.5 – 6 minutes in contrast with previous studies [4].

$\text{CoFe}_2\text{O}_4$  powders were prepared by sol-gel followed by heating at 900°C in air. X-ray diffraction showed the presence of exclusively spinel  $\text{CoFe}_2\text{O}_4$  phase. The resulting mean grain size was 80 nm. This powder was used as starting material for milling experiments

following two different routes: dry milling in air and milling with oleic acid as surfactant media (followed by removal of the surfactant).

Starting material showed a coercivity ( $H_c$ ) of 0.9 kOe, a saturation magnetization ( $M_s$ ) of 74 emu/g and a remanence ( $M_r$ ) of 31 emu/g. Dry milling of this powder for only 1.5 min has led to powders with a high coercivity  $H_c=4.1$  kOe,  $M_s=64$  emu/g and  $M_r=39.5$  emu/g. This combination of magnetic properties results in a remanence ratio of 62% and  $(BH)_{\max}=11$  kJm<sup>-3</sup> [5].

Surfactant-assisted milling of the starting material for 6 min results in a more homogeneous microstructure with a mean grain size of about 10 nm and top values  $H_c=4.1$  kOe, remanence ratio of 64% and  $(BH)_{\max}$  above 13 kJm<sup>-3</sup>.

The achieved large coercivity is due to a combination of a fine microstructure and the stress anisotropy and pinning effects induced on the particles during the milling process. The excellent combination of magnetic properties makes of these isotropic powders good candidates for PM applications.

**Keywords:** *Nanocomposites, magnetic materials, permanent magnets, functional materials*

[1] LEWIS, L.H. & JIMENEZ-VILLACORTA, F. 2013. Perspectives on Permanent Magnetic Materials for Energy Conversion and Power Generation. *Metall. Mater. Trans. A* 44, 2-20.

[2] GUTFLEISCH, O., WILLARD, M.A., BRÜCK, E., CHEN, C.H., SANKAR, S.G. & LIU, J.P. 2011. Magnetic Materials and Devices for the 21st Century: Stronger, Lighter, and More Energy Efficient. *Adv. Mater.* 23, 821–842.

[3] *NANOPYME* website: [www.nanopyme-project.eu](http://www.nanopyme-project.eu)

[4] LIU, B.H. & DING, J. 2006. Strain-induced high coercivity in CoFe<sub>2</sub>O<sub>4</sub> powders. *Appl. Phys. Lett.* 88, 042506-1\_3.

[5] PEDROSA, F.J. *et al.* 2014. High coercive CoFe<sub>2</sub>O<sub>4</sub> powders obtained by ultrafast milling. *Submitted.*

**Acknowledgements:** Research supported by EU-FP7 *NANOPYME* Project (No. 310516).

## **Fabrication and Characterization of Superparamagnetic Maghemite/PMMA Nanofibrous Composite**

**H M Khanlou, B C Ang\*, S Talebian, A M Afifi**

Centre of Advanced Materials, Department of Mechanical, University of Malaya, 50603 Kuala Lumpur, Malaysia

E-mail: amelynang@um.edu.my

**Abstract:** Over the years, the utilization of engineered magnetic composites has been growing, particularly in areas of remediation and water treatments. Also, this development cause to elevate public attention. In this study, PMMA nanofiber was selected to be used as the matrix. PMMA was dissolved in three diverse solvents which were Acetone, THF and DMF, to obtain fine PMMA nanofiber. In due course, the PMMA-DMF unwraps to be the best objective polymer solution among the three solvents, with its impressive defect-free surface morphology results. Meanwhile, production of Maghemite nanoparticles using Massart's procedure showed the average diameter of 6 nm, as observed using transmission electron microscopy (TEM). After that, Maghemite nanoparticle was mixed with a prepared polymer solution in order to fabricate Maghemite/PMMA nanofibrous Composite. Furthermore, the investigation of the morphology and structure of the composite was carried out by using field emission scanning electron microscopy (FESEM), Energy-dispersion X-ray spectroscopy (EDX), Fourier transform infrared spectrometer (FTIR), and X-ray diffraction (XRD). The results indicate the tremendous presence of Maghemite, both in and on the composite's surface. In addition, the distribution eas homogenous which concluded that the composite can be utilized in the sustainable applications.

**Keywords:** Electrospinning, Maghemite, PMMA, Nanofiber, Composite

## **Mechanical Properties of Non-cement Mortars fabricated under Supercritical Carbonation Conditions without Alkali Activators and Composed of Fly Ash and Fused Waste Slag**

Yootaek (Kim)<sup>1</sup> and Kyongwoo (Lee)<sup>1</sup>

<sup>1</sup>Department of Advanced Materials Science and Engineering, Kyonggi University,  
Suwon, South Korea, 433-760

*ytkim@kgu.ac.kr*

The mechanical properties of non-cement mortars that were fabricated without alkali activators and composed of fly ash (FA) produced from fluidized bed boilers mixed with fused waste slag (FWS) were investigated. Although the specimens were only made with the addition of distilled water, the high pH (pH > 13) of the slurry, which was caused by the hydration of the FA, caused the geopolymerization reactions of the FWS to occur and create the non-cement mortar. It was found that non-cement mortars mixed with FWS and fabricated without alkali activators can achieve compressive strengths of over 20 MPa. The compressive strength of the specimens that contained 20 wt% of FWS was the highest. This is because of the formation of geopolymers in these specimens that enhanced their compressive strength. The compressive strength of the other specimens decreased with increasing FWS content. It is thought that the formation of reaction products through carbonation may cause volume expansion inside the specimen, which produces extra cracks, and therefore, the compressive strength is reduced. The carbonation rate of the specimens after undergoing the supercritical carbonation process decreased with increasing FWS content. The maximum carbonation rate after the carbonation process was 4.75%.

***Keywords: Geopolymer, non-cement mortar, fly ash, fused waste slag, compressive strength***

[1] KIM, Y. & PARK, J. 2014. Property Enhancement of Supercritically Carbonated Specimen by Particle-Size Separation of Fly Ash and Cement: J. Ceram. Proc. Res. 15(4), 212-215.

## Comparative study of Iron-catalyzed ATRP Systems Using Various Highly Active Bidentate P-N Ligands

Mohd Yusuf Khan\*

\*Center of Excellence in Nanotechnology (CENT), King Fahd University of Petroleum and Minerals, KFUPM Box 1656, Dhahran 31261, Saudi Arabia.

*E-mail:* [mykhan@kfupm.edu.sa](mailto:mykhan@kfupm.edu.sa); *Tel:* +966 535056891

New substituted P-N ligands such as [2-Di-tert-butylphosphino-2'-(N,N-dimethylamino)biphenyl] (DTBP), [2-Diphenylphosphino-2'-(N,N-dimethylamino)biphenyl] (DPP), [2-Dicyclohexylphosphino-2'-(N,N-dimethylamino)biphenyl] (DCHP) and 4-(Dimethylamino) phenyldiphenylphosphine (DAPDP) were investigated for different ATRP (atom transfer radical polymerization) systems (i.e. ATRP, AGET ATRP and ATRP using oxidation without any additive) using MMA (methyl methacrylate), BMA (butyl methacrylate) and styrene with EBriB (ethyl-2-bromoisobutyrate) as an ATRP initiator at 80 °C in toluene. The effect of catalytic system on different ATRP methods was studied systematically. Most of the polymerizations with these ligands were well controlled with linear increase in the average molecular weight ( $M_n$ ) with monomer consumption and conversion reached over 90% without any complications. In the case of DTBP, experimental molecular weights matched the theoretical values very well and the molecular weight distributions were found narrower (<1.2) compared with other ligands. Furthermore, the most active catalyst (FeBr<sub>3</sub>/DTDB) was used successfully for polymerization of MMA at 50 ppm of catalyst loading. The PMMA synthesized using FeBr<sub>3</sub> was characterized by MALDI-TOF-MS for the first time.

***Keywords: Living Polymerization techniques, High Oxidation State Iron Complexes, Nitrogen-Phosphorous Ligands, NMR and MALDI TOF-MS.***



## Computational Investigation of Multi Phase Formation in Segmented Polyurethane Copolymers

Erol YILDIRIM, Mine YURTSEVER\*  
Istanbul Technical University, Faculty of Science,  
Department of Chemistry, 34469 Maslak, Istanbul, Turkey  
mine@itu.edu.tr

### Abstract

Soft blocks in segmented polyurethane (PU) copolymers have diverse interactions with each other and also with urethane hard segment due to variable compatibilities between them. Incorporation of two different soft blocks provides more flexibility in controlling extent of phase separation, size and shape of the phase domains and offers new possibilities for tuning the final properties of such materials. Coarse grained computer simulations were carried out to elucidate the phase behaviors and morphologies of segmented di- and tri-block polyurethanes. The copolymers modeled are comprised of polytetramethyleneoxide (PTMO) or polyhexylethylcarbonate (PHEC) and polydimethylsiloxane (PDMS) or polyisobutylene (PIB) soft blocks with PU hard block containing diphenylmethane diisocyanate (MDI)-urethane repeating unit. We demonstrate that different morphologies from homogeneous to complete microphase separated one are attainable by varying the composition and the chain lengths of the blocks. The relatively hydrophobic soft blocks such as PIB and PDMS favor better phase separation than the relatively hydrophilic PHEC and PTMO in studied polyurethane copolymers.

### References

- [1] Selim Sami, Erol Yildirim, Mine Yurtsever, Ersin Yurtsever, Emel Yilgor, Iskender Yilgor, Garth L. Wilkes, *Understanding the influence of hydrogen bonding and diisocyanate symmetry on the morphology and properties of segmented polyurethanes and polyureas: Computational and experimental study*, Polymer, 55, 18, 4563-4576 (2014).
- [2] Erol Yildirim, Mine Yurtsever, *The role of diisocyanate and soft segment on the intersegmental interactions in urethane and urea based segmented copolymers: A DFT study*, Computational and Theoretical Chemistry, 1035, 28 –38 (2014).

**Keywords:** polyurethane copolymers; morphology; coarse graining; DPD

# Highly water soluble nanostructured Boron Nitride for anticancer drug delivery

Bikramjeet Singh, Gurpreet Kaur, Paviter Singh, Akshay Kumar\*

*Department of Nanotechnology, Sri Guru Granth Sahib World University, Fatehgarh Sahib-140406 Punjab, India*

## Abstract

Highly water soluble nanostructured Boron Nitride (BN) has been successfully synthesized by reduction of Boric Acid ( $H_3BO_3$ ) in presence of ammonia. It is a relatively low temperature synthesis route, nanoparticles were synthesized at  $700^\circ C$ . This method can be used for large scale production of nanostructured BN. The synthesized nanoparticles have been characterized by X-ray diffraction (XRD), scanning electron microscopy (SEM) and differential thermal analyzer (DTA), Fourier Transformed Infrared Spectroscopy (FTIR). Particle size analyzer was used to find the approximate size of the particles. XRD analysis confirmed the formation of single phase nanostructured Boron Nitride with compressive strain in crystal structure. SEM analysis showed that the particles are spherical in shape. DTA analysis showed that the phase is stable upto  $900^\circ C$ . These particles are highly soluble in water although traditional BN is insoluble in water. Solubility of these particles make it useful as anticancer drug carrier.

**Keywords:** Boron Nitride, nanoparticles, water soluble, scanning electron microscopy.

\* Email: [akshaykumar.tiet@gmail.com](mailto:akshaykumar.tiet@gmail.com)

## The use of Kenaf fiber reinforced polymer to confine the concrete cylinder

Reza Mahjoub<sup>1</sup>, Jamaludin Mohamad Yatim<sup>2</sup>, Abdulrahman Mohd Sam<sup>2</sup>, Zulkarnain<sup>2</sup>,  
Mehdi Raftari<sup>1</sup>

<sup>1</sup>Departement of Civil Engineering, Faculty of Engineering, Khorramabad Branch, Islamic Azad University, Khorramabad, Iran

<sup>2</sup>Faculty of civil Engineering, Universiti Teknologi Malaysia, Johor Bahru, Malaysia  
[r\\_mahjoub@yahoo.com](mailto:r_mahjoub@yahoo.com)

### Abstract

Recently, Fiber Reinforced Polymer (FRP) wrapping technique has been used as an alternative to retrofit concrete members especially in columns. FRP based on natural fibers are new materials used in wrapping technique and are an alternative to synthetic fibers. The ability of natural fibers based FRP (bio-composites) as an element to wrap concrete columns was studied in this study. This research is a laboratory experiment conducted on the performance of concrete columns subjected to axial compression loading. Many samples of plain concrete cylinders were prepared for testing which consists of unwrapped samples, samples wrapped with glass FRP, and samples were wrapped with Kenaf FRP. Then, the results from tests and a confinement theoretical model will be surveyed.

**Keywords: Confined concrete column, Natural fiber, Bio-composite, Compressive strength**

- [1] Yousef, A., Al-Salloum, Tarek, H., Almusallam, (2002). Rehabilitation of the Infrastructure Using Composite Materials: Overview and Applications. J. King Saud Univ., Vol.0, Eng. Sci (2).
- [2] Demers M, Neale KW. (1994). Strengthening of concrete columns with unidirectional composite sheets. In: Mufti AA, Bakht B, Jaeger LG, editors. Development in short and medium span bridge engineering' 94. Proceedings of the fourth international conference on short and medium bridges. Montreal: Canadian Society for Civil Engineering; p895–905.
- [3] Toutanji, H., Balagurce, P., (1998). Durability characteristics of concrete columns wrapped with FRP two sheets. J Mater Civ Eng, p52–57.
- [4] Berthet, J.F., Ferrier, E., Hamelin, P. (2005). Compressive behavior of concrete externally confined by composite jackets. Part A: experimental study. Construction and Building Materials, 19(3), 223–232.
- [5] Almusallam T.H. (2007). Behavior of normal and high-strength concrete cylinders confined with E-glass/epoxy composite laminates. J Composites: Part B, 38, 629–639.
- [6] Elsanadedy, H.M., Al-Salloum, Y.A., Abbas, H., Ahsayed, S.H. (2011). Prediction of strength parameters of FRP-confined concrete. Composites: Part B, 43(2), 228-239.
- [7] Burgueño, R., Quagliata, M.J., Mohanty, A.K., Mehta, G., Drzal, L.T. and Misra, M. (2004). Load-Bearing Natural Fiber Composite Cellular Beams and Panels. Composites Part A: Applied Science and Manufacturing, 35(6), 645-656.
- [8] Burgueño, R., Quagliata, M.J., Mohanty, A.K., Mehta, G., Drzal, L.T. and Misra, M. (2005). Hybrid Biofiber-Based Composites For Structural Cellular Plates. Composites Part A: Applied Science and Manufacturing, 36(5), 581-593.
- [9] Giles, H., Kim, K.H. (2007). Transparent Facade Panel Typologies Based On Hybrid Bio-composite and Recyclable Polymer Materials. University of Michigan.
- [10] Mahjoub, R., Yatim, J. M. and Mohd Sam, A. R. (2013). A Review Of Structural Performance Of Oil Palm Empty Fruit Bunch Fiber In Polymer Composites. Advances in material science and Engineering, Article ID: 415359.
- [11] Mahjoub, R., Yatim, J. M., Mohd Sam, A. R. and Hashemi, S. H. (2014). Tensile Properties Of Kenaf Fiber Due To Various Conditions Of Chemical Fiber Surface Modifications. Construction and Building Materials, 55, 103-113.
- [12] Mahjoub, R., Yatim, J. M., Mohd Sam, A. R. and Raftari, M. (2014). Characteristics Of Continuous Unidirectional Kenaf Fiber Reinforced Epoxy Composites. Materials and Design, 64, 640-649.

# Symposia 4

## Advances in Energy Storage and Conversion Devices

---

- Lithium, Sodium, Magnesium and potassium Ion Batteries
- Electrochemical Supercapacitors
- Fuel Cells
- Solar Cells
- Photocatalytic and electrochemical water splitting
- Artificial photosynthesis
- Advances in electrolyte and electrolyte additives for energy storage devices
- Computational modeling and simulation for energy storage and conversion devices
- Others

# INDEX PAGE

1. Investigations On Ion Transport Behaviour In A Non-Lithium Chemical Based Solid Polymer Electrolyte (Spe): [Peo:Zna]	1
<b>AUTHOR:</b> Prof. Rakesh Agrawal	
2. Designing of F- ions conductors: correlation between the composition/structural features and ionic conductivity	2
<b>AUTHOR:</b> Dr. Belto Dieudonné	
3. A Nanoscale, All Atomistic Model of Photocatalytic Water Splitting on Titanium Dioxide Surfaces	3
<b>AUTHOR:</b> Dr. Srinivas Mushnoori	
4. First-principles determination of the K-conductivity in the low temperature modification of KAlO <sub>2</sub>	4
<b>AUTHOR:</b> Dr. Maxim Peskov	
5. Novel renewable energy converter concept for solar and hydrogen hybridization	6
<b>AUTHOR:</b> Dr. Emmanuel Ollier	
6. Atomic Layer Deposition For On-Chip Supercapacitors	9
<b>AUTHOR:</b> Dr. Kestutis Grigoras	
7. High energy density asymmetric supercapacitor based on nano-architected NiAl layered double hydroxides/functional carbon nanotube composites	10
<b>AUTHOR:</b> Dr. Yan Wang	
8. Synthesis and electrochemical properties of three-dimensional graphene /polyaniline composites for supercapacitor electrode materials	11
<b>AUTHOR:</b> Prof. Dawei He	
9. Development of doped La substituted SrTiO <sub>3</sub> -based anode materials for solid oxide fuel cells	12
<b>AUTHOR:</b> Prof. Jingli Luo	
10. Characterization Of Pemfc Catalytic Layers Based On Carbon Xerogels	14
<b>AUTHOR:</b> Mr. Fabien Deschamps	
11. Further Understanding of Nitrogen-Doped Carbon Catalytic Property Towards Oxygen Reduction Reaction (ORR)	16
<b>AUTHOR:</b> Dr. Belabbes Merzougui	
12. Oxygen Reduction on Hafnium/Hafnium Carbide Nanoparticles	17
<b>AUTHOR:</b> Dr. Olga Baturina	
13. Effect of Fillers on the Electrical and Sealing Properties of Alkali/Alkaline-Earth Borosilicate Glass Composite Sealants	18
<b>AUTHOR:</b> Prof. Jae Chun Lee	
14. Mechanism for Hydrogen Storage Properties of Li <sub>2</sub> Mg(NH) <sub>2</sub> Determined by Gas Back Pressure: A First-Principles Calculation Assisted Experimental Investigation	19
<b>AUTHOR:</b> Dr. Chu Liang	
15. Polybenzimidazole based composite membranes for high temperature proton exchange membrane fuel cells	21
<b>AUTHOR:</b> Prof. Jin Soo Park	
16. Structure fabrication of stable rGO-wrapped Ni <sub>3</sub> S <sub>2</sub> nanobowls with enhanced electrochemical performance in LIBs	22
<b>AUTHOR:</b> Dr. Wei Zhou	
17. GISAXS and TOF-GISANS studies on surface and depth morphology of self-organized TiO <sub>2</sub> nanotube arrays - model anode material in Li-ion batteries	24
<b>AUTHOR:</b> Dr. Neelima Paul	
18. Vanadium Pentoxide-based Composite Synthesized Using Microwave Water	25

Plasma for Cathode Material in Rechargeable Magnesium Batteries <b>AUTHOR:</b> Mr. Masashi Inamoto	
19. A new kind of lithium ion battery with enhanced electrochemical performances <b>AUTHOR:</b> Prof. Weixin Zhang	26
20. Design and fabrication of hierarchically porous electrode materials using biological templates for lithium ion batteries <b>AUTHOR:</b> Dr. Yang Xia	27
21. Electrospinning And Its Application As Electrode And Separator In Lithium-Ion Batteries <b>AUTHOR:</b> Prof. Jun Seo Park	28
22. Real Time Electron Microscopy Studies on Electrode Materials for Lithium Ion Batteries <b>AUTHOR:</b> Dr. Seung Sang Hwang	29
23. Micro- and nanostructured Silicon anodes for Li-battery application <b>AUTHOR:</b> Dr. Thomas Defforge	30
24. Synthesis of Large Surface Area Al <sub>2</sub> O <sub>3</sub> Nanomaterials for Applications to Batteries and Fuel Cells <b>AUTHOR:</b> Dr. Vic Liu	31
25. New Transition Metal Oxyfluorides with HTB network as rechargeable Li-ion battery at high voltage (average > 3V vs Li <sup>+</sup> /Li) <b>AUTHOR:</b> Dr. Alain Demourgues	32
26. Monodisperse MPd (M: Co, Ni, Cu) Alloy Nanoparticles Supported on Reduced Graphene Oxide as Cathode Catalysts for the Lithium-Air Battery Author : Prof. Önder Metin	33
27. Hybrid structure of cobalt monoxide nanorods and reduced graphene oxide nanosheets as anode materials for lithium-ion batteries <b>AUTHOR:</b> Prof. Hui Huang	34
28. A facile fabrication of red phosphorus/ amorphous TiO <sub>2</sub> composites for lithium ion batteries <b>AUTHOR:</b> Prof. Wenkui Zhang	35
29. High electrochemical Li-storage performance of ultrafine Mn <sub>3</sub> O <sub>4</sub> nanocrystal grown on reduced graphene oxide <b>AUTHOR:</b> Prof. Yongping Gan	36
30. Fabrication of layer LiMO <sub>2</sub> (M=Mn, Co, Ni) cathodes with extra-high charge-discharge rate for lithium ion battery <b>AUTHOR:</b> Prof. Liping Li	37
31. Homogeneous and Heterogeneous Approaches to Photochemical Water Splitting: a Fight for the Right Metals <b>AUTHOR:</b> Prof. Peter Brueggeller	39
32. An Earth-Abundant, Double-Metal-Hydroxide-Decorated Core/Shell Array Photoanode for Improved Photoelectrochemical Water Oxidation Efficiency <b>AUTHOR:</b> Prof. Xu Xiang	40
33. Improving photocatalytic performance and visible light respond by integrating two wide-band-gap semiconductors, SnO <sub>2</sub> and Sn <sub>2</sub> Ta <sub>2</sub> O <sub>7</sub> <b>AUTHOR:</b> Prof. Xiaojing Wang	41
34. Iridium Oxide Modified CdSe/CdS/TiO <sub>2</sub> Nanorods for Efficient and Stable Photoelectrochemical Water Splitting <b>AUTHOR:</b> Mr. Bo Sun	42
35. Magnetron Sputtering For Deposition Of Photocatalyst Nanostructures On Transparent Conductive Oxides For Solar Applications <b>AUTHOR:</b> Dr. Angela Kruth	45
36. Passivated N-P Co-Doping Of Niobium And Nitrogen Into Self-Organized TiO <sub>2</sub> Nanotube Arrays For Enhanced Visible Light Photocatalytic Performance	46

<b>AUTHOR:</b> Dr. Weiyi Yang	
37. Photoanodic Hybrid Semiconductorâ€“Molecular Heterojunction for Solar Water Oxidation	
<b>AUTHOR:</b> Dr. Khurram Joya	48
38. Photocatalytic Water Splitting For Hydrogen Production With Y <sub>2</sub> Fesbo <sub>7</sub> And In <sub>2</sub> Fesbo <sub>7</sub> Photocatalysts Under Visible Light Irradiation	
<b>AUTHOR:</b> Prof. Jingfei Luan	50
39. Photocurrent Extraction Efficiency Near Unity In A Thick Polymer Bulk Heterojunction	
<b>AUTHOR:</b> Prof. Jin Young Kim	51
40. Satellite Solar Array With Silicon Laser Downlinks To Denver And The Arctic	
<b>AUTHOR:</b> Mr. Paul Christopher	53
41. Realization of both high efficiency and quantum tunneling in QM-SIS solar cells	
<b>AUTHOR:</b> Dr. Zhongquan Ma	56
42. A new self-adhesive transparent electrode for high efficiency perovskite solar cells	
<b>AUTHOR:</b> Dr. Trystan Watson	57
43. Molecular glasses as hole transporting materials in solid state dye-sensitized solar cells	
<b>AUTHOR:</b> Dr. Thanh-Tuân Bui	59
44. Design Principles in Polymer-Fullerene BHJ Solar Cells: PBDTPD as a Case Study	
<b>AUTHOR:</b> Prof. Pierre Beaujuge	60
45. Effectively Utilizing NIR Light Using Direct Electron Injection from Up-Conversion Nanoparticles to the TiO <sub>2</sub> Photoanode in Dye-Sensitized Solar Cells	
<b>AUTHOR:</b> Prof. Suli Wu	63
46. Quasi Core-Shell Nitrogen-Doped Graphene/Cobalt Sulfide Conductive Catalyst for Highly Efficient Dye-Sensitized Solar Cells	
<b>AUTHOR:</b> Dr. Chen Han	64
47. Calcium Iodide and Hydroxypropyl Cellulose Based Gel Polymer Electrolytes for Dye-Sensitized Solar Cell	
<b>AUTHOR:</b> Prof. Ramesh T Subramaniam	65
48. Effect of pre-annealing on the solar cell performance of Cu <sub>2</sub> ZnSnS <sub>4</sub> thin film prepared by sulfurization of stacked metal precursor with H <sub>2</sub> S gas	
<b>AUTHOR:</b> Dr. Jong Keuk Park	66
49. A Simple Approach to Fabricate Yolk-shell Si/C Nanostructured Materials towards Anode Materials for Lithium Ion Batteries	
<b>AUTHOR:</b>	67
50. Modifying the Surface of Graphitic Materials Using Aryl Diazonium Ion Nitroxides	
<b>AUTHOR:</b> Prof. Steven Bottle	
51. Nanoparticles as nucleating agent to reduce supercooling in phase change	
<b>AUTHOR:</b> Prof. Jianlei Niu	
52. Mechanochemical reactions and processing of nanostructured electrode materials for lithium-ion batteries	
<b>AUTHOR:</b> Dr. Nina Kosova	
53. Polybenzimidazole based composite membranes for high temperature proton exchange membrane fuel cells	
<b>AUTHOR:</b> Prof. Soryong Chae	

## Investigations on Ion Transport Behaviour in a Non-Lithium Chemical Based Solid Polymer Electrolyte (SPE): [PEO:ZnA]

R. C. Agrawal\*, Shrabani Karan, Tripti Bala Sahu, Manju Sahu  
*School of studies in Physics & Astrophysics,*  
*Pt. Ravishankar Shukla University, Raipur 492010, India*  
*\*Corresponding author E-mail: rakesh\_c\_agrawal@yahoo.co.in*

### Abstract

Dry polymer electrolytes such as Solid Polymer Electrolytes (SPE), Composite Polymer Electrolytes (CPEs) etc. in thin / flexible film form show tremendous technological potentials to develop All-Solid-State electrochemical power sources viz. rechargeable batteries in any desired shapes/ sizes including mini/ micro batteries. Such batteries, based on  $\text{Li}^+$  -ion conducting dry polymer electrolytes and Li-metal electrode are being manufactured at a large scale and have captured  $\sim 70\%$  of commercial market worldwide. However, Lithium polymer batteries have recently reported to encounter several safety and environmental issues. The reason identified for this has primarily been the use of Lithium chemicals i.e.  $\text{Li}^+$  -ion complexing salt and Li –metal electrode in these batteries. Also, these chemicals are very toxic, less environment friendly, very reactive, difficult to handle in open ambience, low natural abundance, very expensive etc. Hence, the need for non-lithium chemical based polymer electrolytes and electrodes are being felt very strongly these days.

As an attempt in this direction, this paper reports investigations on non-lithium chemical based dry Solid Polymer Electrolyte (SPE) : [PEO:  $(\text{CH}_3\text{COO})_2\text{Zn}$ ] in which high mol. wt. polar polymer PEO has been used as host and Zinc Acetate (ZnA) as complexing salt. SPE films of varying salt concentration have been hot press cast. The salt- concentration dependent conductivity measurements at room temperature identified SPE film: [95 PEO: 5 ZnA] as optimum conducting film with  $\sigma_{\text{rt}} \sim 1.22 \times 10^{-7}$  S/cm which also appeared to have superior mechanical flexibility. In order to evaluate the suitability of this SPE film in All-Solid-State battery application, ion transport behavior has been characterized in terms of some basic ionic parameters viz. ionic conductivity ( $\sigma$ ), total ionic ( $t_{\text{ion}}$ ) and cationic ( $t_+$ ) transference numbers, activation energy ( $E_a$ ). These ionic parameters have been experimentally determined using different ac/dc techniques. The characterization of materials properties has also been done with the help of SEM/XRD/ FTIR/DSC techniques.



## Designing of F<sup>-</sup> ions conductors: correlation between the composition/structural features and ionic conductivity

B.Dieudonné<sup>1</sup>, J. Chable<sup>1,2</sup>, F. Mauvy<sup>1</sup>, S. Fourcade<sup>1</sup>, V. Maisonneuve<sup>2</sup>, C. Legein<sup>2</sup>, A. Demourgues<sup>1</sup>,

<sup>1</sup>CNRS-ICMCM-Université de Bordeaux UPR 9048, Avenue du Dr A. Schweitzer, 33600 Pessac Cedex, France.

<sup>2</sup> Université du Maine-CNRS UMR 6283, IMMM, Avenue Olivier Messiaen 72085 Le Mans Cedex, France.

[dieudonne@icmcb-bordeaux.cnrs.fr](mailto:dieudonne@icmcb-bordeaux.cnrs.fr) / [demourg@icmcb-bordeaux.cnrs.fr](mailto:demourg@icmcb-bordeaux.cnrs.fr)

Alternative technologies to replace Li-ion batteries using for example Na<sup>+</sup>, Mg<sup>2+</sup> or Cl<sup>-</sup> ions are investigated. Recently F<sup>-</sup> ions batteries have been proposed [1] but one of the key features is the design (composition, structures, morphologies and sintering) of the solid electrolytes. Among the most interesting and performing F<sup>-</sup> ionic conductors, the Tysonite structure (LaF<sub>3</sub>, SG : P-3c1) have been largely quoted. The aliovalent (Ca<sup>2+</sup>, Sr<sup>2+</sup>, Ba<sup>2+</sup>) cations partial substitution for La<sup>3+</sup> to create anionic vacancies have been explored for many years but the occurrence of solid solutions, the relationships between the chemical composition, the structural features and the ionic conductivity remain unclear. Several solid solutions (R<sub>1-x</sub>M<sub>x</sub>F<sub>3-x</sub>, R= La, Ce, Sm and M= Ba, Ca, Sr) have been prepared by solid-state route and quenching at high temperatures allow obtaining pure phases and determining the solubility limits. The variations of cell parameters and atomic positions in this series have been accurately determined on the basis of XRD-data analysis. F<sup>-</sup> NMR investigations lead to identify the various F1/F2/F3 local environments which vary with the compositions. The sintering of ceramics with compactness around 95%, allow determining accurately the ionic conductivities by the complex impedance method. Finally the chemical compositions have been optimized to design the best F<sup>-</sup> ionic conductors and the key role of the Tysonite network has been brought to the fore.

**Keywords:** Fluorides, Tysonite-type, XRD, F- NMR Ionic conductivity

[1] FICHTNER : FIB

## **A Nanoscale, All Atomistic Model of Photocatalytic Water Splitting on Titanium Dioxide Surfaces**

Chong<sup>1</sup>, Mushnoori<sup>1</sup>, Dutt<sup>1</sup>

<sup>1</sup>Department of Chemical and Biochemical Engineering, Rutgers The State University of New Jersey, Piscataway, NJ 08854

*Email : Srinivas Mushnoori (presenting)- [srinivas.mushnoori@rutgers.edu](mailto:srinivas.mushnoori@rutgers.edu)*

*Meenakshi Dutt (corresponding)- [meenakshi.dutt@rutgers.edu](mailto:meenakshi.dutt@rutgers.edu)*

Photocatalytic water splitting has been a subject of considerable interest as a source of alternative energy. Titanium dioxide based catalysts are a popular choice because of their abundance and low cost. Although promising in concept, hydrogen generation rates, in the current state of the art, are not high enough for commercial viability. Despite the abundance of experimental studies on the subject, there are only few computational studies, which are essential to understand the mechanistic aspects of the phenomena involved. In our study, we employ Molecular Dynamics to establish a nanoscale, all atomistic model to capture the mechanistic aspects of the interfacial interactions such as radial distribution functions, diffusion coefficients, adsorption angles and residence times of water with the catalyst surfaces. We study four different surfaces, Anatase (101) and Rutile (110) forms of Titanium Dioxide, each with and without adsorbed Platinum atoms. Additionally, we use the kinetic Monte Carlo method to model the decomposition reaction. The highlight of our model is the large scale: we have simulated systems as large as 30nm x 30nm x 3 nm for about 4 ns.

***Keywords: Photocatalysis, water splitting, atomistic, Molecular Dynamics***

## First-principles determination of the K-conductivity in the low temperature modification of $\text{KAlO}_2$

Maxim Peskov (Peskov)<sup>1</sup>, Udo Schwingenschlögl (Schwingenschlögl)<sup>1</sup>

<sup>1</sup>Physical Sciences & Engineering, King Abdullah University of Science and Technology, Thuwal 23955-6900, Kingdom of Saudi Arabia.

*maxim.peskov@kaust.edu.sa*

Fast ion-conducting materials are indispensable for new generation energy storage and power devices. In many novel ion-conducting structures the computational effort to identify pathways is very high. The tiling method proposed by Blatov and coworkers [1] is a viable alternative to molecular dynamics, allowing to suggest models of the pathway system in crystal structures. It allows to avoid time-consuming simulations, however, the method can lack reliability because of its dependence on crystal structure features and a set of empirical parameters.

We undertake a critical review of the results obtained with the tiling method for the low-temperature modification of  $\text{KAlO}_2$ . Using first-principles simulations, we calculate the potential barriers of the ionic migration between voids in the structure of  $\text{KAlO}_2$  with local framework distortions and compare the results with those of the tiling method.

The calculations were carried out with the VASP package using a plane-wave basis set in conjunction with projector augmented wave pseudopotentials [2]. We use the Perdew–Burke–Ernzerhof functional [3], a cut-off energy of 400 eV, and a  $\Gamma$ -centered Monkhorst-Pack grid of 10x6x4 k-points to obtain fully converged structures and free energies.

$\text{KAlO}_2$  has a diamond-type framework so that the voids are connected with each other by channels of simple shape. We analyze the pathways along the three unit cell vectors by using density functional theory. We find that the tiling method not taking into account framework distortions suffers from low accuracy, as reflected by wrong potential barriers. A significant drop in the potential barriers (up to 40%) is noticed as a result of the framework relaxation, accompanied by a widening of the channel bottlenecks, which is favorable for ion migration.

The potential barriers of the shortest symmetry-inequivalent (elementary) channels are found to determine the pathway characteristics. It would be beneficial for the criteria proposed in ref. [1] for determining the ability of the elementary channels to conduct ions to include estimates of the potential barriers (activation energy). We demonstrate that knowledge of the potential barriers associated with all the elementary channels enables an estimation of the potential barrier for diffusion through a channel of any complexity and length.

**Keywords:** *fast-ion, potential, barrier, tiling, polarization*

[1] BLATOV, V. A., ILYUSHIN, G. D., BLATOVA, O. A., ANUROVA, N. A., IVANOV-SCHITS, A. K. & DEM'YANETS, L. N. 2006. Analysis of migration paths in fast-ion conductors with Voronoi–Dirichlet partition. *Acta Crystallogr. B*, 62, 1010–1018.

[2] KRESSE, G. & JOUBERT, D. 1999. From ultrasoft pseudopotentials to the projector augmented-wave method. *Phys. Rev. B*, 59, 1758–1775.

[3] PERDEW, J. P., BURKE, K. & ERNZERHOF, M. 1996. *Phys. Rev. Lett.*, 77, 3865–3868.

## **Novel renewable energy converter concept for solar and hydrogen hybridization.**

E. Ollier<sup>1</sup>

<sup>1</sup>Institute for New Energy Technologies and Nanomaterials LITEN - French Alternative Energies and Atomic Energy Commission CEA, 17 rue des martyrs, 38054 Grenoble Cedex 9, France

[Emmanuel.ollier@cea.fr](mailto:Emmanuel.ollier@cea.fr) / Phone: +33 7 87 04 65 61

The context of this work is the need for new solutions to overcome the problem of intermittency linked to most renewable energies, especially solar. Both photovoltaic and solar thermal technologies (concentrated or not) are facing this challenge which prevents them from delivering a controlled power output able to follow the demand (dispatchability). The current trend to overcome this intermittency issue is to implement an energy storage which can be based on batteries for photovoltaics or molten salts for concentrated solar power [1]. In both cases, it provides the ability to deliver electrical power without sun, but the complexity of systems is increased and the flexibility is still limited. Thermal technologies offer the possibility of hybridization by producing heat with solar energy and also with different types of fuels. This approach is investigated within Hybrid Concentrated Solar Power technologies [2]. This type of approach is promising but is still based on the combination of two conventional technologies and is also limited in terms of operational temperature and efficiency.

The objective of this work is to propose and describe a new concept of energy converter able to realize the hybridization of two types of renewable energies to obtain an annual capacity factor of almost 100%, thanks to a high solar concentration and micro/mesocombustion of hydrogen or biogas. A high temperature range of 600°C to more than 1300°C is targeted to benefit from a high Carnot limit, far higher than current technologies operating below 550°C.

This work presents the design of hybrid converters able to operate in the two main modes consisting in solar concentration and internal combustion, and also in the hybrid mode.

The size of these novel converters is within a few centimeters in order to concentrate the heat and achieve very high temperatures. They are designed to be used with the same strategy as concentrated photovoltaics with high solar concentration and solar tracking, the difference being that they will operate with the conversion of solar or chemical energies into heat, followed by a thermal to electrical conversion. The latter one can be achieved by thermoelectrical conversion [3] or thermophotovoltaic (TPV) conversion [4] [5], both of them having higher efficiencies at high temperatures.

Multiphysical modelling is used to investigate solar absorption in the converter as well as internal heat source by catalytic combustion. The work explores the converter temperatures, uniformities, thermal fluxes in three modes: solar, combustion, hybrid. An in depth analysis is provided on the following points: designs able to operate in both modes, reduction of thermal losses, improvement of temperature uniformity which is important for the thermal / electrical conversion efficiency. This analysis is presented for different input powers coming both from solar concentration and internal combustion. A particular focus is done on the impact of the solar receiving surface and its selective solar radiation absorption properties [6].

Finally this work presents the prospects for the realization of these novel converters called HRC for Hybrid Renewable Converters and also for their integration in a full system. Used with a TPV solar cell, this converter concept introduces the possibility of Hybrid TPV called HTPV which will provide much more flexibility than recent solar or conventional TPV technologies.

The advancement over previous work is mostly related to the proposal of a small device able to hybridize two types of energies corresponding to renewables. Another major change with respect to the state of the art is the small size of the hybrid converter allowing high heat concentration. The proposed designs allow achieving very high temperatures from 600°C to more than 1300°C, far higher than the current operational temperatures in the Concentrated Solar Power systems. This new concept and technology provides a very efficient hybridization pathway with the possibility to create installations at different scales.

Presenting author: [Emmanuel.ollier@cea.fr](mailto:Emmanuel.ollier@cea.fr); CEA-LITEN; France

Preferred Mode of presentation: Oral

Topic: Symposia 4: Advances in Energy Storage and Conversion Devices  
(Computational modeling and simulation for energy storage and conversion devices)

**Keywords:** *Hybridization, solar, hydrogen, high temperature materials, energy conversion.*

[1] FERNÁNDEZ, A.G., USHAK, S., GALLEGUILLOS, H., PÉREZ, F.J.. Development of new molten salts with LiNO<sub>3</sub> and Ca(NO<sub>3</sub>)<sub>2</sub> for energy storage in CSP plants. *Applied Energy* 119 (2014) 131–140.

[2] SAN MIGUEL, G., CORONA, B.. Hybridizing concentrated solar power (CSP) with biogas and biomethane as an alternative to natural gas: Analysis of environmental performance using LCA. *Renewable Energy* 66 (2014) 580-587.

[3] KARNI J.. Solar energy: The thermoelectric alternative. *Nature Materials* 10, 481–482 (2011) doi:10.1038/nmat3057.

[4] LENERT, A., BIERMAN, D.M., NAM, Y., CHAN, W.R., CELANOVIC', I., SOLJAC'IC', M., WANG E.N.. A nanophotonic solar thermophotovoltaic device. *Nature Nanotechnology*, Vol 9, February 2014 126

[5] DATAS, A., ALGORA, C.. Development and experimental evaluation of a complete solar thermophotovoltaic system. *Prog. Photovolt: Res. Appl.* 2013; 21:1025–1039

[6] OLLIER, E., DUNOYER, N., DELLEA, O., SZAMBOLICS, H.. Nanostructured refractory thin films for solar applications. SPIE Optics + Photonics symposium 17 - 21 August 2014, San Diego.

## Atomic Layer Deposition for On-Chip Supercapacitors

Grigoras, K., Keskinen, J., Grönberg, L., Ahopelto, J., Prunnila, M.

VTT Technical Research Centre of Finland

[kestutis.grigoras@vtt.fi](mailto:kestutis.grigoras@vtt.fi) VTT Technical Research Centre of Finland, P.O.Box 1000, FI-02044 VTT, Finland)

Further success in development and miniaturization of remote, wearable and implantable electronic equipment is greatly related to advances in energy sources. Besides batteries, the supercapacitors are gaining reasonable attention as temporary energy storage in microdevices, especially when high power densities are needed [1]. Unfortunately, standard, active carbon material based supercapacitors are difficult to integrate into silicon chip due their fabrication process. Silicon based supercapacitor electrode would be a great advantage, and porous silicon (PS) with a large surface area looks as a best candidate here. Main obstacle in PS application as electrode material is a large chemical reactivity of this material [2, 3]. Therefore, the coating layer with efficient passivation and conductivity improvement characteristics is needed.

Here we present the on-chip supercapacitor with porous silicon electrodes coated by atomic layer deposition (ALD). Devices with TiN coated PS show almost ideal cyclic voltammetry characteristics and good stability during long operation. Successful device realization inside a single silicon chip is important for further integration steps.

**Keywords:** *supercapacitor, porous silicon, atomic layer deposition, integration*

[1] SIMON, P. & GOGOTSI, Y. 2008. Materials for electrochemical capacitors. *Nature Materials*, 7, 845-854.

[2] DESPLOBAIN. S., GAUTIER. G., SEMAL. J., VENTURA L. & ROY. M. 2007. Investigations on porous silicon as electrode material in electrochemical capacitors. *Phys. Stat. Sol. C*, 4, 2180-2184.

[3] OAKES. L., WESTOVER. A., MARES. J., CHATTERJEE. S., ERWIN. W., BARDHAN. R., WEISS. S. & PINT. C. 2013. Surface engineered porous silicon for stable, high performance electrochemical supercapacitors. *Sci. Rep.*, 3, 3020.



## High energy density asymmetric supercapacitor based on nano-architected NiAl layered double hydroxides/functional carbon nanotube composites

Yan Wang\*, Hai Li, Jijun Zhang, Xinyu Yan, Peili Li, Huifang Lv, Sheng Zhou, Zexiang Chen

School of Opto-electronic Information, University of Electronic Science and Technology of China,

No. 4, Section 2, Jianshe North Road, 610054 Chengdu, People's Republic of China

e-mail address: wangyan127@uestc.edu.cn

**Abstract:** To improve the energy density of supercapacitors, widely investigation have been focusing on developing active pseudocapacitive materials, including transition metal oxides ( $\text{RuO}_2$ ,  $\text{NiCo}_2\text{O}_4$ ) and hydroxides ( $\text{Ni}(\text{OH})_2$ ,  $\text{Co}(\text{OH})_2$ ), and conducting redox polymers etc. Among the pseudocapacitive materials,  $\text{MnO}_2$  and layered double hydroxides (LDH) have demonstrated their superior electrochemical performance due to high power performance and long cycle life. We constructed a positive electrode composite material in which a hierarchical nano-architected NiAl layered double hydroxide nano-flakes grown on functionalized carbon nanotube bundles (NiAl-LDH/CNT) by a hydrothermal process. The electrochemical performance of the composite showed a high specific capacitance of more than 900 F/g at the current density of 4 A/g. An asymmetric supercapacitor based on the prepared NiAl-LDH/CNT composite as the positive electrode and an activated carbon as negative electrode achieved an very high energy density up to 150 Wh/kg with a cell voltage of 1.75 V, presenting much higher than that of traditional electrochemical double-layer capacitors (EDLCs). The rational design, interesting structure and the ideal electrochemical performance of this CNT-based composite suggest its potential applications in high energy storage systems.

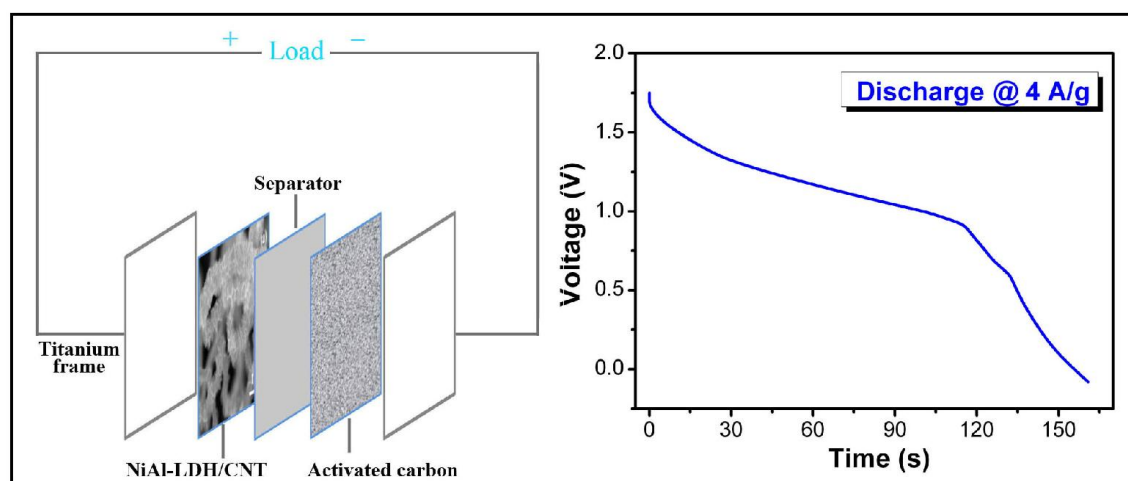


**Figure 1.** Schematic illustration of the asymmetric supercapacitor device based on NiAl-LDH/CNT composite as the positive electrode and activated carbon as the negative electrode.

**Keywords:** supercapacitors, layered double hydroxides, carbon nanotube, composite, electrochemical performance

# Synthesis and electrochemical properties of three-dimensional graphene / polyaniline composites for supercapacitor electrode materials\*

Zhao Wen, He Da-Wei<sup>†</sup>, Wang Yong-Sheng,

Du Xiang, and Xin Hao

*Key Laboratory of Luminescence and Optical Information, Ministry of Education,  
Institute of Optoelectronic Technology, Beijing Jiaotong University, Beijing 100044,  
PR China*

To improve the specific capacitance and rate capability of electrode materials for supercapacitors, three-dimensional graphene/polyaniline (3DGN/PANI) composites were prepared via *in situ* polymerization on GN hydrogel. The PANI content in the composite was controlled by the concentration of reaction monomer, and was grown on the surface of GN surface as a thin film. The specific capacitance of 3DGN/PANI composite containing 10 wt% PANI reached  $322.8 \text{ F g}^{-1}$  at a current density of  $1 \text{ A g}^{-1}$ , nearly twice as large as that of the pure 3DGN ( $162.8 \text{ F g}^{-1}$ ). The capacitance of the composite was  $307.9 \text{ F g}^{-1}$  at  $30 \text{ A g}^{-1}$  (maintained 95.4%), and 89% retention after 500 cycles. This study demonstrates the exciting potential of 3DGN/PANI with high capacitance, excellent rate capability and long cycling life for supercapacitors.

**Keywords:** graphene/polyaniline composites, electrochemical property, three-dimensional graphene

## Development of doped La-substituted SrTiO<sub>3</sub>-based anode materials for solid oxide fuel cells

Jianhui Li<sup>1,2</sup>, Xinwen Zhou<sup>1</sup>, Ning Yan<sup>1</sup> and Jingli Luo<sup>1</sup>

<sup>1</sup> Department of Chemical and Materials Engineering, University of Alberta, Edmonton, Alberta, Canada, T6G 2V4

<sup>2</sup> National Engineering Laboratory for Green Chemical Productions of Alcohols-Ethers-Esters, College of Chemistry and Chemical Engineering, Xiamen University, Xiamen, China, 361005

*E Mail/ Contact Détails :* [jingli.luo@ualberta.ca](mailto:jingli.luo@ualberta.ca) (J.-L. Luo), Tel.: +1-780-492-2232.

The solid oxide fuel cell (SOFC) using sour gas as the feed, rather than traditional H<sub>2</sub>, has drawn increasing attentions in recent years. However, problems remain to be solved before sour gas can be directly used as the fuel in SOFC. For example, trace amount of H<sub>2</sub>S in the feed may cause serious poisoning on the traditional anode catalysts. So far, much effort has been dedicated to developing doping perovskite structure (ABO<sub>3</sub>) materials that can function effectively in the environment under reducing condition and exhibit better resistance against sulfur poisoning. La-substituted SrTiO<sub>3</sub> (LST) based perovskite anodes have been widely investigated because of their adequate electronic conductivity in reducing atmospheres, excellent dimensional and chemical stability upon redox cycling as well as their outstanding sulfur and coking tolerances. However, their ionic conductivity and the electrocatalytic activity need to be improved. In this work, the phase structures, catalytic activities and electrochemical behaviors of Ce-doped LaSrBaTiO<sub>3-δ</sub> (LCSBT) and Co-doped LaSrTiO<sub>3-δ</sub> (LSCT) as the anode catalysts for SOFC were investigated. The doped Ce in LCSBT synthesized by a modified rheological phase reaction (RPR) method could be separated to form nano-CeO<sub>2</sub> after sintering. The catalytic performance of LCSBT was improved in comparison with the pure LaSrBaTiO<sub>3-δ</sub> (LSBT) and LSBT&CeO<sub>2</sub> admixture anodes. The nanostructures of LCSBT and the exsolved nano-CeO<sub>2</sub> might play key roles in contributing to the improvement. The perovskite structure of the Co-doped LST (LSCT) had excellent phase purity and refined particle size. The Co nano-particles with diameter less than 10 nm can be *in-situ* exsolution on the anode surface. These *in-situ* formed Co nano-clusters can increase the catalytic activation in fuel oxidation. The maximum power density of LSCT-based cell was about 300 mW cm<sup>-2</sup> and no obvious degradation and sulfur deposition were detected

during galvanostatic test for 48 h in 5000 ppm H<sub>2</sub>S-H<sub>2</sub> at 900 °C. The experimental results have proven that LSCT is a promising candidate anode material for SOFCs using H<sub>2</sub>S-contaminated fuels. The mechanism of H<sub>2</sub>S-induced enhancement effect for electrochemical reactions on the LSCT-based anode materials is also explored. The challenges related to the future developments of LSCT-based anode materials for SOFCs are also discussed.

***Keywords: Solid oxide fuel cells; Co-doped LST; Perovskite; in-situ exsolution***

## Characterization of PEMFC catalytic layers based on carbon xerogels

F.Deschamps<sup>1</sup>, N.Job<sup>1</sup>

<sup>1</sup> University of Liège, B6a, B-4000 Liège, Belgium,

*fabien.deschamps@ulg.ac.be*

Proton exchange membrane fuel cells (PEMFC) are promising candidates for applications in mobile devices and transportations. The fuel cell market is growing [1]; however, for successful large-scale commercialization, significant cost reduction and durability improvement are needed. An optimization of the electrode [2] structure is required to fulfill these goals.

Catalytic layers are generally prepared by mixing a protonic conductor ionomer, such as Nafion®, with a platinum catalyst supported on carbon black [3]. Nanostructured carbons allow for a better control of the textural properties, such as pore size and pore volume. More precisely, using carbon xerogels as support is a good way to improve the mass transport in catalytic layers [4,5].

In this communication, we present the elaboration and the characterization of catalytic layers based on carbon xerogels. For that purpose, carbon xerogels were synthesized by polymerization of resorcinol and formaldehyde in aqueous solution to form an organic gel. The latter was dried and pyrolysed under inert atmosphere to obtain a porous carbon. By modifying the pH of the initial solution, several carbon xerogels with different pore sizes were synthesized. The milling of these porous carbons in a planetary mill is required to get particle sizes compatible with the thickness of the catalytic layers for fuel cell (~10 µm). After deposition of platinum nanoparticles on carbon xerogels by controlled impregnation method [6], catalytic layers based on these carbons were made.

These catalytic layers were characterized by profilometry on their whole surface to evaluate their homogeneity and their thickness. Then, measurements of electrical and ionic resistances were performed to estimate their influences in fuel cell performances. Finally, characterization of these catalytic layers was performed in fuel cell to evaluate their performances in function of the carbon xerogel pore texture.

***Keywords: Nanostructured carbon, Catalytic layer, Fuel Cells.***

- [1] HORWITZ J., FORD S., Developments in PEM Fuel Cells, 2010, Pira International.
- [2] GASTEIGER H.A., KOCHA S.S., SOMPALLI B., Wagner F.T., 2005, Appl. Catal, 56, 9-35.
- [3] SHARMA S., POLLET B.G., 2012, J. Power Sources, 208, 96-119.
- [4] JOB N., MARIE J., LAMBERT S., et al, 2008, Energ. Convers. Manage, 49, 2461-2470.
- [5] J. MARIE, R. CHENITZ, M. CHATENET, et al, 2009, J. Power Sources, 190, 423-434.
- [6] ZUBIAUR A., CHATENET M., MAILLARD F., et al, 2014, Fuel Cells, 14, 343-349.

## Further Understanding of Nitrogen-Doped Carbon Catalytic Property Towards Oxygen Reduction Reaction (ORR)

Belabbes Merzougui<sup>1</sup>; Saheed Bukola<sup>2</sup>, and Rachid Zaffou<sup>1</sup>

<sup>1</sup>Qatar Environment and Energy Research Institute, Qatar Foundation, Doha, Qatar

<sup>2</sup>Center of Nanotechnology, King Fahd University of Petroleum and Minerals, Dhahran, SA

*E-Mail: bmerzougui@qf.org.qa*

Recently, a great attention has been shifted towards low-cost non-precious metal (NPM) catalysts based on nitrogen modified carbon as potential alternatives to Pt due to their remarkable ORR activities[1]. Many reports have shown that nitrogen precursors, as primary hosts of active sites, play a crucial role in ORR properties when pyrolyzed on carbon matrix at high temperature. Different nitrogen functionalities such as, pyridinic, pyrrolic, and graphitic based sites are generally produced. However, the structure-performance correlation analysis reveals that the graphitic nitrogen function plays a pivotal role in ORR activity. In this presentation, we will demonstrate two catalysts, prepared via pyrolysis of polyaniline and vinazene on carbon, which are rich in graphitic and pyrrolic nitrogen, respectively. ORR activity and potential cycling study confirms that not only the graphitic nitrogen is responsible for high ORR, but also other nitrogen functions, including the pyrrolic one. More details on the subject will be presented.

***Keywords: Nitrogen doped carbon, oxygen reduction reaction, ORR,***

[1] WU, G., MORE, K. L., JOHNSTON, C. M., ZELENAY, P., High-Performance Electrocatalysts for Oxygen Reduction Derived from Polyaniline, Iron, and Cobalt. 2011. *Science*, 332 (6028), 443-447.

## Oxygen Reduction on Hafnium/Hafnium Carbide Nanoparticles

Olga A. Baturina, Albert Epshteyn and Andrew P. Purdy

Chemistry Division, Naval Research Laboratory, 4555 Overlook Ave. SW,  
Washington DC, 20375

[olga.baturina@nrl.navy.mil](mailto:olga.baturina@nrl.navy.mil); [andrew.purdy@nrl.navy.mil](mailto:andrew.purdy@nrl.navy.mil)

Non-precious metal nanoparticles are attractive candidates for oxygen electrocatalytic reduction in electrochemical energy conversion devices, such as fuel cells and batteries. Here we report for the first time electrocatalytic activity of hafnium/hafnium carbide nanoparticles towards the oxygen reduction reaction (ORR). While activity of hafnium oxynitride nanoparticles towards the ORR in acid has previously been reported [1] a little was known about the ability of Hf/HfC nanoparticles to reduce molecular oxygen. Here we demonstrate that molecular oxygen can be reduced on Hf/HfC nanoparticles both in acidic and alkaline environment. However, the reaction mechanism changes from 4 - to 2 - electron pathway, when switching from acidic to alkaline environment. Although the ORR in base occurs through the two-electron pathway, this reaction has a potential for a practical application because Hf/HfC catalyst demonstrates an activity toward the disproportionation of hydrogen peroxide to O<sub>2</sub> and H<sub>2</sub>O. Onset potential for the ORR in 0.1 M KOH for non-optimized catalyst (-0.10 V vs Ag/AgCl) is superior to that of the best reported to date MnO<sub>2</sub> catalyst (-0.13 V vs Ag/AgCl). In acid, moderate catalytic activity towards the ORR is observed. The results suggests that Hf nanomaterials can be considered as a promising candidate for replacing noble metal catalysts in alkaline air electrodes.

**Keywords:** *Hafnium, Nanoparticles, Oxygen Reduction Reaction, Electrochemical Energy Conversion*

[1] CHISAKA, M. & MURAMOTO, H. 2014. Suppression and Evaluation of Hydrogen Peroxide Formation on Carbon-Supported Hafnium Oxynitride. ECS Electrochemistry Letters, 3, F1-F4.



## **Effect of Fillers on the Electrical and Sealing Properties of Alkali/Alkaline-Earth Borosilicate Glass Composite Sealants**

Da-Young Ryu, Yun-Kang Ham, Sung Park and Jae Chun Lee

Dept. of Materials Science and Engineering, Myongji University, Yongin 449-728, Korea

*jcl@mju.ac.kr*

Development of a reliable sealant or sealing system remains one of the top priorities in planar SOFC technology. Recently, a compliant glass seal such as an alkali silicate glass was proposed for SOFCs. In contrast to the conventional glass–ceramic sealant which develops a rigid or semi-rigid microstructure after sealing, the compliant glass shows so called “self-healing” behavior and will remain vitreous without substantial crystallization after sealing and during operation at elevated temperatures. The objective of this study was to investigate the effect of filler in sealant composition on the high temperature viscosities, electrical conductivities and sealing properties of glass composite sealants for solid oxide fuel cells (SOFCs). Alkali/alkaline-earth borosilicate glass-based sealants, both with and without fillers such as Al<sub>2</sub>O<sub>3</sub> and 8YSZ, were heat treated at various temperatures for periods of up to 48 h. Upon 48 hour heat treatment the electrical conductivities of a filler-containing glass were always higher than those of a base glass. The electrical conductivity of a sealant containing Al<sub>2</sub>O<sub>3</sub> filler was higher than that containing 8YSZ filler. This was attributed to the partial dissolution of fillers and increasing mobility of the alkali and alkali-earth ions in sealing glass. Crystallization behavior of sealing glass was affected by fillers and significantly controlled the sealing performance of sealants during seal operation.

***Keywords:*** Sealant, glass, electrical conductivity, viscosity, solid oxide fuel cell

[1] COILLOT, D., MEAR, F. O., NONNET, H., MONTAGNE, L. 2012. New viscous sealing glasses for electrochemical cells. *Int. J. Hydrogen Energy*, 37, 9351-9358.

## Mechanism for Hydrogen Storage Properties of $\text{Li}_2\text{Mg}(\text{NH})_2$ Determined by Gas Back Pressure: A First-Principles Calculation Assisted Experimental Investigation

Chu Liang<sup>\*1,2</sup>, Hongge Pan<sup>2</sup>, Yang Xia<sup>1</sup>, Hui Huang<sup>1</sup>, Yongping Gan<sup>1</sup>, Xinyong Tao<sup>1</sup>, Wenkui Zhang<sup>1</sup>

<sup>1</sup> College of Materials Science and Engineering, Zhejiang University of Technology, Hangzhou 310014, People's Republic of China

<sup>2</sup> Department of Materials Science and Engineering, Zhejiang University, Hangzhou 310027, People's Republic of China

*E Mail* : [cliang@zjut.edu.cn](mailto:cliang@zjut.edu.cn);

Hydrogen storage technology is the major obstacle in implementing the coming hydrogen economy. Solid-state storage offers evidently potential advantages, such as high storage density, low energy consumption and high safety, over current storage technologies of compressed and liquefied hydrogen. Ternary imide  $\text{Li}_2\text{Mg}(\text{NH})_2$  is considered to be one of the most promising on-board hydrogen storage materials in view of its high reversible capacity, favorable thermodynamics and good cycling stability for hydrogenation/dehydrogenation. However, the high kinetic barrier resulted in the dehydrogenation temperatures of the  $\text{Mg}(\text{NH}_2)_2\text{-2LiH}$  mixture much higher than the thermodynamically predicted equilibrium temperature of  $\sim 90$  °C under 1.0 bar hydrogen.

In this work, the  $\text{Li}_2\text{Mg}(\text{NH})_2$  with the primitive cubic and orthorhombic structure was obtained by dynamically dehydrogenating a  $\text{Mg}(\text{NH}_2)_2\text{-2LiH}$  mixture up to 280 °C under different gas atmospheres. The orthorhombic  $\text{Li}_2\text{Mg}(\text{NH})_2$  was converted to a primitive cubic structure as the dehydrogenation temperature was increased to 400 °C or performed by a 36 h of ball milling. Moreover, the primitive cubic phase can be converted to an orthorhombic phase after heating at 280 °C under 9.0 bar  $\text{H}_2$  for 1 h. The crystal structure of  $\text{Li}_2\text{Mg}(\text{NH})_2$  was found to depend on the gas back pressure in the dehydrogenation process. Experimental investigations combined with first-principles calculations showed that the crystal structures of  $\text{Li}_2\text{Mg}(\text{NH})_2$  and dehydrogenation/rehydrogenation properties of the  $\text{Mg}(\text{NH}_2)_2\text{-2LiH}$  system strongly depended on the gas back pressure in

the dehydrogenation process due to the effect of the gas back pressure on hydrogen storage kinetics. This study provides a new approach for improving the hydrogen storage properties of the amide–hydride systems.

***Keywords:*** ternary imide, crystal structure, hydrogen storage properties, thermodynamics, kinetics

## **Polybenzimidazole based composite membranes for high temperature proton exchange membrane fuel cells**

Mun-Sik Shin, Moon-Sung Kang, Jin-Soo Park

Department of Environmental Engineering, College of Engineering, Sangmyung  
University

*E-mail : energy@smu.ac.kr*

Phosphoric acid (PA) doped poly[2,2'-(m-phenylene)-5,5'-bibenzimidazole] (PBI) is one of most interesting electrolyte materials for high temperature proton exchange membrane fuel cells (HTPEMFCs) operating without no external humidification at temperatures from 150 to 200 °C. The proton conductivity of PBI membranes highly depend on the acid doping level (ADL) of the membranes. However, the ADL is limited due to the decrease in mechanical strength at high ADL. The study developed PBI based composite membranes using porous substrate to get low resistance thin membranes instead high ADL membranes. Porous poly(imide benzimidazole) (PIBIs) films was prepared by the random copolymers synthesized by condensation polymerization of biphenyl-4,4'-diyl-di(oxo)-4,4'-bis(1,8-naphthalenedicarboxylic anhydride), 2-(4-aminophenyl)-5-aminobenzimidazole and 4,4'-diaminodiphenyl ether. The PBI based composite membranes were prepared by filling electrolytes in the PIBI porous substrate for HTPEMFCs. Several properties of the membranes were investigated in terms of oxidative stability, acid doping level, swelling ratio, ionic conductivity, mechanical strength, crossover etc.

***Keywords: Fuel Cell, polybenzimidazole, composite membrane, porous substrate***

ACKNOWLEDGEMENT. This research is supported by Basic Science Research Program through the National Research Foundation of Korea (NRF) funded by the Ministry of Science, ICT and Future Planning (NRF-2014R1A1A1006067).

## Structure fabrication of stable rGO-wrapped Ni<sub>3</sub>S<sub>2</sub> nanobowls with enhanced electrochemical performance in LIBs

Wei Zhou, Jin-Long Zheng, Yonghai Yue and Lin Guo

School of Chemistry and Environment, Beihang University, Beijing 100191, China

zhouwei@buaa.edu.cn

### Abstract

Some transition metal oxides or sulfides have been studied instead of traditional graphite anodes as their higher lithium activity and theoretical capacity in lithium ion batteries (LIBs) [1]. However, these anode materials suffer from irreversible expanded volume and easily pulverized structures during lithium ions insertion/extraction processes [2]. It's significant to design stable nanostructures and to seek efficient structure buffer for developing high-performance LIBs. In our work, uniform Ni<sub>3</sub>S<sub>2</sub> nanobowls with an average size of 250 nm and shell thickness of ~30 nm wrapped by rGO sheets were firstly synthesized by a simple wet chemical method. The Ni<sub>3</sub>S<sub>2</sub>-rGO hybrid composite with spatial three-dimensional (3D) structure showed enhanced electrochemical properties in lithium-ion batteries, compared with Ni<sub>3</sub>S<sub>2</sub> hollow chains. Its specific capacity could be up to 443 mAh g<sup>-1</sup> at 0.5 C after 500 cycles (theoretical capacity of Ni<sub>3</sub>S<sub>2</sub> is 462 mAh g<sup>-1</sup>), while Ni<sub>3</sub>S<sub>2</sub> hollow chains faded dramatically to 147 mAh g<sup>-1</sup> after 100 cycles. The improved cycle stability of the composite could be ascribed to the bowl structure with both exposed interior and exterior arch surfaces which could stand much more lithiation-delithiation than quasi-1D hollow chains. The novel stable bowl-like structure, the wrapped flexible rGO sheets served as buffers for the expansion of Ni<sub>3</sub>S<sub>2</sub> bowls [3], the attachment sites provided by bowls keeping rGO from aggregation, and the improved electron transfer rate by rGO sheets, all synergetic effects made the composite a superior anode material. The relationship between persistence of nanostructure and long-term

cycle stability was disclosed, giving suggestion on designing optimal structures for electrode materials with superior electrochemical performance [4].

#### References:

- [1] a) Q. M. Su, J. Xie, J. Zhang, Y. J. Zhong, G. H. Du, B. S. Xu, *ACS Appl. Mater. Interfaces* 6 (2014) 3016-3022; b) S. M. Xu, C. M. Hessel, H. Ren, R. B. Yu, Q. Jin, M. Yang, H. J. Zhao, D. Wang, *Energy Environ. Sci.* 7 (2014) 632-637; c) Y. Wang, L. Zhou, X. W. Lou, *Adv. Mater.* 24 (2012) 1903-1911.
- [2] a) J. F. Liang, Z. Cai, Y. Tian, L. D. Li, J. X. Geng, L. Guo, *ACS Appl. Mater. Interfaces* 5 (2013) 12148-12155; b) G. X. Zhao, T. Wen, J. Zhang, J. X. Li, H. L. Dong, X. K. Wang, Y. G. Guo, W. P. Hu, *J. Mater. Chem. A* 2 (2014) 944-948; c) B. Wu, H. H. Song, J. S. Zhou, X. H. Chen, *Chem. Commun.* 47 (2011) 8653-8655.
- [3] a) Y. C. Yang, X. B. Ji, F. Lu, Q. Y. Chen, C. E. Banks, *Phys. Chem. Chem. Phys.* 15 (2013) 15098-15105; b) S. K. Park, A. H. Jin, S. H. Yu, J. H. Ha, B. C. Jang, S. Y. Bong, S. H. Woo, Y. E. Sung, Y. Z. Piao, *Electrochim. Acta* 120 (2014) 452-459.
- [4] W. Zhou, J. L. Zheng, Y. H. Yue, L. Guo, *Nano Energy*, in revision.

## Abstract

Self-organized anodic titania ( $\text{TiO}_2$ ) nanotube arrays are an interesting model anode material for use in Li-ion batteries due to their excellent rate capability, cycling stability and enhanced safety compared to graphite. A composite material where carbothermally treated conductive  $\text{TiO}_2$  nanotubes are used as support for a thin silicon film has been shown to have the additional advantage of high lithium storage capacity. We present a detailed comparison of the structure, surface and bulk morphology of self-organised conductive  $\text{TiO}_2$  nanotube arrays, with and without silicon coating, using a combination of X-ray diffraction (XRD), X-ray reflectivity (XRR), grazing incidence small-angle X-ray scattering (GISAXS) and time-of-flight grazing incidence small-angle neutron scattering (TOF- GISANS) techniques. XRD shows that the nanotubes crystallise in the anatase structure with a preferred (004) orientation. GISAXS and TOF-GISANS are used to study the morphology of the nanotube arrays delivering values for the inner nanotube radius and intertubular distances with high statistical relevance due to the large probed volume. They reveal the distinct signatures of a prominent lateral correlation of the  $\text{TiO}_2$  nanotubes of  $\sim 94$  nm and a nanotube radius of  $\sim 46$  nm. The porosity averaged over the entire film using TOF-GISANS is 23%. The nanotube radius is reduced to half ( $\sim 23$  nm) through the silicon coating, but the prominent lateral structure is preserved. Such in-depth morphological investigations over large sample volumes are useful towards development of more efficient battery electrode morphologies.

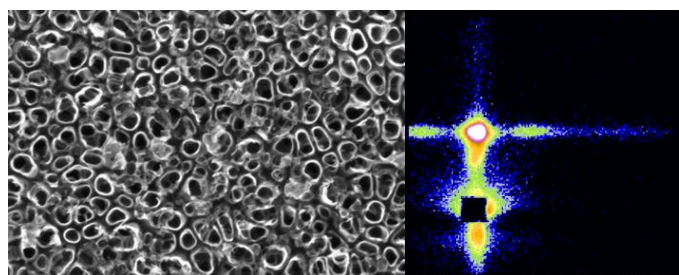


Figure: A ‘real space’ SEM image (left) and a ‘reciprocal space’ GISANS image (right) of the nanorod array.

## Vanadium Pentoxide-based Composite Synthesized Using Microwave Water Plasma for Cathode Material in Rechargeable Magnesium Batteries

Masashi (Inamoto)<sup>1,2</sup>, Hideki (Kuriahra)<sup>2</sup>, Tatsuhiko (Yajima)<sup>1</sup>

<sup>1</sup>Department of Applied Chemistry, Graduate of Engineering, Saitama Institute of Technology, 1690, Fusaiji, Fukaya-shi, Saitama 369-0293, Japan.

<sup>2</sup>Saitama Industrial Technology Center, 3-12-18, Kamiaoki, Kawaguchi-shi, Saitama 333-0844, Japan.

*E Mail/ inamoto-m@saitec.pref.saitama.jp*

Multivalent cation rechargeable batteries are expected to perform well as high-capacity storage devices. Rechargeable magnesium batteries have an advantage in terms of resource utilization and safety. Here, we report on sulfur-doped vanadium pentoxide (S-V<sub>2</sub>O<sub>5</sub>) as a potential material for the cathodes of such a battery; S-V<sub>2</sub>O<sub>5</sub> showed a specific capacity of 300 mAh g<sup>-1</sup>. S-V<sub>2</sub>O<sub>5</sub> was prepared by a method using a low-temperature plasma generated by carbon felt and a 2.45 GHz microwave generator. It is assumed that the water in the raw materials is distributed uniformly enough that the composite is treated uniformly. Furthermore, although the process was performed under reduced pressure and at the evaporating temperature of water, the process did not induce reduction of V<sub>2</sub>O<sub>5</sub> and oxidation of sulfur.

This study investigates the ability of S-V<sub>2</sub>O<sub>5</sub> to achieve high capacity when added to metal oxide. The highest recorded capacity (420 mAh g<sup>-1</sup>) was reached with MnO<sub>2</sub> added to composite SMn-V<sub>2</sub>O<sub>5</sub>, which has a higher proportion of included sulfur than found in S-V<sub>2</sub>O<sub>5</sub>. Results from transmission electron microscopy, energy-dispersive X-ray spectroscopy, Micro-Raman spectroscopy, and X-ray photoelectron spectroscopy show that the bulk of the SMn-V<sub>2</sub>O<sub>5</sub> was the orthorhombic V<sub>2</sub>O<sub>5</sub> structure; the surface was a xerogel-like V<sub>2</sub>O<sub>5</sub> and a solid solution of MnO<sub>2</sub> and sulfur.

**Keywords:** *microwave, rechargeable magnesium battery, vanadium pentoxide, Sulfur-doped*



# A new kind of lithium ion battery with enhanced electrochemical performances

ZHANG Weixin\*, MA Guo, LU Jianbo, YANG Zeheng

(School of Chemistry and Chemical Engineering, Hefei University of Technology, Hefei, 230009, Anhui, China;  
Anhui Key Laboratory of Controllable Chemical Reaction & Material Chemical Engineering, Hefei, 230009, Anhui, China)

\* E-mail: wxzhang@hfut.edu.cn

**Abstract:** To meet the demand in electric vehicles and energy storage applications, it is necessary for next generation lithium-ion batteries to have high energy density and fast charge and discharge capability. This manuscript demonstrates the preparation of transition metal oxide micro/nanostructured arrays on metal substrates as anode and high energy hierarchical cathode materials towards fabricating new lithium-ion batteries with enhanced electrochemical performances. On one hand, a bulk aqueous solution-based process and a microemulsion-mediated process have been developed respectively to control the kinetic and thermodynamic processes for the transition metal oxide micro/nanostructured arrays grown on metal substrates as anode directly. On the other hand, a series of hierarchical cathode materials, including spinel  $\text{LiNi}_{0.5}\text{Mn}_{1.5}\text{O}_4$ , layered  $\text{LiNi}_{1/3}\text{Co}_{1/3}\text{Mn}_{1/3}\text{O}_2$ , and lithium-rich layered  $0.5\text{Li}_2\text{MnO}_3 \cdot 0.5\text{LiNi}_{1/3}\text{Mn}_{1/3}\text{Co}_{1/3}\text{O}_2$ , have been successfully prepared by a controllable stepwise co-precipitation method. This match design for the full cells not only takes advantages of the high specific capacity, high rate capability, good safety and other features related with the anode and cathode materials, but also simplifies the assembly procedures of full cells.

**Key words:** lithium-ion battery; fabrication; transition metal oxide; micro/nanostructured arrays; hierarchical cathode materials

## References:

- [1] Zhang Yingmeng, Zhang Weixin, Li Mei, *et al.* Cosurfactant-mediated microemulsion to free-standing hierarchical CuO arrays on copper substrates as anodes for lithium-ion batteries, *Journal of Materials Chemistry A*, 2013, 1(45): 14368-14374.
- [2] Zhang Weixin, Ma Guo, Gu Heyun, *et al.* A new lithium-ion battery: CuO nanorod array anode versus spinel  $\text{LiNi}_{0.5}\text{Mn}_{1.5}\text{O}_4$  cathode, *Journal of Power Sources*, 2015, 273: 561-565.
- [3] Yang Zeheng, Lu Jianbo, Bian Doucheng, *et al.* Stepwise co-precipitation to synthesize  $\text{LiNi}_{1/3}\text{Co}_{1/3}\text{Mn}_{1/3}\text{O}_2$  one-dimensional hierarchical structure for lithium ion batteries, *Journal of Power Sources*, 2014, 272: 144-151.
- [4] Zhang Weixin, Li Mei, Wang Qiang, *et al.* Hierarchical self-assembly of microscale cog-like superstructures for enhanced performance in lithium-ion batteries, *Advanced Functional Materials*, 2011, 21(18): 3516-3523.
- [5] Zhang Weixin, Yang Shihe, In-situ fabrication of inorganic nanowire arrays grown from and aligned on metal substrates, *Accounts of Chemical Research*, 2009, 42(10): 1617-1627.

## **Design and fabrication of hierarchically porous electrode materials using biological templates for lithium ion batteries**

Yang Xia<sup>1,\*</sup>, Xinyong Tao<sup>1</sup>, Hui Huang<sup>1</sup>, Yongping Gan<sup>1</sup> and Wenkui Zhang<sup>1</sup>

<sup>1</sup>College of Materials Science and Engineering, Zhejiang University of Technology, Hangzhou, 310014, P.R. China.

*E Mail/Contact Détails: nanoshine@zjut.edu.cn (Y. Xia)*

Hierarchically porous micro/nanostructures with high surface area and permeability have attracted tremendous attention. Particularly, the synthesis and structural tailoring of diverse hierarchically porous materials is regarded as a crucial step toward the realization of high-performance electrode materials, which has several advantages including a large contact area with electrolyte, a superior structural stability, and a short transport path for  $\text{Li}^+$  ions. Meanwhile, owing to the inexpensive, abundant, environmentally benign, and renewable biological resources provided by nature, great efforts have been devoted to understand and practice the biotemplating technology, which has been considered as an effective strategy to achieve morphology-controllable materials with structural specialty, complexity, and related unique properties. In this paper, we design and practice the unique hierarchically porous micro/nanostructures derived from several biological templates for  $\text{LiFePO}_4$ ,  $\text{NiO}$ ,  $\text{MnO}$  and  $\text{S}$  electrode materials with high electrochemical performance for lithium ion batteries. We believe that this green, sustainable and economical strategy will trigger more studies for exploring other functional materials in various structure-dependent applications such as catalysis, gas sensing and energy storage.

***Keywords: biological templates, hierarchically porous structure, electrode, lithium ion batteries***

## Electrospinning and its application as electrode and separator in lithium-ion batteries

Jun Seo Park<sup>\*1</sup>, Ok Hee Chung<sup>2</sup>

<sup>1</sup> Department of Chemical Engineering, Hankyong National University, Korea.

<sup>2</sup> Department of Physics, Sunchon National University, Korea.

We introduce an anode material in LIBs, silicon nanoparticles and carbon nanotubes loaded carbon nanofibers (SCNFs), fabricated by the single electrospinning. The one dimension structure of electrospun nanofibers provides porosity for the material. Carbon nanotubes (CNTs) in the electrospun fibers reduce volume expansion of silicon nanoparticles (SiNPs) and improve mechanical stability of the electrode. Both CNTs and carbon nanofibers enhance electronic conduction by connecting SiNPs each other in SCNFs for electrode reactions. These contribute to increase electrochemical performances of SCNF anode-based lithium ion batteries (LIBs) resulting in the enhancement of capacity and cycling ability. Electrospun silicon nanoparticle-carbon nanotube core/carbon shell nanofibers (SCNFs) were fabricated for using as an anode material in LIBs. The precursor of the SCNFs was coaxially electrospun using a blend of SiNPs, CNTs, and polyvinylpyrrolidone (PVP) in the core and polyacrylonitrile (PAN) in the shell. After carbonization at 1000 °C for 1 h in nitrogen, the SCNFs were formed with SiNP-CNT composite core wrapped by carbon shell. The core/shell structure of the SCNFs with different amounts of CNTs in the core, were confirmed by scanning electron microscopy, transmission electron microscopy, and water contact angle. The electrochemical performances of the SCNF anode-based LIBs were evaluated. The results indicated that the SCNF electrode with 1 wt% of CNTs had an initial delithiation capacity as high as 1500 mAh/g at C/10 rate and a retained capability of 50% at high rate (10C).

Thermally stable polyimide (PI) composites non-woven mats were fabricated firstly by electrospinning a mixture of pre-polymer, poly(amic acid) ammoniumsalt (PAAS), and inorganic nanoparticles of SiO<sub>2</sub> and Al<sub>2</sub>O<sub>3</sub> and subsequently imidizing the electrospun nanofibers of PAAS composites at 350 °C for using of the separator of LIBs. The microstructures of PI electrospun nanofiber mats, PI/SiO<sub>2</sub> composite electrospun nanofibers, PI/Al<sub>2</sub>O<sub>3</sub> composite electrospun nanofibers, and commercial separator, SV718, were examined by using a FE-SEM. Test results of thermal properties of PI, PI composites and SV718, conducted by Thermal Gravimetric Analyzer (TGA) and a Differential Scanning Calorimeter (DSC), show superior thermal stability of PI and PI composites, which show no melting peak and no decomposition to 600 °C, while SV718 has melting peak at 137 °C and decompose at 300 °C. Porosity and liquid electrolyte uptake of PI composites showed over 90 % and 790 %, respectively, while porosity and liquid electrolyte uptake of SV718 are 40 % and 101 %, respectively, implying separators of the PI/SiO<sub>2</sub> composite and the PI/Al<sub>2</sub>O<sub>3</sub> composite have lower interfacial resistance than commercial SV718 separator. The electrochemical performance of PI composite separator assembled between LiCoO<sub>2</sub> and Li metal electrodes of the LIBs exhibits more stable cycle performance, higher discharge capacity and better capacity retention compared with those using SV718 separator.

## Real Time Electron Microscopy Studies on Electrode Materials for Lithium Ion Batteries

Sooyeon Hwang<sup>1</sup>, Jinsik Kim<sup>2</sup>, Seung Min Kim<sup>3</sup>, Seong-Min Bak<sup>4</sup>, Se Young Kim<sup>1</sup>, Young Sun Shin<sup>1</sup>, Kyung Yoon Chung<sup>1</sup>, Kyo Seon Hwang<sup>2</sup>, Eric A. Stach<sup>5</sup>, Wonyoung Chang<sup>1</sup>

<sup>1</sup>Center for Energy Convergence, Korea Institute of Science and Technology, Seoul 136-791, Republic of Korea.

<sup>2</sup>Center for Bio Microsystems, Brain Science Institute, Korea Institute of Science and Technology. Seoul 136-791, Republic of Korea.

<sup>3</sup>Carbon Convergence Materials Research Center, Korea Institute of Science and Technology, Wanju-gun 565-905, Republic of Korea.

<sup>4</sup>Chemistry Department, Brookhaven National Laboratory, Upton, New York 11973, United States.

<sup>5</sup>Center for Functional Nanomaterials, Brookhaven National Laboratory, Upton, New York 11973, United States.

*E Mail/ [cwy@kist.re.kr](mailto:cwy@kist.re.kr) (corresponding author), [sooyeon.hw@kist.re.kr](mailto:sooyeon.hw@kist.re.kr) (presenting author)*

The development of novel electrode materials for the next generation of lithium-ion batteries highly requires thorough understanding of structural changes during charge-discharge cycling, aging, and thermal decomposition. In situ analysis using TEM can provide information on local structure as well as chemical information during the electrochemical reactions and thermal-phase transitions in *real time* at high spatial resolution. The goals of this study are to identify and characterize processes that limit lithium-ion battery performance, and ultimately to describe the specific mechanisms that cause performance degradation as well as thermal decomposition. At first, we take advantage of real time electron microscopy to directly investigate the process of thermal decomposition as it occurs at the surface of Ni-based cathode materials that have been charged to different state of charge (SOC). In addition, huge volume expansion of Si anode materials is examined in *real time* during electrochemical reactions using liquid flow holder (from *Hummingbird Scientific*), which enables the direct imaging of electrodes, interfaces, and surfaces under electrochemical exposure through a liquid electrolyte and within TEM. All the details will be available at the meeting.

**Keywords:** *in-situ, transmission electron microscope, lithium ion batteries, electrode materials*

## Micro- and nanostructured Silicon anodes for Li-battery application

T. Defforge<sup>1</sup>, E. Luais<sup>1,2</sup>, J. Santos-Peña<sup>2</sup>, J. Sakai<sup>1</sup>, A. Brugère<sup>2</sup>, F. Ghamouss<sup>2</sup>, F. Tran-Van<sup>2</sup>, D. Lemordant<sup>2</sup>, G. Gautier<sup>1</sup>

<sup>1</sup>Université François Rabelais de Tours, CNRS, CEA, INSA-CVL, GREMAN UMR  
7347, 16 rue P. et M. Curie, 37071 Tours cedex 2, France

<sup>2</sup>Université François Rabelais de Tours, PCM2E (EA 6299), Parc de Grandmont, 37200  
Tours, France

*thomas.defforge@univ-tours.fr*

Silicon is presented as an attractive material for lithium-ion batteries (Li-B) mainly due to its high theoretical capacity (4200 mA.h/g). However, mechanical stress induced by lithium alloying/de-alloying during silicon anode test cycling strongly limits the electrode lifetime. Silicon nanostructures and porous silicon have demonstrated better volume change accommodation during battery cycling and thus enhanced performance stability [1]. In this work, various silicon micro- and nanostructures have thus been studied as Li-B anodes. These structures were obtained by two cost-efficient techniques: wet chemical or electrochemical etching of monocrystalline Si. Macroporous and mesoporous layers obtained by silicon electrochemical etching were peeled off from the silicon substrate to be used as Li-B anodes. Macroporous layers showed interesting cycling stability (600 mA.h/g during 200 cycles @ 1.8A/g). High aspect ratio (> 50) nano-ribbons were also experimented. These 2D structures exhibited interesting behavior as well (high stability up to 50 cycles). Finally, metal-assisted chemical etching technique enabled the growth of high aspect ratio silicon nanowires (1D). Their performances as Li-B anode were then compared with 2D nano-ribbon anodes.

**Keywords:** *porous silicon, silicon nanowires, silicon nano-ribbons, Li-ion batteries*

[1] GE, M., FANG, X., RONG, J., & ZHOU, C. 2013. Review of porous silicon preparation and its application for lithium-ion battery anodes. *Nanotechnology*, 24, 422001.

## Synthesis of Large Surface Area Al<sub>2</sub>O<sub>3</sub> Nanomaterials for Applications to Batteries and Fuel Cells

Vic Liu<sup>1</sup>, Anusorn Kongkanand<sup>2</sup>, Qiangfeng Xiao<sup>1</sup>, Li Yang<sup>1</sup>, and Mei Cai<sup>1</sup>

<sup>1</sup>Chemical and Materials Systems Laboratory, General Motors Global R&D Center, Warren, MI 48090, USA

<sup>2</sup>General Motors Powertrain Engineering, Pontiac, MI 48340, USA

Conference abstract: International Conference on Advances in Functional Materials 2015, Stony Brook University, Long Island NY, USA, from June 29<sup>th</sup>, 2015 to July 3<sup>rd</sup>, 2015.

### Abstract (150 words maximum)

This presentation covers a new simple approach to synthesize Al<sub>2</sub>O<sub>3</sub> nanomaterials and their applications to lithium-sulfur (Li-S) batteries and polymer electrolyte membrane (PEM) fuel cells. The morphology and yield (the amount of product) of the Al<sub>2</sub>O<sub>3</sub> nanomaterials were studied by varying Al precursors, pH levels, temperatures, and types of heterogeneous nucleation sites during hydrothermal synthesis. Flower-like Al<sub>2</sub>O<sub>3</sub> hierarchical nanostructures were successfully synthesized with a very large surface area (~240 m<sup>2</sup>/g) which is 50% to 100% higher than commercially available Al<sub>2</sub>O<sub>3</sub>. The “petals” (nanorods) of the flower-like Al<sub>2</sub>O<sub>3</sub> were decorated with three-dimensional pores (pore size ranging from 1 nm to 5 nm). Such synthesized Al<sub>2</sub>O<sub>3</sub> was tested as functional additives in Li-S batteries and PEM fuel cells. It has been demonstrated that the Al<sub>2</sub>O<sub>3</sub> nanomaterials shown in this presentation have the potential to improve the performance and life of Li-S batteries and PEM fuel cells.

## New Transition Metal Oxyfluorides with HTB network as rechargeable Li-ion battery at high voltage (average > 3V vs Li<sup>+</sup>/Li)

**Demourgues A**, Duttine. M, Chennabasappa. M, Dambournet. M, Durand. E, Penin. N

CNRS, Univ. Bordeaux, ICMCB, UPR9048, F-33600 Pessac, France

[demourg@icmcb-bordeaux.cnrs.fr](mailto:demourg@icmcb-bordeaux.cnrs.fr)

The Fe-based oxyfluorides with HTB (Hexagonal Tungsten Bronze) networks as positive electrode material in lithium battery have been investigated and exhibit outstanding Li intercalation properties depending on the composition and especially the O/F ratio. Various anionic species F<sup>-</sup>/OH<sup>-</sup>/O<sup>2-</sup> have been stabilized into the Fe-based HTB network, prepared by hydrothermal route followed by annealing under Ar below T=350°C. Powder X-Ray Diffraction, Partial Distribution Function (PDF) as well as Mossbauer spectroscopy for the local environment of Fe<sup>3+</sup> and IR and UV-Vis spectroscopies investigations versus temperature, allow solving the complex structural features. For the first time, the stabilization of anionic vacancies into the HTB network has been proposed [1]. Oxygen ions and anionic vacancies seem to play a key role for the performances of the electrode material, as a very poor electrochemical activity (in the 2-4.5V voltage range) was obtained for the pure Fe trifluoride FeF<sub>3</sub> with HTB network. Ti-based oxyfluorides with HTB network have been also obtained by solvothermal routes and the structure as well as the reactivity properties have been investigated.

**Keywords:** Fe, fluoride, Li-ion battery, structure, anionic vacancies

[1] Duttine. M, Dambournet. D, Penin. N, Carrier. D, Bourgeois. L, Wattiaux. A, Chapman. K. W, Chupas. P. J, Groult. H, Durand. E, Demourgues. A. **Tailoring the composition of a mixed anion iron based fluoride compound: Evidence for anionic vacancy and electrochemical performance in lithium cells.** Chem. Mater, 25(14) (2014) 4190-4199

## Monodisperse MPd (M: Co, Ni, Cu) Alloy Nanoparticles Supported on Reduced Graphene Oxide as Cathode Catalysts in the Lithium-Air Battery

*Önder Metin<sup>1,\*</sup>, Tansel Şener<sup>2</sup>, Melike Sevim<sup>1</sup> Emine Kayhan<sup>2</sup>*

<sup>1</sup>Department of Chemistry, Faculty of Science, Ataturk University, Erzurum, TR-25240, Turkey

<sup>2</sup>TUBITAK, Marmara Research Center, Energy Institute, TR-41470 Gebze, Kocaeli, Turkey

Addressed herein is the electrocatalyst performance of the monodisperse MPd (M: Co, Ni, Cu) alloy nanoparticles (NPs) supported on reduced graphene oxide (rGO) in the non-aqueous Li-air battery. MPd alloy NPs were prepared by using the well-established surfactant-assisted organic solution phase protocol comprising the co-reduction of palladium(II) acetylacetonate and M(acetate)<sub>2</sub> or M(acetylacetonate)<sub>2</sub> by borane-based mild reducing agents in oleylamine as surfactant. The as-synthesized Co<sub>3</sub>Pd<sub>7</sub>, Ni<sub>3</sub>Pd<sub>7</sub> and CuPd NPs have the monodisperse particle distribution with the mean particle size of 3.5, 3.4 and 3.1 nm, respectively. The MPd NPs were supported on rGO before their use as cathode catalysts in the non-aqueous Li-air cell. The charge-discharge curves of Li-air electrodes using rGO-CuPd, rGO-Co<sub>3</sub>Pd<sub>7</sub> and rGO-Ni<sub>3</sub>Pd<sub>7</sub> catalysts were investigated at a current rate of 100 mA/gtotal. The specific discharge capacities were found as 4407 mA•h.g<sup>-1</sup> for rGO-CuPd, 3158 for rGO-Co<sub>3</sub>Pd<sub>7</sub> and 2512 mA•h.g<sup>-1</sup> for rGO-Ni<sub>3</sub>Pd<sub>7</sub>, respectively. Ex-situ FTIR analyses convincingly show that Li<sub>2</sub>O<sub>2</sub> is the main component of the discharge products. The lifetime of the cathode electrodes during the first 10 cycles was found to be 130 h for rGO-CuPd, 100 h for rGO-Co<sub>3</sub>Pd<sub>7</sub> and 180 h for rGO-Ni<sub>3</sub>Pd<sub>7</sub> catalyst. The Ni<sub>3</sub>Pd<sub>7</sub> has the highest total capacity of 8175 mA•h.g<sup>-1</sup> over the first 10 cycles.

**Keywords:** Palladium; alloy nanoparticles; reduced graphene oxide; electrocatalyst; Lithium-air battery.



## Hybrid structure of cobalt monoxide nanorods and reduced graphene oxide nanosheets as anode materials for lithium-ion batteries

Hui Huang\*, Wenjun Zhu, Yang Xia, Wenkui Zhang

College of Materials Science and Engineering, Zhejiang University of Technology,  
Hangzhou 310014, China

E Mail: [hhui@zjut.edu.cn](mailto:hhui@zjut.edu.cn)

Graphene-based hybrid nanostructures offer many opportunities for improved lithium storage performance. Herein, we report a facile synthesis of mesoporous CoO nanorods (CoO NRs) on reduced graphene oxide (rGO) substrate by hydrothermal and calcination treatment. Transmission electron microscopy (TEM) investigation reveals that CoO NRs with a size of 20–60 nm are tightly anchored on the surface of rGO sheets. Compared to pure CoO NRs, the CoO NRs/rGO composite shows higher lithium storage capacity and superior rate capability as anode materials for Li-ion batteries. The CoO NRs/rGO composite delivers an initial discharge capacity of 1452 mAh g<sup>-1</sup>, and it can still remain 960 mAh g<sup>-1</sup> after 50 cycles at 0.1 A g<sup>-1</sup>. After each 10 cycles at 0.1, 0.2, 0.5, and 1 A g<sup>-1</sup>, the specific capacities of the composite are about 1096, 1049, 934 and 513 mAh g<sup>-1</sup>, respectively. The enhanced electrochemical performance of the composite can be ascribed to its unique structure, such as 1D mesoporous morphology of CoO NRs and its tightly-contacting with rGO nanosheets, which could shorten the transport pathway for both electrons and ions, enhance the electrical conductivity and accommodate the volume expansion during prolonged cycling.

**Keywords:** *Cobalt monoxide, graphene, hydrothermal, mesoporous nanorods, lithium-ion batteries*

## **A facile fabrication of red phosphorus/ amorphous TiO<sub>2</sub> composites for lithium ion batteries**

Wenkui Zhang<sup>1,\*</sup>, Han Xiao<sup>1</sup>, Yang Xia<sup>1</sup>, Yongping Gan<sup>1</sup>, Hui Huang<sup>1</sup>, Chu Liang<sup>1</sup>

<sup>1</sup>College of Materials Science and Engineering, Zhejiang University of Technology, Hangzhou, 310014, P.R. China.

*E Mail/Contact Détails: msechem@zjut.edu.cn (W.K. Zhang)*

Red phosphorus (RP) is an attractive anode material with an ultrahigh specific capacity of 2596 mAh g<sup>-1</sup>. However, its rapid capacity decay attribute to the volume expansion during the lithiation process presents a noteworthy technical challenge. Meanwhile, titanium oxide (TiO<sub>2</sub>) is a good candidate for lithium ion batteries owing to its high safety and outstanding stability, but it is restricted by the low capacity of 167 mAh g<sup>-1</sup> at room temperature. Inspired by reinforced concrete structure, we fabricate RP built-in amorphous TiO<sub>2</sub> (A-TiO<sub>2</sub>) composite in consideration of achieving complementary effects. Herein, A-TiO<sub>2</sub> could act as “concrete” to prevent RP from escaping the electrode. While RP plays the role of “steel”, which could improve the electrochemical capacity of composite. As a result, RP/A-TiO<sub>2</sub> composite demonstrates an enhanced cycling capacity of 369 mAh g<sup>-1</sup> over 100 cycles as well as an acceptable rate capacity of 202 mAh g<sup>-1</sup> at the current density of 1 A g<sup>-1</sup>. This designed unique reinforced concrete structure may provide a novel strategy to fabricate high electrochemical performance anodic materials for advanced lithium ion batteries.

**Keywords:** *red phosphorus, titanium oxide, anode, lithium ion batteries*

## **High electrochemical Li-storage performance of ultrafine $\text{Mn}_3\text{O}_4$ nanocrystal grown on reduced graphene oxide**

Yongping Gan\*, Liyuan Zhang, Hui Huang, Chu Liang, Xinyong Tao

College of Materials Science and Engineering, Zhejiang University of Technology,  
Hangzhou 310014, China

*E Mail:* [ganyp@zjut.edu.cn](mailto:ganyp@zjut.edu.cn)

Graphene-based hybrid nanostructures offer many opportunities for improved lithium storage performance. Herein, we report a novel synthesis of  $\text{Mn}_3\text{O}_4$ /reduced graphene oxide ( $\text{Mn}_3\text{O}_4/\text{r-GO}$ ) composite based on microexplosion mechanism. It is found that many ultrafine  $\text{Mn}_3\text{O}_4$  particles with a size of about 20 nm are well dispersed on the surface of r-GO sheets. Compared to pure  $\text{Mn}_3\text{O}_4$ , the  $\text{Mn}_3\text{O}_4/\text{r-GO}$  composite delivers higher lithium storage capacity and superior rate capability as promising anode materials for Li-ion batteries. The enhanced electrochemical performance of the  $\text{Mn}_3\text{O}_4/\text{r-GO}$  composite can be attributed to the buffering confining and conducting effects of the r-GO sheets, as well as the small and uniform particle size of  $\text{Mn}_3\text{O}_4$ .

***Keywords:***  $\text{Mn}_3\text{O}_4$ , graphene, nanocrystals, electrochemical performance, lithium-ion batteries

## **Fabrication of layer LiMO<sub>2</sub> (M=Mn, Co, Ni) cathodes with extra-high charge-discharge rate for lithium ion battery**

Liping Li\*, Dong Luo and Guangshe Li

Key Lab of Optoelectronic Materials Chemistry and Physics, Fujian Institute of Research on the Structure of Matter, Chinese Academy of Sciences, Fuzhou 350002, P. R. China. E-mail: lipingli@fjirsm.ac.cn

Li-ion batteries, an ultimate rechargeable energy storage, play more and more important roles in modern people's life and activity. Developing energy storage equipments that can work at very high charge-discharge rate is crucial for efficient use of energy at power-hungry laptops, cameras, mobile phones and electric cars. From the perspective of chemistry, high-rate property of Li-ion batteries can only be achieved by significantly improving the kinetics of lithium ions and electrons in electrode. Here, we report on a simple method to resolve kinetics problems of ultrafast charging-discharging Li-ion batteries by fabrication of layered LiMO<sub>2</sub> (M=Mn, Co, Ni) hexagonal sheet exposing with facets {101}. The synthetic procedure of hexagonal sheets is proceeded via a simple PVP-assisted co-precipitation, which is followed by a heat treatment. All hexagonal sheets LiMn<sub>x</sub>Co<sub>y</sub>Ni<sub>z</sub>O<sub>2</sub> were demonstrated to deliver a superior excellent rate capability and outstanding cycle stability at high current density of 3000 mA g<sup>-1</sup> and under a high cutoff voltage of 4.4 V. The discharge capacity for the composition LiMn<sub>0.075</sub>Co<sub>0.775</sub>Ni<sub>0.15</sub>O<sub>2</sub> at an ultrahigh charge-discharge rate of 10000 mA g<sup>-1</sup> is almost as large as that for LiMn<sub>2</sub>O<sub>4</sub> and commercial LiFePO<sub>4</sub> at low rate of 1 C. Analysis shows that such a superior electrochemical performance could be attributed to the following three aspects: (1) the top-bottom surfaces ({101} facets) of hexagonal sheet form an angle of 80.2° with one of the transport direction of Li-ions, which can greatly shorten the transport distance of lithium ions in layered electrode materials and provide an “express way” for lithium ions rocking; (2) hexagonal sheet is beneficial to the transmission of

electrons, which makes the resistance of hexagonal sheet electrode material very low; and (3) introduction of electrochemically inert  $Mn^{4+}$  can significantly enhance the structural stability of  $LiCoO_2$  at 4.4 V, which ensures the hexagonal sheets to have an excellent cycle life when charge-discharge at a high cutoff voltage. The findings reported here will open up a new way to prepare ultrahigh rate capability and cycle stability electrode materials for advanced lithium-ion batteries.

#### Reference

1. Luo Dong, Li Guangshe, Fu Chaochao, Zheng Jing, Fan Jianming, Li Qi, Li Liping, *Adv. Energy Mater.*, 2014, 1400062
2. Qi Li, Guangshe Li, Chaochao Fu, Dong Luo, Jianming Fan, Liping Li, 8. *ACS Appl. Mater. Interfaces*, 2014, 6, 10330–10341
3. Fu Chaochao, Li Guangshe, Luo Dong, Zheng Jing, Li Liping, *J. Mater. Chem. A*, 2014, 2, 1471-1483
4. Luo Dong, Li Guangshe, Guan Xiangfeng, Yu Chuang, Zheng Jing, Zhang Xinhui, Li Liping, *J. Mater. Chem. A*, 2013, 1, 1220-1227
5. Zhang Xinhui, Luo Dong, Li Guangshe, Zheng Jing, Yu Chuang, Guan Xiangfeng, Fu Chaochao, Li Liping, *J. Mater. Chem. A*, 2013, 1, 9721-9729

## Homogeneous and Heterogeneous Approaches to Photochemical Water Splitting: a Fight for the Right Metals

Peter Brüggeller\*, Christof Strabler, Johannes Prock, and Wolfgang Viertl

*Institute of General, Inorganic and Theoretical Chemistry, University of Innsbruck, Innrain 80–82, 6020 Innsbruck, Austria, E-mail address: [Peter.Brueggeller@uibk.ac.at](mailto:Peter.Brueggeller@uibk.ac.at) (P.Brüggeller)*

Only recently, it has been shown that inexpensive metals like Cu and Fe lead to death and rebirth of a photocatalytic hydrogen production system.<sup>1</sup> The lifetime of the overall catalytic system varied from only 5 to 60 h, being a typical problem for the use of 3d-metals.<sup>1</sup> By contrast, it is well-known that 4d metals like Pd remain stable, when they are connected with soft donors like phosphines even under high pressure conditions.<sup>2</sup> Thus, our work group has developed typical dyads based on Pd and Os containing a bridging bis(bidentate) tetraphosphine (Fig. 1, left) and an excellent stability of about 1000 h has been reached. Attempts are under way to replace the expensive Os-chromophore with an earth-abundant Cu-analogue. In this case its stability is enhanced due to the presence of a tetraphosphine, where the formation of a  $\text{CuP}_4$  species is suppressed.<sup>1,3</sup> Fig. 1, right, shows one coordination moiety of this chromophore. The sterically demanding structure leads to a lifetime of the excited state of 13.8  $\mu\text{s}$  and an emission quantum yield of 0.49 at ambient temperature, indicating that the radiationless decay is reduced. First experiments show very good TON numbers for  $\text{H}_2$  production, when combined with  $[\text{Fe}_3(\text{CO})_{12}]$ .

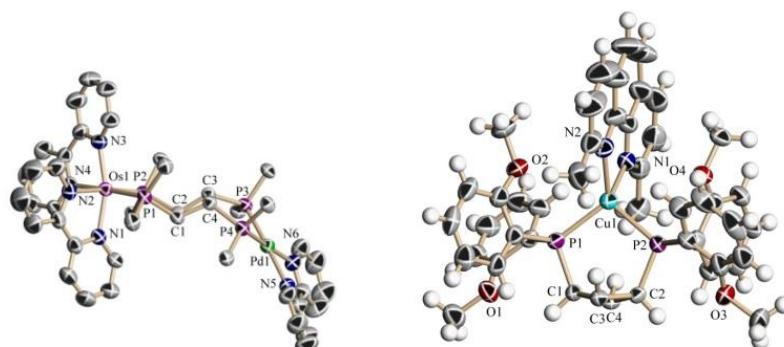


Fig. 1: Crystal structures (simplified views) of a typical dyad (left) and a chromophore (right).

Furthermore, also the 3d metal Co has been tested as water reduction catalyst (WRC). Monophosphines are capable of stabilizing precatalysts of the type  $[\text{Co}(\text{III})\{(\text{DO})(\text{DOH})\text{pn}\}\text{Br}_2]$ ,<sup>4</sup> leading to excellent TON numbers. A whole series of different monophosphines has been investigated, showing that  $\text{Me}_2\text{PhP}$  outperforms  $\text{Ph}_3\text{P}$  for photochemical water splitting. In the case of nanoparticles new 2,0 nm-sized Pd-particles capped with bipyridine have been used, yielding excellent TON numbers above 1000, where this value is related to one Pd-atom. Relating the TON to the active sites produces considerably higher TON values.

<sup>1</sup>S. Fischer, D. Hollmann, S. Tschierlei, M. Karnahl, N. Rockstroh, E. Barsch, P. Schwarzbach, S.-P. Luo, H. Junge, M. Beller, S. Lochbrunner, R. Ludwig, and A. Brückner, *ACS Catalysis* **2014**, *4*, 1845–1849.

<sup>2</sup>W. Oberhauser, G. Manca, A. Ienco, C. Strabler, J. Prock, A. Weninger, R. Gutmann, and P. Brüggeller, *Organometallics* **2014**, *33*, 4067–4075.

<sup>3</sup>C. Bizzarri, C. Strabler, J. Prock, B. Trettenbrein, C.-H. Yang, F. Polo, A. Iordache, P. Brüggeller, and L. De Cola, *Inorg. Chem.* **2014**, *53*, 10944–10951.

<sup>4</sup>P. Zhang, P. A. Jacques, M. Chavarot-Kerlidou, M. Wang, L. Sun, M. Fontecave, and V. Artero, *Inorg.Chem.* **2012**, *51*, 2115–2120.

## **An Earth-Abundant, Double-Metal-Hydroxide-Decorated Core/Shell Array Photoanode for Improved Photoelectrochemical Water Oxidation Efficiency**

Wanhong He<sup>1</sup>, Ye Yang<sup>2</sup>, Xu Xiang<sup>1</sup>

<sup>1</sup> State Key Laboratory of Chemical Resource Engineering, Beijing University of Chemical Technology, Beijing, 100029 China

<sup>2</sup> Chemical and Materials Science Center, National Renewable Energy Laboratory, Golden, Colorado, 80401

**Corresponding author:** [xiangxu@mail.buct.edu.cn](mailto:xiangxu@mail.buct.edu.cn)

The development of earth-abundant, highly-stable semiconductor photoelectrodes is of great importance to high-efficiency and sustainable photoelectrochemical (PEC) water splitting, which achieves solar fuels production in a clean and economic way.<sup>1</sup> To date, the rational fabrication of high-efficiency photoanodes are challenging since the water oxidation (a half reaction of water splitting) is kinetics-sluggish, and it also involves a complex multiple proton-coupled electron transfer (PCET) process. An effective way to expedite the kinetics is to couple efficient electrocatalysts onto the surface of photoanodes. Herein, TiO<sub>2</sub> photoanode was decorated by a simple photochemical modification strategy, for the first time, resulting in an ultrathin-layer-covered core/shell array photoanode. Large cathodic shift of photocurrent onset potential (~220 mV) was achieved for PEC water oxidation. The oxidative efficiency reaches close to 100% over a wide range of potential. The enhanced PEC performances originate from the greatly improved charge separation and suppression of back reactions. The present work supplies a facile and efficient strategy to construct core/shell array semiconductor photoanodes towards improving water oxidation efficiency.

**Keywords:** *Photoelectrochemistry, Photoanode, Water Oxidation, Core/Shell Structure*

[1] MCKONE, J. R., LEWIS, N. S. & GRAY, H. B. 2014. Will Solar-Driven Water-Splitting Devices See the Light of Day? *Chem. Mater.* 26, 407-414.

## Improving photocatalytic performance and visible light respond by integrating two wide-band-gap semiconductors, SnO<sub>2</sub> and Sn<sub>2</sub>Ta<sub>2</sub>O<sub>7</sub>

XiaojingWang, Junyu Liang, Shuwei wang, Chongyan Li

School of Chemistry and Chemical Engineering, Inner Mongolia University, Huhehaote, 010021, P. R. China.

*E Mail : wang\_xiao\_jing@hotmail.com*

It is well documented that NaTaO<sub>3</sub> is superior over other semiconductors such as TiO<sub>2</sub> in photocatalytic oxidation due to its wide band gap and very positive electrochemical potential. Although a larger band gap usually gives rise to a more strong driving force of the photo-redox reaction, while wider band gap would reduce light response range and seriously inhibit solar adsorption. Therefore, enormous efforts have been dedicated to tailoring the electronic structures so as to make the semiconductor sensitive to visible light without loss of the redox ability [1]. A novel heterostructure integrated by two wide-band-gap semiconductors, SnO<sub>2</sub> and Sn<sub>2</sub>Ta<sub>2</sub>O<sub>7</sub>, was successfully prepared in this work. The as-prepared heterostructure exhibits a higher potential edge that yielded an enhanced photo-redox ability. Further, the heterostructure is of Z-type, which effectively separated the photo-generated electron-hole pairs. Although both component semiconductors do not adsorb visible light, the resulted heterostructure was surprisingly observed to show an outstanding photocatalytic performance under visible light illumination(Fig. 2a). That is, methyl orange was completely removed in 20 min, more exceeding commercial photocatalyst N-doped P25. The existence of coupled Sn<sup>2+</sup> and Sn<sup>4+</sup> ions in the heterostructure is responsible for the absence of defeats and the regenerated catalytic activities.

***Keywords: photocatalysis, visible light respond, semiconductor, SnO<sub>2</sub> and Sn<sub>2</sub>Ta<sub>2</sub>O<sub>7</sub>, wide band gap***

[1] A Versatile and Nontoxic Carbon Nanomaterial. ACS Nano, 7, 10552-10562. [1] FUJISHIMA, A., ZHANG, X. T., TRYK, D.A. 2007, Heterogeneous Photocatalysis: From Water Photolysis to Applications in Environmental Cleanup, Int. J. Hydrogen Energ. 32, 2664–2672.



## Iridium Oxide Modified CdSe/CdS/TiO<sub>2</sub> Nanorods for Efficient and Stable Photoelectrochemical Water Splitting

Bo Sun, Tielin Shi, Xianhua Tan, Zhiyong Liu, Youni Wu, Guanglan Liao\*

State Key Laboratory of Digital Manufacturing Equipment and Technology, Huazhong University of Science and Technology, Wuhan 430074, China

*\*corresponding author, tel: +86-27-87793103, fax: +86-27-87793103, e-mail: guanglan.liao@hust.edu.cn*

Sensitizing with CdS and CdSe quantum dots has been regarded as an effective approach to improve the photoactivity of TiO<sub>2</sub> nanorods [1]. However, the use of CdS/CdSe is severely hindered by its terrible photochemical stability caused by hole-induced anodic corrosion [2]. In this paper, we demonstrate the employ of iridium oxide nanoparticles on CdSe/CdS/TiO<sub>2</sub> nanorods for efficient and stable photoelectrochemical water splitting.

The morphology of the iridium oxide modified CdSe/CdS/TiO<sub>2</sub> nanorods is shown in Figure 1a and 1b. TEM image and high resolution TEM image in Figure 1c and 1d directly illustrate the core-shell structure of the nanorods. Nanoparticles with diameter about 2~3 nm at the edge of the shell has an interplanar spacing of 0.225 nm which is correspond to the d-spacing of (200) planes of IrO<sub>2</sub> as shown in the inset. Figure 2 displays the Energy Filter TEM image of an ultimate nanorod and its elemental mappings which further confirm the multiple core-shell structure of the nanorods.

Figure 3a depicts the line sweep voltammograms measured from TiO<sub>2</sub> nanorods, CdSe/CdS/TiO<sub>2</sub> nanorods and IrO<sub>2</sub> modified CdSe/CdS/TiO<sub>2</sub> nanorods. Photocurrent density of the CdSe/CdS/TiO<sub>2</sub> nanorods increases rapidly as applied potential above the onset potential of -1.1 V vs. Ag/AgCl, and saturated at the potential of -0.5 V vs. Ag/AgCl. With the modification of IrO<sub>2</sub> nanoparticles, the onset potential and saturation potential substantially shift to a lower value of -1.45 V and -0.8 V vs. Ag/AgCl, respectively. The negative shift of onset and saturation potential indicates that the charge separation and transportation in the IrO<sub>2</sub> modified CdSe/CdS/TiO<sub>2</sub> nanorods are more efficient than CdSe/CdS/TiO<sub>2</sub> nanorods. Time-dependent measurement reveals that

photocurrent density of CdSe/CdS/TiO<sub>2</sub> nanorods decrease continuously as shown in Figure 3b. In contrast, the ultimate nanorods with IrO<sub>2</sub> modification show a stable photocurrent.

In summary, we have successfully improved the photocatalytic activity and stability of the CdSe/CdS/TiO<sub>2</sub> nanorods via IrO<sub>2</sub> nanoparticles modification. Besides, the onset potential of -1.45 V vs. Ag/AgCl is one of the lowest values achieved by TiO<sub>2</sub>-based photoanode. Moreover, the IrO<sub>2</sub> modification may also be an effective approach in other occasions including solar cells and photocatalysis.

**Keywords:** *Nanorods, quantum dots, iridium oxide, photoelectrochemical water splitting*

- [1] LUO, J., MA, L., HE, T., NG, C., WANG, S., SUN, H., FAN, H. J. 2012. TiO<sub>2</sub>/(CdS, CdSe, CdSeS) Nanorod Heterostructures and Photoelectrochemical Properties. *J. Phys. Chem. C*, 116, 11956–11963.
- [2] CHAKRAPANI, V., BAKER, D., KAMAT, P. V. 2011. Understanding the Role of the Sulfide Redox Couple (S<sup>2-</sup>/Sn<sup>2+</sup>) in Quantum Dot-Sensitized Solar Cells, *J. Am. Chem. Soc.*, 133, 9607–9615.

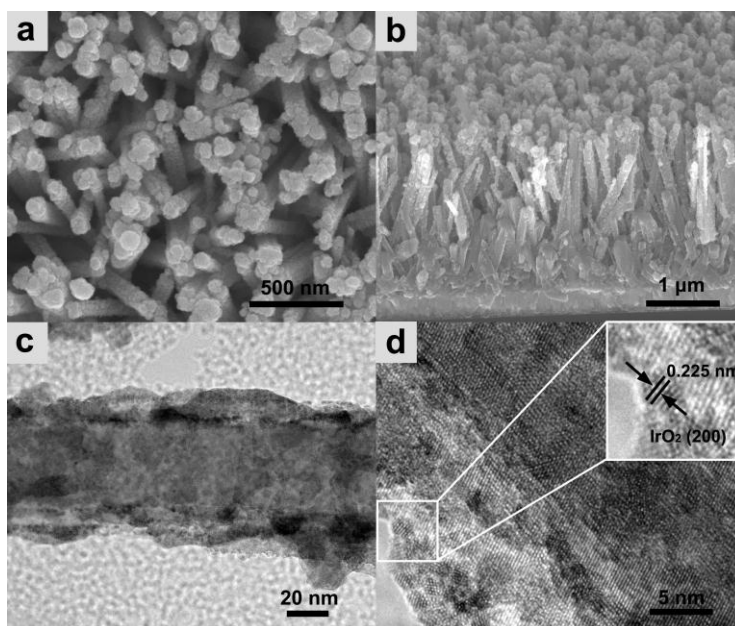


Figure 1. Plane-view (a) and Side-view (b) SEM image of IrO<sub>2</sub> modified CdSe/CdS/TiO<sub>2</sub> nanorods. TEM image (c) and High resolution TEM image (d) of IrO<sub>2</sub> modified CdSe/CdS/TiO<sub>2</sub> nanorods. The inset is a magnified image.

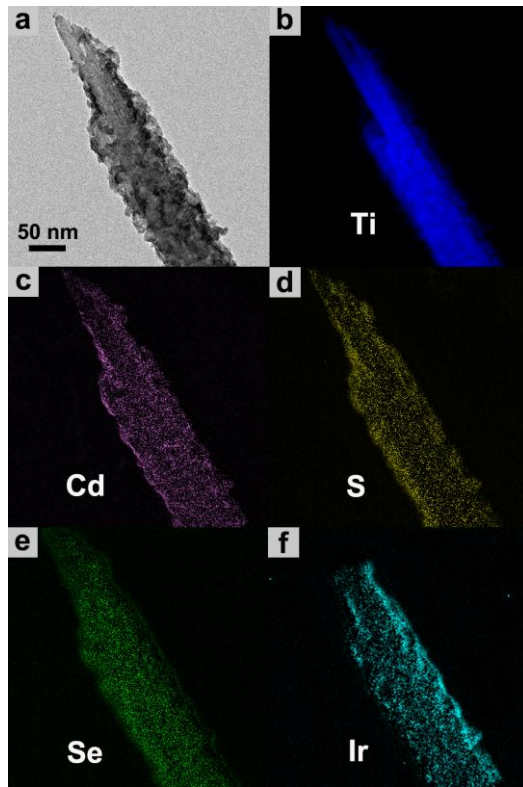


Figure 2. Energy Filter TEM image of  $\text{IrO}_2$  modified  $\text{CdSe/CdS/TiO}_2$  nanorods and its corresponding elemental mappings.

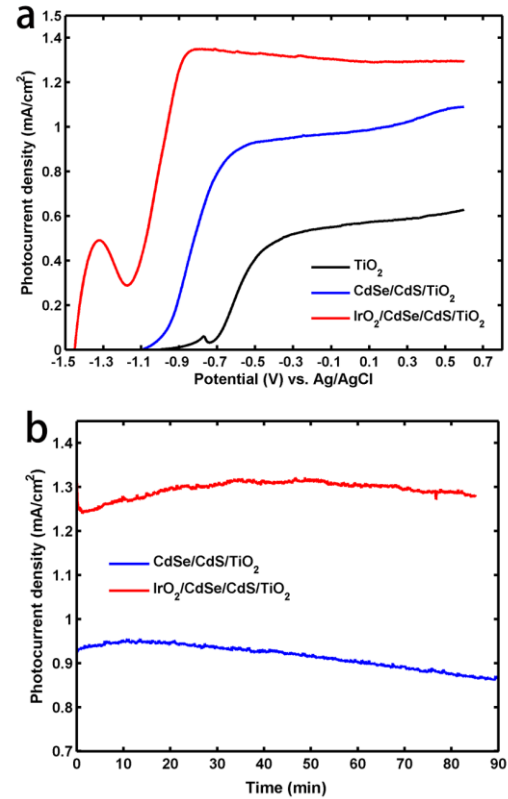


Figure 3. (a) Line sweep voltammograms measured from  $\text{TiO}_2$  nanorods,  $\text{CdSe/CdS/TiO}_2$  nanorods and  $\text{IrO}_2$  modified  $\text{CdSe/CdS/TiO}_2$  nanorods. (b) Time-dependent photocurrent density of  $\text{CdSe/CdS/TiO}_2$  nanorods before and after  $\text{IrO}_2$  modification.

# MAGNETRON SPUTTERING FOR DEPOSITION OF PHOTOCATALYST NANOSTRUCTURES ON TRANSPARENT CONDUCTIVE OXIDES FOR SOLAR APPLICATIONS

A. Kruth<sup>1</sup>, S. Peglow<sup>1</sup>, F. May<sup>1</sup>, S. Müller<sup>1</sup>, M.-M. Pohl<sup>2</sup>, T. Schedel-Niedrig<sup>3</sup>,  
V. Brüser<sup>1</sup>, K-D. Weltmann<sup>1</sup>

<sup>1</sup> Leibniz Institute for Plasma Science and Technology (INP), Greifswald, Germany

<sup>2</sup> Leibniz Institute for Catalysis (LIKAT), Rostock, Germany

<sup>3</sup> Helmholtz Zentrum Berlin, Institute for Solar Fuels, Berlin, Germany

## ABSTRACT

Photocatalysis has attracted an enormous amount of research interest, in especially with regard to applications such as solar hydrogen generation as well as pollutant degradation. Main research target is the development of corrosion-stable core candidate materials that are able to perform under the abundant visible light in the solar spectrum. Two main approaches are being employed, the development of visible light-sensitive semiconductors and sensitisation of wide band-gap semiconductors [1]. In materials synthesis, plasma-enhanced surface modification and layer deposition methods are based on the presence of non-equilibrium states of reactive species in a plasma environment. They are therefore able to overcome limitations of traditional catalyst synthesis methods, giving rise to new reaction pathways and resulting in unique properties of nanomaterials.

This presentation reports on recent work on development of DC magnetron sputtering processes for deposition of TiO<sub>2</sub> and WO<sub>3</sub> semiconductor layers as well as RF magnetron deposition for synthesis of N-doped graphite electrodes on TCO. Electrode properties are characterised by means of XRD, TEM, UV/Vis, XPS, Raman spectroscopy and photoelectrochemical characterisation including IMVS/IMPS and IPCE measurements. Furthermore, plasma-enhanced deposition methods for surface enhancement of photocatalysts layers by nanoparticles and polymer-encapsulation are also discussed.

**Passivated *n-p* Co-doping of Niobium and Nitrogen into Self-organized TiO<sub>2</sub> Nanotube Arrays for Enhanced Visible Light Photocatalytic Performance**

Zhengchao Xu<sup>1</sup>, Weiye Yang<sup>1,\*</sup>, Qi Li<sup>1</sup>, and Jian Ku Shang<sup>1,2</sup>

<sup>1</sup>Environment Functional Materials Division  
Shenyang National Laboratory for Materials Science,  
Institute of Metal Research, Chinese Academy of Sciences, Shenyang, 110016, P. R.  
China

<sup>2</sup>Department of Materials Science and Engineering  
University of Illinois at Urbana-Champaign, Urbana, IL 61801, USA  
Corresponding: Tel.: +86 24 83978837, \*E-mail: [wyyang@imr.ac.cn](mailto:wyyang@imr.ac.cn)

Passivated *n-p* co-doping of niobium and nitrogen was successfully incorporated into self-organized TiO<sub>2</sub> nanotube arrays by anodizing Ti-Nb alloys, followed with the heat treatment in a flow of ammonia gas. Nb was doped into TiO<sub>2</sub> nanotube arrays during the anodization by substituting Ti<sup>4+</sup> with Nb<sup>5+</sup>, while N was doped into TiO<sub>2</sub> nanotube arrays during the heat treatment by substituting O<sup>2-</sup> with N<sup>3-</sup>. Since Nb in TiO<sub>2</sub> enhanced the adsorption of NH<sub>3</sub> molecules onto the nanotube arrays, Nb doping was found to promote the subsequent N doping into the anatase lattice. As predicted by first-principles band structure calculations, Nb/N co-doped titanium oxide nanotube arrays demonstrated a largely enhanced visible light response and visible light photocatalytic performance on the degradation of methylene blue, compared to TiO<sub>2</sub> nanotube arrays or TiO<sub>2</sub> nanotube arrays with either dopant. The passivated *n-p* co-doping approach may also be applied to other material systems and promise a wide range of technical applications.

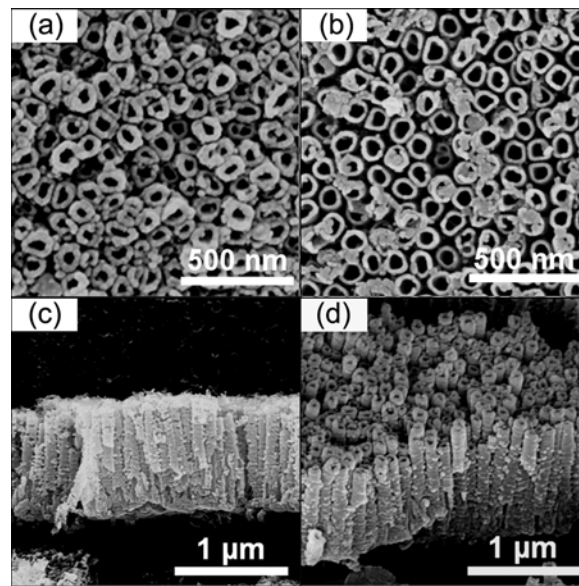


Figure 1: (a) and (b) Top-view FESEM images of TiON and  $\text{Ti}_{0.9}\text{Nb}_{0.1}\text{ON}$  nanotube arrays, respectively. (c) and (d) Cross-sectional view FESEM images of TiON and  $\text{Ti}_{0.9}\text{Nb}_{0.1}\text{ON}$  nanotube arrays, respectively.

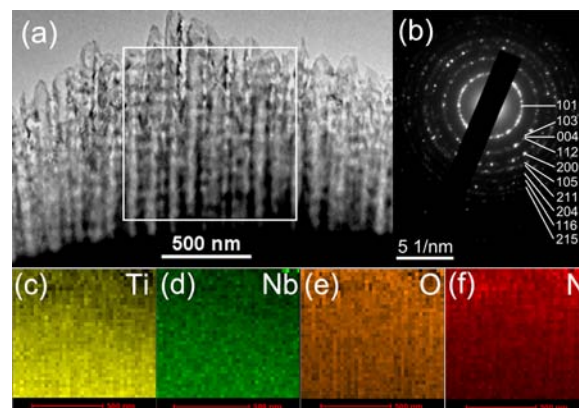


Figure 2: (a) and (b) TEM image and SAED patterns of  $\text{Ti}_{0.9}\text{Nb}_{0.1}\text{ON}$  nanotube arrays, respectively. (c) to (f) The distribution map of Ti, Nb, O, and N elements in  $\text{Ti}_{0.9}\text{Nb}_{0.1}\text{ON}$  nanotube arrays, respectively.

**Preferred contribution: Oral**

## Photoanodic Hybrid Semiconductor–Molecular Heterojunction for Solar Water Oxidation

Khurram Saleem Joya<sup>1,2</sup>, Kazuhiro Takanabe<sup>1</sup>

<sup>1</sup>Division of Physical Sciences and Engineering, KAUST Catalysis Center, King Abdullah University of Science and Technology, Thuwal, 23955-6900, Saudi Arabia.

<sup>2</sup>Leiden Institute of Chemistry, Leiden University, Einsteinweg 55, P.O. Box 9502, 2300 RA, Leiden, The Netherlands.

*E Mail/ [khurram.joya@kaust.edu.sa](mailto:khurram.joya@kaust.edu.sa)*

Inorganic photo-responsive semiconducting materials have been employed in photoelectrochemical (PEC) water oxidation devices in pursuit of solar to fuel conversion.[1] The reaction kinetics in semiconductors is limited by poor contact at the interfaces, and charge transfer is impeded by surface defects and the grain boundaries.[2] It has shown that successful surface functionalization of the photo-responsive semiconducting materials with co-catalysts can maximize the charge separation, hole delivery and its effective consumption, and enhances the efficiency and performance of the PEC based water oxidation assembly.[3] We present here unique modification of photoanodic hematite ( $\alpha\text{-Fe}_2\text{O}_3$ ) and bismuth vanadate ( $\text{BiVO}_4$ ) with molecular co-catalysts for enhanced photoelectrochemical water oxidation (**Figure 1**). These hybrid inorganic–organometallic heterojunctions manifest impressive cathodic shifts in the onset potentials, and the photocurrent densities have been enhanced by > 90% at all potentials relative to uncatalyzed  $\alpha\text{-Fe}_2\text{O}_3$  or  $\text{BiVO}_4$ , and other catalyst-semiconductor based heterojunctions. This is a novel development in the solar to fuel conversion field, and is crucially important for designing a tandem device where light interfere very little with the catalyst layer on top of semiconducting light absorber.

**Keywords:** *Water oxidation, photoelectrochemical, semiconducting materials, heterojunction, solar fuel*

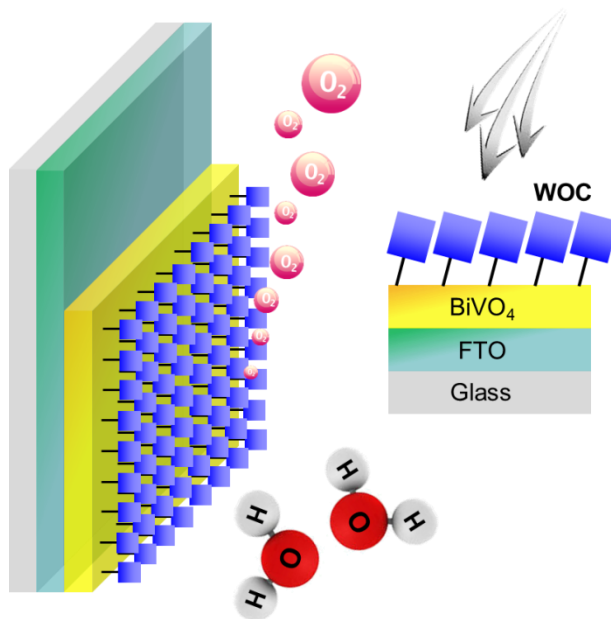


**Figure 1.** Schematic representation of a hybrid molecular-inorganic heterojunction system for photoelectrochemical water oxidation. FTO is fluorine-doped tin-oxide coated glass substrate and WOC is a molecular water oxidation complex.

[1] JOYA, K. S., FAHEEM, Y., OCAKOGLU, K., & KROL, VAN DE R. 2013. Water Splitting Catalysis and Solar Fuel Devices: Artificial Leaf on The Move. *Angew. Chem. Int. Ed.*, 52, 10426–10437.

[2] CHEN, H. M., CHEN, C. K., LIU, R.-S., ZHANG, L., ZHANG, J., & WILKINSON, D. P. 2012, Nano-architecture and material designs for water splitting photoelectrodes. *Chem. Soc. Rev.*, 41, 5654–5671.

[3] MAYER, M. T., LIN, Y., YUAN, G., & WANG, D. 2013. Forming Heterojunctions at the Nanoscale for Improved Photoelectrochemical Water Splitting by Semiconductor Materials: Case Studies on Hematite. *Acc. Chem. Res.*, 46, 1558–1566.



# Photocatalytic Water Splitting for Hydrogen Production with $Y_2FeSbO_7$ and $In_2FeSbO_7$ Photocatalysts under Visible Light Irradiation

Jingfei Luan \* and Yanyan Li

State Key Laboratory of Pollution Control and Resource Reuse, School of the Environment, Nanjing University, Nanjing 210093, China; E-Mail: mg1325050@smail.nju.edu.cn

\* Author to whom correspondence should be addressed; E-Mail: jfluan@nju.edu.cn; Tel.: +86-(0)-13585206718; Fax: +86-(0)-25-83707304.

---

**Abstract:** New photocatalysts  $Y_2FeSbO_7$  and  $In_2FeSbO_7$  were synthesized by the solid state reaction method for the first time. A comparative study about the structural and photocatalytic properties of  $Y_2FeSbO_7$  and  $In_2FeSbO_7$  was reported. The results showed that  $Y_2FeSbO_7$  and  $In_2FeSbO_7$  crystallized with the pyrochlore-type structure, cubic crystal system and space group  $Fd\bar{3}m$ . The lattice parameter  $a$  for  $Y_2FeSbO_7$  or  $In_2FeSbO_7$  was 10.2281 Å or 10.0933 Å. The band gap of  $Y_2FeSbO_7$  or  $In_2FeSbO_7$  was estimated to be 2.129 eV or 1.847 eV. For the photocatalytic water-splitting reaction,  $H_2$  or  $O_2$  evolution was observed from pure water with  $Y_2FeSbO_7$  or  $In_2FeSbO_7$  as catalyst under visible light irradiation (Wavelength > 420 nm). Furthermore,  $H_2$  or  $O_2$  also spilt by using  $Y_2FeSbO_7$  or  $In_2FeSbO_7$  as catalyst from  $CH_3OH/H_2O$  or  $AgNO_3/H_2O$  solutions under visible light irradiation ( $\lambda > 420$  nm).  $In_2FeSbO_7$  showed higher activity compared with  $Y_2FeSbO_7$ . The photocatalytic activities for splitting water into  $H_2$  were further improved under visible light irradiation with  $Y_2FeSbO_7$  or  $In_2FeSbO_7$  being loaded by Pt, NiO or  $RuO_2$ . The effect of Pt was better than that of NiO or  $RuO_2$  for improving the photocatalytic activity of  $Y_2FeSbO_7$  or  $In_2FeSbO_7$ .

## Acknowledgements

This work was supported by a grant from China-Israel Joint Research Program in Water Technology and Renewable Energy (No. 5), by a grant from the Natural Science Foundation of Jiangsu Province (No. BK20141312), by a Project of Science and Technology Development Plan of Suzhou City of China from 2014 (No. ZXG201440).

## Photocurrent Extraction Efficiency Near Unity in a Thick Polymer Bulk Heterojunction

Seo-Jin Ko<sup>1</sup>, Bright Walker<sup>1</sup>, Thanh Luan Nguyen<sup>2</sup>, Hyosung Choi<sup>1,3</sup>, Jason Seifter<sup>3</sup>, Mohammad Afsar Uddin<sup>2</sup>, Seongbum Kim<sup>1</sup>, Taehyo Kim<sup>1</sup>, Gi-Hwan Kim<sup>1</sup>, Shinuk Cho<sup>4</sup>, Alan J. Heeger<sup>3</sup>, Han Young Woo<sup>2</sup>, and Jin Young Kim<sup>1</sup>

<sup>1</sup> School of Energy and Chemical Engineering, Ulsan National Institute of Science and Technology (UNIST), Ulsan 689-798, South Korea.

<sup>2</sup> Department of Cogno-Mechatronics Engineering (WCU), Pusan National University, Miryang 627-706, South Korea.

<sup>3</sup> Center for Polymers and Organic Solids University of California Santa Barbara, Santa Barbara, CA 93106, USA

<sup>4</sup> Department of Physics and Energy Harvest Storage Research Center (EHSRC), University of Ulsan, Ulsan 680-749, South Korea.

*E mail: jykim@unist.ac.kr*

Although most organic solar cell materials produce photocurrents at efficiencies well below theoretical values as films exceed ~100 nm in thickness, we report an dialkoxyphenylene-difluorobenzothiadiazole based conjugated polymer (PPDT2FBT) which closely tracks theoretical photocurrent production while maintaining a high fill factor and producing peak power conversion efficiencies of 9% from remarkably thick films. The unique behavior of thick PPDT2FBT films arises from a combination of physical properties including strong  $\pi$ - $\pi$  stacking, an isotropic morphology and suitable energy band structure. These physical characteristics allow efficient photocurrent extraction while inhibiting the recombination of electrical charges, allowing quantum efficiency near unity from exceptionally thick active layers in both conventional and inverted architectures. The ability of PPDT2FBT to function efficiently in thick cells allows devices to fully attenuate incident sunlight while enabling defect-free films to be processed over large areas, constituting a major advancement towards commercially viable organic solar cells.

***Keywords: conjugated polymer, bulk heterojunction, organic solar cells, quantum efficiency, thick films***

[1] NGUYEN, T. L., CHOI, H., KO, S.-J., UDDIN, M. A., WALKER, B., YUM, S., JEONG, J.-E., YUN, M. H., SHIN, T. J., HWANG, S., KIM, J. Y., & WOO, H. Y. 2014. Semi-crystalline photovoltaic polymers with efficiency exceeding 9% in a ~ 300 nm thick conventional single-cell device. *Energy Environ. Sci.*, 7, 3040-3051.

# Satellite Solar Array with Silicon Laser Downlinks to Denver and the Arctic

Paul Christopher  
Leesburg, VA 20175  
pfchristopher56@gmail.com

**Abstract-** Gerard O'Neill's outstanding satellite solar array concepts are updated from geostationary systems to include sun synchronous low earth orbits and Brandon Molniya orbits. The low earth orbits would offer low cost and Brandon orbits would offer the convenience of stationary ground antennas. Jalali's silicon laser concepts would be useful for ten micron links for low cost and low cloud attenuation.

## 1. Introduction

Gerard K. O'Neill (1) had many important concepts in the mid 1970's, including solar power arrays on geostationary satellites with microwave downlinks to large ground arrays. These were envisioned to supply a sizeable fraction of terrestrial energy needs. Since then, geostationary real estate has come under intense pressure, and low earth orbits and Brandon Molniya elliptic orbits have been examined as geostationary replacements. These Brandon orbits allowed convenient low loss laser links to the northern Temperate Zone. We examine 10 micron satellite laser transmission to northern U.S. and Denver with Jalali's silicon lasers as a potentially important power source. We compare the link performance of the Brandon Molniya orbits with a geostationary satellite.

Fig. 1-1 shows the expected 80<sup>th</sup> percentile attenuation over the Northern Hemisphere for 10 micron laser communication, as derived from Barbaliscia (2) (App A), and the 1999 Ka Conference (3).

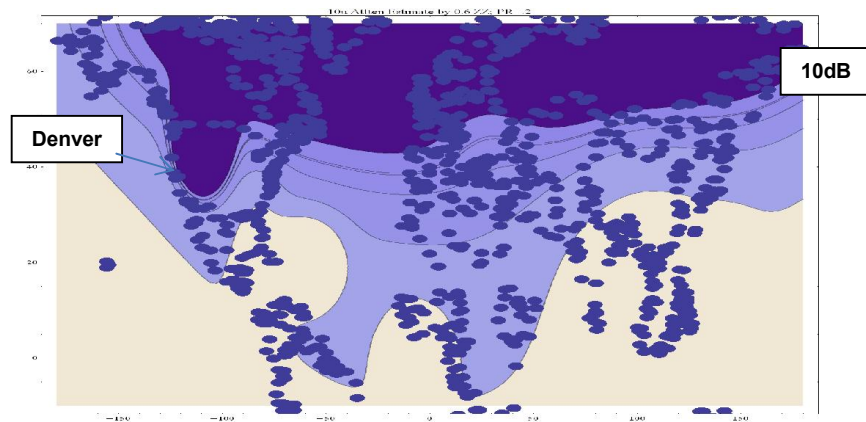


**Fig 1-1 New 10 Micron Attenuation (80%), with Cloud Cover from Barbaliscia (2)**

Mathematica Jan8—lrev2.nb pc.

## *Laser Communication for Nanosatellites*

Low cost nanosatellites are receiving new emphasis for Earth Observation, with the need for restricted costs. We also examine the possibility that high performance optical systems could deliver high downlink power for a small low cost system. Link reliability would suffer, but might be acceptable if large scale

ground site diversity were available. Takayama (4) showed the value of large ground arrays, and Boldyrev's cloud correlation can be used to estimate attenuation for large scale diversity (5).

The Boldyrev cloud correlation function, helpful for laser systems, demands site separation approaching 120 km as in Fig. 1-2. The cloud correlation function actually becomes negative at 200 km, approaching a minimum at 380 km.

The diversity demands for millimeter wave and laser systems appear so diverse, that a compromise on site diversity appears very difficult. The ground site economics for diversity presents its own demands and a resolution for the dilemma may be estimated by good performance with reasonable ground site costs.

We examine millimeter wave satellite systems, and then 10 micron system demands. Ground system economics then suggests reasonable compromises for ground site separation.

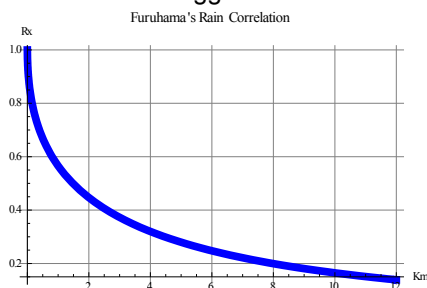


Fig. 1-2a Furuhamas Rain Correlation

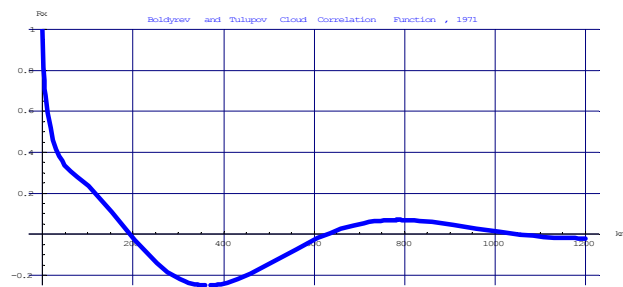


Fig. 1-2b Boldyrev's Cloud Correlation

**Pierce's Bivariate Exponential PDF**

Pierce's bivariate exponential probability density function is helpful in seeing the advantages of two separated ground sites for laser reception. The Pierce pdf may be seen as

$$P(A1,A2)= \frac{p \left[ \frac{A1}{B} + \frac{A2}{r} \right] I_0 \left[ 2 \sqrt{\frac{A1 A2 r}{B^2 \left[ \frac{A1}{B} + \frac{A2}{r} \right]}} \right]}{B^2 \left[ \frac{A1}{B} + \frac{A2}{r} \right]}$$

(1-1)

Where r= correlation coefficient between 2 sites (from Boldyrev)

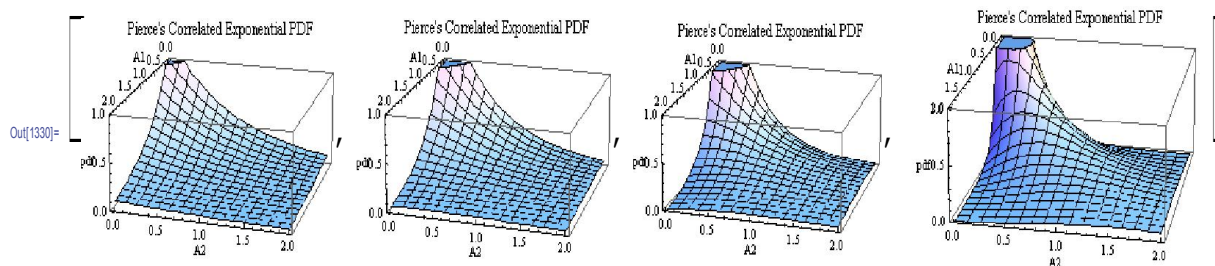


Fig 1-3 Pierce Bivariate Exponential PDF for Range of Correlation (0.7,.8,.9,1.0)

The Pierce probability for two sites showing extreme attenuation

$$P[A1>AR, A2>AR]=$$

$$p = \frac{\int_{A_R} \int_{A_R} e^{-\frac{A_1+A_2}{B(1-r)}} I_0\left(2\sqrt{\frac{A_1 A_2 r}{B^2(1-r)^2}}\right) dA_2 dA_1}{B^2(1-r)}$$

(1-2)

It is helpful to expand the pdf about the correlation rho =0. The first order expansion, as shown by Mathematica (6), is

Quad Diversity for Pierce=

$$\frac{2 \frac{A_1 A_2}{B^2}}{B^4} \left( 2 \left( \frac{2 A_1}{B} \frac{2 A_2}{B} \frac{A_1 A_2}{B^2} \frac{A_1}{B} \frac{A_2}{B} \frac{1}{B^2} \right) + 2 \frac{A_1 A_2}{B^2} \text{Log} \left( \frac{A_1 A_2}{B^2} \right) \right) \frac{1}{B^6}$$

( 1-3 )

The joint probability of all four ground sites suffering large attenuation may be found as a double integral, with results discussed further in App. B.

$$\text{Simple } P_{A_1, A_2, A_3, A_4} = \frac{1}{8} \frac{1}{B^4} \int_{A_R} \int_{A_R} \int_{A_R} \int_{A_R} e^{-\frac{A_1+A_2+A_3+A_4}{B(1-r)}} I_0\left(2\sqrt{\frac{A_1 A_2 r}{B^2(1-r)^2}}\right) I_0\left(2\sqrt{\frac{A_3 A_4 r}{B^2(1-r)^2}}\right) dA_4 dA_3 dA_2 dA_1$$

( 1-4 )

Higher reliability results for 8-ary ground diversity are also underway.

## Realization of both high efficiency and quantum tunneling in QM-SIS solar cells

Z.Q.Ma, H.W.Du, J.Yang, F.Xu, L.Zhao, M.Gao, S.M.Chen and D.D.Wang

SolarE Joint Lab., Dept. of Physics, Shanghai University 200444, PRC

[zqma@shu.edu.cn](mailto:zqma@shu.edu.cn)

Abstract: Among the various photovoltaic (PV) devices with the heterojunction architecture, the intrinsic layer of the thickness in nano-scale is significant for carrier (electron - hole) transportation and efficient tunneling, such as those solar cells of HIT (Heterojunction with intrinsic thin film), SHJ-IBC, QTSC, SIS and so on with multi-layers [1]. However, the controllable synthesis and/or growth of these functional thin films are usually very difficult to get to the goal. Here, a predigested processing used for an ultra-thin silicon oxide layer has been developed in the fabrication of QM-SIS (quasi-metal-semiconductor – insulator - semiconductor) solar cells by a direct sputtering of ITO on crystal Si substrate at an appropriate temperature. The built in field and the carriers tunneling path have been established near the buffer layer and an inversion region within the special changed region on the top of silicon substrate is verified through I-V, C-V and XPS measurement. The apparent thickness of the buffer layer was observed by high resolution TEM together with depth etching of XPS spectroscopies, respectively. The good optoelectronic conversion parameters of the PV device, such as open-circuit voltage, short-circuit current, filled factor, conversion power and thermal stability, have been obtained compared with the former results. In addition, the quantum tunnel of the device was confirmed at low temperature (below 100K) to support the tunneling mechanism of the device.

Reference:

[1] Alan Goodrich, Peter Hacke, Qi Wang, Bhushan Sopori, Robert Margolis, Ted L.James and Michael Woodhouse, **A wafer-based monocrystalline silicon photovoltaics road map: Utilizing known technology improvement opportunities for futher reductions in manufacturing costs**, Solar Energy Materials and Solar Cells 114, (2013) 110-135

## **A new self-adhesive transparent electrode for high efficiency perovskite solar cells**

Daniel Bryant<sup>1</sup>, Joel Troughton<sup>1</sup>, Peter Greenwood<sup>1</sup>, Matthew Davies<sup>1</sup>, Matt Carnie<sup>1</sup>,  
David Worsley<sup>1</sup>, Trystan Watson<sup>1</sup>

<sup>1</sup>SPECIFIC, Baglan Bay Innovation Centre, Baglan Energy Park, Baglan, Port Talbot,  
SA12 7AX, United Kingdom

[t.m.watson@swansea.ac.uk](mailto:t.m.watson@swansea.ac.uk) Tel +44 01792 295509

The field of thin film hybrid organic inorganic photovoltaics has been recently reinvigorated by the development of solid state organolead halide perovskite solar cells achieving over 19% performance at lab-scale. Attention is now starting to turn to the manufacturing processes required to scale these lab devices into modules, for high volume output roll to roll processing on low cost substrates such as metal foils and plastic sheeting. For laboratory devices, charge collection at the counter electrode is achieved via sputtering or evaporating of an opaque metallic contact, typically gold or silver and this renders it inappropriate for high volume manufacturing on flexible metal foils.

Here we describe a major breakthrough in electrode engineering that entails the combination of a polymer embedded nickel grid with a transparent conducting contact adhesive that can be applied to perovskite devices providing conductivity, charge extraction, mechanical adhesion and environmental protection. This has enabled the development of an indium-tin oxide (ITO), Au and Ag free entirely non-vacuum processed perovskite device to be manufactured.

The new system is a blend of an acrylic emulsion pressure sensitive adhesive (PSA) with a very low loading (0.018 volume fraction) PEDOT:PSS. This causes a phase segregation to occur between the PEDOT:PSS and the polymer adhesive domains which is advantageous for achieving conductivity at an order of magnitude lower volume fraction than the conventional percolation threshold. The PEDOT:PSS assembles into a honeycomb arrangement around the larger domains typical of acrylic emulsion, the



spanning network is now more ordered and allows conductivity to be evolved. The low loading gives excellent transparency of over 85%. To complete the electrode design the conducting adhesive is applied onto a corrosion proof Ni mesh electrode embedded into conventional PET film. The whole electrode can be fabricated separately to the perovskite material and then laminated together at room temperature

Device performance is comparable to that of a gold vacuum deposited electrode with champion efficiencies achieving 16.7% for the gold and 15.5% for the laminate on a glass substrate. This paper also presents for the first time a fully flexible indium and silver free perovskite solar cell using metal foil as a substrate incorporating the new laminate.

***Keywords: Functional, laminate, perovskite, adhesive, solar cell***

## Molecular glasses as hole transporting materials in solid state dye-sensitized solar cells

Thanh-Tuân Bui,<sup>1\*</sup> S. K. Shah,<sup>2</sup> M. Abbas,<sup>2</sup> X. Sallenave,<sup>1</sup> G. Sini,<sup>1</sup> L. Hirsch,<sup>2</sup> F. Goubard<sup>1</sup>

<sup>1</sup>Laboratoire de Physicochimie des Polymères et des Interfaces (LPPI), Université de Cergy Pontoise, 5 mails Gay Lussac, 95000 Neuville-sur-Oise (France).

<sup>2</sup>IMS, Université de Bordeaux, Institut Polytechnique de Bordeaux, UMR CNRS 5218, 16 Avenue Pey Berland, F-33607 Pessac (France).

\*E Mail: [tbui@u-cergy.fr](mailto:tbui@u-cergy.fr) (T.-T. Bui)

In recent years, there have been considerable interests in the development of small organic molecules hole transporting materials (HTM) for solid state dye sensitized solar cells (ssDSSCs). Small molecules exhibit many outstanding advantages over polymers (structural versatility, identical molecular weight, relatively easy purification). Despite their tendency to crystallization, small molecules can form stable amorphous materials above ambient temperature if their structures are meticulously designed. In the present communication, we will focus on the design, synthesis, and characterization of new p-type amorphous organic semiconductors based on *N*-alkylated carbazole and star-shaped tris(4-(thiophen-2-yl)phenyl)amine cores. We will also report the application of these molecules as HTMs in ssDSSCs combining with indoline D102 organic dye.

**Keywords:** *arylamine, molecular glass, hole transporting material, dye-sensitized solar cell*

[1] BUI, T.-T., BEOUCH, L., SALLENAVE, X. & GOUBARD, F. 2013 Carbazol-N-yl and diphenylamino end-capped triphenylamine-based molecular glasses: synthesis, thermal and optical properties. *Tetrahedron Lett.* 54, 4277. [2] BUI, T.-T. & GOUBARD, F. 2013 Recent advances in small molecular, non-polymeric organic hole transporting materials for solid-state DSSC. *EPJ Photovolt.* 4, 40402. [3] BUI, T.-T., SHAH, K., ABBAS, M., SALLENAVE, X., SINI, G., HIRSCH, L. & GOUBARD, F. Carbazole-based molecular glasses as hole transporting materials in solid state dye-sensitized solar cells. Manuscript in preparation. [4] BUI, T.-T., SHAH, K., ABBAS, M., SALLENAVE, X., SINI, G., HIRSCH, L. & GOUBARD, F. Star-shaped tris(4-(thiophen-2-yl)phenyl)amine based molecular glasses as hole transporting materials in solid state dye-sensitized solar cells. Manuscript in preparation

## Design Principles in Polymer-Fullerene BHJ Solar Cells:

### PBDTTPD as a Case Study

Pierre M. Beaujuge<sup>1</sup>

<sup>1</sup> Division of Physical Sciences & Engineering, Solar & Photovoltaic Engineering Research Center, King Abdullah University of Science and Technology (KAUST), Thuwal 23955-6900, Saudi Arabia.

*E Mail/ pierre.beaujuge@kaust.edu.sa*

Among *Organic Electronics*, solution-processable  $\pi$ -conjugated polymers are proving particularly promising in bulk-heterojunction (BHJ) solar cells with fullerene acceptors such as PCBM.[1] In recent years, great headway has been made in the development of efficient polymer donors across the community, with published power conversion efficiencies (PCE)  $>8\%$  in single cells and  $>10\%$  in tandems. In most reports, these systems involve elaborate repeat unit and side chain patterns, and deviating from those patterns induces substantial drops in device PCE. While the range of polymer design parameters that impact BHJ solar cell performance remains a matter of some debate, our recent developments indicate that the combination of side-chain substituents appended to the main chain critically impacts polymer performance.

For example, in poly(benzo[1,2-*b*:4,5-*b'*]dithiophene–thieno[3,4-*c*]pyrrole-4,6-dione) (PBDTTPD), side-chain substituents of various size and branching impart distinct molecular packing distances (i.e.,  $\pi$ - $\pi$  stacking and lamellar spacing), varying degrees of nanostructural order in thin films, and preferential backbone orientation relative to the device substrate.[2-5] While these structural variations seem to correlate with BHJ solar cell performance, with power conversion efficiencies ranging from 4% to 8.5%,[2,3] we believe that other contributing parameters – such as the local conformations between the polymer and the fullerene, and the domain distribution/composition across the BHJ (i.e., pure/mixed phases) – should also be taken into account.[6,7] Other discrete modifications of PBDTTPD's molecular structure affect polymer performance in BHJ solar cells with PCBM, and our recent developments emphasize how systematic structure-property

relationship studies impact the design of efficient polymer donors for BHJ solar cell applications.[8-10] It is important to further our understanding of these effects as we look to continue improving BHJ solar cell efficiencies.

**Keywords:** *Polymer, fullerene, bulk-heterojunction, PBDTPD, solar cell*

[1] BEAUJUGE, P. M. & FRECHET J. M. J. 2011. Molecular Design and Ordering Effects in  $\pi$ -Functional Materials for Transistor and Solar Cell Applications. *JACS*, 133, 20009-20029.

[2] PILIEGO, C., HOLCOMBE, T. W., DOUGLAS, J. D., WOO, C. H., BEAUJUGE, P. M. & FRECHET, J. M. J. 2010. Synthetic Control of Structural Order in *N*-Alkylthieno[3,4-*c*]pyrrole-4,6-dione-Based Polymers for Efficient Solar Cells. *JACS*, 132, 7595-7597.

[3] CABANETOS, C., EL LABBAN, A., BARTELT, J. A., DOUGLAS, J. D., MATEKER, W. R., FRECHET, J. M. J., MCGEHEE, M. D. & BEAUJUGE, P. M. 2013. Linear Side Chains in Benzo[1,2-*b*:4,5-*b'*]dithiophene–Thieno[3,4-*c*]pyrrole-4,6-dione Polymers Direct Self-Assembly and Solar Cell Performance. *JACS*, 135, 4656-4659.

[4] BARTELT, J. A., DOUGLAS, J. D., MATEKER, W. R., EL LABBAN, A., TASSONE, C. J., TONEY, M. F., FRECHET, J. M. J., BEAUJUGE, P. M. & MCGEHEE, M. D. 2014. Controlling Solution-Phase Polymer Aggregation with Molecular Weight and Solvent Additives to Optimize Polymer-Fullerene Bulk Heterojunction Solar Cells. *Adv. Energy Mater.*, 4, 1301733, 1-11.

[5] EL LABBAN, A., WARNAN, J., CABANETOS, C., RATEL, O., TASSONE, C. J., TONEY, M. F. & BEAUJUGE, P. M. 2014. Dependence of Crystallite Formation and Preferential Backbone Orientations on the Side Chain Pattern in PBDTPD Polymers. *ACS Appl. Mater. Interfaces*, Article ASAP, DOI: 10.1021/am505280a.

[6] GRAHAM, K. R., CABANETOS, C., JAHNKE, J. P., IDSO, M. N., EL LABBAN, A., NGONGANG NDJAWA, G. O., CHMELKA, B. F., AMASSIAN, A., BEAUJUGE,

P. M. & MCGEHEE, M. D. 2014. Importance of the Donor:Fullerene Intermolecular Arrangement for High-Efficiency Organic Photovoltaics. *JACS*, 136, 9608-9618.

[7] DYER-SMITH, C., HOWARD, I. A., CABANETOS, C., EL LABBAN, A., BEAUJUGE, P. M. & LAQUAI, F. 2014. Interplay Between Side-Chain Pattern, Polymer Aggregation, and Charge Carrier Dynamics in PBDTTPD:PCBM Bulk-Heterojunction Solar Cells. Submitted.

[8] WARNAN, J., EL LABBAN, A., CABANETOS, C., HOKE, E., RISKO, C., BREDAS, J-L., MCGEHEE, M. D. & BEAUJUGE, P. M. 2014. Ring Substituents Mediate the Morphology of PBDTTPD-PCBM Bulk-Heterojunction Solar Cells. *Chem. Mater.*, 26, 2299-2306.

[9] WARNAN, J., CABANETOS, C., BUDE, R., EL LABBAN, A., LI, L. & BEAUJUGE, P. M. 2014. Electron-Deficient *N*-Alkylolyl Derivatives of Thieno[3,4-*c*]pyrrole-4,6-dione Yield Efficient Polymer Solar Cells with Open-Circuit Voltages > 1 V. *Chem. Mater.*, 26, 2829-2835.

[10] WARNAN, J., CABANETOS, C., EL LABBAN, A., HANSEN, M. R., TASSONE, C. J., TONEY, M. F. & BEAUJUGE, P. M. 2014. Ordering Effects in Benzo[1,2-*b*:4,5-*b'*]difuran-thieno[3,4-*c*]pyrrole-4,6-dione Polymers with >7% Solar Cell Efficiency. *Adv. Mater.*, 26, 4357-4362.

## Effectively Utilizing NIR Light Using Direct Electron Injection from Up-Conversion Nanoparticles to the TiO<sub>2</sub> Photoanode in Dye-Sensitized Solar Cells

Jie Chang, Suli Wu\*

State Key Laboratory of Fine Chemicals, Dalian University of Technology

*E Mail/ Contact Details (wusuli@dlut.edu.cn)*

As the infrared and near-infrared light comprises almost half of the energy in the sunlight, utilizing this part of energy by up-conversion nanoparticles (UCNPs) to increase the energy conversion efficiency has been a research hotspot. Current researches mainly focus on two aspects: i) the conversion of NIR light to visible light by UCNPs and how the converted light is absorbed by dye-sensitizer, ii) the reflection of light. Due to the low emission efficiency of UCNPs, the large energy loss during energy transfer from the UCNPs to the dye sensitizer and the apparent charge recombination at the UC/dye/electrolyte interfaces, it is difficult to achieve a higher photocurrent output efficiency. Herein, TiO<sub>2</sub>/NaYF<sub>4</sub>:Yb<sup>3+</sup>,Er<sup>3+</sup> nano-heterostructures are prepared in situ on the TiO<sub>2</sub> photoanode of dye-sensitized solar cells (DSCs). By directly injecting the excited electrons in the high energy level of UCNPs into the conductive band (CB) of TiO<sub>2</sub> through the shared interface of the nano-heterostructures, the overall efficiency ( $\eta$ ) of a DSC device with the nano-heterostructure in the photoanode is 17% higher than that of a device without the up-conversion nanoparticles (UCNPs) and 13% higher than that of a device with only physically mixed TiO<sub>2</sub> and UCNPs. The decisive role of electron injection is carefully explained by comparing the up-converted fluorescence spectrum. Nano-heterostructures of TiO<sub>2</sub>/UCNP containing Tm<sup>3+</sup> and Ho<sup>3+</sup> are also prepared. Their results further reveal that only ones with appropriate energy levels matching can facilitate effectively direct electron injection from the UCNPs to TiO<sub>2</sub>, and result in obvious improvement of the photocurrent and overall efficiency of DSCs while using NIR light.

**Keywords:** *Up-conversion, dye-sensitized solar cells, nano-heterostructures, electron injection*

# Quasi Core-Shell Nitrogen-Doped Graphene/Cobalt Sulfide Conductive Catalyst for Highly Efficient Dye-Sensitized Solar Cells

Han Chen,<sup>a</sup> Enbing Bi,<sup>a</sup> Xudong Yang,<sup>b</sup> and Liyuan Han<sup>a, b</sup>

<sup>a</sup> State Key Laboratory of Metallic Matrix Composites Materials, School of Materials Science and Engineering, Shanghai Jiao Tong University, Shanghai 200240, China. E-mail: [chen.han@sjtu.edu.cn](mailto:chen.han@sjtu.edu.cn). Fax: (+86) 21-54742414, Tel: (+86) 21-54742414

<sup>b</sup> Photovoltaic Materials Unit, National Institute for Materials Science, Tsukuba, Ibaraki 305-0047 (Japan).

## Abstract

To solve the energy crisis and environmental pollution problems, researchers have prompted to intensively investigate solar cells which can provide clean and renewable energy to reduce the consumption of fossil fuels. Dye-sensitized solar cells (DSSCs) are promising solar cells because of their low cost and environmentally friendly characteristics <sup>[1]</sup>. For the purpose of further cost-cutting, Platinum (Pt)-free counter electrode (CE) has been proposed to be used in the DSSCs.<sup>[2]</sup> However, the efficiency of cells fabricated with Pt-free CEs is still lower than that of cells with Pt CEs, especially, in the cell with high efficiency of over 10%. In this work, a novel conductive catalyst was designed based on a quasi core/shell structure of N-doped graphene/cobalt sulfide. This Platinum-free catalyst shows high catalytic activity and conductivity owing to close interactions between the core- cobalt sulphide and the shell- N-doped graphene. It enables dye-sensitized solar cells (DSSCs) to obtain high energy conversion efficiency up to 10.71%, which is as far as we know the highest efficiency for DSSCs based on Platinum-free counter electrode.

Keywords: conductive catalyst; counter electrodes; dye-sensitized solar cells; energy conversion; electrochemistry

## References

- [1] B. O'regan and M. Grätzel. Nature, 1991, 353, 737-740.
- [2] H. Wang, G. Liu, X. Li, et al. Energy Environ. Sci., 2011, 4, 2025-2029.

## Calcium Iodide and Hydroxypropyl Cellulose Based Gel Polymer Electrolytes for Dye-Sensitized Solar Cell

S.Ramesh, M.H.Khanmirzaei, K.Ramesh

Centre for Ionics University of Malaya, Department of Physics, Faculty of Science,  
University of Malaya, 50603 Kuala Lumpur, Malaysia.

[rameshtsubra@gmail.com](mailto:rameshtsubra@gmail.com)

corresponding author. Tel.: +60-3-7967-4391

Dye sensitized solar cells (DSCs) based on gel polymer electrolytes (GPEs) have received significant attention [1-2] due to advantages such as having excellent contact, high conductivity and thermal stability compared with DSSCs based on conventional polymer electrolytes. In this work, environmental friendly biopolymer Hydroxypropyl cellulose (HPC), calcium iodide (CaI), ethylene carbonate (EC) and propylene carbonate (PC) were used for preparation of polymer electrolyte system (HPC:EC:PC:CaI). To provide a redox mediator, iodine (I<sub>2</sub>) was added into the gel polymer electrolyte. The weights of HPC, EC, PC and CaI were kept at 0.5, 5.0, 5.0 and 0.5 g, respectively. Ionic conductivity of  $2.49 \times 10^{-3}$  S/cm was achieved. Temperature-dependent behavior of gel polymer electrolyte was analyzed in this work. Dye sensitized solar cell (DSSC) was fabricated using HPC:EC:PC:CaI gel polymer electrolyte and analyzed under Sun simulator. The GPE sample shows 4.61 % energy conversion efficiency with short-circuit current density, open-circuit voltage and fill factor of  $16.50 \text{ mA cm}^{-2}$ , 470 mV and 59.4 %, respectively.

**Keywords:** *Gel polymer electrolyte, HPC, DSC, calcium iodide*

[1] PARK S. H., WON D. H., CHOI H. J., HWANG W. P., JANG S. I., KIM J. H., JEONG S. H., KIM J. U., LEE J. K. & KIM M. R. 2011. Dye-Sensitized Solar Cells Based on Electrospun Polymer Blends as Electrolytes. *Sol Energy Mat Sol C*, 95, 296-300.

[2] SINGH P. K., BHATTACHARYA B., NAGARALE R. K., KIM K. W., RHEE H. W. 2010. Synthesis, Characterization and Application of Biopolymer - Ionic Liquid Composite Membranes. *Synthetic Metals*, 160, 139-142.



## Effect of pre-annealing on the solar cell performance of $\text{Cu}_2\text{ZnSnS}_4$ thin film prepared by sulfurization of stacked metal precursor with $\text{H}_2\text{S}$ gas

Jung Hun Lee<sup>1</sup>, Heon Jin Choi<sup>2</sup>, Won Mok Kim<sup>1</sup>, Jeung Hyun Jeong<sup>1</sup>, and Jong Keuk Park<sup>1</sup>

<sup>1</sup>Korea Institute of Science and Technology (KIST), Hwarang-ro 14-gil 5, Seongbuk-gu, Seoul 136-791, South Korea

<sup>2</sup>Yonsei University, 50 yonsei-ro, Seodaemun-gu, Seoul, 120-749 Korea

[jokepark@kist.re.kr](mailto:jokepark@kist.re.kr)

$\text{Cu}_2\text{ZnSnS}_4$  (CZTS) is known to be a candidate to replace  $\text{Cu}_2\text{InGaSe}_4$  for low cost thin film solar cell. For the synthesis of CZTS, sulfurization of (S-incorporated) Cu-Zn-Sn precursor is widely used. As for the preparation of the precursor, sputtering process is favorable to obtain uniform film with controllable composition. As for the sulfurization, the annealing with  $\text{H}_2\text{S}$  gas has advantage for the synthesis of CZTS phase under the controlled sulfur partial pressure. In this respect, sulfurization of metal precursor prepared by sputtering of pure Cu, Zn and Sn targets with  $\text{H}_2\text{S}$  gas is suitable for fabrication of CZTS solar cell with large-scale at low cost. However, there are few papers about CZTS solar cells prepared by sulfurization of pure metal precursor with  $\text{H}_2\text{S}$  gas. In this study, we investigated the influence of pre-annealing on the solar cell performance of CZTS thin film prepared by sulfurization of metal precursor with  $\text{H}_2\text{S}$  gas. Cu-Zn-Sn precursor with stacked structure, (Cu,Sn)/Zn, was deposited on the Mo coated glass substrate by magnetron sputtering of pure Cu, Zn and Sn metal targets. The stacked precursor was sulfurized using a rapid thermal annealing (RTA) in the mixed  $\text{N}_2+\text{H}_2\text{S}$  atmosphere at  $550^\circ\text{C}$ . In the process, pre-annealing at various temperatures from  $350^\circ\text{C}$  to  $450^\circ\text{C}$  in the mixed  $\text{N}_2+\text{H}_2\text{S}$  atmosphere was adopted to improve the phase formation of CZTS. The efficiency of the CZTS solar cell was critically dependent on the pre-annealing condition. In contrast to the CZTS solar cell prepared without pre-annealing which showed lower conversion efficiency (2.1~ 2.6%), the CZTS solar cell prepared with pre-annealing at  $450^\circ\text{C}$  showed higher cell efficiency (3.0~3.3%). However, the cell efficiency of CZTS solar cell prepared with pre-annealing in an Ar atmosphere, much lower conversion efficiency (0.9%) was obtained. The change in the cell performance of CZTS thin films by the adoption of various pre-annealing processes will be discussed in terms of CZTS formation through the ZnS and  $\text{Cu}_2\text{SnS}_3$  phases.

**Keywords:** CZTS solar cell, metal precursor, sulfurization,  $\text{H}_2\text{S}$ , pre-annealing

## A Simple Approach to Fabricate Yolk–shell Si/C Nanostructured Materials towards Anode Materials for Lithium Ion Batteries

Huanhuan Li<sup>1</sup> and Jingping Zhang<sup>1</sup>

<sup>1</sup> Faculty of Chemistry, Northeast Normal University, Changchun 130024, China

*jpzhang@nenu.edu.cn*

A novel method was developed to successfully prepare mesoporous Si/C nanocomposites with yolk–shell structures (MSi@C). Different from the previous reported methods, this approach was unique, straightforward and easily scaled up. The MSi@C nanocomposites possessed an M-Si core with diameter ~150 nm and a carbon shell with diameter ~230 nm. Such nano and mesoporous structure combined with voids between the M-Si core and carbon shell not only provides enough space for the volume expansion of M-Si during lithiation, but also accommodates the mechanical stresses/strains caused by the volume inflation and contraction. Moreover, partial graphitization of the carbon contributed to the improved electrical conductivity and rate performance of MSi@C. As a result, the prepared MSi@C exhibited an initial reversible capacity of 2599.1 mA h g<sup>-1</sup> and maintained 1264.7 mA h g<sup>-1</sup> even after 150 cycles at 100 mA g<sup>-1</sup>, with high coulombic efficiency (CE) above 99% (based on the weight of M-Si in the electrode). Therefore, this work provided an alternative method to fabricate yolk–shell nanostructured materials with great potential as anode materials for lithium ion batteries.

**Keywords:** *Si/C nanocomposites, Yolk–shell, anode materials, lithium ion batteries*

# Symposia 5

## Advances in Biosensors and Biomaterials

---

- Advances in Enzymatic and Non-Enzymatic Biosensors
- Functional biomaterials for drug delivery
- Advances in Bioelectronics and Commercial biosensors,
- DNA chips and nucleic acid sensors
- Biomaterials for Cardiovascular Applications
- Environmental biosensors
- Biosensors for Imaging
- Application of Biosensors in Drug Delivery and Clinical Chemistry
- Lab-on-a-chip
- Printed biosensors and microfabrication
- Applications of Biopolymer for Drug Delivery
- Computational modeling and simulation of Biosensors
- Others

# INDEX PAGE

1. Controlled Assembly of Modified DNA Wires <b>AUTHOR:</b> Ms. Colette Whitfield	1
2. Non-Enzymatic Detection Of Carbamate Pesticides Based On Monodisperse Aurh Nanocrystals <b>AUTHOR:</b> Dr. Yuan Zhang	2
3. Active Colloids for Enhanced Analyte Transport in Biosensors <b>AUTHOR:</b> Dr. Richard Archer	3
4. Molecular functionalization of Nanomaterials for Immuno-diagnosis of Cancer <b>AUTHOR:</b> Dr. Kavita Arora	4
5. A New Bifunctional Electrochemical Sensor for Hydrogen Peroxide and Nitrite Based on Bimetallic Porphyrin MOF <b>AUTHOR:</b> Prof. Bo Zhou	6
6. Amyloid-Beta Detection With Mems Fabrication Based Reduced Graphene Oxide Sensor. <b>AUTHOR:</b> Dr. Jinsik Kim	7
7. Preparation and Characterization of Chitonated Fatty Acid Liposome in Carbohydrate-based Gel <b>AUTHOR:</b> Dr. Misni Misran	10
8. MEMBRANES BASED ON QUITOSAN-PULLULAN AND EXTRACTS OF H. virginiana, C. sinensis AND A. adstringens: ANTIMICROBIAL AND CITOTOXIC ACTIVITIES <b>AUTHOR:</b> Dr. Katiushka Arevalo	12
9. Swichable fluorescent materials as probes for sensing and imaging <b>AUTHOR:</b> Prof. Tao Yi	13
10. Poly(amidoamine) dendrimers as a tool for the design of functionalized iron oxide nanoparticles for multimodal MRI imaging and drug delivery <b>AUTHOR:</b> Dr. Adriano Boni	14
11. An investigation on the buckling of soft spherical shells perforated by complex shapes <b>AUTHOR:</b> Dr. Sen Lin	17
12. Impact of self-assembled molecular interconnects on the immobilization and hydridization of DNA at semiconductor substrates <b>AUTHOR:</b> Dr. Bee Min Goh	18
13. Detection of DNA damage by a combined effect of metal oxide nanoparticles and UV-C irradiation using DNA biosensor <b>AUTHOR:</b> Prof. Jan Labuda	19
14. Water-Soluble Conjugated Polymer-Based Chemo- And Biosensors <b>AUTHOR:</b> Prof. Han Young Woo	20
15. Characterization and fabrication of nanocomposite thin films of PANI embedded with Ag-Mn alloy for E. coli sensor <b>AUTHOR:</b> Dr. Norshafadzila Mohammad Naim	21
16. Sensitive and Selective detection of nanotoxic material using resonance sensor <b>AUTHOR:</b> Prof. Juneseok You	22
17. A liquid flow valve made from a functional composite gel <b>AUTHOR:</b> Mr. Christoffer Abrahamsson	23
18. Magnetite Nanoparticles Functionalized with Vitamin E analogues: Anticancer Effects <b>AUTHOR:</b> Dr. Aracely Angulo-Molina	24
19. Bioengineering novel floating nanoparticles for protein and drug delivery <b>AUTHOR:</b> Prof. Shiladitya Dassarma	25

20. Fabrication of drug carrier polyvinyl alcohol/chitosan composite nanofiber and its drug release <b>AUTHOR:</b> Dr. Qianting Wang	26
21. Delivery of mRNA via layer-by-layer biodegradable capsules <b>AUTHOR:</b> Dr. Mitali Kakran	27
22. Evaluation of multiple theranostic properties of polydopamine coated Fe <sub>0.65</sub> Co <sub>0.35</sub> @(Fe <sub>0.65</sub> Co <sub>0.35</sub> ) <sub>3</sub> O <sub>4</sub> nanocubes for cancer nanomedicinal application <b>AUTHOR:</b> Mr. Khachatur Julfakyan	28
23. Paper-Based Scale Bar Readout System for Quantitative Analysis <b>AUTHOR:</b> Ms. Devi Liana	30
24. Detection of microorganisms on a chip <b>AUTHOR:</b> Prof. Gurunath Ramanathan	31
25. Covalent and stable modification of silicon and GaAs surfaces for control of cell adhesion and study of protein–protein interactions <b>AUTHOR:</b> Dr. Surendra Vutti	
26. Assessment of wound infection with different biosensors based on enzymes of the human immune system <b>AUTHOR:</b> Dr. Alexandra Rollett	

## Controlled Assembly of Modified DNA Wires

Colette J Whitfield<sup>1</sup>, Andrew R Pike<sup>1</sup>, Bernard A Connolly<sup>2</sup>, Eimer M Tuite<sup>1</sup>

<sup>1</sup>Chemical Nanoscience Laboratory, Newcastle University, NE1 7RU, UK

<sup>2</sup>Institute of Cellular and Molecular Biology, Newcastle University, NE2 4HH, UK

*c.j.whitfield@newcastle.ac.uk*

*andrew.pike@newcastle.ac.uk*

For several years, the self-assembling nature of DNA has been an attractive property to construct functional wires on the nano-scale. Many groups have successfully assembled metal-based nano-wires using DNA as a template [1], however, site specific deposition is an ongoing challenge. We aim to control the uniform deposition of metal ions at prepositioned functionalities along the helix. Here we report an enzyme based route for the formation of long uniformly functionalised DNA for controlled metal incorporation.

A PCR-based method has been developed, capable of annealing DNA duplexes to form 'sticky ends', resulting in extension of double stranded DNA using a *Thermococcus gorgonarius* Family B Polymerase exonuclease minus variant. Products from 200 to 20,000+ base pairs (68 nm to 6800 nm) of any repeat sequence of DNA are possible. The controlled incorporation of d-6-thio-GTP into such DNA permits the controlled binding of Au(I) to precise arrangements to produce uniform and ordered nano-scale wires.

Due to the ability to extend a range of repeat sequences and the extensive variety of modified nucleotides available, an endless assortment of uniformly functional DNA is possible.

**Keywords:** *Functional, template, DNA, wire*

[1] WATSON, S. M. D., PIKE, A. R., PATE, J., HOULTON, A. & HORROCKS, B. R. 2014. DNA-template nanowires: morphology and electrical conductivity. *Nanoscale*, 6, 4027-4037

## Non-enzymatic detection of carbamate pesticides based on monodisperse AuRh nanocrystals

Chen, Zhang, Xu

Department of Chemistry, Shanghai University, Shanghai 200444, China

*E mail: conanbokc@gmail.com (Presenting author), xujiaqiang@shu.edu.cn (Corresponding author)*

For the first time, monodisperse AuRh bimetallic nanocrystals are employed for the non-enzymatic specific detection of carbamate pesticides. Compared with state of the art, other Au based bimetallic nanocrystals and monometallic analogues, AuRh nanocrystals show their advances in specific electrocatalytic reaction toward carbamate pesticides at nano-molar (nM) level without the assistance of acetylcholinesterase (AChE) or other biochemical recognition elements. According to the electrochemical assessments, we discover that AuRh nanocrystals have considerable response toward 1 nM carbaryl, while there is no response to organophosphorus pesticides over AuRh nanocrystals. The ultra-sensitive and highly selective detection of carbamate pesticides could be attributed to the great catalytic activity of AuRh nanocrystals toward  $-NH_2$  group in carbamate pesticides.

**Keywords:** AuRh, carbamate pesticides, electrochemical sensor

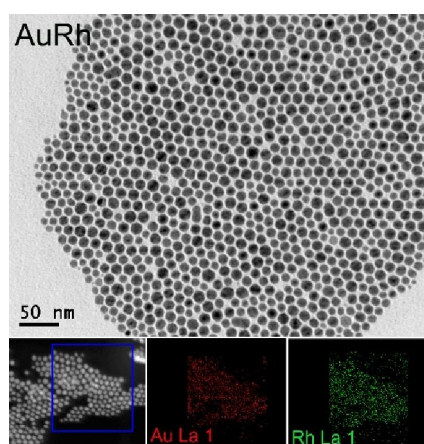


Figure 1: TEM image of AuRh nanocrystals as well as STEM image and corresponding element maps showing the distribution of Au (red) and Rh (green).

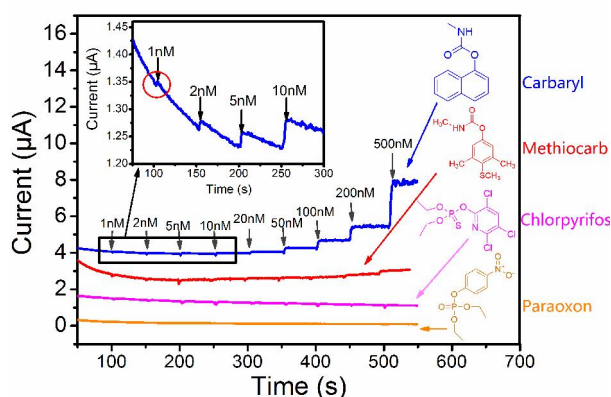


Figure 2: Current-time responses of AuRh toward different pesticides. Inset is the magnified amperometric responses of low concentration of carbaryl.

## Active Colloids for Enhanced Analyte Transport in Biosensors

Dr Andrew Campbell<sup>1</sup>, Richard Archer<sup>1</sup>, Prof. Gavin Buxton<sup>2</sup>, Dr Stephen Ebbens<sup>1</sup>

<sup>1</sup>Chemical & Biological Engineering, University of Sheffield, Sir Robert Hadfield Building, Sheffield, S1 3JD

<sup>2</sup>Department of Science, Robert Morris University, Moon Township, PA 15108

*s.ebbens@sheffield.ac.uk*

Transport processes in biosensing devices are often limited by diffusion. For example, in a common immunoassay sensor geometry, where analytical solution is placed within a microwell containing a spatially well-defined detector region, binding rate is determined by the Brownian diffusion constant of the target molecules. As the detector region is miniaturized, the diffusion limit can lead to accumulation times of several hours.<sup>1</sup> One suggested method to improve transport rate is to coat surfaces surrounding the detector with protein motors, which can bind and carry molecules for analysis at enhanced rates.<sup>2</sup> However, protein motors are difficult to extract, suffer from storage and lifetime, and solution compatibility issues and are limited to 2D transport. In this context, we explore the potential for active colloids, synthetic catalytically driven super-diffusive devices capable of 3D motion to offer an alternative transport system. We show how active colloids modified with anti-bodies can perform selective protein capture from throughout a liquid volume, and at an enhanced rate due to improved volume transport and rotational alignment. We also describe how harnessing active colloids interaction with gravity, and surface topographic and chemical modification can lead to autonomous rapid accumulation of active colloids, and surface bound protein at the detector region, consequently providing a route to overcome the diffusion limit for a wide range of biosensing applications.

**Keywords:** *Biosensor, Colloid, Catalysis*

- [1] KATIRA, P. & HESS, H. 2010. Two-stage capture employing active transport enables sensitive and fast biosensors. *Nano Lett.* 10, 567–72.
- [2] FISCHER, T., AGARWAL, A. & HESS, H. 2009. A smart dust biosensor powered by kinesin motors. *Nat. Nanotechnol.* 4, 162–6.



## Molecular functionalization of Nanomaterials for Immuno-diagnosis of Cancer

Meenakshi Choudhary<sup>1,2</sup>, Anu Singh<sup>1</sup>, Satbir Kaur<sup>2</sup>, S. P. Singh<sup>3</sup>, Kavita Arora<sup>1\*</sup>

<sup>1</sup>Advanced Instrumentation Research Facility, Jawaharlal Nehru University, New Delhi-110067

<sup>2</sup>Department of Human Genetics, Punjabi University, Patiala, Punjab-147002

<sup>3</sup>CSIR-National Physical Laboratory, New Delhi-110067

\*Email: kavitaarora@gmail.com, kavitaarora@jnu.ac.in

Cancer is a major health problem worldwide, where poor prognosis of the disease significantly contributes to its monstrous nature. Survival of a cancer patient is strongly dependent on its early/timely detection coupled with appropriate treatment modalities. Till date majority of cancers remain undetected until advanced stage. Cancer existence can be controlled through evidence-based cancer prevention strategies, improved diagnostic methodologies and patient management. About one-third of the cancer burden could be decreased with the timely diagnosis and treatment. Therefore, research and development of handy devices for early diagnosis and prognosis of disease are receiving much attention. Functionalized nanomaterials based portable and miniaturized, low cost biosensors/ immunosensors can prove a pioneer step in the same direction. These devices offer fast, sensitive, selective and convenient clinical diagnosis and monitoring due to ease of handling. These are small devices incorporated with biomolecules which are used to detect the biological parameters by electrochemical or optical transduction system and facilitate detection of biomarkers (nucleic acid, enzymes and proteins etc.). our work focuses on the synthesis and functionalization of nanomaterials to make them biocompatible for application in biological sensing.

Graphene oxide (GO) due to excellent electrochemical properties, biocompatibility, high defect density and presence of pendant organic functional groups (-OH,-COOH,-CHO) allows easy attachment of various biomolecules such as protein, enzyme and nucleic acids. Graphene Oxide (GO) based electrochemical immunosensor for human telomerase reverse transcriptase (hTERT) for lung cancer was developed exhibiting detection limit of  $10 \text{ ag mL}^{-1}$  ( $10 \times 10^{-18} \text{ g mL}^{-1}$ ) in detection range ( $10 \text{ ag mL}^{-1} - 50 \text{ ng mL}^{-1}$ ) using DPV. Carbon nanotubes (CNTs) are also among attractive low cost matrices available that offer bio-electro-compatibility due to their unique structure, high chemical stability, high surface-to-volume ratio. An immunosensor as successfully demonstrated for simultaneous detection of two analytes (anti-MAGE A11 and anti-MAGE A2) from  $5 \text{ fg mL}^{-1} - 50 \text{ ng mL}^{-1}$  using differential pulse voltammetry. Similarly, cysteine functionalized gold electrodes utilized

towards detection of oral cancer biomarker, CD-59. This immunosensor facilitated improved electron transduction due to cysteine linker serving as 'molecular switch' and showed a specific response to CD-59 in the range of  $0.1 \text{ pg mL}^{-1}$  –  $50 \text{ ng mL}^{-1}$  using EIS with good specificity and reproducibility. Therefore, the simplistic nano based molecular functionalization approaches are opening wonderful opportunities to fine tune and custom design efficient clinical diagnostic platforms for early cancer diagnosis. Such devices also allows low level detection that warrants the realization of point-of-care device for early detection of diseases through biological fluids.

## A New Bifunctional Electrochemical Sensor for Hydrogen Peroxide and Nitrite Based on Bimetallic Porphyrin MOF

Li-Mei Shi, Bo Zhou

Nanjing Normal University, Nanjing 210023, China.

*E Mail: zhoubo@njnu.edu.cn*

Metalloporphyrin molecules are excellent candidates to act as molecular building blocks for the construction of MOFs, because of various functional group substituents in the periphery of the molecule and the huge variety of available derivatives incorporating different centre-coordinated metals.[1] in this work, a new bimetallic porphyrin MOF,  $[\text{Cu}_2(\text{Co-TCPP})(\text{H}_2\text{O})_2] \cdot 0.5\text{DMF} \cdot 5\text{H}_2\text{O}$  (Cu-CoTCPP), consisting of [5,10,15,20-(4-carboxy-phenyl)porphyrin]Co(II) (CoTCPP) struts which were bound by Cu(II)-carboxylate clusters ( $\text{Cu}_2(\text{COO})_4$ ), was prepared solvothermally and characterized by various techniques, including XRD, IR, elemental analysis, TG, and TEM. Cu-CoTCPP showed novel bifunctional electrocatalytic ability toward both the reduction of  $\text{H}_2\text{O}_2$  and the oxidation of  $\text{NaNO}_2$  which might be due to Cu and Co, respectively. With the assistance of multi-walled carbon nanotubes (MWNTs), Cu-CoTCPP showed greatly improved sensing performance in the determination of  $\text{H}_2\text{O}_2$  and  $\text{NaNO}_2$ . Cu-CoTCPP/MWNTs/GCE also showed fast response, and high selectivity, steadiness and reproducibility. Excellent determination performance and high biocompatibility make the metalloporphyrin functionalized MOFs promising in electrochemical biosensing.

**Keywords:** *porphyrin MOF, bimetallic, electrochemical sensing*

[1] LI, Q. W., ZHANG, W. Y., MILJANIC, O. S., SUE, C. H., ZHAO, Y. L., LIU, L. H., KNOBLER, C. B., STODDART, J. F. & YAGHI, O. M. 2009. Docking in Metal-Organic Frameworks. *Science*, 325, 855-859.

The authors thank National Natural Science Foundation of China (Grant No. 21175068) for the financial support.

## **Amyloid-beta detection with MEMS fabrication based reduced graphene oxide sensor**

Jinsik Kim<sup>1</sup>, Myung-Sic Chae<sup>1,2</sup>, Hye Jin Kim<sup>1,2</sup>, Dahye Jeong<sup>1</sup>, Yong Kyoung Yoo<sup>1,3</sup>,  
Gangeun Kim<sup>1,2</sup>, Jung Ho Park<sup>2</sup> and Kyo Seon Hwang<sup>1</sup>

<sup>1</sup>Center for BioMicrosystems, Korea Institute of Science and Technology, Seoul 136-791, Korea

<sup>2</sup>Department of Electrical Engineering, Korea University, Seoul 136-713, Korea

<sup>3</sup>Department of Electrical Engineering, Kwangwoon University, Seoul 139-701, Korea

- *Presentator* : [lookup2@hanmail.net](mailto:lookup2@hanmail.net) / Jinsik Kim
- *Contact Author* : [kshwang@kist.re.kr](mailto:kshwang@kist.re.kr) / Kyo Seon Hwang

The reproducible fabrication of device with graphene was the bottleneck to make the device as practically used device. To improve the reproducibility, a widely used promising nano material, graphene oxide (GO), has been introduced. The reduced GO called rGO has been used in various fields such as flexible display, light emitting diode and field-effect transistor nano-device due to its novel properties [1]. The rGO had great electrical conductivity compared with graphene and it can be used as electrical device. The sites and band gap of rGO could be easily controllable. The rGO nano material's great novel properties which were high conductivity and easy controllable band gap and reaction sites could make the rGO as sufficient sensing material in biosensor applications [2].

Here, we introduced the MEMS (micro electrical and mechanical systems) fabrication method based sensor with reduced graphene oxide for amyloid beta for early diagnosis of Alzheimer's disease. Amyloid-beta is the biomarker related with Alzheimer's disease. The level of amyloid-beta in blood should be detected to early diagnosis of the Alzheimer's disease [3].

The surface modification was tried to enhance the conductivity of GO. Ester group replacement with Dextran was tried as a reduction process. Thermal reduction and

chemical reduction with hydriodic acid were also tried. In case of the replacement using Dextran, the replaced ester groups with Dextran were also reaction sites with biomolecules as a result in reaction site enhancement compare to rGO with other method. The squeezing method was used to form the rGO film on silicon oxide substrate. The rGO film's resistance in range of tens ~ hundreds kilo ohms was optimized to sufficient for detection of biomolecules. Fully reduced GO could have less resistance, however, the adhesion was also going to be poor. The adhesion of rGO layer to substrate is important property to use conventional MEMS fabrication method such as photoresist deposition, developing, etching and washing with deionized water and acetone. The optimization of reduction between resistance and adhesion should be needed to make practical bio sensor with rGO.

Detection of amyloid-beta was tried for early diagnosis for an Alzheimer's disease with the designed rGO based sensors. Antibody of amyloid-beta was immobilized on the rGO surface. The affinity reaction between antibody of amyloid-beta and amyloid-beta induced the changes of conductance of rGO. The conductance was measure to detect the amyloid-beta.

Finally, ultra-low concentration of below ~pg/mL range was the limit of detection point of the rGO biosensor. The sensitivity of rGO based sensor was sufficient to detect the amyloid-beta in blood sample. We hope that the achievement of biosensor device with rGO makes the Alzheimer's disease is not a disease.

***Keywords: rGO biosensor, Alzheimer's disease, Graphene Oxide, Conductance***

[1] Sasha Stankovicha, Dmitriy A. Dikina, Richard D. Pinera, Kevin A. Kohlhaasa, Alfred Kleinhammesc, Yuanyuan Jiach, Yue Wuc, SonBinh T. Nguyenb and Rodney S. Ruoffa, 2007, Synthesis of graphene-based nanosheets via chemical reduction of exfoliated graphite oxide, *Carbon*, 45, 1558–1565

[2] Sung Myung, Perry T. Yin, Cheoljin Kim, Jaesung Park, Aniruddh Solanki, Pavel Ivanoff Reyes, Yicheng Lu, Kwang S. Kim, and Ki-Bum Lee, 2012, Label-free

polypeptide-based enzyme detection using a graphene-nanoparticle hybrid sensor, *Advanced materials*, 24, 6081-6087

[3] Soo Min Cho, Hyunjin Vincent Kim, Sejin Lee, Hye Yun Kim, Woong Kim, Tae Song Kim, Dong Jin Kim and Young Soo Kim, 2014, Correlations of amyloid- $\beta$  levels between CSF and plasma in acute AD mouse model, *Scientific reports*, 4, 6777

## Preparation and Characterization of Chitonated Fatty Acid Liposome in Carbohydrate-based Gel

H.W., Tan, S. X., Tiew, M., Misran and H. M. Ali

*CENAR, Department of Chemistry, Faculty of Science, University of Malaya, 50603 Kuala Lumpur, Malaysia.*

*Email: [misni@um.edu.my](mailto:misni@um.edu.my)*

### ABSTRACT

Liposomes in polymer gel preparation have opened up a new dimension in pharmaceutical formulation especially topical application as gels usually have longer contact time with the skin. In this study, liposomal gel was prepared by mixing oleic acid (OA) liposomes coated acylated chitosan into carbohydrate based gel of iota-carrageenan and carboxymethyl cellulose (*iC*-CMC) gel. The acylated chitosans were prepared by using water soluble low molecular weight (LMW) chitosan (10 and 25 kDa). The coating of the chitosan layer on OA liposomes was confirmed by its microscopic images and physicochemical properties, such as zeta potential and size of the liposomes. After surface modification, we have also observed enhanced liposome structure rigidity and decrease in the average particle size by at least 20 nm as compared to the unmodified OA liposomes. The decrease in the liposome average diameter was also accompanied with an increase of their average zeta potential from -86 mV to -60 mV indicated that successful coating on the surface of OA liposomes. The gel mixture with 5:5 of *iC*-CMC ratio has been found to be the optimum composition. Under the optimum composition, the gel matrix has showed optimum flexibility and elasticity. The liposomal gels were prepared by dispersing the liposomes into the optimized gel matrix individually. Based on the rheological results, the presence of liposomes has been enhanced the elasticity and viscosity of the liposomal gel. The liposomal gels were also showed greater shear thinning effect, which indicated the better spreading ability of the liposomal gels as compared to the pure 5:5 of *iC*-CMC mixed gel. However, the changes in the viscous modulus ( $G''$ ) which described the physical entanglements within the gel matrix were negligible in the presence of liposomes. This result indicated that the liposomes do not alter the internal gel network structure, but accommodated in the void spaces in the gel.

**Keywords:** *Liposomes in gel, oleic acid liposome, acylated chitosan, carrageenan, carboxymethyl cellulose.*

**References:**

- [1] GE, L., ZHU, J.B., XIONG, F. & NI, B. 2007. Preparation, Characterization and Pharmacokinetics of N-Palmitoyl Chitosan Anchored Docetaxel Liposomes. *J. Pharm.Pharmacol.*, 59, 661–667.
- [2] GUO, J., PIN, Q., JIANG, G., HUANG, L. & TONG, Y. 2003. Chitosan-coated Liposomes: Characterization and Interaction with Leuprolide. *Int. J. Pharm.*, 260, 167-173.
- [3] MADY, M.M., DARWISH, M.M., KHALIL, S. & KHALIL, W.M. 2009. Biophysical Studies on Chitosan-coated Liposomes. *Eur. Biophys. J.*, 38, 1127-1133.
- [4] MOURYA, V.K., INAMDAR, N.N. & TIWARI, A. 2010. Carboxymethyl Chitosan and Its Applications. *Adv. Mater. Lett.*, 1, 11–33.
- [5] MOURTAS, S. HAIKOU, M. THEODOROPOULOU, M., TSAKIROGLOU, C. & ANTIMISIARIS, S.G. 2008. The Effect of Added Liposomes on the Rheological Properties of A Hydrogel: A Systematic Study. *J. Colloid Interf. Sci.*, 317, 611-619.
- [6] ORTONA, O., D'ERRICO, G., MANGIAPIA, G. & CICCARELLI, D. 2008. The Aggregation Behavior of Hydrophobically Modified Chitosans with High Substitution Degree in Aqueous Solution. *Carbohydr. Polym.*, 74, 16-22.
- [7] PARK, S.I., LEE, E.O., KIM, J.W., KIM, Y.J., HAN, S.H. & KIM, J.D., 2011. Polymer-Bybridized Liposomes Anchored with Alkyl Grafted Poly(Asparagine). *J. Colloid Interface Sci.* 364, 31-38.
- [8] TAKEUCHI, H., MATSUI, Y., YAMAMOTO, H. & KAWASHIMA, Y., 2003. Mucoadhesive Properties of Carbopol or Chitosan-Coated Liposomes and Their Effectiveness in the Oral Administration of Calcitonin to Rats. *J. Control. Release*, 86, 235-242.
- [9] TAN, H.W. & MISRAN, M. 2012. Characterization of Fatty Acid Liposome Coated with Low Molecular Weight Chitosan, *J. Liposome Res.*, 22(4), 329-335.
- [10] TAN, H.W. & MISRAN, M. 2013. Polysaccharide- anchored Fatty Acid Liposome. *Int. J. Pharm.*, 441, 414-423.
- [11] TAN H.W. & MISRAN, M. 2014. Effect of Chitosan-Modified Fatty Acid Liposomes on the Rheological Properties of the Carbohydrate-Based Gel. *Applied Rheology*, 24(3):34839.



## MEMBRANES BASED ON QUITOSAN-PULLULAN AND EXTRACTS OF *H. virginiana*, *C. sinensis* AND *A. adstringens*: ANTIMICROBIAL AND CITOTOXIC ACTIVITIES

Emmanuel Garza Zaragoza, Alberto Gómez Treviño, María del Socorro Flores González, Carlos Solís Rojas, Katiushka Arévalo Niño\*

Instituto de Biotecnología, Facultad de Ciencias Biológicas, UANL, Cd. Universitaria S/N, San Nicolás de los Garza, Nuevo León, C.P. 66455, México

*katiushka,arevalonn@uanl.edu.mx;karevalo01@hotmail.com*

This work is focused directly to the addition of extracts of traditional medicinal plants (*H. virginiana*, *C. sinensis* and *A. adstringens*) in a chitosan-pullulan platform to generate appropriate based materials for biomedical applications biopolymers. The antimicrobial effect of chitosan based active membranes and pullulan was evaluated against *Streptococcus mutans* ATCC 700610 and *Candida albicans* ATCC 90029 strains [1]. Based on preliminary antimicrobial activity test, the MIC values were determined with 123.9 mg/ml for *C. sinensis*, 30.87 mg/ml for *H. virginiana* and 156.8 mg/ml for *A. adstringens*. The cytocompatibility of active membrane was evaluated by the Neutral Red method using a fibroblast cell line [2]. After 24 hours, cell viability was 82%, 88% and 100% for functionalized membranes *C. sinensis*, *A. adstringens* and *H. virginiana*, respectively.

**Keywords:** *drug delivery, chitosan, pullulan, antimicrobial*

[1] SEDIGHINIA, F., SAFIPOUR, A.A., SOLEIMANPOUR, S., ZARIF, R., ASILI, J., GHAZVINI, K. 2012. Antibacterial activity of *Glycyrrhiza glabra* against oral pathogens: an *in vitro* study. Avicenna Journal of Phytomedicine, Vol. 2, No. 3, 118-124.

[2] SABUDIN, M.A., DERMAN, I.Z., NOORSAL, K. 2012. In Vitro Cytotoxicity and Cell Seeding Studies of a Chitosan-silver Composite for Potential Wound Management Applications. Journal of Engineering Science, 8, 29-37.

## Switchable fluorescent materials as probes for sensing and imaging

Tao Yi,\* Ying Wen, Guanglei Lv, Keyin Liu, Luyan Meng

<sup>1</sup>*Department of Chemistry, Fudan University, Shanghai, 200433, China*

*E-mail: yitao@fudan.edu.cn*

Switchable fluorescent materials whose emission properties can be tuned or even switched by environmental stimuli such as light<sup>[1]</sup> or chemical input,<sup>[2]</sup> can be used as probes for sensing biomolecules. Some of them showed exciting applications in imaging living cells. Herein, naphthalimide based ratiometric fluorescent probes and photoswitchable diarylethene derivatives have been developed for the detection of reactive oxygen species (ROS, including hydroxyl radicals and hydrogen peroxide) and DNA, respectively.

The probes for ROS show high selectivity and sensitivity toward hydroxyl radicals or hydrogen peroxide (H<sub>2</sub>O<sub>2</sub>). Moreover, they have no cellular toxicity, and can be effectively used for intracellular detection of ROS. By introducing a nuclear localization signal (NLS) peptide, the ratiometric H<sub>2</sub>O<sub>2</sub> fluorescent probe can be delivered into nuclei and can monitor nucleus H<sub>2</sub>O<sub>2</sub>.

Photoswitchable molecules can undergo conformational change between two isomers with different photophysical properties triggered by light,<sup>1</sup> which might have significant potential applications in DNA-related bio-events. Herein, thiazole orange-modified diarylethene derivatives were designed and their DNA-gated photochromic properties were explored. Those molecules act as an effective DNA marker, whereas DNA can light-up the chromophore and unlock the photochromic activity of the diarylethene even within cells.

### References

- [1] (a) Y. Zou, T. Yi, S. Xiao, F. Li, C. Li, X. Gao, J. Wu, M. Yu, C. Huang, *J. Am. Chem. Soc.* **2008**, *130*, 15750–15751. (b) Piao, X.; Zou, Y.; Wu, J.; Li, C.; Yi, T. *Org. Lett.* **2009**, *11*, 3818-3821.
- [2] (a) X. Cao, Y. Wu, K. Liu, X. Yu, B. Wu, H. Wu, Z. Gong, T. Yi, *J. Mater. Chem.* **2012**, *22*, 2650 - 2657. (b) J. Wu, Y. Zou, C. Li, W. Sicking, I. Piantanida, T. Yi, C. Schmuck, *J. Am. Chem. Soc.* **2012**, *134*, 1958-1961.

**Poly(amidoamine) dendrimers as a tool for the design of functionalized iron oxide nanoparticles for multimodal MRI imaging and drug delivery**

Adriano Boni,<sup>1</sup> Giovanni Signore,<sup>1</sup> Silvia Villa,<sup>1</sup> Claudia Innocenti,<sup>2</sup> Claudio Sangregorio,<sup>3</sup> Luca Menichetti,<sup>4</sup> Vincenzo Piazza<sup>1</sup>

<sup>1</sup>Center for Nanotechnology Innovation @NEST, Istituto Italiano di Tecnologia, Piazza San Silvestro, 12 - 56127 Pisa, Italy

<sup>2</sup>INSTM and Department of Chemistry, University of Florence, 50019 Sesto F. no, Firenze, Italy

<sup>3</sup>CNR-ISTM and INSTM, via Golgi 19, 20133 Milano, Italy

<sup>4</sup>CNR-IFC, Istituto di Fisiologia Clinica, via Moruzzi 1, 56124 Pisa, Italy

*E Mail/ Contact Détails*

Adriano Boni, PhD

Istituto Italiano di Tecnologia, Center for Nanotechnology Innovation @NEST, Piazza San Silvestro, 12, 56127 Pisa, Italy

+39 050 509 119 (tel)

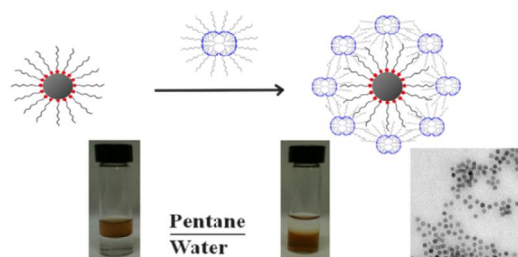
+39 050 509 417 (fax)

[adriano.boni@iit.it](mailto:adriano.boni@iit.it) (e-mail)

Magnetic nanoparticles are often synthesized by decomposition of organometallic precursors into hot surfactant solutions, a technique that results in highly crystalline iron oxide cores with a narrow size distribution. In order to use these nanoparticles for biomedical applications, replacement of the hydrophobic coating with a hydrophilic one

is necessary to obtain stable and injectable aqueous solutions. Among the available hydrophilic coatings, dendrimers, highly monodisperse hyperbranched polymers with a repetitive and perfectly defined structure, have attracted considerable interest.<sup>4-7</sup>

Recently, we presented a novel and facile method to attach commercially available lipid-modified PAMAM dendrimers to the surface of iron oxide nanoparticles. Here we report the latest developments of this work.



By means of this platform, we have been able to tune the relaxometric properties of iron oxide nanoparticles, such as coating thickness and core size, to obtain the best relaxometric efficiency with a high degree of control. Also, we have performed *in vitro* biocompatibility tests and half-life *in vivo* measurements to demonstrate the possibility to use this material as MRI negative contrast agent. Thanks to the versatility of the PAMAM base coating, we have been able to successfully modify the surface of the nanoparticles for specific applications. Lipophilic drugs, such as coumarin-6 and doxorubicin, could be easily loaded on the nanoparticles by entrapping them into the double lipidic shell formed by the oleic acid and the PAMAM C12 chains on the surface. These results are interesting in view of theranostic applications where the PAMAM coated nanoparticles are able to increase the diagnostic efficiency of MRI, and also to perform therapy by specific deliver and release of drugs.

**Keywords:** *Nanoparticles, MRI, Iron oxide, magnetic, drug delivery*

[1] SUN, S., ZENG, H. 2002. Size-Controlled Synthesis of Magnetite Nanoparticles. *Journal of the American Chemical Society*, 124, 28, 8204-8205.

- [2] ROCKENBERGER, J., SCHER, E. C., ALIVISATOS, A. P. 1999 A New Nonhydrolytic Single-Precursor Approach to Surfactant-Capped Nanocrystals of Transition Metal Oxides. *Journal of the American Chemical Society*, 121, 49, 11595-11596.
- [3] HYEON, T., LEE, S. S., PARK, J., CHUNG, Y., NA, H. B. 2001 Synthesis of Highly Crystalline and Monodisperse Maghemite Nanocrystallites without a Size-Selection Process. *Journal of the American Chemical Society*, 123, 51, 12798-12801.
- [4] WANG, S. H., SHI, X., VAN ANTWERP, M., CAO, Z., SWANSON, S. D., CI, X., BAKER, J. R. 2007 Dendrimer-Functionalized Iron Oxide Nanoparticles for Specific Targeting and Imaging of Cancer Cells. *Advanced Functional Materials*, 17, 16, 3043-3050.
- [5] SHI, X., WANG, S. H., SWANSON, S. D., GE, S., CAO, Z., VAN ANTWERP, M. E., LANDMARK, K. J., BAKER, J. R. 2008 Dendrimer-Functionalized Shell-crosslinked Iron Oxide Nanoparticles for In-Vivo Magnetic Resonance Imaging of Tumors. *Advanced Materials*, 20, 9, 1671-1678.
- [6] SHI, X., THOMAS, T. P., MYC, L. A., KOTLYAR, A., BAKER, J. R. 2007 Synthesis, characterization, and intracellular uptake of carboxyl-terminated poly(amidoamine) dendrimer-stabilized iron oxide nanoparticles. *Physical Chemistry Chemical Physics*, 9, 42, 5712-5720.
- [7] LANDMARK, K. J., DIMAGGIO, S., WARD, J., KELLY, C., VOGT, S., HONG, S., KOTLYAR, A., MYC, A., THOMAS, T. P., PENNER-HAHN, J. E., BAKER, J. R., HOLL, M. B., ORR, B. G. 2008 Synthesis, Characterization, and in Vitro Testing of Superparamagnetic Iron Oxide Nanoparticles Targeted Using Folic Acid-Conjugated Dendrimers. *ACS Nano*, 2, 4, 773-783.
- [8] BONI, A., ALBERTAZZI, L., INNOCENTI, C., GEMMI, M., BIFONE, A. 2013 Water dispersal and functionalization of hydrophobic Iron Oxide nanoparticles with lipid-modified poly(amidoamine) dendrimers. *Langmuir*, 29, 35, 10973-10979.

**An investigation on the buckling of soft spherical shells perforated by complex shapes**

Sen Lin<sup>1</sup>, Yi Min Xie<sup>1</sup>, Qing Li<sup>2</sup>, Xiaodong Huang<sup>1</sup>, Shiwei Zhou<sup>1†</sup>

<sup>1</sup>Centre for Innovative Structures and Materials, School of Civil, Environmental and Chemical Engineering, RMIT University, GPO Box 2476, Melbourne 3001, Australia. E-mail: shiwei.zhou@rmit.edu.au; Fax: +61-3-9639-0138; Tel: +61-3-9925-2098

<sup>2</sup>School of Aerospace, Mechanical and Mechatronic Engineering, The University of Sydney, NSW 2006, Australia

The buckling and its related phenomenon have attracted increasing interests recently as they occur ubiquitously in soft materials. The buckling and post-buckling performances of spherical shells perforated by various shapes under external pressure were investigated systematically in this paper. The complex aperture shapes generated from a mathematical superformula in 2D were projected on the spherical shell. The numerical simulation was conducted on Abaqus, in which the velocity-controlled loads and selective geometric imperfection were used to obtain desirable buckling patterns. It has been found the aperture shape is significant to the buckling performance and a spherical shell perforated by the rounded square shape shows maximal volume retraction ratio, together with the lowest energy consumption. This structure was fabricated via 3D printing technique and an experimental platform was developed to validate the simulation results.

**Impact of self-assembled molecular interconnects on the immobilization and hybridization of DNA at semiconductor substrates**

Bee Min Goh, Andrew Pike

Chemical Nanoscience Laboratory, School of Chemistry, Faculty of Science, Agriculture and Engineering, Bedson Building, Newcastle University, NE1 7RU

[bee-min.goh@newcastle.ac.uk](mailto:bee-min.goh@newcastle.ac.uk) and [andrew.pike@newcastle.ac.uk](mailto:andrew.pike@newcastle.ac.uk)

The sensitivity and selectivity of biosensors hinge on the integrity of the immobilisation of DNA probes onto the solid support. This immobilisation step is crucial as it ensures the correct orientation and high accessibility of the probes for binding with complementary strands. This ultimately determines the efficacy of the hybridisation and hence signal strength for biosensor detection. Here, we report our investigations into the effect of different molecular interconnects (length and molecular structure) on the immobilization, and hybridization using electrochemical methods. We covalently attached ferrocenyl-modified amino-terminated DNA onto the self-assembled linkers at different solid supports; silicon oxide, silicon hydride and indium tin oxide. Various characterization techniques, contact angle measurement, X-ray photoelectron spectroscopy and atomic force microscopy and cyclic voltammetry were employed to examine the surface properties. The data gathered provides insights into the development of DNA microarray field and the optimization for biosensor platforms.

***Keywords: DNA, hybridization, immobilization, self-assembly, molecular interconnects.***

## **Detection of DNA damage by a combined effect of metal oxide nanoparticles and UV-C irradiation using DNA biosensor**

Ignat, Labuda

Institute of Analytical Chemistry, Faculty of Chemical and Food Technology, Slovak University of Technology in Bratislava, Radlinského 9, 812 37 Bratislava, Slovakia.

*E Mail/ jan.labuda@stuba.sk*

Due to increasing use of metal oxide nanoparticles with inevitably release into the environment and thereby exposure to human life, an interaction of Fe<sub>3</sub>O<sub>4</sub>, ZnO, TiO<sub>2</sub> with dsDNA was investigated with respect to an effect of nanosized materials on the chemical stability of the most important biomacromolecule. Size of nanoparticles was evaluated by scanning electron microscopy (SEM) and dynamic light scattering (DLS). For the investigation, a nanostructured electrochemical biosensors with immobilized layers of salmon sperm DNA and metal oxide nanoparticles were prepared. Using cyclic voltammetry and electrochemical impedance spectroscopy with the ferrocyanide DNA indicator, a significant effect of the nanoparticles on degradation of DNA in the presence of UV-C irradiation ( $\lambda = 254$  nm) for 20 to 300 s was detected. Two experimental approaches were used, namely irradiation of the metal oxide–DNA layer immobilized on the electrode and irradiation of the metal oxide–DNA dispersion in solution followed by its immobilization on the electrode. The deep DNA degradation was confirmed by square wave voltammetric measurements of intrinsic signals of the DNA bases moieties as well as by gel electrophoresis.

**Acknowledgement:** This work was supported by the Scientific Grant Agency VEGA of the Slovak Republic (Project 1/0361/14), Slovak Research and Development Agency under the contract No. APVV-0797-11, and the National Scholarship Programme of the Slovak Republic (Teodora Ignat).

**Keywords:** *DNA damage, metal oxide nanoparticles, UV irradiation, DNA biosensor*



## Water-soluble conjugated polymer-based chemo- and biosensors

Han Young Woo

*Department of Cogno-Mechatronics Engineering, Pusan National University, Miryang  
627-706, Republic of Korea*

E-mail: hywoo@pusan.ac.kr

Ionic conjugated polyelectrolytes (CPEs) have established themselves as an optical platform in chemical- and biological sensors with high sensitivity by virtue of their light harvesting properties.<sup>1-3</sup> CPEs are described by a  $\pi$ -conjugated backbone with ionic pendant groups, which make them water-soluble and/or bio-compatible. Here, we designed a novel strategy by combining biological molecular beacon aptamers (MBAs) and a synthetic polymer, to tune the detection range for weakly binding target materials and investigated principal factors governing the tuning mechanisms. ATP was selected as a target material due to the weak binding constant with its complementary aptamer. A series of MBAs (MBA1~MBA5) were designed so that the differences in structure lead to different stem stabilities. The MBAs contain the same ATP-specific aptamer sequence within the loop substructure, while their stem interactions were fine-tuned by changing the number of Guanine (G)-Cytosine (C) triple hydrogen bonds. As described in detail, the extension of the detection range depends critically on the competition between opening of the ATP/MBA G-quadruplex by CPEs and the composite influence by ATP/aptamer binding and the stem interactions. With increasing stem stability (MBA1  $\rightarrow$  MBA5), the weak binding affinity of ATP and its aptamer was successfully compensated to show resistance to opening by CPEs, resulting in a significantly broadened detection range with remarkably improved LOD: from millimolar up to nanomolar concentrations.

- [1] Q. Zhou, T. M. Swager, J. Am. Chem. Soc. 117, 7017 (1995).
- [2] B. S. Gaylord, A. J. Heeger, G. C. Bazan, Proc. Natl. Acad. Sci. U. S. A. 99, 10954 (2002).
- [3] B. Kim, I. H. Jung, M. Kang, H.-K. Shim, H. Y. Woo, J. Am. Chem. Soc. 134, 3133 (2012).

## **Characterization and fabrication of nanocomposite thin films of PANI embedded with Ag-Mn alloy for *E. coli* sensor**

H. Abdullah<sup>1\*</sup>, Norshafadzila Mohammad Naim<sup>1</sup>, Aidil Abdul Hamid<sup>2</sup>

<sup>1</sup>Department of Electrical, Electronic and System Engineering, Faculty of Engineering and Built Environment, 43650 UKM, Bangi, Selangor, Malaysia

<sup>2</sup>School of Biosciences and Biotechnology, Faculty of Science and Technology, 43650 UKM, Bangi, Selangor, Malaysia

\*E-mail: [huda@eng.ukm.my](mailto:huda@eng.ukm.my)

Recently, considerable attention has been compensated for the synthesis of polymer-metal nanocomposite materials for detection microbiological organisms such as *Escherichia coli* (*E. coli*). In this study, we presented a simple method of prototype *E. coli* sensor based on polyaniline with Ag-Mn nanocomposite thin films for biosensor. The nanocomposite of polyaniline (PANI) and bimetallic nanoparticles of silver and manganese were prepared by the oxidative polymerization of aniline and the reduction process of bimetallic compound with the presence of nitric acid and PVA. The samples were varied with different concentration of Ag-Mn alloy. The morphology and structure properties of these film sensors were characterized by X-ray diffraction (XRD), UV-Visible spectroscopy and transmittance electron microscopy (TEM). The sensor performance was conducted using current-voltage (*I-V*) measurement. XRD analysis shows the crystallite face-centered cubic structure of Ag, Mn and Ag-Mn. The crystallite sizes are around 30 nm - 40 nm and increases with the increment of Mn concentration. UV-Vis absorption spectra show the maximum peaks at around 420 nm – 430 nm. The microphotograph from TEM image shows the nanospherical of Ag-Mn alloy particles. The sensor performance of PANI-Ag-Mn nanocomposite thin films upon *E. coli* cells in the liquid medium indicates the sensitivity increases when Mn concentration was increased.

**Keywords:** *Polyaniline; Ag-Mn; nanocomposite; thin films; E. coli, biosensor.*

## Sensitive and Selective detection of nanotoxic material using resonance sensor

Kuewhan Jang<sup>1†</sup>, Chanho Park<sup>1†</sup>, Juneseok You<sup>1</sup>, Jinsung Park<sup>2\*</sup>, Sungsoo Na<sup>1\*</sup>

<sup>1</sup>Department of Mechanical Engineering, Korea University, Seoul 136-701, Republic of Korea

<sup>2</sup>Department of Control and Instrumentation Engineering, Korea University, Sejong 339-700, Republic of Korea

### Abstract

For the several decades, various nanomaterials are broadly used in industrial fields, research areas and commercialized products. Among many nanomaterials, silver ion, carbon nanotube, ZnO, and mercury ion etc are of the widely used nanomaterials in real life. However, high toxicity of those materials has been reported and the detection method is required for human health and environment. In present study, high-sensitive, label-free detection methods of nanotoxic materials are described.

We have developed a sensitive and selective quartz crystal microbalance (QCM) based resonance sensor for detection of nanotoxic materials by using frequency shift. In this study, we propose the sensitive in situ detection of nanotoxic materials by using QCM functionalized with a specific DNA for a target material. It also allows the detection of target material rapidly in real time. In contrast to the conventional methods, this method is label-free and sensitive, capable of direct rapid detection and real-time monitoring. The results suggest that QCM-based resonance sensor opens a new avenue for the development of a practical water-testing sensor.

## A liquid flow valve made from a functional composite gel

Christoffer Abrahamsson<sup>1\*</sup>, Hanzhu Zhang<sup>1</sup>, Michael Persson<sup>1,2</sup>, Ellis Meng<sup>3</sup>, Magnus Nydén<sup>4</sup>

<sup>1</sup>Chemical and Biological Engineering, Chalmers University of Technology, Kemivägen 10, 412 96, Gothenburg, Sweden.

<sup>2</sup>Akzo Nobel Pulp and Performance Chemicals AB, 445 80, Bohus, Sweden.

<sup>3</sup>Biomedical Engineering, University of Southern California, 1042 Downey Way, DRB-140, Los Angeles, CA, 90089-1111, USA

<sup>5</sup>Ian Wark Research Institute, University of South Australia, Mawson Lakes Campus, Mawson Lakes, SA, 5095, Australia.

*\*Corresponding author, e-mail: abrahamc@chalmers.se*

Previously, controlled drug delivery<sup>1</sup> has been shown through composite membranes containing stimuli responsive microgels. This study shows that also the rate of a pressurized liquid flow can be controlled with a temperature responsive material acting as a liquid flow valve for use in e.g. drug-delivery and microfluidic applications. The sol-gel material synthesis method used in this study could with relative ease be adapted to other types of colloidal materials as well as bulk material geometries, while the previously used solvent casting<sup>1</sup> method is limited to a membrane geometry. The active component in the material is temperature responsive poly(N-isopropylacrylamide) microgels that are dispersed in a colloidal silica gel matrix. While the matrix remains structurally static, the reversible swelling of the microgel as a response to controlled temperature variations opens or closes porous pathways conductive to liquid flow through the material. The results showed that by varying the temperature the flow rate through the material could effectively be more than doubled.

**Keywords:** *composite, temperature responsive, microgels, flow valve*

[1] TIMKO B., ARRUEBO M., SHANKARAPPA S., MCALVIN B., OKONKWO O., MIZRAHI B., STEFANESCU C., GOMEZ L., ZHU J., ZHU A., SANTAMARIA J., LANGER R., and KOHANE D. 2014. Near-infrared-actuated devices for remotely controlled drug delivery. PNAS, 111, 4, 1349-1354.

## Magnetite Nanoparticles Functionalized with Vitamin E analogues: Anticancer Effects

A. Angulo-Molina<sup>1,2</sup>; M.A. Méndez-Rojas<sup>3</sup>; T. Palacios-Hernández<sup>4</sup>; S. Hernández<sup>5</sup>; O.E. Contreras-López<sup>6</sup>; G.A. Hirata-Flores<sup>6</sup>; A. Delgado<sup>7</sup>; J.R. Reyes-Leyva<sup>8</sup>; J. Hernández<sup>9</sup>; C. Velazquez<sup>1</sup>; A. Garibay<sup>1</sup>; O Valenzuela<sup>1</sup>; M. Barboza<sup>2</sup>; M. Pedroza-Montero<sup>2</sup>

1. Dpto. Químico Biológicas, Universidad de Sonora (UNISON), Hermosillo, Son. Méx.
2. Dpto. de Investigación en Física, Universidad de Sonora (UNISON), Hermosillo, Son. Méx.
3. Universidad de las Américas, Puebla (UDLAP), Puebla, Méx.
4. Johns Hopkins University (JHU), USA.
5. Universidad Panamericana (UP), DF, Méx.
6. Centro de Nanociencias y Nanotecnología CNYN-UNAM, Ensenada, BC, Méx.
7. Hospital de Especialidades, IMSS, Centro Médico Siglo XXI. México, DF.
8. Centro de Investigación Biomédica de Oriente (CIBIOR), IMSS, Metepec, Puebla, Méx.
9. Centro de Investigación en Alimentación y Desarrollo (CIAD), Hermosillo, Son. Méx.

Corresponding author: aracelyam@hotmail.com

### ABSTRACT

Iron oxide nanoparticles (Nps) possess exceptional physical and chemical properties, which led to their potential use in modern anticancer therapies. We reported synthesis and characterization of Nps functionalized with a vitamin E analogue, alpha-tocopheryl succinate (Nps@ $\alpha$ -TOS) to enhance its resistance. Also, we found Nps protect and enhance the *in vitro* and *in vivo* anticancer bioactivity of this vitamin E analogue. Electronic microscopy studies revealed sphere-like nanoparticles with a 15 nm average size. Inorganic chemical composition and magnetite crystalline phase was confirmed by energy dispersive X ray spectroscopy and selected area electron diffraction respectively. Organic and functional groups were analyzed by FTIR. The load drug was estimated by thermogravimetric analysis. *In vitro* evaluation shows that Nps@ $\alpha$ -TOS selectively affected the viability of cervical cancer cells, a resistant cell line, in a dose and time dependent way at 24-72 h ( $p < 0.05$ ) without toxic effects for nonmalignant cells. For *in vivo* evaluation, a melanoma model in BALB/c nude mice was established. The mice were i.t. treated with Nps@ $\alpha$ -TOS (0.075-2 mg) each third day for two weeks. After treatment, the major organs not showed apparently toxic effects and tumor growth was affected in a dose dependent manner ( $p < 0.05$ ). Nps@ $\alpha$ -TOS could be a multifunctional nanopatform candidate with additional biomedical applications; magnetite core can be used for cancer cell ablation through hyperthermia and the vitamin E analogue may induce radiosensitization of cancer cells and to protect the normal cells against radiation induced damage. However, further studies are needed in order to corroborate the potential application and anticancer bioactivity of these multifunctional nanoparticles.

### Reference

A. Angulo-Molina, M. Méndez, T. Hernandez, O.E. Contreras-López, G. Hirata-Flores, et al. Magnetite nanoparticles functionalized with  $\alpha$ -tocopheryl succinate ( $\alpha$ -TOS) promote selective cervical cancer cell death. *Journal of Nanoparticle Research* **16** 2528 (2014)

**Bioengineering novel floating nanoparticles for protein and drug delivery**

Priya DasSarma, Therese Poku, Ram Karan, Jong-Myoung Kim, Wolf Pecher, and Shiladitya DasSarma, University of Maryland School of Medicine, Baltimore MD USA

Introduction: Many microbes produce buoyant nanoparticles called GVNPs which are hollow structures filled with gas and bounded by a thin and extremely stable protein membrane. GVNPs from *Halobacterium* sp. NRC-1, a salt-loving microbe, are non-toxic, easily purified, and may be used as a vehicle for protein delivery (1-5). Foreign proteins may be displayed on GVNPs by insertions in the *gvpC* gene within a large *gvp* gene cluster. Methods and Results: To establish an improved genetic system for bioengineering of GVNPs, we constructed a strain of NRC-1 deleted solely for the *gvpC* gene ( $\Delta gvpC$ ), which resulted in small nanoparticles observable by transmission electron microscopy (6). Next, we introduced expression plasmids containing N-terminal coding portions of *gvpC*, or the complete *gvpC* gene, into the  $\Delta gvpC$  strain. GvpC protein and variants were localized to the GVNPs by Western blotting analysis, and their effect on modulating the size of nanoparticles was established by electron microscopy. Subsequently, a synthetic gene coding for *Gaussia princeps* luciferase was fused to the *gvpC* gene fragments on expression plasmids, and resulted in an enzymatically active GvpC-luciferase fusion protein bound to GVNPs. Discussion: These results represent a significantly improved genetic system for presenting or displaying foreign proteins on *Halobacterium* GVNPs. The luciferase fusion is an ideal reporter for studying protein display on GVNPs. The reported work extends the types of ligands that may be displayed on GVNPs by genetic engineering to peptides, antigenic proteins, and enzymes (1,4-7).

## References:

1. DasSarma S. et al. *J. Bacteriol.* 176:7646-7652, 1993.
2. Ng, et al. *Genome Res.* 8:1131-1141, 1998
3. Shukla, H.D. and S. DasSarma. *J. Bacteriol.* 186:3182-3186, 2004.
4. Stuart, E.S. et al. *J. Biotechnol.* 88:119-128, 2001.
5. Stuart, E.S. et al. *J. Biotechnol.* 114:225-237, 2004.
6. DasSarma, S. et al. *BMC Biotechnol.* 13:112, 2013.
7. DasSarma, P. et al. *Vaccine* 32:4543-4549, 2014.

## **Fabrication of drug carrier polyvinyl alcohol/chitosan composite nanofiber and its drug release**

Zhixiang Cui<sup>1,2</sup>, Qianting Wang<sup>1</sup>, Pingqiang Dai<sup>1</sup>, Qiong Liu<sup>1</sup>, Junhui Si<sup>1</sup>, Wenzhe Chen<sup>2</sup>

( 1 School of Materials Science and Engineering, Fujian University of Technology, Fujian, Fuzhou 350108; 2 School of Materials Science and Engineering, Fuzhou University, Fujian, Fuzhou 350000;)

*E*Mail/ [cuizhixiang2006@126.com](mailto:cuizhixiang2006@126.com); [chenwz@fjut.edu.cn](mailto:chenwz@fjut.edu.cn)

In this study, the polyvinyl alcohol(PVA)/chitosan(CS) composite nanofiber was fabricated by using electrospinning, and the drug release characteristic of PVA/CS composite nanofiber wrapped with amoxicillin was observed through UV-visible spectrophotometer. The morphology and diameter of the electrospun nanofibers were examined by scanning electron microscopy (SEM). The results showed that the morphology and diameter of the nanofibers were mainly affected by weight ratio of PVA/CS blend at constant applied voltage, collection distance and drug content. The average fiber diameter was in the range of 150–215 nm. The drug released rate of PVA/CS composite nanofiber decreases with increasing of release time, CS and drug content in the drug carrier. Moreover, it was observed that the PVA/CS composite nanofiber provided a slower release rate of the entrapped drug in compare to PVA nanofiber.

***Keywords: Electrospinning, Composite nanofiber, Polyvinyl alcohol (PVA)/chitosan (CS), Drug release***

### **Delivery of mRNA via layer-by-layer biodegradable capsules**

Mitali Kakran<sup>1\*</sup>, Maria N. Antipina<sup>1</sup>, John Tng Weiquan<sup>2</sup>, Hongqing Liang<sup>2</sup>, Huck Hui Ng<sup>2</sup>

<sup>1</sup>*Institute of Materials Research and Engineering, A\*STAR, 117602, Singapore*

<sup>2</sup>*Genome Institute of Singapore, A\*STAR, 60 Biopolis Street, Singapore 138672*

\* Presenting author, Email: kakranm@imre.a-star.edu.sg

Viral vectors are efficient systems for nucleotide delivery but they encompass risks of mutagenesis, safety, immunogenicity, and high production costs. This has encouraged researchers to focus on alternative nonviral systems. Currently available cationic lipid-based delivery or cationic complexes of DNA / RNA are often highly toxic for the cells or not efficient for many cell types. In our study to encapsulate and deliver RNA, we propose biodegradable microcapsules by the layer-by-layer (LbL) technique. This technique is based on the sequential adsorption of oppositely charged molecules, such as polyelectrolytes, onto a charged sacrificial template. The template is then dissolved, resulting in hollow capsules with a wall thickness in the nanometer range. Polyelectrolyte microcapsules (PEMs) have the advantages of mild preparation conditions, multifunctionality, and the capacity to encapsulate large amounts of material. Polyelectrolyte microcapsules are produced at room temperature using simple bench-top equipment, without organic solvents or harsh reaction conditions.

In the present study, we employed calcium carbonate microparticles as a sacrificial template. CaCO<sub>3</sub> microparticles represent “bio-friendly” tool for encapsulation of proteins and nucleic acids, enzymes and nanoparticles. Porous morphology of CaCO<sub>3</sub> offers large surface area and, thus, an opportunity to capture macromolecules with high efficiency. RNA was “pre-loaded” into the microspheres by coprecipitation in the process of their synthesis. Inorganic template extraction was performed after layer-by-layer coating by EDTA treatment. As outer shell, we used dextran sulfate (DS) and poly-L-arginine (PArg), which are known to be biodegradable polymers. The capsules prepared were tested for cellular non-toxicity and used for delivery of mRNA.



**Evaluation of multiple theranostic properties of polydopamine coated  
 $\text{Fe}_{0.65}\text{Co}_{0.35}@(\text{Fe}_{0.65}\text{Co}_{0.35})_3\text{O}_4$  nanocubes for cancer nanomedicinal application**

\*Julfakyan K<sup>1</sup>., Fatieiev Y<sup>1</sup>., Alsaiani Sh<sup>1</sup>, Deng L<sup>1</sup>., Ezzeddine A<sup>1</sup>., Abu Samra, D<sup>2</sup>., \*\*Khashab N<sup>1</sup>.

<sup>1</sup>CRD Lab., PSE Division, 4700 King Abdullah University of Science and Technology, Thuwal 23955-6900, Kingdom of Saudi Arabia

<sup>2</sup>CMS Lab., BESE Division, 4700 King Abdullah University of Science and Technology, Thuwal 23955-6900, Kingdom of Saudi Arabia

*\*E Mail - khachatur.julfakyan@kaust.edu.sa / Tel. +966544701780 / Address - 4700 King Abdullah University of Science and Technology, Thuwal 23955-6900, Kingdom of Saudi Arabia*

*\*\*E Mail – niveen.khashab@kaust.edu.sa / Tel. + +966 2 808-2410 / Address - 4700 King Abdullah University of Science and Technology, Thuwal 23955-6900, Kingdom of Saudi Arabia*

The objective of our work was the fabrication of single theranostic agent for cancer nanomedicine, which should be easily producible, cheap, biocompatible, spatially and temporally controllable and should have broader range of diagnostic and therapeutic modalities compared with previous works. Here we present the cost efficient and easy to scale-up, modified procedure of synthesis, controlled thin oxide shell formation and polydopamine coating with basic polymerization of dopamine hydrochloride in aqueous solution. Full characterization (HR-TEM, SEM, XRD, HR-TEM-EDAX, HR-TEM-SAED, SEM-EDAX, FTIR, UV-Vis-NIR, TGA, VSM) of novel system comprising of sub-micrometer sized  $\text{Fe}_{0.65}\text{Co}_{0.35}@(\text{Fe}_{0.65}\text{Co}_{0.35})_3\text{O}_4@PDA$  highly magnetic (with 226 emu/g value for the metal core  $\text{Fe}_{0.65}\text{Co}_{0.35}@(\text{Fe}_{0.65}\text{Co}_{0.35})_3\text{O}_4$ ) nanoparticles was done. In vitro MTT cell viability assay on HeLa cells showed no toxicity up to 100  $\mu\text{g}/\text{ml}$  of nanoparticles concentration. They are dual mode diagnostic agents with MRI ( $r^2=186.44 \text{ mM}^{-1}\text{s}^{-1}$ ) and X-Ray CT contrasting properties. The HeLa cells was used in *in vitro* assays. Doxorubicin delivery to the nuclei (laser fluorescence confocal microscopy) and 55% of death (MTT assay) at the concentration of 10  $\mu\text{g}/\text{ml}$  was registered. The release of doxorubicin

was demonstrated pH sensitive and attenuated in time behavior (temporal control). Specific absorption rate for 470 kHz alternating magnetic field hyperthermia was 180 W/g. Flow cytometry with PI staining demonstrated 60% cell death with 15 min of 808 nm NIR laser exposure at 0.3 kW of laser power and 30  $\mu\text{g/ml}$  of nanoparticles concentration. High magnetic saturation is prerequisite for potential magnetic targeting (special control), the size is within the range of EPR mediated accumulation. Summarizing, above mentioned nanocomposite has 5 theranostic modalities, which is more than previous works and may be considered as good candidate for further *in vivo* studies as “all-in-one” agent.

***Keywords: theranostic nanoparticles, drug delivery, magnetic hyperthermia, photothermal therapy, cancer***

***For poster presentation***

***Topic - Functional Biomaterials in Drug Delivery***

## Paper-Based Scale Bar Readout System for Quantitative Analysis

Devi D Liana<sup>1,2</sup>, Burkhard Raguse<sup>1</sup>, J. Justin Gooding<sup>2,3</sup> and Edith Chow<sup>1\*</sup>

<sup>1</sup> CSIRO Materials Science and Engineering, PO Box 218, Lindfield, NSW 2070, Australia

<sup>2</sup> School of Chemistry, The University of New South Wales, Sydney, NSW 2052, Australia.

<sup>3</sup> Australian Centre for NanoMedicine, The University of New South Wales, Sydney, NSW 2052, Australia.

Presenting author e-mail: [d.liana@student.unsw.edu.au](mailto:d.liana@student.unsw.edu.au)

\*Corresponding author e-mail: [edith.chow@csiro.au](mailto:edith.chow@csiro.au)

Developing a simple and low cost technology that can be used to monitor environmental conditions in-field as well as the health-state of people in resource-limited locations is a significant challenge [1]. Recently, paper has gained much interest as a sensing platform since it is abundant, disposable, lightweight and low in cost. However, interpreting the result of the sensor usually requires pairing with bulky and expensive external electronics which compromises the advantages of using paper-based sensors.

We herein present a simple quantitative scale bar readout system using electrochromic Prussian Blue/polyaniline on top of a paper-based gold nanoparticle film strip. The working principle of the readout is that when a voltage is applied across the gold nanoparticle film strip a voltage gradient is generated which will affect the colour of the electrochromic material at different positions along the strip. When the readout is integrated with a resistive sensor, the readout can be used to determine the resistance of the sensor (or changes in the resistance due to analyte exposure). Depending on the magnitude of the sensor's resistance and the voltage across it, this will affect the voltage across the readout. Quantitative analysis will be based on measuring the distance,  $d$ , along the strip where the colour change occurs. This type of readout could provide a viable alternative for recording the resistance of a sensor in a colorimetric manner without the need for additional instrumentation.

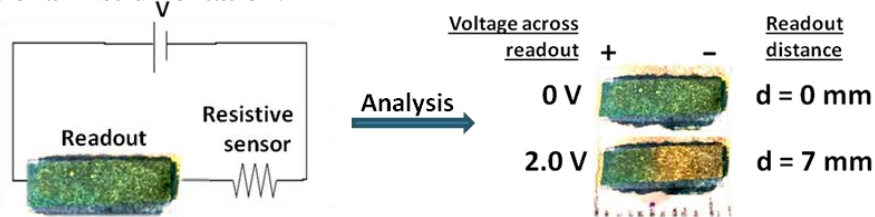


Fig. 1 Paper-based scale bar readout system integrated with a resistive sensor

**Keywords:** paper, gold nanoparticles, electrochromic materials, readout, low cost

Integrated sorting, concentration and real time polymerase chain reaction based diagnostic protocol for rapid detection of microorganisms\*

Monalisha Nayak<sup>1\*</sup>, Deepak Singh<sup>2\*</sup>, Himanshu Singh<sup>1</sup>, Rishi Kant<sup>1</sup>, Ankur Gupta<sup>1</sup>, □ Shashank Shekhar Pandey<sup>1</sup>, Swarnasri Mandal<sup>1</sup>, **Gurunath Ramanathan**<sup>2</sup> & Shantanu Bhattacharya<sup>1</sup>

There is a critical need to address issues related to food and water security as instances of adulteration and poisoning are increasing at an alarming rate around the globe. Therefore a rapid monitoring and testing of food and water quality to prevent contamination and disease outbreaks is a high end immediate need for humanity today. The work in this talk describes a microchip platform that carries out an ensemble of protocols which are otherwise carried in a molecular biology laboratory to achieve the global safety standards. The various steps in the microchip include pre-concentration of specific microorganisms from samples and a highly specific real time molecular identification utilizing a q-PCR process. The microchip process utilizes a high sensitivity antibody based recognition and an electric field mediated capture enabling an overall low LOD. The whole process of counting, sorting and molecular identification is performed in less than 4 hours for highly dilute samples.

\* this work was published in SCIENTIFIC REPORTS | 3 : 3266 | DOI: 10.1038/srep03266

# Symposia 6

## Advances in Catalysis

---

- Homogeneous and Heterogeneous Catalysis
- Nano and Environmental catalysis
- New concepts in catalyst design and preparation
- Industrial and green catalysis
- Theoretical modeling of catalytic reactions
- Catalyst preparation & characterization
- Organo-metallic catalyst
- Catalysis for chemical energy transformation and storage
- Catalysis for clean energy, Transportation, industrial and domestic fuels
- Catalytic transformation of CO<sub>2</sub>
- Others

# INDEX PAGE

1. Promising electrospun carbon fibers material for abiotic and enzymatic catalysis in hybrid biofuel cell for energy conversion <b>AUTHOR:</b> Mr. Sophie Tingry	1
2. Rutile TiO <sub>2</sub> Hierarchical Microspheres: A Promising Multi -Functional Material As High-Rate/Long-Life Anode And Advanced Catalyst <b>AUTHOR:</b> Prof. Guangshe Li	2
3. Development Of Ni Based Nano-Oxyhydride Catalysts: Application To Hydrogen Production From Bioethanol At Room Temperature <b>AUTHOR:</b> Dr. Louise Jalowiecki-Duhamel	4
4. Multi-Wall Carbon Nanotubes As Support Of Copper-Cerium Composite For Preferential Oxidation Of Carbon Monoxide <b>AUTHOR:</b> Prof. Shanghong Zeng	5
5. New complex Manganese-based oxides as oxygen buffer <b>AUTHOR:</b> Dr. Stéphanie Lesturgez	6
6. Platinum Nanocrystals Selectively Shaped Using Interfacial Tension In Novel Two-Phase Synthesis. <b>AUTHOR:</b> Dr. Zhanli Chai	7
7. Structure Of Pt-Decorated Polyacrylonitrile-Based Carbon Nanofibers Designed As Electrodes For Membrane Fuel Cells. <b>AUTHOR:</b> Prof. Olga Zhigalina	9
8. Magnetic Nanoparticles Supported Rh(I)-bis(phosphine) as Recyclable Catalyst for Hydroformylation of Olefines <b>AUTHOR:</b> Dr. Mohammed Nasiruzzaman Shaikh	11
9. Application of homogeneous catalysis and heterogeneous photocatalysis in extremely fast decontamination of real chemical warfare agents <b>AUTHOR:</b> Dr. Nicoleta Petrea	12
10. Oxidation Of 5-Hydroxymethyl Furfural Over Noble Metal Free Heterogeneous Catalysts <b>AUTHOR:</b> Dr. Florentina Neat	14
11. Facile Synthesis of Ceria-based Mixed Oxide Nanoparticles for Environmental Cleanup and Human Health <b>AUTHOR:</b> Prof. Tsugio Sato	15
12. Ionically conducting supports for oxidation catalysis <b>AUTHOR:</b> Dr. Philippe Vernoux	16
13. Copper Nanoparticles Supported by Nanostructured Ceria: A Highly Efficient and Recyclable Catalyst for N-Arylation of Indoles <b>AUTHOR:</b> Prof. Abderrahim Solhy	17
14. Fe <sup>3+</sup> /iron oxide/SiO <sub>2</sub> xerogel catalysts for p-nitrophenol degradation by photo-Fenton effects <b>AUTHOR:</b> Mr. Julien Mahy	18
15. Visible light induced photocatalytic degradation of fungicide with Fe and Si doped TiO <sub>2</sub> nanoparticles <b>AUTHOR:</b> Prof. Amrit Pal Toor	20
16. BiOCl: an efficient photo and fenton-like catalyst for degradation of 2-nitrophenol <b>AUTHOR:</b> Prof. Chunfang Du	21
17. Improved light-free catalytic property by the modulated nanosized Zn/ZnO-CNT porous structure	22

<b><i>AUTHOR:</i></b> Dr. Shengjuan Li	
18. Environmentally Benign TiO <sub>2</sub> nanomaterials for removal of Heavy Metal Ions with interfering ions present in Tap Water	
<b><i>AUTHOR:</i></b> Dr. Nupur Bahadur	23
19. Degradation Of 4-Chlorophenol By Mixed Fe/Fe <sub>3</sub> O <sub>4</sub> Nanoparticles: From The Perspective Of Mechanisms	
<b><i>AUTHOR:</i></b> Dr. Rong Cheng	24
20. Effect of Ce substituted hydrotalcite-derived mixed oxides on total catalytic oxidation of air pollutant	
<b><i>AUTHOR:</i></b> Dr. Renaud Cousin	26
21. Photocatalytic activity of ZnO in the oxidation reaction of nitric oxide	
<b><i>AUTHOR:</i></b> Dr. Azael Martinez-De La Cruz	28
22. Co-Al-Ce mixed oxide materials prepared by Hydrotalcite way for VOCs total oxidation in micro- and semi-pilot scale	
<b><i>AUTHOR:</i></b> Mr. Julien Brunet	29
23. The Development Of Core-Shell, Methane-Oxidation Nano Catalysts	
<b><i>AUTHOR:</i></b> Prof. Mahmoud Khader	30
24. Magnetically separable and reusable nano catalyst for carbon-carbon bond formation reactions	
<b><i>AUTHOR:</i></b> Prof. Vasundhara Singh.	31
25. Synthesis of Catalytically-Active Cu(II) and Zn(II) Coordination Polymer Nanocrystals Using a Microemulsion Method	
<b><i>AUTHOR:</i></b> Dr. Carla Meledandri	32
26. Effect Of Wo <sub>3</sub> Nanoparticles Morphology On The Catalytic Properties	
<b><i>AUTHOR:</i></b> Dr. Madjid Arab	

## Promising electrospun carbon fibers material for abiotic and enzymatic catalysis in hybrid biofuel cell for energy conversion.

S. Tingry<sup>1</sup>, A. Both-Engel<sup>1</sup>, A. Cherifi<sup>1</sup>, D. Cornu<sup>1</sup>,  
Y. Holade<sup>2</sup>, K. Servat<sup>2</sup>, B. Kokoh<sup>2</sup>, T. Napporn<sup>2</sup>

<sup>1</sup> Institut Européen des Membranes, UMR 5635, ENSCM-UMII-CNRS, place Eugène Bataillon, 34095 Montpellier, France.

<sup>2</sup> Université de Poitiers, IC2MP UMR CNRS 7285, 4 rue Michel Brunet–B27, TSA 51106- 86022 Poitiers cedex 09, France

*sophie.tingry@univ-montp2.fr, Tel.: +33 04 67 14 91 57, Fax: +33 04 67 14 91 19*

This work focus on the synthesis of a new functional material based on home-made carbon fibers (CFs) combined with nano-metallic and biological catalysts for its use in catalysis to harvest electrical energy. Such material presents interesting properties, like good conductivity and high specific surface allowing the immobilization of large amounts of catalysts that have been exploited to develop electrodes in biofuel cells to produce electricity from glucose and oxygen. The suitable carbon fibers material was synthesized via electrospinning technique followed by carbonization treatment to achieve a self-standing felt with mean fiber diameter of 330 nm. The material was used to construct both an abiotic anode, modified by di- and trimetallic nanoparticles (Au, Pt, Pd) of different compositions for glucose oxidation, and an enzymatic cathode, modified by the enzyme bilirubin oxidase for O<sub>2</sub> reduction. The optimization of the electrodes has been explored to develop a hybrid biofuel cell that delivered a power density of 90 μW cm<sup>-2</sup> at 0.37 V at pH 7.4 in the presence of glucose [1]. The performance highlights the advantage of the tridimensional structure of the CFs that enables higher amounts of immobilized catalysts in close contact with the fibers surface, and relieves the mass-transfer limitation of the reactive species through the material.

**Keywords:** *carbon nanofibers • enzyme • gold nanoparticles • catalysis • hybrid biofuel cell*

[1] HOLADE, Y., BOTH ENGEL, A., TINGRY, S., CHERIFI, A., CORNU, D., SERVAT, K., NAPPORN, T.W., KOKOH, K.B., 2014. Insights on Hybrid Glucose Biofuel Cell Based on Bilirubin Oxidase Cathode and Gold-Based Anode Nanomaterials. ChemElectroChem 1, 1976-1987.



**Rutile TiO<sub>2</sub> hierarchical microspheres: A promising multi-functional material as high-rate/long-life anode and advanced catalyst**

Chaochao Fu, Liping Li, Jun Zhang and Guangshe Li\*

State Key Laboratory of Structural Chemistry, Fujian Institute of Research on the Structure of Matter, Chinese Academy of Sciences, Fuzhou 350002, P. R. China.

E-mail: guangshe@fjirsm.ac.cn

Multi-functionalities of inorganic solids as energy storage or energy conversion are strongly dependent on the control over the microstructures and the associated charge transfer path. From the perspective of chemistry, the kinetics of charge transfer can be significantly improved by fabricating nano-building-block-assembled microstructures that can give functional materials like high-rate anodes or advanced catalysts. Herein, four types of hierarchically structured rutile TiO<sub>2</sub> microspheres assembled by different subunits such as nanoparticles and nanorods along [001] direction were synthesized using a facile hydrothermal method. The microstructures of subunits were tuned using hydrochloric acid, nitric acid, and oxalic acid during the formation reactions, with an aim to adjust the surface film and charge transfer resistance for optimum electrochemical performance. Comparing to other three hierarchical microspheres, the phase-pure rutile TiO<sub>2</sub> hierarchical microspheres assembled by nanoparticles obtained in the presence of 1 M hydrochloric acid exhibited the best lithium storage properties with a high reversible discharge capacity of 184 mAh/g at a current density of 0.5 C after 450 cycles and 143 mAh/g at a rate of 2 C for up to 500 cycles. Even at an extremely high rate of 10 C, the electrode still delivered a stable capacity of 94.9 mAh/g, the upper capacity so far for rutile TiO<sub>2</sub> and even comparable one with anatase TiO<sub>2</sub>. The superior electrochemical performance may be ascribed to trace amounts of Cl ion strongly adsorbing on the surface of the microspheres, which may prevent the side reactions between the electrolyte and surface of rutile TiO<sub>2</sub> and further result in the lowest surface film resistance and charge transfer resistance. All of these

demonstrate that the as-prepared hierarchically structured rutile TiO<sub>2</sub> microspheres reported herein have the great potential as high-rate and long-life anode materials for lithium-ion batteries. Further, rutile TiO<sub>2</sub> microspheres assembled by nanorods along [001] direction were found to show high photocatalytic activity towards organic removal. These findings demonstrate that rutile TiO<sub>2</sub> hierarchical microspheres, if properly prepared, are promising as multi-functional material for energy storage or energy conversion.

#### Reference

1. Chaochao Fu, Guangshe Li, Qi Li, Jianming Fan, Dongjiu Xie, and Liping Li, unpublished.
2. Hu WB; Li LP; Li GS\*; Liu Y; Withers RL. *Scientific Repots*, 2014, 4, 6582
3. Hu W; Li LP; Tong WM; Li GS\*; *Chem. Commun.* 2010, 46, 3113-3115.
4. Hu W; Li LP; Tong WM; Li GS\*; Yan TJ, *J. Mater. Chem.* 2010, 20, 8659-8667.
5. Zhang, J.; Li, L. P.; Huang, X. S.; Li, G. S.; *J. Mater. Chem.* 2012, 22, 10480.

## Development of Ni based nano-oxyhydride catalysts: application to hydrogen production from bioethanol at room temperature

W. Fang<sup>1,2</sup>, C. Pirez<sup>1,2</sup>, S. Paul<sup>2,3</sup>, H. Jobic<sup>4</sup>, F. Dumeignil<sup>1,2,5</sup>, L. Jalowiecki-Duhamel<sup>1,2</sup>

<sup>1</sup>Université Lille Nord de France, 59000 Lille, France

<sup>2</sup>CNRS UMR8181, UCCS, 59655 Villeneuve d'Ascq, France.

<sup>3</sup>Ecole Centrale de Lille, 59655 Villeneuve d'Ascq, France

<sup>4</sup>IRCELyon, 69626 Villeurbanne Cedex, France

<sup>5</sup>Institut Universitaire de France, 75005 Paris, France

E Mail/louise.duhamel@univ-lille1.fr

Well tuning the preparation, formulation and conditions applied, different series of nickel based nano-oxyhydride catalysts were developed for the highly efficient and sustainable H<sub>2</sub> formation from ethanol in the presence of oxygen and water at room temperature. Once *in situ* treated in H<sub>2</sub> at adequate temperature, the nickel based mixed oxides become oxyhydrides, with the presence of hydrogen species of hydride nature located in the anionic vacancies. In complement to the exothermic partial oxidation reaction of ethanol, by taking advantage of the chemical energy released from the reaction between hydride species stored in the nano-oxyhydride catalysts and O<sub>2</sub>, continuous complete conversion of ethanol specifically at 50 °C (oven temperature), with simultaneously production of H<sub>2</sub>, can be obtained, in agreement with some previous reported results [1, 2]. Correlations between catalytic activity and physico-chemical characterizations allow participating to the open debate on the active site and mechanism.

**Keywords:** oxyhydrides, catalysts, hydrogen, ethanol, nickel

- [1] PIREZ C., CAPRON M., JOBIC H., DUMEIGNIL F. & L. JALOWIECKI-DUHAMEL. 2011. Highly Efficient and Stable CeNiH<sub>2</sub>O<sub>Y</sub> Nano-Oxyhydride Catalyst for H<sub>2</sub> Production from Ethanol at Room Temperature. *Angew. Chem. Int. Ed.* 50, 10193-10197.
- [2] FANG W., PIREZ C., PAUL S., CAPRON M., JOBIC H., DUMEIGNIL F. & L. JALOWIECKI-DUHAMEL. 2013. Room Temperature H<sub>2</sub> Production from Ethanol over CeNi<sub>X</sub>H<sub>Z</sub>O<sub>Y</sub> Nano-Oxyhydride Catalysts. *ChemCatChem* 5, 2207-2216.

## **Cu<sub>x</sub>O-CeO<sub>2</sub>/MWCNTs catalysts for preferential oxidation of carbon monoxide**

Lu Zhang, Nan Jiang, Meiyi Gao, Xiaozhou Zhao, Yueling Yin, Haiquan Su, Shanghong Zeng\*

Inner Mongolia Key Laboratory of Chemistry and Physics of Rare Earth Materials, School of Chemistry and Chemical Engineering, Inner Mongolia University, Hohhot 010021, P. R. of China

**Abstract:** The Cu<sub>x</sub>O/MWCNTs, CeO<sub>2</sub>/MWCNTs and Cu<sub>x</sub>O-CeO<sub>2</sub>/MWCNTs catalysts were synthesized by a simple impregnation method, and characterized via X-ray diffraction, N<sub>2</sub> adsorption-desorption, Fourier transformed infrared spectroscopy, transmission electron microscopy, H<sub>2</sub> temperature-programmed reduction and X-ray photoelectron spectra. The catalytic performance for preferential CO oxidation was carried out in the hydrogen-rich gasses. It is found that the hydrophilic functional groups of hydroxyl and carboxyl in the samples are favorable for the incorporation of Cu<sub>x</sub>O and CeO<sub>2</sub> into the tubes of the MWCNTs. Most of Cu<sub>x</sub>O particles and CeO<sub>2</sub> nanowires are filled in the tubes of MWCNTs, and a small amount of nanoparticles are deposited on the surface of MWCNTs. The MWCNTs have high BET surface area, which is helpful for the dispersion of Cu<sub>x</sub>O and CeO<sub>2</sub> to expose more active surface for CO-PROX reaction over the Cu<sub>x</sub>O-CeO<sub>2</sub>/MWCNTs catalysts. MWCNTs with high BET surface area weaken poisoning effect of H<sub>2</sub>O and CO<sub>2</sub> after 135 °C.

## New complex Manganese-based oxides as oxygen buffer

Lesturgez S.<sup>1</sup>, Goglio G.<sup>1</sup>, Bisson L.<sup>2</sup>, Hernandez J.<sup>2</sup>, Demourgues A.<sup>1</sup>

- 1 CNRS, Univ. Bordeaux, ICMCB, UPR9048, F-33600 Pessac, France  
2 RIC-SOLVAY Recherches, 52 Rue de la Haie Coq, F-93306 Aubervilliers Cedex

[lesturgez@icmcb-cnrs.bordeaux.cnrs/goglio@icmcb-cnrs.bordeaux.fr/demourg@icmcb-bordeaux.cnrs.fr](mailto:lesturgez@icmcb-cnrs.bordeaux.cnrs/goglio@icmcb-cnrs.bordeaux.fr/demourg@icmcb-bordeaux.cnrs.fr)

Complex oxides as oxygen buffers for Three Way Catalysts are the solution for oxygen storage and release to promote oxidation of exhaust gas and reductants like CO. In this research domain, Ceria-Zirconia with  $\text{Ce}^{4+}$  ( $[\text{Xe}]4f^0$ ) /  $\text{Ce}^{3+}$  ( $[\text{Xe}]4f^1$ ) valence states have been investigated for many years. Our objective is to explore new systems based on transition metal. Manganese oxides appear as promising materials because of the high tunability of the manganese valency ( $\text{Mn}^{4+}$   $[\text{Ar}]3d^3$ ,  $\text{Mn}^{3+}$   $[\text{Ar}]3d^4$ ,  $\text{Mn}^{2+}$   $[\text{Ar}]3d^5$ , one might then expect high exchanged oxygen amounts) and to the ability of the metal to accommodate various coordination polyhedra. We focused on the Ca-Mn-O system because it offers the possibility i) to stabilize many line compounds and ii) to vary dimensionality and connectivity of the crystallographic network [1]. The redox properties will then be discussed on the basis of structural changes and the valency of manganese in the stable oxidized phase such as  $\text{CaMn}_3\text{O}_6$  tunnel structure. Doped manganites and  $\text{CaMn}_{3-x}\text{A}_x\text{O}_6$  ( $\text{A} = \text{Al}^{3+}$ ,  $\text{Fe}^{3+}$ ) new compositions will be presented. A special care will be given to the evolution of manganese valency induced by the substitution and the subsequent structural changes.

**Keywords:** *Manganite, tunnel structure, Redox properties, automotive exhaust catalyst*

[1] HOROWITZ, H. S., LONGO, J. 1978. Phase Relation in the Ca-Mn-O System. Material Research Bulletin, 13, 1359–1369.

## Platinum Nanocrystals Selectively Shaped Using Interfacial Tension in Novel Two-phase Synthesis

Quanyu Suo, Hui Wang, Zhanli Chai

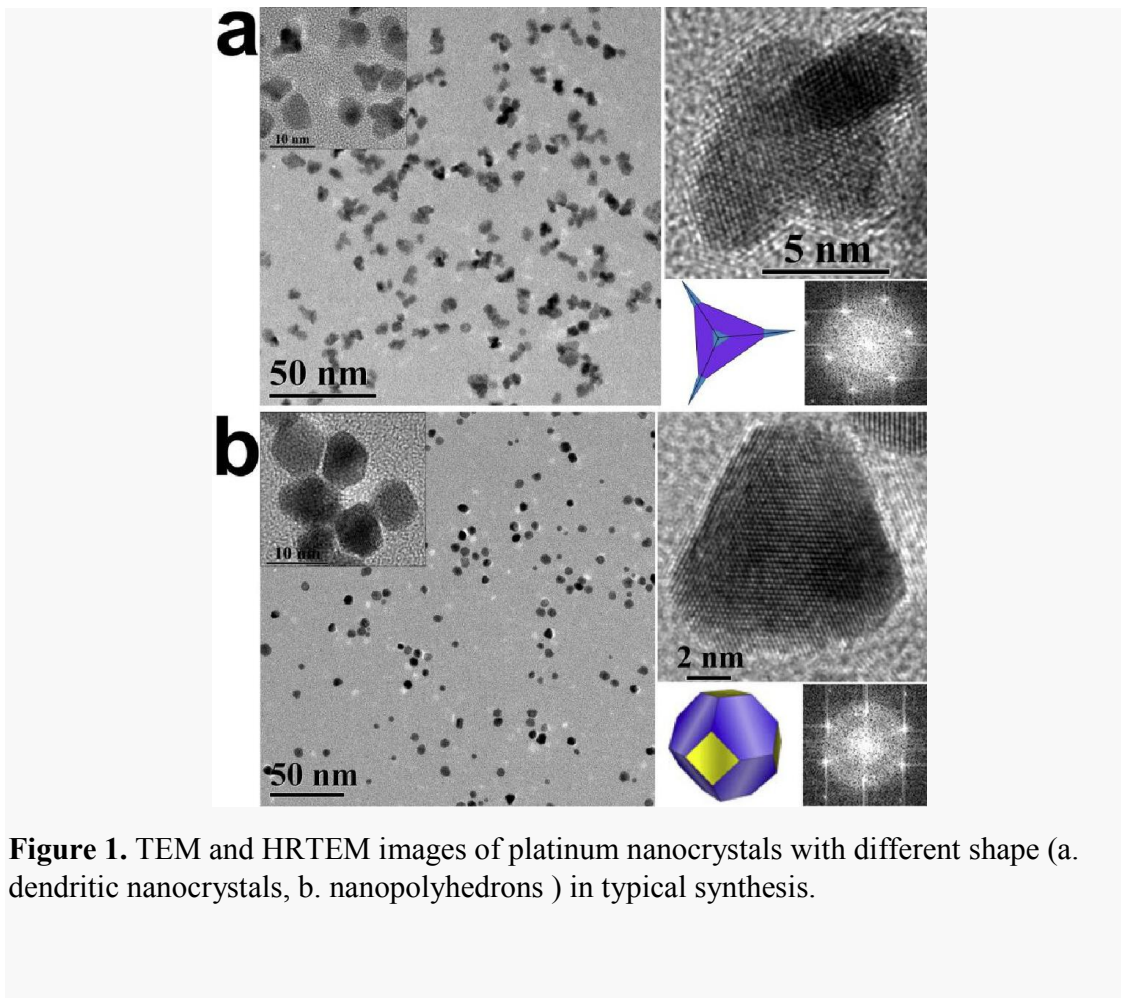
College of Chemistry and Chemical Engineering, Inner Mongolia University, Hohhot  
010021, P. R. China

*E Mail:* chai\_zl@hotmail.com

So far, surfactant-free preparation of shaped Pt nanocrystals have often been obtained by means of a trial-and-error process for identifying the appropriate capping agents and synthetic environments, largely because of the lack of a general approach for synthesizing facet-controllable Pt nanocrystals. Interfacial tension has exquisite specific molecular recognition properties that can be explored for the precise engineering of nanostructured materials. Here, we report the use of facet-specific interfacial tension for the predictable synthesis of platinum nanocrystals with selectively exposed crystal surfaces and particular shapes. The formations of nanopolyhedrons and dendritic nanocrystals were obtained in different type of two-phase synthesis, such as solid-liquid, and gas-liquid solution. In addition, the branched nanocrystals have the highest catalytic active for methanol electro-oxide among the as-obtained different shaped Pt nanocrystals. Our studies unambiguously demonstrate the abilities of variable type of two-phase synthesis in determining nanocrystal shape, representing a critical step forward in the use of interfacial tension for programmable synthesis of nanostructures.

**Keywords:** *Platinum nanocrystals, interfacial tension, two-phase, electrocatalysts*

- [1] DEBE M. K. 2012. Electrocatalyst approaches and challenges for automotive fuel cells. *Nature*, 486, 43-51.
- [2] Porter N. S., WU H., QUAN Z., FANG J. 2013. Shape-Control and Electrocatalytic Activity-Enhancement of Pt-Based Bimetallic Nanocrystals. *Acc. Chem. Res.* 46, 1867-1877.
- [3] LENG M., CHEN Y., XUE J. M. 2014. Synthesis of TiO<sub>2</sub> nanosheets via an exfoliation route assisted by a surfactant, *Nanoscale*, 6, 8531-8534.



## Structure of Pt-decorated Polyacrylonitrile-based Carbon Nanofibers designed as Electrodes for Membrane Fuel Cells

Zhigalina V.<sup>1</sup>, Zhigalina O.<sup>1</sup>, Ponomarev I.<sup>2</sup>, Razorenov<sup>2</sup>, Ponomarev Iv.<sup>2</sup>, Kiselev<sup>1</sup>, Khmelenin<sup>1</sup>

<sup>1</sup>A.V. Shubnikov Institute of Crystallography RAS, Leninskii prospekt 59,  
119333 Moscow, Russia;

<sup>2</sup>A.N. Nesmeyanov Institute of Organoelement Compounds RAS, Vavilova St. 28,  
119991 Moscow, Russia

*zhigal@ns.crys.ras.ru/ Olga Zhigalina*

Thin catalyst layers and their supporting substrates are the most critical components of membrane fuel cells and up to now the problem of their optimisation is far from trivial. It is a well-known fact that good support material must have a high surface area which disperses the nanoparticles over, be porous enough to transmit gas flow and have a good electrical conductivity. Therefore nowadays carbon nanofibers (CNFs) are considered to be very promising support materials [1, 2].

The aim of the present work is to investigate the influence of different treatments on the morphology, metal particle distribution and surface structure of Pt-decorated nanofiber electrospun polyacrylonitrile mats. Pt-decorated CNFs were obtained using different catalytical coating and treatment techniques. To improve the CNF porosity and the process of catalytic nanoparticles deposition the CNFs were obtained on a base of polyvinylpyrrolidone (PVP) and polyimide (PI) polymer mixture with addition of carbon black and annealed at T = 900 and 1200 °C.

The samples structure was characterized by a scanning electron microscopy (SEM) in a FEI Helios 600 Dual Beam TM and a high resolution transmission electron microscopy (HRTEM) in a FEI Titan 80-300 with Cs corrector at an accelerating voltage of 300 kV.

It was shown that PVP/PI treatment with annealing at 900 °C or at 1200 °C stimulated the fiber carbonization process without changes to their morphology or surface destruction. In the structure of fibers the straight graphene planes were mainly observed. In the case



of combined heat and chemical (PVP+PI) treatment the carbon nanofibers consisted of “curly” graphene planes within the whole fiber space. As a result of this process the fibers’ surface became porous which promoted platinum nanoparticles to form a thick layer on the fibers’ surface.

**Keywords:** *carbon, fibers, microscopy, structure, fuel cell*

[1] DONG, Z., SCOTT, J., WU, Y. 2011. Electrospinning Materials for Energy-related Applications and Devices. *J. of Power Sources*, 196, 4886-4904.

[2] PONOMAREV, I. I., PONOMAREV, I. I., FILATOV, I. Y., FILATOV, Y. N., RASORENOV, D. Y., VOLKOVA, Y. A., ZHIGALINA, O. M., ZHIGALINA, V. G., GREBENEV, V. V. & KISELEV, N. A. 2013. Design of Electrodes Based on a Carbon Nanofiber Nonwoven Material for the Membrane Electrode Assembly of a Polybenzimidazole-Membrane Fuel Cell. *Doklady Physical Chemistry*, 448, 2, 23 – 27.

## Magnetic Nanoparticles Supported Rh(I)-bis(phosphine) as Recyclable Catalyst for Hydroformylation of Olefines

M. Nasiruzzaman Shaikh<sup>1,\*</sup>, Abiola Azeez Jimoh<sup>1</sup>, Mahmoud Abdelnaby<sup>1</sup>

Center of Research Excellence in Nanotechnology (CENT), King Fahd University of Petroleum and Minerals (KFUPM), Dhahran-31261, Saudi Arabia

E Mail : [mnschaikh@kfupm.edu.sa](mailto:mnschaikh@kfupm.edu.sa); [oasisshaikh@kfupm.edu.sa](mailto:oasisshaikh@kfupm.edu.sa)

The use of rhodium (I) supported on magnetic nanoparticles (MNPs) for the hydroformylation reaction via heterogenous catalysis is described. Dopamine is first phosphinated with bisphosphine (bp), distributed uniformly on MNPs followed by surface functionalization to give particles of the type MNP@bpd-Rh. The <sup>31</sup>P NMR study corroborated the formation of methylated bisphosphine on the arm of primary amine of dopamine by the *in-situ* reaction involving paraformaldehyde and diphenylphosphine. Anchoring on the magnetic nanoparticle surface was confirmed by the appearance of characteristic Fe-O vibration band at 593 cm<sup>-1</sup> in the FT-IR spectrum, supported by the stepwise weight loss in TGA as a function of temperature. TEM Imaging showed very small about 3-5 nm particles distributed homogeneously, whose crystallinity was confirmed by XRD. The phosphorus content determined by ICP-MS was found to be about 0.39 mmol of phosphine per gram of the nanoparticles. This catalyst (with low loading) was found to be highly active towards the complete conversion of olefins like styrene to its corresponding aldehydes with good selectivity at low pressure; it is also very robust at high temperature and magnetically separable and recyclable without decomposition.

**Keywords:** *Heterogeneous catalysis, hydroformylation, magnetic nanoparticles*

[1] ABU-REZIQ, R., ALPER, H., WANG, D. & POST, L.M. Metal Supported on Dendronized Magnetic Nanoparticles: Highly Selective Hydroformylation Catalysts, J. Am. Chem. Soc. 128, 2013, 5279-5282.

## **Application of homogeneous catalysis and heterogeneous photocatalysis in extremely fast decontamination of real chemical warfare agents**

Nicoleta Petrea<sup>1</sup>, Răzvan Petre<sup>1</sup>, Florentina Neatu<sup>2</sup>, Vasile Somoghi<sup>3</sup>, Stefan Neatu<sup>3,4</sup>

<sup>1</sup>Scientific Research Centre for CBRN Defense and Ecology, 225 Oltenitei Road, 041309  
Bucharest, Romania

<sup>2</sup>University of Bucharest, Department of Organic Chemistry, Biochemistry and Catalysis, 4–12  
Regina Elisabeta Bvd., 030016 Bucharest, Romania

<sup>3</sup>Stimpex SA, 46-48 Nicolae Teclu Street, 032368 Bucharest, Romania

<sup>4</sup>National Institute of Materials Physics, 105bis Atomistilor Street, 077125 Bucharest, Romania

*E Mails:* [nicoleta.petrea@yahoo.com](mailto:nicoleta.petrea@yahoo.com), [stefan.neatu@infim.ro](mailto:stefan.neatu@infim.ro)

Chemical warfare agents (CWAs) are among the most toxic compounds ever used in military conflicts. Currently, the practical methodologies for decontamination involve much effort and high amounts of chemicals and water. All these methods exhibit disadvantages and produce strong environmental pollution. For this reason, the development of a feasible decomposition method is necessary. Starting from the excellent reports of Brown group [1,2] in the field of metal-catalyzed methanolysis of organophosphorous materials, in the present study we describe an extremely efficient system, environmentally benign, which use a suspension based on La, Zn and Cu complexes in corroboration with an extremely powerful photocatalyst, Au/TiO<sub>2</sub> that, at the open atmosphere and under visible light, produces complete decontamination of organophosphorous CWAs (GB, GD, VX) and some of their simulants (paraoxon, parathion, methyl parathion, etc.) in less than 1 minute. In a typical procedure, different amounts of CWAs were dispersed on a surface of 100 cm<sup>2</sup> of different supports (wood, metal, borosilicate glass, Plexiglas, rubber, painted wood, metal). The evolution of the reaction was followed by extracting the suspension with methanol after of daylight exposure and analysing by GC-MS. Taking into account that, at the level of world market of products dedicated to decontamination of toxic

compounds, there is no other photocatalytic system feasible for this purpose, then these results will improve the performances of these necessary countermeasures in the case of occurrences of emergency situations. This work was supported by a grant of Partnerships in priority S&T domains Programme (PNII), MEN–UEFISCDI, project number 306/2014.

**Keywords:** CWAs, fast decontamination, methanolysis, Au/TiO<sub>2</sub> photocatalyst

[1] LEWIS, R. E., NEVEROV, A. A. & BROWN, R. S. 2005. Mechanistic studies of La<sup>3+</sup> and Zn<sup>2+</sup>-catalyzed methanolysis of *O*-ethyl *O*-aryl methylphosphonate esters. An effective solvolytic method for the catalytic destruction of phosphonate CW simulants. *Org. Biomol. Chem.*, 3, 4082-4088.

[2] MELNYCHUK, S. A., NEVEROV, A. A. & BROWN, R. S. 2006. Catalytic decomposition of simulants for chemical warfare V agents: Highly efficient catalysis of the methanolysis of phosphonothioate esters. *Angew. Chem. Int. Ed.*, 45, 1767-1770.

## Oxidation of 5-hydroxymethyl furfural over noble metal free heterogeneous catalysts

Nicoleta Petrea<sup>1</sup>, Vasile Comoghi<sup>2</sup>, Mihaela Florea,<sup>3</sup> Octavian Dumitru Pavel,<sup>3</sup> Vasile I. Pârvulescu,<sup>3</sup> Florentina Neatu<sup>3</sup>

<sup>1</sup>Scientific Research Centre for CBRN Defense and Ecology, 225 Oltenitei Sos., 041309 Bucharest, Romania

<sup>2</sup>S.C. Stimpex S.A., 46-48 Teclu Nicolae Street, 032368 Bucharest, Romania

<sup>3</sup>University of Bucharest, Department of Organic Chemistry, Biochemistry and Catalysis, 4 – 12 Regina Elisabeta Bvd., 030016 Bucharest, Romania

*E-mail:* [florentina.neatu@chimie.unibuc.ro](mailto:florentina.neatu@chimie.unibuc.ro)

The continuous depletion of petrochemical resources for energy and chemical materials production has attracted considerable attention lately especially for environmental concerns. [1] In this context, the replacement of traditional fossil fuels derived commodities, including polyethylene terephthalate (PET), with polymers from renewable sources can significantly contribute to this issue. As valuable product derived from the oxidation of HMF, 2,5-furandicarboxylic acid (FDCA) is a promising biomass-derived chemical building block with a high market potential. Since the chemical synthesis of FDCA requires high pressure and temperature, noble metals and organic solvents, which render the process to be expensive and polluting, a new greener synthetic route is highly desirable. Herein, we present an environmentally benign and safe alternative for FDCA synthesis using MnFe mixed oxides as heterogeneous catalysts. Following an easy to perform co-precipitation synthetic route, several MnFe mixed oxides have been prepared and tested in the oxidation of HMF in water at 90 °C in the presence of NaOH and oxygen, the Mn<sub>0.75</sub>Fe<sub>0.25</sub> catalyst leading to high conversion to FDCA of 90%.

This work was supported by a grant of Partnerships in priority S&T domains Programme (PNII), MEN–UEFISCDI, project number 166/2012.

**Keywords:** *HMF oxidation, heterogeneous catalysis, FDCA synthesis*

[1] LESHKOV-ROMAN, Y., CHHEDA, J. N. & DUMESIC, J. A. 2006. Phase modifiers promote efficient production of hydroxymethylfurfural from fructose. *Science*, 312, 1933-1937.

## Facile Synthesis of Ceria-based Mixed Oxide Nanoparticles for Environmental Cleanup and Human Health

Tsugio Sato, Shu Yin

Institute of Multidisciplinary Research for Advanced Materials, Tohoku University,  
2-1-1, Katahira, Aoba-ku, Sendai 980-8577, Japan

*E Mail/ tsusato@tagen.tohoku.ac.jp*

Since ceria ( $\text{CeO}_2$ ) possesses the oxygen release-absorption ability (oxygen storage capacity: OSC), it has been used as a co-catalyst of the automobile 3-way catalyst to cleanup automobile exhausts. In this application, ceria is required to possess high OSC, high specific surface area and high thermal stability. Ceria can also be used as a UV-shielding material for human health, because of the adequate bandgap energy of ca. 3 eV. When used as the UV-shielding material, ceria is required to be nanoparticles to realize the high visible-light transparency and possess low OSC to decrease the catalytic activity in the oxidation of organic materials. The OSC of ceria is considered to be related to the stability of crystal structure of ceria. The ideal  $r(\text{M}^{n+})/r(\text{O}^{2-})$  ionic size ratio of an eight-coordination metal oxide is 0.732, but the value of  $r(\text{Ce}^{4+})/r(\text{O}^{2-})$  of the fluorite structured ceria, is 0.703, which is smaller than that of the ideal value. To take on a more stable eight coordination structure,  $\text{Ce}^{4+}$  would have a tendency to be reduced to larger  $\text{Ce}^{3+}$  by releasing oxygen. Therefore, it is expected that the OSC of ceria can be increased by doping with smaller size of metal ion, and decreased by doping with larger size and/or lower valence metal ion. According to such design concept, ceria nanoparticles possessing high OSC were fabricated by the solvothermal reaction by doping with smaller size metal ion, such as  $\text{Zr}^{4+}$ ,  $\text{Sn}^{4+}$ , etc. The  $\text{Zr}^{4+}$  and  $\text{Sn}^{4+}$  co-doped ceria also showed excellent thermal stability, therefore, is expected to be applied to form advanced automobile 3-way catalysts. On the other hand, the oxidation catalytic activity of ceria could be greatly reduced by doping with  $\text{Ca}^{2+}$ . In addition,  $\text{Ca}^{2+}$ -doped  $\text{CeO}_2$  showed quite low photocatalytic activity, consequently, is now commercially supplied as new UV-shielding materials.

***Keywords: Ceria, oxygen storage capacity, automobile exhaust gas purification catalyst, UV-shielding***

## **Ionicly conducting supports for oxidation catalysis**

P. Vernoux<sup>1</sup>, M.N. Tsampas<sup>1</sup>, F.M. Sapountzi<sup>1</sup>

<sup>1</sup> Institut de Recherches sur la Catalyse et l'Environnement de Lyon (IRCELYON),

UMR 5256, CNRS, Université Claude Bernard Lyon 1

2 avenue A. Einstein, 69626 Villeurbanne, France.

*philippe.vernoux@ircelyon.univ-lyon1.fr*

This study reports isotopical labelling experiments during propane oxidation on nanodispersed Pt nanoparticles supported either on Ytria-Stabilized Zirconia, an O<sup>2-</sup> ionic conductor, or on non-conductive ceramics (ZrO<sub>2</sub>, SiO<sub>2</sub>) showing high metallic dispersions. <sup>18</sup>O<sub>2</sub> Temperature-Programmed Desorption and oxygen exchange experiments have shown that YSZ lattice oxygen species continuously migrate toward the Pt surface to such an extent that the gas phase oxygen adsorption is strongly inhibited [1]. This is not the case when the Pt nanoparticles are supported on ZrO<sub>2</sub> or SiO<sub>2</sub>, where the propane mainly reacts with gaseous oxygen. This underlines the strong impact of the YSZ oxygen species on the propane combustion mechanism. The oxygen ions containing in the support can act as predominant oxidizing species. This finding open new routes to design smart and efficient high surface specific area metal-supported catalysts for hydrocarbon oxidation reactions involved in environmental catalysis.

***Keywords: ionicly conducting ceramics, hydrocarbon catalytic oxidation, metal/support interactions.***

[1] ALVES FORTUNATO M., PRINCIVALLE A., CAPDEILLAYRE C., PETIGNY N., TARDIVAT C., GUIZARD C., TSAMPAS M.N., SAPOUNTZI F.M., VERNOUX P., 2014. Role of lattice oxygen in the propane combustion over Pt/Ytria-Stabilized Zirconia : Isotopic Studies. Topics in Catalysis, 57, 1277-1286

## Copper Nanoparticles Supported by Nanostructured Ceria: A Highly Efficient and Recyclable Catalyst for N-Arylation of Indoles

O. Amadine,<sup>a</sup> H. Maati,<sup>a</sup> A. Fihri,<sup>b</sup> K. Abdelouahdi,<sup>c</sup> C. Len,<sup>d</sup> A. Solhy<sup>b\*</sup>

<sup>a</sup> FST, Université Hassan II-Mohammedia B.P. 146, 20650, Morocco.

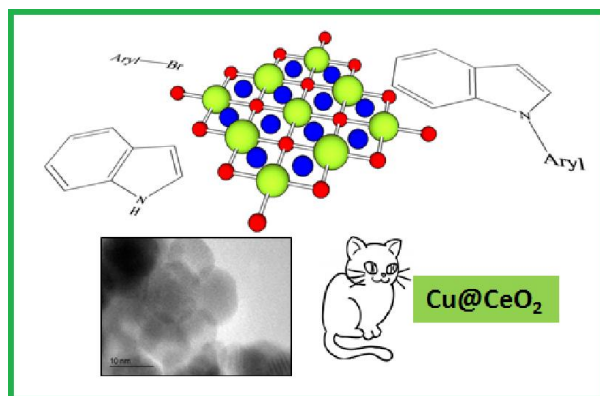
<sup>b</sup> Université Polytechnique Mohammed VI, Lot 660 - Hay Moulay Rachid. 43150 Ben Guerir, Morocco.  
E-mail address: [Abderrahim.Solhy@um6p.ma](mailto:Abderrahim.Solhy@um6p.ma)

<sup>c</sup> Centre National pour la Recherche Scientifique et Technique (CNRS), Division UATRS, Angle Allal Fassi/FAR, B.P.8027, Hay Riad, 10000-Rabat, Morocco.

<sup>d</sup> Transformations Intégrées de la Matière Renouvelable, UTC/ESCOM, Centre de Recherche Royallieu, B.P. 20529, 60205 Compiègne, France.

Over the last years, apart from homogeneous catalysis or heterogeneous catalysis, the nanocatalysis is a third way, which combines the advantages of both previously mentioned catalysis, and that is currently being developed both from the academic and industrial point of view.<sup>1</sup> A large part of the searches into this category of the catalysis has focused often on the metal nanoparticles supported on nanostructured materials specifically mesoporous non-silicious oxides. Indeed, ceria fits into this category. It is one of the most important functional rare earth oxides, who attracted significant interest thanks to their wide applications in cutting-edge technology sectors. However, this oxide has been widely used as a catalyst or support-catalyst of several metal nanoparticles for various chemical transformations. The impregnation of ceria by copper nanoparticles or copper oxide, or vice versa (ceria supported on copper nanoparticles) is widely studied for oxidation of CO,<sup>2</sup> and organic volatile compounds,<sup>3</sup> but especially for Water-Gas-Shift reaction.<sup>4</sup>

On the other hand, N-aryl indoles have attracted a keen interest over the last few years due to their diverse biological activities already revealed and exploited.<sup>5</sup> However, in homogeneous systems this reaction poses significant issues related to product purification and toxic waste produced after separation of copper catalyst. One of the most favorable ways to overcome these problems is the realization of the N-arylation reaction via heterogeneous catalysts.<sup>6</sup> It is against this background that this work is situated and which has as objective the synthesis and characterization of ceria doped with copper nanoparticles, and then its use as a nanocatalyst in the reaction of N-arylation of indole with bromo-aryl derivatives (Scheme 1).



Scheme 1.

### References

1. V. Polshettiwar, R. Luque, A. Fihri, H. Zhu, M. Bouhrara, J.-M. Basset, *Chem. Rev.* 111 (2011) 3036.
2. F. Yang, J. Graciani, J. Evans, P. Liu, J. Hrbek, J.F. Sanz, J.A. Rodriguez, *J. Am. Chem. Soc.* 133 (2011) 3444.
3. R. Dziembaj, M. Molenda, L. Chmielarz, M. Drozdek, M.M. Zaitz, B. Dudek, A. Rafalska-Lasocha, Z. Piwowarska, *Catal. Lett.* 135 (2010) 68.
4. P. Gawade, B. Mirkelamoglu, U.S. Ozkan, *J. Phys. Chem. C* 114 (2010) 18173.
5. I. Salama, C. Hocke, W. Utz, O. Prante, F. Boeckler, H. Hubner, T. Kuwert, P. Gmeiner, *J. Med. Chem.* 50 (2007) 489.
6. O. Amadine, H. Maati, K. Abdelouahdi, A. Fihri, C. Len, A. El Bouari, A. Solhy, *J. Mol. Catal. A: Chem.*, 395 (2014) 409.



## **Fe<sup>3+</sup>/iron oxide/SiO<sub>2</sub> xerogel catalysts for *p*-nitrophenol degradation by photo-Fenton effects**

Julien Mahy<sup>1\*</sup>, Ludivine Tasseroul<sup>1</sup>, Anthony Zubiaur<sup>1</sup>, Jérémy Geens<sup>1</sup>, Magali Brisbois<sup>2</sup>, Marcus Herlitschke<sup>3,4</sup>, Raphael P. Hermann<sup>3,4</sup>, Benoit Heinrichs<sup>1</sup>, Stéphanie D. Lambert<sup>1</sup>

<sup>1</sup>Laboratoire de Génie chimique, Nanomatériaux, Catalyse, Electrochimie, B6a, Université de Liège, B-4000 Liège, Belgium

<sup>2</sup>Département de Chimie, LCIS GreenMat, B6a, Université de Liège, B-4000 Liège, Belgium

<sup>3</sup>Jülich Center for Neutron Science JCNS and Peter Grünberg Institut PGI, JARA-FIT, Forschungszentrum Jülich GmbH, D-52425 Jülich, Germany

<sup>4</sup>Faculté des Sciences, Université de Liège, B-4000 Liège, Belgium

\*Corresponding author: [julien.mahy@ulg.ac.be](mailto:julien.mahy@ulg.ac.be)

**Keywords** : Sol-gel, Cogelled xerogels, iron oxide nanoparticles, Photo-Fenton effects, *p*-nitrophenol degradation.

### **Abstract**

Since the beginning of the industrial era, the various human activities have increased steadily, leading to a rapid technological development and a high population growth. Thus, the expansion of the industry has heavily polluted the atmosphere, soil and water with negative consequences for humans and environment [1]. To decrease this pollution, it exists various treatment methods: chemical, physical and biological [2,3]. Among all these methods, a recent way of treatment is the degradation of pollutants in soils or waters by Fenton and photo-Fenton reactions [3] which use H<sub>2</sub>O<sub>2</sub>, iron-based compounds and UV light.

In this way, several iron xerogel catalysts were synthesized by hydrolysis and condensation of tetraethoxysilane (TEOS) and 3-(2-aminoethylamino)propyltrimethoxysilane (EDAS) which is able to form a chelate with iron ions [4]. The EDAS/TEOS ratio strongly influences the texture of xerogel catalysts. The specific surface area and the micro- and mesoporous volume increase with this ratio. It seems that EDAS plays a nucleating agent role for silica particles [5,6] and allows to anchor Fe-based moieties inside the silica network [4]. Iron oxide nanoparticles of diameter 1–1.5 nm and Fe<sup>3+</sup> ions result, encapsulated in silica particles with sizes of about 10–30 nm in diameter. The iron species was determined by Mössbauer spectroscopy and magnetometry measurements and only Fe<sup>3+</sup> species were observed in xerogel catalysts. The Fenton and photo-Fenton effect of these catalysts were evaluated on the degradation of *p*-nitrophenol in aqueous media under different conditions. Results show that in the presence of H<sub>2</sub>O<sub>2</sub>, iron xerogel catalysts present a photo-Fenton effect, reaching 99% of degradation after 24 h.

[1] M. A. Khan, A. M. Ghouri, *Environmental pollution: its effects on life and its remedies*, Journal of Arts, Science & Commerce (Vol. 2), 2011, pg 276-285.

[2] M. S. Kuyukina, I. B. Ivshina, *Biology of rhodococcus: chapter 9*, Springer, 2010, pg 232-256.

- [3] J. J. Pignatello, E. Oliveros, A. MacKay, *Advanced Oxidation Processes for Organic Contaminant Destruction Based on the Fenton Reaction and Related Chemistry*, Critical Reviews in Environmental Science and Technology (Vol. 36), 2006, pg 1-84.
- [4] B. Heinrichs, L. Rebbouh, J.W. Geus, S. Lambert, H.C.L. Abbenhuis, F. Grandjean, G.J. Long, J.-P. Pirard, R.A. van Santen, *Iron (III) species dispersed in porous silica through sol-gel chemistry*, Journal of Non-Crystalline Solids (Vol. 354), 2008, pg 665-672.
- [5] S. Lambert, C. Alié, J.-P. Pirard, B. Heinrichs, *Study of textural properties and nucleation phenomenon in Pd/SiO<sub>2</sub>, Ag/SiO<sub>2</sub> and Cu/SiO<sub>2</sub> cogelled xerogel catalysts*, Journal of Non-Crystalline Solids (Vol. 342), 2004, pg 70-81.
- [6] B. Heinrichs, S. Lambert, N. Job, J.-P. Pirard, in "Catalyst Preparation: Science and Engineering, J. R. Regalbuto (Ed.)", CRC Press, Taylor & Francis Group, Boca Raton, 2007, p. 163-208.

## Visible –light induced photocatalytic degradation of fungicide with Fe and Si doped TiO<sub>2</sub> nanoparticles

Amrit Pal Toor<sup>a</sup>, Taranjeet Kaur<sup>b</sup>, Abhishek Sraw<sup>b</sup> and R.K. Wanchoo<sup>a</sup>

<sup>a</sup>Dr. SSB University Institute of Chemical Engineering and Technology

<sup>b</sup>Energy Research Centre, Panjab University, Chandigarh-160014, India

Panjab University, Chandigarh-160014, India

Email: [aptoor@yahoo.com](mailto:aptoor@yahoo.com)

### Abstract

Iron (Fe) and Silica (Si) doped TiO<sub>2</sub> nanoparticles were synthesized by wet impregnation method. The concentration of dopants Fe (1%, 2%, 3% and 4%) and Si (3%, 5%, 7% and 9%) were varied for the preparation of doped TiO<sub>2</sub> which were characterized by, XRD, SEM, TEM, and EDS. Doped TiO<sub>2</sub> (Fe, Si) were calcinated at different temperature (200°C, 300°C, 400°C and 500°C) to achieve the optimum dopant activation. The TEM measurements show that the particle size is in the range of 3-18 nm. With the optimum dopant concentration i.e 2% for Fe and 5% for Si, doped TiO<sub>2</sub> showed 98% degradation of fungicide under sunlight. Optical measurements indicated that the absorption band edge of Fe and Si dopants were shifted towards visible wavelength. Band gap of doped and undoped TiO<sub>2</sub> nanoparticles was measured by UV-Vis spectroscopy. Fe doped TiO<sub>2</sub> and Si doped TiO<sub>2</sub> degrades fungicide much faster than the undoped TiO<sub>2</sub> at optimum catalyst loading of 1g L<sup>-1</sup>. This signified that doped TiO<sub>2</sub> (Fe, Si) have better efficiency to degrade complex fungicide into smaller molecules in the presence of sunlight. The photocatalytic transformation products were identified by using gas chromatography-mass spectrometry (GC/MS).

**Keywords:** *Photocatalytic degradation, TiO<sub>2</sub>, dopants, fungicide*

## **BiOCl: an efficient photo and fenton-like catalyst for degradation of 2-nitrophenol**

Qihang Zhao<sup>1</sup>, Menglin Sun<sup>1</sup>, Chunfang Du<sup>1,\*</sup>

<sup>1</sup>Department of College of Chemistry and Chemical Engineering, University of Inner Mongolia, No.235 West College Road, Hohhot, Inner Mongolia, P.R.C, 010021

*E-mail: cedchf@imu.edu.cn. Fax: +86-471-4995414; Tel: +86-471-4995414*

2-nitrophenol is usually existed in the production of dyes, pesticides, photochemicals and wood preservatives, which is highly hazardous as well as toxic to human health and should be treated carefully before discharge.<sup>[1,2]</sup> Bismuth oxychloride (BiOCl) composed of asymmetric round nanoplates with a diameter of 25-50 nm and a width of 10 nm was successfully synthesized through a solvothermal route and thermal treatment at 400 °C. The XRD result indicated that all the diffraction peaks of the product could be indexed to tetragonal BiOCl (JCPDS 06-0249) and the relative strong peak suggested the favorable growth along the [110] orientation. The thermal treatment could improve the crystallinity of BiOCl, which consequently led to the enhanced catalytic activity than the counterpart without calcination. The synthesized BiOCl nanoplates after thermal treatment showed excellent activity in degradation of 2-nitrophenol under UV light irradiation, nearly 100 % within 40 min. Furthermore, 2-nitrophenol could be decomposed about 50 % within 120 min in the presence of H<sub>2</sub>O<sub>2</sub> at 60 °C without UV light irradiation. This finding expands the application fields of BiOCl and opens the possibilities for designing novel catalytic systems.

**Keywords:** *Bismuth oxychloride, 2-nitrophenol, photocatalytic activity, fenton*

[1] AKTAŞ, Ö. & ÇEÇEN, F. 2010. Adsorption and Comatabolic Bioregeneration in Activated Carbon Treatment of 2-Nitrophenol. *Journal of Hazardous Materials*, 177, 956-961.

## Improved light-free catalytic property by the modulated nanosized Zn/ZnO-CNT porous structure

Shengjuan Li<sup>a,\*</sup>, Xi Zhang<sup>a</sup>, Xiang Ning<sup>a</sup>, Yulai Gao<sup>b,\*</sup>, Mei Zhang<sup>c</sup>, Shulin Wang<sup>a</sup>

<sup>a</sup> School of Materials Science and Engineering, University of Shanghai for Science and Technology, Jungong Road 516, Shanghai 200093, P.R. China.

<sup>b</sup> Shanghai Key Laboratory of Modern Metallurgy and Materials Processing, Shanghai University, 149 Yanchang Road, 200072 Shanghai, P.R. China

<sup>c</sup> High-Performance Materials Institute, Florida State University; Department of Industrial and Manufacturing Engineering, FAMU-FSU College of Engineering, Tallahassee, FL 32310, USA

\* Corresponding author. Email: usstshenli@usst.edu.cn; ylgao@shu.edu.cn

### Abstract

We demonstrate a newly developed three-dimensional (3D) ZnO-Zn/CNT porous framework, which can be used as light-free nanocatalyst in degradation reaction. Such 3D ZnO-Zn/CNT hybrid tunable porous morphology was prepared by using carbon nanotubes and ZnO-Zn powders, including ZnO nanorods (NRs) and ZnO-Zn heterogeneous structures obtained by hydrolyzing Zn nanoparticles (NPs). The 3D ZnO-Zn/CNT porous structure was obtained by weaving ZnO-Zn/CNTs on polymethyl methacrylate (PMMA) spheres and the subsequent thermal decomposing of PMMA, which constructed crisscrossed micro-, meso- and macro-pores and channels. The hybrid porous framework has provided a new architecture with light weight, high porosity, and thus offering great potential application as catalyst. In the present study, the hybrid porous structure exhibited effective catalytic property in degrading methylene blue in aqueous solution without special light control at ambient temperature. The 3D tunnel morphology with high specific surface areas and modulated pores offers obvious deformation and enough reaction channels, which contribute more possibility to the deformation of ZnO NRs induced by flow impact, producing higher degradation efficiency than that prepared by CNT membrane. In particular, the degradation efficiency is not only related to the catalyst content but also the deformation of ZnO NRs. It is deemed that the piezoelectric effect of the ZnO NRs plays a crucial role in this degradation process. The faster the solution flows, the larger deformation of the ZnO NRs embedded in the porous structure occurs, which induces higher ionic charges to effectively degraded the methylene blue. This novel 3D hybrid porous structure really opens a new approach to develop light-free catalyst to degrade organic contaminant.

Keywords: Light-free, Modulated porous structure, ZnO nanorods, Carbon nanotubes, Catalytic property

**Environmentally Benign TiO<sub>2</sub> nanomaterials for removal of Heavy Metal Ions with interfering ions present in Tap Water**

Nupur Bahadur<sup>a\*</sup>, Tanushree Godara<sup>a</sup>, V.K. Jain<sup>a</sup>, A.K. Shukla<sup>a</sup>, Rajini Singh<sup>a</sup>, Nahar Singh<sup>b</sup>

<sup>a</sup>Amity University, Sector-125, Noida-201303, India

<sup>b</sup>CSIR-National Physical Laboratory, Dr. K.S. Krishnan Road, New Delhi-110060, India

\*Corresponding and Presenting author's: email: nupurbahadur@ymail.com; Tel: +919911023050

Availability of clean drinking water is a great challenge in developing countries like India. Time to time there have been numerous strategies adopted by Scientific community for the removal of heavy metal ions present in waste waters so as to make it available for recycle and reuse and more importantly for drinking purposes. However, with the presence of interfering ions, it always seems to be an insurmountable task of removing heavy metal ions in the presence of tap water. Undertaking nanotechnology initiatives, herein we present a case study of TiO<sub>2</sub> nanoparticles which were successfully utilized for the removal of arsenic (As), antimony (Sb) and cadmium (Cd). Since Cd was completely removed within 20 min of adsorption, therefore it was chosen for further study to be removed in the presence of interfering ions present in regular tap water. The results were very exciting as there was complete removal of Cd within few minutes of contact of TiO<sub>2</sub>. The quantitative analysis was carried at ppb level with Atomic Absorption Spectroscopy. The bare TiO<sub>2</sub> was prepared using simple sol-gel synthesis and had irregular shape morphology. However, believing that more regular and spherical shape morphology might give better results, the TiO<sub>2</sub> was further prepared using different types of cationic and anionic surfactants like CTAB and SDS, respectively but when they were tested for Cd removal, it was found that the bare TiO<sub>2</sub> having irregular shape were more efficient for the purpose. Thus this simple study clearly rules out the need of costly and harmful surfactants. Moreover it also clearly establishes a moderate role for TiO<sub>2</sub> to be an efficient adsorbent not necessary to be a photocatalyst requiring dedicated UV light sources or need for band gap tuning of TiO<sub>2</sub> in order to harness solar radiation. Further, having nil antibacterial activity, the bare TiO<sub>2</sub> could be considered environmentally benign. Thus the overall study opens up numerous possibilities of simple and efficient means of removing heavy metal ions even in the presence of interfering ions of tap water in areas especially having lack of resources.

## Degradation of 4-chlorophenol by mixed Fe/Fe<sub>3</sub>O<sub>4</sub> nanoparticles: from the perspective of mechanisms

Rong Cheng (Cheng), Can Cheng (Cheng), Lei Shi (Shi), Zhong Ma (Ma)

School of Environment and Natural Resources, Renmin University of China, Beijing  
100872, China.

*Chengrong@ruc.edu.cn*

Nanosized iron particles have been widely studied for pollution abatement these years; however, the mechanism for pollutants degradation was mainly focused on the reductive dechlorination by Fe<sup>0</sup>, and the dynamic process has not been clarified completely. It's reported that some organics could be degraded during the oxidation of Fe<sup>0</sup> by O<sub>2</sub> and H<sub>2</sub>O<sub>2</sub> was supposed to be produced. In this study, Fe<sub>3</sub>O<sub>4</sub>, the main oxidation product of nanosized Fe<sup>0</sup>, was used to treat the pollutant combining with nanosized Fe<sup>0</sup>; and 4-chlorophenol, a representative persistent organic pollutant which is highly toxic and recalcitrant towards chemical and biological degradation in the environment, was used as the model compound. The results showed that both of the removal efficiency and dechlorination efficiency were lower in the system with mixed Fe/Fe<sub>3</sub>O<sub>4</sub> nanoparticles than those with Fe<sup>0</sup> nanoparticles alone under anoxic conditions, which suggested that the addition of Fe<sub>3</sub>O<sub>4</sub> nanoparticles hindered the degradation of 4-chlorophenol by Fe<sup>0</sup> nanoparticles. Nevertheless, under aerobic conditions, the reused Fe<sub>3</sub>O<sub>4</sub> nanoparticles would improve the removal and dechlorination of 4-chlorophenol. And the Fe<sub>3</sub>O<sub>4</sub> nanoparticles which were ever used in acidic conditions showed the strongest facilitation. Fe<sup>0</sup> nanoparticles were transformed to Fe<sub>3</sub>O<sub>4</sub> and FeOOH during the process. And Fe<sub>3</sub>O<sub>4</sub> was the main product under anoxic conditions; however, the proportion of FeOOH was increased under aerobic conditions. Fe<sub>3</sub>O<sub>4</sub> nanoparticles remained as Fe<sub>3</sub>O<sub>4</sub> during the reaction, and Raman spectrum reflected that 4-chlorophenol, the acids with low molecular weight (products of 4-chlorophenol) and some other chlorinated by-products could be adsorbed on the surface of Fe<sub>3</sub>O<sub>4</sub> nanoparticles. It's proposed that the removal of 4-chlorophenol was due to the both effects of nanosized Fe<sup>0</sup> and Fe<sub>3</sub>O<sub>4</sub>—reducing action of Fe<sup>0</sup> and catalytic oxidation action of Fe<sub>3</sub>O<sub>4</sub>. The reducing action of Fe<sup>0</sup> was the

major factor under anoxic conditions. And the catalytic oxidation action of  $\text{Fe}_3\text{O}_4$  became an important reason that could not be ignored under aerobic conditions.

***Keywords:***  $\text{Fe}^0$  nanoparticles,  $\text{Fe}_3\text{O}_4$  nanoparticles, dechlorination, mechanism, catalytic oxidation

[1] KEENAN, C. R., SEDLAK, D. L. 2008. Factors affecting the yield of oxidants from the reaction of manoparticulate zero-valent iron and oxygen. Environ Sci Technol, 42, 1262-1267.



## Effect of Ce substituted hydrotalcite-derived mixed oxides on total catalytic oxidation of air pollutant.

Genty E.<sup>1</sup>, Brunet J.<sup>1</sup>, Pequeux R.<sup>1</sup>, Capelle S.<sup>1</sup>, Siffert S.<sup>1</sup>, Cousin R<sup>1\*</sup>.

<sup>1</sup> UCEiV - Université du Littoral Côte d'Opale, Dunkerque, France.

\* [Renaud.Cousin@univ-littoral.fr](mailto:Renaud.Cousin@univ-littoral.fr)

Emission of Volatile Organic Compounds (VOCs) into the environment is now strictly regulated due to harmful on public health and atmospheric environment. Among many technologies available for VOCs control, the catalytic oxidation of these pollutants to carbon dioxide and water has been recognized as one of the most promising technologies. In the aim to obtain a reaction economically competitive, it is necessary to explore higher active catalysts performing at low temperatures. Transition metal oxides, especially cobalt, copper and manganese oxides, offer a low cost alternative to metal noble based catalysts which are presently the most active catalysts in the complete oxidation of VOCs at low temperatures. An interesting way to obtain mixed oxides catalysts is through the use of hydrotalcites or layered double hydroxides as precursors. Indeed, after calcination treatment mixed oxides are formed and possess unique properties like a high surface area, good thermal stability, good mixed oxides homogeneity and basic properties. The partial or the total substitution of  $Mg^{2+}$  and  $Al^{3+}$  is possible by divalent cation or trivalent cation in the hydrotalcite structure. Cerium oxide ( $CeO_2$ ) is widely used as a promoter in various redox reactions due to its reducibility and high oxygen storage capacity. The introduction of Ce ions in the hydroxide layer of LDHs is difficult because of their large ionic radius, when compared to  $Mg^{2+}$  and  $Al^{3+}$ . In the present study, Co-Al-Ce hydrotalcite as precursors are characterized and investigated for total oxidation of toluene.

Hydrotalcite like compounds called  $Co_6Al_{2-x}Ce_xHT$  (with  $0 \leq x \leq 0.8$ ) were prepared by co-precipitation with several cerium content. The calcination treatment was performed under air (4 hours at  $500^\circ C$ ). The solids were characterized by several physicochemical technics ( $N_2$  sorption, XRD,  $H_2$ -TPR, XPS). The toluene total oxidation was conducted at atmospheric pressure in a quartz flow micro reactor containing 100 mg of catalyst using a gas mixture containing of 1000 ppm  $C_7H_8$  and 20%  $O_2$  in He.

For the dried samples, the hydrotalcite phase was observed on XRD patterns. Concerning calcined samples,  $\text{CeO}_2$ ,  $\text{Co}_3\text{O}_4$ ,  $\text{CoAl}_2\text{O}_4$  and  $\text{Co}_2\text{AlO}_4$  spinel phases were revealed by XRD for the  $\text{Co}_6\text{Al}_{2-x}\text{Ce}_x\text{HT500}$  samples. Mixed oxides obtained by calcination present several textural differences. A better catalytic activity for toluene total oxidation was observed for the solids when cerium is incorporated. Thus, the presence of cerium in the Hydrotalcite structure is very interesting and promising for the development of performing catalysts for the VOCs abatement.

**Keywords:** *Layered double hydroxide; catalytic oxidation; cerium, cobalt*

## Photocatalytic activity of ZnO in the oxidation reaction of nitric oxide

E. Luévano-Hipólito<sup>1</sup>, [A. Martínez-de la Cruz](#)<sup>1</sup>

<sup>1</sup> CIIDIT, Facultad de Ingeniería Mecánica y Eléctrica, Universidad Autónoma de Nuevo León, Ciudad Universitaria, C.P. 66451, San Nicolás de los Garza, N. L., México.

[azael.martinezdl@uanl.edu.mx](mailto:azael.martinezdl@uanl.edu.mx), [azael70@yahoo.com.mx](mailto:azael70@yahoo.com.mx)

Zinc oxide is a very important material in the ceramic industry due to its excellent properties as chemical stability, broad range radiation absorption, photostability, hardness, rigidity, low toxicity, and low cost [1]. Besides the classical TiO<sub>2</sub> oxide, ZnO is a semiconductor oxide that it has proven be an efficient photocatalyst in the reaction of degradation of numerous organic pollutants in wastewater. In this work the ability of ZnO to act as photocatalyst in the air purification will be evaluate.

ZnO samples were prepared by several synthesis routes such as sol-gel, precipitation, solvothermal, and solvothermal assisted with polyethylene glycol. The physical properties of ZnO samples were studied by X-ray powder diffraction (XRD), scanning electron microscopy (SEM), UV Vis diffuse reflectance spectroscopy (DRS) and adsorption-desorption N<sub>2</sub> isotherms (BET). The photocatalytic activity of oxides prepared was compared by means the oxidation reaction of nitric oxide (NO) under UV light irradiation. The conversion degree of NO reached by each oxide was associated with their physical properties. In this sense, ZnO sample prepared by sol-gel exhibited the highest conversion of nitric oxide under steady state reaching a removal of 70%. This situation was associated with the fact that this sample exhibited the lowest particle size, highest surface area, and highest radiation adsorption among the ZnO samples studied. The presence of nitrate ions as product of deep oxidation of NO was successfully confirmed by a simple reduction method of nitrate to nitrite ions using a colorimeter.

**Keywords:** ZnO, heterogeneous photocatalysis, NO<sub>x</sub>, nitric oxide

[1] RADZIMSKA, A. K., JESIONOWSKI, T. 2014. Zinc Oxide-From Synthesis to Application: A Review. Materials, 7, 2833-2881.

## Co-Al-Ce mixed oxide materials prepared by Hydrotalcite way for VOCs total oxidation in micro- and semi-pilot scale

J. Brunet<sup>1</sup>, E. Genty<sup>1</sup>, G. De Weireld<sup>2</sup>, D. Thomas<sup>2</sup>, A. Decroly<sup>2</sup>, S. Siffert<sup>1</sup>, R. Cousin<sup>1\*</sup>

<sup>1</sup>Unité de Chimie Environnementale et Interactions sur le Vivant, Université du Littoral Côte d'Opale (ULCO), 59140 Dunkerque (France)

<sup>2</sup>Département Chimie - Science des Matériaux, Université de Mons (UMons), B-7000 Mons (Belgium).

*E-mail address: Renaud.Cousin@univ-littoral.fr*

The removal of VOCs, done by catalytic oxidation, is an expensive process. Indeed, the supported noble metals have been generally regarded as the most desirable catalysts, in terms of their catalytic activity for catalytic oxidation. However, transition metal based oxides can replace traditional noble-metal-based catalysts, because of their low cost and stability. Recently some hydrotalcites have been reported [1] as precursors for obtaining catalysts for VOCs elimination and they exhibit promising results. Thus, a ternary mixed oxide Co-Al-Ce has been developed in the laboratory by synthesis method using hydrotalcite way. This material was studied as a catalyst for the total oxidation of VOCs (toluene and/or methyl ethyl ketone) alone or in mixtures. It showed very interesting performances in comparison with catalysts based on noble metals.

This work focuses on preparing of the mixed oxide Co-Al-Ce in large quantities for his study in a semi-pilot. The method of synthesis has been adapted to combine repeatability and uniformity of the material. It was then shaped and has been studied for the catalytic oxidation of VOCs in a semi-pilot.

**Keywords:** *VOCs oxidation, transition metal, mixed oxide, hydrotalcite way, scaling-up*

[1] Genty, E., Cousin, R., Capelle, S., Gennequin, C. and Siffert, S. 2012. Catalytic Oxidation of Toluene and CO over Nanocatalysts Derived from Hydrotalcite-Like Compounds ( $X_6^{2+}Al_2^{3+}$ ): Effect of the Bivalent Cation. *Eur. J. Inorg. Chem.*, 2012: 2802–2811.

## The Development of Core-Shell, Methane-Oxidation Nano Catalysts

M. Khader<sup>1\*</sup>, S. Ali<sup>1</sup>, P. Fornasiero<sup>2</sup> and R. J. Gorte<sup>3</sup>

(1) Gas Processing Center, Qatar University, Doha, Doha 2713, Qatar, (2) Department of Chemical and Pharmaceutical Sciences, University of Trieste, Trieste, Trieste, Italy, (3) Department of Chemical and Biomolecular Engineering, University of Pennsylvania, Philadelphia, Pennsylvania 19104, United States

The development of methane-combustion nano catalysts that showed high rates at lower temperatures and good stability at higher temperatures would have a significant impact on a number of energy-based technologies. We have demonstrated that core-shell catalysts, with metal nano-particles surrounded by a nano oxide shell, can be synthesized in solution and then deposited onto various oxide supports. In the case of Pd@ceria/alumina and Pd@TiO<sub>2</sub>/alumina, the materials have shown very interesting activities and high stabilities. Under dry conditions, both Pd@TiO<sub>2</sub> and Pd@CeO<sub>2</sub> were highly active and showed nearly identical reaction rates; however, unlike Pd@CeO<sub>2</sub>, the Pd@TiO<sub>2</sub> catalysts did not experience deactivation due to hydroxide formation during methane oxidation under wet conditions. The high activity of both Pd@TiO<sub>2</sub> and Pd@CeO<sub>2</sub> is partially due to the reducibility of the oxide shells.

This presentation will show that data, along with recent investigations into the effects of water on the oxidation rates.

\*Corresponding author: mmkhader@qu.edu.qa

### Acknowledgement

This research was made possible by an NPRP Grant #6-290-1-059 from the Qatar National Research Fund (a member of Qatar Foundation). The statements made herein are solely the responsibility of the authors.

## Magnetically separable and reusable nano catalyst for carbon-carbon bond formation reactions

Vasundhara Singh<sup>1</sup>, Amanpreet Kaur<sup>1</sup>

<sup>1</sup> Department of Applied Sciences (Chemistry), PEC University of Technology, Chandigarh, INDIA

vasun7@yahoo.co.in, vasundhara@pec.ac.in

One of the important challenges in the chemical industry and for the development of green chemical processes is the design of catalysts which can be reused and can be easily separated from the reaction mixture. The inherent limitation of homogeneous catalysis wherein the catalyst cannot be reused has resulted in the development of new strategies like heterogenisation of Pd on a solid support which facilitates catalyst recycling and recovery. A variety of materials such as carbon, clay, metal oxide, silica, zeolite and polymer resins have been explored in Pd mediated catalysis, in which Pd complex or Pd nanoparticle acts as an active species.

Recently, magnetic nanoparticles (MNPs) have emerged as ideal supports due to their large surface area, low preparation cost, low toxicity, and good stability for anchoring catalysts for facile separation by an external magnet. Literature records several examples of a magnetic catalytic system which provides more effective separation of the catalyst than is possible by traditional filtration and centrifugation methods and also avoids catalyst loss [1].

In the present work a palladium based catalyst has been synthesized by anchoring the complex moiety on the surface of magnetic  $\text{Fe}_3\text{O}_4@\text{SiO}_2$ . The as prepared catalyst was well characterized and evaluated in carbon-carbon bond formation reactions in terms of its high activity in ionic liquid media. The catalyst was easily recoverable from the reaction medium by an external magnet and recycled upto seven cycles without loss in activity.

**Keywords:** *Palladium catalysts, magnetic supports, carbon-carbon bond formation, easy separation*

[1] ZHANG, L., LI, P., LIU, C., YANG, J., WANG, M., & WANG, L. 2014. A highly efficient and recyclable  $\text{Fe}_3\text{O}_4$  magnetic nanoparticle immobilized palladium catalyst for the direct C-2 arylation of indoles with arylboronic acids. *Catal. Sci. Technol.*, 4, 1979-1988.

## Synthesis of catalytically-active Cu<sup>II</sup> and Zn<sup>II</sup> coordination polymer nanocrystals using a microemulsion method

Carla Meledandri,<sup>1,2</sup> Nigel Lucas,<sup>1,2</sup> Kiattipoom Rodpun,<sup>1,2</sup> Eng Tan<sup>1</sup>

<sup>1</sup> Department of Chemistry, University of Otago, Dunedin 9054, New Zealand; cmeledandri@chemistry.otago.ac.nz

<sup>2</sup> MacDiarmid Institute for Advanced Materials and Nanotechnology, University of Otago, Dunedin 9054, New Zealand

Ultra-small nanocrystals composed of either Zn<sup>2+</sup>- or Cu<sup>2+</sup>-coordination polymers with uniform shape and controllable size have been synthesised within confined nanoscale water droplets using a specifically-tailored modification of the microemulsion method (Figure 1). Notably, under optimised conditions, it is estimated that each nanocrystal contains < 5 repeating units. The nanocrystals have been observed to form solvent-dispersible aggregate structures of controlled size and shape, in the range of 50 – 80 nm. In contrast to macroscopic coordination polymer crystals of identical composition, the nanocrystals demonstrate high catalytic activity, as evidenced through their use in a ring opening reaction of cyclohexene oxide with aniline. Furthermore, a reduced form of the Cu<sup>I</sup> NCPs has been successfully employed as a catalyst for an azide-alkyne cycloaddition “click” reaction in nonpolar solvent. The synthetic method described in this work represents a convenient approach to the synthesis of coordination polymer nanocrystals with tunable properties, as the ligands can be independently modified and selectively combined with desired metal ions to prepare materials for various applications.

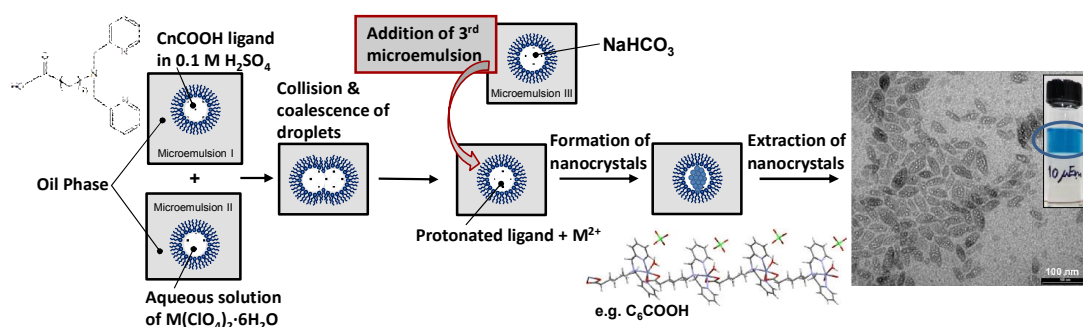


Figure 1. Synthesis of Cu(II) coordination polymer nanocrystals composed of polydentate bridging ligands, and TEM image of the resulting nanostructures.

# Symposia 7

## Low dimensional, Nano and 2D materials

---

- Structural, electrical, mechanical and optical of low dimensional, nano and 2D-layered oxides, nitrides and sulfides
- Advances in the Synthesis and Characterization of low dimensional, nano and 2D materials
- Large Scale Growth & Characterization of 2D-layered oxides, nitrides, carbides and sulfides
- Spectroscopy studies of low dimensional, nano and 2D materials Carbon Based materials
- Advanced Nuclear Materials
- Magnetic Materials
- Applications of low dimensional, nano and 2D materials
- Nano-optics, Nano-optoelectronics, Nano-Photonics and Nano-photonics
- Computational modeling and simulation of low dimensional, nano and 2D materials
- Low dimensional, nano and 2D materials for optical devices, Flexible Electronics, Sensors & Composites
- Nanomedicine, Nanobiotechnology, Environment and Nanotoxicology
- Photonic and optoelectronic device applications of low dimensional, nano and 2D materials
- Exfoliation and unzipping 2D materials
- Others



# INDEX PAGE

1. Everything but the kitchen sink: delamination of layered silicates using a kitchen blender, a freezer, and microwave heating	1
<b>AUTHOR:</b> Dr. Antoine Hervier	
2. Elaboration of Nano-SiC / Carbon Nanotubes Composites : Mechanical, Thermal and Electric Properties	4
<b>AUTHOR:</b> Dr. Yann Leconte	
3. Non-Classical Crystal Growth of Decorated ZnO Microstadiums	5
<b>AUTHOR:</b> Ms. Katherine Self	
4. Synthesis of BNNTs from Residual Materials by chemical vapor deposition technique	6
<b>AUTHOR:</b> Dr. Pervaiz Ahmad	
5. Template-Assisted and Electrochemical Synthesis of Novel Nanostructures	7
<b>AUTHOR:</b> Prof. Lichun Liu	
6. 34 nanoparticles for application in MRI: mastering size and magnetism through a new coprecipitation route	9
<b>AUTHOR:</b> Dr. Clara Pereira	
7. 2D Nanomaterials	11
<b>AUTHOR:</b> Prof. Eileen Fong	
8. Catalytic Conversion Reaction of Hexagonal Boron Nitride to Graphene for Graphene/Boron Nitride Lateral Heterostructure	12
<b>AUTHOR:</b> Prof. Gwangwoo Kim	
9. Silver Chalcogenide-Based Hybrid Nanocrystals With Enhanced Thermoelectric Properties	13
<b>AUTHOR:</b> Dr. Albert Figuerola	
10. Advanced Microchannel System Design for Homogeneous Size and Morphology of Nanomaterials	14
<b>AUTHOR:</b> Prof. Ali Canlier	
11. 2001)Si-based compressively strained sGe- Quantum Wells	15
<b>AUTHOR:</b> Prof. Oleg Mironov	
12. 3 devices.	16
<b>AUTHOR:</b> Prof. Marc Fontana	
13. A Direct Growth of Wafer-Scale Monolayer Graphene using Microwave Plasma CVD	17
<b>AUTHOR:</b> Prof. Zexiang Chen	
14. Simulation of Quantum Dot Growth: Towards Rational Development of Nanomaterials With Predictable Properties	18
<b>AUTHOR:</b> Dr. Pavel Samokhvalov	
15. DNA-promoted polymerization of pyrrole; a route to templated DNA origami conductive networks	20
<b>AUTHOR:</b> Dr. Andrew Pike	
16. Large Scale Interlayer Carbon Bonding in Multilayer Graphene via Surface Hydrogenation	21
<b>AUTHOR:</b> Prof. Seong In Yoon	
17. Green synthesized noble metals for biological applications	22
<b>AUTHOR:</b> Dr. Jakub Siegel	
18. Carbon Nanotube based Three Stage Operational Amplifiers, a Simulation Study	24
<b>AUTHOR:</b> Prof. Shuja Abbasi	
19. 3D graphene foam electrode	25
<b>AUTHOR:</b> Mr. Hongyan Yue	
20. Water through Graphynes' Pores: First-Principles Penetration Barrier and Force Field	27

Optimization <b>AUTHOR:</b> Dr. Massimiliano Bartolomei	
<b>21.</b> Bismuth Telluride Based Nanowires For Direct Thermoelectric Energy <b>AUTHOR:</b> Dr. Massimiliano Bartolomei	28
<b>22.</b> Graphene for spin transport <b>AUTHOR:</b> Prof. Pierre Seneor	29
<b>23.</b> 2 nanopencils as electron source <b>AUTHOR:</b> Dr. Dilip Joag	31
<b>24.</b> Boron Nitride Nanosheets <b>AUTHOR:</b> Prof. Ying Chen	32
<b>25.</b> 2 Hybrid Device <b>AUTHOR:</b> Prof. Gil Ho Kim	33
<b>26.</b> Investigation Of Accommodation Mechanisms Using A Three Dimensional Finite Element Rve Model Of Polycrystalline Nanostructured Niti <b>AUTHOR:</b> Mr. Manuel Petersmann	34
<b>27.</b> 2D Nanostructures <b>AUTHOR:</b> Prof. Petr Kral	36
<b>28.</b> Catalyst-Free Growth of multi-layer h-BN on Sapphire Substrate <b>AUTHOR:</b> Prof. A-Rang Jang	37
<b>29.</b> Catalyst-Free Growth of multi-layer h-BN on Sapphire Substrate <b>AUTHOR:</b> Prof. Hyeon Suk Shin	38
<b>30.</b> 34 Nanofibers for A Fast Responsive Selective Ammonia Sensor <b>AUTHOR:</b> Dr. Xiaogan Li	39
<b>31.</b> Nanocrystalline Graphene/Hematite Composites: Rational Synthesis and Catalytic Gas Sensing Behavior <b>AUTHOR:</b> Prof. Joerg Schneider	40
<b>32.</b> Towards printable, conductive and functionalised graphene based inks <b>AUTHOR:</b> Mr. Tom Bamford	41
<b>33.</b> 3Ht To Produce P/N Hetero-Junction Array Of Zno Nanowires <b>AUTHOR:</b> Mr. Yi-Chieh Chao	42
<b>34.</b> 3Ht To Produce P/N Hetero-Junction Array Of Zno Nanowires <b>AUTHOR:</b> Mr. Yi-Chieh Chao	43
<b>35.</b> 06043 ilmenite oxide <b>AUTHOR:</b> Dr. Johannes Frantti	44
<b>36.</b> 514 System <b>AUTHOR:</b> Dr. Andre Pereira	45
<b>37.</b> Synthesis of metallic magnetic nanorods protected by noble metal shell <b>AUTHOR:</b> Dr. Soulantica Katerina	47
<b>38.</b> Superparamagnetic Iron Oxide Nanoparticles Investigated By Nuclear Magnetic Resonance And Magnetization Measurements <b>AUTHOR:</b> Mr. Petr Kristan	49
<b>39.</b> The Particle Size Dependent Cation Distribution And Magnetization Of Lithium Ferrite <b>AUTHOR:</b> Prof. Vladimir Sepelak	50
<b>40.</b> 24 <b>AUTHOR:</b> Mr. Munish Gupta	51
<b>41.</b> Biocompatible Gold Nanorods: One-step Surface Functionalization and Complete Detoxification <b>AUTHOR:</b> Dr. Yuanhui Zheng	52
<b>42.</b> 34 Nanoparticles Interfere Spore Germination Of Clostridium Difficile: An In Vitro And In Vivo Study <b>AUTHOR:</b> Prof. Dar-Bin Shieh	53
<b>43.</b> Conventional antibiotics in form of nanospheres for the prevention of biofilm	55

formation and provide infection control <b>AUTHOR:</b> Dr. Margarida Fernandes	
<b>44.</b> 2 Nanoparticles For Uv Protective, Antibacterial, Mosquitocidal And Seed Germination Inducing Potentials <b>AUTHOR:</b> Dr. Brindha Durairaj	56
<b>45.</b> Porous Silicon Based Mass Spectrometry Platform for Biomarker Diagnosis <b>AUTHOR:</b> Dr. Frédéric Gaillard	58
<b>46.</b> Controlling neuronal and glial cell behavior by patterning vertical gallium phosphide nanowires <b>AUTHOR:</b> Dr. Maria-Thereza Perez	60
<b>47.</b> Making structured metals transparent for ultrabroadband electromagnetic waves <b>AUTHOR:</b> Prof. Ru-Wen Peng	62
<b>48.</b> White quantum dot light emitting diode by mixed blue-green-red QDs <b>AUTHOR:</b> Dr. Jing Chen	63
<b>49.</b> Structural Investigation on Catalyst-Free Si-Doped InAs Nanowires <b>AUTHOR:</b> Mr. Dong Woo Park	64
<b>50.</b> 2D nanowires by thermal oxidation method and their application in solar cells <b>AUTHOR:</b> Prof. Yang Ju	65
<b>51.</b> 5-nm Graphene Nanowrinkles <b>AUTHOR:</b> Dr. Hyunseob Lim	67
<b>52.</b> Nanophotonics with Nanocarbon Materials: From Bio-sensing to Remote Heat Removal (keynote) <b>AUTHOR:</b> Prof. Vyacheslav V. Rotkin	68
<b>53.</b> 2D(ZnO) <sub>n</sub> Nanostructures With Tunable Compositional And Optical Properties <b>AUTHOR:</b> Ms. Yujie Guo	70
<b>54.</b> 2D Hall effects of individual ZnO microwire <b>AUTHOR:</b> Prof. Sang Wook Lee	71
<b>55.</b> Laser-Assisted Processing And Diagnostics Of Functional Micro/Nanomaterials <b>AUTHOR:</b> Prof. David Hwang	72
<b>56.</b> Strain induced energy level engineering in semiconductor nanocrystals <b>AUTHOR:</b> Mr. Chinmay Phadnis	74
<b>57.</b> 3-LDH) prepared at different pH values <b>AUTHOR:</b> Dr. Abdullah Ahmed Ali Ahmed	76
<b>58.</b> Electrical And Structural Properties Of Octahedral Layered Manganese Oxides Materials Substituted With Cobalt <b>AUTHOR:</b> Ms. Monica Maria Gomez Hermida	78
<b>59.</b> 2 van der Waals Heterostructures <b>AUTHOR:</b> Prof. Yongsheng Wang	80
<b>60.</b> Tuning Sulfur Doping in Graphene for Highly Sensitive Dopamine Biosensors <b>AUTHOR:</b> Dr. He Zhao	81
<b>61.</b> SERS study of plasmon induced functionality of aryl azo heterocycles <b>AUTHOR:</b>	82
<b>62.</b> Graphene Oxide Networks As The Illuminated Carriers <b>AUTHOR:</b> Ms. Elham Bidram	
<b>63.</b> Bioinspired Structure Materials to Control Water-collecting Properties <b>AUTHOR:</b> Prof. Yongmei Zheng	

## **Everything but the kitchen sink: delamination of layered silicates using a kitchen blender, a freezer, and microwave heating**

Antoine Hervier<sup>1</sup>, Souhir Boujday<sup>1</sup>, Juliette Blanchard<sup>1</sup>

<sup>1</sup> UPMC-CNRS, UMR 7197, Laboratoire de Réactivité de Surface, F-75005, Paris,  
France

*Presenting author:* [antoine.hervier@upmc.fr](mailto:antoine.hervier@upmc.fr)

*Corresponding author:* [juliette.blanchard@upmc.fr](mailto:juliette.blanchard@upmc.fr)

Layered silicates are inexpensive and versatile materials with already several industrial applications, particularly in the polymer industry. They consist of silicate sheets, several microns across and just a few nanometers thick, stacked on top of each other, and separated by layers of cations. With an effective delamination method, these materials could serve as a source of large amounts of functionalized, nanometer thin sheets. This could be of use in the production of biosensors, which require large, nanostructured surfaces produced at low cost.

Another material with a similar geometry, graphene, has generated tremendous attention because of its highly unusual physical properties. One of the strategies currently being considered for the mass production of graphene sheets is in fact the delamination of graphite or graphite oxide, with already many different methods reported in the literature<sup>1-3</sup>. These same methods may prove to be just as useful for the production of silicate sheets.

We report on the use of several of these methods, all of them inexpensive and simple to implement, in the delamination of layered silicates. The kitchen blender is used because high speed mixing creates shear strain within the material, causing the layers to come apart. As for freezing and microwave heating, the mechanisms at play are still not well understood, but may involve the expansion of water trapped between the silicate layers.

This study focuses on ilerite and magadiite, two commonly studied layered silicates. As synthesized, the electrostatic interactions holding the sheets together are too strong for delamination to occur. The sodium ions were exchanged with much bulkier cetyltrimethylammonium ions in order to increase the distance between the sheets, allowing for the insertion of functionalization agent, cyanopropyltrichlorosilane. Once the surface has been silanized, the surface charge is significantly reduced, and the sheets can be separated.

The extent of the delamination was characterized using atomic force microscopy of solutions dropcast onto a substrate. At the appropriate silicate concentration, and after optimizing the delamination process, a near monolayer deposition of large fragments ( $\approx 1 \mu\text{m}$ ) of functionalized silicates is observed with very little overlap, over large areas, on the order of a  $1 \text{ cm}^2$ .

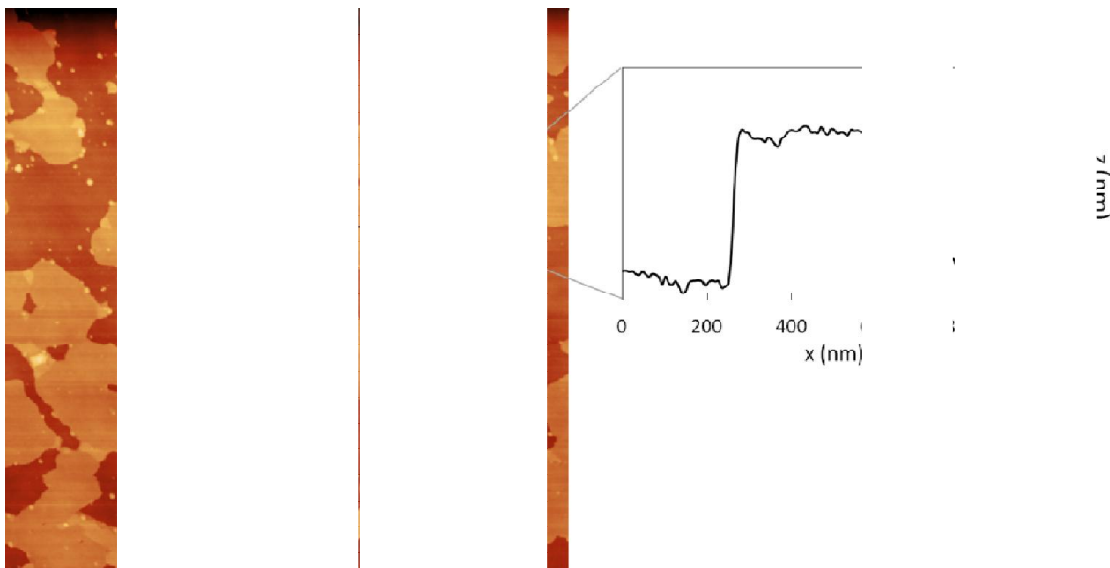


**Fig.1** – AFM image and cross-section of ilerite sheets delaminated with a kitchen blender and dropcast onto a silicon substrate

**Keywords:** Layered silicates, delamination, atomic force microscopy

- [1] ZHU, Y.; MURALI, S.; STOLLER, M. D.; VELAMAKANNI, A.; PINER, R. D.; RUOFF, R. S. 2010. Microwave assisted exfoliation and reduction of graphite oxide for ultracapacitors. *Carbon*, 48, 2118-2122.
- [2] PATON, K. R.; VARRLA, E.; BACKES, C.; SMITH, R. J.; KHAN, U.; O'NEILL, A.; BOLAND, C.; LOTYA, M.; ISTRATE, O. M.; KING, P.; others. 2014. Scalable production of large quantities of defect-free few-layer graphene by shear exfoliation in liquids. *Nature materials* 13, 624–630.
- [3] OGINO, I.; YOKOYAMA, Y.; IWAMURA, S.; MUKAI, S. R. 2014. Exfoliation of Graphite Oxide in Water without Sonication: Bridging Length Scales from Nanosheets to Macroscopic Materials. *Chemistry of Materials*, 26, 3334–3339.

## **Elaboration of Nano-SiC / Carbon Nanotubes Composites : Mechanical, Thermal and Electric Properties**

B. Lanfant<sup>1</sup>, Y. Leconte<sup>1</sup>, M. Pinault<sup>1</sup>, M. Mayne-L'Hermite<sup>1</sup>, G. Bonnefont<sup>2</sup>, V. Garnier<sup>2</sup>, Y. Jorand<sup>2</sup>, G. Fantozzi<sup>2</sup>, S. Le Gallet<sup>3</sup>, F. Bernard<sup>3</sup>

<sup>1</sup> DSM/IRAMIS/NIMBE/LEDNA, CEA Saclay, Bât. 522, 91191 Gif sur Yvette, France.

<sup>2</sup> MATEIS, Université de Lyon, INSA de Lyon, UMR CNRS 5510, Bât. Blaise Pascal, 7 Av. Jean Capelle, 69621 Villeurbanne Cedex, France.

<sup>3</sup> ICB, Université de Lyon, UMR CNRS 6303, 9 Av. Alain Savary, BP 47870, 21078 Dijon Cedex, France.

*yann.leconte@cea.fr*

Carbides materials such as SiC, due to their refractory nature and their low neutron absorption are believed to be promising candidates for high temperature nuclear or aerospace applications. However, SiC brittleness has limited its structural application. In order to overcome this drawback, a reduction of grain size below 100 nm is expected to enhance mechanical properties. Reinforcement by carbon nanotubes (CNTs) could also be of great interest because of their interesting mechanical, thermal and electric properties. We report here the elaboration of nanoSiC/CNTs composites together with the study of their related properties.  $\beta$ -SiC nanopowders (15-20 nm) differing in surface composition (C or O controlled contamination) were synthesized by laser pyrolysis. CNTs several hundred microns in length were grown by catalytic CVD. Thanks to spark plasma sintering process, SiC matrix grain size was kept below 100 nm while final densities were higher than 96%. Finally, the obtained composites were subjected to hardness, toughness, and thermal and electric conductivities measurements performed in different directions, as the orientation of CNTs upon sintering lead to anisotropy.

**Keywords:** *Silicon carbide, Carbon nanotubes, Ceramic Matrix Composites, Nanomaterials*

## Non-Classical Crystal Growth of Decorated ZnO Microstadiums

Katherine Self\* and Wuzong Zhou

EaStChem, School of Chemistry, University of St Andrews, Fife, KY16 9ST, United Kingdom  
Email: ks478@st-andrews.ac.uk

Hexagonal microdisks of zinc oxide (Figure 1a) have been synthesized via a hydrothermal method which appear single crystalline. A reversed crystal growth mechanism (1) has been revealed for the microdisks by analysing specimens across a range of time intervals. It was found that initially the precursor materials aggregate into disordered quasi spherical particles on the glass substrate and then undergo surface crystallization. The seemingly single crystal disks, therefore, are actually composed of a “core-shell” structure with a disordered, polycrystalline core encased in a layer of single crystal.(2) This structure allows the selective dissolution of the core, resulting in ZnO microstadiums (Figure 1b). Furthermore, nanocones of ZnO were grown on the surfaces of the ZnO structures giving rise to ZnO decorated microstadiums (Figure 1c). This structure is unusual as it would be more energetically favourable for additional ZnO to form simply as an extension of the existing ZnO structure (via classical crystal growth).It was determined, however, that a polymer layer coats the surfaces of the ZnO microstadiums which enhances the aggregation of precursor ions. These aggregates grow larger over time and recrystallize to form the single crystal cones. The nanocones also, therefore, follow a non-classical growth route, challenging our existing knowledge of crystal growth.

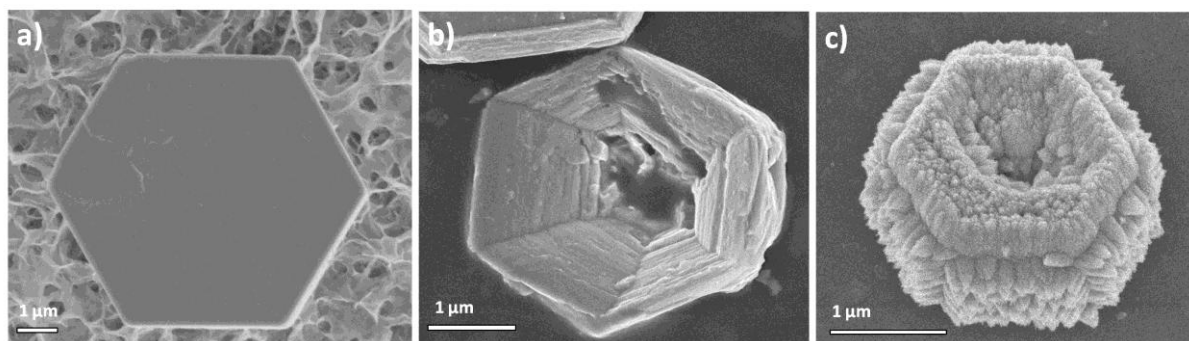


Figure 1. SEM images displaying the 3 step formation mechanism of ZnO decorated microstadiums.

### References

- (1) X. Y. Chen, M. H. Qiao, S. H. Xie, K. N. Fan, W. Z. Zhou and H. Y. He, *J. Am. Chem. Soc.*, 2007, 129(43), 13305.
- (2) K. Self, H. Zhou, H. F. Greer, Z. R. Tian, W. Z. Zhou, *Chem. Commun.*, 2013, 49(47), 5411.



**Synthesis of BNNTs from Residual Materials by chemical vapor deposition technique**

Pervaiz Ahmad , Mayeen Uddin Khandaker, Yusoff Mohd Amin, Ziaul Raza Khan

*Department of Physics, Faculty of Science University of Malaya 50603 Kuala Lumpur Malaysia*

*Corresponding author. Tel.: +601115402880; Fax: +60379674146.*

*E-mail: [mu\\_khandaker@yahoo.com](mailto:mu_khandaker@yahoo.com), [mu\\_khandaker@um.edu.my](mailto:mu_khandaker@um.edu.my) (MU Khandaker)*

**Abstract**

Chemical vapor deposition technique is used with some modifications for the synthesis of BNNTs at 1200 °C in a conventional horizontal tube furnace. Ar gas is used as a reaction atmosphere inside the chamber. After BNNTs synthesis the residual materials left in alumina boat is covered with a few new Si substrate and tried for another (BNNTs) synthesis. The synthesized BNNTs are thinner at the bottom and thicker at the top with a thick bulb-like tip. The synthesized nanotubes have internal bamboo like structures with an interlayer spacing of 0.34 nm. XPS and Raman confirmed the Boron and Nitrogen components of synthesized nanotubes with  $E_{2g}$  mode of h-BN.

**Keywords:** BNNTs, Residual material, Synthesis.

**PACS:** 81.07.De

## Graphene Oxide networks as the illuminated carriers

Elham (Bidram<sup>1</sup>)\*, Adrian (Putro Sulistio<sup>1</sup>), Dave (Dunstan<sup>1</sup>), Alastair (Stewart<sup>2</sup>)

<sup>1</sup> Chemical and Biomolecular Engineering, university of Melbourne

<sup>2</sup>Pharmacology and Therapeutics, Medical building, university of Melbourne

\**elhamb@student.unimelb.edu.au*

The recently discovered carbon polymer, Graphene oxide (GO), is one of the most attractive two dimensional polymer especially in medical and clinical applications due to its large surface area, adsorption affinity with the variety of biomolecules and its optical properties. In this study, GO biomedical derivatives [poly-ethylen-glycol functionalized (PEGylated) GO with Folic acid (GOPEGFA) and poly-ethylen-glycol functionalized GO (PEGylated) with RGD peptide (GOPEGRGD)] have been synthesized and studied spectroscopically. The observed emission spectrum varies widely depending on the applied excitation wavelengths over the range of 200 nm to 488 nm. Notably, these derivatives exhibit the fluorescence phenomenon more intensely than pristine Graphene Oxide. Fluorescence microscopy also shows the strong and bright fluorescence in three main fluorescence regions (blue, green and red) when different excitation ranges (filters) put on for the same sample. We also found that the attached targeting ligand seems to affect the observed fluorescence in cell media. As a result, these produced networks have the potential to be used as a probe for dye free fluorescence imaging and tracking. Removing the potential toxic effects of dyes is the most important advantages of this system. Taken together, initial observation shows the potential application of Functionalized GO sheets as a traceable component in cell media as well as the appropriate carrier for drug delivery purposes. Therefore these unique characteristics of GO can decrease the complexity and toxicity of the therapeutical systems.

***Keywords: Graphene Oxide (GO), fluorescence property, functionalized sheets, biomedical derivatives, traceable component***

## Tailored design of high-performance Fe<sub>3</sub>O<sub>4</sub> nanoparticles for application in MRI: mastering size and magnetism through a new coprecipitation route

Clara (Pereira)<sup>1</sup>, André (Pereira)<sup>2</sup>, Mariana (Rocha)<sup>1</sup>, Cristina (Freire)<sup>1</sup>, Carlos (Geraldes)<sup>3</sup>

<sup>1</sup>REQUIMTE, Chemistry and Biochemistry Department, Faculty of Sciences of Porto University (FCUP), 4169-007 Porto, Portugal

<sup>2</sup>IFIMUP and IN, Physics and Astronomy Department, FCUP, 4169-007 Porto, Portugal

<sup>3</sup>Life Sciences Department and Coimbra Chemistry Center, Faculty of Sciences and Technology, Coimbra University, 3001-401 Coimbra, Portugal

*clara.pereira@fc.up.pt*

Superparamagnetic iron oxide nanoparticles (NPs) are a family of magnetic nanomaterials with a wide range of applications such as in biomedicine, environmental remediation and data storage. Among iron oxides, magnetite (Fe<sub>3</sub>O<sub>4</sub>) and maghemite ( $\gamma$ -Fe<sub>2</sub>O<sub>3</sub>) NPs are of prime importance as contrast agents in MRI due to their nanoscale dimensions, high saturation magnetization, non-toxicity and biocompatibility.[1] Several strategies have been developed to achieve efficient  $T_2$  iron oxide-based contrast agents with controlled size and improved magnetic properties, mostly based on coprecipitation, thermal decomposition and polyol processes.[1] The aqueous coprecipitation route continues to be one of the prime choices for the production of this type of contrast agents since it is eco-sustainable, less time consuming, cost effective and easily scalable.[2] However the control of the nanomaterials size and magnetic properties through this route is still challenging.

This work reports a new one-pot aqueous coprecipitation process for the tailored design of superparamagnetic Fe<sub>3</sub>O<sub>4</sub> NPs. Through the use of a new generation of polyfunctional alkanolamine bases, we were able to master the particles size and magnetic properties, improving the saturation magnetization (up to 65.1 emu g<sup>-1</sup>) while reducing the nanomaterials dimensions (from 9.0 to 4.8 nm). The alkanolamines not only acted as coprecipitation agents, but also had a crucial role on the improvement of the surface spin order (magnetic dead layer) due to their complexation with the the subcoordinated metal

atoms on the NPs surface. These tuned characteristics led to an enhancement of the relaxometric properties, reaching a maximum value of transverse relaxivity  $r_2$  of 300.30  $\text{mM}^{-1} \text{s}^{-1}$  (at 25 °C, 20 MHz, 0.47 T), which is significantly higher than the  $r_2$  values reported for commercially available  $T_2$  contrast agents and other iron oxides with identical particle size.[3] Finally, a relation between relaxivity – particle size – saturation magnetization was established, opening new horizons in the design of high-performance MRI contrast agents.

**Keywords:** *iron oxides, magnetic nanoparticles, coprecipitation, contrast agents, MRI*

[1] LAURENT, S., FORGE, D., PORT, M., ROCH, A. ROBIC, C., ELST, L. V. & MULLER, R. N. 2008. Magnetic Iron Oxide Nanoparticles: Synthesis, Stabilization, Vectorization, Physicochemical Characterizations, and Biological Applications. *Chem. Rev.*, 108, 2064–2110.

[2] PEREIRA, C., PEREIRA, A. M., FERNANDES, C., ROCHA, M., MENDES, R., FERNÁNDEZ-GARCÍA, M. P., GUEDES, A., TAVARES, P. B., GREÑÈCHE, J.-M., ARAÚJO, J. P. & FREIRE, C. 2012. Superparamagnetic  $\text{MFe}_2\text{O}_4$  (M = Fe, Co, Mn) Nanoparticles: Tuning the Particle Size and Magnetic Properties through a Novel One-Step Coprecipitation Route. *Chem. Mater.*, 24, 1496–1504.

[3] LEE, N. & HYEON, T. 2012. Designed synthesis of uniformly sized iron oxide nanoparticles for efficient magnetic resonance imaging contrast agents. *Chem. Soc. Rev.*, 41, 2575–2589.

**Genetically engineered biomolecules for synthesis of functional 2D and 3D nanomaterials**

Yanping Zhou, Yan Lu, Eileen Fong\*

Nanyang Technological University, Singapore

**ABSTRACT**

Genetically engineered biomolecules have attracted tremendous attention for their tunable mechanical and chemical properties. These advantages have rendered biomolecules popular as materials and scaffolds for tissue engineering and repair. Recently, efforts to utilize genetically engineered biomolecules for synthesis of inorganic materials nanostructures have been reported. Unlike traditional chemical molecules, both the morphologies and chemical composition can be controlled through carefully designed templates made out of genetically modified biomolecules. In this work, we report novel strategies to synthesize nanostructured inorganic materials through the use of both genetically modified bacteria and fusion proteins. We showed that the nanostructured materials obtained from both routes exhibit electronic properties when evaluated as lithium-based batteries.

## Catalytic Conversion Reaction of Hexagonal Boron Nitride to Graphene for Graphene/Boron Nitride Lateral Heterostructure

Gwangwoo Kim<sup>1,4</sup>, Hyunseob Lim<sup>2,4,5</sup>, A-Rang Jang<sup>1</sup>, Gyeong Hee Ryu<sup>3</sup>, Kyoungyeol Ma<sup>1</sup>, Zonghoon Lee<sup>3,5</sup>, Hyeon Suk Shin<sup>1,2,4,5</sup>

<sup>1</sup>Department of Energy Engineering, <sup>2</sup>Department of Chemistry, <sup>3</sup>Department of Mechanical & Advanced Materials Engineering, <sup>4</sup>Low Dimensional Carbon Materials Center, and <sup>5</sup>Center for Multidimensional Carbon Materials, Ulsan National Institute of Science and Technology (UNIST), UNIST-gil 50, Ulsan 689-798, Republic of Korea.

*Presenting author's e-mail: kw820@unist.ac.kr*

*Corresponding author's e-mail: shin@unist.ac.kr*

The lateral heterostructure of graphene and hexagonal boron nitride (h-BN) has attracted particular attention in research of 2D materials. Among various synthetic methods, there have been several attempts to develop the substitution reaction to convert graphene to h-BN or boron carbonitride (h-BNC). However, the reverse reaction converting h-BN to graphene has never been reported, which might be originated by the thermodynamic instability because the reaction is endothermic. Here, we report a new chemical route for the substitution reaction from h-BN to graphene for the first time, in which Pt substrate plays a role of catalyst to overcome the thermodynamic difficulty of the reaction. The conversion reaction was characterized by Raman spectroscopy, Kelvin probe microscopy and high-resolution transmission electron microscopy (HRTEM). The detail reaction mechanism has been investigated by systematic control experiments. We also show the controlled-formation of lateral graphene/h-BN heterostructure by lithographic techniques.

**Keywords:** *Graphene, boron nitride, lateral heterostructure, platinum, conversion reaction*

## Silver chalcogenide-based hybrid nanocrystals with enhanced thermoelectric properties

Albert Figuerola,<sup>\*,1,2</sup> Mariona Dalmases,<sup>1,2</sup> Maria Ibáñez,<sup>3</sup> Andreu Cabot,<sup>4,5</sup> Pau Torruella,<sup>2,6</sup> Sònia Estradé,<sup>2,6</sup> Francesca Peiró,<sup>2,6</sup> Jordi Llorca,<sup>7</sup> Víctor Fernández-Atable<sup>2</sup>

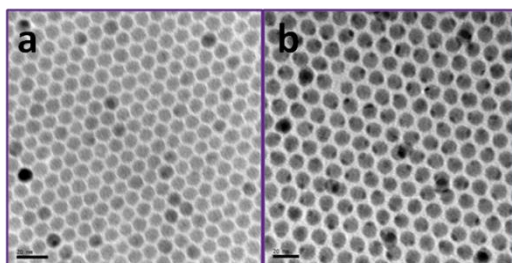
<sup>1</sup>Inorganic Chemistry Department, University of Barcelona (Spain); <sup>2</sup>Nanoscience and Nanotechnology Institute (IN2UB), University of Barcelona (Spain); <sup>3</sup>Eidgenössische Technische Hochschule Zürich, ETH Zürich (Switzerland); <sup>4</sup>Catalonia Energy Research Institute (IREC) (Spain); <sup>5</sup>Institució Catalana de Recerca i Estudis Avançats (ICREA) (Spain); <sup>6</sup>Laboratory of Electron Nanoscopies (LENS)-MIND/IN2UB, Electronic Department, University of Barcelona (Spain); <sup>7</sup>Institute of Energy Technologies, Technical University of Catalonia (Spain)

albert.figuerola@qi.ub.es

Noble metal-semiconductor heterostructures are currently devised as potentially efficient materials for energy conversion technologies. [1] In particular, silver selenide ( $\text{Ag}_2\text{Se}$ ) is a narrow band-gap semiconductor that shows chemical and physical interesting properties such as high electronic and ionic mobility, infrared emission, high ionic diffusion and good thermoelectric performance. [2] Although this material has been extensively studied in the bulk, the potential of nanostructured  $\text{Ag}_2\text{X}$ -based particles ( $\text{X}=\text{S}, \text{Se}, \text{Te}$ ) in technology is yet to be examined.

In this work we present a general method for the synthesis of size-controlled  $\text{Au-Ag}_2\text{X}$  hybrid nanocrystals through the room temperature heterogeneous nucleation of  $\text{Au}$  on the surface of pre-synthesized  $\text{Ag}_2\text{X}$  nanoparticles. Silver chalcogenide nanoparticles are prepared in solution through the thermal decomposition of a  $\text{Ag}^+$ -oleylamine complex in the presence of the corresponding chalcogen, using trioctylphosphine oxide as solvent. The exhaustive structural characterization of the samples indicated the formation of the dimeric nanoparticles as well as the occurrence of high diffusion phenomena of  $\text{Au}^+$  ions through the  $\text{Ag}_2\text{X}$  lattice at room temperature. This low energy barrier process induces the formation of novel nanostructured  $\text{Au-Ag}_3\text{AuX}_2$  nanoparticles with modified properties.

The followed synthetic protocol proved to be highly reproducible and readily scalable. Thus, sufficient amounts of  $\text{Ag}_2\text{Se}$ -based hybrid nanoparticles could be easily prepared for the assembly of lab-scale thermoelectric devices. The results show the superiority and enhanced thermal-to-electrical energy conversion of the hybrid systems with respect to single  $\text{Ag}_2\text{Se}$  nanoparticles, and evidence the potential of this new nanostructured material within the search for efficient renewable energy sources.



$\text{Ag}_2\text{Se}$  nanocrystals (a) and  $\text{Au-Ag}_3\text{AuSe}_2$  hybrid nanoparticles (b)

[1] Costi, R.; Cohen, G.; Salant, A.; Rabani, E.; Banin, U. *Nano Lett.* **2009**, *9*, 2031-2039.

[2] Ferhat, M.; Nagao, J. *J. Appl. Phys.* **2000**, *88*, 813-816.



## Advanced Microchannel System Design for Homogeneous Size and Morphology of Nanomaterials

Huseyin Uvet<sup>a</sup>, Ali Canlier<sup>\*b</sup>

<sup>a</sup>Department of Mechatronics Engineering, Yildiz Technical University, Istanbul, Turkey

<sup>b</sup>Department of Materials Science and Nanotechnology Engineering, Abdullah Gul University, Kayseri, Turkey

E-mail: ali.canlier@agu.edu.tr

### ABSTRACT

Solvothermal methods and simple reduction reactions are widely used for the synthesis of metal nanoparticles and nanowires. Large-scale production requires the use of large amounts of reactants. This generally results in low homogeneity distribution of nanoparticle size and a rise in side products. We designed a channel system in order to mix reactants in little amounts homogeneously within channels which help maintain a regular flux of fluids. We succeeded in narrowing particle size distribution highly in several syntheses. (1) Ag nanoparticle synthesis through simple reduction of Ag(I) salt (2) Cu nanoparticle synthesis through simple reduction of Cu(II) salt (3) Metal@metal core/shell nanowire synthesis-inert metal shell coating through galvanic exchange reaction, i.e. Ag@Au core/shell nanowire via reaction between Ag nanowire and Au complex compound (4) Metal@metal core/shell nanoparticle synthesis etc.. This method works excellent for homogeneous size distribution. We succeeded in i.e.,  $10\pm 1$  nm and  $20\pm 1$  nm Ag nanoparticle synthesis at very narrow distribution. We will report other results as well and introduce our system design. Our metal nanoparticles can be used in numerous applications successfully such as solar cells, sensors, catalysis etc. Inert metal coated Ag and Cu nanowires are useful in durable transparent electrode design, fuel-cell electrode design, solar cell and OLED electrode design etc.

**KEYWORDS:** transparent electrode, fuel cell, sensor, Ag, Cu, Au, Pt, Pd, nanoparticle, nanowire



**Fig.** A photograph of our microchannel device in order to mix two reactants simultaneously and a third one in the middle of the flow track.

## 2DHG Fractional Quantum Hall Effect and Composite Fermions in a SiGe/(001)Si-based compressively strained sGe- Quantum Wells

Oleg A. Mironov<sup>1,2</sup>, Nicholas d'Ambrumenil<sup>1</sup>, and David R. Leadley<sup>1</sup>

<sup>1</sup> Department of Physics, University of Warwick, Coventry, UK

<sup>2</sup> International Laboratory of High Magnetic Fields and Low Temperatures, Wroclaw, PL.

*E Mail: oamironov@yahoo.co.uk; O.A.Mironov@warwick.ac.uk*

The extremely high 2DHG mobility of over  $1.3 \times 10^6 \text{ cm}^2/\text{Vs}$  ( $P_s = 2.9 \times 10^{11} \text{ cm}^{-2}$ ) [1-4] and low hole effective mass ( $0.060 \pm 0.001 m_o$ ) determined from Shubnikov-de Haas oscillations has enabled the fractional quantum Hall effect (FQHE) to be observed **for the first time** in a compressively strained (0.65%) sGe-QW (20 nm) selectively doped by boron (single-sided doping with 26 nm spacer between QW and B-layer). The SiGe/(001)Si-based heterostructures grown using the RP-CVD method (ASM, Epsilon 2000) [1-2]. The 2DHG mobility in our system is more than ten times higher than previously reported for similar SiGe-based heterostructures grown by use of LEPE-CVD [3] and MBE [5, 6]. Firstly, these results confirm that the FQHE is a truly universal and material independent phenomenon while secondly, allows us to study the energy gap between the states of Composite Fermions (CF) in a sGe 2DHG. The FQHE features observed at 25 mK and around one half filling factor (at  $B \sim 23\text{T}$ ) include five CF Landau levels (LLs) ranging from  $\nu=1/3$  to  $\nu=5/11$ , while further states are observed in higher LLs around  $\nu=3/2$  (at  $B \sim 8\text{T}$ ) and  $5/2$  (at  $B \sim 4.8\text{T}$ ). We also report CF mass and spin splitting by means of temperature and angle dependent magneto-transport experiments.

**Keywords:** 2DHG, sGe-QW on SiGe/(001)Si, FQHE, Composite Fermions.

[1] DOBBIE, A., *et al.*, 2012. APL 101, 172108. [2] MIRONOV O.A. *et al.*, 2014. Thin Solid Films, 557, 329–333. [3] HASSAN A.H.A., MIRONOV O.A. *et al.*, 2014. APL 104, 132108. [4] MIRONOV O.A., *et al.*, 2014. Phys. Status Solidi C 11, No. 1, 61–64. [5] ROSSNER, B.,ISELLA, G., Isella and VON KANEL, H., 2003. APL 82,754. [6] IRISAWA,T, MYRONOV M.,MIRONOV,O.A. *et al*, 2003. APL 82,1425 (2003).

## **Investigation by Raman micro-probe of local structural changes in various LiNbO<sub>3</sub> devices.**

Fontana Marc D., Kokanyan Ninel, Chapron David and Bourson Patrice.

Laboratoire Matériaux Optiques, Photonique et Systèmes, Université de Lorraine – Metz and Supélec, 2 rue Edouard Belin, 57070 Metz (France).

*fontana@metz.supelec.fr*

Authors LiNbO<sub>3</sub> is a material which is widely used in a great variety of applications for optoelectronics such as electro-optic modulators, optical parametric oscillators and wave guiding, thanks to its large piezoelectric, electro-optical and nonlinear optical coefficients properties. It presents two remarkable advantages. At first, it is a versatile material since some of its properties strongly depend on the nature and concentration of dopant ions introduced in the host lattice. Furthermore fabrication of various 2D or 3D integrated optical devices require specific and complicated processes. Various kinds of reversible or irreversible damages can be induced by the preparation and the various treatments (annealing, redox...): formation of point or extended defects, lattice strains, partial amorphization ... It is of prime importance that structural and optical properties are preserved by the preparation process. The control of material in the different stages of the process is consequently an important challenge to improve reliability and/or characteristics of devices. Here it is shown that Raman microprobe can be efficiently used to control the local structure and to detect any damage caused by the process. For this, several bands in the Raman spectrum can be analyzed as markers of various physical changes in the structure. The incorporation of point defects is revealed by the broadening of some lines. Strains are reflected by shift in the position of lines, especially associated to oxygen octahedral. Extended defects of ablated material can be detected from the change in the whole line shape. It is thus demonstrated that the Raman probe can be thus useful to improve the quality of the structure and improve device properties.

***Keywords: defects, optoelectronics, optical materials, Raman spectroscopy.***

## A Direct Growth of Wafer-Scale Monolayer Graphene using Microwave Plasma CVD

Zexiang Chen\*, Jun Li, Yugong Zeng, Jijun Zhang, Shen Jiang, Yan Wang

School of Opto-electronic Information, University of Electronic Science and Technology of China, Chengdu, China

E-mail address: zxchen@uestc.edu.cn

Graphene shows various fascinating physical properties which promise applications in future electronics, such as transistors, transparent electrodes, optoelectronic devices and supercapacitors. Therefore, preparation of high-quality graphene has been playing the key role for graphene-based devices. Several approaches have been developed, such as high temperature annealing of single crystalline SiC, CVD based methods and so on. However, it is hard to transfer the prepared graphene onto desired substrates or to integrate with other materials without suffering from structural defects. We reported a direct growth graphene on wafer-scale substrate at low temperature of 600 °C using microwave plasma CVD, and proposed a back growth mechanism of graphene coordinately. The Raman spectrums of the prepared graphene show that there are three major peaks around 1345  $\text{cm}^{-1}$  (D band), 1585  $\text{cm}^{-1}$  (G band), and 2683  $\text{cm}^{-1}$  (2D band) respectively. The quite weak D band at 1350  $\text{cm}^{-1}$  indicates very low concentration of defects. The ratio of intensity of the 2D band to the G band  $I_{2D}/I_G$  is about 2, combining the narrow linewidth of 2D which can be fitted by single Lorentzian, confirm the growth of single-layer graphene. The Hexagonal diffraction spots in TEM SAED image of as-prepared graphene demonstrate the monolayer nature of the graphene again. The presented direct graphene growth could provide a low cost batch fabrication approach for potential high performance graphene-based device.

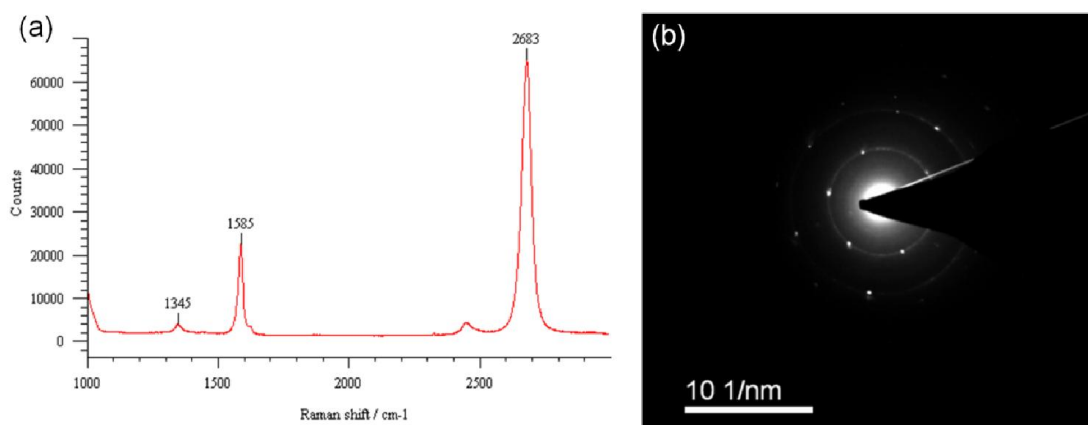


Fig. 1 Raman Spectroscopic Characterization (a) and the TEM SAED patterns (b) of as-grown Graphene

**Keywords:** graphene, microwave plasma CVD, direct growth, wafer-scale size, monolayer

## **Simulation of Quantum Dot Growth: Towards Rational Development of Nanomaterials With Predictable Properties**

Pavel Samokhvalov<sup>1</sup>, Pavel Linkov<sup>1</sup> and Igor Nabiev<sup>1,2</sup>

<sup>1</sup> Laboratory of Nano-Bioengineering, National Research Nuclear University MEPhI (Moscow Engineering Physics Institute), 31 Kashirskoe shosse, 115409 Moscow, Russian Federation

<sup>2</sup> Laboratoire de Recherche en Nanosciences, LRN-EA4682, Université de Reims Champagne-Ardenne, 51 rue Cognacq Jay, 51100 Reims, France

*E-mail: igor.nabiev@gmail.com*

Technological applications of photoluminescent (PL) semiconductor nanocrystals (NCs) or quantum dots (QDs) require not only advanced optical parameters (such as a 100% PL quantum yield), but also high uniformity of the size and shape throughout the NC ensemble. Although methods for production of monodisperse CdSe QD cores exist, there is still a need for the development of procedures for deposition of uniform high-band-gap shells confining charge carriers in QD cores and protecting them from the environment. A layer-by-layer (L-b-L) technique for controllable deposition of inorganic shells onto QD cores, Successive Ionic Layer Adsorption and Reaction (SILAR), has been developed [1]. The real QDs are typically faceted, as seen in TEM, so the simple spherical model of a QD that lies in the basis of the SILAR method, becomes its major drawback. The incorrect estimation of the required shell precursor quantities according to SILAR method may result in excess precursor accumulation in reaction mixture, what, in turn, leads to the formation of core-shell QDs with imperfect structure or nucleation of shell nanocrystals as by-product.

We have developed an approach to the construction of atomistic models of CdSe nanocrystals based on crystallographic parameters of QD material, which allows one to inspect the formation of these NCs in the L-b-L mode. The construction of the models is started from a "monomer" of

CdSe, followed by successive addition of atomic shells from the adjacent crystallographic space. Using this algorithm, we have obtained atomistic models of CdSe QDs up to 10 nm in size.

To test our approach, we have performed the overgrowth of small CdSe NCs whose diameter was in correspondence with a particular growth stage in our model. We have succeeded in predicting the evolution of the optical properties of CdSe QDs during their overgrowth and demonstrated close correlation between the experimental positions and calculated values of the first excitonic transitions.

We conclude that our model is physically relevant and can be used for calculation of precursor quantities for SILAR-like coating procedures. Finally, we have used this approach to synthesize novel CdSe/ZnS/CdS/ZnS core-multishell QDs with a PL quantum yield of almost 100%.

This study was supported by the Russian Science Foundation (grant no. 14-13-01160). We thank Vladimir Ushakov for help in the preparation of this manuscript.

***Keywords: quantum dots, core-shell nanocrystals, structure, modeling, predictable properties***

[1] LI J. J., WANG Y. A., GUO W., KEAY J. C., MISHIMA T. D., JOHNSON M. B., PENG X. 2003. Large-scale synthesis of nearly monodisperse CdSe/CdS core/shell nanocrystals using air-stable reagents via successive ion layer adsorption and reaction, *J. Am. Chem. Soc.* 125, 12567-12575.

## **DNA-promoted polymerization of pyrrole; a route to templated DNA origami conductive networks**

Joseph Hedley, Jennifer Hannant, Joshua Nock, Scott D. Watson, and Andrew Pike

Chemical Nanoscience Laboratory, School of Chemistry, Newcastle University,  
Newcastle-upon-Tyne, Tyne and Wear, UK, NE1 7RU

andrew.pike@ncl.ac.uk

Here we report the polymerization of pyrrole onto DNA origami ‘T’-nanostructures. The templating of  $\lambda$ -DNA with a range of conductive materials has been explored and the conductivity of the 1D nanowires produced has been demonstrated.<sup>[1]</sup> The fabrication of these 1D nanostructures is relatively straightforward but their integration into electronic circuits is more challenging. Circuit junctions and interconnects are required and recent work has shown that origami ‘T’ can be metalized, suggesting that DNA origami has a role to play in complex architectures. However, the formation of polymer templated DNA origami structures carries a further challenge that needs to be addressed. The conditions required to polymerize pyrrole onto densely packed dsDNA within the origami structures (ca 60 nm  $\times$  80 nm compared to 2 nm  $\times$  17  $\mu$ m of  $\lambda$ -DNA), This poster describes our efforts to fabricate DNA origami templated conducting polymers and deposit them on a silicon wafer in order to develop conductive origami materials.

***Keywords: DNA origami, polypyrrole, nanojunctions, molecular electronics***

[1] WATSON S. M. D., PIKE A. R., PATE J., HOULTON A., HORROCKS B. R., 2014. DNA-templated nanowires: morphology and electrical conductivity. *Nanoscale*, 6, 4027-4037.

## Large Scale Interlayer Carbon Bonding in Multilayer Graphene via Surface Hydrogenation

Seong In Yoon<sup>1</sup>, Hyunseob Lim<sup>2</sup>, Hu Young Jeong<sup>3</sup>, Hyeon Suk Shin<sup>1,2</sup>

<sup>1</sup>Department of Energy Engineering, <sup>2</sup>Center for multidimensional Carbon Materials, Institute of Basic Science, <sup>3</sup>UNIST Central Research Facilities, Ulsan National University of Science and Technology (UNIST), UNIST-gil 50, Ulsan 688-798, Republic of Korea

*Presenting author's e-mail: qwopasl@unist.ac.kr*

*Corresponding author's e-mail: shin@unist.ac.kr*

As a diamond synthesis, the direct conversion of graphite to diamond under high pressure and high temperature has been widely investigated. The discovery of graphene layer provided an idea of ultrathin diamond synthesis which is the direct conversion from multilayer graphene to that.<sup>1</sup> The surface hydrogenation on multi-layer graphene was recently reported as a chemical conversion method into  $sp^3$  structure without extreme experimental conditions.<sup>2</sup> However, the number of researches is still limited, as well as the large scale conversion reaction has not been demonstrated yet.

Herein, we present our attempts for the large scale interlayer carbon bonding formation in multi-layer graphene. Multi-layer graphene were prepared by chemical vapor deposition method and transfer method, and surface hydrogenation on surface, interlayer C-C bonding and C-metal bonding were successfully characterized by scanning electron microscope (SEM), Raman spectroscopy, X-ray photoelectron spectroscopy (XPS), near-edge X-ray absorption fine structure (NEXAFS) spectroscopy, and electron energy loss spectroscopy (EELS).

**Keywords :** *Ultrathin diamond,  $sp^3$ -conversion, Hydrogenation, Multilayer graphene*

[1] ODKHUU, D., SHIN, D., RUOFF, R.S. & PARK, N. 2013. Conversion of multilayer graphene into continuous ultrathin  $sp^3$ -bonded carbon films on metal surfaces. *Sci. Rep.* 3, 3276.

[2] RAJASEKARAN, S., ABILD-PEDERSEN, F., OGASAWARA, H., NILSON, A. & KAYA, S. 2013. Interlayer Carbon Bond Formation Induced by Hydrogen Adsorption in Few-Layer Supported Graphene. *Phys. Rev. Lett.* 111, 085503.



## Green synthesized noble metals for biological applications

Jakub Siegel<sup>1</sup>, Marek Staszek<sup>1</sup>, Alena Řezníčková<sup>1</sup>, Silvie Rimpelová<sup>2</sup>, Václav Švorčík<sup>1</sup>

<sup>1</sup>Department of Solid State Engineering, Institute of Chemical Technology, 166 28 Prague,  
Czech Republic

<sup>2</sup>Department of Biochemistry and Microbiology, Institute of Chemical Technology, 166 28  
Prague, Czech Republic  
*[jakub.siegel@vscht.cz](mailto:jakub.siegel@vscht.cz)*

Over the past decades, noble metal nanoparticles have been widely studied due to their unique optical, catalytic, electromagnetic and bactericidal properties, which are strongly influenced by their shape and size [1,2]. Besides extensively studied metals such as silver (Ag) and gold (Au) which bactericidal effect is well known, there are other metals worth to be explored i.e. platinum (Pt) and Palladium (Pd). There are, however, only few research studies addressing biological applications of pure Pt and Pd nanoparticles and their antibacterial properties are almost unknown.

Recently, our group has published a unique approach for silver and gold nanoparticle synthesis which consists in direct metal sputtering into glycerol [1]. This study shows that proposed approach may be used even in case of Pt and Pd nanoparticles (NPs). The novelty of this work lies in evaluation of Pd and Pt antibacterial effect, as well as in addressing their cytotoxicity towards selected cell cultures which is of crucial importance when applying such man-made entities into living tissues. Both average nanoparticle size and size-distribution were measured by transmission electron microscopy, dynamic light scattering and UV-Vis absorption spectroscopy. Inhibition effect of nanoparticles was investigated *in vitro* on two common bacterial strains of *Escherichia coli* (Gram-negative bacteria) and *Staphylococcus epidermidis* (Gram-positive bacteria), frequently involved in infections associated with a biofilm formation. Cytotoxicity of Ag, Au, Pd, and Pt nanoparticles (NPs) was assessed by WST-1 assay (Roche, Germany) using HaCaT (human keratinocytes), Hep G2 (human hepatocyte cells), CHO-K1 (hamster Chinese ovary cells), RAW 264.7 (mouse macrophages), NIH 3T3, and L929 (mouse embryonic fibroblasts) cell lines.

In contrast to PtNPs, PdNPs exhibited at similar concentration considerable higher bactericidal effect towards tested pollutants. However, this work suggested that Ag and Au NPs

are more appropriate antimicrobial agents due to their significantly lower cytotoxicity compared with much higher activity of Pd and Pt NPs.

Financial support of this research from the GACR project No. 14-18131S is gratefully acknowledged.

***Keywords: Metal nanoparticles, sputtering, antibacterial properties, cytotoxicity***

[1] SIEGEL, J., KVITEK, O., ULBRICH, P., KOLSKA, Z., SLEPICKA, P. & SVORCIK, V. 2012. Progressive approach for metal nanoparticle synthesis. *Mater Lett*, 89, 47-50.

[2] SIEGEL, J., KOLAROVA, K., VOSMANSKA, V., RIMPELOVA, S., LEITNER, J. & SVORCIK, V. 2013. Antibacterial properties of green-synthesized noble metal nanoparticles. *Mater Lett*, 113, 59-62.

## Carbon Nanotube based Three Stage Operational Amplifiers, a Simulation Study

Sajad A. (Loan)<sup>1</sup>, M. Nizamudin <sup>1</sup>, Abdulrahman M.(Alamoud)<sup>2</sup>, Shuja A. (Abbasi)<sup>2</sup>

<sup>1</sup>Electronics Engineering, Jamia M. Islamia (Central University) New Delhi-India.

<sup>2</sup>Electrical Engineering Department, King Saud University, Saudi Arabia.

[alamoud@ksu.edu.sa](mailto:alamoud@ksu.edu.sa), [sajadiitk@gmail.com](mailto:sajadiitk@gmail.com)

Carbon nanotubes are envisioned as one of the promising candidates for beyond-silicon electronics. They possess unique properties, like high tensile strength, huge electrical and thermal conductivities, and have nearly one dimensional ballistic transport capability. One of the important applications of CNT includes carbon nanotube field effect transistor (CNTFET). A CNTFET is similar to a conventional MOSFET; however, the channel is made up of parallel combination of SWCNTs. The advantages of CNTFET include 1D ballistic transport of charge carriers, large mobility, large drive current and very low power consumption. To cash the advantages of CNTFET, we design and simulated a novel three stage operational amplifiers (3SOA) using  $n$  and  $p$  type 45 nm technology node CNTFETs, along with the conventional MOSFETs. The two proposed 3SOA structures include the one employing  $n$  CNTFETs as sinks and conventional PMOS transistors as sources, named as NCNT-PMOS-OP-AMP. The other one employs conventional NMOS as sinks and  $p$  CNTFETs as sources, named as PCNT-NMOS-OP-AMP. The simulations have shown a significant improvement in the performance of CNTFET based 3SOAs. In the NCNT-PMOS-OP-AMP, DC gain has increased by 17 %, Output resistance decreased by 90 % and the power consumption is 34 % less in comparison to the conventional OP AMP. Similarly, a significant improvement is seen in PCNT-NMOS-OP-AMP, due to CNTs. It has been observed that the performance of CNTFET devices can be further improved by using an optimum number of CNTs.

**Keywords:** Carbon nanotube, CMOS, CNTFET, Operational amplifier, Power Consumption

## Highly selective and sensitive determination of dopamine using a 3D graphene foam electrode

Hongyan Yue<sup>1,\*</sup>, Shuo Huang<sup>2</sup>, Jin Zhou<sup>2</sup>, Jianjiao Zhang<sup>1</sup>, Chunyu Zhang<sup>1</sup>, Xin Gao<sup>1</sup>, Jing Chang<sup>1</sup>

<sup>1</sup>*School of Materials Science and Engineering, Harbin University of Science and Technology, Harbin 150040, China*

<sup>2</sup>*Department of Neurology, The First Affiliated Hospital of Harbin Medical University, Harbin 150001, China*

Graphene, a two dimensional monolayer of sp<sup>2</sup> carbon atoms, has received tremendous attention from both the experimental and theoretical scientific communities in recent years since its discovery in 2004 by Geim and co-workers [1-2]. Due to its fascinating physical properties, graphene electrodes have constructed one of the most important and ideal electrochemical sensing and biosensing platforms [3-5].

Graphene can be obtained so far by several techniques including micromechanical exfoliation of graphite [6], chemical oxidation of graphite followed by exfoliation and oxygen elimination [7] and chemical vapor deposition (CVD) onto catalytic metallic substrates [8, 9]. Among the various methods, chemically derived graphene has been extensively used due to the low-cost and large-scale production of graphene. However, this integrated graphene shows poor electrical conductivity. CVD represents a promising fabrication process to produce large area graphene in a controlled manner and with a low level structural defects. A single to few layer continuous graphene films grown directly onto a Ni film deposited on an oxidized silicon wafer via CVD was used to detect biologically relevant molecules [8]. However, the electrode is planar. Therefore, the active surface area is limited. Recently, Cheng et al [9] presented a 3D graphene foam (GF) fabricated by using a Ni skeleton upon, then the underlying skeleton was etched away to leave a free-standing graphene. The unique 3D graphene structure was demonstrated to give rise to high quality graphene with outstanding electrical conductivity.

Dopamine (DA) is one of the most important clinical neurotransmitters which plays a vital role in the function of central nervous, renal, and cardiovascular systems of mammals [10]. Deficiency of DA is associated with various neurodegenerative diseases [11, 12]. Therefore, monitoring the concentration of DA is of great importance. However, the primary challenge is that the oxidation peak potentials of DA overlaps with ascorbic acid (AA) at the bare electrodes [13-15]. Moreover, DA concentration is lower than AA and DA coexists with AA under physiological conditions, providing a large challenge for detection of DA in the presence of AA [16, 17]. Therefore, it is desirable for diagnostic applications to develop a simple, reliable and effective electrode with enhanced characteristics to distinguish AA and DA.

In the present study, a 3D GF was synthesized by CVD on a Ni foam as the template. After etching Ni, it was transferred onto ITO coated glass. Figure 1 shows the schematic of electrochemical oxidation reactions of AA and DA at GF electrode. The GF electrode showed a high selectivity for the detection of dopamine in the presence of AA. This electrode will have a wide range of potential application prospect in electrochemical detection.

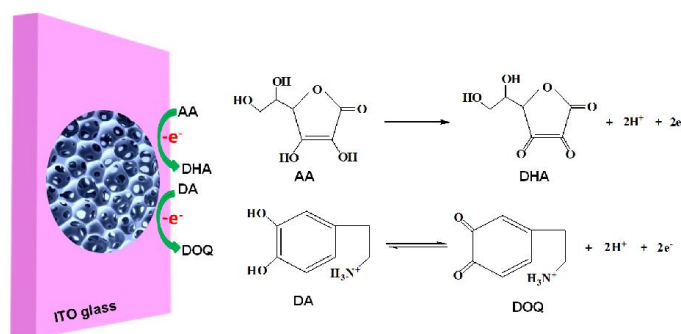


Figure 1 Schematic of electrochemical oxidation reactions of AA and DA at GF electrode

## References

- [1] Z.K Liu, J.H. Li, Z.H. Sun, G.A. Tai, S.P. Lau, F. Yan. *ACS Nano*, 2012, 6, 810-818.
- [2] C.H. Xu, B.H. Xu, Y. Gu, Z.G. Xiong, J. Sun, X.S. Zhao. *Energy Environ. Sci.*, 2013, 6, 1388-1414.
- [3] Y.X Liu, X.C. Dong, P. Chen. *Chem. Soc. Rev.*, 2012, 41, 2283-2307.
- [4] Y. Wang, Y.Y. Shao, D.W. Matson, J.H. Li, Y.H. Lin. *ACS Nano*, 2012, 4, 1790-1798.
- [5] Y.R. Kim, S.Y. Bong, Y.J. Kang, Y.T. Yang, R.K. Mahajan, J.S. Kim, H.S. Kim. *Biosens. Bioelectron.*, 2010, 25, 2366-2369.
- [6] K.S. Novoselov, A.K. Geim, S.V. Morozov, D. Jiang, Y. Zhang, S.V. Dubonos, I.V. Grigorieva, A.A. Firsov. *Science*, 2004, 306, 666-669.
- [7] V. Mani, A.P. Periasamy, S.M. Chen. *Electrochem. Commun.*, 2012, 17, 75-78.
- [8] D.A.C. Brownson, M. Gómez-Mingot, C.E. Banks. *Phy. Chem. Chem. Phy.*, 2011, 13, 20284-20288.
- [9] Z.P. Chen, W.C. Ren, L.B. Gao, B.L. Liu, S.F. Pei, H.M. Cheng. *Nature Mater.*, 2011, 10, 424-428.
- [10] Palraj Kalimuthu, S. Abraham John. *Talanta*, 2010, 80, 1686-1691.
- [11] T.V. Sathisha, B.E.K. Swamy, B.N. Chandrashekar, N. Thomas, B. Eswarappa. *J. Electroanal. Chem.*, 2012, 674, 57-64.
- [12] D. Jia, J.Y. Dai, H.Y. Yuan, L. Lei, D. Xiao. *Talanta*, 2011, 85, 2344-2351.
- [13] I.D.O. Matos, W.A. Alves. *ACS App. Mater. Interfaces*, 2011, 3, 4437-4443.
- [14] M. Noroozifar, M. Khorasani-Motlagh, R. Akbari, M.B. Parizi. *Biosens. Bioelectron.*, 2011, 28, 56-63.
- [15] P. Wang, Y.X. Li, X. Huang, L. Wang. *Talanta*, 2007, 73, 431-437.
- [16] S.J. Hong, L.Y.S. Lee, M.H. So, K.Y. Wong. *Electroanalysis*, 2013, 25, 1-10.
- [17] S. Komathi, A.I. Gopalan, K.P. Lee. *Analyst*, 2010, 135, 397-404.

# Water through Graphynes' Pores: First-Principles Penetration Barrier and Force Field Optimization

M. Bartolomei,<sup>1,\*</sup> E. Carmona-Novillo,<sup>1</sup> M. I. Hernández,<sup>1</sup> J. Campos-Martínez,<sup>1</sup> F. Pirani,<sup>2</sup> G. Giorgi,<sup>3</sup> K. Yamashita<sup>3</sup>

<sup>1</sup>Instituto de Física Fundamental-CSIC, Madrid, Spain

<sup>2</sup>Dipartimento di Chimica, Università di Perugia, Italy

<sup>3</sup>Department of Chemical System Engineering, School of Engineering, University of Tokyo, Japan

**Abstract:** Graphynes are novel two-dimensional carbon-based materials, naturally presenting a nanoweb-like structure characterized by triangular and regularly distributed pores. These intriguing features make them appealing for molecular filtering, especially for water purification technologies. First principles calculations are carried out at the MP2C level of theory to properly assess the interaction between water and graphyne, graphdiyne and graphtriyne pores. The computed penetration barriers (see Figure) suggest that water transport is unfeasible through graphyne while being unimpeded for graphtriyne. Nevertheless for graphdiyne, which presents a pore size almost matching that of water, a low barrier is found which in turn disappears if an active hydrogen bond with an additional water molecule on the opposite side of the opening is taken into account (see Figure). These results confirm the possibility of an efficient use of graphtriyne (and larger pore homologues) membranes for water filtration and purification, as very recently suggested by molecular dynamics investigations[1-4]. Still, in contrast with these studies[1-4], present findings do not exclude graphdiyne since the related first principles penetration barrier leads to water permeation probabilities which are at least two orders of magnitude larger than those estimated by employing commonly used force fields[2-4]. The computed energy profiles for graphdiyne have also served to build a new pair potential for the water-carbon non-covalent component of the interaction which better represents the water-pore behaviour[5] and it is recommended for molecular dynamics simulations involving graphdiyne and water.

**Keywords:** graphyne, graphdiyne, porous materials, nanofiltration, water purification, ab-initio calculations

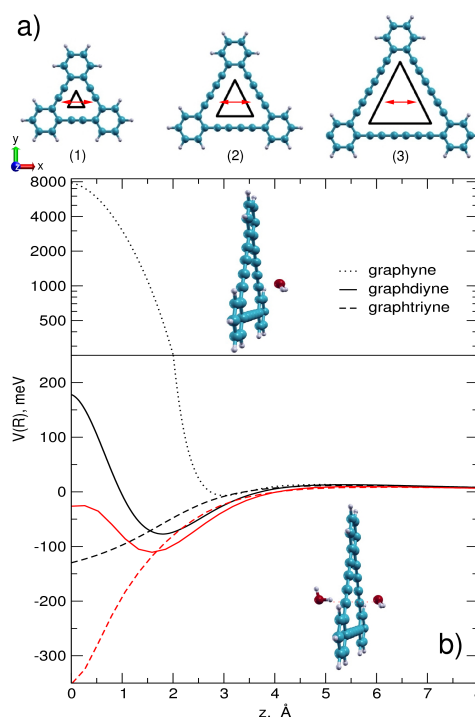


Figure: a) Annulenic molecular structures used to study the nano-pores of graphyne(1), graphdiyne(2) and graphtriyne(3). The black triangles depicted inside the pores represent their effective available area to be compared with the van der Waals diameter of the water molecule (red double-headed arrow).

b) Energy profiles obtained at the MP2C level of theory for water perpendicularly approaching the geometric center of graphyne, graphdiyne and graphtriyne pores. Black lines correspond to the case of a single water molecule approaching the pore. Red lines refer to the case in which a second water molecule fixed on the other side of the pore is added. A catalyzing effect is noticed due to the presence of an active hydrogen bond, which for graphdiyne leads to the suppression of the penetration barrier.

## References:

- [1] Lin. S. and Buehler M. J., *Nanoscale*, **5** (2013) 11801.
- [2] Kou J. et al., *J. Chem. Phys.*, **139** (2013) 064705.
- [3] Zhu C. et al., *Sci. Rep.*, **3** (2013) 3163.
- [4] Xue M. et al., *Nanotechnology*, **24** (2013) 505720.
- [5] Bartolomei M. et al., *J. Phys. Chem. Lett.*, **5**, 751 (2014).

## Bismuth Telluride based Nanowires for Thermoelectric Power Generation

I.K. Ng<sup>1</sup>, K. Y. Kok<sup>1</sup>, C.Z. Che Abd Rahman<sup>1</sup> and T.F. Choo<sup>1</sup>

<sup>1</sup>Malaysian Nuclear Agency, Bangi, 43000 Kajang, Selangor Darul Ehsan, Malaysia.

*E Mail/ Contact Details (kyk1000@nm.gov.my)*

### Abstract

Nanostructured materials systems such as thin-films and nanowires (NWs) are promising for thermoelectric power generation and refrigeration, compared to traditional counterparts in bulk, due to their enhanced thermoelectric figures-of-merit. BiTe and its derivative compounds, in particular, are well-known for their near-room temperature thermoelectric performance. In this work, both the binary BiTe and ternary BiSbTe nanowires were synthesized using template-assisted electrodeposition. Stoichiometric depositions of the p and n-types nanowires were achieved via systematic study on compositional change as a function of applied potential using Linear Sweep Voltammetry (LSV). Chemical compositions of the nanowires were evaluated using Energy Dispersive X-ray Spectrometry (EDXS) and their microstructures and morphologies characterized using diffraction and imaging techniques. Electrical and thermal transport properties of the nanowires were studied using a custom-designed suspended micro-electro-thermal system. Results from chemical analysis on the nanowires indicated that while the Sb contents in BiSbTe nanowires increased with more negative deposition potentials, the formation of Te<sup>0</sup> and Bi<sub>2</sub>Te<sub>3</sub> were favorable at more positive potentials. Thermoelectric test modules constructed from pairs of p- and n-types BiTe based nanowire arrays thermocouples were demonstrated to produce a power output of ~ 0.36 nW per a pair of p-n thermocouples at a maximum temperature difference of ~ 50 K.

**Keywords:** *Thermoelectric Nanowires, bismuth telluride, electrodeposition*

## Graphene for spin transport

M.-B. Martin<sup>1</sup>, B. Dlubak<sup>1</sup>, M. Piquemal<sup>1</sup>, A. Anane<sup>1</sup>, C. Deranlot<sup>1</sup>, R. Mattana<sup>1</sup>, H. Jaffrès<sup>1</sup>, H. Yang<sup>1</sup>, M. Sprinkle<sup>2</sup>, C. Berger<sup>2</sup>, W. de Heer<sup>2</sup>, P. Kidambi<sup>3</sup>, S. Hofmann<sup>3</sup>, J. Robertson<sup>3</sup>, F. Petroff<sup>1</sup>, A. Fert<sup>1</sup>, P. Seneor<sup>1</sup>

<sup>1</sup>Unité Mixte de Physique CNRS/Thales and Université Paris-Sud, 91767 Palaiseau, FR

<sup>2</sup>GeorgiaTech, Atlanta, USA/Institut Néel, Grenoble, FR

<sup>3</sup>Department of engineering, University of Cambridge, Cambridge CB3 0FA, UK

*pierre.seneor@thalesgroup.com*

Spintronics is a paradigm focusing on spin as the information vector. Ranging from quantum information to zero-power non-volatile magnetism, the spin information can be also translated from electronics to optics. Several spintronics devices (logic gates, spin FET, etc) are based on spin transport in a lateral channel between spin polarized contacts. We want to discuss, with experiments in support, the potential of graphene for the transport of spin currents over long distances in such types of devices.

We will present magneto-transport experiments on epitaxial graphene multilayers on SiC [1]. The measured spin signals are in the mega-ohms range, and the analysis of the results in the framework of drift/diffusion equations leads to large spin diffusion length in graphene in the 100 microns range. The high spin transport efficiency of graphene can also be acknowledged up to 75% in our devices. These results will be compared to previous studies on carbon nanotubes and to our on-going study on large scale CVD grown graphene. A unified picture of spin transport in nanotubes and graphene will be presented [2].

**Keywords:** *Graphene, Spintronics*

[1] DLUBAK, B. et al. 2012. Highly Efficient Spin Transport in Epitaxial Graphene on SiC. Nature Physics 8, 557.



[2] SENEOR, P. et al. 2012. Spintronics with Graphene. MRS Bulletin 37, 1245.

## Low turn on field CuInTe<sub>2</sub> nanopencils as electron source

Padmashree (Joshi)<sup>1</sup>, Manorama (Lakhe)<sup>2</sup>, Nandu (Chaure)<sup>2</sup>, Dilip (Joag)<sup>1</sup>

<sup>1</sup>Center for Advanced Studies in Material Science and Condensed Matter Physics,  
Department of Physics, Savitribai Phule University of Pune, Pune, India.

<sup>2</sup>Department of Physics, Savitribai Phule University of Pune, Pune, India.

[dsj@physics.unipune.ac.in](mailto:dsj@physics.unipune.ac.in)

CuInTe<sub>2</sub> (CIT) thin film was electrochemically deposited from aqueous electrolyte onto a molybdenum substrate. A conventional three-electrode geometry consisting working, counter and reference electrodes was used to perform the electrochemical deposition. The film was deposited at - 0.9 V with respect to Ag/AgCl electrode which was optimized by cyclic voltammetry experiment. On annealing the as-deposited film, nanopencil-like structures were obtained. The vertically aligned morphology of the rods with tapering ends is a favorable geometry for the field emission investigations and applications. The field emission study was carried out in Ultra High Vacuum (UHV) *all metal* chamber. A maximum current density of 1.58 mA/cm<sup>2</sup> was attainable at an applied electric field of 1.67 V/μm. The turn field defined as electric field required to draw a current density of 1 μA/cm<sup>2</sup> was found to be 0.97 V/μm. The emitter shows a stable electron emission which was monitored over a period of 3 hours. Thus, vertically aligned CIT nanopencils are a potential candidate for a use as an electron source.

**Keywords:** CuInTe<sub>2</sub>, nanopencils, field emission.

1] LAKHE M. & CHAURE N. 2014. Characterization of electrochemically deposited CuInTe<sub>2</sub> thin films for solar cell applications. Solar Energy Materials and Solar Cells. 123, 122-129 .

2] WILLIAM R.S. 1962. High-Field Electron Emission from Cadmium Telluride. J Appl. Phys. 33, 3198.

# Boron Nitride Nanosheets

Ying Chen, Weiwei Lei, Luhua Li and Dan Liu

Institute for Frontier Materials, Deakin University, Waurn Ponds, Victoria 3216, Australia

e-mail: ian.chen@deakin.edu.au

Atomically thin boron nitride (BN) nanosheets, a structure analogue of graphene, have superior mechanical and thermal conducting properties and thus have been used as reinforcing fillers in composites to improve their mechanical and thermal performances. In contrast to zero band gap graphene, BN nanosheets are a wide band gap semiconductor suitable for optoelectronics or as a dielectric substrate for high-performance graphene electronics. Graphene sandwiched by monolayer BN is predicted to have a tunable band gap without sacrificing its mobility. However, many intrinsic properties of few-layer BN nanosheets as well as their applications have not been systematically investigated. The presentation presents the synthesis of BN nanosheets [1], new physical properties [2-4] and applications in hydrogen storage, oil-water separation and water purification [5].

1. Lu Hua Li, Ying Chen, Gavin Behan, Hongzhou Zhang, Mladen Petracic and Alexey M. Glushenkov, "Large-scale mechanical peeling of boron nitride nanosheets by low-energy ball milling", *Journal of Materials Chemistry*, 21 (2011) 11862-11866.
2. Lu Hua Li, Elton J. G. Santos, Tan Xing, Emmanuele Cappelluti, Rafael Roldán, Ying Chen, "Dielectric Screening in Atomically Thin Boron Nitride Nanosheets", *Nano Lett.*, Article ASAP
3. Lu Hua Li, Jiri Cervenka, Kenji Watanabe, Takashi Taniguchi, and Ying Chen#, "Strong Oxidation Resistance of Atomically Thin Boron Nitride Nanosheets", *ACS Nano*. 8 (2) (2014) 1457-1462.
4. Lu Hua Li, Xing Tan, Ying Chen,\* and Rob Jones, "Boron Nitride Nanosheets for Metal Protection", *Adv. Mater. Interfaces* 2014, 1300132
5. Weiwei Lei, David Portehault, Dan Liu, Si Qin and Ying Chen#, "Porous Boron Nitride Nanosheets for Effective Water Cleaning", *Nature Communications* 4 (2013) 1777

## Electrical Properties for Graphene and MoS<sub>2</sub> Hybrid Device

Servin Rathi, In-yeal Lee, and Gil-Ho Kim

School of Electronics and Electrical Engineering and Sungkyunkwan Advanced Institute of Nanotechnology (SAINT), Sungkyunkwan University, Suwon 440-746, Korea  
ghkim@skku.edu (Gil-Ho Kim)

Two-Dimensional (2D) Transitional Metal dichalcogenides heterostructures with graphene presents a unique combination of 2D materials due to modulation in Fermi-level of graphene with both lateral and longitudinal electric-field. In case of MoS<sub>2</sub> and graphene heterostructure, rectification behavior due to asymmetrical barrier-height formation can be controlled by the lateral field in addition to applied longitudinal field which gives rise to controlled rectification properties. For device fabrication, both graphene and MoS<sub>2</sub> layers were exfoliated and transferred using polymer based transfer techniques. The hybrid device consist of cross-connected MoS<sub>2</sub> and graphene layers connected to metal electrodes at the ends. In this case, the device can be independently measured in both asymmetrical and symmetrical contacts mode. The end-connected MoS<sub>2</sub> with symmetrical metal contacts shows good transistor behavior with good on/off ratio of the order of 10<sup>4</sup>. However, if the configuration is changed to asymmetrical mode with one electrode being the metal while other connected via graphene layer, the simple I-V curve showed rectifying characteristics, which can further be modulated by applying the back-gate bias. This behavior can be considered as a back-gate-controlled schottky diode, with gate-dependent rectification. These contacts behavior adds new functionalities to the 2D devices for tunneling, photo-detectors, and photo-voltaic applications.

**Keywords:** *graphene, MoS<sub>2</sub>, two-dimensional material, diode*

[1] BRITNELL, L., GORBACHEV, R. V., JALIL, R., BELLE, B. D., SCHEDIN, F., MISHCHENKO, A., GEORGIU, T., KATSNELSON, M. I., EAVES, L., MOROZOV, S. V., et al. 2012. Field-Effect Tunneling Transistor Based on Vertical Graphene Heterostructures. *Science*, 335, 947–950.

## Investigation of accommodation mechanisms using a three dimensional finite element RVE model of polycrystalline nanostructured NiTi

M. Petersmann<sup>1</sup>, T. Antretter<sup>1</sup>, T. Waitz<sup>2</sup>

<sup>1</sup>Institute of Mechanics, Montanuniversitaet Leoben, Franz-Josef-Straße 18, Leoben, 8700 Austria

<sup>2</sup>Physics of Nanostructured Materials, Faculty of Physics, University of Vienna, Boltzmanngasse 5, Vienna, 1090 Austria

*E-mail:* [manuel.petersmann@unileoben.ac.at](mailto:manuel.petersmann@unileoben.ac.at) *Tel:*+43 3842 402 - 4011

The present work deals with the modeling of a temperature driven or stress induced martensitic transformation in nano- and poly-crystalline NiTi. The cubic, ordered, high-temperature phase, i.e. the austenite (B2 according to its Strukturbericht designation) transforms upon cooling into the monoclinic lower symmetry phase, the martensite (B19'). The lattice change entails a considerable amount of shear, which is most efficiently accommodated by twinning. In nanostructured NiTi twelve possible martensite variants determined from the phases' symmetries form six unique compound twins [1] which arrange as twin laminates. For grain diameters around one hundred nm these laminates may, in turn start forming a larger self-similar structure, known as «herringbone structure» [2]. Furthermore, contrary to larger grain sizes, nanograins transform instantly and completely into martensite [1]. For martensite it is well known that its specific local morphology as well as the transformation kinetics, depend mainly on the strain energy introduced into the material by the local transformation strain [3]. The Bain strains reflecting the macro deformation via the Cauchy-Born Rule [4] are calculated, using the crystallographic non-linear theory of martensitic transformations [4] starting from the lattice parameters of the two phases. Since the martensite exhibits a considerable elastic anisotropy the full set of 13 elastic constants from ab initio calculations are taken into account and adopted to describe the twin structures. Although the applicability of calculated elastic constants to twinned structures is currently being discussed [5] they will be used here as a starting point. At any rate, accurate data for the elastic constants are vital in order to properly predict the evolving microstructure. The model also accounts for

surface and interface energies via semi-analytical expressions [6]. The microstructure is approximated by means of a representative volume element (RVE) consisting of 150 randomly oriented grains, created by means of a three-dimensional Voronoi cell generator, and subjected to periodic boundary conditions. Each grain in the RVE is toggled from the parent phase to the product martensite phase following a transformation strategy termed « incrementally energy minimizing algorithm (IEMA) » coded in Python. It searches for an optimum sequence of transforming grains such as to minimize the system's total free energy [6], where the term « increment » refers to an increment of the martensitic fraction expressed in terms of the number of product phase grains relative to the total number of grains in the model. From the simulation a realistic kinetics is obtained. Strain energy measurements from differential scanning calorimetry (DSC) experiments are compared with the numerically computed values.

**Keywords:** *NiTi, nanostructure, martensite, twinning, anisotropy, finite elements,*

[1] WAITZ, T., 2005. The self-accommodated morphology of martensite in nanocrystalline NiTi shape memory alloys. *Acta Mater*, 53, 2273-2283.

[2] WAITZ, T., PRANGER, W., ANTRETTTER, T., FISCHER F.D., & KARNTHALER H.P. 2008. Competing accommodation mechanisms of the martensite in nanocrystalline NiTi shape memory alloys. *Mater. Sci. Eng. A*.481, 479-483.

[3] WANG, YU U., JIN Y. M. & KHACHATURYAN A.G. 2004. The effects of free surfaces on martensite microstructures: 3D phase field microelasticity simulation study. *Acta Mater*, 52, 1039-1050.

[4] BHATTACHARYA, K. 2003. *Microstructures of martensite*. Oxford University Press

[5] WANG, T. & SEHITOGLU, H. 2014. Martensite modulus dilemma in monoclinic NiTi-theory and experiments. *International Journal of Plasticity*, 61, 17-31.

[6] WAITZ, T., ANTRETTTER, T., FISCHER F.D., SIMHA N.K. & KARNTHALER H.P. 2007. Size effect on the martensitic phase transformation of NiTi nanograins. *J. Mech. Phys. Solids*, 55, 419-444.

## Molecular Sensing and Catalysis in 2D Nanostructures

Petr Král, University of Illinois at Chicago

First, we discuss our modeling of molecular sensing at graphene grain boundaries (GBs) [1]. The sensing platform is a grain boundary of two graphene grains deposited on amorphous SiO<sub>2</sub> substrate. We uncovered that an isolated graphene GB has ~300 times higher sensitivity to gas molecules (dimethyl methylphosphonate) than a single crystalline graphene grain. Our hybrid modeling of an electronic structure and transport in realistic GBs reveals that the ultra-sensitivity in GBs is caused by a synergetic combination of gas molecules accumulation at GB, together with the existence of ultrasensitive switchable transport channels in GBs. The discovered sensing platform opens up new pathways for the design of nanometer scale highly sensitive chemical detectors. We also discuss our modeling of CO<sub>2</sub> reduction on MoS<sub>2</sub> edges [2].

[1] P. Yasaei et al., Nat. Comm., 5, 4911 (2014).

[2] M. Asadi et al., Nat. Comm. 5, 4470 (2014).

## Catalyst-Free Growth of multi-layer h-BN on Sapphire Substrate

A-Rang Jang<sup>1</sup>, Gwangwoo Kim<sup>1</sup>, Kyoungyeol Ma<sup>1</sup>, Hu Young Jeong<sup>2</sup>, and

Hyeon Suk Shin<sup>1</sup>

<sup>1</sup>Department of Energy Engineering, Department of Chemistry, Low Dimensional Carbon Materials Center, and Center for Multidimensional Carbon Materials, <sup>2</sup>UNIST Central Research Facilities (UCRF), Ulsan National Institute of Science and Technology (UNIST), UNIST-gil 50, Ulsan 689-798, Republic of Korea.

*Presenting author's e-mail: arjang@unist.ac.kr*

*Corresponding author's e-mail: shin@unist.ac.kr*

Hexagonal boron nitride (h-BN) has been regarded as a good substrate for two-dimensional (2D) material based electronic, because ultra-flatness of h-BN surface can reduce the substrate-induced degradation in carrier mobility of 2D materials. Therefore, various approaches have been attempted for the large area growth of high-quality h-BN on metal substrate. However h-BN synthesized on metal substrate need to be transferred onto the other insulating substrate for device applications, as well as this process generally induces wrinkle formation on the surface. Hence, direct growth of h-BN on insulating substrate is promising for the transfer-free process. Herein, we present the catalyst free growth of multi-layer h-BN sheet on insulating sapphire substrate by low pressure chemical vapor deposition method. The surface roughness of synthesized multi-layer h-BN on sapphire substrate was measured as  $\sim 0.168$  nm, and an optical band gap was estimated as 5.65 eV from UV visible absorption spectroscopy.

**Keywords:** *hexagonal boron nitride, Chemical vapor deposition, Ammonia borane, sapphire*



## Catalyst-Free Growth of multi-layer h-BN on Sapphire Substrate

A-Rang Jang<sup>1</sup>, Gwangwoo Kim<sup>1</sup>, Kyoungyeol Ma<sup>1</sup>, Hu Young Jeong<sup>2</sup>, and

Hyeon Suk Shin<sup>1</sup>

<sup>1</sup>Department of Energy Engineering, Department of Chemistry, Low Dimensional Carbon Materials Center, and Center for Multidimensional Carbon Materials, <sup>2</sup>UNIST Central Research Facilities (UCRF), Ulsan National Institute of Science and Technology (UNIST), UNIST-gil 50, Ulsan 689-798, Republic of Korea.

*Presenting author's e-mail: arjang@unist.ac.kr*

*Corresponding author's e-mail: shin@unist.ac.kr*

Hexagonal boron nitride (h-BN) has been regarded as a good substrate for two-dimensional (2D) material based electronic, because ultra-flatness of h-BN surface can reduce the substrate-induced degradation in carrier mobility of 2D materials. Therefore, various approaches have been attempted for the large area growth of high-quality h-BN on metal substrate. However h-BN synthesized on metal substrate need to be transferred onto the other insulating substrate for device applications, as well as this process generally induces wrinkle formation on the surface. Hence, direct growth of h-BN on insulating substrate is promising for the transfer-free process. Herein, we present the catalyst free growth of multi-layer h-BN sheet on insulating sapphire substrate by low pressure chemical vapor deposition method. The surface roughness of synthesized multi-layer h-BN on sapphire substrate was measured as  $\sim 0.168$  nm, and an optical band gap was estimated as 5.65 eV from UV visible absorption spectroscopy.

**Keywords:** *hexagonal boron nitride, Chemical vapor deposition, Ammonia borane, sapphire*

## Thin-layered rGO Wrapped $\text{Co}_3\text{O}_4$ Nanofibers for A Fast Responsive Selective Ammonia Sensor

Qiuxia Feng<sup>a,b</sup>, Xiaogan Li<sup>a\*</sup>, Jing Wang<sup>a\*</sup>

a. School of Electronic Science and Technology, Institute for Sensing Technologies, Key Laboratory of Liaoning for Integrated Circuits Technology, Dalian University of Technology, Dalian 116024, China

b. Department of Electronic Engineering, Dalian Neusoft University of Information, Dalian 116023, China

Abstract:

Thin-layered reduced graphene oxide (rGO) was successfully assembled onto the surface of  $\text{Co}_3\text{O}_4$  nanofibres forming rGO-wrapped  $\text{Co}_3\text{O}_4$  coaxial nanocabled microstructure for the first time by using the electrospinning technique. The resistive type chemical gas sensing properties of as-electrospun rGO wrapped- $\text{Co}_3\text{O}_4$  nanofibres were studied in detail and the sensors showed a good sensitivity and selectivity to different concentrations of ammonia from 10-100 ppm at room-temperature. The response time to ammonia is as fast as ~4 s which is the fastest one reported so far. This may be attributed to the excellent  $\text{NH}_3$  adsorption ability of the surface-coated rGO and porous microstructure of the electrospun intertwined nanofiber networks.

**Key words:** Reduced Graphene oxide (rGO); rGO wrapped- $\text{Co}_3\text{O}_4$  Nanofibres; Electrospun, Ammonia Sensors

**Submitted to Symposia 7: Low dimensional, Nano and 2D materials****Nanocrystalline Graphene/Hematite Composites:  
Rational Synthesis and Catalytic Gas Sensing Behavior**

Joerg J. Schneider, Peter Kraus

Technische Universität Darmstadt, Eduard-Zintl-Institut für Anorganische und Physikalische  
Chemie, Alarich-Weiss-Str. 12, 64287 Darmstadt, Germany

joerg.schneider@ac.chemie.tu-darmstadt.de

The sensitivity of graphene-based chemical gas sensors can be drastically improved by introducing appropriate dopants or defect sites which are able to enhance the interactions between the adsorbed gas molecules and the graphene material. Such modified graphene promotes the charge transfer between specific gas species and functionalized graphene, proving effective in giving faster response, and better selectivity. Our own earlier studies corroborate these findings. Nearly defect free CVD derived graphene shows p-type behaviour towards H<sub>2</sub> gas and a sensitivity in the ppm range, albeit with high response and recovery beginning at temperatures above 200°C [1]. Herein we report that a transfer of low layer CVD graphene to various substrates, represents a selective way to obtain highly defective large area nanocrystalline graphene. In contrast it shows gas sensing behaviour under ambient conditions at 25°C, e.g. 5 ppm NO<sub>2</sub>. By further modifying the particular synthesis conditions it is possible to obtain metal oxide decorated nanocrystalline graphene under controlled conditions. The crystalline oxide nanoparticles (2-3 nm diameter) reside preferentially at highly defective graphene sites. This material is candidate for heterogeneous catalyst, allows to study theoretically and experimentally disputed transparency effects of graphene as well as shed light into electronic and magnetic interactions of quasi zero dimensional nanoparticles on 2D surfaces.

**Keywords:** *Graphene, nanocrystalline, gas sensing, catalytic, graphene composites*

[1] MAO, S., LU, G.H., CHEN, J.H.. 2014.

Nanocarbon-based gas sensors: progress and challenges, Chem Mater. Chem. A, 2, 5573-5576

[2] KAYHAN, E., PRASAD, R., GURLO, A., YILMAZOGLU, O., PAVLIDIS, D., ENGSTLER, J., IONESCU, I., YOON, S., WEIDENKAFF, A., SCHNEIDER, J.J.. 2012.

Synthesis, Characterization, Electronic and Gas Sensing Properties towards H<sub>2</sub> and CO of Transparent, Large Area, Low Layer Graphene, Chem. Eur. J., 18, 14996-15003

## Towards printable, conductive and functionalised graphene based inks

Thomas Bamford, John Hedley, Andrew Pike

Newcastle University, Newcastle-upon-Tyne, Tyne and Wear, UK, NE1 7RU

[t.bamford@ncl.ac.uk](mailto:t.bamford@ncl.ac.uk), [john.hedley@ncl.ac.uk](mailto:john.hedley@ncl.ac.uk), [andrew.pike@ncl.ac.uk](mailto:andrew.pike@ncl.ac.uk)

Graphene, with its low cost and potential high electrical performance, suggests that widely-available, functionalised and printable graphene inks are on the horizon. This poster presents our efforts to develop printable, functionalised graphene inks in order to efficiently produce flexible electrical components for use in bio-sensors and super-capacitors.<sup>[1]</sup>

Graphene oxide ink has been widely researched but problems still exist with regards to conductivity and printability.<sup>[2]</sup> Here we present detailed studies into the formulation of printable graphene inks with robust characterisation by AFM, TEM and probe station measurements. Initial investigations into their functional and conducting properties are also reported and indicate that these functional materials can have applications in bio-MEMS sensor systems.

**Keywords:** *graphene, conductivity, functionalisation, inkjet-printing, bio-sensors*

[1] Li, J., YE, F., VAZIRI, S., MUHAMMED, M., LEMME, M. C. & ÖSTLING, M. 2013. Efficient Inkjet Printing of Graphene. *Advanced Materials*, 25, 3985-3992.

[2] TORRISI, F., HASAN, T., WU, W., SUN, Z., LOMBARDO, A., KULMALA, T. S., HSIEH, G., JUNG, S., BONACCORSO, F., PAUL, P. J., CHU, D. & FERRARI, A. C. 2012. Inkjet-Printed Graphene Electronics. *ACS Nano*, 6, 2992-3006.

# Fabrication of gas sensor based on P3HT to produce P/N hetero-junction array of ZnO nanowires

Chin-Kuo Kuo<sup>a</sup>, Chia-Ching Wu<sup>b</sup>, Ming-Jenq Twu<sup>c</sup>, Yi-Hsuan Hung<sup>a</sup>,  
Tzeng-Feng Liu<sup>a</sup>, Yi-Chieh Chao<sup>a\*</sup>

<sup>a</sup>Department of Industrial Education, National Taiwan Normal University,  
Taipei City 10610, Taiwan (R.O.C.)

<sup>b</sup>Department of Electronic Engineering, Kao Yuan University,  
Kaohsiung City 82151, Taiwan (R.O.C.)

<sup>c</sup>Department of Mechatronic Engineering, National Taiwan Normal University,  
Taipei City 10610, Taiwan (R.O.C.)

\*Correspondence author: [qxes5404@hotmail.com](mailto:qxes5404@hotmail.com) (Yi-Chieh Chao)

Poly(3-hexylthiophene) (P3HT) provides low processing cost and gas sensing operations at room temperature. Zinc Oxide (ZnO) has also demonstrated a high degree of sensitivity to gasses. This study combined organic and inorganic materials in the assembly of a gas sensor with high sensitivity to ammonia, in which ZnO nanowires provide a p-type semiconductor material and P3HT provides an n-type semiconductor. Physical vapor deposition (PVD) was used to deposit Al onto a substrate of indium tin oxide (ITO). Oxalic acid was then used as an electrolyte in anodization, resulting in a template of nano-holes comprising anodized aluminum oxide (AAO) with a pore diameter of 50 nm. Atomic layer deposition (ALD) was then used to fill the holes with ZnO to produce an array of ZnO nanowires. The AAO template was removed by wet etching and field-emission scanning electron microscopy was used to verify the successful formation of nanowires. Finally, a semiconducting layer of P3HT was spin coated onto the nanowires to enable gas sensing. Observations of microstructure and electrical analysis demonstrated that gas sensitivity decreased with an increase in the thickness of the P3HT layer.

**Keyword** : AAO, ZnO, ALD, P3HT, sensor, ammonia

# Fabrication of gas sensor based on P3HT to produce P/N hetero-junction array of ZnO nanowires

Chin-Kuo Kuo<sup>a</sup>, Chia-Ching Wu<sup>b</sup>, Ming-Jenq Twu<sup>c</sup>, Yi-Hsuan Hung<sup>a</sup>,  
Tzeng-Feng Liu<sup>a</sup>, Yi-Chieh Chao<sup>a\*</sup>

<sup>a</sup>Department of Industrial Education, National Taiwan Normal University,  
Taipei City 10610, Taiwan (R.O.C.)

<sup>b</sup>Department of Electronic Engineering, Kao Yuan University,  
Kaohsiung City 82151, Taiwan (R.O.C.)

<sup>c</sup>Department of Mechatronic Engineering, National Taiwan Normal University,  
Taipei City 10610, Taiwan (R.O.C.)

\*Correspondence author: [qxes5404@hotmail.com](mailto:qxes5404@hotmail.com) (Yi-Chieh Chao)

Poly(3-hexylthiophene) (P3HT) provides low processing cost and gas sensing operations at room temperature. Zinc Oxide (ZnO) has also demonstrated a high degree of sensitivity to gasses. This study combined organic and inorganic materials in the assembly of a gas sensor with high sensitivity to ammonia, in which ZnO nanowires provide a p-type semiconductor material and P3HT provides an n-type semiconductor. Physical vapor deposition (PVD) was used to deposit Al onto a substrate of indium tin oxide (ITO). Oxalic acid was then used as an electrolyte in anodization, resulting in a template of nano-holes comprising anodized aluminum oxide (AAO) with a pore diameter of 50 nm. Atomic layer deposition (ALD) was then used to fill the holes with ZnO to produce an array of ZnO nanowires. The AAO template was removed by wet etching and field-emission scanning electron microscopy was used to verify the successful formation of nanowires. Finally, a semiconducting layer of P3HT was spin coated onto the nanowires to enable gas sensing. Observations of microstructure and electrical analysis demonstrated that gas sensitivity decreased with an increase in the thickness of the P3HT layer.

**Keyword** : AAO, ZnO, ALD, P3HT, sensor, ammonia

## Structure and magnetic properties of triclinic $\text{Ni}_{0.6}\text{Co}_{0.4}\text{TiO}_3$ ilmenite oxide

Yukari Fujioka<sup>1</sup>, Johannes Frantti<sup>1</sup>, Anna Llobet<sup>2</sup>, Graham King<sup>2</sup>, and Steven N. Ehrlich<sup>3</sup>

<sup>1</sup> Finnish Research and Engineering, Helsinki, Finland

<sup>2</sup> Lujan Neutron Scattering Center, Los Alamos National Laboratory, Los Alamos, New Mexico 87545, USA

<sup>3</sup> National Synchrotron Light Source, Brookhaven National Laboratory, Upton, New York 11973, USA

*E Mail : johannes.frantti@fre.fi*

Forming a solid-solution of  $\text{NiTiO}_3$  and  $\text{CoTiO}_3$ , two isostructural (ilmenite) and isosymmetrical (space group  $R-3$ ) compounds, result in a single-phase compound with a remarkably low crystal symmetry. By neutron and X-ray synchrotron powder diffraction techniques, the space group symmetry of the  $\text{Ni}_{0.6}\text{Co}_{0.4}\text{TiO}_3$  sample was found to be triclinic  $P-1$  at room temperature, far above the magnetic transition temperature. Ni and Co ions were found to prefer positions close to the octahedron center, whereas Ti ions took off-center positions. This structural distortion is the first known case in ilmenites and opens up ways to modify functional properties of magnetic oxides. Origin of the symmetry lowering is discussed. Temperature dependent DC magnetic measurements revealed two transitions. The first transition took place at around 27 K and the second at 63 K. The low-temperature phase was antiferromagnetic. The phase observed between 27 and 63 K is characteristic to the solid-solution and is not found in either of the constituent members. The origin of the transitions is explained in terms of in-plane and out-of-plane magnetic moments.

**Keywords:** *Ilmenite, neutron diffraction, x-ray diffraction, magnetic ordering*

## Effect of the Scale Miniaturization on the Magnetocaloric Effect for $R_5(\text{Si}_x\text{Ge}_{1-x})_4$ System

A.M. Pereira<sup>1\*</sup>, J.H. Belo<sup>1</sup>, A.L. Pires<sup>1,2</sup>, G.N.P. Oliveira<sup>1</sup>, A. M. Lopes<sup>1,2</sup>, J.P. Araújo<sup>1</sup>

<sup>1</sup>IFIMUP and IN - Institute of Nanoscience and Nanotechnology, Departamento de Física e Astronomia da Faculdade de Ciências da Universidade do Porto, Rua campo Alegre, 687, 4769-007 Porto, Portugal.

<sup>2</sup>CFNUL - Centro de Física Nuclear da Universidade de Lisboa, Av. Prof. Gama Pinto, 2, 1649-003 Lisboa, Portugal.

*ampereira@fc.up.pt*

A magnetic refrigeration (MR) at room temperature (RT) was a mirage for science during several decades due to the considerable low magnetocaloric effect obtained by magnetic materials near RT. This limitation was overcome when the Giant Magnetocaloric Effect (GMCE) near RT was discovered on the  $\text{Gd}_5\text{Si}_2\text{Ge}_2$  compound [1], followed by several families of compounds such La-Fe-Si, Mn-Si-Co, and  $\text{LaCaMnO}_3$  materials.

Besides de GMCE, the  $R_5(\text{Si},\text{Ge})_4$  compounds are considered a playground on condensed matter area since they exhibit several different types of phase transitions (magnetic, structural, electronic) and colossal magnetostriction, being considered a multifunctional materials. The control and tuning of magnetostructural transitions responsible for the magnetocaloric effect are of vital scientific and technological items. On MR the heat exchange and the magnetic losses hysteresis are crucial parameters for MR efficiency. New strategies are being addressed that challenges, namely by increasing the surface exchange and by geometrical design. In order to overcome these barriers, in this work we will study the reduction scale effect on the  $R_5(\text{Si},\text{Ge})_4$  compounds down to the nanoscale size.

Micrometric ball milling samples were studied of two materials: one exhibiting a fully coupled magnetostructural transition -  $\text{Gd}_5\text{Si}_{1.3}\text{Ge}_{2.7}$  and one exhibiting an individual magnetic and structural transition -  $\text{Tb}_5\text{Si}_2\text{Ge}_2$ . At nanoscale, a thin film was prepared by femto-second pulsed laser deposition with same composition of the Gd compound



(Gd<sub>5</sub>Si<sub>1.3</sub>Ge<sub>2.7</sub>). Concerning the Gd sample, the MCE decrease (up to 60%) when reducing the scale. Additionally, an increase of the O(I) phase at RT was observed combined with a volume reduction of the unit cell (up to 1%) when compared with the bulk counterpart. These observations are fingerprints of internal stress in the samples arising probably from the scale down of the magnetic materials. Concerning the Tb compound, a fully coupling of the structural and the purely magnetic transition is achieved in the ball milling for long time preparation revealing again the presence of strain by mimicking the external pressure effect [3]. Concerning the magnetic hysteresis, there is a drastic reduction of the magnetic hysteresis with scale down of the nanomaterials, thus showing that this strategy could be a good choice for the increase of efficiency of the magnetic refrigeration.

[1] V. K. Pecharsky & K. A. Gschneidner, Jr. Phys. Rev. Lett. 78, 4494–4497 (1997)

[2] J. H. Belo, A. M. Pereira, C. Magen, L. Morellon, M. R. Ibarra, P. A. Algarabel and J. P. Araújo J. Appl. Phys. 113 , 133909 (2013)

[3] A. M. Pereira, A. M. dos Santos, C. Magen, J. B. Sousa, P. A. Algarabel, Y. Ren, C. Ritter, L. Morellon, M. R. Ibarra and J. P. Araújo Appl. Phys. Lett. 98 , 122501 (2011)

**Keywords:** *Magnetic refrigeration, MultiFunctional magnetic material, thin film*

## Synthesis of metallic magnetic nanorods protected by noble metal shell

Lentijo-Mozo<sup>1</sup>, Tan<sup>1</sup>, Hungria-Hernandez<sup>1</sup>, Garcia Marcelot<sup>1,2</sup>, Altantzis<sup>3</sup> Cormary<sup>1</sup>, Miller<sup>4</sup>, Gallagher<sup>4</sup>, Martinez<sup>5</sup>, Fazzini<sup>1</sup>, Respaud<sup>1</sup>, Bals<sup>3</sup>, Van Tendeloo<sup>3</sup>, Gatel<sup>2</sup>, Soulantica<sup>1</sup>.

<sup>1</sup> Laboratoire de Physique et Chimie des Nano-objets (LPCNO), Université de Toulouse; INSA, UPS, CNRS, 135 avenue de Rangueil, 31077 Toulouse (France)

<sup>2</sup> Centre d'Elaboration de Matériaux et d'Etudes Structurales (CEMES-CNRS), 29 rue Jeanne Marvig, B.P. 94347, 31055 Toulouse (France)

<sup>3</sup> Electron Microscopy for Materials Research (EMAT), University of Antwerp, Groenenborgerlaan 171, 2020 Antwerp, (Belgium)

<sup>4</sup> Chemical Science and Engineering Division, Argonne National Laboratory, 9700 S Cass Ave., Argonne, IL, 60439 (USA)

<sup>5</sup> IPREM-ECP CNRS UMR 5254, Université de Pau, Hélioparc Pau Pyrénées, 2 av. Pierre Angot, 64053 Pau Cedex 9, (France)

*ksoulant@insa-toulouse.fr*

Anisotropically shaped Co nanocrystals such as nanorods or nanowires are ideal candidates for applications concerning information storage and permanent magnets. Metallic Co single-crystalline nanorods of hexagonal close packed (*hcp*) structure, prepared by the reduction of a coordination Co precursor under hydrogen,<sup>1</sup> exhibit particularly attractive magnetic properties<sup>2</sup> for implementation in domains requiring materials with both high magnetization and high coercivity. They are excellent candidates for applications requiring “hard” magnetic nanoparticles (information storage, permanent magnets), however their use is compromised by their increased sensitivity towards oxygen and water that transforms them to cobalt oxides and/or hydroxides with a concomitant deterioration of their advantageous magnetic properties. The development of

a continuous noble metal shell around the cobalt cores would be an ideal solution for rendering the nanorods appropriate for use in an aqueous environment. The growth of a full shell is not straightforward, since segregation of the noble metal on the surface of cobalt results to noble metal decorated nanorods and not to a continuous full shell. However, even small discontinuities are enough for cobalt oxidation to take place in an aqueous solution. The introduction of an intermediate buffer layer between the magnetic core and the noble metal is a key step for the development of a full noble metal shell. Indeed the compatibility of the intermediate layer with both core and shell materials allows the formation of energetically favorable interfaces that are not disrupted. After noble metal protection, the nanorods are air and water resistant and can be transferred to an aqueous solution and be functionalized by standard antibody immobilization protocols without losing their magnetic properties.

***Keywords: Core-shell, ferromagnetic, nanorods, cobalt, water-resistant.***

[1] WETZ, F., SOULANTICA, K., RESPAUD, M., FALQUI, A.; CHAUDRET, B. Synthesis and Magnetic Properties of Co Nanorod Superlattices. *Mater. Sci. Eng. C* 27, 1162-1166.

[2] SOULANTIKA, K., WETZ, F., MAYNADIE, J., FALQUI, A., TAN, R. P., BLON, T., CHAUDRET, B., RESPAUD, M. *Appl. Phys. Lett.* 95, 152504.

## Superparamagnetic iron oxide nanoparticles investigated by nuclear magnetic resonance and magnetization measurements

P. Křišťan<sup>1</sup>, H. Štěpánková<sup>1</sup>, J. Prokleška<sup>1</sup>, R. Müller<sup>2</sup>, K. Kouřil<sup>1</sup>, V. Chlan<sup>1</sup>

<sup>1</sup> Charles University in Prague, Faculty of Mathematics and Physics,  
V Holešovičkách 2, 18000 Prague 8, Czech Republic

<sup>2</sup> Leibniz Institute of Photonic Technology,  
Albert-Einstein-Str. 9, 07745 Jena, Germany

*Petr.Kristan@mff.cuni.cz*

Magnetic particles of nanoscale or submicron dimensions are widely used in many applications such as recording devices, drug delivery, radiofrequency heating etc. In case of nanoscale dimensions, superparamagnetism plays a considerable role. While superparamagnetic particles were studied by various physical methods, nuclear magnetic resonance (NMR) was employed only rarely. In this paper we report results obtained by <sup>57</sup>Fe NMR and the comparison with macroscopic magnetic properties.

The series of five nanocrystalline iron oxide samples with various mean particle sizes were prepared by glass crystallization. The nanoparticles grew inside a glass matrix to prevent their agglomeration and to reduce magnetic interaction between them. The X-ray diffraction was used to determine the mean particle sizes (5, 7, 8.5, 9 and 10 nm) and phase compositions. Zero-field cooled (ZFC) and field cooled (FC) dependences of sample magnetic moment on temperature (from 4 K to 400 K) were measured in applied magnetic fields of 30, 100 and 300 Oe. From ZFC/FC curves we calculated distribution of blocking temperatures for each sample. <sup>57</sup>Fe NMR spectra were recorded in zero external magnetic field at 4.2 K. The spectral line shape corresponded to magnetite for samples with smaller particles and to maghemite for those with bigger particles. Temperature dependences of NMR spectra displayed a rapid decrease of NMR signal intensity with increased temperature and vanishing of the signal around the average blocking temperature determined from ZFC/FC curve for 30 Oe.

**Keywords:** *nanoparticles, superparamagnetism, glass crystallization, iron oxide, NMR*

## The Particle Size Dependent Cation Distribution and Magnetization of Lithium Ferrite

V. Šepelák<sup>1,2</sup>, I. Bergmann<sup>3</sup>, H. Hahn<sup>1</sup>, K.-D. Becker<sup>4</sup>

<sup>1</sup>Institute of Nanotechnology, Karlsruhe Institute of Technology, Hermann-von-Helmholtz-Platz 1, 76344 Eggenstein-Leopoldshafen, Germany.

<sup>2</sup>Slovak Academy of Sciences, 04353 Košice, Slovakia.

<sup>3</sup>Volkswagen AG, 38436 Wolfsburg, Germany.

<sup>4</sup>Institute of Physical and Theoretical Chemistry, Braunschweig University of Technology, Hans-Sommer-Str. 10, 38106 Braunschweig, Germany.

*vladimir.sepelak@kit.edu*

Interest in nanosized spinel ferrites has greatly increased in the past few years due to their importance in understanding the fundamentals in nanomagnetism and their wide range of applications such as high-density data storage, ferrofluid technology, sensor technology, spintronics, magnetocaloric refrigeration, heterogeneous catalysis, magnetically guided drug delivery, and magnetic resonance imaging. In the present work, lithium ferrite ( $\text{Li}_{0.5}\text{Fe}_{2.5}\text{O}_4$ ) nanoparticles of various sizes were prepared by mechanochemical routes [1]. In-field  $^{57}\text{Fe}$  Mössbauer spectroscopy and high-resolution TEM studies revealed a nonuniform structure of the as-prepared nanoparticles consisting of ordered regions surrounded/separated by disordered grain boundary/surface regions with the thickness of about 1 nm. The as-prepared nanoparticles are found to be structurally and magnetically disordered due to the far-from-equilibrium cation distribution and the canted spin arrangement. As a consequence of frustrated superexchange interactions, the nanosized  $\text{Li}_{0.5}\text{Fe}_{2.5}\text{O}_4$  exhibits a reduced nonsaturating magnetization, an enhanced coercivity, and a shifted hysteresis loop.

**Keywords:** *Ferrite, nanoparticle, cation distribution, spin canting, magnetization*

[1] ŠEPELÁK, V., DÜVEL, A., WILKENING, M., BECKER, K.-D., HEITJANS, P. 2013. Mechanochemical Reactions and Syntheses of Oxides. *Chem. Soc. Rev.*, 42, 7507-7520.

## Aqueous Ammonia as CPCA in Sol-gel Combustion Method for Nanofabrication of CdFe<sub>2</sub>O<sub>4</sub>

Munish Gupta<sup>1,2</sup>, Anu<sup>3</sup>, BS Randhawa<sup>1</sup>

<sup>1</sup>Department of Chemistry, Centre for Advanced Studies-II, Guru Nanak Dev University,  
Amritsar, Punjab, India-143005

<sup>2</sup>Department of Chemistry, D A V College, Amritsar, Punjab, India-143001

<sup>3</sup>Department of Chemistry, B U C College, Batala (Gurdaspur), Punjab, India-143505

e-mail: balwinderrandhawa@yahoo.co.in ☎ +91-9878136639

A comparative study on nanofabrication of Cd ferrites by sol-gel method using citric acid as a complexing agent in the presence and without aqueous ammonia as combustion process chemical additive” (CPCA) have been carried out. Ferrites obtained by different methods were characterized by various spectroscopic techniques and reveal that in the presence of CPCA, ferrites in nanorange (30-38nm) are obtained at lower temperature (500<sup>0</sup>C), with high surface area (14.5067m<sup>2</sup>/g) and novel electro-magnetic ( $M_S = 5.4273$  emu/g). Aqueous ammonia increases the extent of cation chelation with citrates, controls pH of the solution and extend porous three-dimensional (3D) network structures in nitrate-citrate xerogels [1]. Combustion method used has an advantage over other conventional methods as ferrites in the nano-range are obtained whereas in other conventional method like ceramic method, sintering over prolonged period gives rise to formation of bulk ferrites [2].

**Keywords:** *Nanofabrication, CPCA, Sol-Gel method, Ferrites, Xerogels.*

- [1] SUTKA, A., MEZINKIS, G., JAKOVLEVS D. & KORSACKS, V. 2013. Sol-gel combustion synthesis of CdFe<sub>2</sub>O<sub>4</sub> ferrite by using various reducing agents, J. Austr. Ceram. Soc., 49, 136 – 140.
- [2] GUPTA, M., GUPTA, M., SHEEL, V. & RANDHAWA, B.S. 2013. Mössbauer Studies on Thermal Decomposition of Rubidiumbis(citrato)ferrate(III) Precursor Prepared by Precursor Method. J. Anal. & Appl. Pyrol., 104, 73–76.

The conjugation of gold nanorods (AuNRs) with biocompatible polyethylene glycol (PEG) molecules has triggered an emerging application in therapeutics and diagnostics. The AuNRs are generally synthesized by the seed-mediated method that takes advantage of cetyl trimethylammonium bromide (CTAB) and silver nitrate to control over the nanorod formation and the aspect ratio. The PEGylation usually happens only at the tips, resulting in partially modified AuNRs. These AuNRs are found to be toxic to cells due to the residual CTAB and silver. To solve this problem, we report herein a novel, facile, scalable one-step surface functionalization method to produce completely biocompatible (i.e. CTAB and Ag free) AuNRs. The method involves the use of a nonionic, biocompatible surfactant – Tween 20 to stabilize the nanorods, bis(*p*-sulfonatephenyl)phenylphosphine (BSPP) to activate the AuNR surface for the subsequent thiolated PEG attachment and sodium chloride (NaCl) to etch silver from the AuNRs. Highly colloidal stable and nontoxic PEGylated AuNRs were obtained. This method allows for quantitative functionalization of AuNRs with PEG molecules and can be easily extended to other PEG derivant and nanoparticle systems.

# Fe<sub>3</sub>O<sub>4</sub> nanoparticles Interfere spore germination of *Clostridium difficile*: an *in vitro* and *in vivo* study

Wei-Ting Lee,<sup>1</sup> Ya-Na Wu,<sup>2</sup> Yi-Hsuan Chen,<sup>3</sup> Tsai-Miao Shih,<sup>2</sup> Tsung-Ju Li,<sup>1</sup>  
Chen-Sheng Yeh,<sup>4</sup> Pei-Jane Tsai,<sup>1,3</sup> Dar-Bin Shieh<sup>1,2</sup>

<sup>1</sup>Institute of Basic Medical Sciences, National Cheng Kung University, Tainan 70101, Taiwan

<sup>2</sup>Institute of Oral Medicine and Department of Stomatology, National Cheng Kung University Hospital, National Cheng Kung University, Tainan 70101, Taiwan

<sup>3</sup>Department of Medical Laboratory Science and Biotechnology, National Cheng Kung University, Tainan 70101, Taiwan

<sup>4</sup>Department of Chemistry, National Cheng-Kung University, Tainan 70101, Taiwan

## Abstract:

*Clostridium difficile* infection (CDI) has emerged to be a major cause of Healthcare-associated infection in the world. CDI usually occur in patients subject to long-term use of antibiotics, and it is often initiated by the spores acquired from healthcare workers. Current CDI clinical management is still far from satisfactory as the spores are resistant to many chemical agents and physical approaches. Nanotechnology has been explored for potential applications in anti-microbials such as silver and zinc oxide nanoparticles. In this study, germination inhibitory activities of various kinds of nanoparticles were evaluated spectrometrically. We discovered the Fe<sub>3-δ</sub>O<sub>4</sub> nanoparticles present significant inhibition to *C. difficile* spore germination *in vitro* compared to other types of iron containing nanoparticles, zinc oxide, and silver nanoparticles. We previously developed 22 nm truncated octahedral Fe<sub>3-δ</sub>O<sub>4</sub> nanoparticles through thermal decomposition of iron acetylacetonate with oleic acid and trioctylamine. The nanoparticles show a dose dependent inhibition of *C. difficile* spores germination. In an exposure condition of 0.5 mg/mL for 20 minutes, the nanoparticles showed a 64% inhibition to the spores from transforming into the vegetative cells closed to that of sodium hypochloride positive control. CDI animal model was established in NF-κB-reporter mice using oral gavage with *C. difficile* spores. After 3 days, inflammation level was recorded non-invasively by In Vivo Imaging System. *C. difficile* spores without Fe<sub>3-δ</sub>O<sub>4</sub> nanoparticles treatment tripled the inflammatory level of the Fe<sub>3-δ</sub>O<sub>4</sub> nanoparticles treatment group in mice quantified by the luminous intensity. Histopathology analysis revealed intense neutrophil accumulation in the colon tissue of the control group compared to the nanoparticles-treated mice. With images showed that Fe<sub>3-δ</sub>O<sub>4</sub> nanoparticles could bind



to *C. difficile* spores and then interfere in germination. In summary, we demonstrated the potential development of  $\text{Fe}_{3-\delta}\text{O}_4$  nanoparticles as an effective clinical therapeutic agent for CDI.

## **Conventional antibiotics in form of nanospheres for the prevention of biofilm formation and provide infection control**

Margarida M. Fernandes, Kristina Ivanova, Antonio Francesko, Tzanko Tzanov

Group of Molecular and Industrial Biotechnology, Department of Chemical Engineering, Universitat Politècnica de Catalunya, Rambla Sant Nebridi 22, 08222, Terrassa, Spain

Bacterial biofilms are formed when unicellular organisms come together to form a community that is attached to a solid surface and encased in an exopolysaccharide matrix. When growing in the biofilm phenotype, bacteria are able to survive in hostile environments and acquire increased antibiotic tolerance and resistance to clearance by the host immune system. Currently there is an urgent need for new antibacterial agents with low susceptibility to resistance development. In this study, two conventional antibiotics, to which pathogenic bacteria such as *Pseudomonas aeruginosa* and *Escherichia coli* are resistant, were processed into nanospheres using a one-step, environmentally friendly sonochemical technology. The penicillin G and vancomycin nanospheres were shown to possess improved antibacterial and antibiofilm activity compared to the non-processed antibiotics. Their effect was further related to the enhanced membrane permeability of the spheres, studied by their interaction with cell membrane models - Langmuir monolayers - allowing minimum diffusion limitations and maximum surface area per unit mass. Importantly, the studied nano-structured materials selectively killed bacteria, without imparting toxicity to human cells. It is believed that bacteria do not recognize antibiotic nanospheres as a threat, hence their efficiency is improved and a delay in the development of bacteria resistance mechanisms probable.

## **Synthesis, Characterization, and application of TiO<sub>2</sub> Nanoparticles for UV protective, antibacterial, mosquitocidal and seed germination inducing potentials**

**Brindha Durairaj**<sup>1</sup>, Santhoshkumar Muthu<sup>2</sup>

<sup>1</sup>Associate Professor & Head, <sup>2</sup>PhD Scholar, Department of Biochemistry, PSG College of Arts and Science, Coimbatore- 641014. T.N. India

E-mail: [brindhavenkatesh@gmail.com](mailto:brindhavenkatesh@gmail.com) Mobile: +91-98422-98546

### Abstract

The field of nanotechnology has revolutionized the applicability of nanoparticles in various areas ranging from textiles, electronics, medicine, forestry etc. The present work also focuses on harnessing the potentials of TiO<sub>2</sub> nanoparticles in niche biological applications. Nanoparticles, in particular metallic nanoparticles like TiO<sub>2</sub> has now been researched for exploring its application in the field of biology, textile technology, for development of products for conscious human use. The aim of the study was to synthesize Titanium dioxide (TiO<sub>2</sub>) nanoparticles by using *Aspergillus niger*. A concentration of 0.1 M TiO<sub>2</sub> was added to the cell free filtrate prepared from the fungal culture. The entire mixture was incubated in shaker at 28°C for 48 hrs at 150 rpm. Biologically synthesized nanoparticle was characterized by UV visible spectroscopy, SEM, and XRD. After characterization, the TiO<sub>2</sub> nanoparticles were screened for various applications such as antimicrobial activity, larvicidal potential, seed growth promotion, bacterial resistance and UV protective fabrication.

A concentration of 50µg titanium dioxide nanoparticles were found to induce germination significantly in Fenugreek seeds when compared with control seedlings. This was further validated by germination characteristics such as shoot length (19.77 cm), root length (2.81 cm), germination percentage (98.75%), and seed vigor index (2229.7) and biochemical parameters including protein (52.57 mg/g shoot and 51.10 mg/g root), carbohydrates (22.72 mg/g shoot and 17.08 mg/g root), reducing sugars (20.75 mg/g shoot and 18.97 mg/g root), chlorophyll (1.33 mg/g leaf) in the germinating seedlings. The values were found to be significantly higher when compared to 25 µg TiO<sub>2</sub> treatment and control.

TiO<sub>2</sub> nanoparticles impregnated 100% cotton fabric was proven to have best UV protective ability with UPF value of 30. The bactericidal activity of the treated fabric was assessed and a zone of inhibition of 49.12 mm and 40.13 mm was obtained against *Staphylococcus aureus* and *Escherichia coli* respectively. The same cotton fabric was found to exhibit antifungal activity against *Aspergillus niger* and *Trichoderma reesei* with a zone diameter of 60 mm and 65 mm respectively.

The antibacterial activity of the TiO<sub>2</sub> nanoparticles was tested against *Bacillus* (18 mm), *Klebsiella* (19 mm), *Pseudomonas* (21 mm), *Streptococcus sp* (19 mm). Maximum zone of inhibition was observed against *Pseudomonas* (21mm).

The larvicidal activity of TiO<sub>2</sub> nanoparticles against II and III instar larvae of *Aedes aegypti* was deciphered to be concentration dependant (IC<sub>50</sub> = 6.7 ppm and 8.4 ppm for II and III instar). Biochemical profiling in the treated larvae revealed that TiO<sub>2</sub> toxicity reduced the levels of protein, cholesterol, and activities of acid/alkaline phosphatases, and lactate dehydrogenase whereas carbohydrate content increased in the treated larvae. Fungal synthesized TiO<sub>2</sub> strongly induced the larval mortality and altered the metabolism of essential biomolecules leading to development of an effective strategy to control *Aedes aegypti* at its early larval stage. Hence, it can be inferred that there is a vast potential for TiO<sub>2</sub> nanoparticle in biological application ranging from development of a UV protective , antibacterial, mosquitocidal agents, and plant growth inducer.

Keywords : Titanium nanoparticles, *Aspergillus niger* , UV Protection, *Aedes aegypti* , Mosquitocide, cotton fabric.

## Porous Silicon Based Mass Spectrometry Platform for Biomarker Diagnosis

F. Gaillard<sup>1</sup>, V. Aiello<sup>1</sup>, A. Bouamrani<sup>2</sup>, M. Dreyfus<sup>2</sup>, A. Mombrun<sup>2</sup> and F. Berger<sup>2</sup>

<sup>1</sup>CEA-Leti, Minatec Campus, 17 Rue des martyrs – 38054 Grenoble (France).

<sup>2</sup>CEA-Leti, Clinatec, 17 Rue des martyrs – 38054 Grenoble (France).

*frederic-x.gaillard@cea.fr / +33. (0)4.38.78.26.62*

Molecular analysis of biological fluids is a clinical challenge. For instance, detection of peripheral biomarkers is valuable for early detection, prognosis and therapeutic response prediction in many pathologies. The Low Molecular Weight (LMW) proteome of the human blood serum is a promising source for biomarkers discovery [1]. Because 1% of the serum contains potential LMW biomarkers while the remaining 99% is composed of ubiquitous high molecular weight species, their detection and the pre-analytical bias due to sample handling and stability are critical issues in proteomic profiling approaches for clinical applications [2]. Innovative technologies solving these issues are mandatory to find new biomarkers related to the onset of a disease.

In this work, we demonstrate that mesoporous silicon (PSi) layer, used as a platform for direct MALDI-ToF detection (Matrix-Assisted Laser Desorption/Ionization Time-of-Flight mass spectrometry), represents an efficient strategy for molecular size-exclusion, fast and sensitive acquisition of discriminant proteomic profiles, and detection of potential biomarkers in biological samples. We study the influence of porous material characteristics (morphology, thickness...) on the enrichment of LMW species. On the one hand, we present the interest to use this platform to individualize specific proteomic profiles of different pathological states (cardiovascular, lymphoma...). On the other one, we show that *in vivo* exploration can also be considered using this PSi platform. A specific tool for *in vivo* sampling and analysis has consequently been developed on 200mm silicon wafer for surgical intraoperative assistance. Its fabrication mode will be discussed.

**Keywords:** *Porous Silicon, Mass Spectrometry, Biomarker, Proteomic, Pathology*

[1] LIOTTA, L.A., FERRARI, M., PETRICOIN, E. 2003. Written in blood. *Nature*, 425, 905.

[2] FINDEISEN, P., SISMANIDIS, D., RIEDL, M., COSTINA, V., NEUMAIER, M. 2005. Preanalytical impact of sample handling on proteome profiling experiments with matrix-assisted laser desorption/ionization time-of-flight mass spectrometry. *Clin. Chem.* 51, 2409-2411.

## Controlling neuronal and glial cell behavior by patterning vertical gallium phosphide nanowires

Maria-Thereza Perez<sup>1,2</sup>, Gaëlle Piret<sup>1,2,3</sup>, Christelle N. Prinz<sup>2,3,4</sup>

<sup>1</sup>*Department of Clinical Sciences, Division of Ophthalmology,  
Lund University, Lund, Sweden*

<sup>2</sup>*Nanometer Structure Consortium (nmC@LU), Lund University, Lund, Sweden*

<sup>3</sup>*Division of Solid State Physics, Lund University, Lund, Sweden*

<sup>4</sup>*Neuronano Research Center (NRC), Lund University, Lund, Sweden*

± *Current address: Clinattec Laboratory, Biomedical Research Center  
Edmond J. Safra, Grenoble, France*

*E-mail contact: maria\_thereza.perez@med.lu.se*

The ultimate objective of the work is to develop implantable nanowire-based devices for restoring function in patients with retinal degenerative diseases. One of the factors limiting the functionality of neural prosthetics comes from the fact that they need to integrate with tissue that is undergoing degeneration. Nervous tissue consists of two main types of cells, neurons and glia, with the latter being essential for the maintenance of the former. At the same time, glial cell activation (gliosis), which occurs naturally in response to disease and trauma, limits the efficacy of neural implants, since a glial scar, which forms as the glial cells proliferate and migrate, eventually surrounds the device.

We have shown that both retinal neurons and glial cells survive when grown *in vitro* on dense arrays of vertical gallium phosphide (GaP) nanowires and that these promote neurite outgrowth to an exceptional extent<sup>1</sup>. In the present study, we examined whether it is possible to pattern the GaP nanowire substrates such that proliferating glial cells become restricted to particular regions on the surface. Retinal cells were derived from 4-day-old mice and cultured for 8 and 18 days *in vitro* (DIV) on substrates containing regions with different topographies that were generated using electron beam lithography to pattern gold nanoparticle catalysts and metal organic vapor phase epitaxy to grow the nanowires. The regions consisted of 100  $\mu\text{m}$  wide dense and regular arrays of vertical nanowires (4  $\mu\text{m}$  long; 80 nm in diameter) separated by 100 or 25  $\mu\text{m}$  wide regions with a flat topography (referred to as substrates

*100n/100f* and *100n/25f*, respectively). We examined, in addition, whether the outgrowth of retinal neuronal processes could be guided by arranging the nanowires in rows spaced 10  $\mu\text{m}$  apart within the 100  $\mu\text{m}$  nanowire arrays (substrate *100n-rows/100f*).

Using specific markers for neurons and glia, we found that in *100n/100f* substrates, glial cells were observed predominantly within the flat regions and only rarely over the nanowires, both at 8 and 18DIV. In *100n/25f* substrates, most glial cells were still found within the flat regions, although a greater number of them were observed on the nanowires, as compared to *100n/100f* substrates. Using the *100n-rows/100f* substrate, we found that neuronal processes aligned along the nanowire rows, as if guided by the nanowires, and that at least some of the guided processes belonged to retinal ganglion cells.

The study thus shows that, by designing substrates of vertical nanowires with distinct surface topographies, it is possible to control neuronal and glial cell behavior, an important parameter in the design of implants with better biocompatibility and functionality.

**Keywords:** *prosthetics, nanowires, retina, gallium phosphide, gliosis*

[1] PIRET, G., PEREZ, M. T., PRINZ, C. N. 2013. Neurite outgrowth and synaptophysin expression of postnatal CNS neurons on GaP nanowire arrays in long-term retinal cell culture. *Biomaterials*, 34, 875–887.



# Making structured metals transparent for ultrabroadband electromagnetic waves

Ru-Wen Peng<sup>1,\*</sup>, Ren-Hao Fan<sup>1</sup>, Xian-Rong Huang<sup>2</sup>, and Mu Wang<sup>1</sup>

1) *National Laboratory of Solid State Microstructures and School of Physics, Nanjing University, Nanjing 210093, China*

2) *Advanced Photon Source, Argonne National Laboratory, Argonne, Illinois 60439, USA*

## Abstract

In this work, we present our recent progress on making structured metals transparent for broadband electromagnetic waves via excitation of surface plasmons. First, we theoretically show that one-dimensional metallic gratings can become transparent and completely antireflective for extremely broadband electromagnetic waves by relying on surface plasmons or spoof surface plasmons. Second, we experimentally demonstrate that metallic gratings with narrow slits are highly transparent for broadband terahertz waves at oblique incidence and high transmission efficiency is insensitive to the metal thickness. Further, we significantly develop oblique metal gratings transparent for broadband electromagnetic waves (including optical waves and terahertz ones) under normal incidence. In the third, we find that the principles of broadband transparency for structured metals can be extended from one-dimensional metallic gratings to two-dimensional cases. These investigations may provide guidelines to develop many novel materials and devices, such as transparent conducting panels, antireflective solar cells, and other broadband metamaterials and stealth technologies.

## References:

- 1) X.R. Huang, R.W. Peng, R.H. Fan, *Phys. Rev. Lett.* 105 (2010) 243901.
- 2) R.H. Fan, R.W. Peng, X.R. Huang, J. Li, Y. Liu, Q. Hu, Mu Wang, and X. Zhang, *Adv. Mater.* 24 (2012) 1980.
- 3) D.X. Qi, R.H. Fan, R.W. Peng, X.R. Huang, M.H. Lu, X. Ni, Q. Hu, and Mu Wang, *Appl. Phys. Lett.* 101 (2012) 061912.
- 4) R.H. Fan, L.H. Zhu, R.W. Peng, X.R. Huang, D.X. Qi, X.P. Ren, Q. Hu, and Mu Wang, *Phys. Rev. B* 87 (2013) 195444.
- 5) R.H. Fan, J. Li, R.W. Peng, X.R. Huang, D.X. Qi, D.H. Xu, X.P. Ren, and Mu Wang, *Appl. Phys. Lett.* 102 (2013) 171904.
- 6) Xiao-Ping Ren, Ren-Hao Fan, Ru-Wen Peng, and Mu Wang, manuscript submitted (2014).

\*Email: rwpeng@nju.edu.cn

**Symposia 7: Low dimensional, Nano and 2D materials**

**Presentation: oral**

## White quantum dot light emitting diode by mixed blue-green-red QDs

Jing Chen<sup>1</sup>, Jiangyong Pan<sup>1</sup>, Qianqian Huang<sup>1</sup>, Wei Lei<sup>1</sup>

School of Electronic Science and Engineering, Southeast University, Nanjing, China, 210096

### Abstract

White quantum dot light-emitting diodes (QD-LEDs) have been a promising candidate for high-efficiency and color-saturated displays. Here, we report a simply solution-processed white QD-LED using the mixed blue-green-red QDs as the emitting layer. The device is demonstrated with a maximum luminance of  $150 \text{ cd/m}^2$  and power efficiency of  $0.34 \text{ lm/W}$ , exhibiting the Commission Internationale de l'Enclairage (CIE) coordinates of (0.33, 0.33). The unencapsulated white QD-LED has a long lifetime of 60 h at its initial luminance of  $150 \text{ cd/m}^2$ .

## Structural Investigation on Catalyst-Free Si-Doped InAs Nanowires

D. W. Park<sup>1,2</sup>, J. S. Kim<sup>1,\*</sup>, S. K. Noh<sup>2</sup>, J. O. Kim<sup>2</sup>, S. W. Kang<sup>2</sup> and S. J. Lee<sup>2</sup>

<sup>1</sup>Division of Advanced Materials Engineering & Research Center of Advanced Materials Development, Chonbuk National University, Jeonju 561-756, Korea

<sup>2</sup>Nano Materials Evaluation Center, Korea Research Institute of Standards and Science, Daejeon 305-340, Korea

*E-Mail : [dwpark@kriss.re.kr](mailto:dwpark@kriss.re.kr) and [kjinsoo@jbnu.ac.kr](mailto:kjinsoo@jbnu.ac.kr)*

To realize devices using Si-based InAs nanowires (NWs) as an active medium or a channel region, reliable doping profiles should be defined at the NW itself. In the previous works, when Si doping was introduced to InAs NWs, the heights of Si-doped InAs NWs were decreased with relatively thick features compared to those of undoped NWs [1]. In this paper, we report the influences of HF/BOE surface treatment and Si-doping on structural properties of catalyst-free InAs NWs formed on Si(111) substrates. Before depositing InAs, Si substrates were cleaned separately by using HF and BOE solutions. For the formation of InAs NWs, indium was supplied at the pressure of  $3 \times 10^{-8}$  torr and V/III ratio was changed from 50 to 400 by changing arsenic flux for 60 min. Si with the nominal concentration of  $1 \times 10^{19} \text{ cm}^{-3}$  was introduced to form Si-doped InAs NWs. The spatial density of the NWs was increased from  $8 \times 10^6$  to  $1.5 \times 10^8 \text{ cm}^{-2}$  with increasing V/III ratio from 50 to 200. With further increase in V/III ratio, the NW density was not increased. However, the average height of InAs NWs was increased from 0.6 to 5.8  $\mu\text{m}$  with increasing V/III ratio. At the V/III ratio of 400 for 120 min, the average height and diameter of Si-doped InAs NWs were measured to be 10  $\mu\text{m}$  and 80 nm, respectively, which are almost same to those of undoped NWs. In addition, since various shapes of InAs NWs were observed in transmission electron microscopy images, we will statistically discuss electrical properties depending on their structural properties.

**Keywords:** *InAs, nanowires, MBE, catalyst-free*

[1] DIMAKIS, E., RAMSTEINER, M., HUANG, C., TRAMPERT, A., DAVYDOK, A., BIERMANN, A., PIETSCH, U., RIECHERT, H. & GEELHAAR, L. 2013. *In situ* Doping of Catalyst-Free InAs Nanowires with Si: Growth, Polytypism, and Local Vibrational Modes of Si. Applied Physics Letters, 103, 143121.

## Preparation of Cu<sub>2</sub>O nanowires by thermal oxidation method and their application in solar cells

Dongyun Guo and Yang Ju

Department of Mechanical Science and Engineering, Nagoya University

Furo-cho, Chikusa-ku, Nagoya 464-8603, Japan

ju@mech.nagoya-u.ac.jp

The worldwide quest for clean and renewable energy sources has encouraged large research activities and developments in the field of solar cells. It is currently dominated by bulk crystalline Si-based solar cells. But the high specific cost of this technology is a barrier to its widespread dissemination. Cuprous oxide (Cu<sub>2</sub>O), p-type semiconductor with direct band gap ( $E_g$ ) of 2.1 eV, is investigated for solar cells in the early 1900's due to the non-toxic nature, abundance of the copper and cheap production processing. The theoretical energy conversion efficiency of Cu<sub>2</sub>O-based solar cells is about 20%. [1] Many groups have developed Cu<sub>2</sub>O-based solar cells. Recently, Minami *et al* [2] fabricated Ga<sub>2</sub>O<sub>3</sub>/Cu<sub>2</sub>O hetero-junction solar cell and got the highest efficiency of 5.38%. There is still much scope to further improve the energy conversion efficiency.

The single-crystal Cu<sub>2</sub>O nanowire array with large scale can be prepared by thermal oxidation at low cost with simple equipment. We prepared the p-type Cu<sub>2</sub>O nanowire array by thermal oxidation method on glass substrate with Al-doped ZnO transparent electrode, as shown in Fig. 1. The n-type ZnO nanocrystals were prepared according to the method of Guo *et al*. [3] The p-type Cu<sub>2</sub>O nanowire array was filled with n-type ZnO nanocrystals to form the p-n junction. Finally, the Au electrode was deposited by electron-beam evaporation to fabricate the nanostructured Cu<sub>2</sub>O/ZnO solar cells, and the performance of the solar

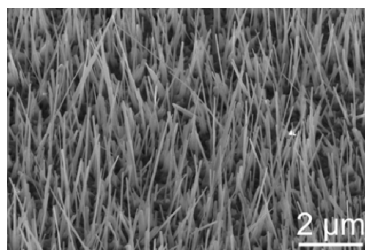


Fig. 1 Cu<sub>2</sub>O nanowire array prepared by thermal oxidation.

cells was obtained employing a solar simulator. In this study, we developed a novel process to prepare Cu<sub>2</sub>O-based solar cells at low cost, which has a potential application in photovoltaic power generation.

**Keywords:** *Cu<sub>2</sub>O nanowire, thermal oxidation, solar cell, ZnO nanocrystal*

[1] RAI, B. P. 1988. Cu<sub>2</sub>O solar cells: A review. *Solar Cells*, 25, 265-272.

[2] MINAMI, T., MIYATA, T., NISHI, Y. 2014. Efficiency improvement of Cu<sub>2</sub>O-based heterojunction solar cells fabricated using thermally oxidized copper sheets. *Thin Solid Films*, 559, 105-111.

[3] GUO, D., SATO, K., HIBINO, S., TAKEUCHI, T., BESSHO, H., KATO, K. 2014. Transparent conductive Al-doped ZnO thin films prepared by a novel sol-gel method. *Journal of Materials Science*, 49, 4722-4734.

## One-dimensional Electron Confinement in Sub-5-nm Graphene Nanowrinkles

Hyunseob Lim<sup>1,2,3</sup>, Rodney S. Ruoff<sup>2,3</sup> Yousoo Kim<sup>1,\*</sup>

<sup>1</sup>Surface and Interface Science Laboratory, RIKEN, 2-1 Hirosawa, Wako, Saitama 351-0198 Japan. <sup>2</sup>Center for Multidimensional Carbon Materials, Institute of Basic Science, UNIST-gil 50, Ulsan 689-798, Korea. <sup>3</sup>Department of Energy Engineering, Department of Chemistry, Ulsan National Institute of Science and Technology (UNIST), UNIST-gil 50, Ulsan 689-798, Republic of Korea.

*Presenting author's e-mail: hslim@ibs.re.kr*

*Corresponding author's e-mail: ykim@riken.jp*

Graphene-based carbon materials such as fullerenes, carbon nanotubes, and graphenes have distinct and unique electronic properties that depend on their dimensionality and geometric structures. Graphene wrinkles with pseudo one-dimensional (1D) structures have been observed in a graphene sheet. However, their 1D electronic properties have never been observed because of their large widths. Here, we present the unique electronic structure of graphene nanowrinkles (GNW) in a graphene sheet grown on Ni(111), the width of which was small enough (less than 5 nm) to cause 1D electron confinement. Use of spatially resolved, scanning tunneling spectroscopy revealed band-gap opening and a 1D van Hove singularity in the GNW, as well as the chemical potential distribution across the GNW. Our demonstration of 1D electron confinement in a graphene creates the novel possibility of controlling its electronic properties not by chemical modification but by “mechanical structuring in a controlled manner”.

**Keywords:** *Graphene, wrinkle, scanning tunneling microscopy, van Hove singularity*

## **Nanophotonics with Nanocarbon Materials: From Bio-sensing to Remote Heat Removal (keynote)**

Slava V. Rotkin

Department of Physics & Center for Advanced Materials and Nanotechnology,  
Lehigh University, 16 Memorial Dr. E., Bethlehem, PA 18015, USA.  
*E Mail : rotkin@lehigh.edu*

Among new materials that have been (re)discovered during last decade, nanocarbons (graphene and nanotubes) stand out for their mechanical, electronic, optical and thermal properties. This talk will cover several featured examples, focusing on the new physics behind fascinating materials properties.

One of the key signatures of the layered materials is their strong anisotropy. For example, in-plane thermal conductivity of nanocarbons approaches or even exceeds those of the best thermal conductors, like diamond. Even though, implementing them for energy management is inhibited by inefficient coupling to the substrate. Such a coupling which is due to the interface (cross-plane) thermal conductance, aka Kapitza conductance, is orders of magnitude lower and often presents a thermal bottleneck.

Last decade our understanding of the nanoscale heat transport has been substantially extended beyond basic thermal physics [1]. Recently the theory of a novel near-field radiation mechanism received significant attention [2]. Using methods established in Quantum Electrodynamics (QED), one can approach understanding of heat radiation and/or remote energy dissipation across nanoscale gap between thermal materials. This heat tunneling process often constitutes main mechanism of the heat exchange between graphene [3a] or nanotube [3b] film and a substrate. Physics of the effect will be outlined to explain major experimental observations, including remote Joule heating [4ab], and to make predictions for engineering of thermal interconnect materials.

Infrared plasmonics of nanocarbon materials explains most of the QED heat transport effects, while the optical properties in visible range are associated with their unique electronic structure: Dirac spectrum, following from the honeycomb lattice symmetry.

Universal optical conductivity of graphene materials has a potential for controlling the surface reflectivity by chemical or electrostatic doping of an atomically thin coating layer. For bio-sensing applications non-metallic nanotube materials are most attractive,

presenting a class of near-infrared optical dyes in their pristine form and demonstrating visible range photo-physics in complexes with other materials, like DNA and rare earths. The talk will touch upon the physics of solvation [5a] and functionalization of nanotube materials [5b] which is a dynamically developing field, rich for applications.

**Keywords:** *nanocarbon materials, near-field Kapitza conductance, remote Joule heat, nanotube bio-sensing, rare-earth-DNA-nanotube complexes*

[1] D.G. CAHILL, W.K. FORD, K.E. GOODSON, G.D. MAHAN, ET.AL 2003. Nanoscale thermal transport. Journal of Applied Physics 93, 793-818. D.G. CAHILL, P.V. BRAUN, G. CHEN, D.R. CLARKE, ET.AL 2014. Nanoscale thermal transport. II. 2003–2012. Applied Physics Reviews 1, 011305.

[2] A.I. VOLOKITIN, AND B.N.J. PERSSON 2007. Near-field radiative heat transfer and noncontact friction. Reviews of Modern Physics 79, 1291-1329.

[3] (a) V.B. SVETOVOY, P.J. VAN ZWOL, AND J. CHEVRIER 2012. Plasmon enhanced near-field radiative heat transfer for graphene covered dielectrics. Physical Review B 85, 155418. (b) A.M. NEMILENTSAU, AND S.V. ROTKIN 2012. Vertical Single-Wall Carbon Nanotube Forests as Plasmonic Heat Pipes. ACS Nano 6, 4298.

[4] (a) K.H. BALOCH, N. VOSKANIAN, M. BRONGEEST, AND J. CUMINGS 2012. Remote Joule heating by a carbon nanotube. Nat Nano 7, 316-319. (b) Z.-Y. ONG, AND M.V. FISCHETTI 2013. Theory of remote phonon scattering in top-gated single-layer graphene. Physical Review B 88, 045405.

[5] (a) T. IGNATOVA, H. NAJAFOV, A. RYASNYANSKIY, I. BIAGGIO, ET.AL 2011. Significant FRET Between SWNT/DNA and Rare Earth Ions: A Signature of Their Spatial Correlations, ACS Nano, 5, 6052-6059. (b) SV. ROTKIN 2010. Electronic Properties of Nonideal Nanotube Materials: Helical Symmetry Breaking in DNA Hybrids, Ann Rev of Phys Chemistry Vol. 61, pp. 241-261.

Work is partially supported by AFOSR (FA9550-11-1-0185) and NSF (ECCS-1202398).



## Low Dimensional Single Crystalline $\text{In}_{2-x}\text{Ga}_x\text{O}_3(\text{ZnO})_n$ Nanostructures with Tunable Compositional and Optical Properties

Yujie (Guo)<sup>1</sup>, Yang (Song)<sup>1</sup>, Jean-Pierre (Locquet)<sup>2</sup>, Jin Won (Seo)<sup>1</sup>

<sup>1</sup>Department of Materials Engineering, KU Leuven, 3001 Leuven, Belgium

<sup>2</sup>Laboratory of Solid State Physics and Magnetism, KU Leuven, 3001 Leuven, Belgium

[yujie.guo@mtm.kuleuven.be](mailto:yujie.guo@mtm.kuleuven.be)

Single crystalline  $\text{In}_{2-x}\text{Ga}_x\text{O}_3(\text{ZnO})_n$  (IGZO) nanostructures hold considerable technological promises for applications owing to their superior properties especially high carrier mobility and high optical transparency<sup>[1]</sup>. However, fabrication of single crystalline IGZO is highly demanding because of the complex “natural superlattice” structure and high volatility of involved metal components at high temperatures<sup>[2]</sup>. In this study, we propose a non-vacuum route to produce low dimensional single crystalline IGZO nanostructures. Because of their confined dimension, the single crystalline structure can be stabilized at lower temperatures. For the first time, highly periodic crystalline structure and homogenous composition are achieved. The growth process, which involves reactive diffusion between single crystalline ZnO nanostructures and solution-based IGZO precursor, is studied systematically. The resulting chemical composition can be modulated by adjusting the thickness of the IGZO precursor. Optical measurements reveal tunable optical band gap with the variation of IGZO composition, indicating that controllability over the nanostructure composition enables precise modification of the optical performances.

**Keywords:** IGZO, natural superlattice, diffusion, optical band gap

[1] NOMURA, A., OHTA, H., UEDA, K., KAMIYA, T., HIRANO, M., HOSONO. 2003. Thin-Film Transistor Fabricated in Single-crystalline Transparent Oxide Semiconductor. *Science*, 300, 1269-1272.

[2] ANDREWS, S. C., FARDY, A. M., MOORE, M. C., ALONI, S., ZHANG, M., RADMILOVIC, V., YANG, P. 2011. *Chemical Science*, 2, 706-714.

## Piezotronic and 2D Hall effects of individual ZnO microwire

Hakseong Kim<sup>a</sup>, Ho Ang Yoon<sup>a</sup>, Hoyoel Yun<sup>a</sup>, Kirstie McAllister<sup>a</sup> and Sang Wook Lee<sup>a</sup>

<sup>a</sup>School of Physics, Konkuk University, Seoul 143-701, Korea

We studied the electrical and electromechanical properties of individual ZnO microwire. To attach the nanoscale electrodes on the ZnO microwire, a suspended PMMA (Poly methyl methacrylate) ribbon structures were fabricated for making electrical connection between the micro wire and the bottom substrate. The estimated contact resistance by 4-probe measurement for ZnO microwire FETs fabricated by our method was found to be much lower than that of device fabricated by standard E-beam lithography and evaporation. We realized a suspended ZnO microwire based electromechanical device by using this fabrication method and investigated **its** piezoelectric properties. An efficient piezoelectric-induced current was detected when the individual suspended microwires were vibrating at their resonant frequency. Using the PMMA ribbons, the Hall probes were also defined only on the top facet of the hexagonal surfaces. The 2-dimensional charge carrier density and mobility of ZnO microwire were studied from the Hall measurements.

## International Conference on Advances in Functional Materials

**Laser-assisted processing and diagnostics of functional micro/nanomaterials**David J. Hwang<sup>1\*</sup> and Costas P. Grigoropoulos<sup>2</sup><sup>1</sup>Assistant Professor, Department of Mechanical Engineering at State University of New York, Stony Brook NY 11794<sup>2</sup>Professor, Department of Mechanical Engineering, University of California, Berkeley CA 94720

\*Speaker

**ABSTRACT**

Lasers have proven to be efficient tools in a variety of micro/nanoscale materials processing and diagnostics. This talk will be focused on presenting recent progress on producing functionalized micro/nanomaterials for various application fields via multiple laser-assisted processing routes including ablation, crystallization, sintering, activation and chemical vapor deposition. In addition, demonstrated strategies on the scalable processing and the advanced *in-situ* monitoring under electron microscope will be also shown.

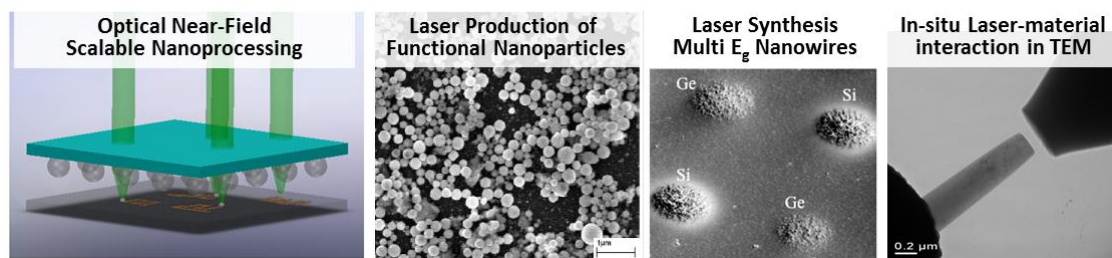


**Figure S1.** Representative examples of laser-assisted processing and diagnostics of functionalized nanomaterials

**Keywords:** Laser-assisted processing and diagnostics, In-situ electron microscope diagnostics of laser-material interactions, Functionalized nanostructures

**Speaker's Bio-sketch: Dr. David J. Hwang**

(Assistant Professor, Department of Mechanical Engineering, Stony Brook University)

David J. Hwang is an assistant professor in Mechanical Engineering department at State University of New York at Stony Brook. He received his BSE and MSE degrees from Seoul National University, Korea (1995 and 1997), and Ph.D. degree in Mechanical Engineering from University of California at Berkeley (2005), followed by postdoctoral researcher (2005-2007) and a research scientist (2008-2010) in University of California at Berkeley. He was a guest scientist in Lawrence Berkeley National Laboratory (2007-2010). He also worked for Samsung (1997-2000), where he was involved in automotive engine control, superconductor related cryogenics and micro-jetting device. His research interests are on the micro- and nanoscale heat transfer, and laser-assisted processing and diagnostics in micro/nanoscale for wide range of applications including display, optoelectronics, energy, materials and bio-engineering. He also has strong expertise in the advanced characterization based on optical near-field, spectroscopy, and in-situ electron microscopy.

## Strain induced energy level engineering in semiconductor nanocrystals

Chinmay Phadnis<sup>1</sup>, Kiran G. Sonawane<sup>1,2</sup>, Shailaja Mahamuni<sup>1</sup>

<sup>1</sup>Department of Physics, SP Pune University, Pune, India

<sup>2</sup> CEES Department, MIT College of Engineering, Kothrud, Pune 411038, India  
[phadnischinmay@gmail.com](mailto:phadnischinmay@gmail.com)/[shailajamahamuni@yahoo.co.in](mailto:shailajamahamuni@yahoo.co.in)

In quest of improving the optoelectronic properties of quantum dots multi-domain nano-heterostructures are being studied. Very often one meets with a challenge of handling lattice strain while designing artificial atoms or heterostructured quantum dots. Lattice constant of CdS is 0.58 nm which is larger than ZnS (0.54 nm) by 7 % in zinc blend phase making it a good example for studying the strain induced effects in semiconductor nanocrystals (NCs). These strain induced NCs are potential candidates for engineering the electron energy levels, besides size and composition. The effects of strain on electron energy levels are studied theoretically in earlier reports. Here, we present experimental evidence to the modifications in the hierarchy of hole energy levels.

CdS NCs were prepared by high temperature wet chemical route. These NCs were coated by higher band-gap ZnS to form core-shell NCs. Growth of four monolayers ZnS on CdS NCs of size 3.8 nm reveals strain of 3.5%. Optical absorption studies indicate red-shift in the first excited state ( $1P_{3/2} \rightarrow 1S_e$ ) by 0.12 eV, while the second excited state ( $1S_{3/2} \rightarrow 1S_e$ ) blue shifts by 0.05 eV. Concomitantly relative oscillator strength of the first excited state increases by 19%, while the same for the second excited state increases by 46%, resulting substantial increase in the intensity of the second excited state. The experimental observations are evaluated on the basis of reported semi-empirical model useful for quantitatively mapping carrier location. Analyses clearly imply lowering of  $1P_{3/2}$  hole level with respect to  $1S_{3/2}$  hole level as a manifestation of induced strain in the lattice. Moreover, intensity rise of the second excited state indicates preferential localization of electron and hole in the core CdS region. These findings are reconfirmed by the electron energy level hierarchy elucidated from low temperature photoluminescence excitation spectroscopy (PLE). Strain induced change in the  $P$  type symmetry of the ground hole state to  $S$  type hole state is also reported based on the empirical tight binding calculations. The present work emphasizes engineering of the energy levels of NCs as a manifestation of interfacial strain in nanoheterostructures. In particular, as anticipated from the calculations, strain induced flipping of ground state hole wavefunction is experimentally demonstrated.

**Keywords:** *Functional materials, II-VI semiconductors, lattice strain, optical properties*

# Synthesis and optimization of electric conductivity and thermal diffusivity of Zinc-Aluminum hydroxide (Zn-Al-NO<sub>3</sub>-LDH) prepared at different pH values

Abdullah Ahmed Ali Ahmed<sup>a,\*</sup>, Zainal Abidin Talib<sup>b,\*\*</sup>, Mohd Zobir Hussein<sup>c</sup>

<sup>a</sup> Department of Physics, Faculty of Applied Science, Thamar University, Dhamar 87246, Yemen,

<sup>b</sup> Department of Physics, Faculty of Science, Universiti Putra Malaysia, 43400 UPM Serdang, Selangor, Malaysia

<sup>c</sup> Advanced Materials and Nanotechnology Laboratory, Institute of Advanced Technology (ITMA), Universiti Putra Malaysia, 43400 UPM Serdang, Selangor, Malaysia

\*Corresponding author. Tel.: +60173372785; fax: +60389454454. E-mail address: [abdullah2803@gmail.com](mailto:abdullah2803@gmail.com) (Abdullah Ahmed)

\*\*Corresponding author. Tel.: +6038946603; fax: +60389454454. E-mail address: [zainalat@science.upm.edu.my](mailto:zainalat@science.upm.edu.my) (Zainal Abidin Talib)

## Abstract

Zn-Al layered double hydroxide (Zn-Al-NO<sub>3</sub>-LDH) was synthesized using the co-precipitation method at Zn<sup>2+</sup>/Al<sup>3+</sup> molar ratio of 4 and at different pH values of 6, 7, 8, 9 and 10. The structural, textural and morphological properties of samples were studied using X-ray diffraction, scanning electron microscopy, nitrogen gas adsorption-desorption technique and Fourier transform infrared spectroscopy (FTIR). The crystallinity of LDH samples increased as pH value increased until pH 9. At pH 10, Zn-Al-NO<sub>3</sub>-LDH and Zn-Al-CO<sub>3</sub>-LDH phases were observed due to the excess addition of NaOH during the preparation of LDH. All prepared LDH samples were mesoporous materials with average pore diameters of between 8 and 25 nm. The thermal stability of LDH samples was studied using thermogravimetric analysis (TGA). The dielectric response of Zn-Al-NO<sub>3</sub>-LDH samples can be described by anomalous low frequency dispersion (ALFD) due to LDHs have two carriers; the first carrier is the proton of the polarized water clusters in the LDH interlayer and the second one is the gallery anions

(NO<sub>3</sub><sup>-</sup>) of LDH interlayer. Thermal diffusivity of samples has been measured as a function in *in situ* temperature at 27, 60, 90, 120, 150, 180 and 210 °C. The optimized electrical conductivity and thermal diffusivity has been found with the synthesized Zn-Al-NO<sub>3</sub>-LDH sample at pH 8.



**ELECTRICAL AND STRUCTURAL PROPERTIES OF OCTAHEDRAL  
LAYERED MANGANESE OXIDES MATERIALS SUBSTITUTED WITH  
COBALT**

M. M. Gómez-Hermida<sup>1,2</sup>, A. Rosales-Rivera<sup>3</sup>, N.P. Arias<sup>4</sup> and O. Giraldo<sup>3</sup>

*1Facultad de Minas, Universidad Nacional de Colombia, Sede Medellín, Medellín,  
Colombia.*

*2 Departamento de Ciencias Básicas, Facultad de Ciencias Básicas e Ingeniería,  
Universidad Católica de Pereira, Colombia*

*3Departamento de Física y Química, Facultad de Ciencias Exactas y Naturales,  
Universidad Nacional de Colombia, Sede Manizales, Manizales, Colombia.*

*4Departamento de Ingeniería Eléctrica, Electrónica y Computación, Facultad de  
Ingeniería y Arquitectura, Universidad Nacional de Colombia, Sede Manizales, Manizales,  
Colombia*

*E-mail: monica.gomez@ucp.edu.co (M. M. Gómez-Hermida)*

**ABSTRACT:**

Layered manganese oxide material has attracted extensive attention of researchers due to its advantages such as structure flexibility, porous structure, mixed valence and specific physicochemical properties in addition to its applications in areas such as catalysts, ion exchange, magnetic storage media and batteries materials. Doping various elements into manganese oxides has been proven to be an effective way to improve their potential for the applications stated above. In this work, Cobalt substituted and no-substituted lamellar manganese oxide materials were studied. Lamellar manganese oxide were synthesized by

oxide-reduction method, the fraction  $x$  of the cobalt was added in the following proportions,  $x = 0, 20\%, 40\%, 60\%, 80\%$  and  $100\%$ , with relation to manganese content in the no-substituted material. The synthesized materials were studied using various techniques, including: Atomic Absorption (AA), electrical impedance spectroscopy (EIS), X ray diffraction (XRD), scanning electron microscopy (SEM), and thermal gravimetric analysis (TGA). The chemical formulas of these synthesized materials were obtained by combining results of thermal gravimetric analysis (TGA) and Atomic Absorption (AA). The XRD pattern shows that the crystal structure of these materials is birnessite type. The SEM and EIS results suggest that the cobalt doping has an effect on the morphologies and the AC response of these materials.

**Keywords:** Birnessite, layered material, electrical properties, impedance spectroscopy.

## Electron Transfer and Coupling in Graphene-WS<sub>2</sub> van der Waals Heterostructures

Jiaqi He<sup>1,2</sup>, Nardeep Kumar<sup>2</sup>, Matt Bellus<sup>2</sup>, Hsin-Ying Chiu<sup>2</sup>, Dawei He<sup>1</sup>,  
Yongsheng Wang<sup>1,\*</sup> & Hui hao<sup>2,\*</sup>

<sup>1</sup>Key Laboratory of Luminescence and Optical Information, Ministry of Education,  
Institute of Optoelectronic Technology,  
Beijing Jiaotong University, Beijing 100044, China

<sup>2</sup>Department of Physics and Astronomy, The University of Kansas,  
Lawrence, Kansas 66045, USA

The newly discovered two-dimensional materials can be used to form atomically thin and sharp van der Waals heterostructures with nearly perfect interface qualities, which can transform the science and technology of semiconductor heterostructures. Owing to the weak van der Waals interlayer coupling, the electronic states of participating materials remain largely unchanged. Hence, emergent properties of these structures rely on two key elements: electron transfer across the interface and interlayer coupling. Here we show, using graphene WS<sub>2</sub> heterostructures as an example, evidences of ultrafast and highly efficient interlayer electron transfer and strong interlayer coupling and control. We find that photocarriers injected in WS<sub>2</sub> transfer to graphene in one picosecond and with near-unity efficiency. We also demonstrate that optical properties of WS<sub>2</sub> can be effectively tuned by carriers in graphene. These findings illustrate basic processes required for using van der Waals heterostructures in electronics and photonics.

## Tuning Sulfur Doping in Graphene for Highly Sensitive Dopamine Biosensors

Mingjie Li<sup>1,2,3</sup>, Chenming Liu<sup>\*1,3</sup>, Hongbin Cao<sup>1,3</sup>, Yi Zhang<sup>1,2,3</sup>

<sup>1</sup> Key Laboratory of Green Process and Engineering, Institute of Process Engineering, Chinese Academy of Sciences, Beijing 100190, PR China

<sup>2</sup> School of Chemical Engineering & Technology, Tianjin University, Tianjin 300072, PR China

<sup>3</sup> Beijing Engineering Research Center of Process Pollution Control, Beijing 100190, PR China

*\*E-mail address for corresponding author: chmliu@ipe.ac.cn (Chenming Liu)*

*E-mail address for presenting author: limingjie19870210@163.com (Mingjie Li)*

S-doped graphene has attracted extensive interest in recent years due to its high catalytic activity. However, most previous reports on S-doped graphene materials present diverse types of S-bonding configurations, it is hard to distinguish which configuration is largely responsible for catalytic activity from many kinds of sulfur species. Herein, homogeneous thiophene S-doped graphene can be synthesized through heating the mixture of graphene oxide and magnesium sulfate, and the doping amount can be easily tuned by the dosage of magnesium sulfate. More importantly, abundant micropores and some in-plane pores are formed in the surface of graphene sheets during S-doping, which are useful for the mass transfer. Due to its high S-loading mass, thiophene S-containing species and porous structure, S-doped graphene shows high electrocatalytic activity toward the redox reaction of dopamine, such as high selectivity, high sensitivity and low detection limit ( $3.94 \mu\text{M} \mu\text{A}^{-1}$ ,  $0.15 \times 10^{-7} \text{ M}$  at S/N=3). Therefore, this work is anticipated to open a new possibility for the further investigation of S-doped graphene with specific S-containing species and could have potential applications in electroanalysis and electrocatalysis.

**Keywords:** Sulfur-doped graphene, electrocatalysis, biosensors

## SERS study of plasmon induced functionality of aryl azo heterocycles

Uttam K Sarkar<sup>1</sup>

<sup>1</sup> Department of Physics, Malda College, Malda-732101, WB, India

E Mail : [chairman\\_uks@yahoo.com](mailto:chairman_uks@yahoo.com), [dr.uttamkumar@maldacollege.ac.in](mailto:dr.uttamkumar@maldacollege.ac.in)

Metal nanoparticles, much smaller than the wavelength of light, have been significant for the massive signal enhancement achieved in surface-enhanced Raman spectroscopy (SERS)<sup>1</sup> —a technique that can now detect a single molecule<sup>2</sup>.

Azobenzene (AB) and its derivatives are active components in various applications, such as liquid crystals, optical switching, memory storage, and photofunctional ionic liquids. Recently, it has been recognized that the photoinduced isomerisation of AB can regulate biological processes that have important implications in pharmacology, nanotechnology, and cell biology.<sup>3</sup>

One of the phenyl rings in AB being replaced by heterocyclic imidazole ring, the phenylazo-imidazole is obtained which constitute an interesting class of heterocyclic azo compounds as a potential switching group in biological applications and in coordination chemistry. These molecules with N-heteroatom have azoimine –N==N– functional group which has interesting properties including electrochemical behaviour, stabilization of low valent metal redox state due to its  $\pi$ -acidity and the presence of low lying azo centred  $\pi$  molecular orbitals, formation of azo-metal complexes, and activation of the C–H function of the pendant aryl group in metal co-ordinate state. Because of the imidazole group and the azo group metal complexes of these molecules are formed which act as a molecular switch. The trivalent imidazole nitrogen offers a site for functionalization of the compound and consequently imidazole is a ubiquitous and essential group in biology especially as a metal coordination site. Interaction of these molecules with the nano structured metal surface has, thus been important to study. SERS study of silver nano particle induced dark isomerisation in aryl azo imidazoles<sup>4</sup> and their plasmon induced and pH controlled semiconductive conformation<sup>5</sup>, manifested as “first layer effect”<sup>6-8</sup> have further substantiated the possibility of using these AAHs as significant functional materials.

**Keywords:** SERS, plasmon, aryl azo heterocycles, first layer effect

1. M. Moskovits, *Rev. Mod. Phys.* 1985, **57**, 783
2. E.C.L. Ru and P.G. Etchegoin, *Annu. Rev. Phys. Chem.* 2012, **63** 65.
3. J.A. Mondal, G. Saha, C. Sinha and D.K. Palit, *Phys. Chem. Chem. Phys.*, 2012, **14**, 13027.
4. W. Hossain, M. Ghosh, C. Sinha, D.K. Debnath, U.K. Sarkar, *Chem. Phys. Lett.*, 2013, **586**, 132.
5. U.K. Sarkar, D.K. Debnath, W. Hossain, *Journal of Molecular Structure* 1061 (2014) 104–109]
6. U.K. Sarkar, *Chem. Phys. Lett.* 2003, **374**, 341.
7. U.K. Sarkar, A.J. Pal, S. Chakrabarti, T.N. Misra, *Chem. Phys. Lett.* 1992, **190**, 59.
8. U.K. Sarkar, S. Chakrabarti, T.N. Misra, A.J. Pal, *Chem. Phys. Lett.* 1992, **200**, 55.
9. U.K. Sarkar, *J. Mol. Struct.* 2013, **1045**, 42.

# Symposia SP1

# INDEX PAGE

1.	Enhanced Gas-Sensing Performance of Hierarchical Metal Oxide Nanocomposites with Ultrahigh Surface Areas	1
	<b>AUTHOR:</b> Prof. Deliang Chen	
2.	Advanced One Dimensional Metal Oxides For Chemical Sensors	3
	<b>AUTHOR:</b> Prof. Giorgio Sberveglieri	
3.	Sweat For The Discrimination Of Humanâ€™S Habit Using Nws Gas Sensors Technology	5
	<b>AUTHOR:</b> Dr. Veronica Sberveglieri	
4.	Hierachical Nanostructures as gas sensors for volatile organic compounds	7
	<b>AUTHOR:</b> Prof. Jinhua Zhan	
5.	Synthesis and Gas-Sensing Performance of Column-shaped Zinc Oxide with Doped-Graphene	8
	<b>AUTHOR:</b> Prof. Jianping Du	
6.	Enhanced Btex Gas-Sensing Performance Of Copper Modified Sno2	10
	<b>AUTHOR:</b> Prof. Jiaqiang Xu	
7.	Metal Oxide Nanowires Chemical Sensor System For Microbial Contamination Screening Of Industrial Food Production	11
	<b>AUTHOR:</b> Dr. Matteo Falasconi	
8.	Synthesis and Charcterization of CuO doped ZrO2 Hollow Sphere for Gas Sensing Application	12
	<b>AUTHOR:</b> Mr. Sudhakar Deshmukh	
9.	Synthesis, Characterization and Acetone Sensing Performance of Nanostructured Cd doped ZrO2 Thin Films	13
	<b>AUTHOR:</b> Dr. Ramesh Bari	
10.	Dimethyl Methyl Phosphonate detection using Pt-modified nanostructured ZnO thick films	14
	<b>AUTHOR:</b> Dr. Anil Bari	

## Enhanced Gas-Sensing Performance of Hierarchical Metal Oxide Nanocomposites with Ultrahigh Surface Areas

Deliang Chen, Li Yin, Lianfang Ge, Rui Zhang

School of Materials Science and Engineering, Zhengzhou University, 100 Science Road,  
Zhengzhou 450001, P.R. China.

*E-Mail* : dlchen@zzu.edu.cn (D.L. Chen, Prof. Dr.)

Small particle sizes and high specific surface areas are the key to achieve high-performance chemical sensors based on metal oxide semiconductors. But nanoparticles with smaller sizes usually suffer from more serious aggregation. We therefore have to design some special nanostructures to overcome the aggregating problem. In this presentation, we will introduce some novel hierarchical nanostructures that constructed by assembling zero-dimensional nanoparticles (0D-NPs: Fe<sub>2</sub>O<sub>3</sub>, SnO<sub>2</sub>, Ag, Au) on two-dimensional nanosheets (2D-NSs: WO<sub>3</sub>, GO). Such hierarchical 0D-NPs/2D-NSs nanostructures can not only overcome the aggeration of 0D-NPs, but also enhance the specific surface areas by pillaring the 2D-NS using 0D-NPs. We synthesize 2D WO<sub>3</sub> and graphene oxide (GO) nanosheets, which are then used as the backbones to in-situ grow 0D-NPs under special conditions (e.g., microwave irradiation, photoreduction, etc). Typically, the as-obtained nanocomposites of Fe<sub>2</sub>O<sub>3</sub>/WO<sub>3</sub> and SnO<sub>2</sub>/rGO have ultrahigh specific surface areas (BET) of ~1200 m<sup>2</sup>/g and ~2100 m<sup>2</sup>/g, respectively, determined by N<sub>2</sub> adsorption-desorption measurement. The enhancement in surface areas highly improves the H<sub>2</sub>S-sensing performance. In addition, the assembly of metal NPs highly enhances the NO<sub>x</sub>-sensing performance at low temperature.

***Keywords:*** Gas sensors, tungsten oxide nanoplates, hierarchical nanocomposites, microwave-assisted synthesis and characterization

[1] YIN, L., CHEN, D., et al.. 2014. Hierarchical Fe<sub>2</sub>O<sub>3</sub>@WO<sub>3</sub> Nanostructures with Ultrahigh Specific Surface Areas: Microwave-Assisted Synthesis and Enhanced H<sub>2</sub>S-Sensing Performance. RSC advances, in press.



[2] YIN, L., CHEN, D., et al.. 2014. Normal-Pressure Microwave Rapid Synthesis of Hierarchical SnO<sub>2</sub>@rGO Nanostructures with Superhigh Surface Areas as High-Quality Gas-Sensing and Electrochemical Active Materials. *Nanoscale*, **6**, 13690-13700.

[3] YIN, L., CHEN, D., et al.. 2014. Microwave-Assisted Growth of In<sub>2</sub>O<sub>3</sub> Nanoparticles on WO<sub>3</sub> Nanoplates to Improve H<sub>2</sub>S-Sensing Performance. *Journal of Materials Chemistry A*, **2**, 18867-18874.

[4] CHEN, D., GE, L., et al.. 2014. Solvent-Regulated Solvothermal Synthesis and Morphology-Dependent Gas-Sensing Performance of Low-Dimensional Tungsten Oxide Nanocrystals. *Sensors & Actuators: B. Chemical*, **205**, 391-400.

[5] YIN, L., CHEN, D., et al.. 2014, In Situ Formation of Au/SnO<sub>2</sub> Nanocrystals on WO<sub>3</sub> Nanoplates as Excellent Gas-Sensing Materials for H<sub>2</sub>S Detection. *Materials Chemistry and Physics*, **148**, 1099-1107.

[6] CHEN, D., YIN, L., et al.. 2013. Low-Temperature and Highly Selective NO-Sensing Performance of WO<sub>3</sub> Nanoplates Decorated with Silver Nanoparticles. *Sensors & Actuators: B. Chemical*, **185**, 445-455.

**Preferred Mode of presentation : Oral**

**Topic : Special Session (Nano MOX sensors for detecting very low concentration of volatile compounds for diverse advanced applications)**

## Advanced One Dimensional Metal Oxides for Chemical Sensors

E. Comini, A. Bertuna, D. Zappa, M. Donarelli, A. Ponzoni, V. Sberveglieri and G. Sberveglieri

<sup>1</sup> SENSOR Lab, Department of Information Engineering , University of Brescia & CNR-INO, Via Valotti 9, Brescia, Italy

*giorgio.sberveglieri@unibs.it*

After the first method proposed for the preparation of metal oxide in forms of nanobelts, plenty of literature was devoted to different experimental techniques that may lead to the formation of these quasi one-dimensional structures. At the beginning, the research was focusing on the vapour phase methods that were producing, with cheap instrumentation, high quality nanostructures in terms of crystallinity and stoichiometry. We have thoroughly studied the synthesis using evaporation and condensation from powder in controlled environment using different experimental set up. Metal oxide nanowires were integrated in functional devices for chemical sensing and then tested towards a wide range of chemicals, including odorous molecules such as ammonia and hydrogen sulphide.

The ability to prepare metal oxide in form of single crystalline nanowire has pushed further the research on this topic especially for the integration in functional devices such as chemical and gas sensors. There is still a lot of work going on regarding the preparation of oxides, like controlling their morphology and position at the nanoscale level. A big issue concerning the development of sensors is their reliable integration on the specific transducers, assuring stable electrical contacts over long-term operation. The ability to prepare stable single crystal quasi one-dimensional metal oxide nanostructures is having an impact on different aspects of science and technology. In particular, their integration in gas sensing devices lead to a significant improvement in stability providing stable and reliable electrical contacts. Furthermore, the possible miniaturization of these devices may produce a strong decrease in power consumption, the use of self heating devices allow the sensing even without the presence of a heater on the transducers.

Combining experimental and simulations techniques in a multidisciplinary and complementary approach, will result in a maximization of the understanding and therefore in the preparation of reliable chemical sensing devices for diverse applications like food safety, security and environment monitoring

### **ACKNOWLEDGEMENTS**

The work has been partially supported by the Italian MIUR through the FIRB Project RBAP115AYN “Oxides at the nanoscale: multifunctionality and applications” and by the European Community’s 7th Framework Programme, either under the grant agreement n° 611887 “MSP: Multi Sensor Platform for Smart Building Management” or the grant agreement n° 313110 “SNOOPY: Sniffer for concealed people discovery”.

***Keywords: Metal oxide, nanowires, chemical sensors***

## Sweat for the discrimination of human's habit using NWs Gas Sensors technology

Veronica Sberveglieri<sup>1,2</sup>, Estefania Nunez Carmona<sup>1</sup>, Dario Zappa<sup>2,3</sup>, Elisabetta Comini<sup>3,2</sup>, Andrea Pulvirenti<sup>1,2</sup>, Andrea Ponzoni<sup>2,3</sup>

Presenting author should be underline

<sup>1</sup>University of Modena and Reggio Emilia, Dep. of Life Sciences, 42124 Reggio Emilia, Italy.

<sup>2</sup>CNR-INO Sensor Lab, Brescia, Italy.

<sup>3</sup>University of Brescia, Dep. of Information Engineering, Brescia, Italy.

[Veronica.sberveglieri@unimore.it](mailto:Veronica.sberveglieri@unimore.it) / Via Kennedy 17, 42124 Reggio Emilia, Italy

The main primordial form of our distal senses is Human olfaction, providing information and knowledge of different chemicals from remote sources in real time [1]. Humans emit a complex array of non-volatile and volatile molecules, depending on their genetics, diet, stress, and immune status. Numerous volatile compounds may be emitted from several areas of the body that are prone to odor production [2]. Used to evaluate food and environmental toxins as well as recognize kin and potential predators. Many body odors evolved to be olfactory messengers, which convey information between individuals.

In this study we have applied an electronic nose (EN) based on metal oxide chemiresistors to distinguish the humans odor and to correlate humans habitude to their sweat odors. In particular the proposed EN is based on a mixed array, composed by sensors prepared by both nanoparticles (NPs) and nanowire (NWs) technologies, exploiting the different response spectra of NPs and NWs [3].

The EN was used in parallel with classical microbiological and chemical techniques, like GC-MS with SPME [4].

Microbiological technique like Petri dish was used for isolating and growing the humans' microbiota useful for the training of nanowire gas sensors able to reproduce, during the training step, an "artificial" sweat odor. Extended literatures of publications demonstrate the advantage of GC-MS with SPME technique for the identification of volatile compounds classes.

The results obtained with a cooperation of different technique strongly suggest the use of metal oxide nanostructures to develop gas sensing devices for the humans detection, like pathology, wrong habitude in a clinical test or the early detection of volatile biomarkers of internal disease (like diabetes, lung cancer, asthma, etc).

**Keywords:** *Nanowire Gas Sensors, GC-MS, Sweat, Microbiota, electronic nose.*

#### ACKNOWLEDGEMENTS

The work has been partially supported by the 7FP European Project “SNOOPY: Sniffer for concealed people discovery” grant agreement n° 313110.

[1] WHITTLE, C.L., FAKHARZADEH, S., EADES, J., PRETI, G., 2007. Human breath odors and their use in diagnosis. *Annals of the New York Accademy Sciences*, 1098, 252-266.

[2] MEBAZAA, R., REGA, B., CAMEL, V., 2011. Analysis of human male armpit sweat after fenugreek ingestion: Characterisation of odour active compounds by gas chromatography coupled to mass spectrometry and olfactometry. *Food Chem*, 128, 227-235.

[3] SBERVEGLIERI, V., NUNEZ CARMONA, E., COMINI, E., PONZONI, A., ZAPPA, D., PIRROTTA, O., PULVIRENTI, A., 2014. A Novel Electronic Nose as Adaptable Device to Judge Microbiological Quality and Safety in Foodstuff. *BioMed research international*, 2014,1-6.

[4] NUNEZ CARMONA, E., SBERVEGLIERI, V., PULVIRENTI, A., 2012. Detection of microorganisms in water and different food matrix by Electronic Nose, *Proceedings of the 2013 Seventh International Conference on Sensing Technology*, 2013, 703-707.

## Hierarchical Nanostructures as gas sensors for volatile organic compounds

Zhihong Jing, Yingju Fan, Zhipeng Li, Jinhua Zhan

Department of Chemistry, Shandong University

[jhzhan@sdu.edu.cn](mailto:jhzhan@sdu.edu.cn); 86-0531-88365017

Explosive or toxic volatile organic compounds (VOCs) are well known to be dangerous for environmental and public safety, as well as human health. It has been attracting the intensive research interest to explore the applications of nanostructured semiconductor metal oxides in detecting VOCs. The surface areas of sensor materials is a crucial parameter affecting their sensitivity and response time for the gas-sensing reaction occurs at the surface of metal oxides. Hierarchical nanomaterials can significantly facilitate the gas diffusion and mass transportation in sensor materials, and then remarkably enhance the gas-sensing performance, which are usually believed as the excellent candidate due to their high surface areas and ordered nanoarchitectures,

In our group, various hierarchical nanostructures including porous ZnO nanoplates, porous SnO<sub>2</sub> hollow nanospheres and hierarchical In<sub>2</sub>O<sub>3</sub> microstructures have been prepared. These nanostructures exhibited excellent gas sensing performance for VOCs detection. The results demonstrated that the morphologies and structures have the obvious influences in the gas sensing properties. The porous ZnO nanoplates sensor exhibits high response to chlorobenzene at relatively low temperature, and also strong response to ethanol at relatively high temperature, implying their multifunctional properties and selectivity. Porous SnO<sub>2</sub> hollow nanospheres have been prepared via a template-free solvothermal route. The porous SnO<sub>2</sub> nanospheres possess a high BET surface area of 76.4 m<sup>2</sup>/g and mesoporous structures of 32.8 nm, showing excellent gas sensing performance toward 2-chloroethanol and formaldehyde vapour with The lowest detection limit of down to 0.5 ppm. Hierarchical In<sub>2</sub>O<sub>3</sub> microstructures also have been fabricated by the cationic-surfactant-assisted solvothermal process and Pluronic F127-assisted micelle-template methods, which display high response to VOCs. Recently, we further develop these gas sensors for detection of diseases.

**Keywords:** *gas sensors, nanostructures, porous, volatile organic compounds*

- [1] Jing, Z. H., Zhan, J. H. 2008, *Adv. Mater.* 20, 4547.
- [2] Li, Z. P., Zhao, Q. Q., Fan, W. L., Zhan, J. H. 2011, *Nanoscale* 3, 1646-1652
- [3] Fan, Y. J., Li, Z. P., Zhan, J. H. 2009, *Nanotechnology*, 20, 285501.
- [4] Li, Z. P., Fan, Y. J., Zhan, J. H. 2011, *J. Colloid. Inter. Sci.* 354, 89.
- [5] Zhang, Z. L., Zhang, J. Y., Fan, W. L.; Zhan, J. H. 2014, submitted.

## Synthesis and Gas-Sensing Performance of Column-shaped Zinc Oxide with Doped-Graphene

Jianping Du<sup>1</sup>, Huanli Yao<sup>1</sup>, Siyuan He<sup>1</sup>, Ruihua Zhao<sup>2</sup>, Jinping Li<sup>1</sup>

<sup>1</sup> Taiyuan University of Technology, Shanxi China

<sup>2</sup> Shanxi Kunming Tobacco Limited Liability Company, Taiyuan, Taiyuan China.

*E-mail: dujp518@163.com; jpli211@hotmail.com*

Toxic volatile substances have caused serious environment pollution. Especially, volatile organic compounds (VOCs), including aldehydes [1], acetone [2] and amines [3-4] are harmful to human health. So it is necessary to detect VOCs gases with low concentration effectively. Metal oxide semiconductors are ideal candidate used as gas-sensing materials. Graphene decorated metal oxide such as ZnO can enhance the gas-sensing properties [5]. However, graphene-doped metal oxides used for detection of VOCs are still lack of wide research. Therefore, it is significant to synthesize novel sensing materials for detecting toxic volatile gases. In addition, the study on detecting toxic glycol gas has not been addressed. Here, graphene-doped zinc oxide with column-like morphology was synthesized and graphene oxide was reduced in-situ by hydrothermal method. The gas-sensing properties were also studied. The results indicate that zinc oxide with doping graphene exhibits high selectivity of glycol upon exposure to various volatile gases, and it has an enhanced response to glycol with different concentrations at 160 °C. The response and recovery times for 5 ppm glycol are 1s and 14s respectively, implying the unique-shape zinc oxide with graphene doping was effective to detect low-concentration VOCs.

**Keywords:** *zinc oxide, morphology, graphene doping, synthesis, gas sensing*

[1] BACHMATIUK, A., MENDES, R. G., HIRSCH, C., JÄHNE, C., LOHE, M. R., GROTHE, J., KASKEL, S., FU, L., KLINGELER, R., ECKERT, J., WICK, P. & RÜMMELI, M. H. 2013. Few-Layer Graphene Shells and Nonmagnetic Encapsulates: A Versatile and Nontoxic Carbon Nanomaterial. *ACS Nano*, 7, 10552-10562.

- [1] GIBERTIA, A., CAROTTA, M. C., FABBRI, B., GHERARDI, S., GUIDI, V., MALAGU, C. 2013. High-Sensitivity Detection of Acetaldehyde. *Sens. Actuators B Chem.*, 174, 402-405
- [2] LI, X. B., MA, S. Y., LI, F. M., CHEN Y., ZHANG, Q. Q., YANG, X. H., WANG, C. Y., ZHU, J. 2013. Porous Spheres-Like ZnO Nanostructure as Sensitive Gas Sensors for Acetone Detection. *Mater Lett.*, 100, 119-123.
- [3] DU, J. P., WANG, H. Y., ZHAO, R. H., XIE, Y. J., YAO, H. L. 2013. Surfactant-Assisted Synthesis of the Pencil-Like Zinc Oxide and its Sensing Properties. *Mater. Lett.*, 107, 259-261.
- [4] XIE, Y. J., DU, J. P., ZHAO, R. H., WANG, H. Y., YAO, H. L. 2013. Facile Synthesis of Hexagonal Brick-Shaped SnO<sub>2</sub> and its Gas Sensing Toward Triethylamine. *J. Environ. Chem. Eng.*, 1, 1380-
- [5] YI, J., LEE, J. M., PARK, W. II. 2011. Vertically Aligned ZnO Nanorods and Graphene Hybrid Architectures for High-Sensitive Flexible Gas Sensors *Sens. Actuators B Chem.*, 155, 264-269.



## Enhanced BTEX gas-sensing performance of Copper modified SnO<sub>2</sub>

Liping Gao, Yang Chen, Yuan Zhang, and Jiaqiang Xu

NEST Lab, Department of Chemistry, Shanghai University, Shanghai, 200444, China.

Crossponding author : E-mail:[xujiaqiang@shu.edu.cn](mailto:xujiaqiang@shu.edu.cn); Tel: +86 21 66132701

**Abstract:** Copper-modified SnO<sub>2</sub> were fabricated by a one-pot microwave synthesis by using glycol, SnC<sub>2</sub>O<sub>4</sub> and Cu (NO<sub>3</sub>)<sub>2</sub>·6H<sub>2</sub>O as raw materials, followed by a calcination treatment. The microwaves synthesis is a fast, simple, and efficient method. The synthesized 3% CuO modified SnO<sub>2</sub> revealed good gas sensitive to 50 ppm benzene at 250 °C. Modified different CuO showed different response to 50 ppm BTEX. At the same time, it can be seen that 3% CuO modified SnO<sub>2</sub> sensor can obtained better property to BTEX, and displays good response to 2-200 ppm BTEX and good selectivity to VOCs than pure SnO<sub>2</sub>. The results suggest the gas sensor a good candidate for the detection of BTEX.

**Keywords:** Copper -modified, SnO<sub>2</sub> , Gas sensor, BTEX

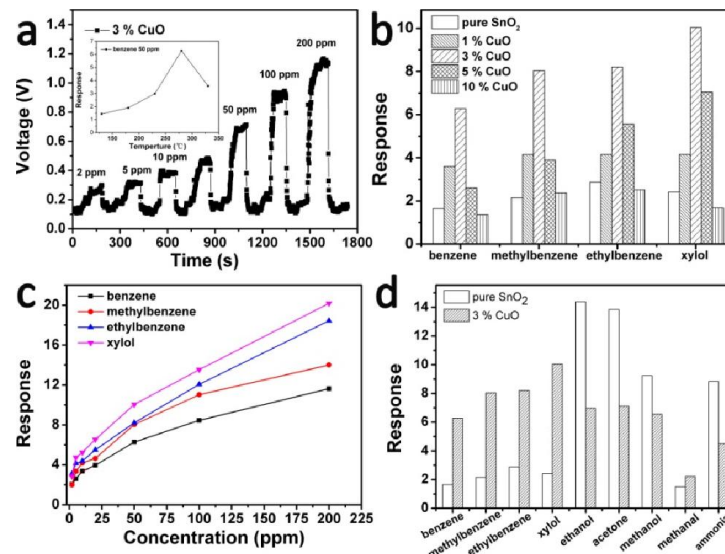


Fig.1 ((a) Responses of copper-modified SnO<sub>2</sub> sensors to 2-200 ppm benzene vapor, (Inset is the response of the sensor to 50 ppm benzene vapor at different test temperature), (b) Response of different copper modification proportion of SnO<sub>2</sub> and pure SnO<sub>2</sub> to BTEX of 50 ppm, (c) 3% CuO modified SnO<sub>2</sub> to 2-200 ppm BTEX, (d) Response value of 3% CuO modified SnO<sub>2</sub> and pure SnO<sub>2</sub> to VOCs of 50 ppm.

## Metal Oxide Nanowires Chemical Sensor System for Microbial Contamination Screening of Industrial Food Production

Giulia Zambotti<sup>1,2</sup>, Veronica Sberveglieri<sup>2,3</sup>, Matteo Falasconi<sup>1,2</sup>

<sup>1</sup> University of Brescia, Dept. of Information Engineering, Via Branze 38, Brescia, Italy

<sup>2</sup> CNR-INO Istituto Nazionale di Ottica, Largo Enrico Fermi, 6, 50125 Firenze, Italy

<sup>3</sup> University of Modena and Reggio Emilia, Dept. of Life Sciences, Via Amendola 2, Padiglione Besta 42122 Reggio Emilia, Italy

*matteo.falasconi@unibs.it; phone : +39 030 3715876*

Modern food industry demands more effective, faster and affordable technologies to perform on-line controls of food processing operations for microbial contamination screening. Currently, quality controls are performed through post-production quarantine tests or by conventional laboratory techniques. Sensitive, rapid and reliable chemical sensor systems (Artificial Olfactory Systems) could be promising to fill the existing gap by exploiting the link between the food contamination and the patterns of emitted volatile compounds [1]. In this work, for the first time, an AOS was used to perform a rapid screening of industrially produced tomato paste and vegetable soups contaminated by yeasts and bacteria. The superior sensitivity and stability of MOX-NW sensors were exploited. The AOS procedure is simple and automated; the instrument, once trained, can recognize contaminated food samples without the human operator support. The AOS provided excellent classification performance: about 98% of contaminated samples were correctly recognized. The implemented approach allowed for a time saving of up to 90% compared to conventional methods and tremendous cost saving for the end-user. The application of AOS on industrial food production represents a breakthrough innovation.

***Keywords: Metal Oxide Nanowires, Chemical sensors, Electronic Nose, Food screening***

[1] M. FALASCONI, I. CONCINA, E. GOBBI, V. SBERVEGLIERI, A. PULVIRENTI, AND G. SBERVEGLIERI. 2012. Electronic Nose for Microbiological Quality Control of Food Products, International Journal of Electrochemistry, Article ID 715763, doi:10.1155/2012/715763.

## Synthesis and Characterization of CuO doped ZrO<sub>2</sub> Hollow Sphere for Gas Sensing Application

Deshmukh S.B.<sup>1</sup>, Bari R.H.<sup>2</sup>

<sup>1</sup>Department of Physics, M. S. G. College, Malegaon, 423105, M.S., India.

<sup>2</sup>Department of Physics, G D.M. Arts, K .R. N. Com. and M.D. Science College, Jamner, 424206, M.S., India.

*E Mail* : [mesudhakar\\_deshmukh@rediffmail.com](mailto:mesudhakar_deshmukh@rediffmail.com) , [rameshbari24@yahoo.com](mailto:rameshbari24@yahoo.com)

CuO doped ZrO<sub>2</sub> hollow sphere were synthesized using spray pyrolysis deposition technique. The films were deposited from mixture of two precursors spraying solution of CuCl<sub>2</sub>.2H<sub>2</sub>O and ZrO<sub>2</sub>.8H<sub>2</sub>O with same concentration (0.05M), in which Cu solution acts as doping solution. It was dissolved in equal volumetric proportion of distilled water (solvent) and mixed surfactant 1N N-dimethylformamide-glycol. In this mixed precursor and doping solution, Cu- volumetric wt% was varied as 3%, 5%, 7%, 9% and sprayed on glass substrates at temperature 350<sup>0</sup>C in air atmosphere with same spray rate. The distance between spray gun nozzle and substrate is optimized. The samples were annealed at temperature 500<sup>0</sup>C for a 1 hour. The analytical techniques XRD, FE-SEM, EDAX were used to characterize and examine the elemental composition, morphology, crystallite size, crystal structure of synthesized films. These films were tested in various gases at different operating temperature ranging from 50-500<sup>0</sup>C. These films showed maximum sensitivity to H<sub>2</sub>S gas .The quick response and fast recovery, hollow and shell structure are the main features of these films. The electrical, optical, structural, morphological and gas sensing properties of the films were studied and discussed.

**Keywords:** *Hollow sphere, spray pyrolysis, H<sub>2</sub>S gas*

## Synthesis, Characterization and Acetone Sensing Performance of Nanostructured Cd doped ZrO<sub>2</sub> Thin Films

Bari R.H.<sup>1</sup>, Deshmukh S.B.<sup>2</sup>, Jain G.H.<sup>3</sup>

<sup>1</sup> Department of Physics, G D.M.Arts, K .R. N. Com. and M.D.Science College, Jamner, 424206, M.S., India.

<sup>2</sup> Department of Physics, M.S.G.College, Malegaon, 423105, M.S., India.

<sup>3</sup> SNJBs K.K.H.A. Arts, S. M .G .G .L .Commerce and Science College, Chandwad, M.S., India

E Mail : [rameshbari24@yahoo.com](mailto:rameshbari24@yahoo.com) , [mesudhakar\\_deshmukh@rediffmail.com](mailto:mesudhakar_deshmukh@rediffmail.com)

This paper presents Cd doped ZrO<sub>2</sub> nanostructured thin films have been deposited on glass substrate at 300<sup>0</sup>C using the spray pyrolysis technique. The films were deposited from mixed precursor spraying solution of cadmium chloride and zirconium oxychloride having same concentration (0.05M) dissolved in equal volumetric proportion of distilled water and triethylene glycol (solvents). The % of (CdCl<sub>2</sub>-ZrOCl<sub>2</sub>) solution was varied as 3-97%, 5-95%, 7-93% and 9-91% .It was sprayed at fixed spray rate and optimized distance between spray gun nozzle and substrate. The films were annealed in air at temperature 550<sup>0</sup>C for an hour. The films were characterized by x-ray diffraction (XRD), FE-SEM, and Optical absorption spectroscopy technique. The films were tested in various gases at different operating temperature. The film showed maximum gas response to acetone gas ( S=93.63) for 500ppm at 300<sup>0</sup>C operating temperature. The several parameters like grain size, activation energy, micro-strain , band gap, response and recovery time was reported, interpreted and discussed.

**Keywords:** nanostructure, spray pyrolysis, acetone gas, sensitivity.

## Dimethyl Methyl Phosphonate detection using Pt-modified nanostructured ZnO thick films

Anil R. Bari<sup>1</sup>, Lalchand A. Patil<sup>2</sup>

<sup>1</sup> Department of Physics, Arts, Commerce and Science College, Bodwad 425 310, Maharashtra, India

<sup>2</sup> Nanomaterials Research Lab., Department of Physics, Pratap College, Amalner, 425 401, Maharashtra, India

*E Mail/ Contact Details [anilbari\\_piyu@yahoo.com](mailto:anilbari_piyu@yahoo.com), "Piyush" House No. 2380/81, Bari Wada Yawal, At. Post. Tal. Yawal, Dist. Jalgaon, Pin: 425301, Maharashtra, India*

Nanostructured ZnO powder is prepared using ultrasonic atomization technique. As prepared powder were characterized using XRD and TEM. The average grain size was observed to be near about 20 nm. Thick films of this powder were prepared using screen printing technique. Pt-modified-nanostructured ZnO films were obtained by dipping pure ZnO films into an aqueous solution of chloroplatnic acid for different intervals of time, followed by firing at 500°C for 30 min. The sensing performance of the unmodified and Pt-modified nanostructured ZnO films was tested on exposure of chemical warfare agents (CWA) simulants, such as, dimethyl methyl phosphonate (DMMP), 2-chloroethyl ethyl sulfide (CEES) and 2-chloroethyl phenyl sulfide (CEPS). Both unmodified ZnO and Pt-ZnO films showed higher response to DMMP. The results are discussed and interpreted.

***Keywords: Ultrasonic atomization; Nanostructured ZnO thick films; Pt-modified ZnO films; CWA simulant sensing; DMMP sensor.***

### References

- [1] T. Z. TZOU, S. W. WELLER, J. Catalysis, 146, 370-375.
- [2] A. R. BARI, M. D. SHINDE, V. DEO, L.A.PATIL, Journal of Pure & Applied Physics, 47, 24-27.
- [3] L. A. PATIL, A. R. BARI, M. D. SHINDE, VINITA DEO, Sensors and Actuators B: Chemical, 149, 79-86.